The Anatomy of the Dodo (*Raphus cucullatus*) and the Solitaire (*Pezophaps solitaria*): A Description and Atlas

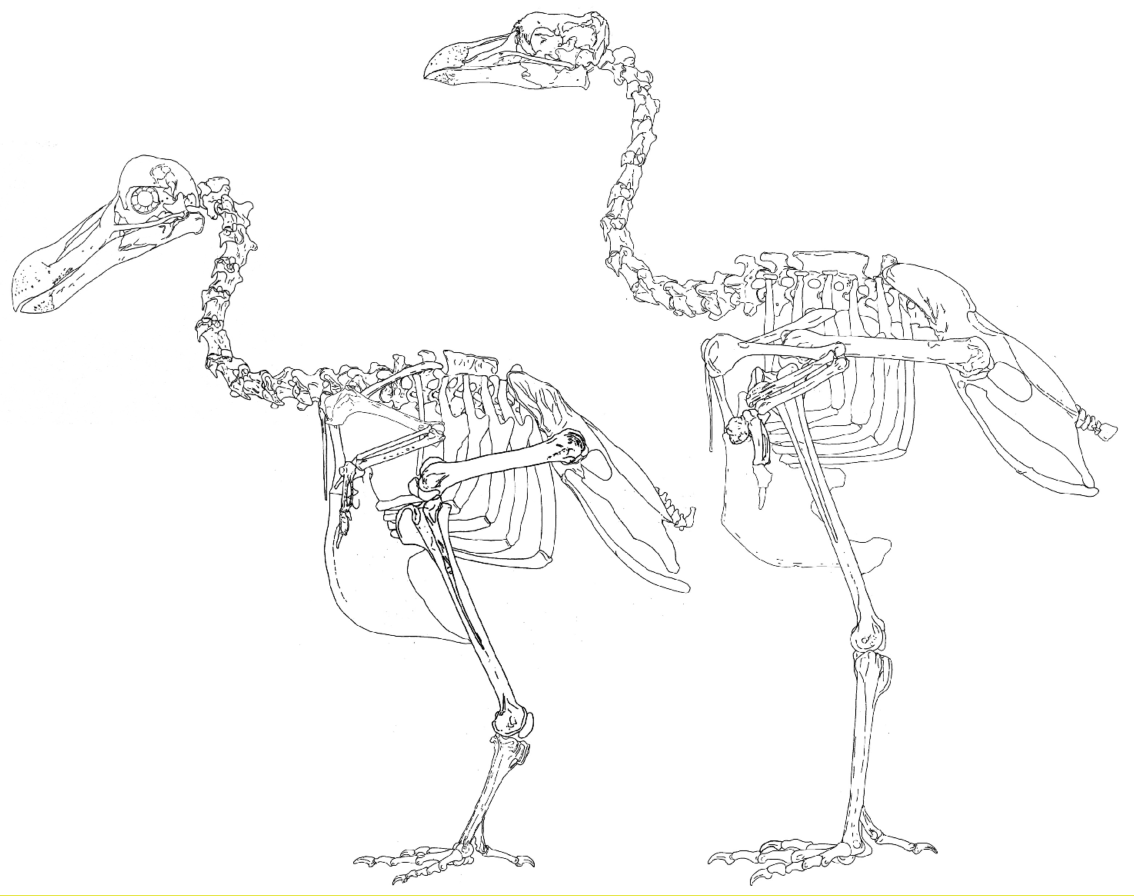

Jolyon C. Parish

The Dodologist's Miscellany 5
December 2020

The Anatomy of the Dodo (*Raphus cucullatus*) and the Solitaire (*Pezophaps solitaria*): A Description and Atlas

Abstract

The osteology of the dodo (*Raphus cucullatus*) and the solitaire (*Pezophaps solitaria*) is redescribed and revised. The present work comprises a description of the anatomy of the dodo, with additonal comments on that of the solitaire. It includes information from specimens from both Mare aux Songes (from where the majority of dodo bones originate) and from other localities. It is noted that the middle part of the mandible of *Raphus* is reinforced by a bony 'brace' (formed by a portion of the supra-angular), which was likely related to feeding on large and/or hard objects. In addition to possible hyoid elements for the dodo, the present work includes previously undescribed elements for the solitaire: columella, hyoid bones, ulnare, distal alar phalanges, patella, tarsal sesamoid and tracheal rings, as well as documenting variation and pathologies in these species. Comparisons are made between the exostoses of *Pezophaps* and hereditary osteochondromas. Possible juvenile specimens are also discussed. A short description of the reconstructed musculature of the dodo is given, although it is by no means complete.

Introduction

> A more wonderful structure than the Dodo's skeleton it is not easy for the ornithologist to conceive! (A. Newton 1866b, p.128).
>
> We have certainly never made a close study of such an extensive series of bones of any one other species as we have done of the Solitaire (Newton & Newton 1869, p.331).
>
> The osteology of the pigeons was given little attention and would have been perhaps altogether neglected up till now, had not the controversy concerning the relationship of *Didus* and *Pezophaps* forced their study (Martin 1904, p.174).
>
> Some of the smaller Dodo-bones are of great rarity, and at least one of them (the pygostyle) had not been found before. M. Thirioux has disposed of his considerable series of these bones to the Museum of Mauritius. Prof. Newton expresses a hope that some competent person may be found to publish a scientific description of this important collection (Sclater & Evans 1905, p.142).

Much has been written on the subject of the dodo and the solitaire, including on the anatomy of these species, notably Melville (1848), Owen (1867, 1871b, 1878, 1879), Newton & Newton (1869), Newton & Clark (1879), Newton & Gadow (1893), Martin (1904), Lüttschwager (1959a, b), Livezey (1993), Janoo (1996) and, more recently, Claessens *et al.* (2015). Indeed, Newton & Clark (1879) remarked: "We are not aware that the osteology of any other vertebrate, other than man, has been studied with the same wealth of materials as that of the Solitaire" (p.451). Cheke & Hume (2008) likewise noted: "the extinct Rodrigues Solitaire had become osteologically almost the best known animal on the planet!" (p.150). However, they are still poorly understood. The descriptions of Alexander Gordon Melville (Melville 1848), made shortly after the dissection of the Tradescant dodo specimen (OUMNH 11605), are comprehensive and detailed, but were written over 170 years ago. Melville's work was described as "very skillfully worked out" (Wilson 1849, p.94); "the patience and ability displayed in working out the osteological details will be admitted by everyone" (Anon. 1848d, p.446); "an account which is quite a model for such kind of work, both for its conscientious accuracy and minute detail" (Wright 1866, p.32).

The present work was begun some years prior to the publication of Claessens *et al.* (2015). This latter work comprises a monograph of the osteology of the dodo, and in particular of two skeletons composed of a majority of elements likely belonging to single individuals. I decided to complete the present work, as although the two cover much of the same ground, there are areas unique to each.

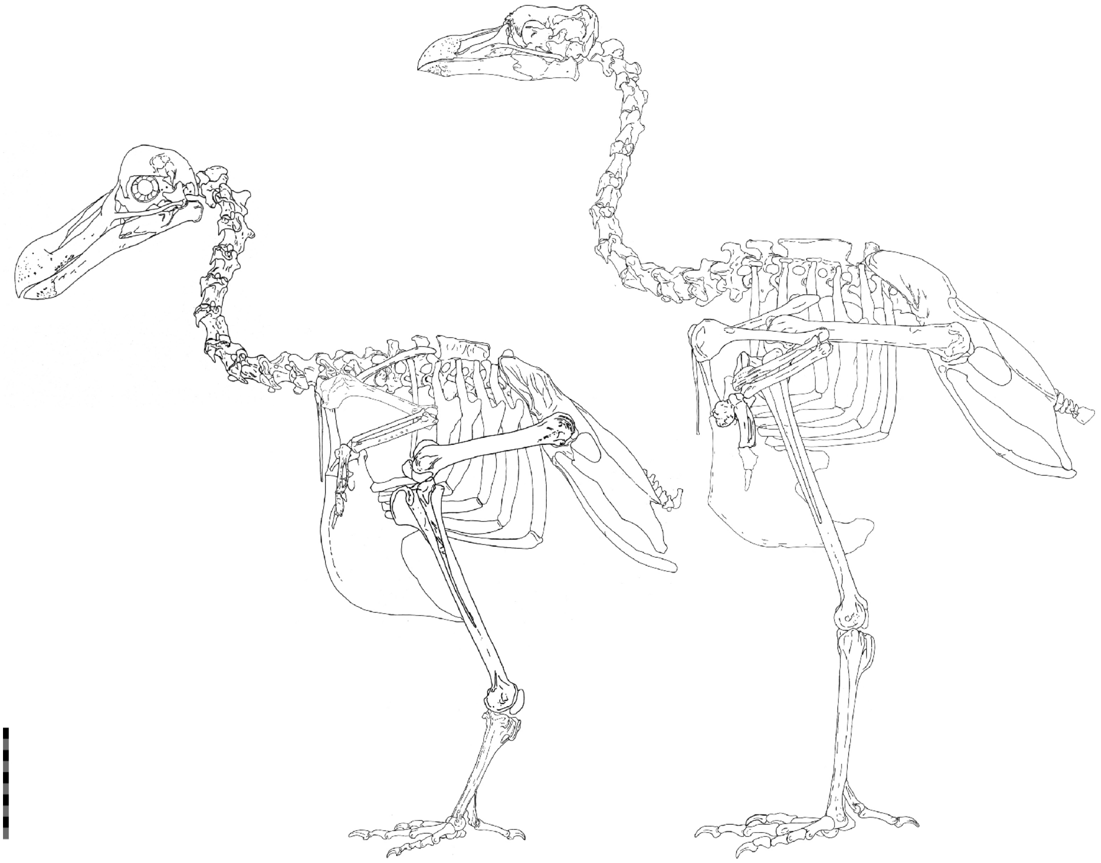

Reconstructed skeletons of the dodo (*Raphus cucullatus*; *left*) and male solitaire (*Pezophaps solitaria*; *right*). Scale in cm. ○ Jolyon C. Parish, 2020.

The present work contains details on osteological variation and pathologies in the dodo and solitaire, both island-dwelling species with no endemic predators. There is little information available on the interplay between such morphological disparity, lack of natural predators and insularization in flightless birds. The present work also includes information on possible juvenile specimens and musculature. A small sample of osteological measurements is also included.

Associated material for *Raphus* is limited: OUMNH 11605, elements from UMZC 415.KK, Thirioux's Port Louis skeleton, the Kanaka dodo skeleton, material from Plaine des Roches described by Janoo (2005), and three partly associated dodo bone constellations from Mare aux Songes, including a partial leg (Rijsdijk *et al*. 2009, Meijer *et al*. 2012). The only known skeleton likely composed mostly of elements belonging to a single individual is Thirioux's Port Louis skeleton (Claessens *et al*. 2015).[1]

---

[1] Thirioux's Port Louis skeleton has been described as representing a nearly complete single individual (Claessens & Hume 2015). Claessens & Hume (2015) noted that "Coloration, (relative) size, fit, and the extreme rarity of several of the elements [in Thirioux's Port Louis skeleton] strongly suggest that (almost) all of the surviving elements belong to a single individual" (p.25).

Donald d'Emmerez de Charmoy (1903) noted that "The most important pieces [of the dodo] found by Mr. Thirioux mostly belong to one and the same individual, which gives them greater value" (p.2). He added: "Mr. Thirioux has the bones of this bird [the dodo], some of which have never been found so far and which I have listed above [the coccygeal vertebrae, pterygoids, hyoid, and some sternal and ventral ribs], these bones if the Museum could acquire them would absolutely complement the skeleton found there, which would then be an excessively important single piece" (p.6). In a letter to Alfred Newton, dated 30th December 1904 (Letter 22), D'Emmerez de Charmoy noted that he had constructed the skeleton of the dodo "almost completely". Similarly, in a letter to Alfred Newton dated 11th January 1907 (Letter 29) Thirioux said "in addition to the full complement of the Dodo I also gave a complete Aphanapterix [*sic*]". However, it should be noted that although Thirioux states that he gave a "full complement" of dodo bones he does not say whether these were from one individual or not (although in a later letter he refers to owl specimens as being from single individuals).

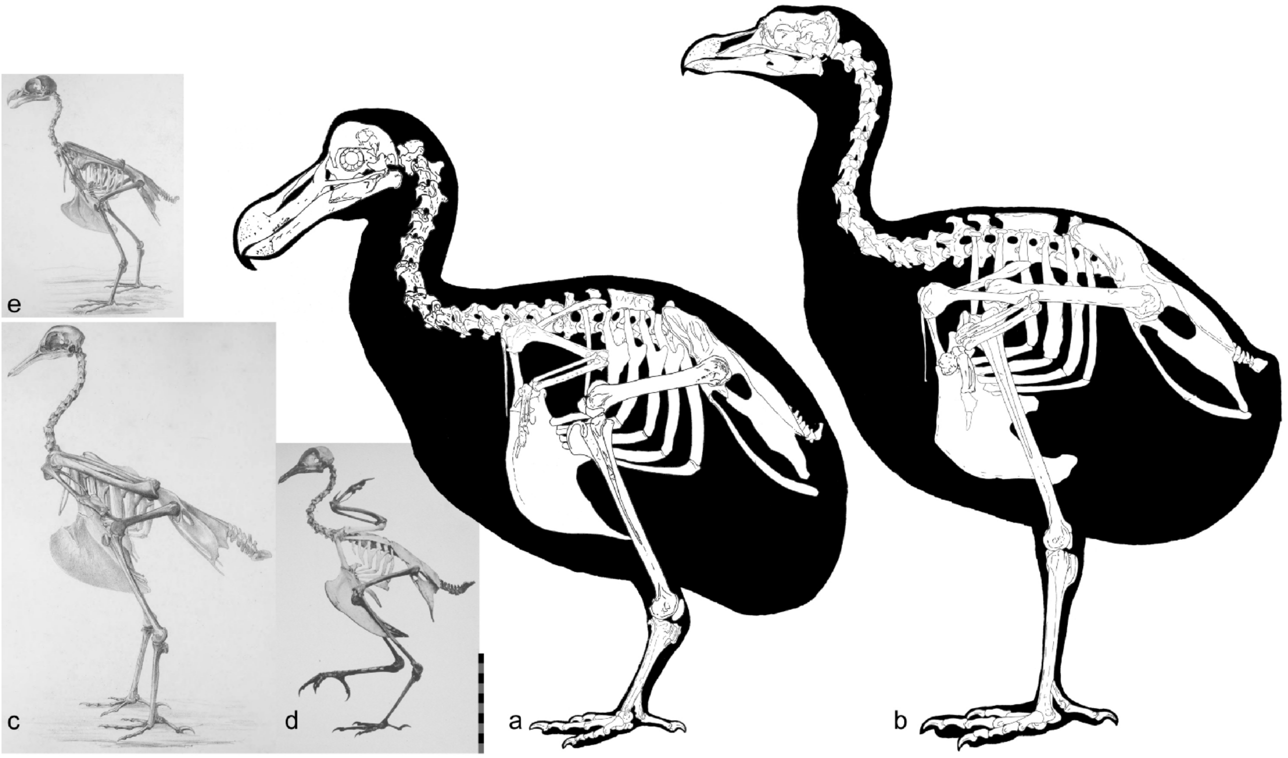

Reconstructed skeletons of the dodo (*Raphus cucullatus*; a) and male solitaire (*Pezophaps solitaria*; b) with body outlines added (○ Jolyon C. Parish, 2020), compared with the skeletons of extant pigeons: c: *Goura cristata* (Eyton 1867, pl.1.G; artist: James Erxleben), d: *Otidiphaps nobilis* (Meyer 1879-1888, Tafel viii), e: *Didunculus strigirostris* (Eyton 1869, pl.22; artist: James Erxleben). Scale in cm.

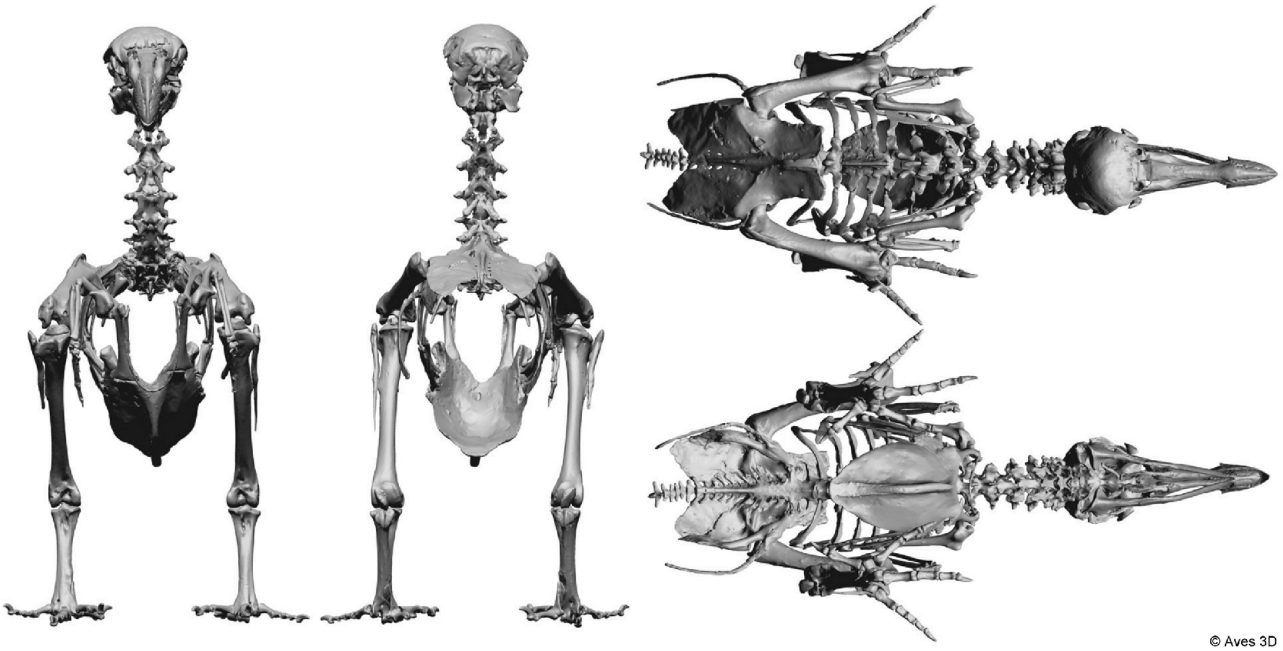

© Aves 3D

Skeleton of *Raphus* (Thirioux's Port Louis skeleton) in cranial, caudal, dorsal and ventral views (Claessens *et al*. 2015, pl.PL3, figs.B, D. F, H; © Aves 3D).

Skeletons of *Pezophaps* belonging to single individuals include NHMUK A.3505 and A.3506 (Claessens *et al*. 2015; near-complete skeletons of male and female respectively, both containing rare elements such as hyoid bones).

Newton & Gadow (1896) stated that the hyoid apparatus, the tip of the wing and the tail are lacking for the solitaire. In the collections of the NHMUK there are examples of part of the hyoid apparatus, the columella, ulnare, the proximal phalanx of digit II of the wing, and the tail bones, including pygostyle. In the UMZC collections there is a possible radiale and a specimen of the distal phalanx of alar digit II. Thus, all that is wanting in the skeleton of *Pezophaps* are: the phalanges of alar digits I and III, the sclerotic bones, and the remainder of the hyoid apparatus. That which is lacking for the dodo amounts to only the proximal hyoid elements (the columella appears to be present in the Copenhagen skull (see below) although is not described herein).

It is hoped that the labelled figures and accompanying text will be of use to students of avian anatomy, and that the synonyms from previous works will be of use to those using nineteenth-century anatomical texts, as well as providing additional information on the historical aspect of the study of the osteology of the dodo and solitaire. Thirioux wished that Newton, or some other, describe the specimens he discovered (see his letter of 11th January 1907). Hopefully those of the dodo, at least, will have now been figured and described.

This work is part of a larger corpus, which includes a comprehensive bibliography and a catalogue of dodo and solitaire specimens in collections worldwide.[2] For further illustrations of dodo osteology and measurements of dodo and solitaire specimens the reader is referred to the excellent monograph by Claessens *et al*. (2015).

Abbreviations
AMNH: American Museum of Natural History, New York
CT: Computed Tomography
GLAHM: The Zoology Museum, Hunterian Museum, University of Glasgow
GUEMG: Guernsey Museum & Art Gallery
lig.: ligamentum
m.: musculus
MAD: Madagascan Region [MHNH specimens]
m. a. m. e.: musculus adductor mandibulae externus
MAS: Dodo Research Project (Mare aux Songes). Specimens housed at Mon Desert Mon Tresor Sugar Estate (Omnicane)
MCZ: Museum of Comparative Zoology, Harvard University
m. d. m.: musculus depressor mandibulae
MGL: Lausanne Geological Museum
MNHN: Muséum national d'Histoire naturelle, Paris[3]
NHMUK: Natural History Museum, London

The ratio of hindlimb element lengths (femur:tibiotarsus:tarsometatarsus) is similar in Thirioux's Port Louis skeleton (0.31:0.44:0.25) and an associated dodo leg described by Janoo (2005) (0.30:0.44:0.26). However, the ratio of tarsometatarsus length to skull length in Thirioux's Port Louis skeleton is 1:1.76 whereas it is 1:1.56 in OUMNH 11605. In addition, Claessens & Hume (2015) noted that the sternum and pelvis are of a darker colour (externally) than other elements of Thirioux's Port Louis skeleton. The presence of an extra pair of (unfused) lacrimals (pers. obs., Claessens *et al*. 2015) also indicate that the skeleton is composed of elements from more than one individual, likely put together by D'Emmerez de Charmoy.

Claessens & Hume (2015) stated that "a supply of disarticulated remains to 'build' this skeleton, especially the rare elements of the skull, wing, and leg bones, would simply not have been available at this time" (p.25). However, D'Emmerez de Charmoy remarked "Do you know the Sesamoid bones of the Dodo, I have a lot of them" (letter to Alfred Newton dated 30th January 1906; Letter 26), suggesting that at least certain of such elements were not extremely rare.

[2] See https://sites.google.com/site/dodologistsmiscellany/ References to other works in this corpus are indicated by a coloured font.

[3] In this work the "MNHN skeleton" refers to that which bears the beak MAD 6530 and the cranium MAD 5971.

NMING: Natural History Museum, Dublin
NMP: Národní Museum, Prague
OUMNH: Oxford University Museum of Natural History, Oxford
RCSHM: Royal College of Surgeons, Hunterian Museum, London
UMZC: University Museum of Zoology, Cambridge
USNM: United States National Museum, Washington, D.C.
YPM: Peabody Museum of Natural History, Yale University, New Haven
ZMUK: Zoologisk Museum, University of Copenhagen

Abbreviations for figure labels are given in Appendix 1.

Notes

The majority of lithographs illustrated herein were photocopied, electronically scanned and (for the most part) have had the backgrounds to the illustrations removed. Some very light retouching of the borders to the illustrations was made in some cases in order to facilitate background removal. Some of the lithographic illustrations retain labels and pointers from the originals.

As the genera *Raphus* and *Pezophaps* are monospecific they will be referred to by their generic or vernacular names only. In older literature the dodo is referred to as *Didus ineptus*.

Owen’s paper on the osteology of the dodo was first published in Owen & Broderip (1866) and later reprinted in the *Transactions of the Zoological Society of London* (1867). The source referenced here is the 1867 one, although the osteology text and plates of the two are identical in all except page and plate numbering.

The terminology used herein follows that of Baumel & Witmer (1993), Butendieck & Wissdorf (1981, 1982), Butendieck, Wissdorf & Ballman (1981), Wissdorf & Butendieck (1982), Livezey & Zusi (2006) and Mayr (2020). Anatomical features were identified using a combination of the literature and examination of specimens (dodo and solitaire (see below) and other bird species).

Bibliographic references are either to be found in the *Bibliography of the Didinæ* or in the Additional References section at the end of this work. Further details on individual specimens are to be found in the Catalogue of Specimens.

Material Examined

In addition to the literature, specimens of *Raphus* and *Pezophaps* in the collections of the AMNH, Booth Museum, NHMUK, OUMNH, UMZC, USNM and YPM were studied (see Parish 2015 Catalogue of Specimens). Photographs of the Copenhagen skull (ZMUK AVES-105485; Harri Kallio, pers. comm.), Prague beak (NMP P6V-004389; photographs by Jiří Moravec) and Louis Etienne Thirioux’s Port Louis and Durban skeletons (Jan den Hengst, pers. comm.) were also examined, as well as images of numerous other specimens sent by museum curators (see Parish 2015 Catalogue of Specimens). Correspondence between Alfred Newton (at Cambridge) and (Louis) Etienne Thirioux (in Mauritius), housed at the UMZC,[4] and CT scan data resulting from the University of Warwick/OUMNH investigations of the Tradescant dodo head[5] yielded further information.

Skeleton

(*Raphus*: Owen 1867, pl.xv, fig.1 [reproduced: Van Wissen 1995; Koenig *et al*. 2004; Hume; Parish 2013, fig.3.8]; Owen 1871b, pls.lxiv [reproduced: Woodruff 2014, fig.13f], lxv; Owen 1879, pls.i, ii; Newton & Gadow 1893, pl.xxxvi, fig.1; Ogilvie-Grant 1905, pl.ii, fig.2; Pitot 1905, pl.19; True 1905, pl.lxxvi; Lankester 1909, fig.17; Newton & Gadow 1910, fig.1; Creizenach

---

[4] See Transcriptions: Thirioux-Newton Correspondence.

[5] https://www.tandfonline.com/doi/suppl/10.1080/08912963.2020.1782396/suppl_file/ghbi_a_1782396_sm7376.mpeg
https://www.morphosource.org/Detail/MediaDetail/Show/media_id/55320

1913, p.9; Pitot 1914, p.87; Dixon 1917; Chubb 1919a, pl.xvii; Chubb 1919b; Killermann 1915, fig.7; Mertens 1925, pl.iv; Pycraft 1931, p.699; Lambrecht 1933, pl.i; Anon. 1934a; De Wit 1940, p.199; Chubb 1948, p.189; Hachisuka 1953, pls.viii, ix ["after Owen" (1871b)]; Keynes 1956, p.90; Lüttschwager 1961, fig.15; Fisher & Peterson 1964, p.273; Shuttlesworth 1968, p.16; Kuhn 1971, fig.36; Carié 1976, p.viii; Fuller 1987, fig. 121; Quickelberge 1987, p.86; Brom & Prins 1988, figs.1, 2; Coffey 1991, p.3; Staub 1993, pl.1, fig.1; Van Wissen 1995, pp.76-77, 83; Ziswiler 1996, covers, p.67; Aan de Brugh 1997, p.3; Cornuault 1997, p.77; Fuller 2000, p.202; Gill & West 2001, pp.64, 96, 139; Fuller 2002, pp.126, 127; Den Hengst 2003, pp.86, 103; Fuller 2003, p.38; Seymour 2003, pp.38-39; Van Oppen 2003; Koenig *et al*. 2004; Grihault 2005, pp.38, 41, 79; Kallio 2005, pp.19, 28-29, 31, 32-33; 54, 55; Hume 2006, figs.23, 24; Grihault 2007, p.101; Parker 2007, p.65; Tabouelle 2007, p.15; Middleton 2008, photo 10; Anon. 2009 [Liverpool]; Hume 2009a, p.50; Powell 2009, p.10; Claessens & Allan 2012, pp.39, 40, 41; Hume 2012a, fig.5; Parish 2013, figs.5.42, 5.45 5.47, 5.48, 5.49, 6.1, 6.4, 6.15. Ohlenbusch 2002-2007 [skeleton reconstruction]; Claessens & Hume 2015, figs.4, 5, 8-10; Claessens *et al*. 2015, figs.1, 16A-D, 65, pls.PL1-3, D1-3.

Pezophaps: Newton & Newton 1869, pl.xxiv, figs.177-179; Owen 1878, pl.vii, fig.1; Owen 1879, pl.iv, figs.1, 2; Oustalet 1874;[6] Oliver 1891, frontispiece; Newton & Gadow 1910, fig.3; Pycraft 1931, p.699; Mortensen 1933, pls.i, ii; Hachisuka 1953, pl.xiv; Lüttschwager 1961, figs.16, 28; Staub 1993, pl.1, fig.2; Fuller 2002, p.164; Grihault 2005, p.114; Grihault 2007, pp.50, 51, 52, 86; Middleton 2008, photo 8; Hume & Steel 2013, fig.2; Parish 2013, figs.5.44, 5.45, 5.46, 5.47, 5.54, 6.9, 6.15)[7]

The dodo exhibited a certain amount of laterality, with bones from the right side of the body frequently being slightly longer than their corresponding elements on the left. This can be seen in Thirioux's Port Louis skeleton as well as specimens from Mare aux Songes and is also apparent in extant columbids (Claessens *et al*. 2015).

- Thirioux's Port Louis skeleton: elements of right side longer (scapula, coracoid, humerus, femur, first metatarsal, palatine); elements equal in length (radius, ulna, carpometacarpus, alar phalanx of digit I, proximal phalanx of alar digit II, tibiotarsus, tarsometatarsus); elements of left side longer (pterygoid, mandibular ramus).

Skull

(*Raphus*: Strickland & Melville 1848, pls.viii, ix, pl.ix*, fig.1, pl.x, 2-2a; Reuss 1855, pl.i; Owen 1867, pl.xxiii, fig.1; Walker & Ward 1992, p.262; Janoo 1996, figs.1-4, 5a-f; Janoo 2005, figs.2i, 2j; Kallio 2005, pp.30, 31, 62-63; Holden 2010, p.765; Claessens *et al*. 2015, figs.6-9, 11, 65; pls.PL4, D4; Warnett *et al*. 2020, figure on p.1 (graphical abstract), figs.2, 3, 4, 5, 6.[8] *Pezophaps*: Strickland & Melville 1848, pl.xiii, figs.1-4; Newton & Newton 1869, pl.xxi, figs.139-147, pl.xxii, figs.149-158; Newton & Clark 1879, pl.l, figs.1-6; Owen 1878, pl.vii, fig.2, pl.viii, figs.1, 2; Owen 1879, pl.v, figs.1-5; Simonetta 1960, fig.12; Lüttschwager 1961, fig.27)

General

The ratio of cranium length to width is approximately 0.74 in *Raphus* and 1.22 in *Pezophaps*. The angle between the plane of the foramen magnum and the base of the skull is 57° (NHMUK A.1338) to 63° (UMZC 415.J) in *Raphus* and 56° (UMZC 648) in *Pezophaps* (Martin 1904 gives 55° and 58° respectively), compared to 25-35° in extant columbids (*ibid*.; pers. obs.). The facial skeleton (ossa faciei) of *Raphus* is proportionately longer compared to the cranium than in *Pezophaps*, the ratio of the

---

[6] This illustration is rather inaccurate.

[7] With the exception of Thirioux's dodo skeleton at Port Louis (see below), all mounted dodo skeletons are composites. Many contain duplicated vertebrae and often elements are fabricated to fill in for missing bones. Many solitaire skeletons are also composites, made up of elements from more than one individual.

[8] A 3D digitized model of the Oxford (Tradescant) dodo head, created by Roger Benson in May 2018, can be found here: https://sketchfab.com/models/1fc58bcf355846d6a942c77daa10b716/embed

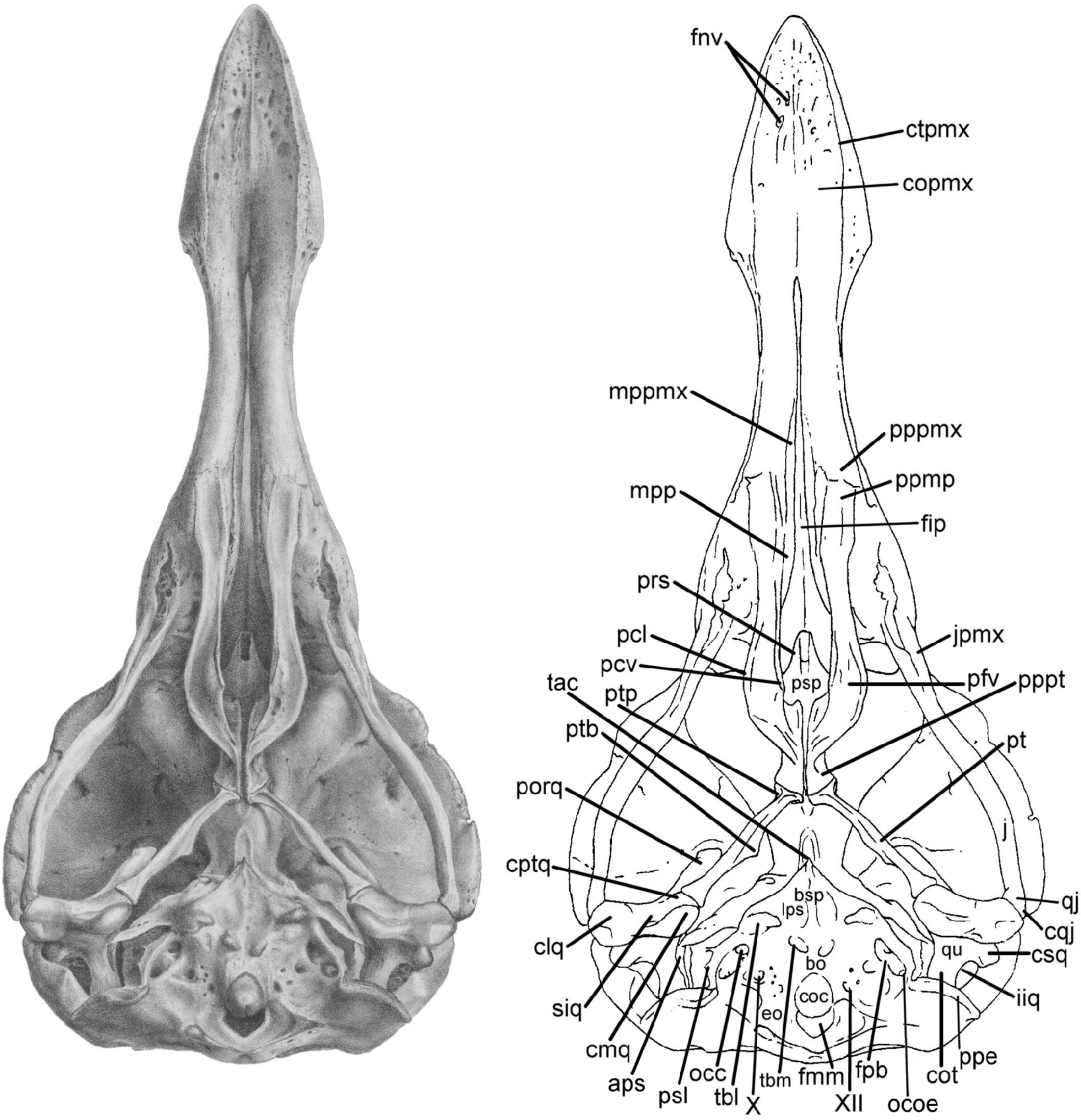

Skull and mandible of the dodo in ventral view (lithograph from Strickland & Melville 1848, pl.ix, fig.2; by Joseph Dinkel; “Reeve, Benham & Reeve, Lithographers.”)

length of the cranium to that of the facial skeleton being around 0.5 in *Raphus* and approximately 1.0 in *Pezophaps*. The jugal arch descends at an angle of around 160° to the plane of the palatine in *Raphus* (UMZC "Dodo Book" Archive[9]); this angle is 145°-155° in other columbids (*ibid.*). As in other pigeons, a septum nasale is absent.

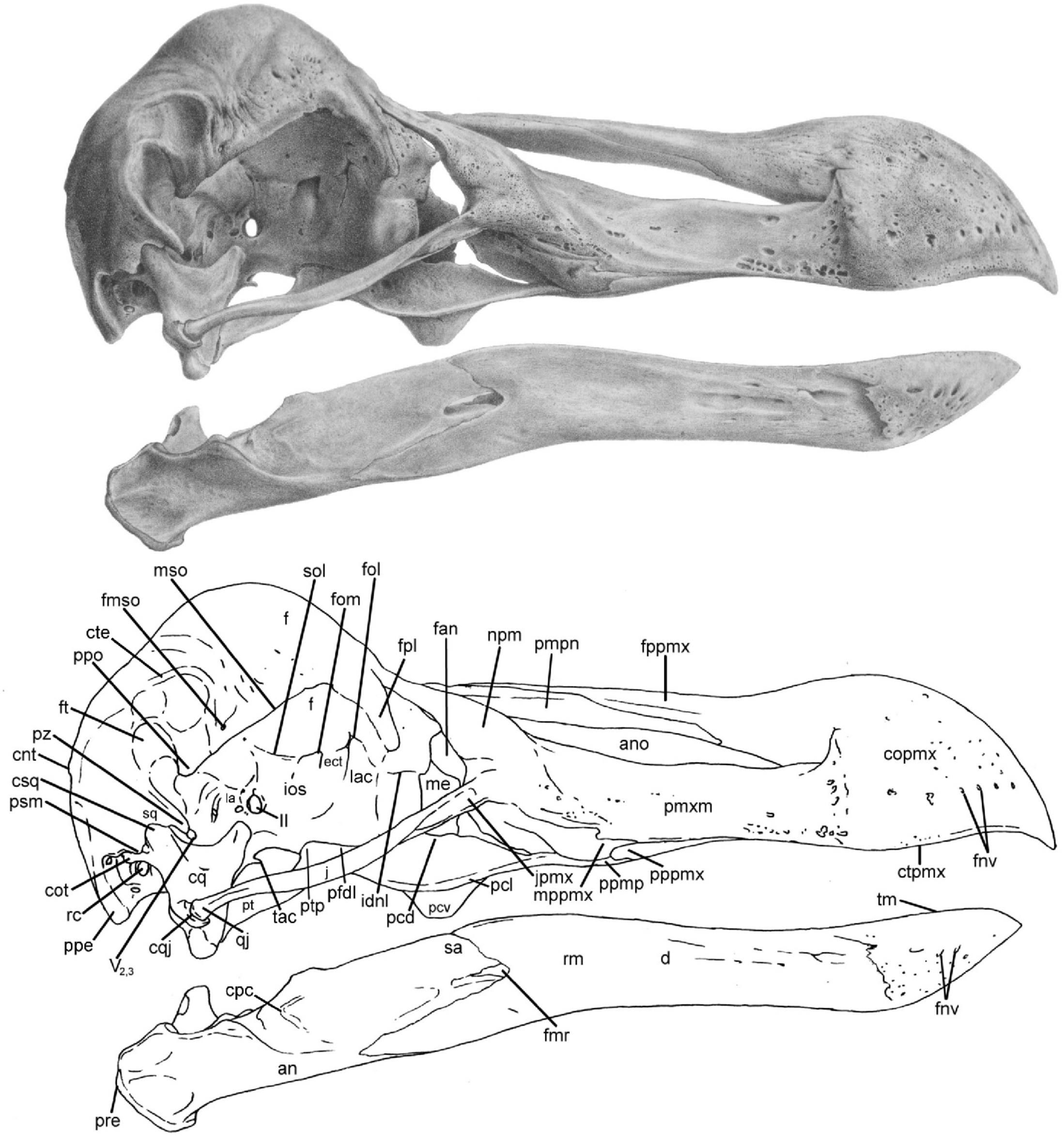

Skull and mandible of the dodo in lateral view (lithograph from Strickland & Melville 1848, pl.viii; by Joseph Dinkel; "Reeve, Benham & Reeve, Lithographers.")

The cranium figured by Owen (1867, pl.xxiii, fig.1 [NHMUK A.1338]) probably does not belong with the bill figured with it (concluded from the ratio of the cranium : bill compared with that of OUMNH 11605), so the reconstruction of the skull in his plate xv is probably inaccurate and disproportionate. The cranium figured by Janoo (1996) may or may not belong to the bill it is associated with, although the cranium is not in proportion with the bill if OUMNH 11605 is taken as a standard. However, the bill shows a slightly different form from that of the Oxford specimen, being more robust (see discussion on variation, below).

---

[9] See Rookmaaker 2010.

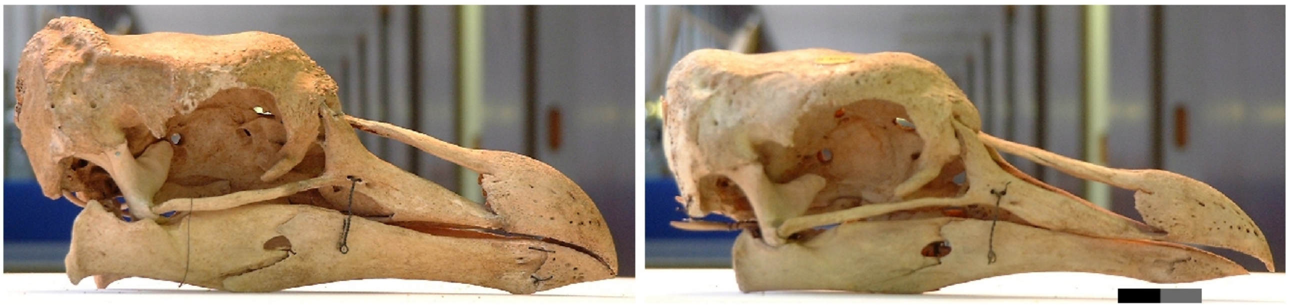

Skulls of *Pezophaps* in lateral view: *left*: male (NHMUK A.3505), *right*: female (NHMUK A.3506), scale: 2cm. ○ Jolyon C. Parish.

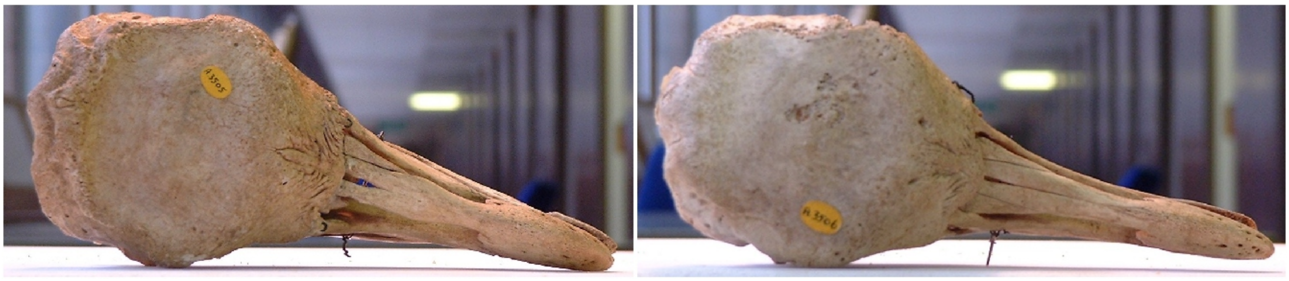

Skulls of *Pezophaps* in dorsal view: *left*: male (NHMUK A.3505), *right*: female (NHMUK A.3506). ○ Jolyon C. Parish.

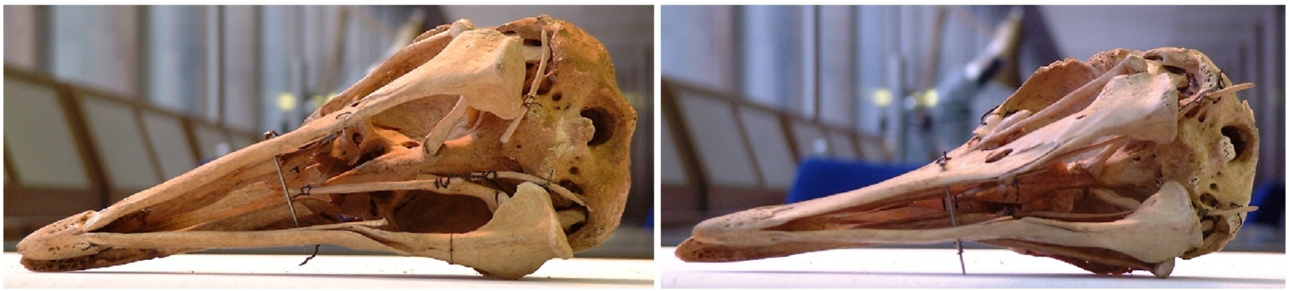

Skulls of *Pezophaps* in ventral view: *left*: male (NHMUK A.3505), *right*: female (NHMUK A.3506). ○ Jolyon C. Parish.

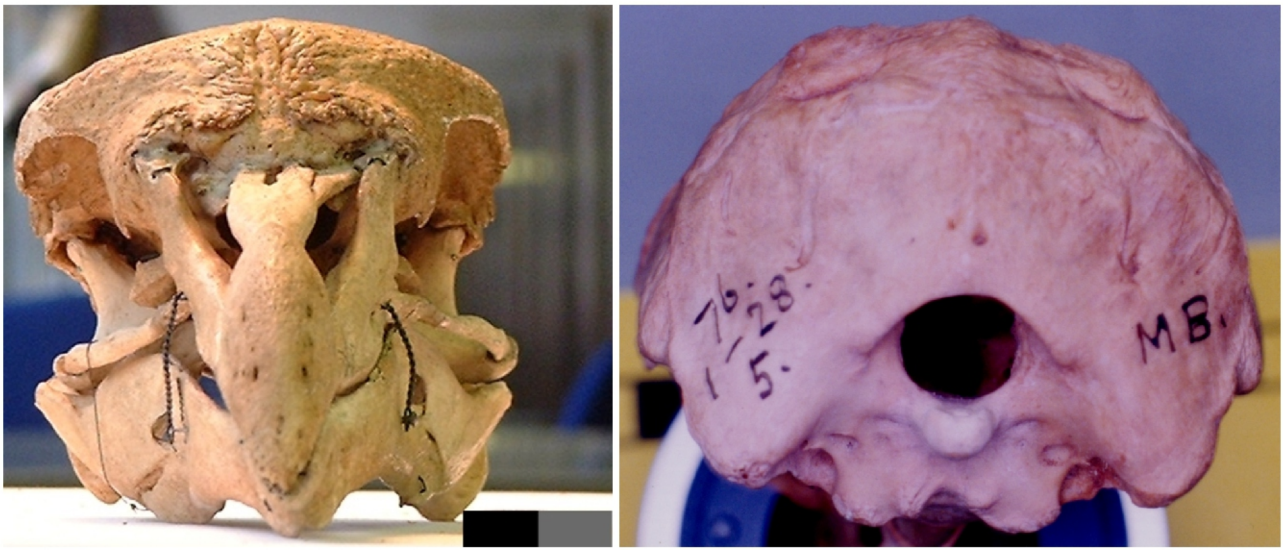

Skulls of *Pezophaps*: *left*: rostral view (NHMUK A.3505; male), scale: 2cm; *right*: caudal view (NHMUK A.1375). ○ Jolyon C. Parish.

The skull of *Pezophaps* displays osseous swellings at the rostral and caudal part of the cranium, these are not pathological, but a feature seen, to differing degrees, in all skulls of *Pezophaps*. Such osseous growths are diagnostic of *Pezophaps* and are are seen in other parts of the skeleton.

Martin (1904) distinguished six basic forms of beak in pigeons, identified from their length, strength and position in relation to the skull. He grouped these as follows: 1) *Ducula* (*Carpophaga*) with *Goura* and *Otidiphaps*, 2) *Treron* with *Raphus* and *Pezophaps*, 3) *Columba*, 4) 'Peristeridae' (including such forms as *Caloenas*, *Columbina*, *Gallicolumba*, *Geopelia*, *Geotrygon*, *Leptotila, Leucosarcia*, *Metriopelia*, *Starnoenas*, *Streptopelia*, *Turtur* and *Zenaida*) and 'Ptilinopodinae' (*Ptilinopus*, *Alectroenas*), 5) *Phaps*, and 6) *Didunculus*.

Using discriminant analyses and variation partitioning, Gussekloo & Cubo (2013) found a relationship between skull morphology and flightlessness in birds, which they suggested could be due to reduced selction pressures for light-weight skulls in nonvolant birds. They also found that the skull morphology of the dodo resembles that of the pre-hatching chicken (*Gallus gallus*), stating: "Principal component scores of adult neognathous flightless birds fall within the range of chicken development, so no clear conclusions about the ontogenetic trajectories leading to their sturdier skull morphology could be drawn" (p.75).[10] This is in contrast with the results of Livezey (1993), who found that the skull of the dodo was peramorphic. Gussekloo & Cubo commented: "The reason why the results obtained when using a classical morphological approach differ from those obtained when using PC analyses may be that in a principal component analysis all data are combined to a single parameter, while in the classical approach individual characters are assessed individually, which might lead to different results" (p.83).

Cranium

Caudal Aspect

The flat, almost vertical, caudal (occipital) face of the skull is of approximately semicircular form, with the transverse nuchal crest and the curved edges of the exoccipitals forming the curved portion and the basioccipital and the medial parts of the exoccipitals completing the form. The caudal face is bounded dorsally by the transverse nuchal crest. This crest slightly overhangs the supraoccipital plate below the parietal region and provided attachment for m.complexus. Continuing laterally from the extremities of the crest are the convex edges of the paroccipital processes. The paroccipital process, formed by the exoccipital, the opisthotic medially, and the metotic laterally (Baumel & Witmer 1993), creates a lateral, stubby, ventromedially directed flattened flange and forms the caudal wall of the tympanic cavity. The convex lateral margin of the paroccipital process provided attachment for lig. occipitomandibulare, which passed to the apex of the medial mandibular process. The exoccipital joins the basioccipital medially on the ventral part of the cranium, the supraoccipital dorsomedially and the squamosal laterally on the posterior aspect of the cranium.

The foramen magnum is vertically sub-oval to sub-rectangular, with small lateral projections constituting the internal processes of the exoccipitals, "rendering it fiddle-shaped" as Melville (1848, p.78) described it.[11] The foramen is bounded dorsally by the supraoccipital, laterally by the exoccipitals and ventrally by the basioccipital. There is variation in the shape of the foramen magnum in both *Raphus* and *Pezophaps*: for example, in Thirioux's Port Louis skeleton it is "rectangular with rounded corners and is deeper than wide" (Claessens *et al.* 2015, p.46), whereas in OUMNH 11605 it more pointed dorsally and its ventral part is wider than its dorsal part. Similarly, in a male specimen of *Pezophaps* mentioned by Newton & Newton (1869) the foramen magnum is wider ventrally than it is dorsally; normally the dorsal and ventral parts of the foramen are approximately equal in width (*ibid.*). The internal exoccipital processes are more developed in *Raphus* than in *Pezophaps* and extant pigeons, making the foramen magnum more laterally compressed. The sagittal nuchal crest overhangs the fossa containing the foramen magnum and has the approximate form of a right angle with the apex rounded. Its ventral extremities curve into the medial edges of the paroccipital processes. The sagittal crest is separated from the margin of the foramen magnum by a groove that probably accommodated the sinus foraminis magni in life.

---

[10] In contrast, they found that the skulls of palaeognathous birds are not similar to those of juvenile chickens and appear peramorphic.

[11] See Rotthowe & Starck (1998) for further information regarding the internal processes of the exoccipitals.

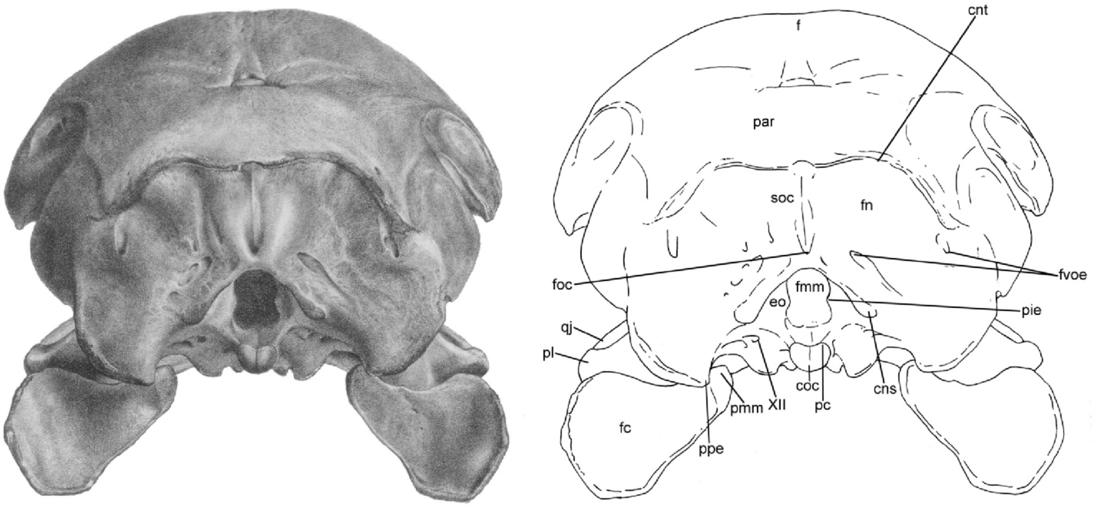

Skull and mandible of the dodo in caudal view (lithograph from Strickland & Melville 1848, pl.ix*, fig.1; by Joseph Dinkel; "Reeve, Benham & Reeve, Lithographers.")

The supraoccipital presents several foramina. Medially, just dorsal to the sagittal nuchal crest, is the median supraoccipital foramen which transmitted the v. occipitalis dorsomediana from the endocranial cavity.[12] The foramen perforates the ventral apical part of a median inverted subtriangular "cerebellar elevation". This elevation, whose ventral apex merges with the sagittal nuchal crest and whose base approaches the transverse nuchal crest, presents a median vertical depressed area that shows a slight vertical ridge at the midline. The prominentia cerebellaris, commonly present in columbids, is absent (Janoo 1996), or at least only weakly developed; the occipital being relatively flat and with the occipital condyle being in line with the paroccipital processes (Claessens *et al*. 2015). Lateral to the median supraoccipital foramen are two others, one on each side, which are the terminations of grooves running parallel to the sagittal nuchal crest (*i.e.*, dorsomedially). These foramina, the foramina venae occipitalis externae, transmitted the vv. occipitalis externae in life. Sometimes the groove leading to the fonticulus occipitalis presents a narrow osseous bridge adjacent (ventrolateral) to it (this is seen only on the left side of OUMNH 11605 (Melville 1848) and on the right side of MAD 5971 (Janoo1996)). A small canal, that would have contained a "muscular vein", opens just dorsomedial to this bridge in OUMNH 11605 (Melville 1848). In OUMNH 11605 the groove leading to the foramen occipitalis venae externae curves around the ventrolateral margin of the sagittal nuchal crest "a narrow tract, one line [2.1mm] in breadth, separating its termination from the groove for the bulb of the jugular vein" (*ibid*., p.77). Just ventral to the termination of the transverse nuchal crest, on each side, is a fonticulus occipitalis, directed ventrolaterally. Dorsal to the median supraoccipital foramen are a pair of very small apertures, ventromedially directed, and probably for the nutrition of the diploë (*ibid*.). The supraoccipital plate also shows a pair of elevations running ventromedially towards the origin of the sagittal nuchal crest, from the dorsal part of the transverse nuchal crest, according to Melville (1848) these correspond to the position of the semicircular canals inside the skull. In *Pezophaps* the supraoccipital plate is vertical and weakly convex vertically.

The occipital condyle is sub-reniform and slightly more than hemispheroid; it is convex ventrally and caudally, and bilobed (or partly so) with a median vertical groove seen posteriorly. In Thirioux's Port Louis skeleton it is between semicircular and reniform in form (Claessens *et al*. 2015). The caudodorsal border of the condyle presents a raised feature in the form of a 'W' (Janoo 1996). The occipital condyle is sub-pedunculate and non-sessile (it is sessile in extant columbids), the articular surface separated laterally from the peduncle by a groove but continuous with it ventrally. The condyle lies above the level of the basisphenoid plate. In Thirioux's Port Louis skeleton the occipital condyle "appears to originate from the same level as the lamina parasphenoidalis, but projects posteriorly and ventrally from it" (Claessens *et al*. 2015, p.46). Dorsally the condyle shows a slight concavity for the medulla oblongata, continuous with that of the dorsal surface of the basioccipital plate. In some specimens of *Pezophaps* the occipital condyle appears unpedunculate (or only weakly pedunculate), sloping gradually from its base (pers. obs.; Newton & Newton 1869). The height to width ratio of the occipital condyle is approximately one in *Pezophaps* and greater than one in *Raphus* (Martin 1904).

---

[12] Parker (1861) commented: "on the eighth day [pigeons] have a large single 'supra-occipital' deeply notched in the middle, inferiorly, in the place of the oval membranous deficiency, or *fontanelle*, in the primordial occipital wall. In adult Pigeons, and also in the Dodo and Didunculus, traces of this structure still remain (see Strickland and Melville), – all the Columbinæ hitherto examined having a mesial 'supra-occipital' foramen" (p.273).

Projecting downwards from the ventral surface of the cranium are the basilar tubercles, the smaller rostromedial and the larger caudolateral tubercles of the lamina basisphenoidalis.

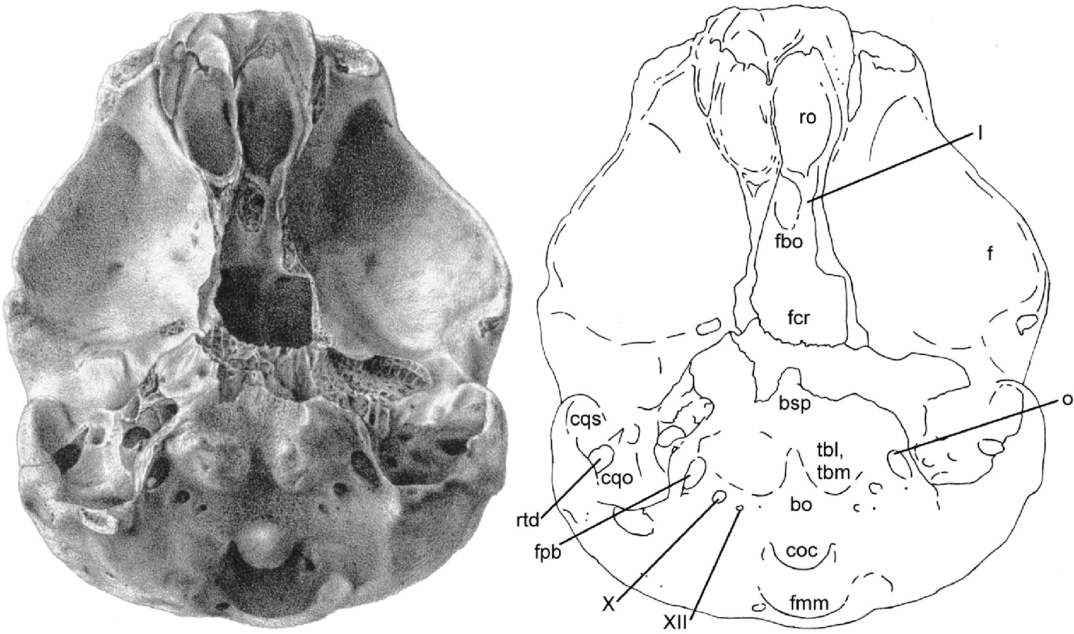

Cranium of male *Pezophaps* in ventral view (lithograph from Newton & Newton 1869, pl.xxi, fig.143; artist: George Henry Ford).

Comparing the posterior face of the cranium of *Pezophaps* with that of *Raphus* it can be seen that in the former the transverse nuchal crest is less developed and the laterally convex edges of the elevetions corresponding to the semicircular canals within, more apparent. In *Pezophaps* the median "cerebellar elevation" seems to be more ridge-like rather than subtriangular and swollen, as it is in *Raphus*. It separates two vertically sub-oval parts, the lateral boundaries of which are marked by the fonticuli occipitalia. *Pezophaps* shows the median supraoccipital foramen and both lateral pairs of fonticuli occipitalia, as occur in *Raphus*. The general form of the caudal face of the skull appears more semicircular in form in *Pezophaps* than in *Raphus*, which shows more lateral expansion. The posterior face of the cranium of *Pezophaps* also often shows marked pachyosteosis, especially in male specimens.

Ventral Aspect

The ventral face of the cranium presents the two large orbital cavities on each side, separated by the parasphenoid and ethmoidal regions. The narrowest part of the ethmoid-parasphenoid complex is ventral to the optic foramina, caudoventrally it broadens to its junction with the basisphenoid. The parasphenoid-ethmoid complex expands rostrolaterally from the narrowest part, forming a pair of 'bulbs'. These then contract and form a thin narrow medial plate in the choanal region. These 'bulbs' are not developed in *Pezophaps*. In *Pezophaps* the ectethmoid projects slightly rostrolaterally from the parasphenoid rostrum, similar to the condition in *Goura* and other columbids. Between the ectethmoid and the parasphenoid rostrum, on each side, is a longitudinally elongate fissure leading up into the posterior olfactory chamber above. The distal end of the parasphenoid is broken in OUMNH 11605, but is present in the Copenhagen skull (ZMUK AVES-105485). It forms a swollen, lanceolate structure, apparently bifid at its anterior end (pers. obs from photograph).[13]

A caudoventrally directed wide but shallow groove, with distinct lateral edges and rounded rostral extremity (which lies just rostral to the narrowest part of the parasphenoid rostrum) leads to the common auditory tube. The groove would have been lined with a sinus in life (Melville 1848). Rostral to this groove are the flat oblong facets for the articulation of the pterygoids and palatines. The articulatory faces on each side, separated by a low median ridge, allow movement of the pterygoids and palatines during cranial kinesis (prokinesis).

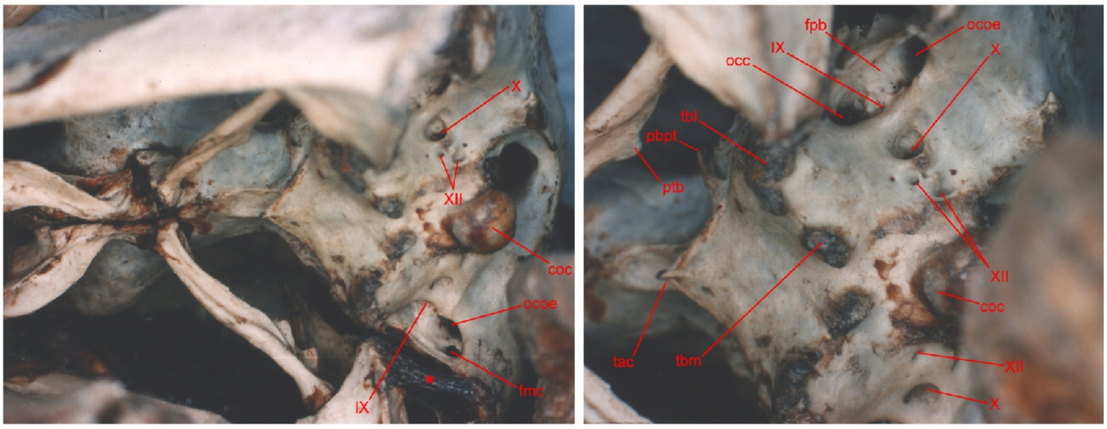

Basicranium of OUMNH 11605. * = Lig. occipitomandibulare. Note: the rostrolateral foramen of cranial nerve XII on the left side of the skull has another foramen for cranial nerve XII caudolateral to it, which is not labelled (see text for details). ○ Jolyon C. Parish, January 2001.

The rostral part of the basisphenoid plate is triangular, pointing forwards. The rostral apex of the basisphenoid plate is sharp and unattached to the parasphenoid; it forms the ventral border of the ostium tuba auditiva (pharyngotympanica) communis. From the apex the plate increases in width caudolaterally and forms a pair of tubercles, one on each side, these are the basilar tubercles. According to Owen (1866), the basilar tuberosities are developed where the basisphenoid joins the basioccipital. The lateral basilar tubercles are wider lateromedially than rostrocaudally; their lateral edges curve medially, whilst their medial edges are more vertical. The depression for m. rectus capitis ventralis is located rostromedial to the lateral basilar tubercles. Caudomedial to the large lateral basilar tubercles are a pair of smaller ones, which are elongate in a rostrolateral-caudomedial direction. These smaller tubercles are not present in all specimens (Owen 1867): they are developed in OUMNH 11605 and in Thirioux's Port Louis skeleton (Claessens *et al.* 2015), but in NHMUK A.1338 they are reduced to narrow ridges. The basilar tubercles, both lateral and medial, are more rounded and rugose in *Pezophaps* compared with *Raphus* (pers. obs.). The basilar tubercles provided attachment for m. rectus capitis dorsalis (Baumel & Witmer 1993, Snively & Russell 2007).[14]

Caudolateral to the smaller tubercles, on each side, is a semi-oval fossa, which presents caudally the shallow oval depression for the v. jugularis interna. Opening into this fossa is the outlet for n. vagi (X) and n. accessorius (XI). Lateral to this is the parabasal fossa (see Mayr 2020). This caudolaterally directed shallow oval concavity (described by Melville (1848) as the remnants of the "foramen lacerum posterius") presents the foramen for the internal carotid artery and its accompanying sinus (Melville 1848), directed rostromedially, at its rostral extremity. Medially it houses the foramen for n.

---

[13] However, the parasphenoid rostrum only has a single centre of ossification (Jollie 1957).

[14] These tubercles are most developed in birds with long skulls (Baumel & Witmer 1993). Melville (1848) stated that "the basilar protuberances [were] for the insertion of the *M. recti capitis laterales*" (p.97).

glossopharyngealis (IX)[15] and the caudal part of the parabasal fossa presents the ostium canalis ophthalmicus externus, which runs dorsally to open in the tympanic cavity.[16] Just lateral to the ostium of the external ophthalmic canal, in the lateral wall[17] of the parabasal fossa, is the medial opening of the foramen m. columellae. The foramina for the hypoglossal nerve (XII) lie at the base of the peduncle of the occipital condyle on each side. Melville (1848) stated that in OUMNH 11605 "[t]wo minute apertures separated by an osseous line, and probably giving exit to small venules, perforate the lower part of the interspace between the condyloid [XII] and pneumogastric foramina [X] on the left side; on the right side they are a line and a half [3.2mm] apart" (p.78); these are interpreted herein as foramina for branches of the hypoglossal nerve.

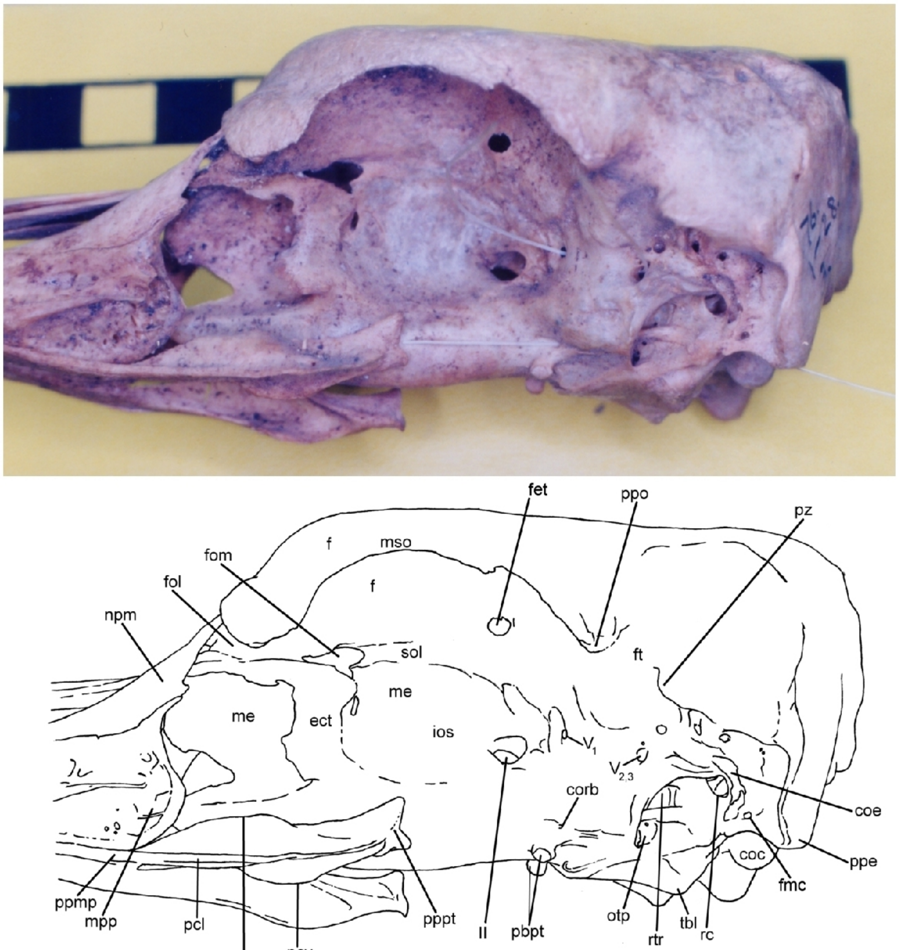

Cranium of *Pezophaps* in left lateral view (NHMUK A.1373). ○ Jolyon C. Parish.

The paroccipital process of the exoccipital flares out on each side, caudolateral to the parabasal fossa, forming the caudal wall of the tympanic cavity. The lateral process of the parasphenoid projects lateral to the parabasal fossa.

---

[15] This is erroneously labelled 'XI' in Claessens *et al.* (2015, fig.11).

[16] Melville (1848) stated that: "curving forwards round the vestibule [= recessus columellae] just mentioned, [is] a canal [= canalis ophthalmicus externus], which transmits an artery and accompanying vein, with the glosso-pharyngeal and sympathetic nerves" (p.78). However, this canal does not transmit the glossopharyngeal nerve, which passes through the glossopharyngeal foramen medial to the ostium canalis ophthalmicus externus.

[17] The lateral wall of the concavity was referred to as the metotic process (processus métotique) by Janoo (1997).

The basipterygoid processes of the parasphenoid are very reduced in *Raphus* (in OUMNH 11605 one is present on the left side as a "minute, thin and flexible upwardly-curved style" (Melville 1848, p.82), but is reduced to a low stub on the right). They are variably reduced in *Pezophaps*: basisphenoid processes can be seen on the parasphenoid as short, stubby projections in some specimens (for example in NHMUK A.1373 and A1441) and they are almost or entirely absent in others (NHMUK 76.1.28.9). The cranium of *Pezophaps* displays the lateral basilar tubercles and the smaller more medial ones, although in some specimens at least the latter seem less distinct from the former compared with those of *Raphus* (as in NHMUK A.3506; Newton & Newton 1869, pl.xxi, figs.140, 143). Between the medial pair of tubercles there is a slight depression. The parasphenoid rostrum of *Pezophaps* does not show the same degree of constriction ventral to the optic foramina, as in *Raphus*, and is not as expanded as that of the latter.

In *Raphus* the general aspect of the ventral surface of the cranium is slightly concave upwards, with the rostral part of the parasphenoid rostrum and the ventral surface of the occipital condyle more ventral than the narrow area below the optic foramina; in *Pezophaps* it is less concave.

Lateral Aspect

The lateral aspect of the cranium is dominated by the orbital fossa. Dorsal to this the frontals of *Raphus* form a large rounded protuberance, made up of diploic bone, which gives the dorsal margin of the cranium a domed appearance. This doming is variable: in Thirioux's Port Louis skeleton the frontals are less convex in lateral view than those of OUMNH 11605 (Claessens *et al*. 2015). Behind this protuberance the skull curves downwards to form the parietal region and supraoccipital plate; the latter forming an angle of approximately 100° with the former (Claessens *et al*. 2015).

Orbit

The orbits of *Raphus* and *Pezophaps* are proprtionally small, compared with other columbids, due to the ventral extension of the frontals. The vertically oval optic nerve foramen (II) is located caudoventrally in the orbital fossa, in its deepest part, approximately halfway between the rostral and caudal margins of the cranium. The dorsal margin of the foramen is notched by a vascular groove. The rostral margin of the foramen corresponds to the caudal border of the interorbital septum. Just caudal to the caudoventral part of the margin of the optic nerve foramen is that for the oculomotor (III) and abducens (VI) nerves. It is longitudinally oval and directed obliquely upwards; it is divided into three orifices by thin struts: the caudal orifice is that for the abducens nerve, and the two rostral orifices transmitted branches of the oculomotor nerve, which passed into a vertical groove that is separated from that running upwards from the caudal orifice by a ridge. These grooves end at a level with the dorsal margin of the optic nerve foramen. Between the optic nerve foramen and that for the oculomotor and abducens nerves is a very small orifice (seen in, for example, OUMNH 11605), opening into the sella turcica; it probably conducted A. ophthalmica (Midtgård 1984; A. ophthalmica interna of Baumel 1993; orbital artery of Porter & Witmer 2016).[18]

The small foramen for the trochlearis (IV) nerve is located at the apex of the rostral groove running dorsally from the oculomotor foramina, just caudodorsal to the optic nerve foramen. In OUMNH 11605 a small groove curves rostrodorsally away from the trochlear nerve foramen (Melville 1848). This feature is also seen in *Pezophaps* (*e.g.*, NHMUK 76.1.28.9), although it is variably defined.

Caudal to the oculomotor and abducens nerve foramen, and in a line with it and the optic nerve foramen, is that for the ophthalmic branch of the trigeminal nerve (V_1). It is approximately circular and larger than that of the trochlear nerve, but smaller than that of the optic nerve; it is sharp edged. Caudoventral to the ophthalmic nerve foramen is the maxillomandibularis foramen ($V_{2,3}$), which is vertically oval and slighly larger than the former. In OUMNH 11605 a small foramen is located rostral to the rostroventral margin of the maxillomandibularis foramen, separated from the latter by a vertical strut.

---

[18] Melville (1848) stated that it probably conducted a branch of the internal carotid (entocarotid) artery.

Caudodorsal to the optic nerve foramen, and in the caudodorsal part of the orbit, is the inflated convexity of the laterospenoid, passing caudodorsally into the ventral part of the postorbital process. This elevation is bounded caudally in part by the origin of m. pseudotemporalis superficialis (see section on musculature). Rostrally the convexity is deeply grooved, this groove, which curves ventrally from the ethmoid foramen, probably conducted the V. ophthalmica (see Porter & Witmer 2016). A continuation of this groove runs just above the optic nerve foramen, curving round the elevation mentioned above, entering the optic nerve foramen, indenting its dorsal border and curving backwards (Melville 1848). In OUMNH 11605 a groove, probably for the surpraorbital vascular vessels (A. et V. supraorbitales; Porter & Witmer 2016), runs parallel to the caudal border of the orbit (Melville 1848) and joins the ethmoid foramen. It shows a number of small foramina along its path.

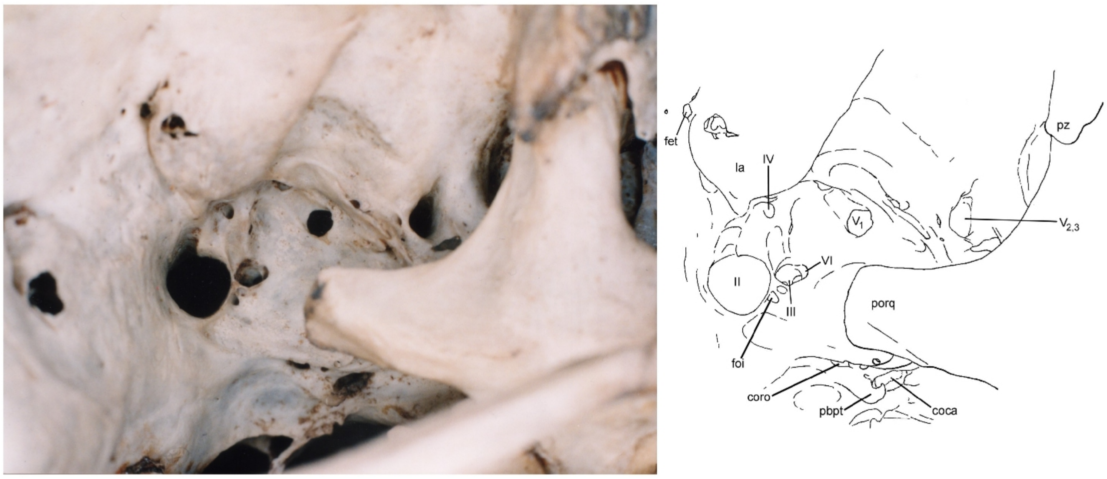

Left orbital region of OUMNH 11605. ○ Jolyon C. Parish, January 2001.

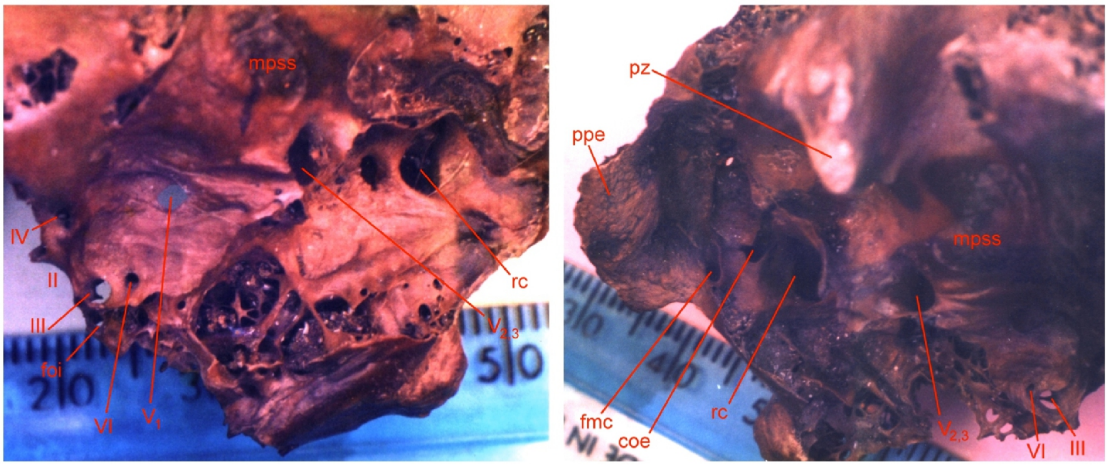

Cranium of NHMUK A.1338, caudal orbital and tympanic region. *Left*: left side, *right*: right side. ○ Jolyon C. Parish.

Ventral to the optic nerve foramen is the narrowest part of the parasphenoid, where the dorsally convex fossa for the maxillary vein (V. maxillaris) is located, sloping ventromedially. The left and right fossae for the maxillary veins are separated from each other medially by the groove leading to the common auditory tube (tuba auditiva communis). Caudoventral to the optic nerve foramen are two small foramina, the ostia of the rostal and caudal orbital canals (Porter & Witmer 2016), which would have transmitted blood vessels in life: the rostral one transmitted A. sphenomaxillaris and the caudal one A. sphenopalatinus (Porter & Witmer 2016; Baumel 1993; Midtgård 1984). These foramina are located caudodorsal to the depression for the maxillary vein. The rostral and dorsal of the two is longitudinally oval and the caudal is larger and vertically oval; they are separated by a thin bar, which shows two capillary orifices dorsally and the remnant of the basipterygoid process ventrally (Melville 1848).

Dorsal to the optic nerve foramen is a small foramen, the foramen ethmoidale, for A. et V. ethmoidales (Porter & Witmer 2016), the olfactory sulcus curving from this foramen to the foramen orbitonasale mediale.[19]

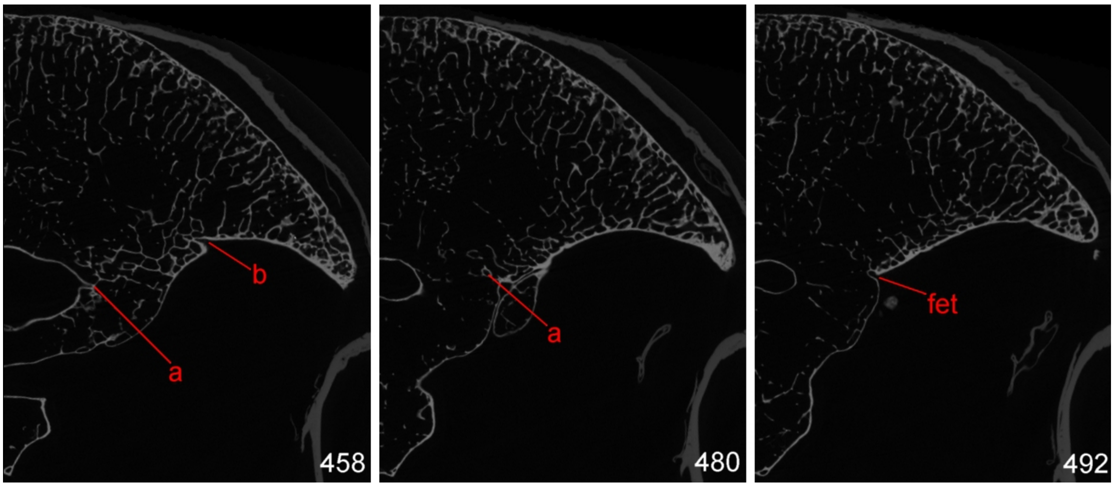

The ethmoid foramen in OUMNH 11605, right orbit (CT data relating to Warnett *et al*. 2020; MorphoSource Media: M55320). a: canal for A. et V. ethmoidalis, b: groove for A. et V. supraorbitalis.

The laterosphenoid[20] forms the ventral part of the caudal wall of the orbit and extends from the interorbital septum laterally to the temporal fossa and the postorbital process. The triangular area for the attachment of m. protractor pterygoidei et quadrati is ventral to the optic nerve foramen and extends caudally towards the ophthalmic nerve foramen (see section on musculature).

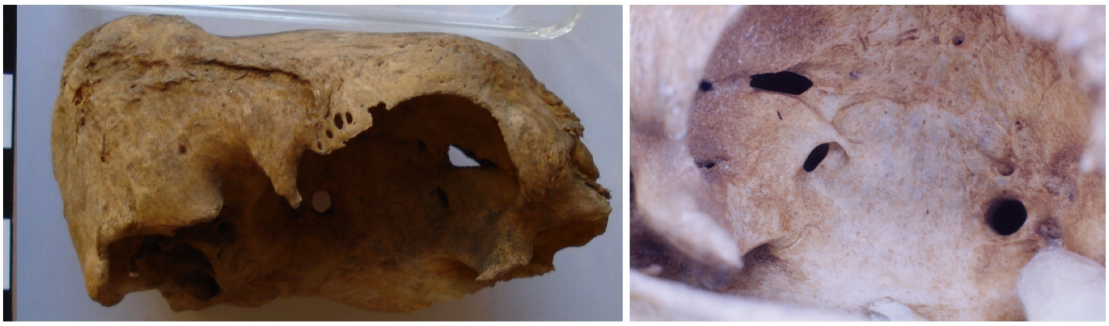

Crania of *Pezophaps*. *Left*: right side; Natural History Museum, Dublin, specimen; scale in cm (© David Gonzalez). *Right*: left orbit of NHMUK A.3505 (○ Jolyon C. Parish).

The interorbital septum is thick, pneumatic and complete in *Raphus*. The rostral wall of the orbit is sub-concave, its dorsal part is formed by the lacrimal and the ventral part by the ectethmoid, which joins the interorbital septum caudally. The roof of the orbit is formed by the frontal, which merges with the interorbital septum ventrally, and by the laterosphenoid caudally. The surface of the roof of the orbit is rounded-off into the interorbital septum due to the expansion of the diploe of the frontal internally. The rostral wall of the orbit slopes gradually caudally due to the large size of the posterior olfactory chambers in front. According to Claessens *et al*. (2015), the lacrimal-ectethmoid complex does not extend rostrally beyond the nasofrontal region in Thirioux's Port Louis skeleton, but in OUMNH 11605 and the Copenhagen skull it projects more rostrally along the midline.

---

[19] Note: the olfactory nerve (I) did not enter the orbit in *Raphus* and *Pezophaps* and as such did not run along the sulcus olfactorius.

[20] Ali-sphenoid, ala-sphenoid of Melville (1848); alisphenoid of Claessens *et al*. (2015).

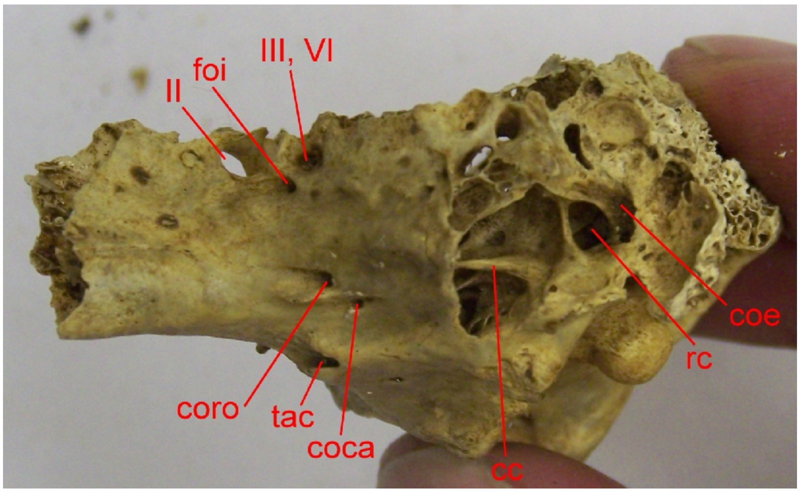

Ventral part of the cranium of *Pezophaps* (UMZC specimen), left side. ○ Jolyon C. Parish, December 2008.

The orbit of *Pezophaps* is more excavated and relatively larger than that of *Raphus*, due to the lesser degree of expansion of the antorbital elements in the former. The interorbital septum is complete, but relatively thinner (resembling that of *Goura*). As in *Raphus*, *Pezophaps* also possesses a rostral and a caudal orbital canal. The supraorbital margin of *Pezophaps* is frequently irregular, with exostotic growths projecting from the rim (for example in NHMUK A.1375 and 76.1.28.12, and a NMING:F21701 specimen). In NHMUK A.1375 the postorbital process on the left side is elongated ventrally due to the extra growth of exostotic bone, or maybe due to partial ossification of the postorbital ligament. The males show a greater tendency for, and more marked development of, exostotic growth of the supraorbital margins and postorbital processes than do the females of the solitaire (pers. obs.).

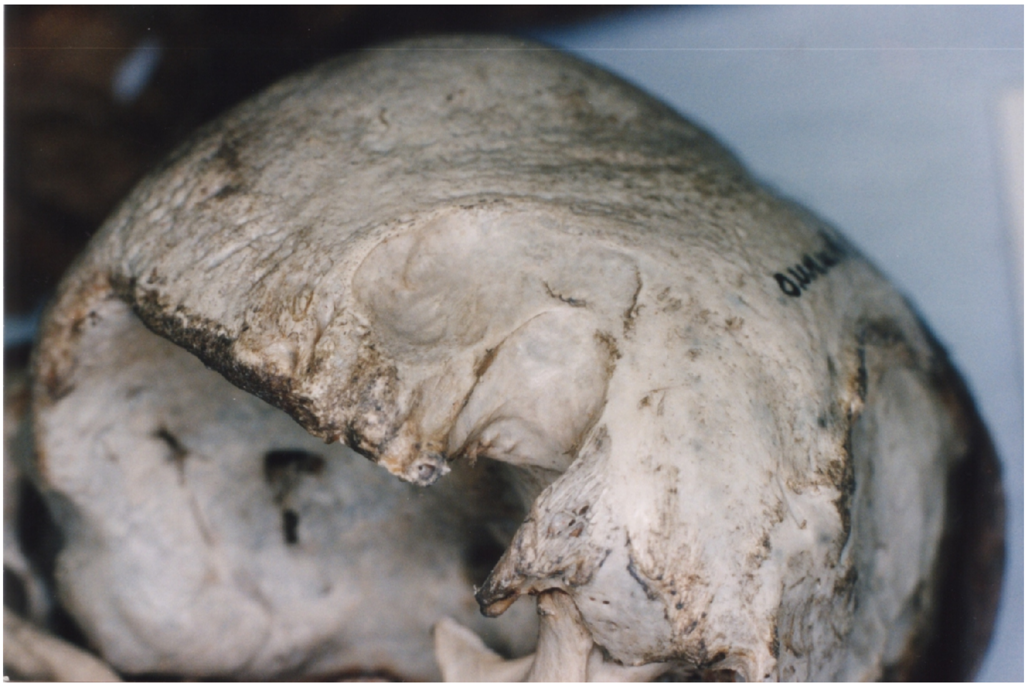

Temporal region of OUMNH 11605. ○ Jolyon C. Parish, January 2001.

Temporal Region

The temporal fossa (fossa musculorum temporalium of Livezey & Zusi 2006) is bounded rostrally by the postorbital process and caudally by the zygomatic process; it has a convex dorsal margin and is narrow. The upper and outer part of the fossa is occupied by the sub-crescentic concave origin of m. a. m. e. superficialis. The limbs of the upwardly facing crescent extend to the postorbital process rostrally and the zygomatic process caudally. Medial to the origin of the m. a. m. e. superficialis is that of m. pseudotemoralis superficialis, which has a convex dorsal margin and extends caudoventrally towards the maxillomandibular foramen. Medial to the impression for m. pseudotemporalis superficialis is the ophthalmic foramen of the trigeminal nerve (V_1). Between the rostral margin of the origin of m. pseudotemporalis superficialis and the ophthalmic foramen is the smooth sub-vertical elongate area corresponding to the "post-orbital vascular flexus" of Melville (1848, p.82), which stretches ventrally to the maxillomandibular foramen.

Surrounding the rostrodorsal part of the origin of the origin of m. a. m. e. superficialis is the sub-pyriform depression for m. cucullaris capitis (see section on musculature). The robust postorbital process is subtriangular with a truncated downwardly pointing apex; it forms the rostral border of the temporal notch and lies ventral to the origin of m. cucullaris capitis. The zygomatic process of the squamosal is elongate and styliform, projecting rostroventrally in front of the squamosal articular facet for the quadrate; in *Pezophaps* it is not well developed. The base of the zygomatic process is defined in a cranium of the dodo studied by Owen (1867) by a transverse ridge rostral to the squamosal articular facet for the quadrate. The short, subtriangular suprameatic process of the squamosal overhangs laterally the dorsal pneumatic foramen of the tympanic cavity, and lies caudal to the squamosal articular facet of the quadrate.

The squamosal adjoins the exoccipital caudoventrally and caudomedially, the parietal dorsally, the laterosphenoid rostrally and the prootic ventromedially. It forms the rostral articular facet for the quadrate. Its outer surface is smooth and convex. The origin of m. d. m. pars superficialis (Bhattacharyya 1989) occupies the squamosal region. The parietal surface bears small vascular impressions (Melville 1848); rostrally it joins the frontal.

The dorsal margin of the orbit would form two sides of a right angle triangle if a line were to be drawn (corresponding to the hypotenuse of the triangle) from the postorbital process to the ventral extremity of the projecting part of the lacrimal process of the frontal. The second longest side would be the near straight orbital margin from the postorbital process to the supraorbital notch; the shortest side would correspond mainly to the projecting part of the lacrimal process of the frontal. The orbital margin is perforated by a small supraorbital foramen rostral to the postorbital process and rostroventral to the origin of m. cucullaris capitis. This foramen, which probably transmitted the supraorbital arteries and veins to the scalp, and leads internally to the groove on the roof of the orbit which curves around the elevation of the laterosphenoid at the base of the postorbital process.

Tympanic Region

The tympanic cavity is bounded caudally by the paroccipital process (ala tympanica), ventrally by the parasphenoid and dorsally by the prootic[21] and squamosal. Dorsally the cavity presents the squamosal and otic articular facets for the quadrate, the squamosal facet being anterior and the otic facet being posterior. The otic facet is approximately oblong in form and composed of a smaller inner and a larger posterior part at right angles with each other. A notch separates it from the paroccipital process, caudal to it. Between the two articular facets is the large pneumatic dorsal tympanic recess, which is approximately quadrate in outline. Medial to the dorsal tympanic recess is a small foramen, separated from the former by a rounded strut; this feature can be observed in NHMUK A.1338 and some specimens of the cranium of *Pezophaps*; it probably transmitted the ramus occipitalis of A. ophthalmica externa (Mayr 2002). Caudal to the otic facet for the quadrate is a venous? foramen, seen in both *Raphus* and *Pezophaps*.[22]

Caudoventral to the dorsal tympanic recess is the sub-oval columellar recess. Three openings can be seen within this recess: rostroventral is the fenestra vestibuli, caudoventral is the fenestra cochlearis, and caudodorsal is the caudal pneumatic foramen. The fenestra vestibuli, into which the base plate

---

[21] Ex-occipitale of Melville (1848).

[22] See Mayr (2020, p.77) for a discussion of this foramen in other birds.

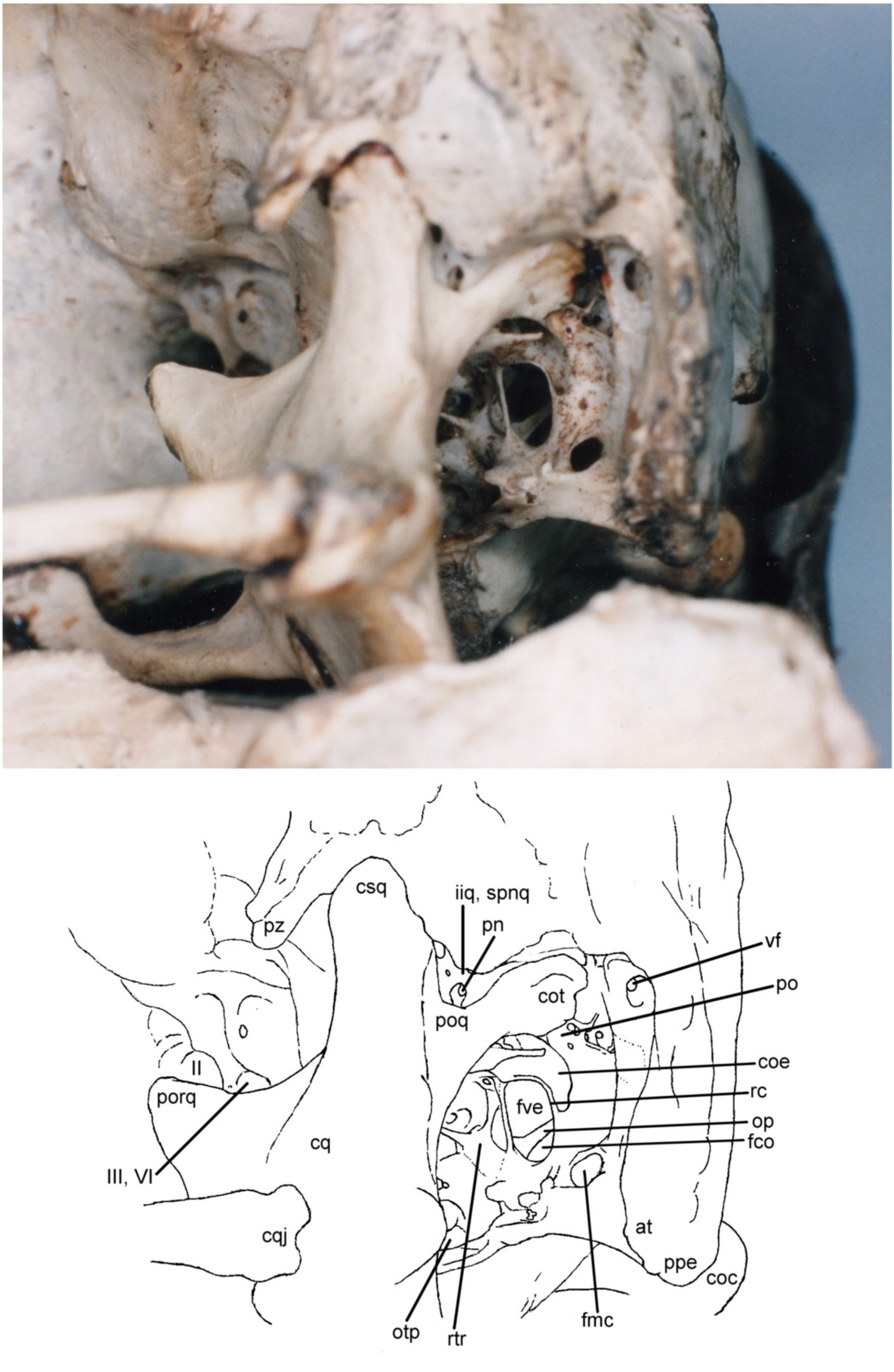

Tympanic region of OUMNH 11605, left side. ○ Jolyon C. Parish, January 2001.

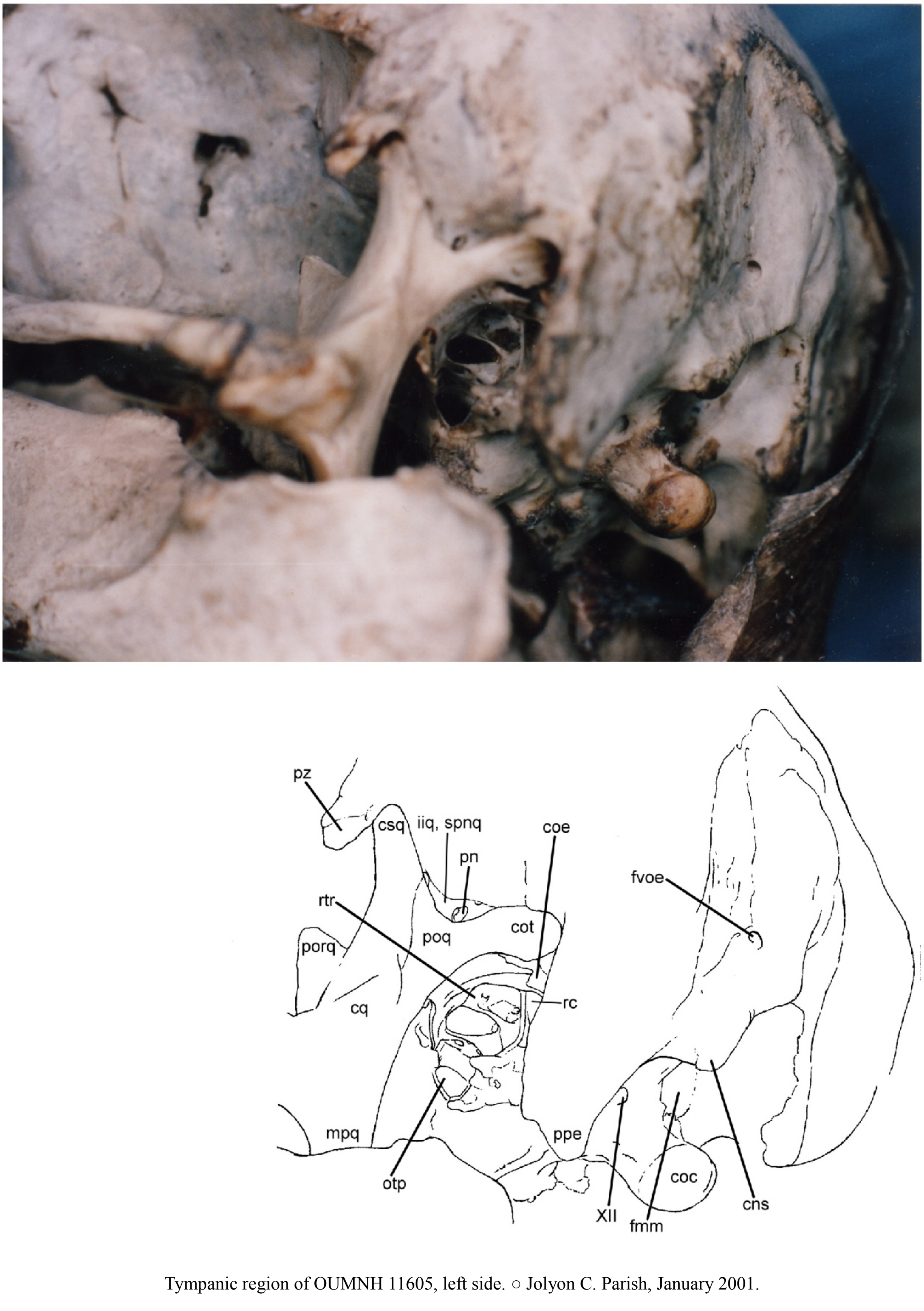

Tympanic region of OUMNH 11605, left side. ○ Jolyon C. Parish, January 2001.

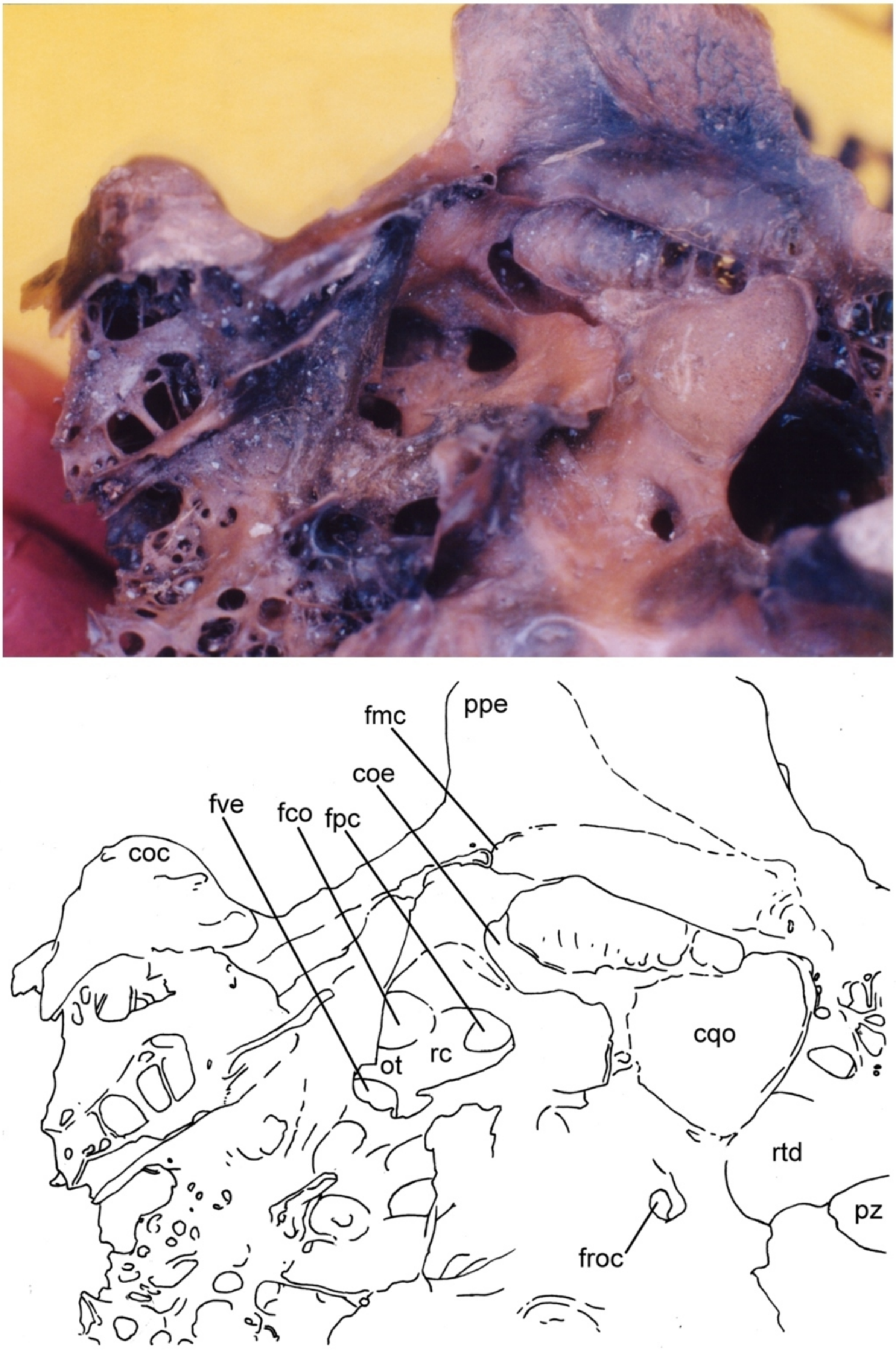

Tympanic region of *Raphus*, NHMUK A.1338, right side. ○ Jolyon C. Parish.

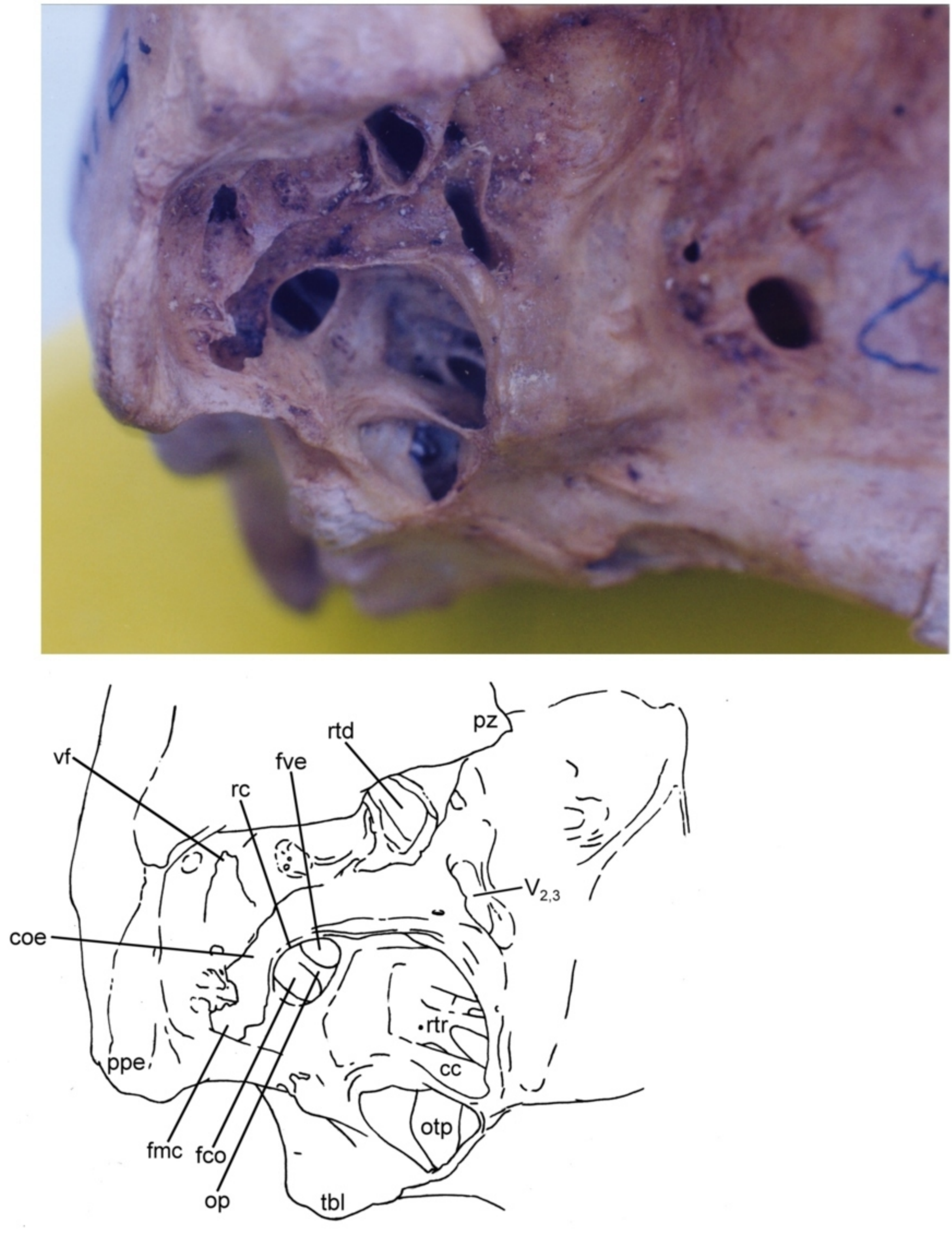

Tympanic region of *Pezophaps*, NHMUK A.1375, right side. ○ Jolyon C. Parish.

(clipeolus) of the columella fits, is separated from the fenestra cochleae by the narrow rostroventrally directed promontorium tympani (Mayr 2020), formed by the opisthotic. The fenestra vestibuli is located between the prootic and opisthotic (Jollie 1957) and the fenestra cochleae opens within the opisthotic (Baumel & Witmer 1993). The caudal pneumatic foramen lies dorsal to the fenestra cochleae and leads caudally into a chamber ventrolateral to the rostral semicircular canal (Baumel & Witmer 1993). In one specimen of the cranium of the dodo examined (NHMUK A.1338), the rostral edge of the columellar recess shows a small slightly projecting styloid process directed downwards.

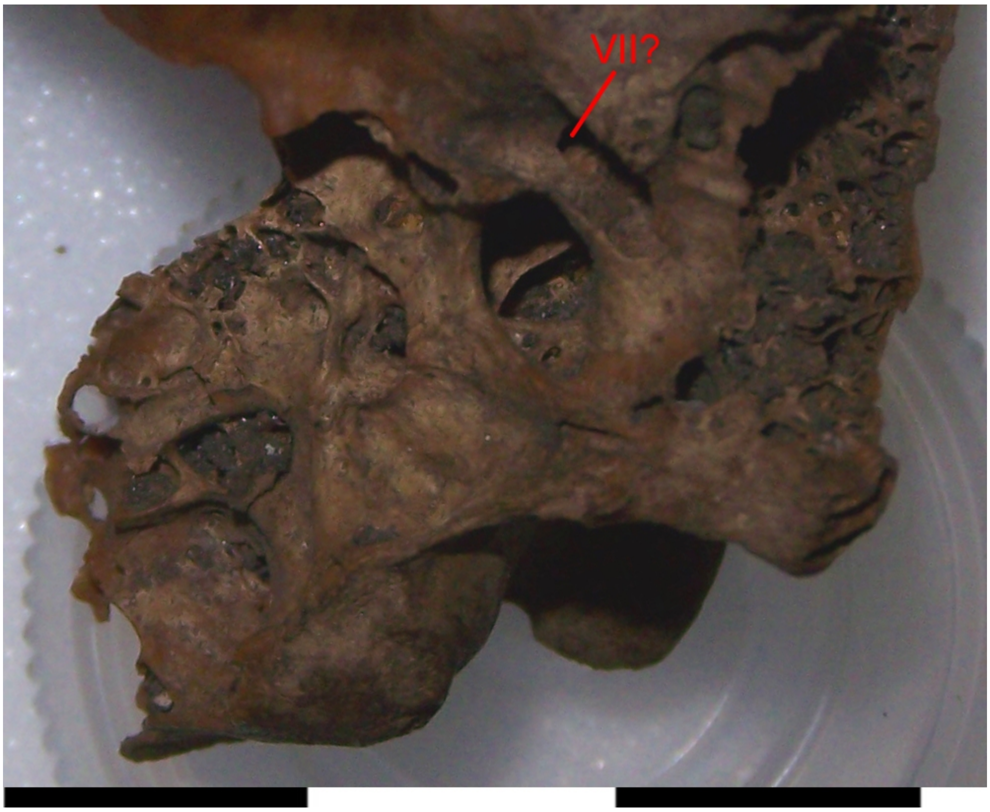

Left tympanic region of *Raphus* (UMZC 415.J). Scale in cm. ○ Jolyon C. Parish, December 2008.

The external ophthalmic canal runs dorsally from the ostium canalis ophthalmicus externus, which opens in the caudal part of the parabasal fossa; it passes caudal to the fenestra vestibuli, which it arches dorsal to. The groove for the occipital ramus of the external ophthalmic artery curves backwards to the ventral part of the dorsal tympanic recess, “terminating in a narrow canal which traverses the diploe at the floor of that orifice, emerges at the canalicular convexity on the occipital aspect” (Melville 1848, p.83). This groove joins the external ophthalmic canal.

The external ophthalmic canal is open laterally for much of its length in *Raphus* and *Pezophaps*.[23] In most specimens the canal is closed over laterally in its ventral part, however in one specimen of *Pezophaps* examined (NHMUK A.1375) it is open laterally and merges with the foramen m. columellae, this foramen[24] usually being separate from the external ophthalmic canal. In life the external ophthalmic canal carried the external ophthalmic artery and vein from the ostium canalis ophthalmicus externus towards the orbit (Baumel & Witmer 1993; Midtgård 1984).

---

[23] In adult specimens of other columbids it is closed over in its caudal part (in sub-adult specimens it is open caudally; pers. obs.).

[24] The foramen m. columellae may correspond to the “rounded aperture leading to a broad groove on the base of the paroccipital process anteriorly” which “transmits the venous sinus of the membrana tympani to the internal jugular vein” of Melville (1848, p.78).

The small foramen for the hyomandibular branch of the facial nerve (VII) is located dorsal to the columellar recess, in the ventral part of the canalis ophthalmicus externus, as can be observed in NHMUK A.1338 and several crania of *Pezophaps* (for example NHMUK 76.1.28.11).

Rostral to the columellar recess is the large pneumatic rostral tympanic recess, containing the rostral pneumatic foramen. Ventral to the rostral tympanic recess, and separated from it by a narrow sub-horizontal bar, is the large caudal opening of the auditory tube, which lies near the ventral surface of the cranium. The bony canal of the auditory tube is directed rostromedially. Apertures of the auditory canal open into the cells of the lateral basal tubercle, which it passes dorsal to. The left and right auditory tubes join and exit the cranium together via the common auditory tube, which, as stated previously, is located dorsal to the free apex of the basisphenoid plate in the midline of the skull. The columellar recess, the rostral tympanic recess and the caudal opening of the auditory tube all lie within a rounded subtriangular area. In lateral view of the tympanic region of *Pezophaps* the enclosed osseous canal for the cerebral carotid artery and vein can been seen passing between the rostral tympanic recess above and the opening of the auditory tube below.

There is extensive pneumatization of the tympanic region in *Raphus* and *Pezophaps*. The degree of pneumaticity of the tympanic region in *Raphus* is variable: in OUMNH 11605 it is highly pneumatized, whereas in NHMUK A.1338 it is much less so. Variation is also seen in the tympanic region of *Pezophaps* in the form and number of foramina.

In lateral view the base of the cranium in the tympanic region is concave downwards, with the paroccipital processes and the basal tubercles being more ventral than the intervening area between them. The paroccipital process forming the ala tympanica in lateral view is very slightly convex backwards. The rostral and caudal orbital canals, offshoots of the carotid canal, open on the side of the base of the parasphenoid rostrum, at the base of the remnant basipterygoid process (see above).

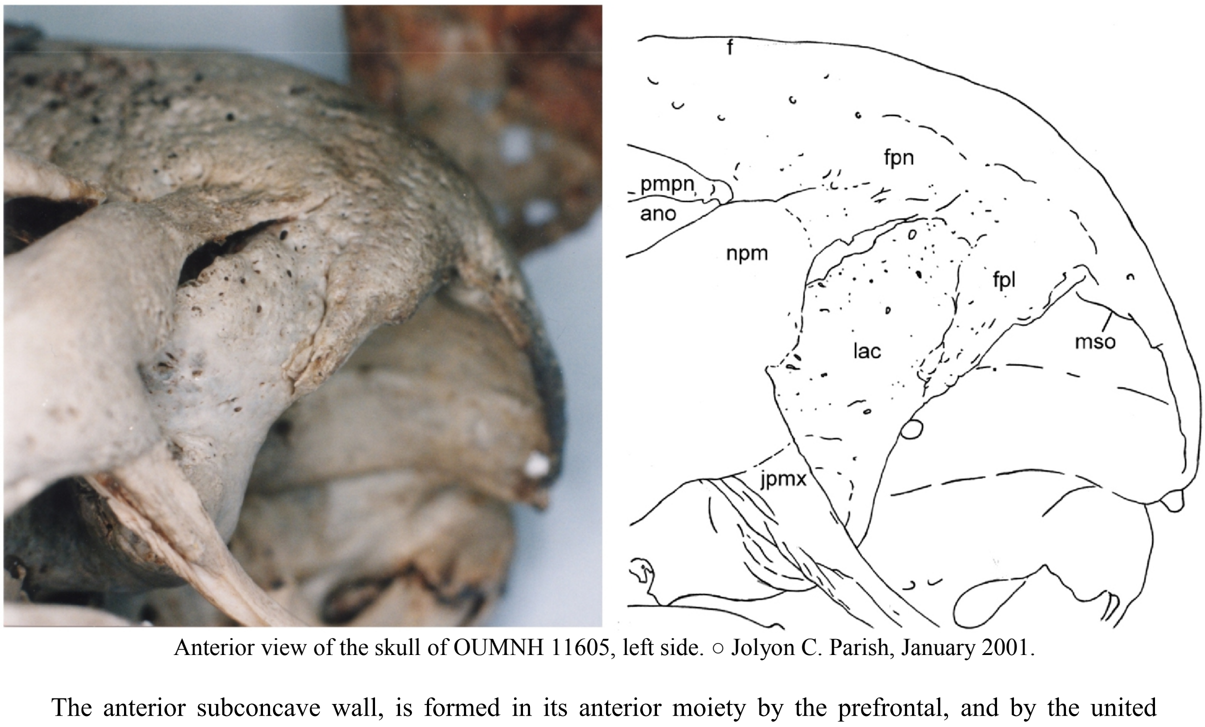

Anterior view of the skull of OUMNH 11605, left side. ○ Jolyon C. Parish, January 2001.

The anterior subconcave wall, is formed in its anterior moiety by the prefrontal, and by the united turbinated and inferior alse of the ethmoid; posteriorly it is constituted by the enormously thick, but contracted, interorbital septum; it slopes gradually inwards and backwards, and above is rounded off into the roof of the orbit.

Anterior Part of the Cranium

The anterior wall of the orbit is sub-concave and is formed from the lacrimal,[25] ectethmoid, mesethmoid and frontal bones. The lacrimal lies wedged between the lacrimal process of the frontal and the maxillary process of the nasal, the former of which it is fused to. It is subtriangular in shape and medially it fuses with the ectethmoid. The lacrimal is separated medially by a fissure from the maxillary process of the nasal. The foramen orbitonasale laterale lies between the lacrimal, frontal, ectethmoid and the "turbinated ala of the ethmoid" (Melville 1848; probably the turbinated part of the mesethmoid). In *Raphus* the foramen orbitonasale laterale is almost completely obliterated due to the upward extension of the ectethmoid, contributing to the large posterior olfactory chambers. The foramen orbitonasale laterale is reduced to a narrow fissure, a "tripartite chink slightly wider at the centre [...] the inner branch of which probably corresponding to the notch between the turbinated and inferior alae [...] the upper indicates the union of the prefrontal [= lacrimal] to the turbinated ala" (Melville 1848, p.81). The foramen orbitonasale laterale transmitted the lateral ramus of N. ophthalmicus, the lateral branches of the common nasal artery and vein, and duct(s) of glandula nasalis (Baumel & Witmer 1993, Porter & Witmer 2016).[26] The lacrimal diverticulum of the antorbital sinus pneumatizes the lacrimal bone (Witmer 1990) and evidence of this can be seen in *Pezophaps* in the form of a pneumatic foramen or foramina on the rostromedial face of the lacrimal (as in NHMUK A.1454). The lacrimal of *Raphus* is also pneumatized on its medial aspect by a large foramen (Melville 1848; CT scans of OUMNH 11605).

In *Columba* the ectethmoid does not reach the foramen orbitonasale laterale, in contrast to the condition in *Raphus*, where the ectethmoid forms part of its margin. In *Raphus* the foramen orbitonasale laterale has been reduced by the dorsal expansion of the ectethmoid and lacrimal. The differing position of the foramen orbitonasale laterale in *Columba* and *Raphus* suggests that the latter evolved from a form where the foramen orbitonasale laterale was open (as is the case in *Caloenas* and *Goura*) and was later diminished, causing the foramen to become restricted to a more medial position than that seen in *Columba*.

An interrupted groove passes from the dorsal extremity of the foramen orbitonasale laterale rostroventrolaterally to the dorsal margin of the lacrimal groove. The lacrimal groove runs sub-horizontally along the lateral margin of the lacrimal, conducting the lacrimal duct to the orbitonasal hiatus, and defines the ventral apex of the lacrimal process of the frontal. It slopes medially to the lateral margin of the posterior olfactory chamber and is deepest ventrally. In *Raphus* the groove is wide and shallow. The wide lacrimal groove in *Pezophaps* is deeper and better defined than that of *Raphus* and *Columba*. Ventral to the lacrimal groove the lacrimal of *Pezophaps* presents a rounded caudolaterally directed ridge running to the end of the bone. The ventral part of the lacrimal of *Raphus* is slightly roughened opposite the jugal arch; Melville (1848) stated that these would probably meet during cranial kinesis.

The lacrimal of *Pezophaps* is attached to the lacrimal process of the frontal by a long articular surface, the suture being distinguishable in some specimens (NHMUK A.3506; Newton & Clark 1879). The lacrimal process varies in shape between individuals but is generally pointed. In *Pezophaps* the lacrimal curves backward and its ventral extremity projects caudoventrally. The main body of the lacrimal is sub-conical and recurved, with a spongy internal texture. The lacrimal is less expanded, especially ventrally, than that of *Raphus*. It joins the mesethmoid by a thin process, ventral to the foramen orbitonasale laterale. The lacrimal of *Pezophaps* is often fused with the other elements of the cranium, as in *Raphus*, but in some specimens (for example NHMUK A.1454 and A.1373) the

---

[25] The designation of the bone forming the rostrolateral part of the orbit follows that of Baumel & Witmer (1993). In theropod dinosaurs leading to birds the prefrontal becomes progressively reduced in size and the lacrimal becomes the main element in the rostral wall of the orbit. Thus the prefrontal of Melville (1848) is here regarded as the lacrimal.

[26] Melville (1848) stated that it transmitted the "upper diverticulum of the suborbital sinus" in most birds.

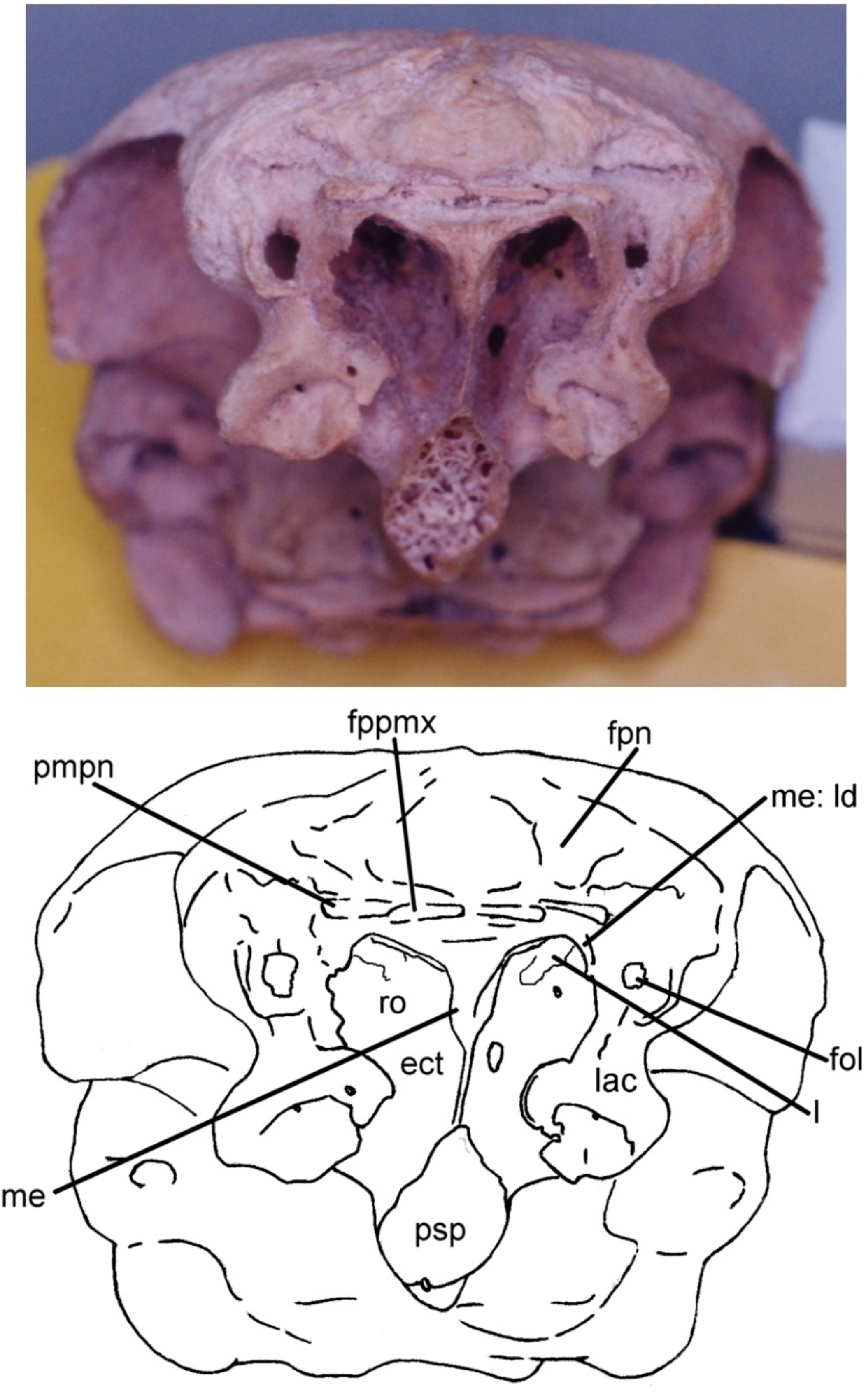

Cranium of *Pezophaps*, rostral view (NHMUK 76.1.28.9), female. (○ Jolyon C. Parish).

lacrimals are unfused and can be separated from the rest of the skull.[27] The "turbinated ala" is also less expanded than that of *Raphus*.

The interorbital septum of the mesethmoid joins the frontal dorsally and the ectethmoid laterally, and forms most of the medial wall of the orbit. From the supraorbital notch a capillary groove runs caudomedially; this probably contained a branch of a supraorbital cutaneous artery in life (Melville 1848). Between the foramen orbitonasale laterale and the optic nerve foramen is the foramen orbitonasale mediale, which transmitted the medial ramus of N. ophthalmicus and the medial branches of the common nasal artery and vein from the orbit into the nasal cavity; it lies at the junction of the frontal, interorbital septum and ectethmoid. The foramen is directed rostrodorsally and is approximately transversely oval in shape. The shallow olfactory sulcus runs rostroventrally from the ethmoid foramen to the foramen orbitonasale mediale. Unlike in other columbids, the sulcus did not transmit the olfactory nerve in *Raphus* and *Pezophaps*; this ran from the olfactory bulbs to the olfactory chamber without entering the orbit.[28] In OUMNH 11605 there are minute foramina along the course of the olfactory sulcus. The foramen orbitonasale mediale lies at the caudodorsal extremity of a sub-quadrate depression situated between the foramen orbitonasale laterale and the optic nerve foramen. This depression is open ventrally but has well defined edges rostrally, caudally and dorsally, as seen in OUMNH 11605.

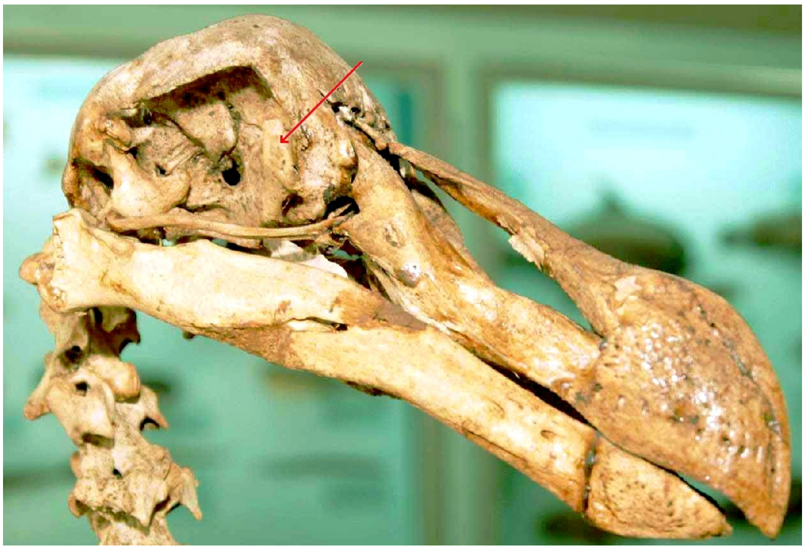

The skull of Thirioux's Port Louis dodo skeleton, showing one of the pair of additional lacrimals (marked by an arrow). (© Naturalis). [http://www.naturalis.nl/nl/over-ons/pers/persberichten/dodo-massagraf-opnieuw-open-voor-minutieus-graafwerk/ Accessed 7 February 2012]

The foramen orbitonasale mediale of *Pezophaps* is much more transversely elongate, along the olfactory sulcus, than that of *Raphus*. The olfactory sulcus is well defined rostral to the foramen orbitonasale mediale and can be observed running rostrally into the foramen orbitonasale laterale. In some specimens (for example NHMUK A.3505, A.1375; Newton & Clark 1879, pl.l, fig.3) there is a foramen present ventral to the foramen orbitonasale mediale which is sub-oval and located in a shallow depression. It is not present in all specimens and is sometimes found in only one orbit (it is only found

---

[27] Both these specimens appear to be otherwise osteologically mature. There are also a pair of unfused lacrimals present in the skull of Thirioux's Port Louis skeleton (pers. obs.; Claessens *et al*. 2015). They are attached to the sides of the skull, lateral to the fused lacrimals of the cranium itself. They are apparently left and right lacrimals of similar size and form to those fused to the skull and of similar preservation and colour (pers. obs. from photographs and video) and presumably belong to a separate individual. See Claessens *et al*. (2015, figs.6A-E, H-L; 9C, D).

[28] The olfactory nerve also passes to the olfactory chamber without entering the orbit in Dinornithiformes, *Struthio*, *Casuarius*, *Dromaius*, *Apteryx*, *Diomedea*, *Puffinus*, *Pachyptila*, *Oceanites*, *Pelecanoides*, *Spheniscus*, *Cathartes* and *Aptornis* (Livezey & Zusi 2006).

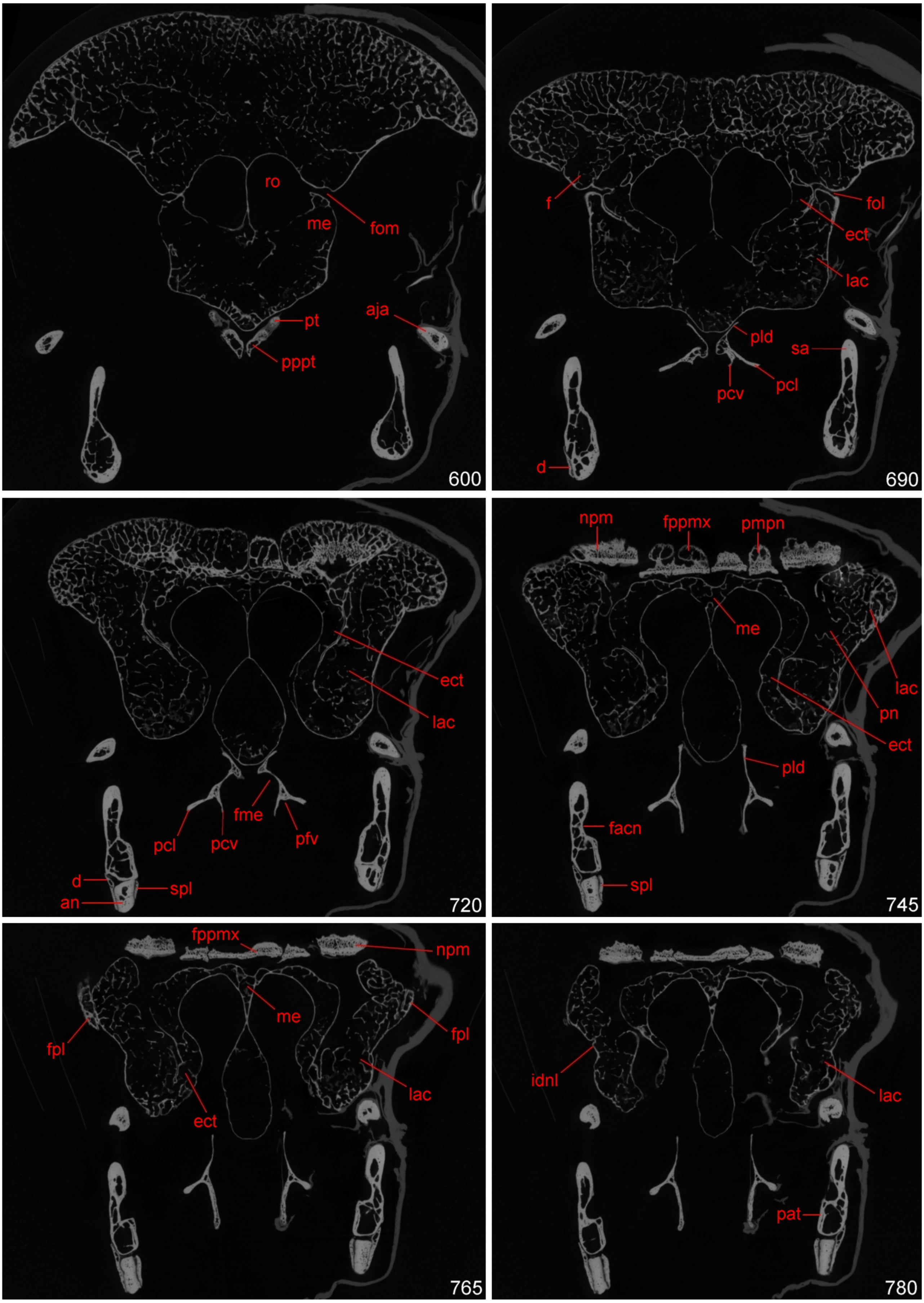

Transverse CT sections of OUMNH 11605 (CT data relating to Warnett *et al*. 2020; MorphoSource Media: M55320).

in the right orbit of NHMUK 76.1.28.9, for example). In other specimens only a depression is seen. A fissure between the ectethmoid and the lacrimal, ventral to the olfactory sulcus can be seen in some specimens of *Pezophaps* (NHMUK A.3506; Newton & Clark 1879, pl.l, fig.3). In *Pezophaps* the foramen orbitonasale laterale is not diminished by the dorsal expansion of the ectethmoid as is the case in *Raphus*.

Ventrally the rounded parasphenoidal rostrum forms a horizontal spike. Dorsal to this is a wide incisure in the rostral margin of the cranium, above which the mesethmoid projects rostral to the lacrimal as a thin vertical plate.

The anterior aspect of the cranium presents the posterior olfactory chambers, partially separated by the mesethmoid which forms the dorsal median septum between them. They housed the concha nasalis caudalis in life. Ventrally the mesethmoid merges with the parasphenoid rostrum. Projecting ventrally, lateral to the posterior olfactory chambers, are the lacrimals and ectethmoids. Melville (1848) stated that the foramen orbitonasale mediale is "diminished by an extension forwards of an osseous plate, from the interorbital septum outside of the foramen olfactorium; it forms the outer part of the floor of the olfactory fossa" (p.88). The olfactory foramen, on each side, opens into the base of the posterior olfactory chamber and is inclined outwards. Grooved impressions of branches of the olfactory nerve diverge upon the caudal and dorsal wall of the fossa and proceed rostrally towards the craniofacial hinge (zona flexoria craniofacialis). The posterior olfactory chambers of *Pezophaps* are, like those of *Raphus*, situated just rostral to the cerebral cavity, albeit proportionately not as close, and are also partially separated by a dorsal median septum.

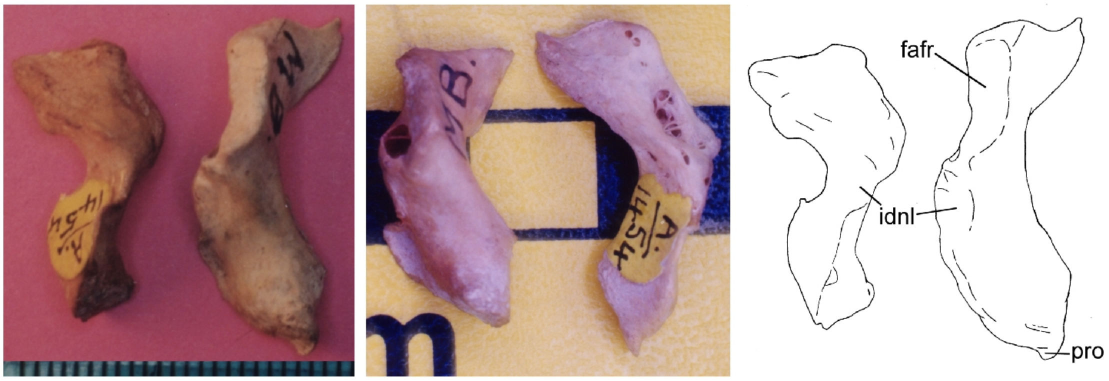

Lacrimals of *Pezophaps* (NHMUK A.1454). Scale in mm (left) and cm (right). Note: the right image shows the pneumatic foramina on the medial face of the lacrimal. (○ Jolyon C. Parish).

In anterior view the cranium of *Pezophaps* presents the foramen orbitonasale laterale lateral to the posterior olfactory chamber, on each side. In anterior view the foramen is small and sub-round. Ventral to this can be seen the concavity of the lacrimal groove and below this the lacrimal expands below the posterior olfactory chamber. The fissure between the lacrimal, ventral to the lacrimal groove, and the interorbital septum and parasphenoid rostrum is visible (this fissure can be seen in the ventral view of the cranium of *Raphus* and leads up into the posterior olfactory chamber). The paired arches of the mesethmoid forming the dorsal part of the posterior olfactory chambers can be seen; these arches are fused to the proximal ends of the frontal processes of the premaxillae and the nasals dorsally (just caudal to the craniofacial hinge), the lacrimals dorsolaterally and the ectethmoids caudolaterally. In *Raphus* the flat mesethmoidal arch (formed by the "turbinated alae of the ethmoid") projects as a thin plate ventral to the dorsal beam of the mandible (formed from the frontal processes of the premaxillae and the premaxillary processes of the nasals), separated from it by a space (allowing downward flexion of the mandible during cranial kinesis).

The extension of the lacrimal diverticulum of the antorbital sinus in *Raphus* probably pneumatized the ectethmoid and the mesethmoid, frontal and parasphenoid rostrum. Witmer (1990) stated that "communication of the air cells in the lacrimal and frontal takes place later in ontogeny of many birds and obliterates the suture between the bones" (p.338). A comment in the UMZC "Dodo Book" noted that the interorbital septum is composed of large pneumatic cavities connected with the "frontal sinuses".

Dorsal Aspect

The dorsal aspect of the cranium of *Raphus* is approximately hexagonal in shape, with the rostral edge, between the apices of the lacrimals, being around half the length of the caudal edge, and the rostrolateral edges (corresponding mainly to the orbital margins) being around twice the length of the caudolateral edges. The cranium is slightly broader than it is long, and has a maximum width just rostral to the postorbital processes. Laterally it shows the impressions of m. cucullaris capitis and the origin of m. a. m. e. superficialis. Caudally it is composed of the parietals, and laterally the squamosals. The dorsal aspect of the cranium is dominated by the inflated frontals. The frontal processes of the nasals are separated medially by the frontal process of the premaxillae. The cranium of *Pezophaps* is also sub-hexagonal in dorsal view, although it is slightly longer than it is wide.

The parietals are short and broad, and are bounded laterally by the squamosals, caudally by the supraoccipital and rostrally by the frontals. Medially, between the parietals and the frontals, is a small foramen where the coronal fontanelle existed (Melville 1848), which leads to a small canal opening into the endocranial cavity towards the apex of the cerebellar fossa; it probably transmitted a vein from the scalp to the "posterior cerebellar sinus" (*ibid.*; probably the sinus occipitalis). Caudal to this foramen is a transversely oblong band which is defined caudally by "an ungueal fissure-like groove, the angles of which extend outwards, curving backwards: its extremities are also defined by grooves" (*ibid.*, p.85). From the foramen a vascular groove passes laterally and defines the caudal margin of the frontal protuberance. The groove curves caudally in its lateral part to the foramen or notch on the supraorbital margin corresponding to the groove on the roof of the orbit. The parieto-squamosal region is gently convex transversely but proceeds rapidly towards the frontal protuberance from the supraoccipital.

The dome-shaped frontal protuberance is large. Its rostral margin is undefined where the frontals meet the frontal processes of the nasals and those of the premaxillae. Its caudal margin follows nearly that of the combined frontals. In OUMNH 11605 the protuberance shows a broad shallow longitudinal furrow, which gives it an almost bilobed form. Melville (1848) stated that in juveniles of *Raphus* the frontal protuberance would not be developed, and that if the protuberance were not present then "the cranium would present a gentle slope, descending from the vertex (somewhat in front of the coronal fontanelle, and corresponds to the most elevated part of the cerebrum) to the upper surface of the mandible. The profile would hence resemble that in the skull of the *Caloenas*, &c., but would be relatively much shorter, from the abbreviation of the frontal" (p.84).

The inflated frontal processes of the nasals are bent upwards at approximately 45° to the plane of the upper beak to fuse with the frontals, the sutures between the frontals and nasals being obliterated. The frontal processes of the nasals are subtriangular and separated medially by the triangular apex of the combined frontal processes of the premaxillae, which extend caudally to meet the frontals, the apices of the premaxillae joining the obliterated suture between the frontals. The boundary between the frontal processes of the nasals and those of the premaxillae is indicated by a longitudinal fissure-like groove on each side.

Between the lacrimal process of the frontal and the frontal process of the nasal, on each side, is wedged the subtriangular lacrimal, which is separated from the premaxillary process of the nasal by a fissure continuous with the orbitonasal hiatus. The anterior part of the lacrimal projects rostral of the craniofacial hinge. Livezey (1993) stated that the lacrimal process of the frontal in *Raphus* is small, whereas that of *Pezophaps* is comparatively large. This appears to be linked to the development of the lacrimal groove and the degree of inflation of the lacrimal-ectethmoidal region. Livezey (*ibid.*) also stated that the reduction in size of the lacrimal process is a derived state, thus in this respect *Raphus* and columbids such as *Columba* are more derived than *Pezophaps*.

The sub-crescentic supraorbital region shows numerous vascular foramina. A series of these can be seen running from the notch on the lacrimal process to the supraorbital foramen or notch as if the

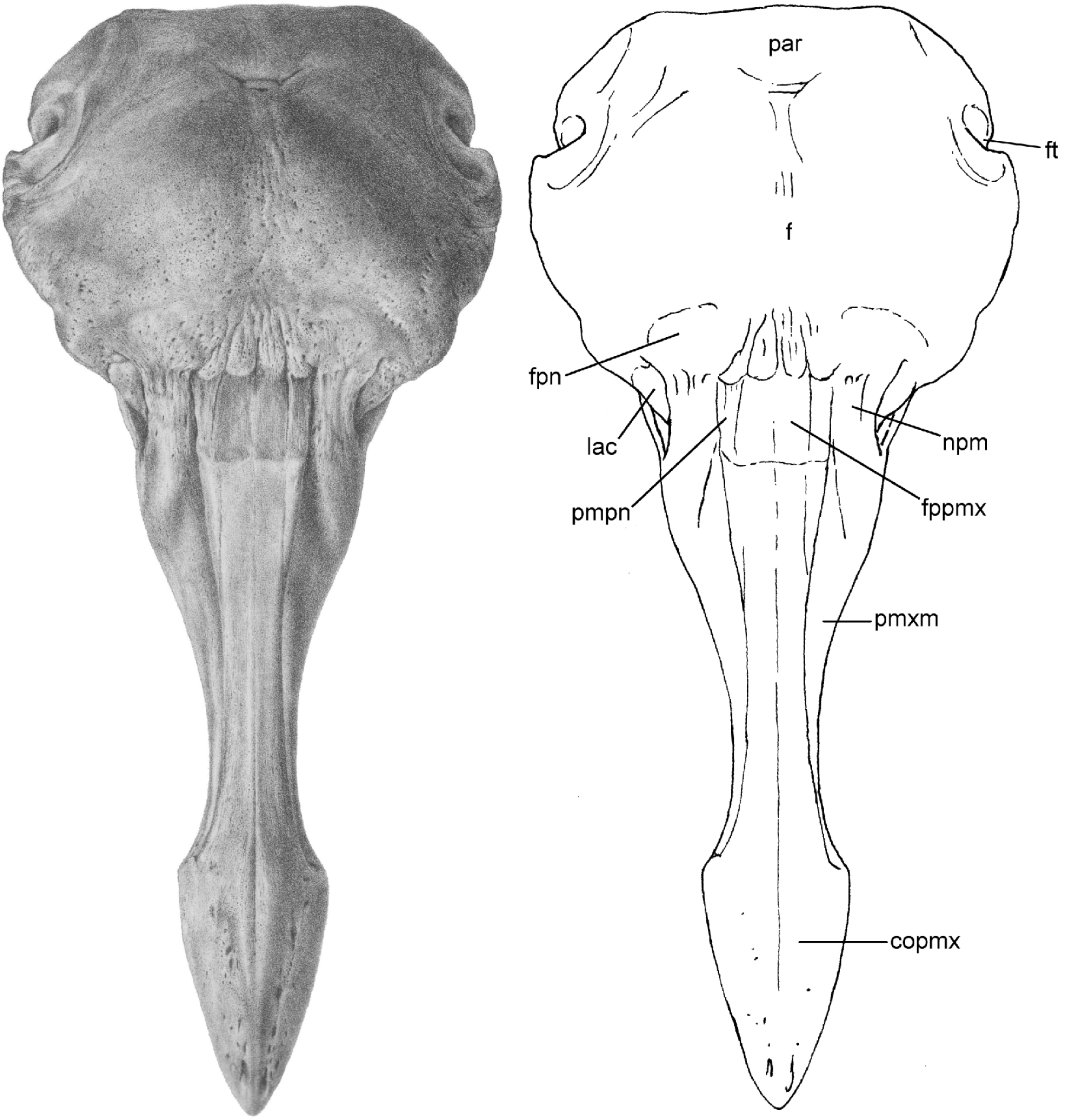

Skull and mandible of the dodo in dorsal view (lithograph from Strickland & Melville 1848, pl.ix, fig.1; by Joseph Dinkel; “Reeve, Benham & Reeve, Lithographers.”)

"supra-orbital plate appears formed, as it were, by a separate ossification of the periosteum extending outwards to protect the eyeball" (Melville, p.86). Melville (1848) also stated that "the tabula externa of the pneumatic diploe, on the frontal slope, is thinned and inflated opposite the individual cells; and some of these have opened out; these appearances indicate that the skull in question [OUMNH 11605] belonged to a domesticated individual" (*ibid.*).

The dorsal surface of the cranium of *Pezophaps* does not show the great expansion of the frontals, or the slight median furrow as seen in *Raphus*, but instead there is a depression of the central region of the dorsal surface of the cranium. This depressed region lies between the elevated rostral and caudal ridges (consisiting internally of cancellous structure) which continue laterally to meet each other, thus forming a dish-like form, the centre of which is flat (or slightly concave in some individuals, or divided into two parts by a low transverse elevation in others). The frontals rise rapidly from the craniofacial hinge, more so than in *Raphus*.

The frontal ridge of *Pezophaps*, which forms the rostral boundary of the depressed dorsal region, is divided into a central portion comprising the frontal processes of the nasals and the frontal process of the premaxillae and two lateral protuberances, formed by the frontals, which show variably developed exostoses. These lateral prominences meet in the midline in some specimens (Newton & Clark 1879). The frontal ridge is also in some specimens "raised into warty protuberances separated by deep depressions" (*ibid.*, p.445). In *Pezophaps* the frontals are separated rostrally by a depressed tract corresponding to the frontal processes of the nasals and the frontal process of the premaxillae, as stated above. Projecting over this depressed tract, on each side, is a bony fringe formed of exostotic bone. This fringe is more marked in the male than in the female. The supraorbital tract is also more rugose in the former than in the latter (pers. obs.; Owen 1878). The rugosity of the cranium in the region of the craniofacial hinge indicates "the position of the caruncular ridge, which, from Leguat's figure and description, we already knew the bird possessed at the base of its bill" (Newton & Newton 1869, p.347). Likewise, Ottow (1950) remarked that the pitting and unevenness present in the craniofacial hinge region represented the "strong expression of individual feathers on the head (tuft formation and other)" (p.9). In one specimen examined (NHMUK A.3506) there are a pair of foramina on the dorsal surface of the frontal at, or near, the fronto-nasal junction (foramen rostral du frontal of Janoo 1997, pl.5). Their function is unknown, but they may have been to transmit vascular vessels.

The transverse nuchal crest of *Pezophaps* is more elevated than the frontal ridge, and forms the caudal boundary to the depressed dorsal region. It shows much exostotic development, especially in the male, although Ottow (1950) remarked that this feature, in addition to the rugosities of the craniofacial region, is not due to pathology. The occipital region of *Pezophaps* shows extensive pachyosteosis, especially in the male. Martin (1904) described this part of the skull as "bovine [*bovin*]". The cranium of *Pezophaps* is proportionately longer and narrower than that of *Raphus* and the surface for muscle attachment slopes down more rapidly in *Pezophaps* than in *Raphus*, but to less an extent than in extant columbids. The cranium is widest in front of the postorbital processes, although proportionately further in front of these than in *Raphus*. The individual elements of the cranium are also less inflated compared with those of *Raphus*. Newton and Clark (1879) stated that in old specimens the temporal crest is always present, forming the lateral boundary to the depressed central region of the cranium, caudal to the orbits. The temporal notches of *Pezophaps* are less apparent, compared with *Raphus*, in dorsal view.

Endocranial Cavity

The endocranial cavity of *Raphus* is relatively small compared to its body size, being not much larger than that of *Goura*, a much smaller bird (see Parish 2013, fig.6.2). Warnett *et al.* (2020) calculated it to be 14.6 cm^3 in OUMNH 11605.[29] The longitudinal axis of the endocranial cavity is more horizontal than that of extant pigeons and is linked to the occipital face of the cranium being more vertical with respect to the base than in that group. Martin (1904) stated that the angle between the brain axis (longitudinal axis of the endocranial cavity) and the longitudinal axis of the basicranium in *Pezophaps* is *c.*30° (however, it seems to be closer to 20° upon examination of Newton & Clark's figure (1879,

---

[29] Endocasts of bird crania are taken to be reliable proxies for brain size and form (Early *et al.* 2020).

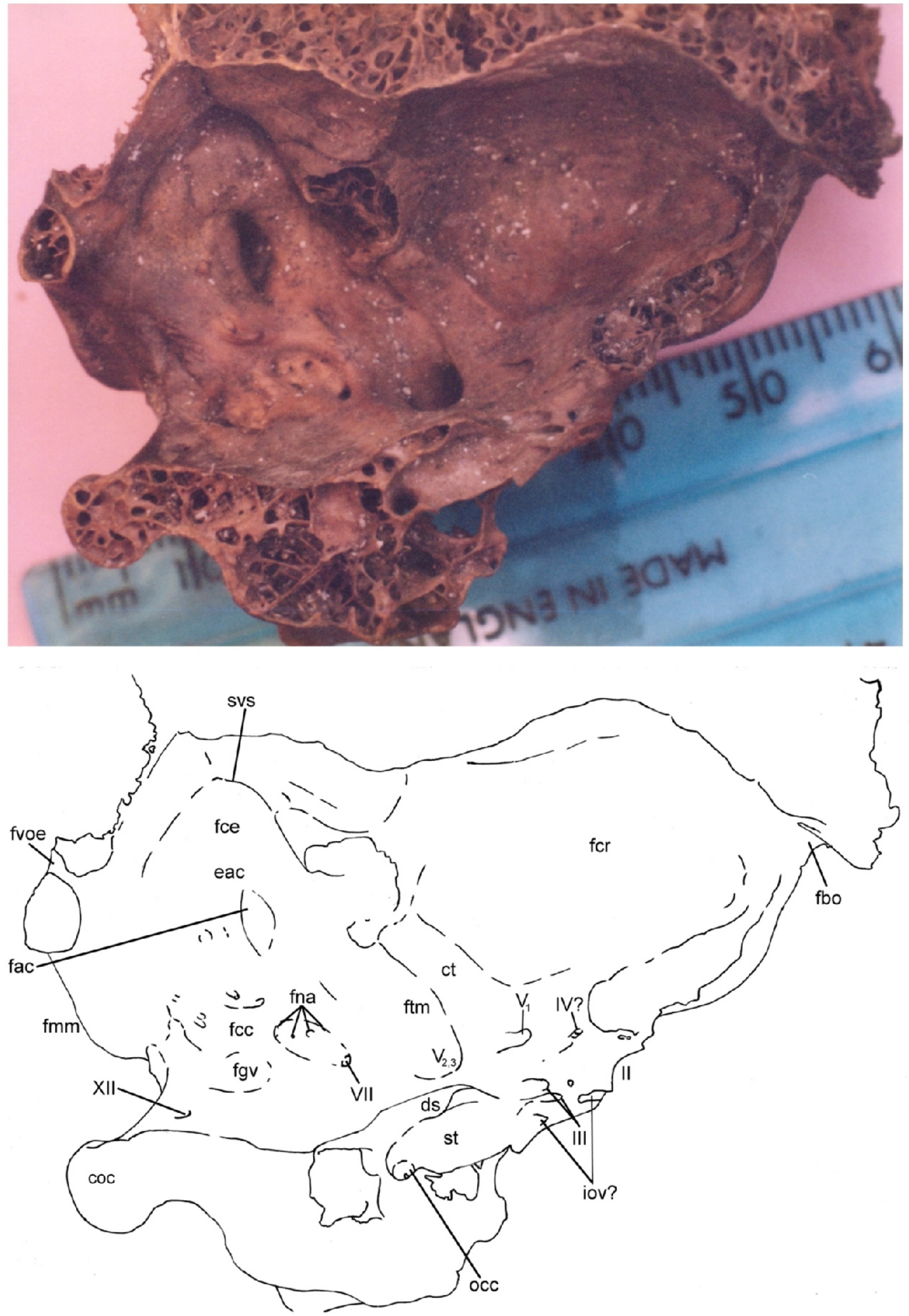

Endocranium of *Raphus* (NHMUK A.1338), left side. Note: N. accessorius (XI) exits the endocranial cavity with n. vagus (X). The basal ganglion of $V_{2,3}$ is housed in the fossa ganglii trigemini (labelled as $V_{2,3}$). ○ Jolyon C. Parish.

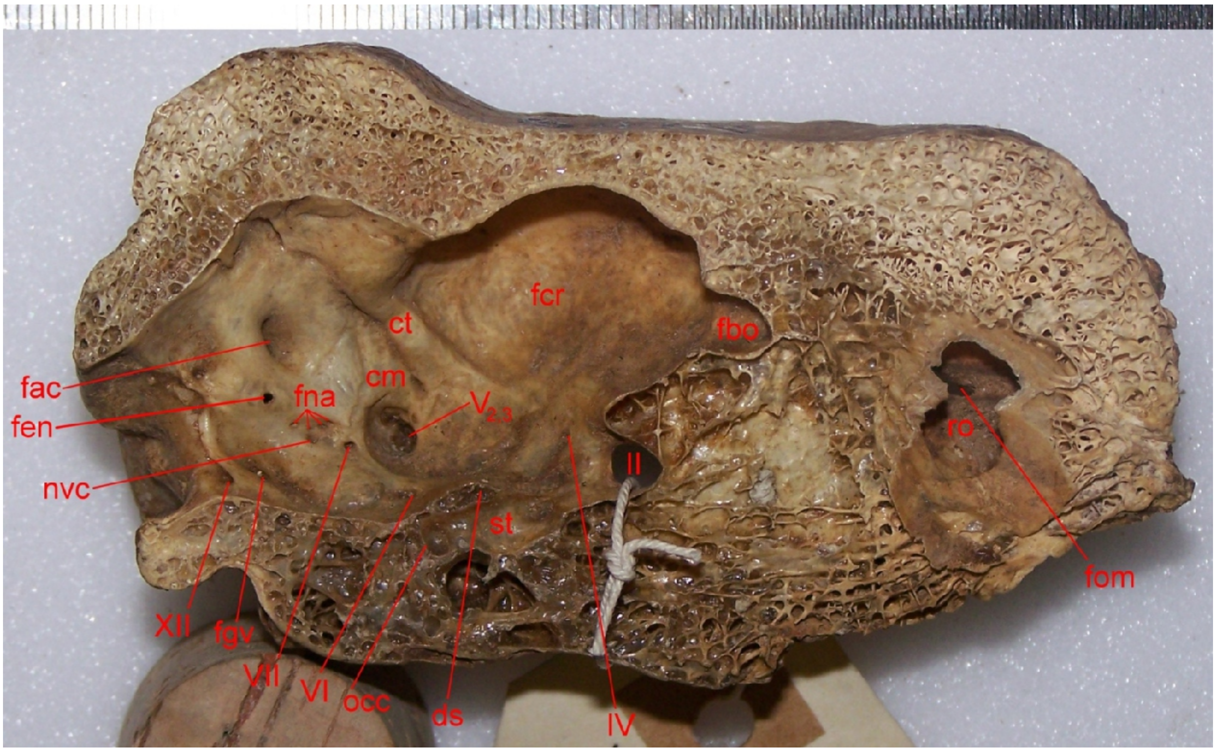

Endocranium of *Pezophaps* (UMZC 648), left side. ○ Jolyon C. Parish, December 2008.

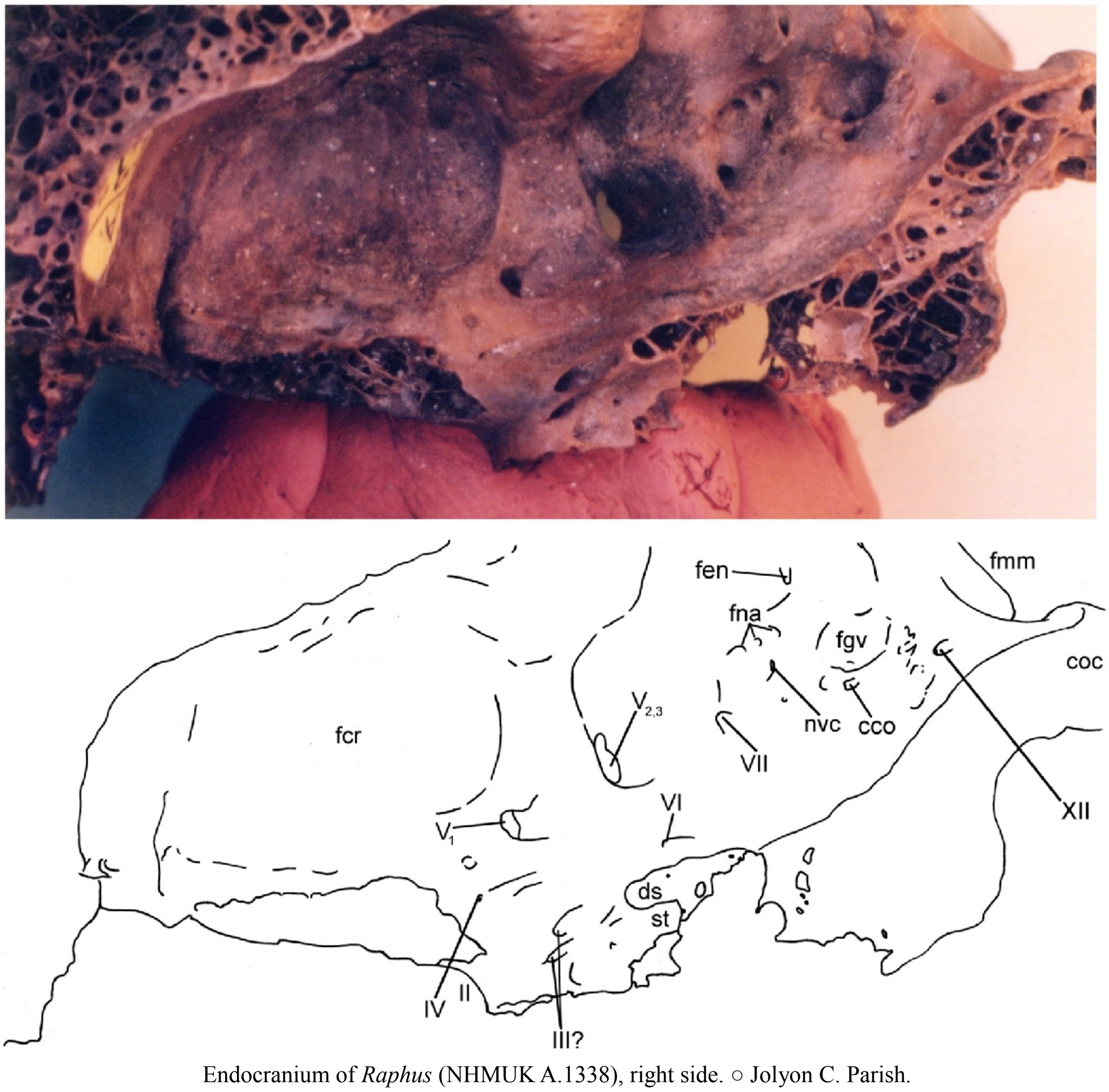

Endocranium of *Raphus* (NHMUK A.1338), right side. ○ Jolyon C. Parish.

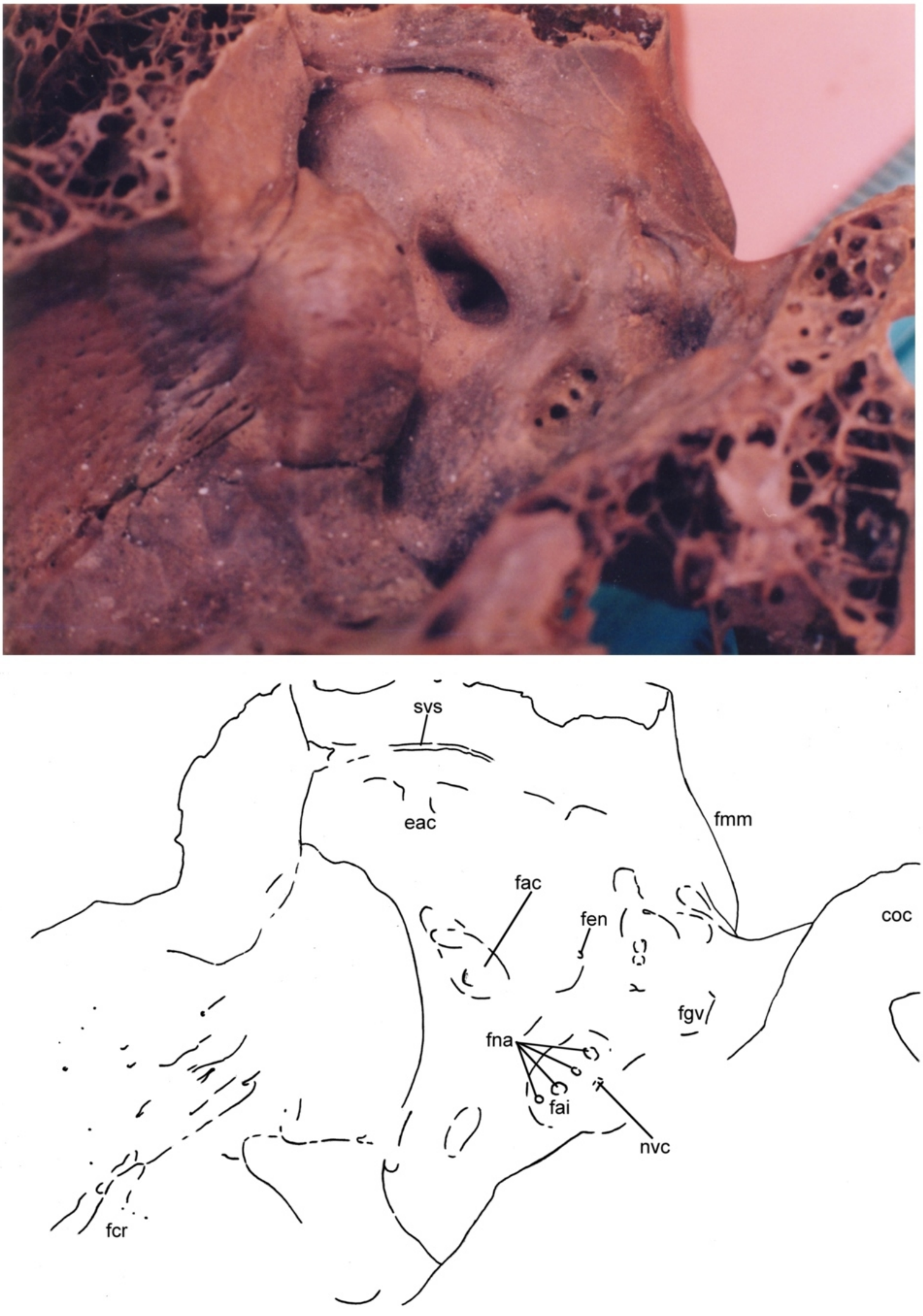

Endocranium of *Raphus* (NHMUK A.1338), right side. ○ Jolyon C. Parish.

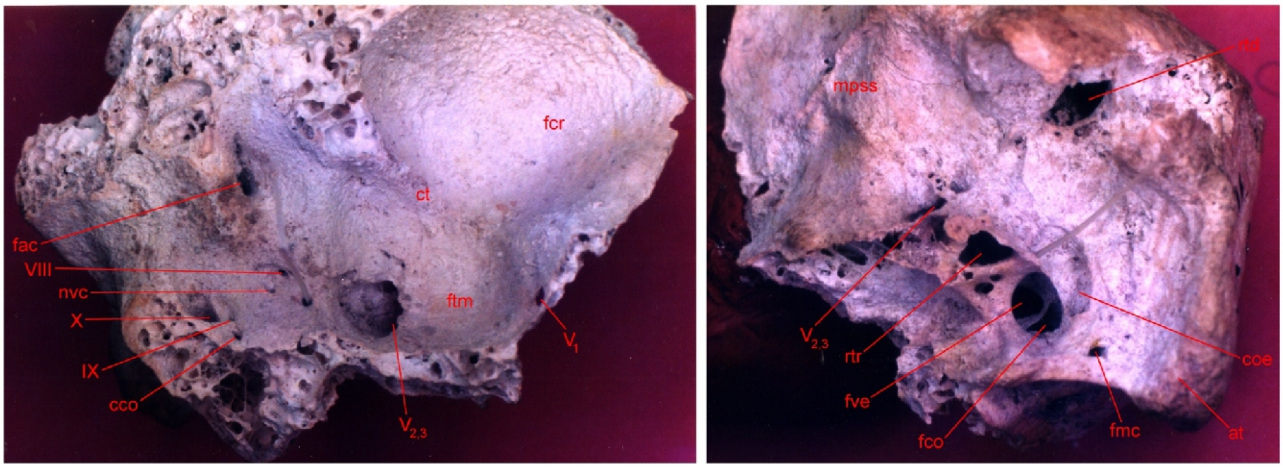

The endocranium (*left*) and tympanic region (*right*) of *Pezophaps* (NHMUK 76.1.28.11), left side. Note: the plastic bristle emerges from the foramina for the facial nerve (VII); the foramen opening into the tympanic region (right image) is for the hyomandibular branch of the facial nerve (VII_h). ○ Jolyon C. Parish.

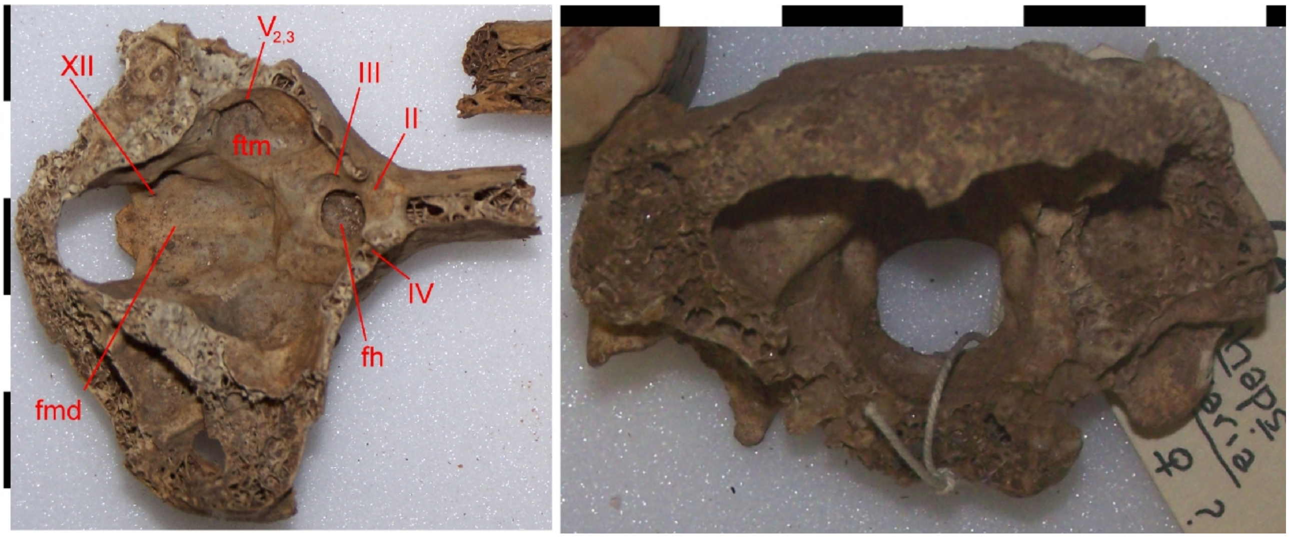

The endocranium of *Pezophaps* (UMZC specimens). *Left*: dorsal view, *right*: rostral view of caudal part of endocranium (UMZC 642), female. Scales in cm. Note: UMZC 642 was figured by Newton & Newton (1869, pl.xxi, fig.146). ○ Jolyon C. Parish, December 2008.

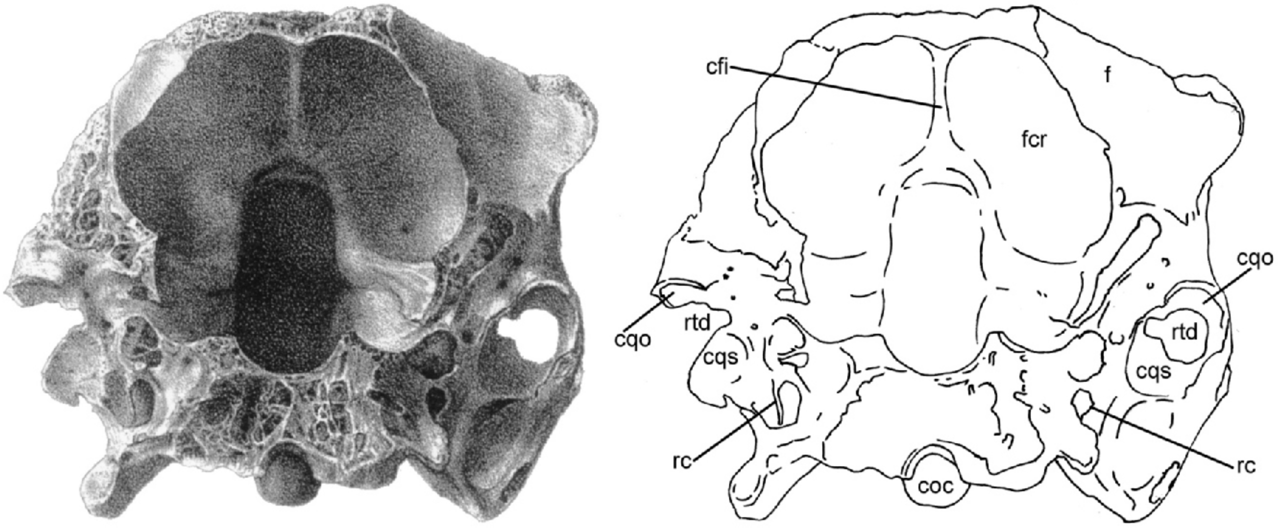

Endocranium of *Pezophaps*, ventral view, female (UMZC 641. Lithograph: Newton & Newton 1869, pl.xxi, fig.145. Artist: George Henry Ford. "G. H. Ford ad nat. lith." "W. West imp.").

pl.l, fig.2)). This is less than the corresponding angle in *Raphus*, which approaches that of extant columbids.

The endocranial cavity is longer than it is wide (length measured from the olfactory septum to the margin of the foramen magnum) and its greatest width is in the cerebral fossa, the largest of the three endocranial cavities, which housed the cerebrum in life. In sagittal section the great thickness of the frontals, and to a lesser extent the parietals, can be seen, as can the large open pneumatic vacuities in these regions (as evident in NHMUK A.1338).

The internal exoccipital process is small and emarginates the middle of the lateral border of the foramen magnum on each side. The fossa for the medulla oblongata, in the base of the cranial cavity, is slightly convex transversely and rises to the dorsum sellae, which projects with a sub-convex margin over the caudal part of the broad, shallow sella turcica. In the caudoventral part of the sella turcica are the pair of openings of the carotid canals. The dorsum sellae presents, at its base, the canal for the abducens nerve (VI). The transverse width of the fossa for the medulla oblongata is equal to that of the ventral part of the foramen magnum. Caudolaterally the fossa presents the hypoglossal nerve (XII) foramen on each side. Rostral to the hypoglossal foramen is the large depression, the fovea ganglii vagoglossopharyngealis, containing the vagal (X) and glossopharyngeal nerve (IX) foramina.[30] The internal exoccipital process overhangs this depression. The fovea ganglii vagoglossopharyngealis is located in the junction between the exoccipital and opisthotic bones (Baumel & Witmer 1993).

There are two small foramina close together, separated by a minute distance, at the rostral end of the fossa ganglii vagoglossopharyngealis:[31] the caudal one is the foramen for cranial nerve IX and the rostral one the opening of the canaliculus cochleae (which opens laterally into the medial wall of the scala tympani (opposite the fenestra cochleae) via the apertura lateralis; see Ewald 1892, Starck 1995, Mayr 2020).[32]

The internal acoustic fossa (fossa acustica interna) contains the facial nerve (VII) and vestibulocochlear nerve (VIII) foramina, which pierce the prootic. Dorsally it presents four foramina in a sub-horizontal line; these are (rostral to caudal): foramen n. ampullaris anterior, foramen n. ampullaris horizontalis, foramen n. sacculus and foramen n. ampullaris posterior (Ewald 1892, Dubbeldam 1993). Ventral to the third of the four foramina and caudal to the most rostral one is another which connects with the columellar recess: the foramen n. cochlearis. The largest foramen, at the rostroventral extremity of the fossa is that of the facial nerve.[33] This is the same arrangement as in extant columbids. The internal acoustic fossa is located rostral to the fovea ganglii vagoglossopharyngealis and is separated from it by a narrow convex ridge. Caudal to, and between, the internal acoustic fossa and the fossa auriculae cerebelli is a small foramen at the end of a groove: the endolymphatic foramen. In birds the endolymphatic duct usually opens at the juncture of the prootic, opisthotic and epiotic bones (Larry Witmer, pers. comm., 2nd September 2020).

The cerebellar fossa is relatively narrow and its apex is below the level of that of the cerebral cavity. Caudodorsally it presents the canal for the v. semicircularis rostralis. The caudal part of the cerebellar fossa shows the internal opening of the median supraoccipital foramen, in the midline of the cranial cavity just above the foramen magnum. Owen (1867) remarked that "the size of the cerebellar division [...] of the cranial cavity accords with the generally accepted physiology of the superincumbent mass of the epencephalon [= cerebellum]" (p.70). Melville (1848) stated that the "great posterior cerebellar sinus" is located in a groove between the margin of the foramen magnum and the sagittal nuchal crest,

---

[30] Owen (1867) stated that the fossa contained the foramen for the vagal nerve and entojugular vein.

[31] Slice numbers 258-260 and 263-264 of the transverse CT data of the Oxford dodo head.

[32] In the endocranial cavity of *Columba palumbus* the foramen for cranial nerve IX and canaliculus cochleae are also separate (pers. obs.).

[33] In a specimen of *Pezophaps* (NHMUK 76.1.28.11) a bristle has been inserted into the cranium; one end emerges from the foramen in the ventral part of the canalis ophthalmicus externus and the other from the rostralmost foramen of the fossa acustica interna.

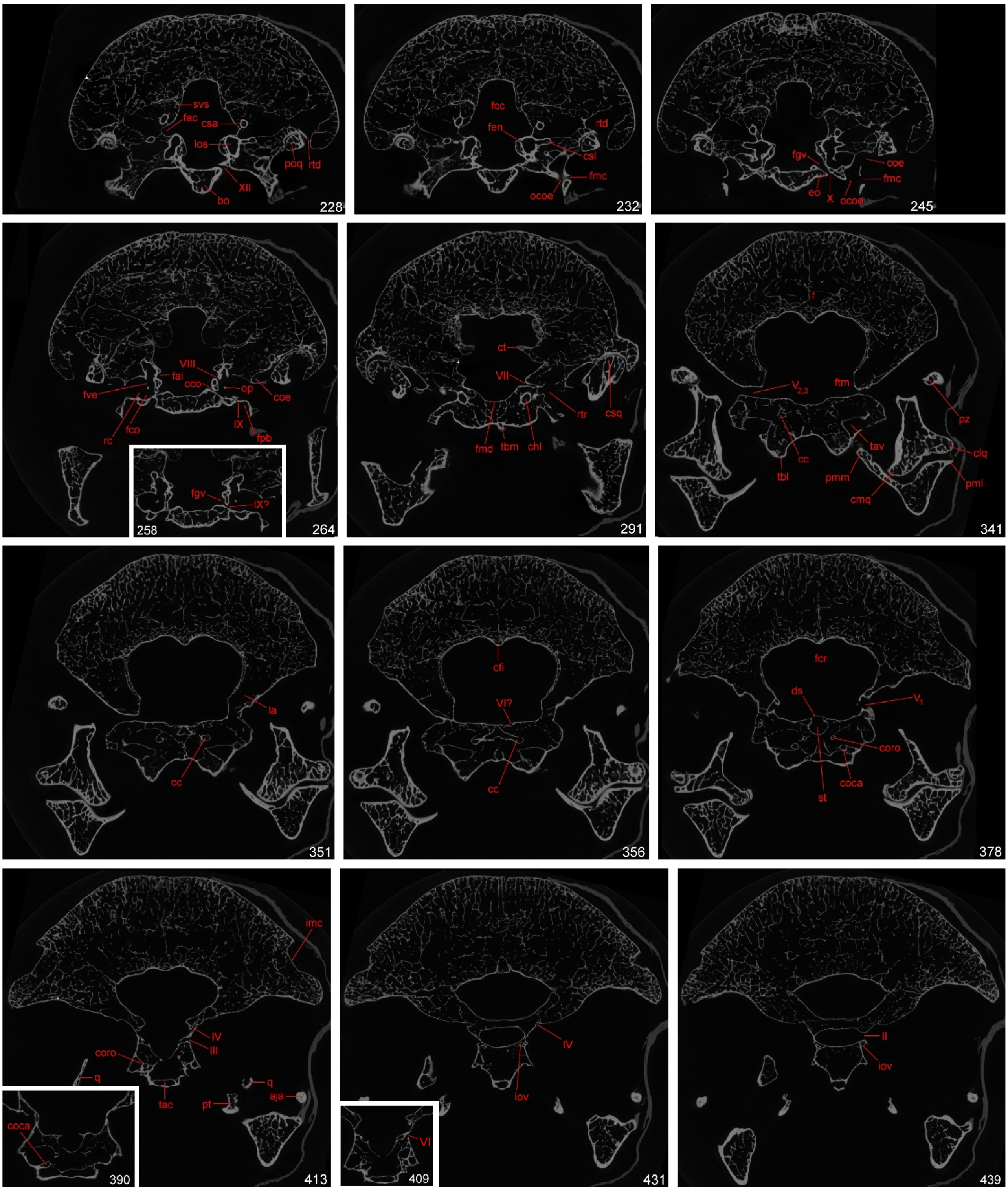

Transverse CT sections of OUMNH 11605 (CT data relating to Warnett *et al*. 2020; MorphoSource Media: M55320).

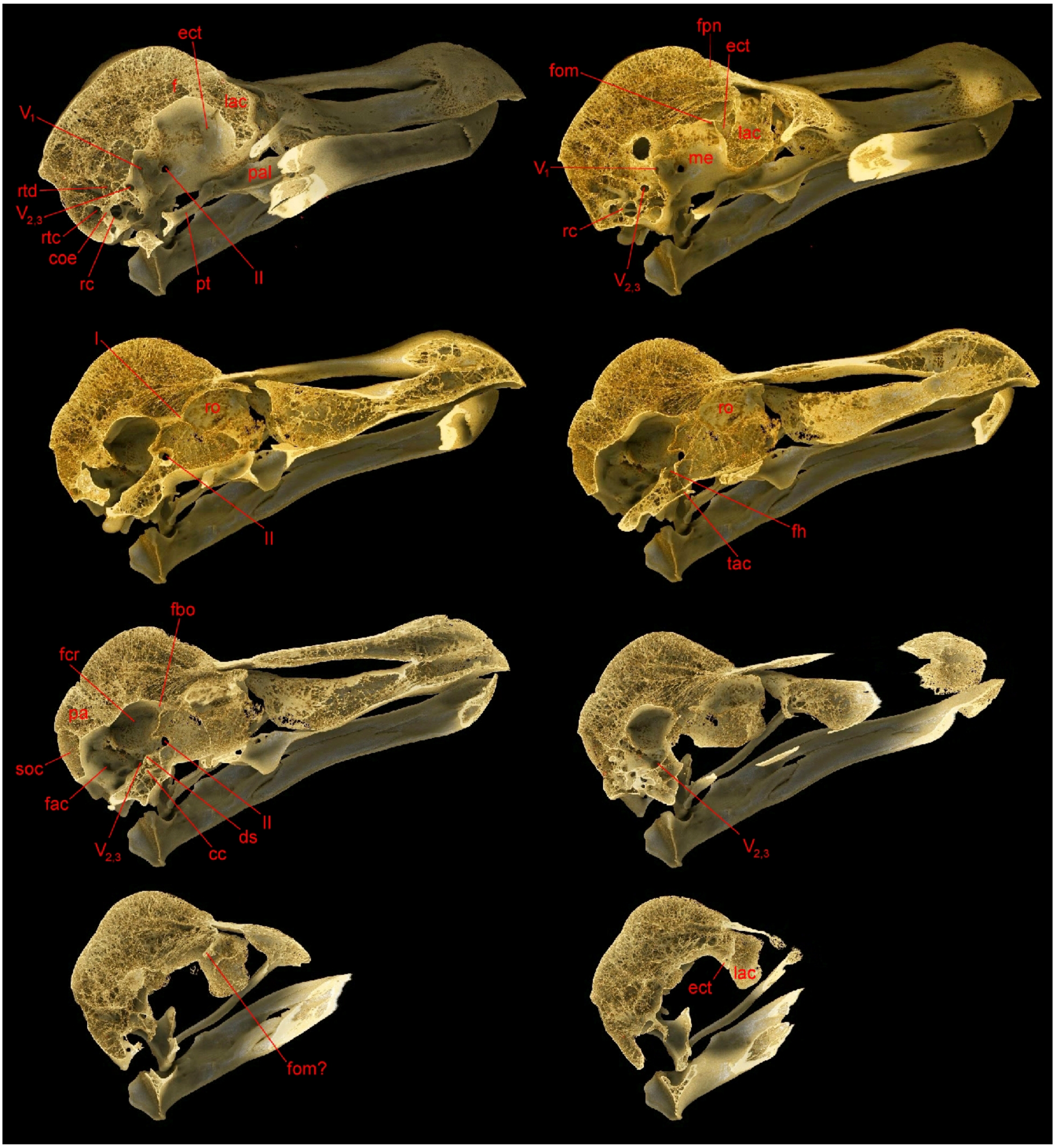

3D CT data of OUMNH 11605, sagittal sections (after Warnett *et al*. 2020, supplementary data).

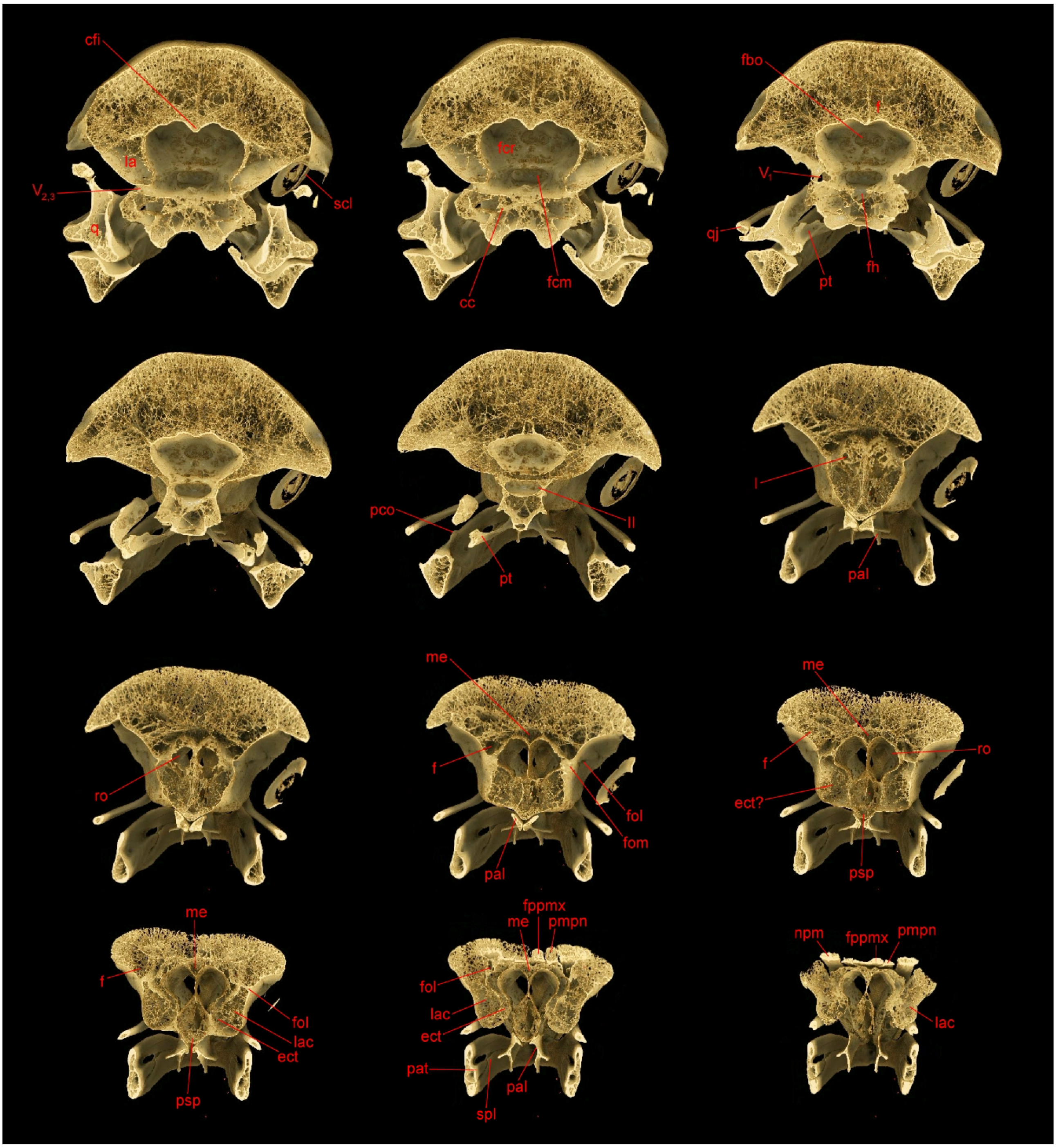

3D CT data of OUMNH 11605, transverse sections (after Warnett *et al*. 2020, supplementary data).

this part of the "posterior cerebellar sinus" may correspond with the sinus supraforaminalis. The vein passing through the supraoccipital foramen to join this sinus (this part of the sinus is probably the sinus occipitalis) is the v. occipitalis dorsomediana.

The cerebral fossa is broad and sub-rounded rostrally. Its dorsal surface presents the low median crista frontalis, indicating the division of the cerebrum into two hemispheres. The crista frontalis shows a narrow sagittal groove, possibly for a longitudinal sinus (Owen 1867; possibly the mid dorsal sinus of Richards (1968)) and a transverse linear groove defines the rostral part of the ridge (Owen 1867). The crista frontalis subsides rostrally towards the septum between the olfactory fossae. The cerebral fossa shows a longitudinally slightly curved groove, possibly for a vein (shown in NHMUK A.1338), near its dorsal surface and running the length of the cavity. The internal surface of the cerebral fossa is smooth.

The fossa tecti mesencephali is shallow and its margins are undefined. The crista marginalis is weakly developed, if at all; it is more distinct in *Pezophaps*. At the apex of the fossa tecti mesencephali, beneath the groove for the v. semicircularis rostralis, is a "tumid pneumatic projection" (Melville 1848), the "tentorial tuberosity" of Owen (1867, p.77), which overhangs the fossa. This tuberosity is developed on the crista tentorialis and lies at the dorsal ends of the crista marginalis and crista tentorialis. The groove for the v. semicircularis rostralis marks the caudal margin of this tuberosity, above which it bifurcates: the lower branch defining the wall of the rostral semicircular canal. Ventral to the arch formed by the groove is the vertically oblong fossa auriculae cerebelli, housing in life the flocculus and associated blood vessels. Owen (1867) stated that it "appears to have received veins from the cranial diploë" (p.71).

The floor of the fossa tecti mesencephali is thin and perforated by the foramen for the ophthalmic nerve (V_1). Caudal to this, below the tentorial tuberosity and rostral to the internal acoustic fossa, is the large depression containing the maxillomandibular foramen ($V_{2,3}$), which is larger than that for the ophthalmic nerve. Rostromedioventral to the ophthalmic nerve foramen is the groove for the trochlear nerve (IV). The trochlear nerve foramen lies at the rostral end of this groove and pierces the thin lamina which forms the caudal margin of the optic nerve foramen (II). Ventral to the trochlear nerve foramen and close to the caudal border of the optic nerve foramen are those of the oculomotor nerve (III). The oculomotor nerve appears to exit the cranial cavity via two foramina, which lie at the rostral ends of two parallel grooves. One foramen is slightly rostroventral of the other. The thick plate formed by the interorbital septum, between the olfactory nerve foramen (I) and that for the optic nerve is slightly convex longitudinally and transversely. Its caudal margin is thick and rounded and projects over the groove for the optic chiasma (Melville 1848). The optic chiasma, the fossa ganglii trigemini and the fossa tecti mesencephali are housed in the fossa cranii media.

The olfactory fossae (for the olfactory bulbs; rhinencephalon of Owen 1866) are separated by a median septum. On each side, the olfactory nerve proceeded rostroventrolaterally from the olfactory fossa and entered the posterior olfactory chamber.

In *Pezophaps* a sagittal section of the skull shows the strong spongiosa development and pneumatization of the skull roof (Ottow 1950). The frontal diploë is thinnest above the centre of the cerebral fossa. The diploë is thickest over the olfactory fossae and posterior olfactory chambers, and to a lesser extent in the region of the transverse nuchal crest. The diploë close to the dorsal surface of the cranium of *Pezophaps* is of "close, firm texture, consisting of small sub-equal and sub-spherical cells" (Newton & Clark 1879, p.446). Around the olfactory fossae and posterior olfactory chambers, and in the body of the basisphenoid and parasphenoid, the pneumatic cells are larger. In contrast, the diploë is thickest over the cerebral fossa and olfactory fossae in *Raphus*. This pneumatic diploë exceeds the length of the cranial cavity. The thickness of pneumatic diploë between the dorsal surface of the cerebral fossa and the dorsal surface of the cranium is great, approaching in size the longitudinal length of the cerebral fossa, and exhibits severallarge pneumatic vacuities. The diploë is composed mainly of small sub-equal sub-spherical pneumatic cells in both the dorsal, ventral and lateral walls of the cranium (Owen 1867). A longitudinally sectioned cranium of *Raphus* (NHMUK A.1338) shows that the internal structure of the basilar processes also consists of larger cells, probably the result of pneumatization. In addition, the suture line between the frontal and parietal can be seen in the sectioned cranium of *Raphus* (NHMUK A.1338). Martin (1904) gave the ratio of the length of the base of the skull ("der Länge der Schädelbasis") to the length of the endocranial cavity ('Gehirnaxe') as 4.5 for *Raphus*. For *Pezophaps* it is approximately 3.3 (pers. obs.).

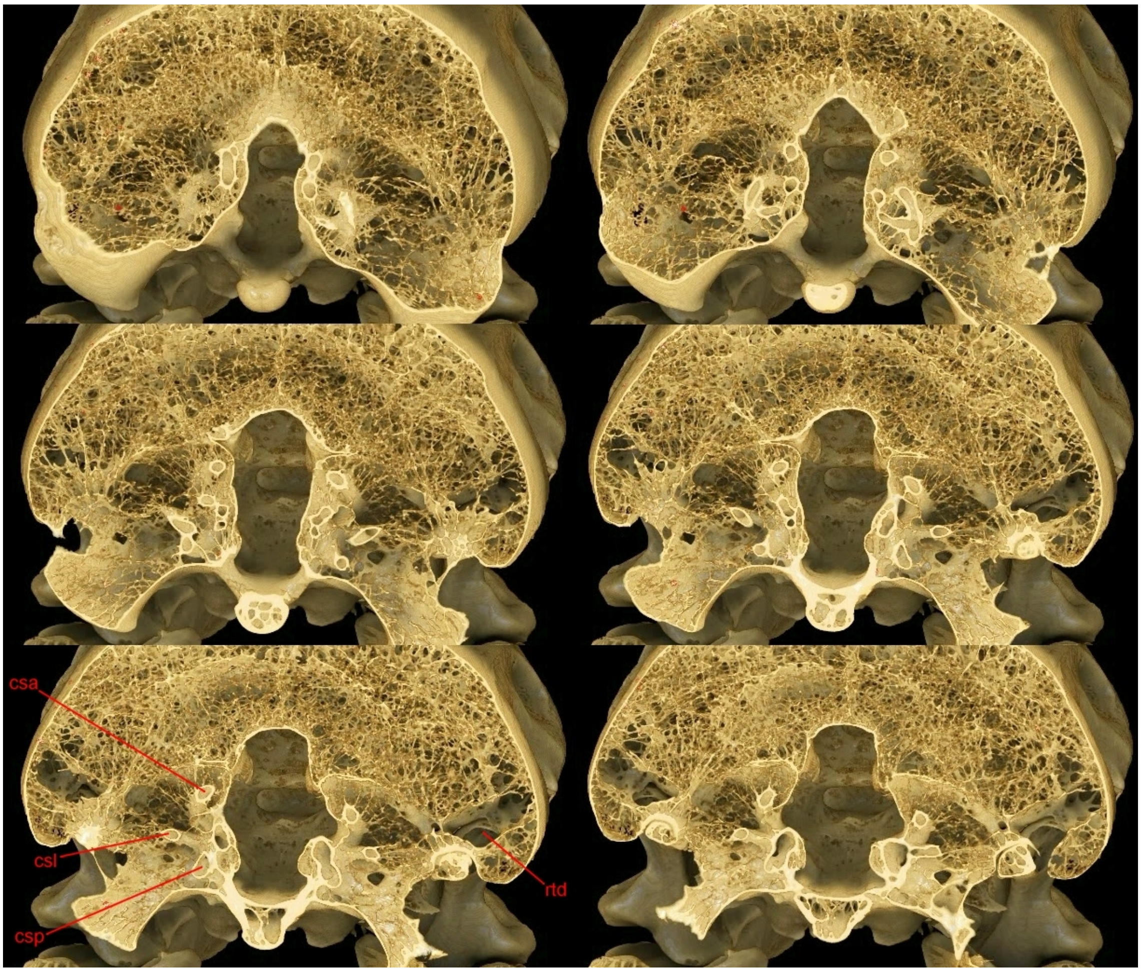

3D CT data of OUMNH 11605, transverse sections, showing the osseous labyrinth (after Warnett *et al*. 2020, supplementary data).

Owen (1867) provided his interpretation as to the expansion of the cranial diploë: "the true explanation rests on the size, weight, and power of the bill, and the concomitant necessity for adequate extent of attachment of the facial to the cranial part of the skull, and of the muscles from the trunk destined to sustain and wield the long and heavy-beaked head" (p.70). However, Behn (1868b) noted firstly that cristae would have been sufficient for muscle attachment and secondly that there are no muscle attachments in the areas where the diploë is most developed. In fact, an increase in cranial diploë may have been, at least in part, a sexually selected character, increasing the area of the facial and bill region. This would be associated with the naked face and well-developed cutaneous muscles. Although the cranium is expanded, the attachment for jaw muscles is not extensive. The mechanics of the skull are discussed below.

The cranial cavity of *Pezophaps* is similar to that of *Raphus*, although the apex of the cerebellar fossa does not appear to be as well defined as it is in the former (comparing the sectioned cranium of NHMUK A.1338 (*Raphus*) with UMZC 648 (*Pezophaps*)). The dorsal surface of the endocranial cavity of *Pezophaps* exhibits the median, low, rounded crista frontalis, caudal to which the cavity deepens into the cerebellar fossa. A cast of the endocranial cavity of *Pezophaps* was figured by Newton & Clark (1879, pl.xlv, fig.14).

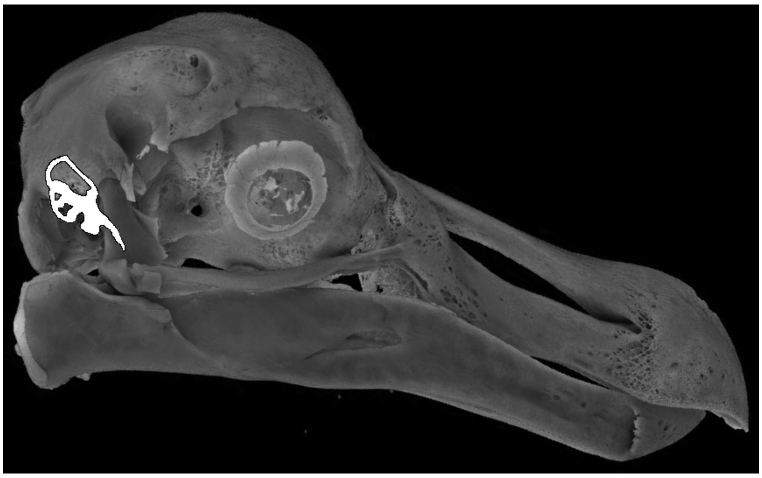

Skull (OUMNH 11605) showing approximate location of the osseous labyrinth (approximate due to the sagittal axis of the skull not being orthogonal), with the skull oriented such that the horizontal semicircular canal is approximately horizontal (skull image: Warnett *et al*. 2020 CT data; labyrinth image: after Gold *et al*. 2016, fig.6A).

Osseous Labyrinth

(*Raphus*: Janoo 1997, pl.10; Gold *et al*. 2016, fig.6)

The medial part of the osseous labyrinth is covered and enclosed by the prootic. The middle part of the anterior semicircular canal is enclosed by the epiotic, and the posterior semicircular canal, its ampulla and part of the horizontal semicircular canal are enclosed by the opisthotic (Jollie 1957).

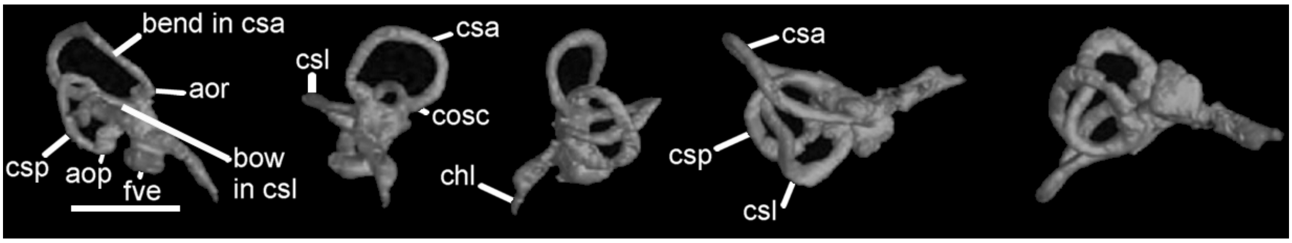

Osseous labyrinth of *Raphus* in lateral, rostral, caudal, dorsal and ventral views. Scale = 1cm. (After Gold *et al*. 2016, fig.6).

The relative proportions of the semicircular canals in *Raphus* resemble those of other columbids (Gold *et al*. 2016). The anterior semicircular canal of *Raphus* is larger than the horizontal and caudal ones (Janoo 1997) and is very caudally inclined (Gold *et al*. 2016). Its rostral part has a caudal bend, as in other columbids. The horizontal semicircular canal bears a concavity around its midpoint, rendering it bow-shaped; a weak concavity is seen in *Goura crista* and *Chalcophaps indica*, however such a developed bend is not seen in other neornithines (*ibid*.).[34] *Pezophaps* also appears to show a developed bow-shape of the horizontal canal, as well as a slight bend in the anterior canal (pers. obs. from unpublished CT data from Larry Witmer, pers. comm., 2nd September 2020). The horizontal semicircular canals do not meet in the sagittal plane, a feature in common with other Columbiformes (Janoo 1997).

The cochlea is relatively straight in *Raphus* and *Pezophaps* compared with other columbids (see Gold *et al*. 2016, fig.6). This condition is similar to that seen in *Rhynchops niger*, *Alca torda*, *Uria aalge*, and the flightless *Pinguinus impennis* and Mancallinae in comparison with other charadriiforms (Smith & Clarke 2012). Smith & Clarke (2012) noted that "[c]urvature of the cochlear duct may reflect an elongation of the basilar papilla and an increase in the range of hearing frequency as has been shown in

---

[34] Gold *et al*. (2016) speculated that this bend might "represent an increase in variability of the semicircular canals resulting from a release from the need for high sensitivity" (p.12).

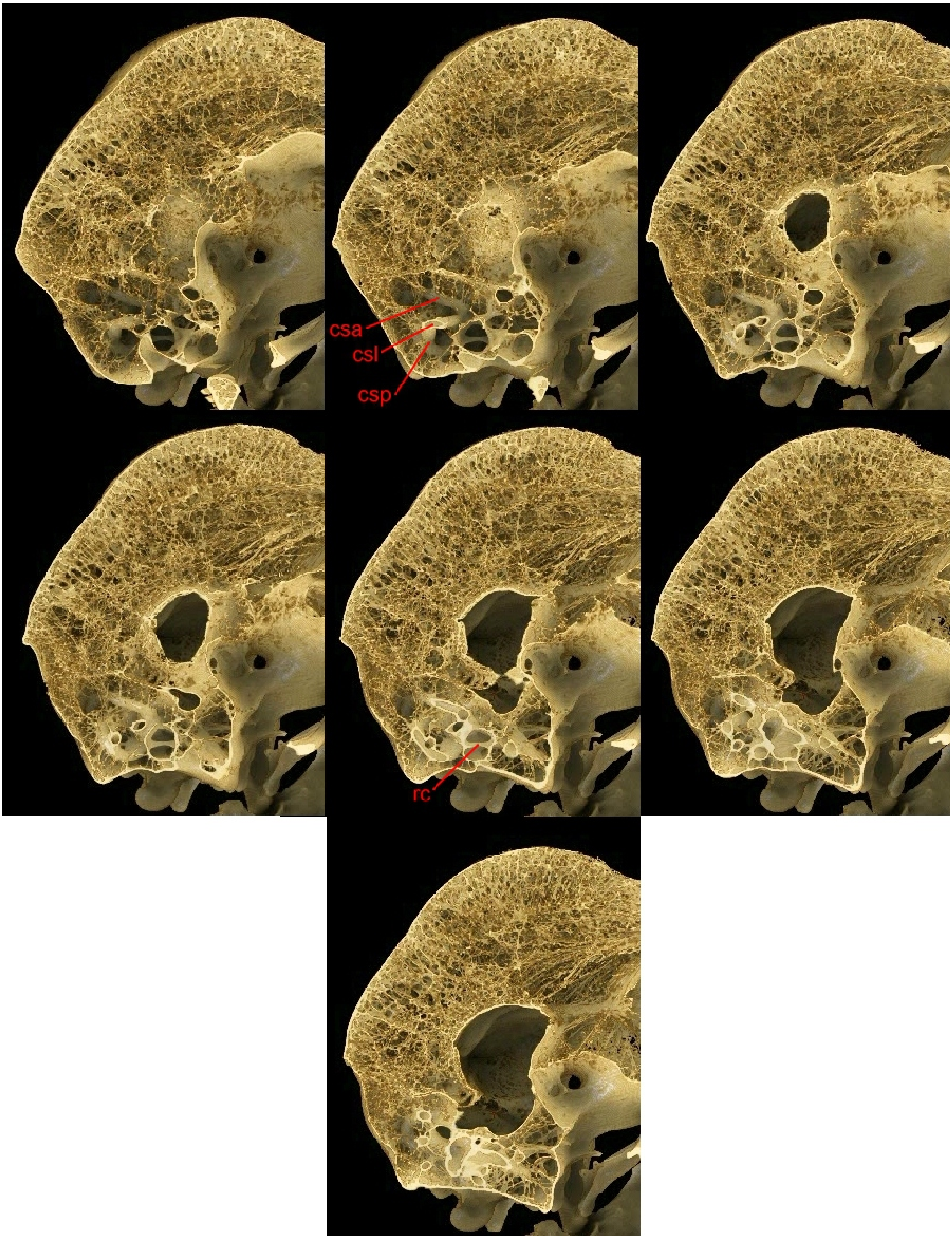

3D CT data of OUMNH 11605, sagittal sections, showing the osseous labyrinth (after Warnett *et al*. 2020, supplementary data).

other birds” (p.19). The distal end of the cochlea is narrow in *Raphus* and *Pezophaps* in comparison to the more bulbous end seen in other columbids. The proportionately similar lengths of the endosseous cochlear duct in *Raphus* and other columbids studied by Gold *et al.* (2016) suggests that the former had a range of hearing similar to that of the latter. The osseous labyrinth is also more inclined (when the horizontal semicircular canal is placed horizontally) than in other columbids (see Gold *et al.* 2016, fig.6), which may be related to the orientation of the longitudinal endocranial axis.

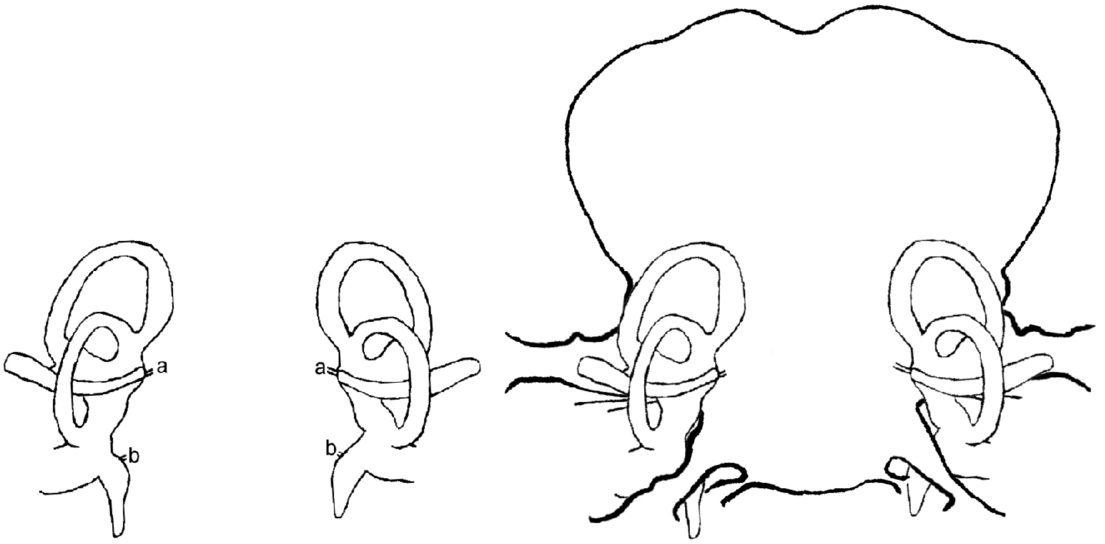

Left: outline of the osseous labyrinth of *Raphus* in caudal view (traced from CT data; Warnett *et al.* 2020). a: foramen endolymphaticum, b: canaliculus cochleae. *Right*: outline of the osseous labyrinth of in *Raphus* superimposed on the outline of the endocranium in caudal view (traced from CT data; Warnett *et al.* 2020). Note: the flocculi are not shown.

Quadrate

(*Raphus*: Claessens & Hume 2015, fig.2; Claessens *et al.* 2015, fig.12; *Pezophaps*: Newton & Newton 1869, pl.xxii, figs.163-168)

Quadrates of *Raphus* are present in (amongst other specimens) OUMNH 11605, UMZC 415.KK, the Copenhagen skull (ZMUK AVES-105485), the MNHN skeleton, MNHN MAD 5993 to MAD 6000, AMNH SKEL 6258, CM Av6281, MAS11-11020, the Port Louis skeletons, Paul Carié’s skeleton, the Summers Place Auctions skeleton and Thirioux’s collection. In lateral view the quadrate of *Raphus* shows the typical columbiform cruciform shape, with the orbital and otic processes forming the dorsal arms and the lateral and medial condyles forming the ventral arms. The dorsal extremity of the otic process is divided into the caudomedial otic condyle and the rostrolateral squamosal one, which articulate with the otic and squamosal bones of the cranium respectively. The axes of the otic and squamosal condyles form an angle of 40° (Claessens *et al.* 2015).

The otic articular facet of the quadrate is triangular in dorsal view and presents several foramina around its base (Melville 1848, Claessens *et al.* 2015). The squamosal articular facet is larger than the otic one and is covered by a thin triangular synovial surface in OUMNH 11605 (*ibid.*). The condyles are joined by a ridge (Claessens *et al.* 2015)[35] lying within the saddle-shaped intercondylar incisure, just ventral to which, on the caudal face of the quadrate, is a deep circular fossa containing numerous pneumatic apertures; these would have been orifices of the paratympanic sinus (see Witmer & Ridgely 2008). *Pezophaps* lacks this pneumatic fossa, and if pneumatic foramina are present they are minute. All other columbids examined possess a pneumatic foramen on the caudal face of the quadrate, just ventral to the intercondylar incisure. Melville (1848) stated that in OUMNH 11605 a “ligamentous groove” is most defined rostrally and laterally in both condyles (p.94). The otic process (pars oticus) of the quadrates of *Raphus* and *Pezophaps* are bicephalic (*i.e.*, showing both squamosal and otic condyles), but in the latter, at least, there is variation: the intercapitular incisure being more developed in some specimens (for example OUMNH 19635), thus making them slightly bicervical.

---

[35] Claessens *et al.* (2015) refer to this as the vallecula intercapitularis. However, a vallecula is a depression or furrow.

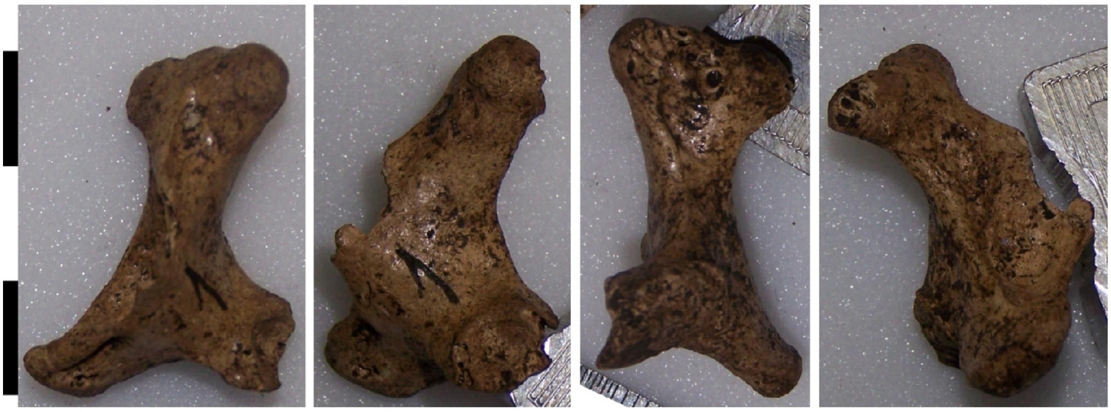

Left quadrate of *Raphus* (UMZC 415.KK) in rostral, lateral, caudal and medial views; scale in cm. Note: most of the orbital process is missing in this specimen. ○ Jolyon C. Parish, December 2008.

The attachment of the membrana tympani to the quadrate, the tympanic crest, is indicated by a slight ridge passing from the squamosal condyle ventromedially towards the medial condyle. In MAS11-11020 it is thick and broad (Claessens *et al*. 2015). In some specimens (for example, OUMNH 19635) of *Pezophaps* the sharp ridge for the attachment of the membrane on the caudal face of the quadrate, running from the medial part of the squamosal condyle towards the medial edge of the medial condyle, is distinct. The orbital process is thin, slightly curved and subtriangular and its apex is truncated and slightly expanded. The dorsal part of the apex is slightly turned laterally. The lateral surface of the orbital process is convex provided attachment for m. pseudotemporalis profundus (see section on musculature); in a specimen in Thirioux's collection (photograph (9B) accompanying a letter to Alfred Newton dated 5th September 1900) a curving crista can be seen which may have been for the attachment of this muscle. The medial face of the orbital process is slightly concave. Its dorsal margin extends caudally to the squamosal condyle, and the ventral margin is bent medially slightly and passes into the pterygoid process, which lies ventromedial to the orbital process. The thickened ventral margin of the orbital process forms the crista orbitalis. Medially the orbital process is concave, the concavity deepening into the basiorbital fossa.

The angle between the orbital process and the otic process is more open in *Raphus* compared with *Pezophaps* (Janoo 1997). In OUMNH 11605 the apex of the narrow pterygoid process presents a pneumatic foramen (Melville 1848). The lateral aspect of the body of the quadrate (corpus quadrati) is smooth and convex.

The ventrolateral arm of the quadrate is formed by the projecting lateral process, which presents the quadratojugal fossa with which the quadratojugal of the jugal arch connects. The mandibular extremity (pars mandibularis) of the quadrate is expanded laterally and medially to form the condyles. The medial condyle is narrow and ventromedially pointing. The quadratojugal condyle is compressed rostrodorsally-caudoventrally. The medial face of the lateral condyle is sub-concave due to a broad shallow groove directed obliquely forwards which passes onto the lateral face of the medial condyle. In OUMNH 11605 the caudally sloping ventral surface of the lateral condyle is covered with articular cartilage, which dips into this groove and increases over the thick rounded edge of the medial condyle (which shows a large reticulated pneumatic foramen), and over its rostral surface, at the lateral angle of which it is narrowest (Melville 1848). In both *Raphus* and *Pezophaps* the lateral condyle is continuous with the caudal one; the latter "forms a flattened, rounded surface" on the caudal face of the lateral process (Claessens *et al*. 2015, p.47). The mandibular condyles are separated by the poorly-defined intercondylar sulcus, and exhibit a single "transverse cartilage-coated surface" in *Raphus*, as in most pigeons (Parker 1866, p.192). The medial condyle extends further ventrally than the lateral one; a transverse groove lies in the intercondylar sulcus, its lateral end impressing the lateral face of the medial condyle. In rostral view the lateral and medial processes are approximately 90° to each other (Claessens *et al*. 2015). In ventral view the quadrate of *Pezophaps* is more similar to that of extant pigeons than that of *Raphus* is. The lateral and caudal condyles of the quadrate of *Pezophaps* are continuous with the medial condyle.

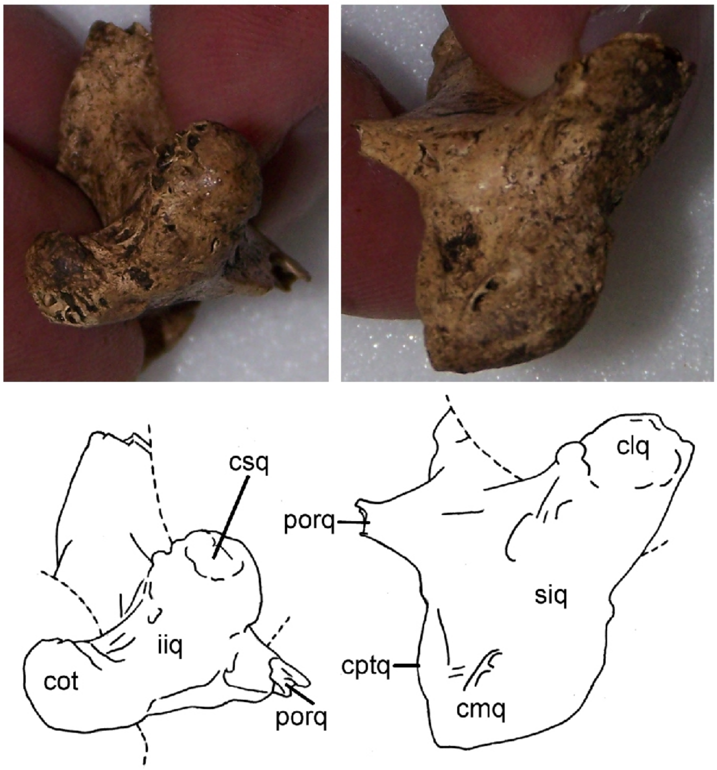

Left quadrate of *Raphus* (UMZC 415.KK) in dorsal and ventral views. Note: most of the orbital process is missing in this specimen. ○ Jolyon C. Parish, December 2008.

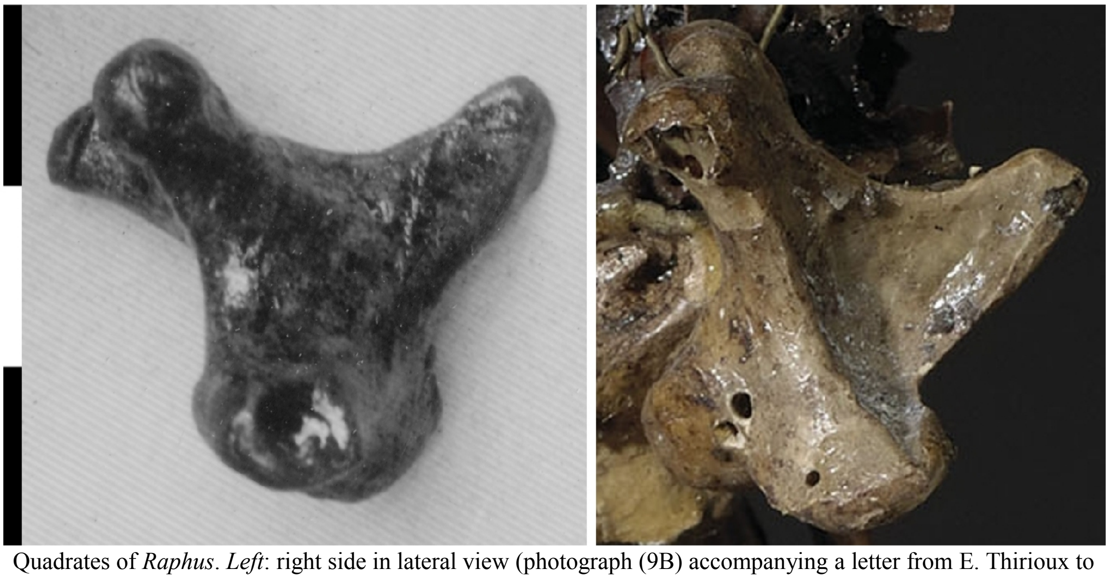

Quadrates of *Raphus*. *Left*: right side in lateral view (photograph (9B) accompanying a letter from E. Thirioux to Alfred Newton, dated 5th September 1900; scale in cm; © UMZC). *Right*: left side, medial view (Paul Carié's dodo skeleton, Christie's London, Sale 17492, lot 155; © Christie's 2019).

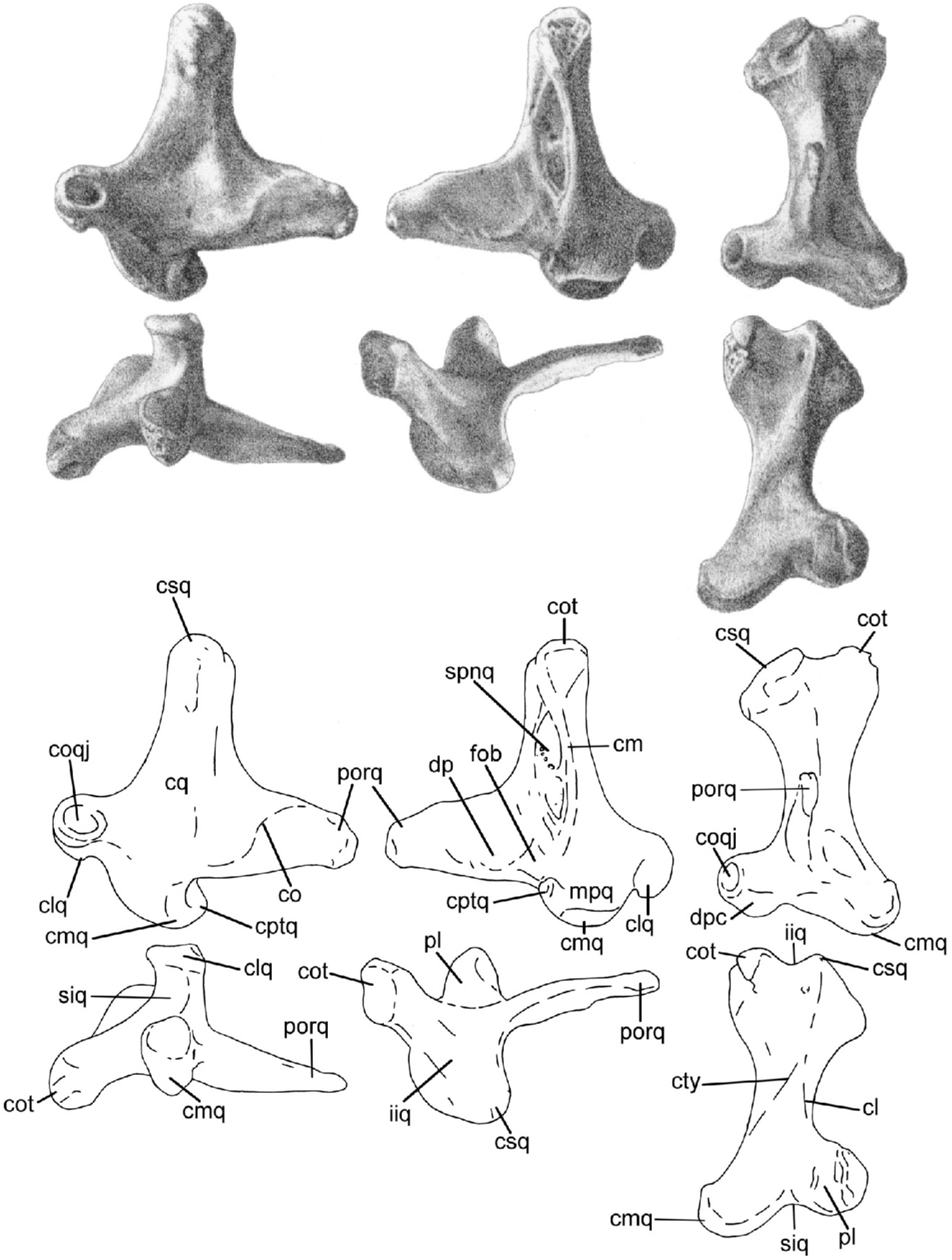

Right quadrate of *Pezophaps*, male (lithograph: Newton & Newton 1869, pl.xxii, figs.163-168. Artist: George Henry Ford. “G. H. Ford ad nat. lith.” “W. West imp.”).

The caudal face of the quadrate is 'X'-shaped with the medial and lateral condyles projecting transversely more than the condyles of the otic process. The lateral margin, between the otic process and the quadratojugal condyle, is more concave in outline than the medial margin between the otic process and the medial condyle. The medial surface of the quadrate shows a tripartite depression, the basiorbital fossa, for m. protractor pterygoidei et quadrati that is deepest ventrally and rough internally. The rostral extremity of this fossa is truncated "the expansion of the diploë of the orbital process, which is subtranslucent" in OUMNH 11605 (Melville 1848, p.95). The basiorbital fossa is bordered caudally by the tympanic crest. The fossa lacks pneumatic foramina in Thirioux's Port Louis skeleton (Claessens *et al.* 2015). In *Pezophaps* it varies in shape and size between individuals and may be subdivided (Newton & Newton 1869). In some specimens there is a pneumatic foramen on the medial face in *Pezophaps*, at the base of the orbital process (Janoo 1997). The lateral surface of the quadrate is convex, with a slight concavity along the dorsal margin extending onto the orbital process.

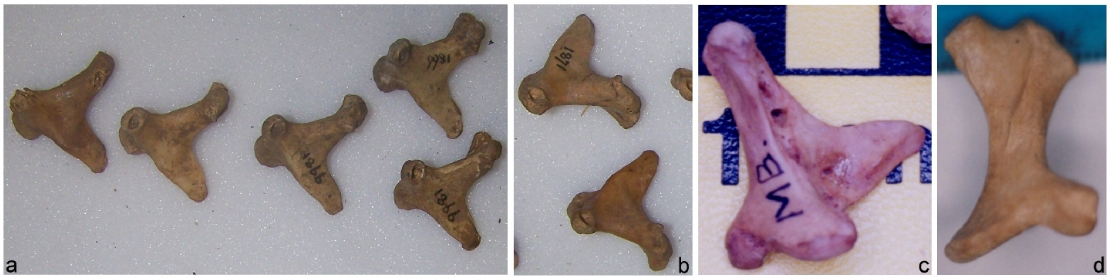

Quadrates of *Pezophaps*. a, b: UMZC specimens in lateral view; c: left side (NHMUK A.1373), medial view (scale in cm); d: right side (OUMNH 19635), caudal view. ○ Jolyon C. Parish.

The pterygoid condyle is separated from the medial condyle by a shallow V-shaped fossa (Claessens *et al.* 2015).

The mandibular extremity of the quadrate of *Pezophaps* is more elongate and relatively wider transversely than that of *Raphus*, and the abutment for the quadratojugal does not project as far caudally as in *Raphus* (Newton & Newton 1869). The quadrate of *Pezophaps* is nearly as large as that of *Raphus* in absolute size. In *Raphus* the quadrate articulation with the mandible is situated proportionately more caudally on the cranium, compared with *Pezophaps* and volant columbids (pers. obs.; Livezey 1993).

Pterygoid

(*Pezophaps*: Newton & Clark 1879, pl.l, figs.10, 11)

Pterygoids of *Raphus* are present in OUMNH 11605, UMZC 415.H and 415.KK, the Copenhagen skull (ZMUK AVES-105485), the MNHN collections, the Port Louis skeletons and Thirioux's collection.

The apneumatic pterygoids of *Raphus* are elongate and are slightly curved "like the human clavicle" (Melville 1848, p.94). They adjoin the palatines rostrally and the quadrates caudally, each passing caudoventrolaterally from its rostral articulation to its articulation with the quadrate. The angle between the articulated pterygoids in *Raphus* (OUMNH 11605) is approximately 92°. Approximately the rostral two-thirds of the pterygoid is convex laterally and slightly concave ventromedially. The main body of the pterygoid is narrow and rounded and twists upon itself as it continues caudally from its rostral extremity. Both the rostral and caudal extremities are slightly expanded for articulation with the palatines and parasphenoid rostrum and the quadrates respectively. The rostral part of the ventrolateral surface presents the facet for the articulation of the palatine. The lateral edge of the pterygoid is thick and rounded caudally and thinner rostrally; the caudal part of the lateral face provided attachment for m. protractor pterygoidei et quadrati (see section on musculature). The medial flat edge, about halfway along the pterygoid, presents a wide, short projection which represents the remnants of the peduncle of the pterygobasipterygoid articulation which in most other columbids (one exception being *Pezophaps*) articulates with the parasphenoid basipterygoid process. Thirioux noted that there were two forms of the pterygoid of *Raphus*. There is a ventromedial projection approximately midway along the bone, slightly nearer the quadrate end (UMZC 415.KK), which is probably the remnant of the peduncle of the pterygobasipterygoid articulation. This is variably developed: in one of Thirioux's specimens, of approximately adult size, it is prominent and may well have been functional; indeed, it is more prominent than in many other columbids. In Thirioux's Port Louis skeleton "a triangular, dorsomedially oriented facies articularis basipterygoidea projects from the middle of the right pterygoid" (Claessens *et al*. 2015, p.46).[36] In other specimens studied herein, however, it is absent or only very slightly developed (this variation is discussed further in the section on variation). Dorsally the pterygoid presents a ridge with two peaks, passing from the caudolateral extremity rostromedially; it forms the lateral margin of a lanceolate area (Melville 1848). The parasphenoid articular face is triangular and slightly convex, the rostral extremity was joined to the palatine bone in front by a ligament in life. The articular face for the quadrate, located at the caudal extremity of the pterygoid, consists of a deep oval concavity. M. pterygoideus dorsalis medialis probably originated in part from the rostral part of the pterygoid (see section on musculature).

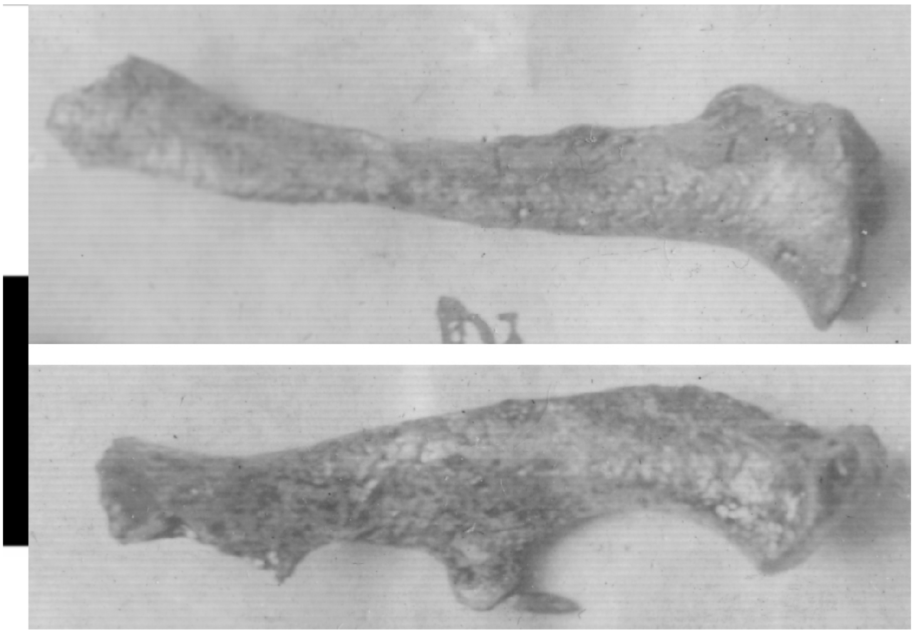

Pterygoids of *Raphus* (photograph (13A) accompanying a letter from E. Thirioux to Alfred Newton, dated 31st January 1901; scale in cm (Thirioux stated that the images were very close to natural size); © UMZC). Note the large peduncle of the pterygobasipterygoid articulation in the lower image (right pterygoid).

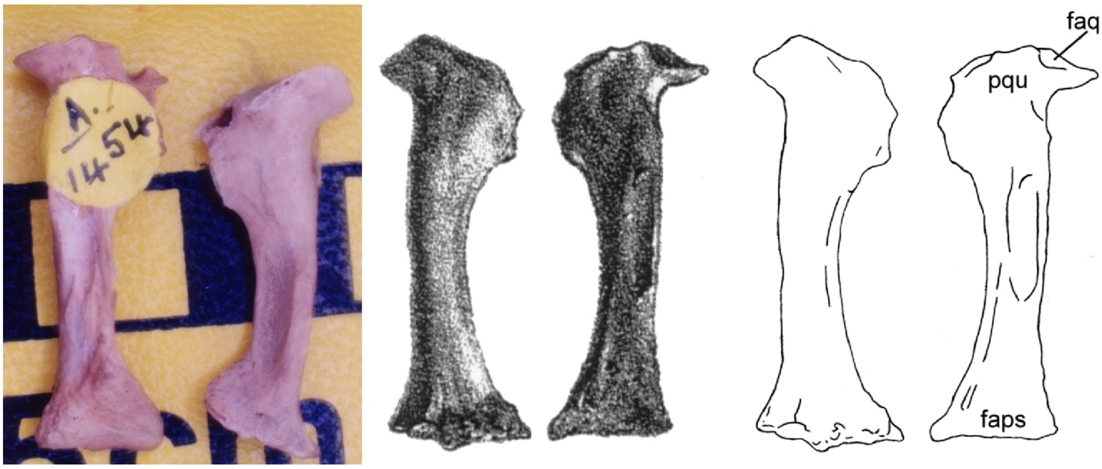

Pterygoids of *Pezophaps*. *Left*: left side (NHMUK A.1454; scale in cm; ○ Jolyon C. Parish). *Right*: right side (lithographs: Newton & Clark 1879, pl.xlv, figs.10, 11; "R. Mintern del." "Mintern Bros. lith.").

---

[36] That of the left side is missing "and likely to have been broken off" (*ibid*.).

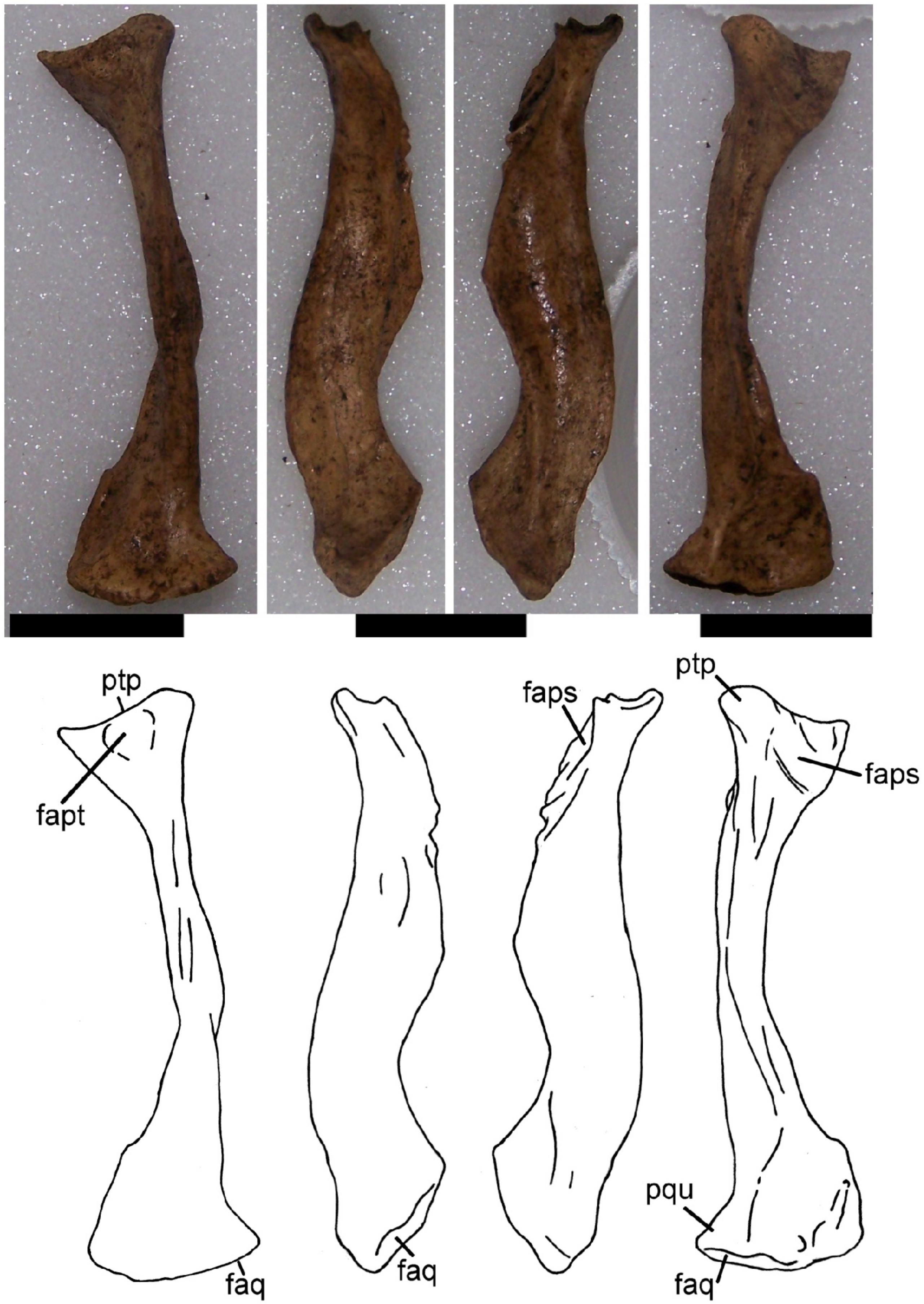

Right pterygoid of *Raphus* (UMZC 415.KK), scale in cm. ○ Jolyon C. Parish, December 2008.

In *Pezophaps* the pterygoid is short, stout and almost straight. The articulation process for the quadrate is almost at right angles to the plane of the pterygoid (Newton & Clark 1879). The parasphenoid articular surface is large, flat and triangular. The rostral extremity of this surface is sharp and joins the palatine bone in front without a distinct articular facet. According to Martin (1904), there is evidence for the hemipterygoid (the pars palatina, or 'mesopterygoid', of the pterygoid which joins the palatine) in *Pezophaps*. However, in the specimens examined in the present work, no evidence of a distinct hemipterygoid could be found. Martin stated that the reduction of the pterygoid seen in some pigeons is accompanied by a stretching of the bone, which reaches a maximum in *Raphus* and *Pezophaps*.

Palatine

(*Raphus*: Claessens & Hume 2015, fig.2)

Palatines of *Raphus* are present in OUMNH 11605, UMZC 415.H and 415.KK, the Copenhagen skull (ZMUK AVES-105485), the Port Louis skeletons and possibly also in Thirioux's collection. The palatine of *Raphus* is almost apneumatic (Melville 1848). The palatines are attached to the parasphenoid rostrum caudally, where they are separated from each other by a narrow gap. Rostrally they contact the palatal processes of the premaxillae: in OUMNH 11605 and the Copenhagen skull they fuse with these, whereas in Thirioux's Port Louis skeleton they do not (Claessens *et al*. 2015). Claessens *et al*. (2015) noted that in Thirioux's Port Louis skeleton the rostral ends of the palatines are broad and flat, but in the Durban skeleton there is a medially-placed ventrally projecting ridge.

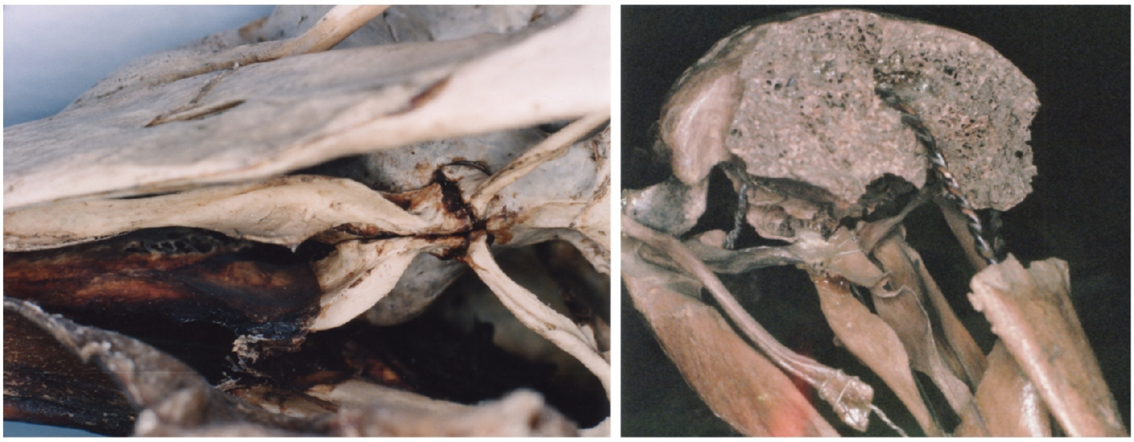

Palatines of *Raphus*. *Left*: ventral view of OUMNH 11605. *Right*: UMZC 415.H. ○ Jolyon C. Parish January 2001, December 2008.

Each palatine is approximately scimitar-shaped, excluding the parasphenoid articulation area, with the tip of the blade corresponding to the caudal extremity and the cutting edge to the lateral edge of the palatine (crista lateralis). The palatine is horizontal rostrally and almost perpendicular, inclined slightly inward, caudally (Reuss 1855). The palatines diverge slightly as they proceed rostrally and enclose the choanae[37] medially. They converge very slightly at their rostral extremities, at the rostral margin of the choanae, where they join the maxillae and premaxillae. The palatines are closer together at their caudal ends than at their rostral ends.

The rostral extremity of the palatine is flat and horizontal, where it joins the maxilla dorsally and the palatal process of the premaxilla rostrally. The lateral crest is thin and flexible (Melville 1848); proceeding caudally it thickens and becomes ventrolaterally directed; caudally its lateral edge curves dorsomedially. The thin lateral crest is broadly rounded off caudally, as it is in *Pezophaps* and other columbids.

---

[37] The choanae correspond to the inferior nasal fissure, posterior nares of Melville (1848), and probably also the naso-palatal aperture of Owen (1867).

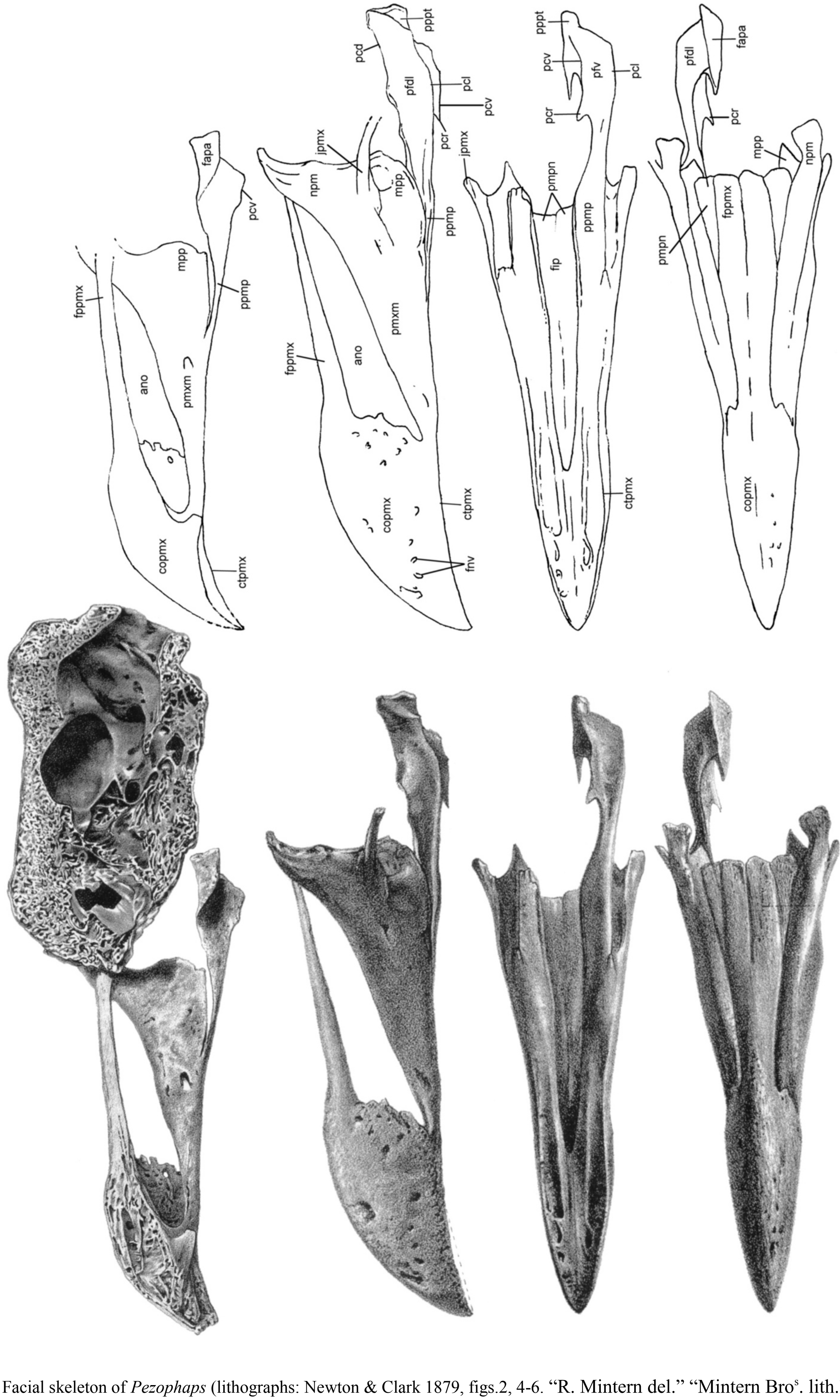

Facial skeleton of *Pezophaps* (lithographs: Newton & Clark 1879, figs.2, 4-6. “R. Mintern del.” “Mintern Bro^{s}. lith.”).

The dorsal lamella (lamella dorsalis)[38] is thin and subtriangular elongate, pointing forwards, and slightly inclined medially (Reuss 1855). It is concave towards the nasal cavity and rises from the medial edge of the lateral crest to project into the ventral part of the orbitonasal hiatus. The rostral part of the dorsal margin of the dorsolateral crest is separated from the palatal process of the maxilla by a narrow fissure. Caudal to this the dorsal margin is slightly irregular (as seen in OUMNH 11605), and provided attachment for the fibrous membrane of the antorbital sinus in life (Melville 1848). The rostral choanal process is present in *Pezophaps* as a sharp rostrally directed spur on the ventral process of the palatine, as in most extant columbids; this process is absent in *Raphus*. The development of the rostral choanal process varies in *Pezophaps*: in some specimens it is prominent (for example, Newton & Clark 1879, pl.l, figs.4, 6: *a*), whilst in others it is much reduced (for example, NHMUK A.3506).

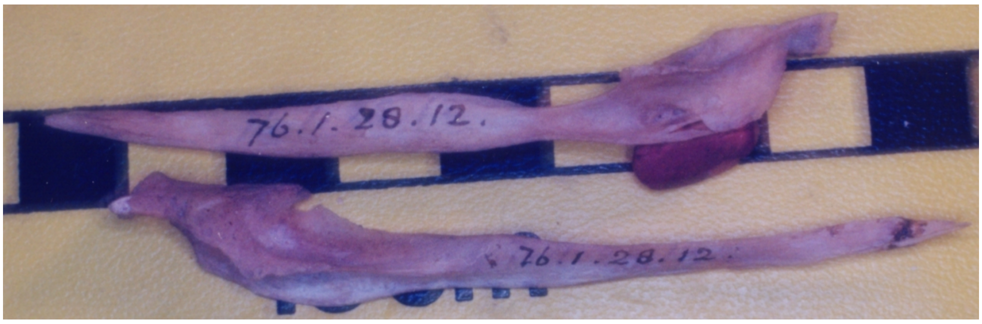

Left and right palatines of *Pezophaps* (NHMUK 76.1.28.12; male; scale in cm; ○ Jolyon C. Parish.

At the caudodorsal part of the dorsolateral face of the palatine of *Raphus* are fossae (seen in OUMNH 11605 and the Copenhagen skull ZMUK AVES-105485), similar to those seen in other columbids, which may be pneumatic or vascular. These appear to be absent in *Pezophaps*, although other foramina and fossae may be present on the dorsolateral face.

The lamella choanalis bounds the choana laterally. Its ventral crest (crista ventralis) projects ventrally and is subtriangular with a rounded truncate apex in lateral view (this is variable: in Thirioux's Port Louis skeleton it is more squared, but in the Copenhagen skull it is of a rounded triangular outline; Claessens *et al*. 2015); it is slightly curved. The caudal margin is sub-concave and extends almost to the caudal extremity of the palatine. The medial surface of the ventral crest is slightly concave rostrocaudally but sub-convex dorsoventrally. The junction of the concavity of the medial surface with that of the dorsal lamella is marked by a groove, which corresponds to the lateral crest laterally (Melville 1848). The ventral crest of the palatine in *Pezophaps* does not project as far ventrally as in *Raphus*, thus the palatines are less ventrally concave in the former compared with the latter. The fossa ventralis of the palatine, between the lateral and ventral crests, provided origin for m. pterygoideus (Melville 1848; see section on musculature). Martin (1904) remarked that the reduction of the lateral, medial and ventral crests of the palatine, seen in the 'Treroninae' and *Didunculus*, to a greater degree, is apparent in *Raphus* and *Pezophaps*, being more developed in the former than the latter.

The parasphenoid articulation surface of the palatine is subtriangular, pointing forwards. It faces dorsomedially. The palatine attaches to the ventral surface of the parasphenoid rostrum, just rostral to the pterygoid articulation. The parasphenoid articulation surfaces in *Pezophaps* are broad and slightly concave and, as in *Raphus*, do not meet medially. The articulations of the palatines and pterygoids with the parasphenoid rostrum allowed movement of these two bones during cranial kinesis.

Jugal arch

(*Raphus*: Claessens & Hume 2015, fig.2; *Pezophaps*: Newton & Clark 1879, pl.l, fig.12)

Jugal arches of *Raphus* are present in OUMNH 11605, UMZC 415.H and 415.KK, the Copenhagen skull (ZMUK AVES-105485), MNHN MAD 7115 and 7117, the Port Louis skeletons, the Summers

---

[38] The lamella dorsalis (and crista dorsalis) corresponds to the following: nasal process (Melville 1848); Nasenfortsatz (Reuss 1855); lames palatinales internes (pl.) (Verheyen 1957)?; crista palatina nasalis (Janoo 1997).

Place Auctions skeleton and Thirioux's collection. The jugal arch is composed of three fused elements: the quadratojugal, the jugal and the jugal process of the maxilla. The quadratojugal joins the quadrate by means of a convex articulatory surface directed medially which articulates with the quadratojugal cup[39] of the lateral aspect of the quadrate. A groove surrounds the articulatory surface and is for the attachment of the "capsular ligament" of Melville (1848). The lateral edge, rostral to the groove, was covered by articular cartilage in life, on which lig. zygomaticomandibulare moved. The jugal arch descends at an angle of 125° from the caudal part of the maxilla. It is slightly sigmoidal, curving slightly ventrally below the orbit. In OUMNH 11605 the rostral part of the lateral surface, between its merging with the main body of the maxilla and the part of the jugal arch directly below the lacrimal process of the frontal shows a longitudinal groove; its caudal extremity is better defined than its rostral one. The underside of the rostral part of the jugal arch presents a long fissure in OUMNH 11605, in the dorsal part of which is a large pneumatic foramen. Ventral to this foramen are several smaller ones; these are due to the pneumatization of the bone by the antorbital sinus. The jugal arch is externally curved in *Raphus*, whereas it is straight in *Pezophaps* and other columbids. However, there is evidently variation: in the Durban dodo skeleton the left jugal arch[40] is more sigmoid than that of OUMNH 11605, ZMUK AVES-105485 or Thirioux's Port Louis skeleton, a difference which Claessens *et al*. (2015) considered to likely represent individual variation.. A separate jugal (and fused quadratojugal?) of *Pezophaps* was figured by Newton & Clark (1879, pl.xlv, fig.12). It is thin and flattened and exhibits a long sutural surface for articulation with the jugal process of the maxilla, extending almost two-thirds of the length of the element. On the dorsal surface of the proximal end is a slight process (*ibid*.).

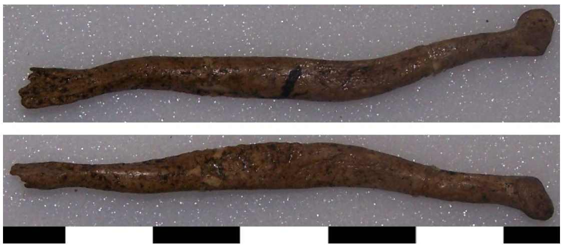

Jugal arch of *Raphus* (UMZC 415.KK; scale in cm; ○ Jolyon C. Parish, December 2008).

Maxilla

The maxilla forms the ventral part of the rostral margin of the orbitonasal hiatus; it is taller than wide. Dorsally it presents the jugal process of the jugal arch. Its dorsal extremity fuses with the premaxillary process of the nasal; rostrally the maxilla joins the palatal process of the premaxilla and ventrally the palatine. The caudomedial part of the maxilla is thin and presents a pneumatic fossa formed by the intrusion of the caudal maxillary sinus. The inner surface slopes outward and is vertically convex. In OUMNH 11605, just beneath the jugal process is a deep groove, at the caudodorsal extremity of which is a large pneumatic foramen and ventrally several smaller ones, formed by the pneumatization of the maxillopalatine process of the maxilla by the maxillary diverticulum of the antorbital sinus. The lateral surface of the base of the jugal arch and surrounding area of the maxilla of OUMNH 11605 presents numerous foramina, both large and small. The palatal surface of the maxilla is narrow and very convex transversely. The maxillaries do not meet medially but are separated by the rostral part of the interpalatine fissure. The maxillopalatine processes of the maxilla are medial to the jugal process and main body of the maxilla, the jugal process arching dorsolateral to the pneumatic fossa of the maxillopalatine process. The well-developed maxillopalatine process lies medial to the base of the jugal arch, with the main body of the lateral beam of the upper mandible arching rostrodorsal to the maxillopalatine process in lateral view. Caudally there is commonly a large, deep pneumatic fossa (OUMNH 11605; Reuss 1855), divided into numerous cells by thin struts of bone traversing it in different directions. A similar feature is also seen in *Pezophaps* (as in, for example, NHMUK A.1375, A.3506). The degree of pneumatization varies between individuals and even on opposite sides of the same skull (Newton & Clark 1879; compare NHMUK A.1375 with NHMUK 76.1.28.12 which shows less pneumatization).

---

[39] Processus jugalis of the quadrate of Martin (1904)?

[40] The right jugal arch is reconstructed (Claessens *et al*. 2015).

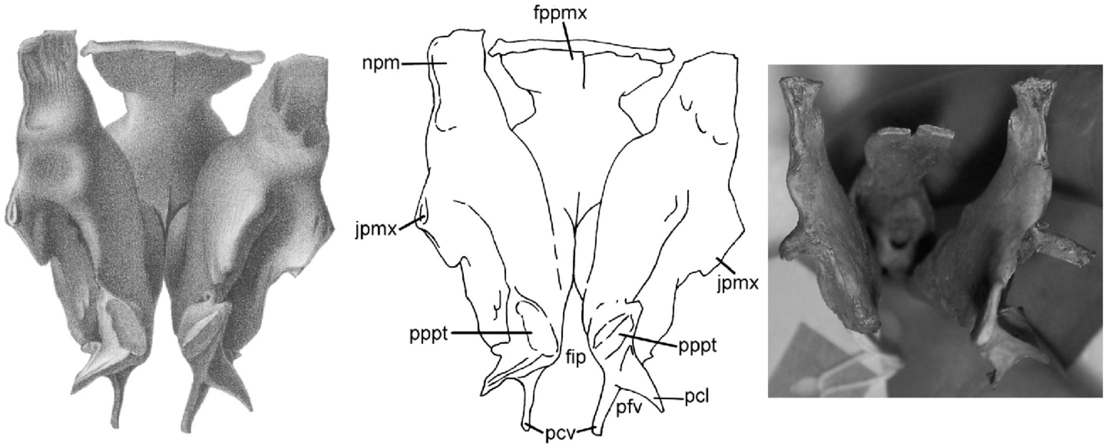

Left: facial skeleton of *Raphus*, caudal view (lithograph: Reuss 1855, taf.I, fig.4; "Lith. u. gedr. i. d. k. k. Hof-u. Staatsdruckerei."). *Right*: facial skeleton of *Pezophaps* (UMZC 649), caudal view (○ Jolyon C. Parish, December 2008).

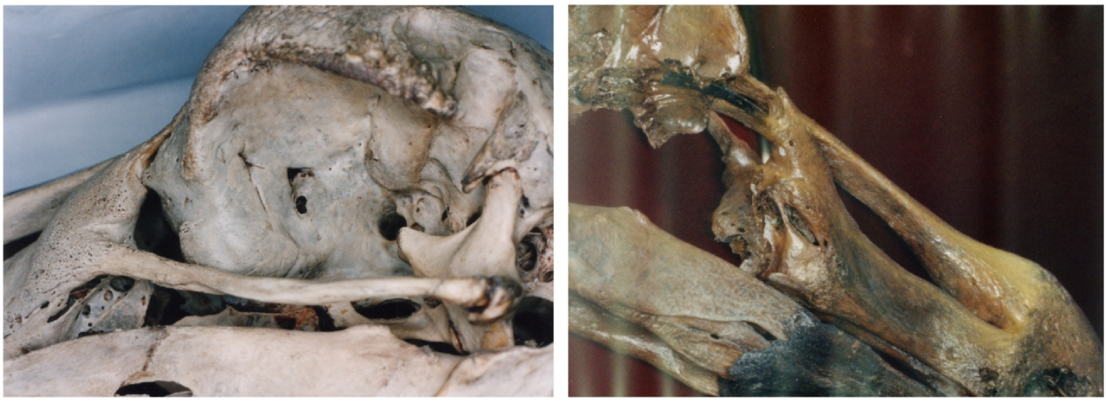

Maxilla of *Raphus*. *Left*: OUMNH 11605, left side; *right*: NHMUK A.9040, right side (○ Jolyon C. Parish).

On the lateral surface of the lateral beam of the upper mandible, rostral to the base of jugal process of the maxilla, is an elongate approximately horizontal depression containing a foramen at its caudal extremity. This foramen appears to be found consistently in specimens of *Pezophaps* (both male and female); in *Raphus* it seems to be located rostroventral to the base of the jugal arch. The skull of the mounted skeleton of *Raphus* NHMUK A.9040 shows a deep elongate depression with a foramen at its rostral exremity in this position. There may be more than one pneumatic foramen in this region and there is individual variability in number and size of foramina, with pneumaticity being least developed in the Prague beak (NMP P6V-004389). All other columbids examined also appear to possess a foramen in this location. The suture between the maxilla and the maxillary process of the nasal is distinct in some specimens of *Pezophaps* (for example NHMUK A.1373, A.3506), lying just dorsal to the base of the jugal arch. It runs from a slight process on the caudal margin of the lateral beam of the upper mandible, curving rostroventrally as it progreeses rostrally, to become sub-horizontal for most of its length before terminating at the caudoventral margin of the osseous external naris.

Vomer

The vomer appears to be absent in *Raphus* and *Pezophaps*.[41] Melville (1848) stated that it was absent in the dodo. However, Janoo (1996) pointed out that in OUMNH 11605 "the apex of the parasphenoid rostrum which normally adjoins the vomer, appears to be broken as shown in their [Strickland & Melville's (1848)] illustration [pl.ix, fig.2]" (p.70). The vomer is usually absent in columbids (pers.

---

[41] Pers. obs. Claessens *et al*. (2015) stated that the vomer in *Pezophaps* "is a rostrally directed spur" (p.43), but gave no reference or specimen number.

obs.; Parker 1866; Verheyen 1957). This region is intact in the Copenhagen skull of *Raphus* (ZMUK AVES-105485; see Parish 2013, pp.190-195) and a vomer is not present (Jon Fjeldså, pers. comm., 1st May 2006; Claessens *et al*. 2015). Meijer *et al*. (2014) also noted that an ossified vomer was absent in the Durban and Thirioux's Port Louis skeletons.[42]

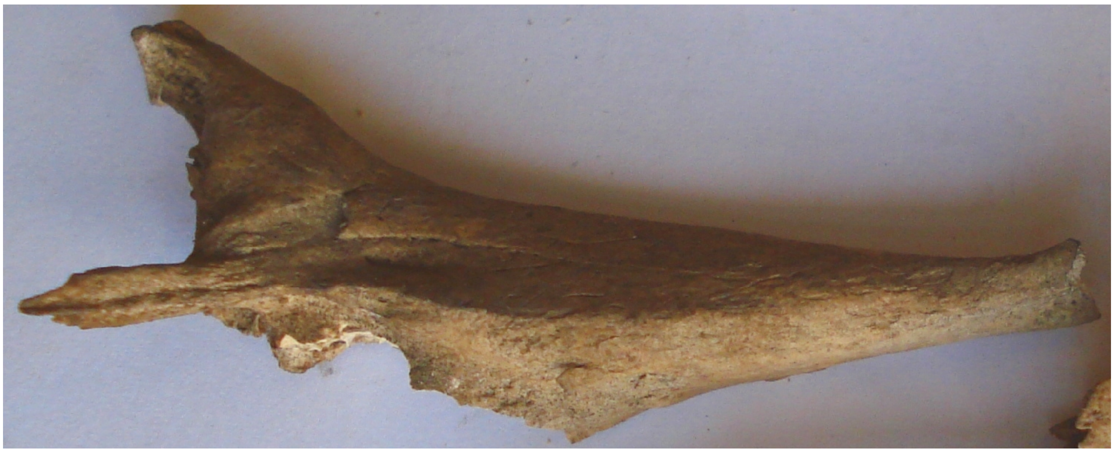

Right maxilla of *Pezophaps* (Natural History Museum, Dublin; © David Gonzalez).

In his osteology of columbids, Martin (1904) stated that the presence of a vomer was possibly individually variable and that it was possible that "its last remnants are taken up by the hemipterygoids" (p.209). He had only noted one in *Didunculus* and remarked that in this genus the vomer ossifies latest. He described it as an oblong median bone plate, triangular rostrally. In contrast, a vomer was not observed by Verheyen (1957) in *Didunculus*. Huxley (1867) stated that the vomer was "very slender" and figured it in the skull of *Columba palumbus*. Claessens *et al*. (2015) stated that a vomer was present in *Caloenas* and *Goura*.

Nasal and Premaxilla

The dorsal border of the longitudinal external osseous nasal aperture is formed by the bar (pila supranasalis) constituting the conjoined frontal processes of the premaxillae and, on either side, the premaxillary process of the nasal. The nasal fissure is bounded, on each side, ventrally and caudoventrally by the lateral bars, formed by the maxillary processes of the nasals and the maxillary processes of the premaxillae. The boundaries between the premaxillae and the nasals are indicated by faint impressions. The nasal-premaxillary suture is longitudinal and runs rostrally and rostromedially. In lateral view it can be seen to progress rostrally from the craniofacial hinge then bend, passing more rostromedially, bending again to progress to the apex of the nasal. It then passes caudomedially to meet with the corresponding suture of the opposite side. In the Copenhagen skull (ZMUK AVES-105485) these sutures are more-or-less obliterated, whereas in *Pezophaps* they are apparently invariably present. The caudal extremity of the dorsal bar joins with the cranium, the caudal end of the frontal process of the premaxilla projecting between the frontal processes of the nasals, as mentioned before. Caudally the frontal processes of the premaxillae meet without a gap between the medial margins in *Raphus*, whereas in *Pezophaps* they may be separated by a short narrow space (in, for example, NHMUK A.3505, A.3506). The craniofacial hinge area is around 1.5cm long and both the premaxillary processes of the nasals and frontal processes of the premaxillae show a striated surface, with longitudinal grooves and pits (as seen in OUMNH 11605, ZMUK AVES-105485, MNHN MAD 5971 and Thirioux's Port Louis skeleton; Claessens *et al*. 2015). In the Copenhagen skull the maxillary process of the nasal also shows a striated surface (*ibid*.).

Rostrally the dorsal bar is formed only of the frontal processes of the premaxillae, where it is subcircular in section but becomes dorsoventrally flattened as it progresses caudally, eventually becoming a flat thin plate at its caudal extremity. From its rostral end the dorsal bar decreases slightly in width and then continues with the same width up to the craniofacial hinge. The premaxillary processes of the nasals lie ventral and ventrolateral to the fused frontal processes of the premaxillae and meet medially on the ventral surface of the dorsal bar. The caudal half of the premaxillary processes of the nasals can be seen in the dorsal aspect of the skull on either side of the frontal processes of the premaxillae. They increase the width of the dorsal bar, the width of the premaxillae being fairly constant in this region.

---

[42] However, Claessens *et al*. (2015) noted that in Thirioux's Port Louis skeleton the parasphenoid rostrum "appears broken and it cannot be excluded that the rostrum parasphenoidalis may have supported a vomer" (p.42). They also added that as the cranium of the Durban skeleton has been reconstructed this sheds no light on the matter.

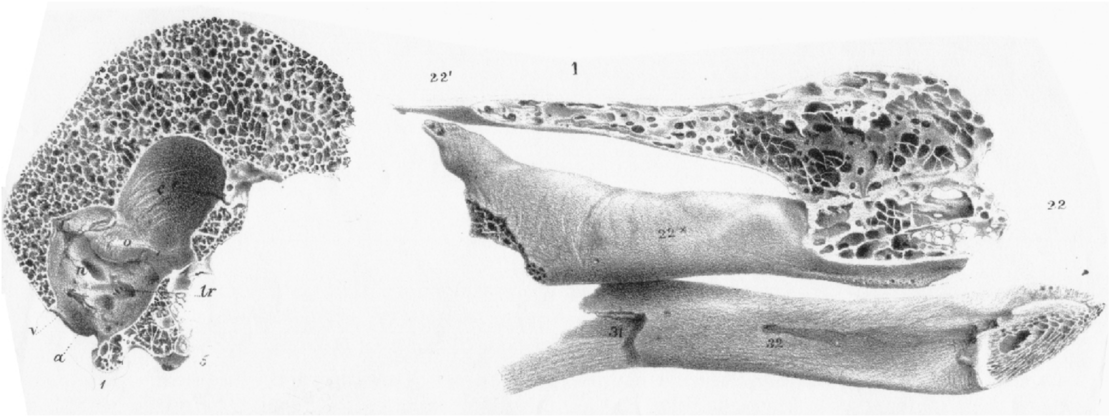

Sectioned cranium, upper beak and distal mandible (Owen 1867, pl.xxiii, fig.1. Artist: Joseph Smit; “J Smit lith” “M & N Hanhart imp”).

The premaxillary process of the nasal is elongate and triangular in lateral view. Melville (1848) stated that the premaxillary processes of the nasals “continue to meet [medially] as far backwards as the free edge of the inter-olfactory septum; but where the mesial beam [= pila supranasalis] covers that septum and the turbinated alae [of the ethmoid], they diverge to pass into the respective bodies of the nasals” (p.92). At the craniofacial hinge region the dorsal bar and proximal ends of the maxillary processes of the nasals are thinned dorsoventrally, allowing flexion during cranial kinesis.

The frontal processes of the premaxillae present, on their transversely convex ventral surface, a median longitudinal rounded ridge between the nasals. This ridge becomes less prominent caudally and shows a groove in its caudal part. Thus, the fused frontal processes of the premaxillae have an approximately triangular cross section, with the apex pointing downwards. The premaxillary processes of the nasals meet in the midline on the ventral surface of the dorsal nasal bar. The sutures between the nasals and the frontal processes of the premaxillae are very indistinct in the Prague beak (NMP P6V-004389; Reuss 1855).

The dorsal bar is narrowest, in dorsal view, in its centre (where its width constitutes only that of the premaxillae). In dorsal view a faint median impression can be seen running longitudinally, marking the suture between the fused frontal processes of the premaxillae. This median groove is better defined where the premaxillae are attached to the cranium. This longitudinal groove, seen in OUMNH 11605 and the Copenhagen skull (ZMUK AVES-105485), is absent in the Prague beak (NMP P6V-004389) and the sutures between these and the premaxillary processes of the nasals are more-or-less obliterated. The dorsal surface of the dorsal bar is flat, or very slightly convex, with rounded lateral edges.

The maxillary process of the premaxilla is fused to the maxilla and maxillary process of the nasal, the sutures being obliterated. The lateral part of the premaxilla, below the nasal aperture, divides just caudal to the main body of the bone (corpus ossis premaxillare) into the maxillary process (dorsal) and the palatine process (ventral). The lateral bar of the upper mandible (composed of the maxilla and maxillary process of the premaxilla) is subtriangular, with a truncated rostral apex that merges with the main body of the premaxilla. In dorsal view the lateral margins of the upper mandible are convex where maxillary processes of the nasals expand to meet the maxillary processes of the premaxillae. Passing rostrally the lateral margins become concave for most of their length, the upper mandible being narrowest just behind the main body of the premaxilla, and finally the lateral border becomes convex to the rostral extremity. In dorsal view the dorsal bar joins the main body of the premaxilla with the maxillary processes of the premaxillae ventrolateral to it.

In ventral view the maxillary processes of the premaxillae are narrowest and closest together where the upper mandible is narrowest. The lateral surface of the maxillary process of the premaxilla is deep vertically and slightly concave longitudinally, “a structure not known in *Didunculus* or any other Dove, and related, like most other deviations from the Columbine cranial characteristics, to the provision of unwonted strength of beak in the Dodo” (Owen 1867, p.68). The maxillary processes of the premaxillae are sub-parallel in ventral view. The interpalatine fissure rostrally, between the maxillary processes, is very narrow. It constricts at the narrowest part of the upper mandible, then slightly broadens rostral to this, providing passage for the palatine nerves and vessels in life, and finally terminates at the region where the maxillary processes join the main body of the premaxilla. The medial faces of the maxillary processes are smooth and slightly convex vertically and the dorsal and ventral borders are thickened.

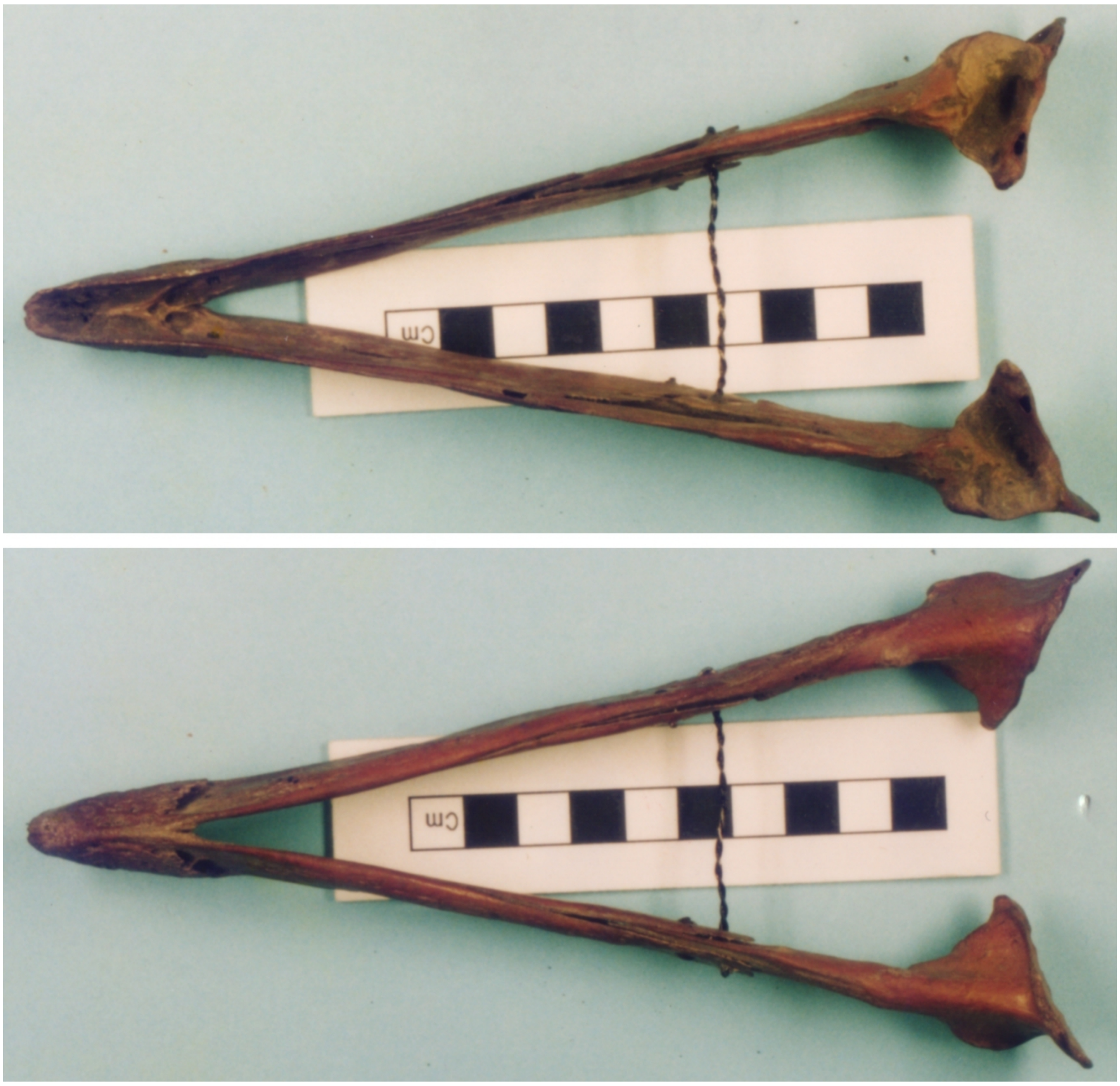

Mandible of *Raphus* in dorsal (*top*) and ventral (*bottom*) views (UMZC 415.K; © E. C. Parish).

The main body of the premaxilla, the corpus ossis premaxillare, is enlarged. The lateral surfaces are moderately convex, whilst the dorsal surface is very much so. The ventral part of the lateral surface shows several foramina in a line (in OUMNH 11605 the rostralmost is the largest), which are the ostia of a vascular canal. In the Prague beak (NMP P6V-004389) there are eight foramina on the left side and nine on the right (Reuss 1855). Several other foramina can be seen, in a series running parallel with the rostrodorsal border of the corpus ossis premaxillae. In OUMNH 11605 the caudalmost is the largest and the more rostral ones are narrow and slit-like. These are also the ostia of vascular canals, branching from the main one; between these two series of foramina are other smaller ones, this area being also "minutely grooved by the impressions of venous radicles" (Melville 1848, p.92). In Thirioux's Port Louis skeleton the neurovascular foramina on the dorsal part of the rostrum maxillare are joined and form grooves running subparallel to the longitudinal axis of the upper beak (Claessens *et al*. 2015). A similar arrangement of vascular and neurovascular foramina are also visible on the lateral surface of the corpus ossis premaxillare of *Pezophaps*. The dorsal border of the corpus ossis premaxillare of OUMNH 11605 is grooved longitudinally caudodorsally, a continuation of the medial groove of the frontal processes of the premaxillae. In both *Raphus* and *Pezophaps* the distal terminus is slightly decurved and the tip is rounded off, in the ventral aspect, but appears pointed in lateral view.

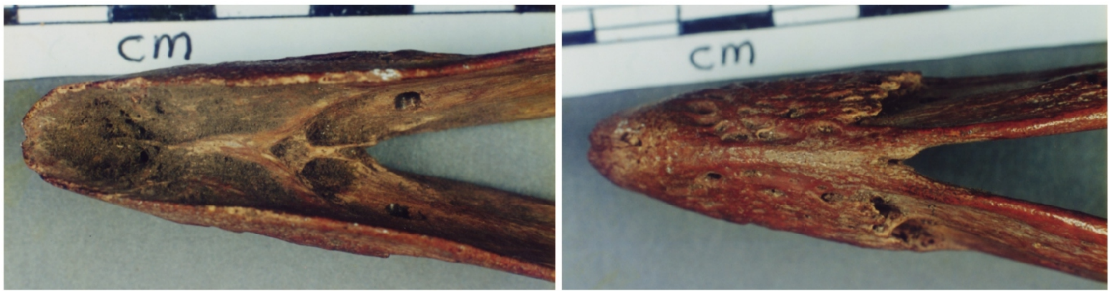

The distal end of the mandible of *Raphus* in dorsal (*left*) and ventral (*right*) views (UMZC 415.K; © E. C. Parish).

In ventral view the palatal surface is concave and bounded externally by the sharp premaxillary tomia. The lateral surfaces of the proximal end of the corpus ossis premaxillare curve laterally (lateral to the maxillary tomia), the curvature receding rostrally until the lateral surfaces can no longer be seen in ventral view. The ventrolateral surfaces of the corpus ossis premaxillare curve more ventrolaterally in OUMNH 11605 and the Copenhagen skull (ZMUK AVES-105485) than in the Prague beak (NMP P6V-004389), where they are more vertical. The palatal surface of the corpus ossis premaxillare shows a medial longitudinal ridge, separated caudally by a short space from the groove representing the distal end of the interpalatine fissure. The surface either side of the medial ridge shows numerous large neurovascular foramina, the ostia of the neurovascular canal (the caudal opening of which is at the junction between the frontal and maxillary process of the premaxilla).

The premaxillary tomium progresses caudally and ascends slightly, passing into a line leading towards the base of the jugal process of the maxilla. In lateral view the tomium, from the distal terminus to the rostral end of the palatine, shows a very slight sigmoidal profile. The ratio of the length of the corpus ossis premaxillare to that of the frontal process of the premaxilla is about half for *Raphus* and approximately two-thirds to five-sixths for *Pezophaps* (Martin 1904; pers. obs.).

The lateral surface of the maxillary process of the premaxilla of OUMNH 11605 presents 'opened-out' features, which according to Melville (1848) are indicative of the domestication of the individual; the Prague beak (NMP P6V-004389) does not show these foramina (pers. obs.; Reuss 1855).[43] The caudal margins of the corpus ossis premaxillare project laterally to the rostral ends of the maxillary processes, forming a fossa on each side, visible in posterior view but not in anterior view. Melville (1848) stated that "the upper angle [of the fossa] is also seen to curve obliquely backwards and inwards, grooving the upper border of the [lateral] stem [= lateral bar]. On tracing the groove downwards, it is seen to be continuous with a distinct broad impression, occupying the deepest part of the fossa, separated posteriorly from a narrow tract of the general excavation by a faint ridge, which curves downwards and forwards, becoming more distinct below; its concavity looks upwards and forwards, and its anterior angle corresponds to the most constricted part of the mandible" (p.91). Caudal to the caudolateral projection of the corpus ossis premaxillare, mentioned above, is a wide foramen, the caudal ostium of the vascular canal that runs to the rostal end of the beak (Reuss 1855). The rostral ostia open on the ventral part of the lateral face of the corpus ossis premaxillare (see above).

---

[43] The life history of OUMNH 11605 is unknown. There are no records of dodos being bred in captivity, which occurrence is highly unlikely.

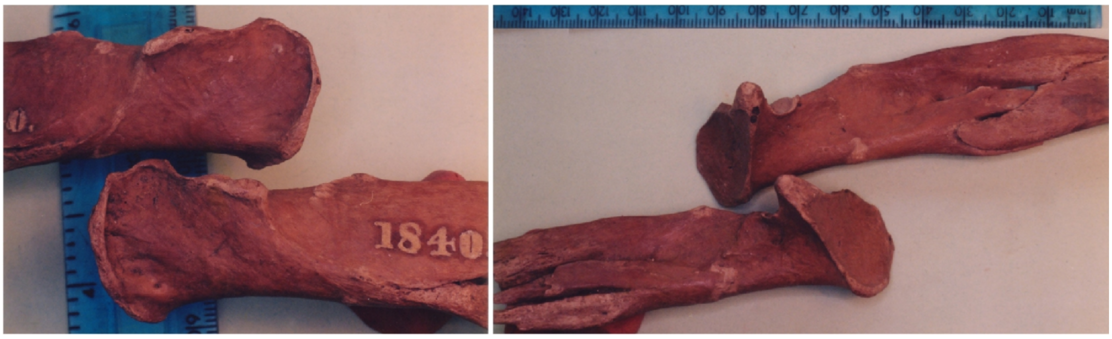

Mandibular rami of R*aphus* (NHMUK A.1840). *Left*: lateral views, *right*: medial views (○ Jolyon C. Parish).

In sagittal section the corpus ossis premaxillare displays a large pneumatic cavity within the cancellous structure of the bone, as exhibited in a specimen studied by Owen (Owen 1867, pl.xxiii, fig.1). The maxillary process of the premaxilla in sagittal section shows a cancellous interior enclosed by a thin outer lamina of bone (*ibid*.). The premaxillary diverticulum of the antorbital sinus extended into the bill (Witmer 1990), so that the interior of the corpus ossis premaxillare is formed into a large lattice of trabeculae. The dorsal bar of the beak of *Raphus* shows an open, trabecular internal structure, in contrast to that of *Pezophaps*, which is much more solid (Newton & Clark 1879, pl.l, fig.2).

The beak of *Raphus* shows a certain degree of individual variation. Thirioux suggested that there were two forms of skull, albeit from very limited material: one with a beak that is narrower at its base, and the other being broader, but of the same length and shape. He also reported an anomaly in one of his specimens, where both upper 'apophyses' of the beak were fused behind. This, with the labelling of his accompanying sketch (Transcriptions: Thirioux-Newton Correspondence, fig.5), is taken to indicate that the premaxillary processes of the nasals were fused to the frontal processes of the premaxillae.

The corpus ossis premaxillare of *Pezophaps*, being less enlarged, resembles those of extant columbids, especially *Treron*, more than it does that of *Raphus*. The frontal and maxillary processes of the premaxillae of *Pezophaps* do not meet with an acute angle at the rostral extremity of the external nasal aperture as they do in *Raphus*, due to the intervention of the laminar caudal margin of the corpus ossis premaxillare. Thus, the nasal aperture in *Pezophaps* is subtriangular (as it is in *Treron*), whereas in *Raphus* it is lanceolate.

Mandible

(*Raphus*: Strickland & Melville 1848, pl.ix*, figs.2-4; Janoo 1996, fig.5g. *Pezophaps*: Newton & Newton 1869, pl.xxii, figs.159-162; Ottow 1950, pl.i, figs.1, 2; Claessens & Hume 2015, fig.2; Claessens *et al*. 2015, figs.13, 14)

The rami of the lower jaw diverge from each other at an angle of approximately 22° in *Raphus* (UMZC 415.K, NHMUK A.729). In *Pezophaps* this angle is approximately 23° (NHMUK A.3505) to 15° (NHMUK A.3506).[44] The symphysis[45] rises at an angle of around 45° with the ventral border. It is longer than wide and presents a median ridge from which diverge two caudolaterally directed ridges.

---

[44] However, the artificial articulation of these specimens might have increased or decreased this angle; Claessens *et al*. (2015) gave it as approximately 25° for *Raphus*. In dorsal view, the rami of Thirioux's Port Louis skeleton bend slightly inwards caudal to the coronoid process, whereas in OUMNH 11605 and the Copenhagen skull they are straight (Claessens *et al*. 2015). A similar condition is seen in *Pezophaps*. This may be, at least in part, *post-mortem* (pers. obs. of modern avian mandibles).

[45] Claessens *et al*. (2015) erroneously stated that symphysis "is formed by the symphysis of the anterior parts of the dentary and the splenial" (p.47) – it is formed of the dentary only.

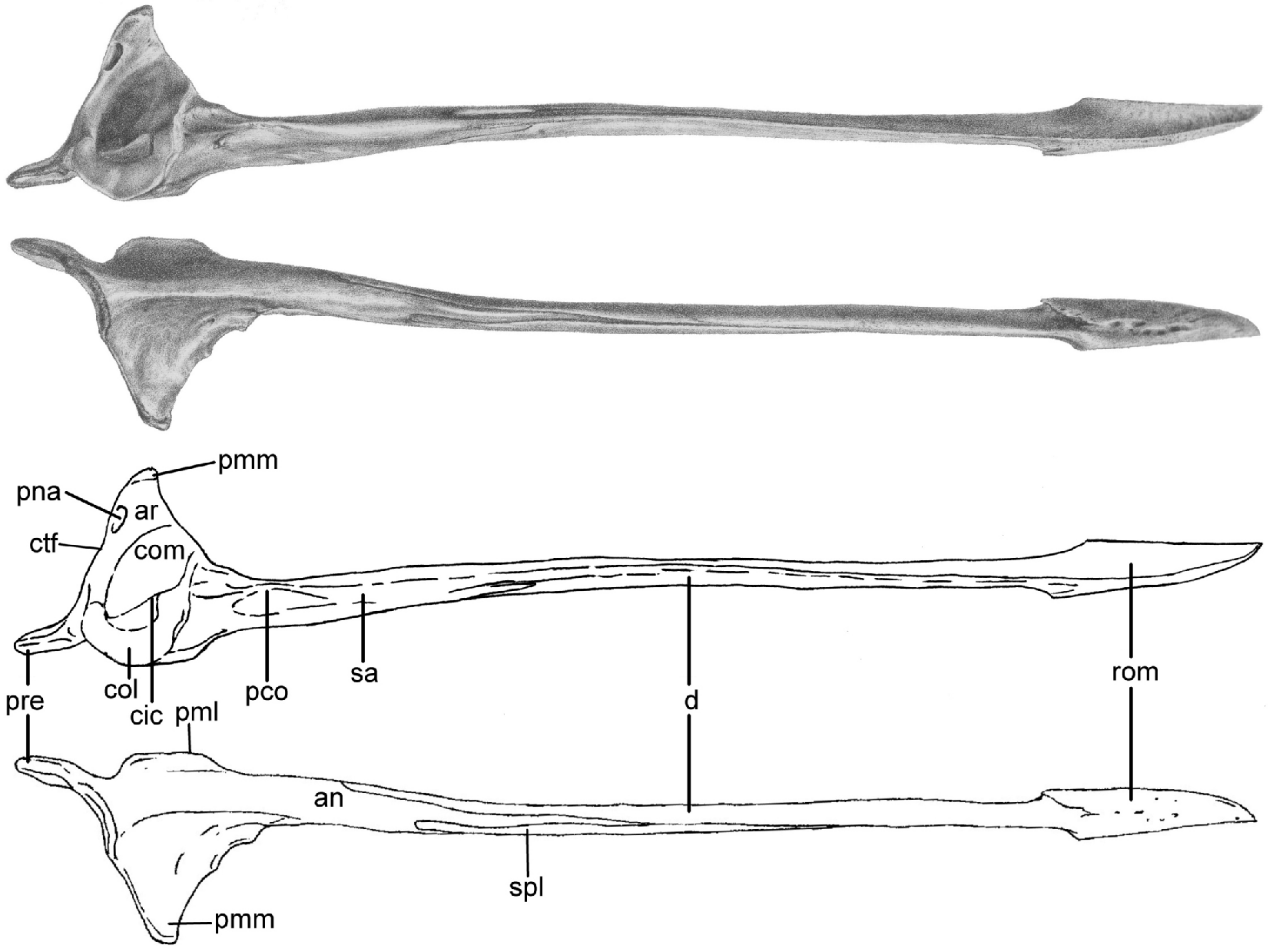

Mandible of *Raphus*, dorsal and ventral views (lithograph: Strickland & Melville 1848, pl.ix*, figs.2, 3. Artist: Joseph Dinkel; "Reeve, Benham & Reeve, Lithographers.").

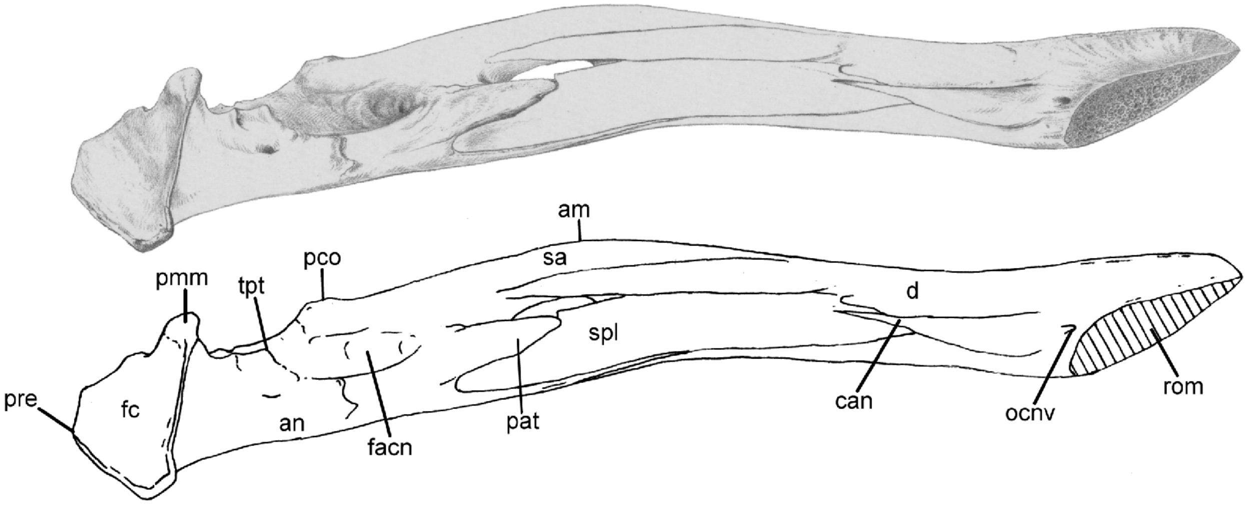

Mandible of *Raphus*, medial view (lithograph: Strickland & Melville 1848, pl.ix*, fig.4, "partly in outline, as it could not be viewed directly by the artist" (*ibid*., p.136). Artist: Joseph Dinkel; "Reeve, Benham & Reeve, Lithographers.").

The caudal margin of the symphysis, when seen in dorsal view, shows a depression on each side of the median ridge, between it and the caudolaterally directed ridge. These depressions are open caudally and may have provided attachment for m. genioglossus. The symphysis is concave dorsally and sub-angularly rounded ventrally. The caudal margin of the lateral surface of the symphysis projects slightly laterally and shows an irregular edge. The lateral surfaces of the symphyseal region present several large neurovascular foramina which open from a pair of horizontal neurovascular canals whose caudal ostia lie at the caudomedial border of the symphysis, close to its ventral edge. Melville (1848) described these neurovascular foramina in OUMNH 11605: “externally, a series of five large apertures open upwards from it; three or four downwards, and one on the rough concave symphyseal surface” (p.96). The symphyseal region is well developed in *Pezophaps*, although the distal end of the mandible is not as expanded as in *Raphus*. The dorsal surface of the symphysis in *Pezophaps* shows a median longitudinal channel (the canal symphysaire of Janoo 1997), which narrows rostrally.

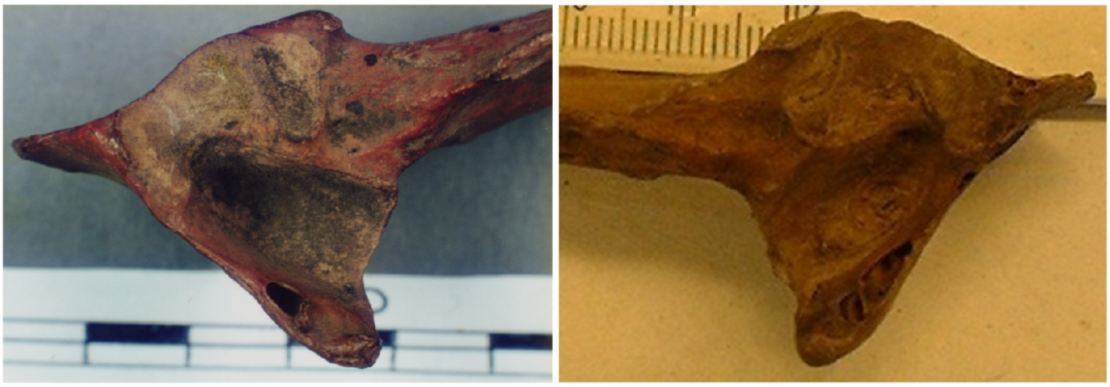

The proximal end of the mandible of *Raphus* in dorsal view. *Left*: UMZC 415.K, left ramus (scale in cm; © E. C. Parish), *right*: AMNH 3852, right ramus (scale in cm and mm; ○ Jolyon C. Parish, January 2002).

In a specimen studied by Owen (1867) the sagittal section of the symphysis showed a small vacuity within a cancellous structure that was denser than that of the upper mandible (pl.xxiii, fig.1). He stated that the walls were thicker and more compact than those of the upper mandible, especially dorsally and caudally.

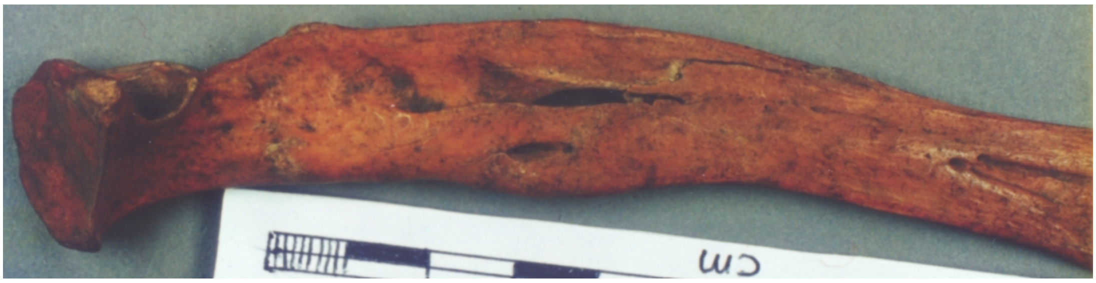

Medial view of the left mandibular ramus of *Raphus* (UMZC 415.K; © E. C. Parish).

The mandibular ramus is widest vertically at approximately halfway along its length, and at the caudal extremity. The dorsal margin of the mandible is slightly sigmoidal, concave rostrally and convex caudally. The ventral margin of the mandible is mostly slightly concave with a very slight convexity caudoventral to the mandibular fenestra. The dentary is the largest bone in the mandible and forms its rostral part. At its caudal end the dentary splits into a dorsal and a ventral portion (processus dorsalis and processus ventralis respectively), the mandibular fenestra being at the bifurcation point; the dorsal part is shorter than the ventral part. The ventral part passes caudally along the lateral surface of the angular. Both parts are approximately triangular in lateral view. The dorsal part of the dentary joins the rostrodorsal part of the supra-angular. The thick ventral margin of the angular thins rostrally and passes forwards between the dentary and the splenial as far as the centre of the ventral edge of the mandibular ramus (Melville 1848). The width of the mandibular ramus, in ventral view, decreases from the proximally to distally (excluding the symphysis).

The angle of the mandible (angulus mandibulae), located dorsal to the rostral end of the mandibular fenestra in both *Raphus* and *Pezophaps*, is around 161° in the former and around 167-168° in the latter. In *Pezophaps* the angular and supra-angular portions of the ventral margin of the mandible slope rostroventrally to the dentary from the caudal end, and then rise again as steeply, forming an angle on the ventral margin below the mandibular fenestra. This angle is not well developed in *Raphus*. The ventral border of the dentary, in lateral view, is concave from this angle to the caudal end of the symphysis.

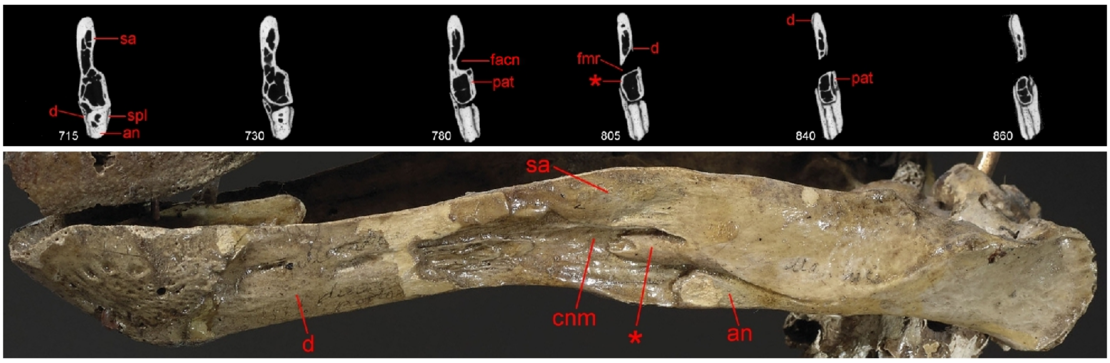

Top: transverse CT slices through the left mandibular ramus of OUMNH 11605 (CT data relating to Warnett *et al*. 2020; MorphoSource Media: M55320). *Bottom*: mandible of Paul Carié's dodo skeleton (Christie's London, Sale 17492, lot 155; © Christie's 2019). * = rostrally-directed spur of the supra-angular ventral to the mandibular fenestra.

The mandibular fenestra is elongate rostrocaudally. In lateral view its rostral extremity, which indicates the caudal opening of the mandibular canal,[46] is at the point of bifurcation of the dentary into its dorsal and ventral parts. The supra-angular evidently forms both dorsal and ventral margins of the mandibular fenestra. The ventral extension can be seen in the left ramus of Paul Carié's dodo skeleton.[47] In OUMNH 11605 a slight ridge can be seen running caudoventrally from the caudal end of the fenestra. It may be of note that this ventral extension of the supra-angular is in the same area (around the angulus mandibulae) as the evidently calcified tissue of the lower jaw (see below). In lateral aspect the mandibular fenestra of OUMNH 11605 shows two structures at the ventral part of its medial side, one rostral to the other: the caudal one is presumed to be the prearticular and the rostral one the splenial (cf. Strickland & Melville 1848, pl.ix*, fig.4). In *Pezophaps* (see, for example, NHMUK A.3505, A.3506; RCSHM/Aves 706, 707; UMZC 635; NMING specimen) the supra-angular extends as a rostrally pointing spur a little way along the ventral margin of the mandibular fenestra, overlying the prearticular laterally.

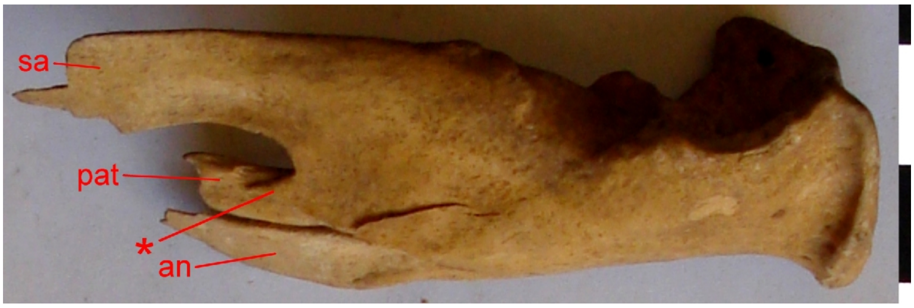

Caudal end of the left ramus of the mandible of *Pezophaps* (Natural History Museum, Dublin). * = spur of the supra-angular ventral to the mandibular fenestra (scale in cm; © David Gonzalez).

---

[46] The "foramen du nerf mandibulaire" of Janoo (1997, fig.9, fnm).

[47] https://www.christies.com/img/LotImages/2019/CKS/2019_CKS_17492_0155_004%28a_dodo_skeleton_mauritius_before_1690%29.jpg

The mediolaterally compressed lamina of the prearticular separates from the supra-angular at around the level of the caudal end of the medial branch of the dorsal fork of the dentary. It narrows at it progresses rostrally and its rostral termination is around midway along the mandibular fenestra. It covers the rostral projection of the supra-angular medially. Remnants of this lamina can be seen in NHMUK A.1840 (both rami). The fissure between the prearticular and the angular is visible in the medial aspect of the mandibular ramus in some specimens (NHMUK A.1840, UMZC 415.K) due to the curvature of the dorsal margin of the caudal end of the splenial.

The thin sheet of the splenial is seen in the medial aspect of the mandibular ramus and is irregularly elongate rostrocaudally. It is longer ventrally than dorsally. Its rostral extremity is pointed and its rostral margin is irregular with forward-pointing splints. Its caudal extremity is more rounded and passes over the medial surface of the angular, ventral to the rostral projection of the prearticular. The dorsal margin of the splenial meets the dorsal part of the dentary. The splenial partly covers the medial surfaces of the dentary and prearticular and covers the mandibular canal laterally, which contained the mandibular ramus of the trigeminal nerve (V_3) and other vessels in life. The mandibular fenestra lies above its caudodorsal border. Melville (1848) stated that the splenial in OUMNH 11605 "begins to coalesce with the dentary, along the anterior part of its lower edge" (pp.95-96), and that the splenial "remains distinct, perhaps, to a late period of life" (*ibid*., p.95), unlike in extant columbids. In some specimens the dorsal margin of the splenial is marked by a series of fairly evenly-spaced foramina set in a shallow horizontal groove (as in UMZC 415.K).

The CT data of OUMNH 11605 (Warnett *et al*. 2020) shows that a short distance rostral to the caudal extremity of the splenial the angular separates from the prearticular, the junction between the two becoming a narrow gap. The splenial and dentary remain distinct from the other caudal mandibular elements, with essentially no sign of fusion to them.

In OUMNH 11605 a large sub-horizontal vascular canal passes rostrally from the mandibular canal on the medial face of the mandible to open on the lateral surface, closer to the dorsal margin than to the ventral one (Melville 1848). It opens into the caudal part of a groove that passes horizontally towards the symphysis. The lateral face of the rostral end of the mandible of OUMNH 11605 exhibits a horizontal groove approximately midway between the dorsal and ventral margins, pierced by two foramina, one rostral and one caudal. The rostral opening of the mandibular canal lies above the rostral extremity of the splenial and in OUMNH 11605 is sub-divided by a small process of the latter (*ibid*.). Rostrally it widens, progressing towards the mandibular symphysis.

The suture between the angular and the prearticular is covered by the dentary laterally and (in part) by the splenial medially. The angular forms the ventral margin of the caudal part of the mandible; it widens caudally to meet the articular caudomedially; rostrally it tapers, passing along the ventromedial edge of the mandible. The rostral part of the angular is wedged between the dentary (lateral) and the splenial (medial). The supra-angular forms the dorsal margin of the caudal part of the mandible. Its caudal end joins the angular and its rostral end is wedged between the lateral and medial parts of the dorsal fork of the dentary. The angular and articular are large in *Pezophaps*, as in *Raphus*, but the retroarticular process and medial mandibular process are not as well developed; in this respect it approaches the condition in the majority of other columbids. The angle between the caudal margin of the mandible and the long axis of the caudal part of the mandibular ramus, as seen in dorsal view, is around 60° in *Raphus*, but 65-70° in *Pezophaps*.

The caudal part of the mandible is expanded. The retroarticular process in lateral view shows a convex and thickened caudal margin, which passes ventrally into the smooth rostrodorsomedially directed crest marking the margin between the fossa caudalis and the rostral face of the medial mandibular process. The medial mandbular process is sub-pyramidal, its apex pointing medially. Its caudal surface forms part of the fossa caudalis and its dorsal surface presents, near its caudal border, a pneumatic foramen (foramen pneumaticum articulare), for the articular diverticulum of the middle ear sac (Witmer 1990). *Pezophaps* also possesses such a foramen, as do all other columbiforms. The caudal and rostral surfaces of the medial mandibular process slope medially. M. pterygoideus would have inserted on the ventromedial surface of the mandible. The insertion site of m. pterygoideus is defined rostrally by a ridge that passes from the tuberculum pseudotemporale,[48] rostroventromedially towards a groove running along the ventral part of the angular; this ridge defines the caudoventral margin of the mandibular fossa (see section on musculature).

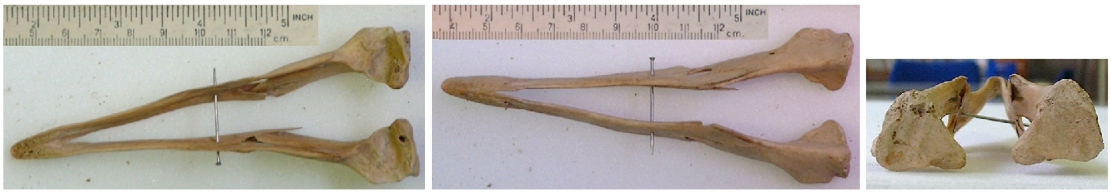

Mandible of *Pezophaps* (NHMUK A.3506). *Left*: dorsal view, *middle*: ventral view, *right*: caudal view ○ Jolyon C. Parish).

The crista transversa fossae is craniocaudally narrow; its medial part, along the caudal border of the medial mandibular process, provided attachment for lig. occipitomandibulare (see section on musculature). The fossa caudalis is triangular, with its rough obtuse medial apex being that of the medial mandibular process and its lateral apex being that of the retroarticular process. The sub-concave fossa provided insertion for m. d. m. medialis (Van Gennip 1986). The caudal aspect of the mandible of *Raphus* is subtriangular, with the form of an isosceles triangle: the longer sides being the dorsal and ventromedial margins and the lateral margin being convex, with the ventral apex truncated. In *Pezophaps* the posterior aspect of the mandible has the form more of an equilateral triangle, its width only slightly greater than its height. The posterior surface is near vertical and is less concave than that of *Raphus*, which forms an acute angle with the horizontal plane.

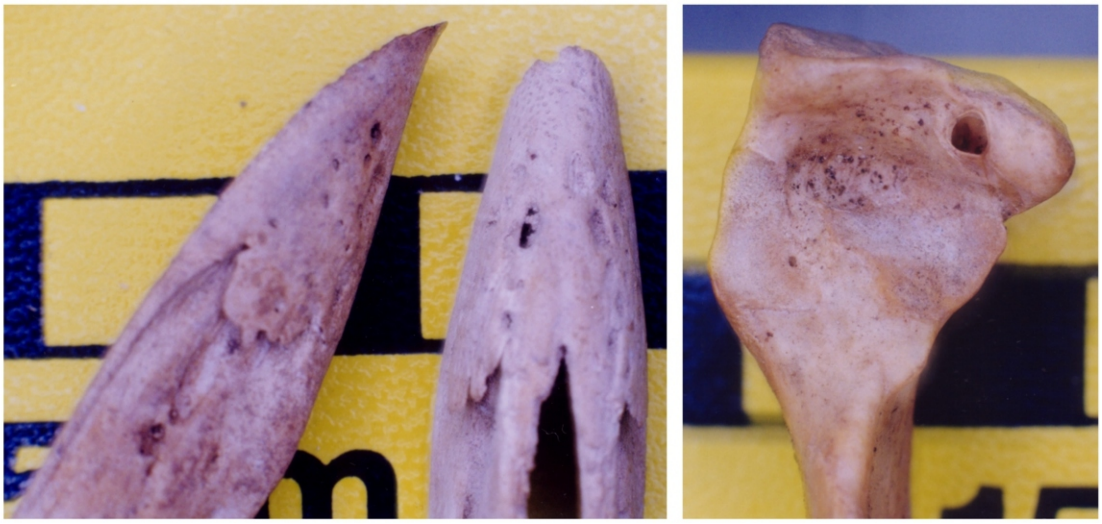

Mandible of *Pezophaps*. *Left*: distal end in lateral and ventral views (NHMUK 76.1.28.12 and A.1375), *right*: proximal end of right ramus in dorsal view (NHMUK A.1373). Scale in cm (○ Jolyon C. Parish).

The coronoid process is short and low, much longer than it is high; it provided insertion for the strong aponeurosis of m. a. m. e. superficialis. It is generally more developed in *Raphus* than in *Pezophaps*. The dorsal margin of the supra-angular, rostral to the coronoid process is smooth and rounded.

The articular surface is lateromedially sub-oval. The lateral cotyle for articulation with the quadrate is approximately rostrocaudally aligned, slightly concave and reniform in outline, its lateral margin is convex and projects laterally over the lateral face of the mandible. The medial cotyle is deeply concave, subcircular, and is directed rostromedially, becoming wider and shallower rostromedially. The rostral depressed edge descends and the caudal edge rises medially into a rough projection. In OUMNH 11605 the medial half of its floor and rostral surface is covered by synovial cartilage, as is the lateral cotylar surface. The walls of the articular surface are thicker absolutely and more so proportionately in *Pezophaps* compared with *Raphus* (Newton & Newton 1869, p.348).

---

[48] *Contra* Claessens *et al*. (2015), the tuberculum pseudotemporale is present (*e.g.*, in OUMNH 11605, ZMUK AVES-105485, NHMUK A.1840).

A ridge[49] runs from the lateral extremity of the cotyle rostroventrally down the lateral surface of the mandible to the caudal extremity of the ventral part of the dentary. Caudal to this ridge the mandible is concave, and slightly roughened, and may have provided muscular attachment, perhaps for the lateral extension of m. pterygoideus ventralis. Rostral to this ridge is another, running caudally from the caudal end of the mandibular fenestra; it may mark the ventral boundary of the supra-angular. M. pseudotemporalis profundus inserted rostrodorsal to the insertion of m. pterygoideus (see section on musculature).

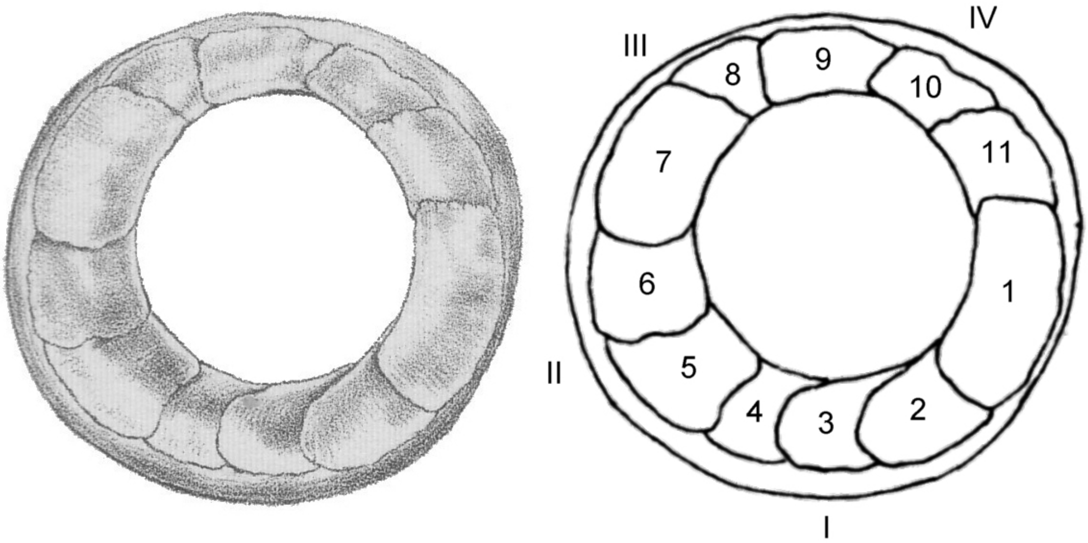

Sclerotic ring of *Raphus* "with the sclerotic coat of the eye-ball"(Strickland & Melville 1848, p.136. Lithograph: Strickland & Melville 1848, pl.ix*, fig.5. Artist: Joseph Dinkel; "Reeve, Benham & Reeve, Lithographers.")

Martin (1904) stated that the mandibular elements fuse late in ontogeny in pigeons and are only coossified imperfectly in *Raphus* and *Pezophaps*. Mandibular sutures are distinct in OUMNH 11605, the Copenhagen skull, Thirioux's Port Louis skeleton and Mare aux Songes specimens (pers. obs.; Claessens *et al*. 2015) and the rostral and caudal parts of the mandible do not fuse (or at least only weakly) in *Raphus* and *Pezophaps*. Martin noted that mandibular elements are 'always' found separate in *Raphus* (which is incorrect, although the rostral and caudal parts of the mandibular rami are commonly found separately),[50] but that fusion appeared to have progressed further in *Pezophaps*.

Sclerotic plates

(Strickland & Melville 1848, pl.ix*, fig.5; Lambrecht 1933, fig.23; Claessens *et al*. 2015, fig.15)

The sclerotic ring (Anulus [Annulus] ossicularis sclerae) of *Raphus*, as preserved in OUMNH 11605 and the Copenhagen skull (ZMUK AVES-105485; Claessens *et al*. 2015, fig.15), consists of eleven plates. No other dodo specimens with sclerotic plates are known. Some of these plates slightly overlap; the arrangement of plates is the same as in other columbiforms (Claessens *et al*. 2015; Curtis & Miller 1938, table 1) and is of Lemmrich's (1931) typus A. The plates vary in size, the two largest being the lateral plates (lateral ossiculae) on either side of the ring. Slater (1879, p.295) mentioned that "plates of sclerotic" had been found with other solitaire bones in a cave on 6th November 1874. However, these have not been located in the NHMUK collections (pers. obs.).[51]

---

[49] Masseteric ridge of Owen (1848a).

[50] Claessens *et al*. (2015) likewise stated that rostral and caudal portions of mandibular rami from Mare aux Songes have only been found separately. However, there are rare complete mandibles from the locality (*e.g.*, a specimen in the UMZC 415.K collection).

Columella

Both columellae appear to be intact in the Copenhagen *Raphus* skull (ZMUK AVES-105485; Jon Fjeldså, pers. comm., 1st May 2006). In OUMNH 11605 the columella is missing from the left ear and also apparently from the right (pers. obs. from CT data).

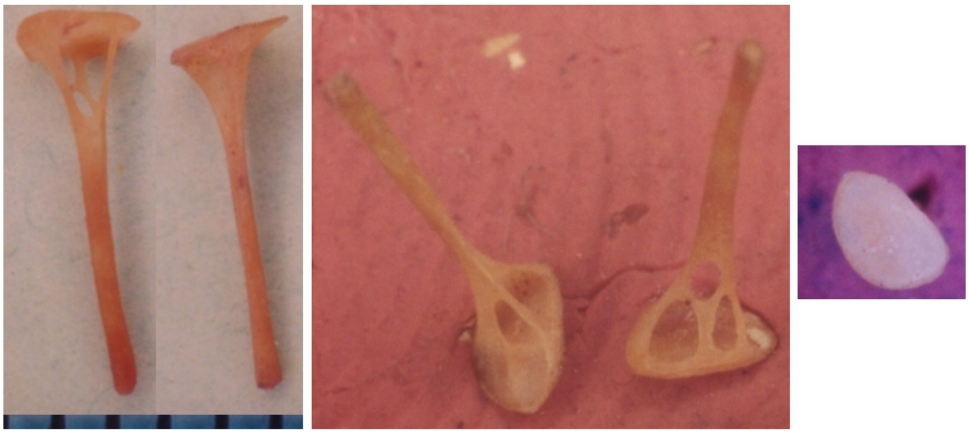

Columellae of *Pezophaps* (NHMUK A.1440). Scale in mm (○ Jolyon C. Parish).

The columella of *Pezophaps* is known only in NHMUK A.1440. The scapus is long, thin and tubular; in life it provided attachment for the extracolumella cartilage. The proximal end, or footplate (clipeolus; columellar base), which adjoined the fenestra vestibularis, is sub-oval in end-on view. The scapus widens proximally, becoming cone-shaped as it joins the flat footplate. The proximal end of the scapus shows several large foramina or fenestrae.[52]

Apparatus hyobranchialis

The ceratobranchial (os ceratobranchiale) and epibranchial I (os epibranchiale I) are known for Pezophaps (NHMUK A.3505, A.3506; RCSHM/Aves 706, RCSHM/Aves 707). The ceratobranchial is long and almost straight and the epibranchial is shorter and more slightly curved, but of approximately the same calibre.

A possible rostral basibranchial (os basibranchiale rostrale)[53] and two possible paraglossals (ossa paraglossae)[54] are known for *Raphus* from the Thirioux Collection (see Transcriptions: Thirioux-Newton correspondence. In a letter to Alfred Newton, dated 5th September 1900, Thirioux mentioned that he had found the complete 'tongue' in good condition.[55] Accompanying a letter dated 29th November 1900 Thirioux sent Newton a sketch of "a small bone found with the carpometacarpus/manus [*metacarpiens*] of the Dodo", which he related to the hyoid, and in another dated 13th November 1901, he listed "1 os hyoïd" in his collection[56] – this appears to be a rostral basibranchial. It shows an impression on the lateral surface, presumably for muscle attachment and is very similar to that of other columbids (for example *Streptopelia*: pers. obs.). The elements that may be paraglossals are separate elements; they were not fused in the midline as in other taxa.

---

[51] Sclerotic bones were also mentioned in a list of previously unknown bones given in a MS. by Slater (Abstract from H. H. Slater's Reports on Rodriguez – Collection. 9pp. In: Royal Society Transit of Venus Expeditions Correspondence and papers relating to distribution of collections and preparation of reports 1875-1876, NHMUK Archives, DF 202/9).

[52] These fenestrae are absent in the columellae of other columbids examined: *Caloenas nicobarica* (NHMUK S/1985.26.2), *Goura cristata* (NHMUK S/1966.52.61), *Columba palumbus* and *Streptopelia decaocto* (both in the author's collection).

[53] Shown in a photograph (13A, no. '4') in the Thirioux-Newton Correspondence accompanying a letter dated 31st January 1901.

[54] Although the paraglossals appear to be from *Raphus*, Gadow remarked that they "cannot well belong to the hyoid apparatus if [the specimen referred to the rostral basibranchiale] is the corpus" (see Transcriptions: Thirioux-Newton Correspondence). They were shown in a photograph (13A, nos. '9' and '10') in the Thirioux-Newton Correspondence accompanying a letter dated 31st January 1901. They look different to, and are larger than, the alar phalanx 1 of digit III seen in the same photograph (no. '7').

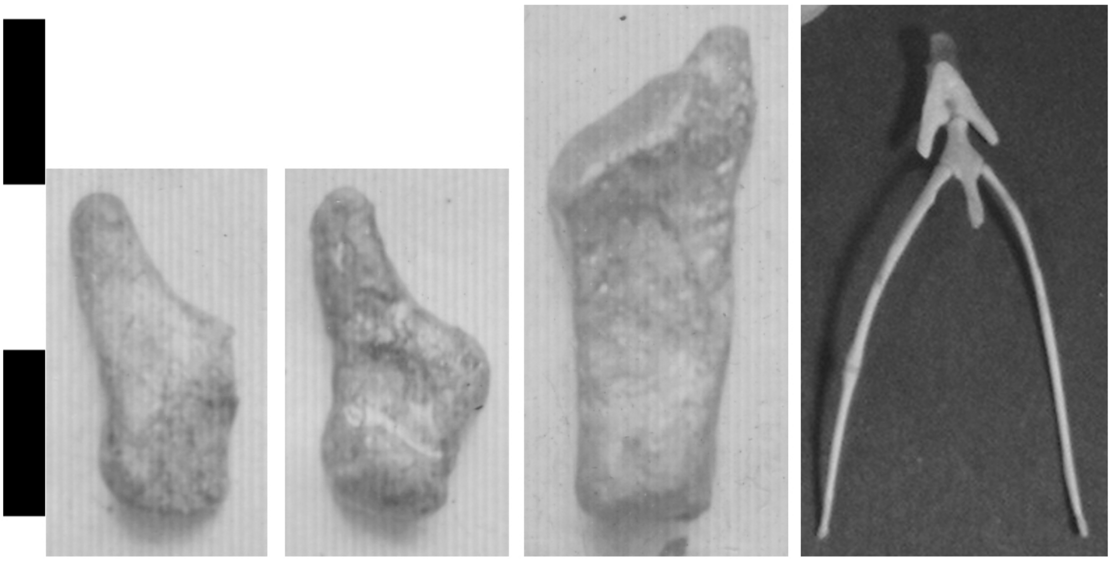

Left: two possible paraglossals and a rostral basibranchial of *Raphus* (photograph (13A) accompanying a letter from E. Thirioux to Alfred Newton, dated 31st January 1901; scale bar: 0.5cm units; © UMZC). *Right*: apparatus hyobranchialis of *Goura victoria* (USNM 489410; ○ Jolyon C. Parish).

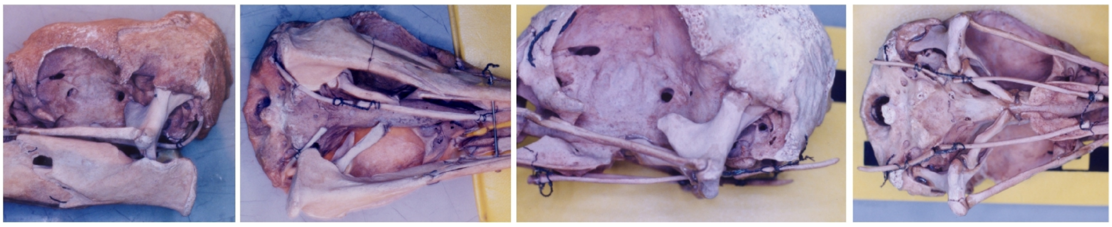

Apparatus hyobranchialis of *Pezophaps*. Left two images: NHMUK A.3505, lateral and ventral views; right two images: NHMUK A.3505, lateral and ventral views (○ Jolyon C. Parish).

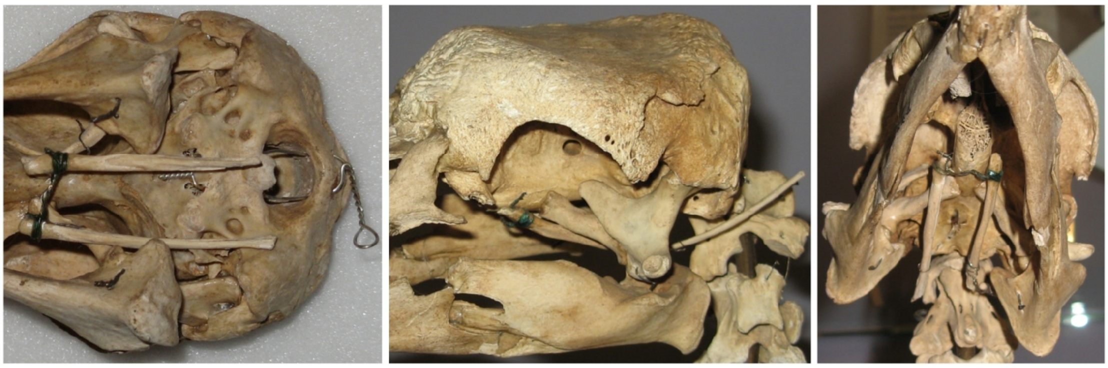

Apparatus hyobranchialis of *Pezophaps*. *Left*: female (RCSHM/Aves 707); *middle* and *right*: male (RCSHM/Aves 706; Simon Chaplin, pers. comm., 20th March 2008; © The Hunterian Museum at the Royal College of Surgeons).

---

[55] "j'ai trouvé la langue complète et en bon etat. Je l'ai mise dans l'alcool faut il vous l'envoyer [I found the tongue complete and in good condition. I put it in alcohol [and] must send it to you]"

[56] No dodo hyoid remains have been found in the collections of the Mauritius Institute or Durban Natural Science Museum (Claessens et al. 2015), or in the UMZC (*ibid.*; pers. obs.).

Cranial Kinesis

(*Raphus*: Zusi 1984, fig.12c)

Raphus and *Pezophaps*, like all other pigeons, were schizognathous (the palatal processes of the maxillae do not meet in the midline) and schizorhinal (the external osseous nasal aperture extends caudally to the craniofacial hinge). Both the dodo and the solitaire appear to have had prokinetic skulls.[57] Zusi (1984) suggested that the dodo might have evolved from a rhynchokinetic ancestor, due to the fact that the osseous nasal aperture terminates at the craniofacial hinge, adding that "the craniofacial hinge is still slightly separated into two axes" (p.30). The craniofacial flexion zone (zona elastica craniofacialis) allowed vertical movement of the facial skeleton with respect to the cranium during cranial kinesis. During prokinesis, bending the facial skeleton downwards, the jugal arch (the "outer beam" of Owen 1878) moved backward at its caudal end, flexing downward at its rostral end. The caudal ends of the palatines moved backward, sliding on the parasphenoid rostrum. The rostral ends allowed flexion at the palatine flexion zone (zona elastica palatina). The pterygoids also moved backward, sliding on the parasphenoid rostrum, and the quadrate rotated – the orbital process moving downwards and the mandibular end backwards. The reverse to the above-described actions occurred when the facial skeleton moved upward with respect to the cranium.

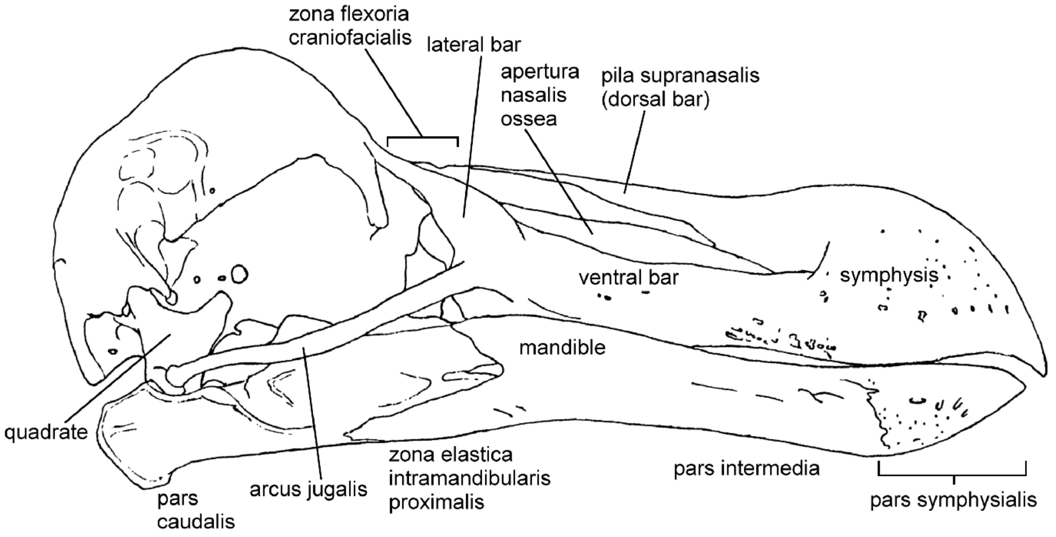

The skull of *Raphus* (traced from Strickland & Melville 1848, pl.viii).

Melville (1848) stated that the pterygoids and palatines glided on "flattened oblong surfaces [...] in the movements of the upper mandible" (p.79). Melville also observed that the projection of the lacrimal (his prefrontal) beyond the level of the anterior margin of the cranium is "separated by a notch, from the inner angle of the prefrontal [= lacrimal] above, and below from its inferior extremity; which is slightly flattened and roughened opposite the zygoma [= jugal arch], with which it would probably come into contact, in the great downward flexion of the upper mandible" (*ibid.*, p.81). In *Raphus* the lacrimal extends ventrally medial to the jugal bar, although there was still space for the arch to move in life. In *Pezophaps* the lacrimal does not extend ventrally medial to the bar, with a small gap existing between the bar and the ventral extremity of the lacrimal.

Bock (1960) stated that the medial brace (an articulation between the medial process of the mandible and the lateral process of the parasphenoid) appeared to be present in *Raphus* (from examination of published figures of the skull). He added that "the mb [medial brace] would be with the mpm. [medial process of the mandible] articulating with the well-developed lbp. [lateral basitemporal process = os parasphenoidale: processus lateralis]" (p.48).[58] Claessens *et al.* (2015) also noted that in OUMNH 11605 the medial process of the mandible "appears to abut the lateral aspect of the lateral basitemporal process" (p.46). Bock (*op. cit.*) also noted that the medial brace is absent in Columbidae, as are the lateral processes of the parasphenoid and the lateral basilar tubercles (his medial basitemporal processes). The lateral process of the parasphenoid of OUMNH 11605 shows remnants of a soft tissue attachment, which may be the remains of the medial brace ligament. This was apparently well developed in *Raphus* and both the lateral process of the parasphenoid and the medial process of the mandible were well developed. The presence of a well-developed medial brace in *Raphus*, and possibly also in *Pezophaps*, would have prevented disarticulation of the mandible when breaking up or swallowing large fruits and seeds.

---

[57] Claessens *et al.* (2015) stated that the dodo had a rhynchokinetic skull. However, the only zone of flexion in the upper beak is at the craniofacial hinge (see Zusi 1984, fig.12c).

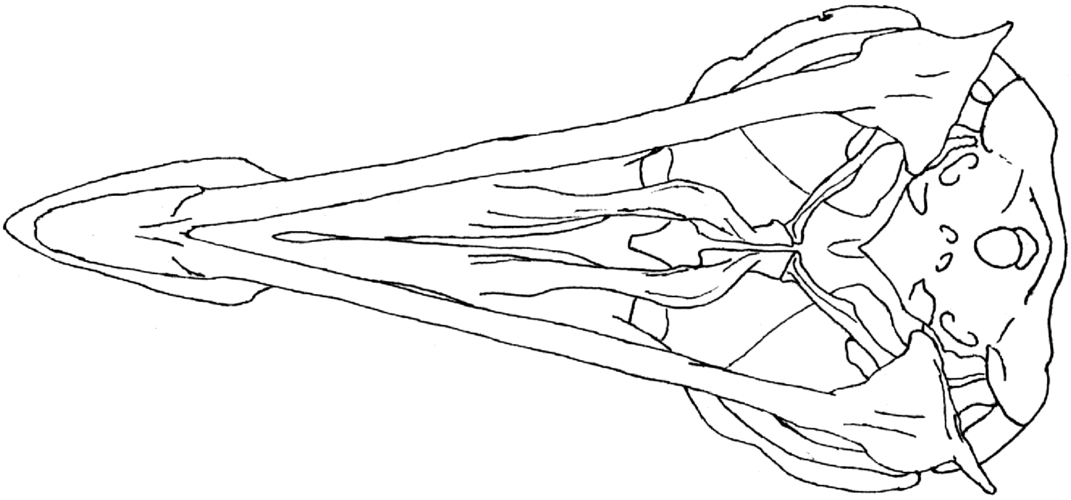

The skull and mandible of *Raphus* in articulation (based on Strickland & Melville 1848, pls.ix, fig.2; pl.ix*, fig.3; with additional data from a UMZC 415.K specimen).

In *Pezophaps* small basipterygoid processes of the parasphenoid are variably developed (see above), but when present they do not articulate with the pterygoids.[59] Nevertheless, they may perhaps have provided attachment for a ligament connected to the pterygoid (cf. Simonetta 1960). Likewise, the peduncle of the pterygobasipterygoid articulation of the pterygoid seen in a specimen in the Thirioux Collection might have either connected with the parasphenoid basipterygoid process or provided ligamental attachment. The medial brace would appear to have been fairly well developed in *Pezophaps*.

The loss of basipterygoid processes would have allowed a greater degree of movement during cranial kinesis (Fisher 1955). The medial brace of the mandible would have prevented disarticulation. Intramandibular flexion (aided by the large m. pterygoideus) may have been present in *Raphus*, with bending occuring in the zona elastica intramandibularis proximalis. It was perhaps more developed in *Pezophaps* due to the presumed greater flexibility of the intramandibular region. The width of the mandible was slightly greater than that of the upper beak just rostral to the craniofacial hinge, as also seen in the frugivorous pigeons *Ducula*, *Ptilinopus*, *Treron*, *Didunculus*, *Caloenas* and others

---

[58] Baumel & Witmer (1993) stated that the medial and lateral basitemporal processes of Bock (1960) were synonymous with their processus medialis parasphenoidalis and processus lateralis parasphenoidalis. However, this is not the case, as shown by Bock's figures. Furthermore, Bock added that medial to his medial basitemporal processes were sometimes found a pair of smaller tubercles (herein the medial basilar tubercles), thus showing that his medial basitemporal processes are the lateral basilar tubercles and not the lateral processes of the parasphenoid.

[59] In *Goura cristata* the development of the basipterygoid processes is also variable, the basipterygoid articulation varying from being functional to being absent (Verheyen 1957). *Goura* feeds on fallen fruits and seeds and occasionally invertebrates.

(Verheyen 1957; pers. obs.). These factors might have aided in the ingestion of larger food objects. As noted by Claessens *et al*. (2015), a kinetic upper jaw aids in the feeding on larger food items.[60]

As the m. a. m. musculature was probably not developed to the extent that tough seeds could be cracked, such food items were probably swallowed whole and processed in the gizzard. The elongate beaks of *Raphus* and *Pezophaps*, in contrast to the proportionately shorter ones of columbids such as *Treron* and *Didunculus*, were not well adapted to providing a strong bite force, further suggesting that tough seeds and fruits were swallowed whole. The mention by L'Estrange (see Parish 2013, p.40) of a bird swallowing many pebbles is supportive of this. Furthermore, the internal structure of the osseous upper beak of *Raphus* is composed of light trabecular bone, the distribution and arrangement of which is probably not particularly adapted to cope with large stresses (unlike that of *Didunculus*: Martin 1904, fig.R). The solitaire, at least, had a relatively robust hyoid apparatus (at least as regards the known elements), suggesting a muscular tongue.

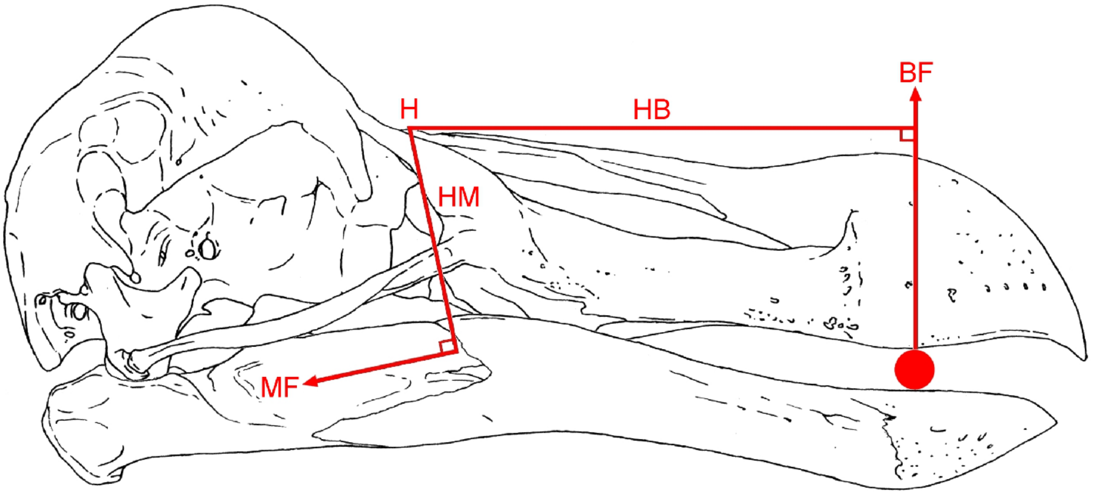

The skull of *Raphus* showing elements mentioned in the text (based on Witmer & Rose 1991, fig.4). Note: the red spot represents a food item. BF = bite force, H = craniofacial hinge (axis of rotation for upper jaw), HB = moment arm of bite force in upper jaw, HM = moment arm of pterygoideus muscle force, MF = muscle force of pterygoideus musculature.

The curved jugal arch of *Raphus*, which was presumably shaped to accommodate the adductor muscles, differs from the straight elements seen in other columbids.

The paraglossals attributed to *Raphus* are not fused in the midline, as in *Ducula* (Bhattacharyya 1990) or *Goura* (USNM 489410), which may have had implications for the use of the tongue in the processing of food.

Biomechanical Analysis and Feeding

Regarding the skulls of *Raphus* and *Pezophaps* as prokinetic, a simple biomechanical model can be applied to examine the forces involved in biting. The model used is that given by Witmer & Rose (1991, after Bock 1966). It is stated that "when a bird [...] adducts its upper jaw as in biting, there are two major forces involved: an adductor muscle force (MF) and the bite force (BF)" (Witmer & Rose 1991, p.99). The adductor muscle force is supplied by m. pterygoideus. This muscle complex acts to retract the palatine bridge, which in turn depresses the upper jaw, which rotates about the craniofacial hinge (H). Following this model, the equation given for the biting force is BF = (MF) (HM) / (HB). Witmer & Rose stated that the bite force can be increased by 1) increasing the pterygoideus muscle force, 2) increasing the moment arm of the pterygoideus (HM), or, 3) decreasing the moment arm (HB) at which the bite force is applied. The moment arm of the bite force can be decreased by moving the bite to a more caudal position. In *Raphus* and *Pezophaps* the rhamphothecae are restricted to the rostral part of the beak, therefore limiting the moment arm of bite force. However, the dodo is known to have had an area of dense tissue (presumed to be calcified) in the region of the angulus mandibulae (see below). This may have enabled strong bite forces to be habitually applied closer to the jaw joint by significantly reducing HB.

---

[60] Claessens *et al*. (2015) stated that "the skull was highly kinetic and adapted to withstand high force loads" (p.79). This is not the case: the only zone of flexion of the upper mandible was at the craniofacial hinge (there were no flexion zones of the dorsal nasal bar distally as in rhynchokinetic skulls) and the skull was probably not as suited to withstand high force loads as those of *Didunculus* and parrots.

Having used high-resolution CT scanning and Finite Element Analysis (FEA) to investigate the mandible of the dodo, Bright *et al*. (2017) stated that "dodos experience lower and more evenly distributed mandibular feeding stresses than Nicobar pigeons [*Caloneas nicobarica*], especially during unilateral biting. While this indicates that dodos were capable of forceful bites along the entire length of the jaw, stresses are particularly low when biting at the back of the jaw where lever mechanics dictate that bite forces will be highest. This suggests that dodos were well adapted for crushing, asymmetrical bites" (p.86).

Vertebral Column

The number and arrangement of vertebrae in the skeletons of *Raphus* and *Pezophaps* can be determined from examination of associated skeletons composed of elements from single individuals. For *Raphus* the only skeleton that can be said to be mainly composed of bones from one individual is that of Thirioux's Port Louis skeleton.[61] For *Pezophaps* there are a few such skeletons (*e.g.*, NHMUK A.3505 and A.3506) that are assumed to be composed of bones from single individuals.

The number of vertebrae found in the vertebral columns of *Raphus* and *Pezophaps* are given in the table below:

	Cervical	Cervicodorsal	Thoracic	Synsacral	Caudal
Raphus cucullatus	14	1	4	14-18	6
Pezophaps solitaria	13	2	3	17-18[62]	5-6

Note: the pygostyle is not included in the count of caudal vertebrae.

Cervical vertebrae are those having fused ribs (*i.e.*, having complete transverse foramina, the atlas and axis[63] excepted), cervicodorsal vertebrae are those having articulations for attached ribs which are not connected to the sternum (*i.e.*, the vertebral rib has no sternal rib attaching to it) and thoracic vertebrae are those which have articulations for attached ribs which are connected to the sternum, either directly or indirectly (*i.e.*, the vertebral rib has a sternal rib attaching to it).

The vertebral column of *Raphus* (as seen in Thirioux's Port Louis skeleton and the Durban skeleton[64]) consists of nineteen presynsacral vertebrae. These are divided into fourteen cervical, one cervicodorsal and four thoracic vertebrae. The first three thoracic vertebrae are fused to form a notarium.[65] In

---

[61] Claessens *et al*. (2015) stated that the presynsacral vertebral series of Thirioux's Port Louis skeleton "appears to derive from a single bird, without additions, removals, or substitutions" (p.79).

[62] Slater ("Abstract from H. H. Slater's Report, on Rodriguez-Collection", Royal Society Transit of Venus Expeditions. Correspondence and papers relating to distribution of collections and preparation of reports 1875-1876, DF 202/9, NHMUK General Library) remarked: "I agree with [Alfred Newton] as to the eighteen coalesced sacral vertebræ, though I believe one specimen in my collection has nineteen."

[63] The atlas and axis constitute the vertebrae cervicales speciales, whilst the remainder of the cervical vertebrae constitute the vertebrae cervicales communis.

[64] Note: the vertebral count given by Chubb (1919a) for the Durban skeleton differs from that given by Claessens *et al*. (2015). This is due to the fact that in 1919 the skeleton was remounted and the tenth vertebra was removed (Claessens & Hume 2015).

[65] In the outgroups to Columbiformes: sandgrouse (Pteroclididae) have nineteen or twenty presynsacral vertebrae (thirteen or fourteen cervical, one or two cervicodorsal and four or five thoracic vertebrae, with four vertebrae forming the notarium) (Verheyen 1957); Mesites (Mesitornithidae) have 22 presynsacral vertebrae (fifteen

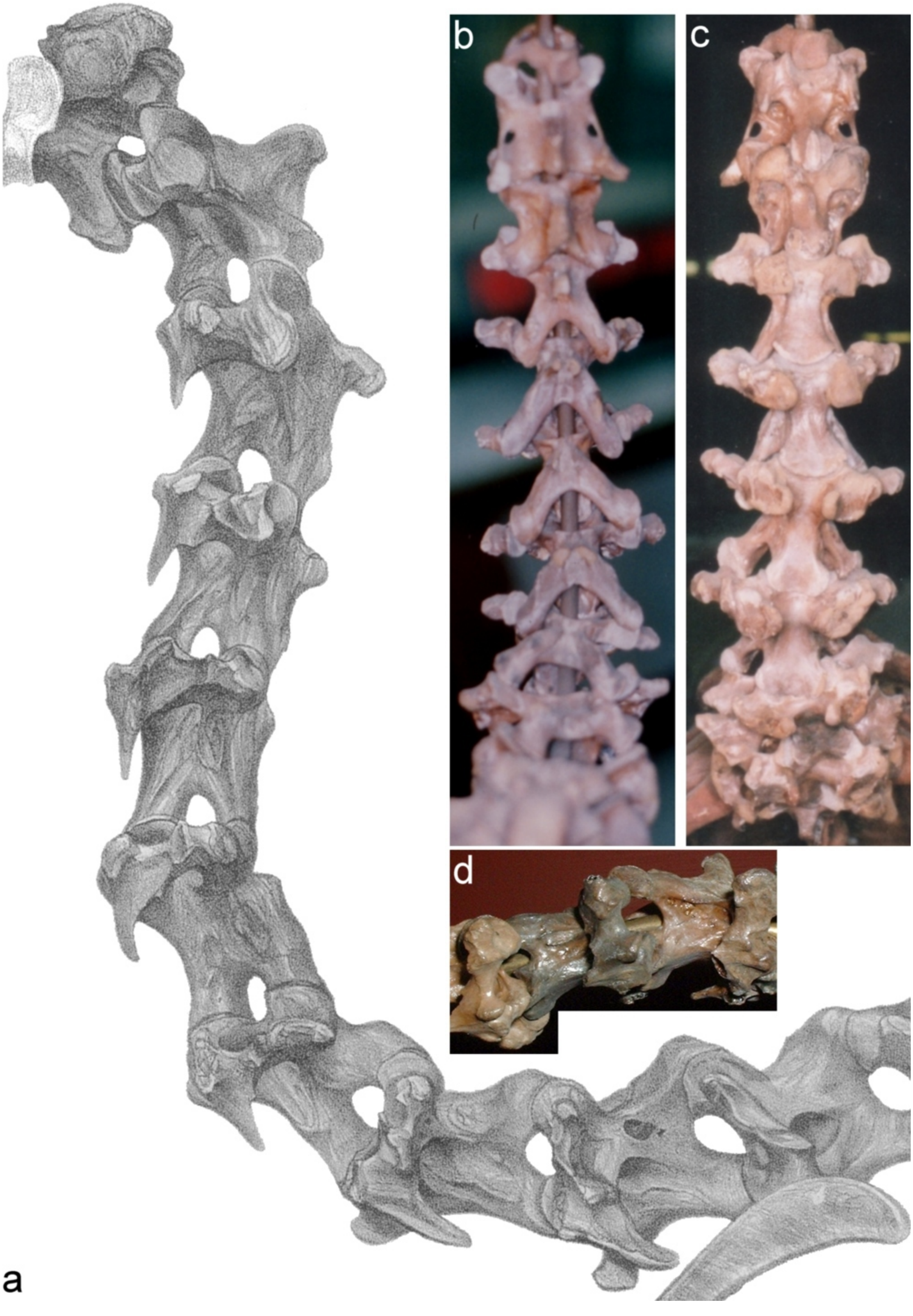

Cervical vertebrae of *Raphus*. a: lateral view, after Owen (1867, pl.xv, fig.1; artist: James Erxleben; “From nat on Stone by J.Erxleben.” “M. & N. Hanhart. imp.”); note: the atlas was unknown at the time and has been lightened here. b and c: dorsal and ventral views (NHMUK A.729; ○ Jolyon C. Parish). d: lateral views of C4 and C5 (NHMUK A.9040; ○ Jolyon C. Parish).

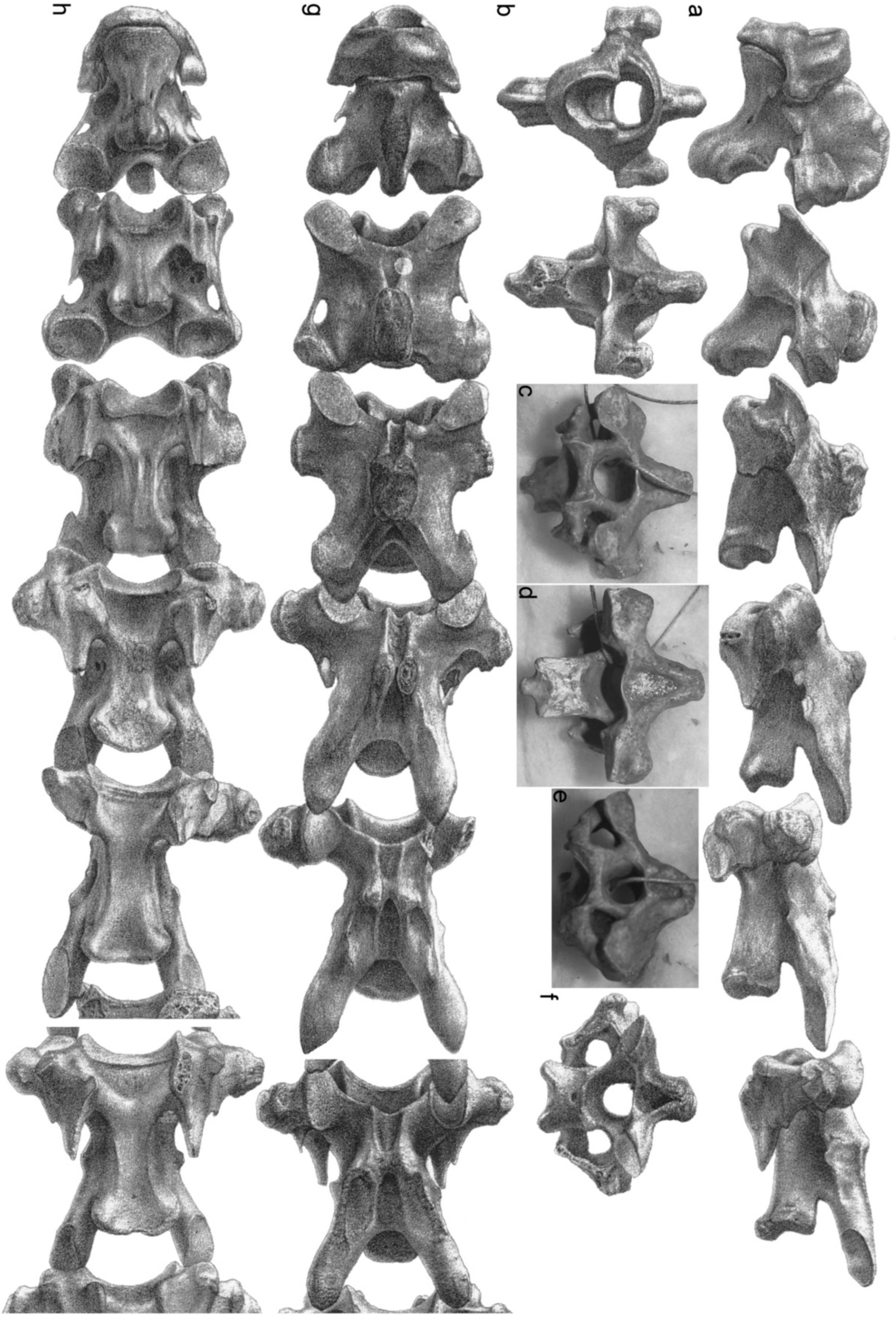

Cervical vertebrae of *Pezophaps*. a: C1-C7, lateral views (Newton & Newton 1869, pl.xv, figs.1, 6, 9, 13, 17, 24); b: atlas and axis, cranial and caudal views (Newton & Newton 1869, pl.xv, figs.2, 3); c: C3, cranial view (UMZC specimen); d: C3, caudal view (UMZC specimen); e: C4, cranial view (UMZC specimen); f: C4, caudal view (Newton & Newton 1869, pl.xv, fig.10); g: C1-C7, dorsal views (Newton & Newton 1869, pl.xv, figs.4, 7, 11, 15, 19, 25); h: C1-C7, ventral views (Newton & Newton 1869, pl.xv, figs.5, 8, 12, 16, 20, 26). Newton & Newton (1869, pl.xv): artist: George Henry Ford; “G. H. Ford ad nat. lith.” “W. West imp.”) Photographs of UMZC specimens: ○ Jolyon C. Parish, December 2008.

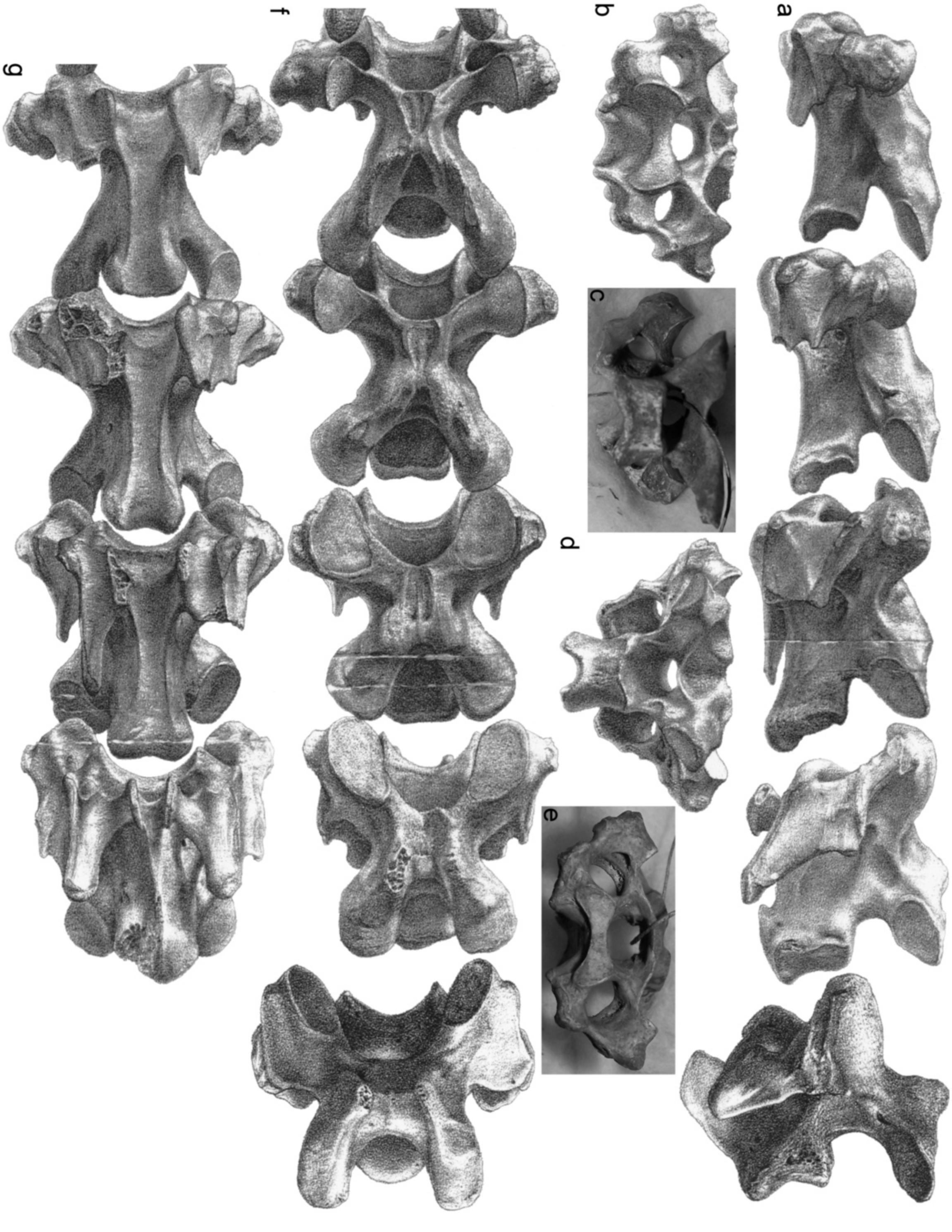

Cervical vertebrae of *Pezophaps*. a: C8-C12, lateral views (Newton & Newton 1869, pl.xv, figs.27, 31, 35, 38; Newton & Clark 1879, pl.xliv, fig.5); b: C8, cranial view (Newton & Newton 1869, pl.xv, fig.28); c: C8, caudal view (UMZC specimen); d: C9 caudal view (Newton & Newton 1869, pl.xv, fig.32); e: C10, cranial view (UMZC specimen); f: C8-C12, dorsal views (Newton & Newton 1869, pl.xv, figs.29, 33, 36, 40; Newton & Clark 1879, pl.xliv, fig.6); g: C8-C11, ventral views (Newton & Newton 1869, pl.xv, figs.30, 34, 37, 41). Newton & Newton (1869, pl.xv): artist: George Henry Ford; "G. H. Ford ad nat. lith." "W. West imp.") Newton & Clark (1879, pl.xliv): "R. Mintern del." "Mintern Bro^{s}. lith." Photographs of UMZC specimens: ○ Jolyon C. Parish, December 2008.

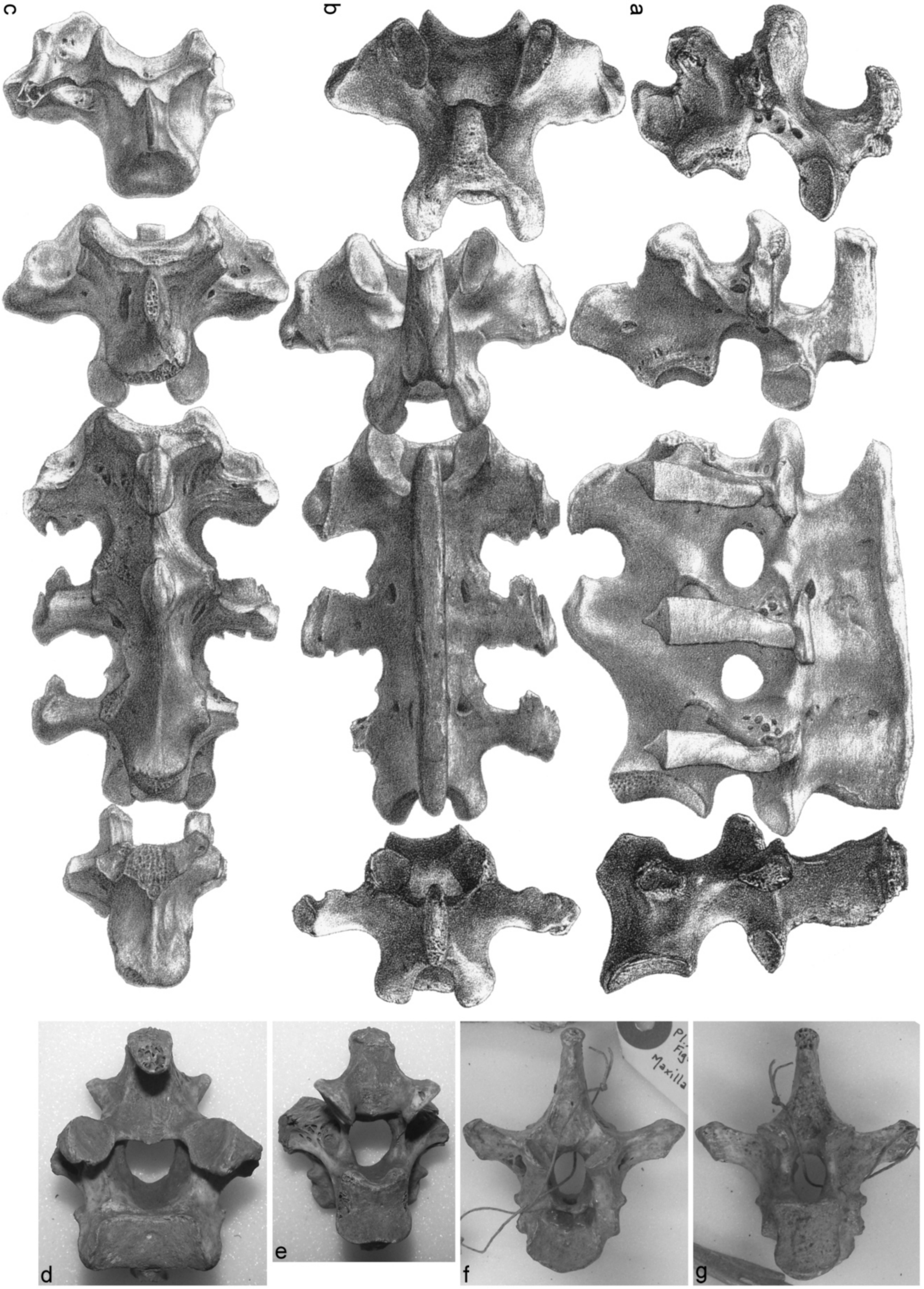

Vertebrae of *Pezophaps*. a: C13, 14th-18th vertebrae, lateral views (Newton & Clark 1879, pl.xliv, fig.3; Newton & Newton 1869, pl.xv, figs.48, 51; Newton & Clark 1879, pl.xliv, fig.1); b: C13, 14th-18th vertebrae, dorsal views (Newton & Clark 1879, pl.xliv, fig.4; Newton & Newton 1869, pl.xv, figs.49, 54; Newton & Clark 1879, pl.xliv, fig.2); c: C13, 14th-18th vertebrae, ventral views (Newton & Newton 1869, pl.xv, figs.47, 50, 55, 59); d and e: 14th vertebra, cranial and caudal views (UMZC specimen); f and g: 18th vertebra, cranial and caudal views (UMZC 646; not to scale). Newton & Newton (1869, pl.xv): artist: George Henry Ford; "G. H. Ford ad nat. lith." "W. West imp.") Newton & Clark (1879, pl.xliv): "R. Mintern del." "Mintern Bros. lith." Photographs of UMZC specimens: ○ Jolyon C. Parish, December 2008.

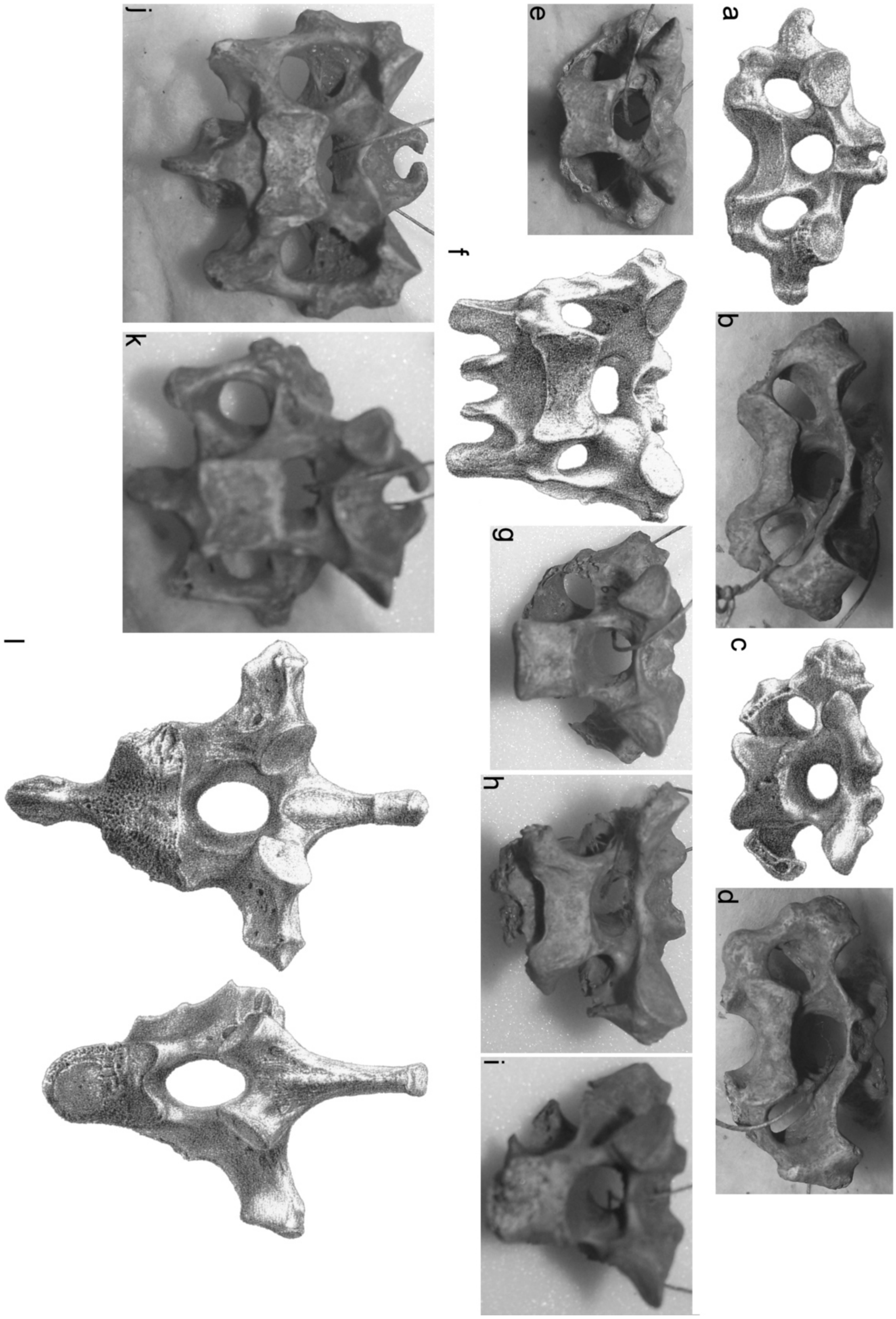

Vertebrae of *Pezophaps*. a: C5, cranial view (Newton & Newton 1869, pl.xv, fig.14); b: C6, cranial view (UMZC specimen); c: C6, caudal view (Newton & Newton 1869, pl.xv, fig.18); d and e: C7, cranial and caudal views (UMZC specimen); f: C11, cranial view (Newton & Newton 1869, pl.xv, fig.39); g: C11, caudal view (UMZC specimen); h and i: C12, cranial and caudal views (UMZC specimen); j and k: C12, cranial and caudal views (UMZC specimen); l: notarium, cranial and caudal views (Newton & Newton 1869, pl.xv, figs.52, 53). Newton & Newton (1869, pl.xv): artist: George Henry Ford; "G. H. Ford ad nat. lith." "W. West imp.") Photographs of UMZC specimens: ○ Jolyon C. Parish, December 2008.

Pezophaps there are eighteen presynsacral vertebrae, as in other columbids.[66] The closest living relatives of *Raphus* and *Pezophaps* (*Caloenas* and *Goura*) also have thirteen cervical vertebrae.

However, birds show some intraspecific variation as to the number of cervical vertebrae, and indeed the number of presynsacral vertebrae as a whole.[67] The possible differing morphology of the eleventh cervical in *Raphus* (see below) suggests that there could have been intraspecific variation as regards numbers of cervical and presynsacral vertebrae, perhaps with some individuals having fourteen cervicals (as in Thirioux's Port Louis skeleton) and others thirteen (as in *Pezophaps*, *Caloenas* and *Goura*). This, however, remains conjecture. As Claessens *et al.* (2015) concluded: "it is also important to note that presynsacral, synsacral, and caudal vertebral counts vary intraspecifically in almost all birds, including columbids such as *Goura* and *Columba* (Claessens, pers. observ.; Fürbringer, 1888; Martin, 1904). Thus, establishing an absolute, fixed, and immutable vertebral count for *Raphus* (e.g., Newton and Gadow, 1893), or any bird for that matter, is likely impossible considering the inherent plasticity of vertebral development in birds. Minor deviations from the total vertebral number as well as the borders between different axial regions as observed in the Thirioux specimens is certainly possible in the light of intraspecific variation" (p.81).

Owen's figure of the skeleton of Raphus (1867, pl.xv) shows twelve cervical, two cervicodorsal and five thoracic vertebrae.[68] Newton & Newton (1869) gave the number of cervical and 'dorsal' vertebrae for *Pezophaps* as twelve and eight respectively,[69] on the basis that the genus had the same number as in Owen's figure. However, Owen shows only seven cervicodorsal/thoracic vertebrae in his plate; this difference may be explained by counting the first synsacral vertebra as a thoracic one. Newton & Newton (1869) stated that "Owen himself does not offer any opinion as to the number of vertebrae in *Didus*. We prefer citing his draughtsman as the authority for the number assigned to the bird, because the on the same plate *Didunculus* appears to be represented as possessing fourteen cervical and seven dorsal vertebrae, being altogether two *more* than we are able to count in the very specimen, now in the Museum of the Royal College of Surgeons, which served as the subject for his pencil" (p.332). The latter part of this statement is erroneous, as noticed by Owen (1879): James Erxleben, the artist, only figures twelve cervicals and seven cervicodorsal/thoracic vertebrae in *Didunculus* (the correct number). Thus, there seems to have been some confusion over the numbers of vertebrae assigned by various authors to various genera. Newton & Newton (*op. cit.*) figured nineteen vertebrae in the vertebral column of *Pezophaps* (pl.xv), one too many, and this series appears to show two specimens of the seventh cervical. Owen (1878) enumerated the vertebrae in *Pezophaps* as follows: twelve cervical, six cervicodorsal/thoracic, sixteen (syn)sacral, and seven caudal. Newton & Clark (1879) correctly gave the number of cervical vertebrae for *Pezophaps* as thirteen, although they indicated that there were nineteen vertebrae between the skull and the synsacrum. Gadow & Selenka (1891) gave the following:

	All cervical	Cervico-dorsal	'Dorsal'	Sternal ribs
Raphus	14	2	4	5

---

cervical, two cervicodorsal and five thoracic vertebrae, with four vertebrae fused into the notarium) (Milne-Edwards & Grandidier 1879, 1881; Lowe 1924).

[66] In other columbids these are divided into twelve or thirteen cervical, two cervicodorsal and three or four thoracic (Verheyen 1957). The composite skeleton of *Pezophaps* in the Mauritius Institute has nineteen presynsacral verebrae.

[67] Verheyen (1957) gave the following: *Phaps chalcoptera*: thirteen cervicals (nineteen presynsacrals; n= 1 out of 3); *Stigmatopelia senegalensis*: thirteen cervicals (nineteen presynsacrals; n=1 out of 4); *Patagioenas speciosa*: twelve cervicals (seventeen presynsacrals; n=1); *Patagioenas subvinacea*: twelve cervicals (seventeen presynsacrals; n=1); *Oena capensis*: twelve cervicals (seventeen presynsacrals; n= 1 out of 2); *Columbigallina passerina*: twelve cervicals (nineteen presynsacrals; n=1).

[68] As they were unknown at the time the atlas, eighteenth, free caudal vertebrae and pygostyle of *Raphus* were interpolated in Owen's figure (pl.xv).

[69] Although Newton & Newton (1869) refer to the twelfth to fourteenth vertebrae as the "anterior dorsal vertebrae" (p.333).

Pezophaps	14	2	3, 4	4, 5

Newton & Gadow (1893) gave *Raphus* thirteen cervical and two cervicodorsal vertebrae (as seen in UMZC 415.H and Sauzier's dodo skeleton at Port Louis); they also gave *Pezophaps* thirteen cervical and two cervicodorsal vertebrae. Newton & Gadow (1896) incorrectly gave the vertebral formula of the 'Dididae' [*Raphus* and *Pezophaps*] as: fifteen cervical, two cervicodorsal, three 'dorsal' and four 'thoracic' vertebrae.[70] Beddard (1898) stated that in the dodo: "There are 15 cervical vertebrae [...] The last cervical and first two dorsals are fused. Four ribs reach the sternum, of which the last belongs, as in *Pezophaps* only, to the first pelvic vertebra" (pp.314-315). Martin (1904) stated that *Raphus* possesses thirteen cervical, two cervico-thoracic and three thoracic vertebrae. This was followed by Lambrecht (1933), who stated that *Raphus* possessed two cervicothoracic and three thoracic vertebrae.

Verheyen (1957) gave the following:

	Cervical	Notarium		Thoracic	Complete thoracic ribs	Dorso-sacrum	Synsacrum	Caudal
		Cervical	Thoracic					
Raphus	13 (+2)	1	2	3	3	4	16	6 (+1)
Pezophaps	13 (+2)	1	2	3	3	5	17	5 (+1)

The correct number of vertebrae is now known, having been determined from specimens belonging to the same individuals (see above).[71]

Cervical Vertebrae

C1-C14 (*Raphus*: Owen 1867, pl.xv; Claessens *et al*. 2015, figs.16A-D, 65). C1-13 (*Pezophaps*: Newton & Newton 1869, pl.xv)

There are fourteen cervical vertebrae in *Raphus* and thirteen in *Pezophaps*; Owen incorrectly gave both *Raphus* (1867, pl.xv) and *Pezophaps* (1878) twelve cervical vertebrae, as in *Didunculus*, even though he figured no rib on the thirteenth vertebra of *Pezophaps* (1878, pl.vii, fig.1).

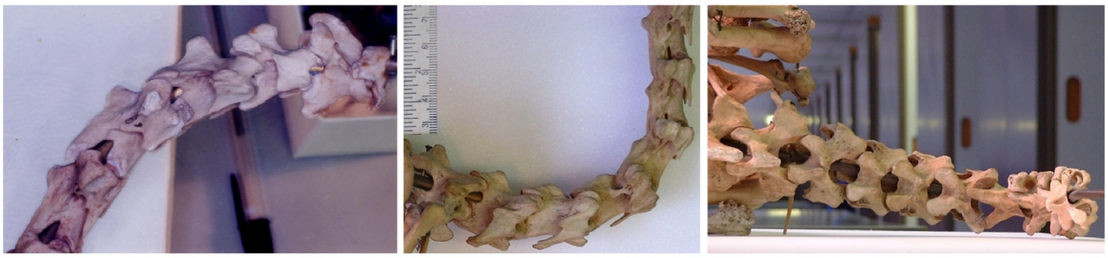

Cervical vertebrae of *Pezophaps*. *Left* and *middle*: NHMUK A.3506, lateral views; *right*: NHMUK A.3505, dorsal view (○ Jolyon C. Parish).

The neck of *Pezophaps* is longer than that of *Raphus*, and the vertebrae generally larger (Newton & Newton 1868). Newton & Newton (1869) remarked that "from the gradual elongation [of the cervical vertebrae] the neck [of *Pezophaps*] when living, must have been absolutely longer than that of *Didus*, a

---

[70] Cervical vertebrae were defined as those with fused ribs, cervicodorsal as those with unfused ribs that do not meet the sternum, and dorsal as those with "begin at the first that is connected with the sternum by a pair of complete ribs, and end at the last that is not fused with the ILIUM." They added that thoracic vertebrae "or those which are connected with the sternum, are not necessarily Dorsal Vertebræ" (p.849). They gave *Columba livia* fourteen cervical, two cervicodorsal and four 'dorsal' vertebrae, and *Treron olax* fifteen cervical, two cervicodorsal and three 'dorsal' vertebrae.

[71] The figure of the dodo skeleton given in Parish (2013, fig.6.1) only has eighteen presynsacral vertebrae (thirteen cervical, two cervicodorsal and three thoracic). The author had only seen Thirioux's Port Louis skeleton in photographs and (television) video clips and had based the presynsacral vertebral count and arrangement on those of *Pezophaps* and other columbids, as well as Newton & Gadow (1893).

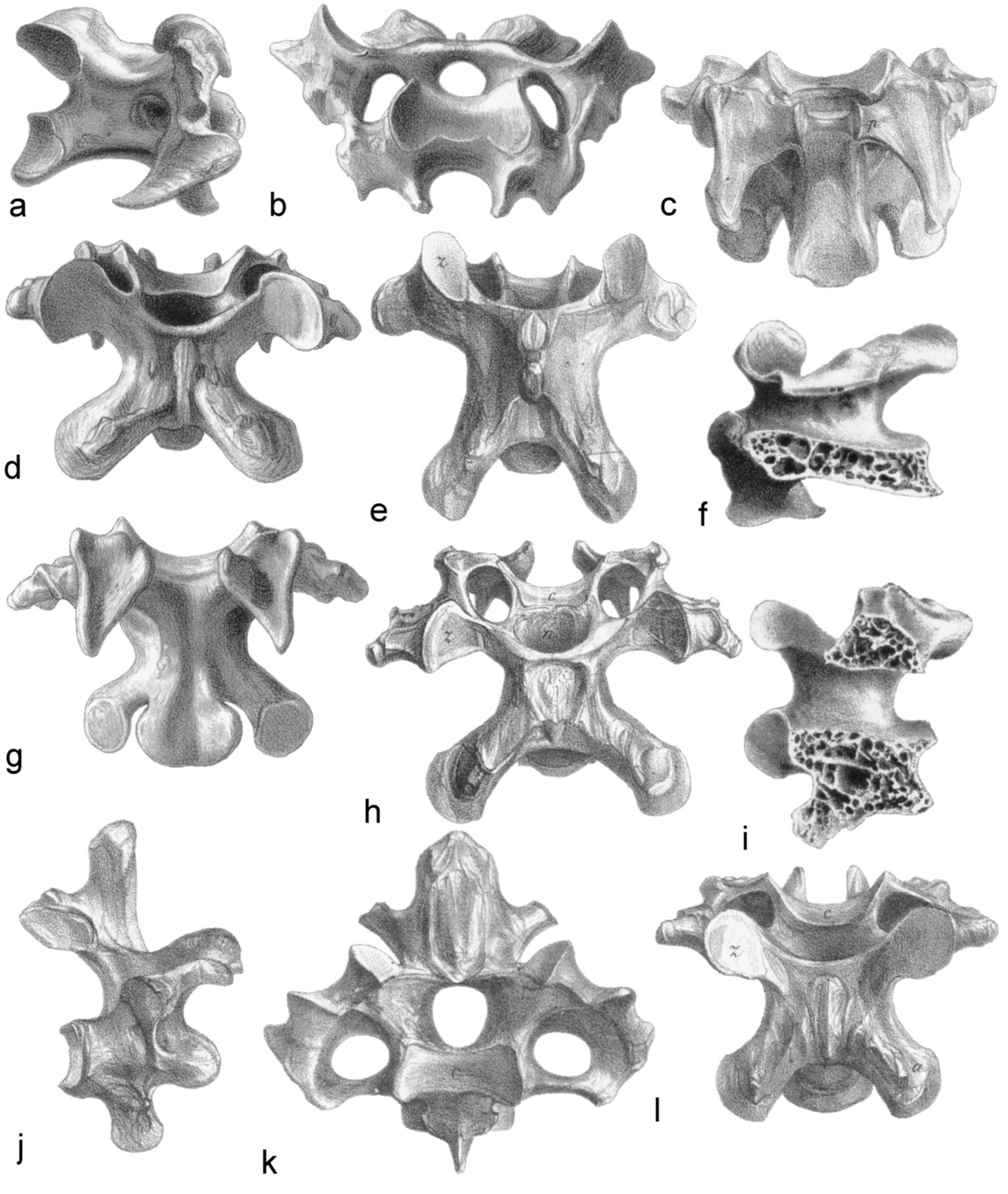

Cervical vertebrae of *Raphus*. a: cf. C9, lateral view (Milne-Edwards 1866b, pl.14, fig.4b); b: cf. C9, cranial view (Milne-Edwards 1866b, pl.14, fig.4c); c: cf. C11, ventral view (Owen 1867, pl.xvii, fig.11); d: cf. C9, dorsal view (Milne-Edwards 1866b, pl.14, fig.4a); e: C5, dorsal view (Owen 1867, pl.xx, fig.2); f: C3? in sagittal section (Owen 1867, pl.xxiii, fig.2); g: cf. C9, ventral view (Milne-Edwards 1866b, pl.14, fig.4); h: cf. C8, dorsal view (Owen 1867, pl.xx, fig.1); i: C13? in sagittal section (Owen 1867, pl.xxiii, fig.3); j: C14, lateral view (Owen 1867, pl.xvii, fig.6); k: C14, cranial view (Owen 1867, pl.xvii, fig.7); l: cf. C11, dorsal view (Owen 1867, pl.xvii, fig.10). Milne-Edwards 1866b: “Louveau del et lith.” “Imp. Becquet à Paris.” Owen 1867, pls.xvii, xx: “From nat on Stone , by J Erxleben” “M & N Hanhart , imp”; pl.xxiii: “J Smit lith” “M & N Hanhart imp”.

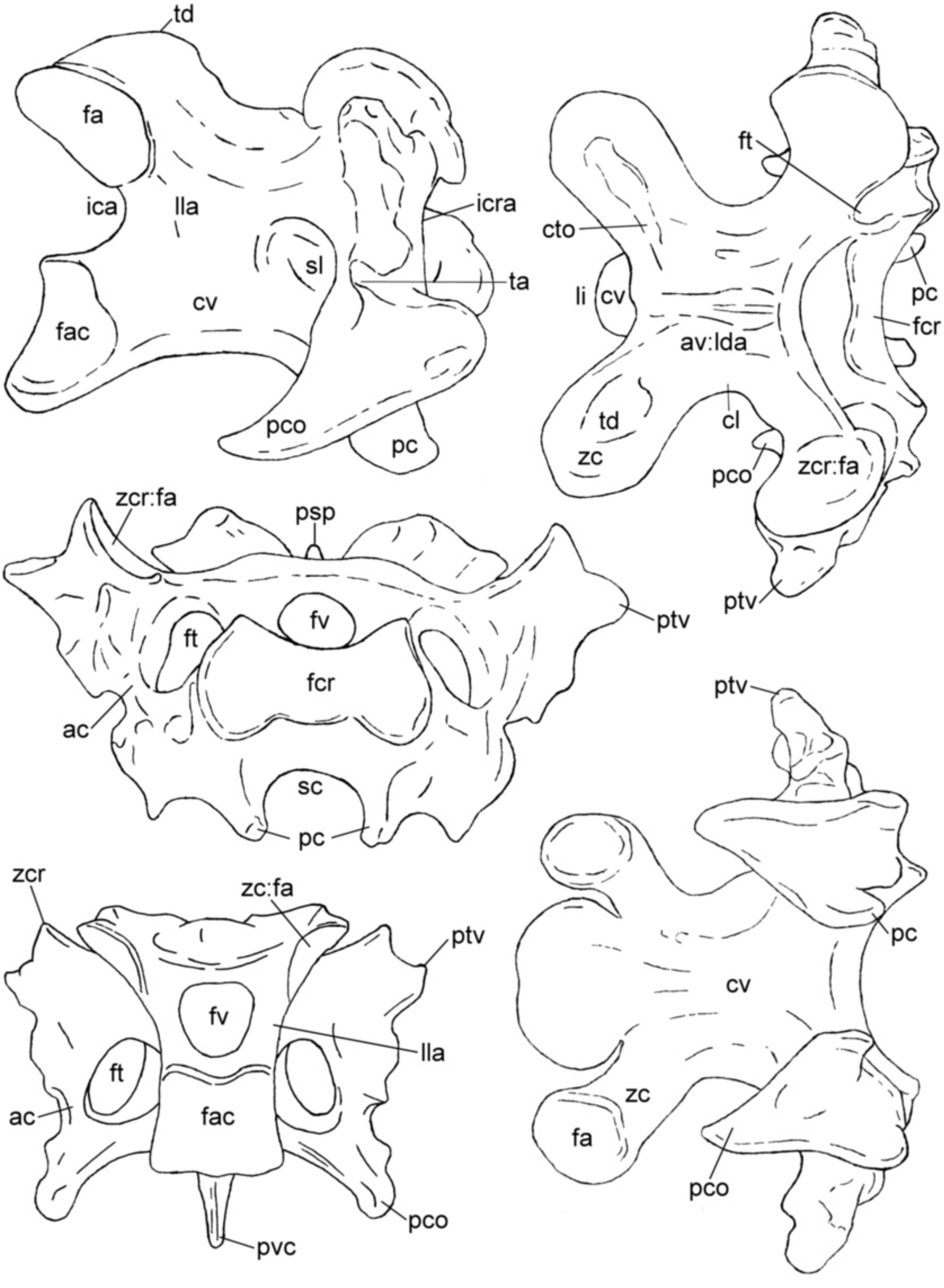

Cervical vertebrae of *Raphus* (traced from Milne-Edwards 1866b, pl.14, figs.4-4c and Owen 1867, pl.xvii, fig.9).

conclusion which testifies in another point of fidelity of LEGUAT'S figure" (p.333). The cervical vertebrae of *Raphus* and *Pezophaps* are similar to those of other columbids in proportion and development of the neural spines, hypapophyses and other features. The majority of the cervical vertebrae lack both hypapophyses and pronounced neural spines, as in extant pigeons. In *Raphus* a neural spine is lacking in cervicals eight to thirteen. The mid- to proximal cervicals (fifth to twelfth) of *Pezophaps* have bifurcated neural spines (see, for example, NHMUK A.3505, A.3506; Newton & Newton, pl.xv), which is thought to be a possible biomechanical adaptation to sustain a large mobile weight near the pectoral girdle, and is associated with the lig. elasticum interspinale (Tsuihiji 2004, Woodruff 2014).[72] In *Raphus* only cervicals six and seven have bifurcate neural spines (present as a pair of low tubercles). Bifurcate neural spines of the cervical vertebrae are also found in Aepyornithidae, *Casuarius*, Dinornithidae, *Rhea*, *Andalgalornis*, *Cnemiornis*, Gastornithidae, *Sylviornis* and *Theristicus* – all birds with long necks (Woodruff 2014, Tsuihiji 2004, Tambussi *et al.* 2012, Worthy *et al.* 1997, Worthy *et al.* 2016).[73]

The fifth and sixth in *Raphus* (Thirioux's Port Louis skeleton; Claessens *et al.* 2015, table5), and the fifth to seventh and tenth in *Pezophaps* (Newton & Newton 1869; pers. obs.), appear to be the longest vertebrae.

The carotid sulcus runs from the upper cervicals to the tenth or eleventh cervical in *Raphus* and the eleventh cervical in *Pezophaps*. In *Pezophaps* the carotid processes are well developed in the ninth to eleventh vertebrae, progressively becoming closer together and narrowing the carotid sulcus between them. The carotid sulcus is never completely closed over (except in rare circumstances of individual variation: see below). In *Raphus*, those cervicals that lack hypapophyses and pronounced neural spines are "broader and more massive in proportion to their length than in the winged Doves" (Owen 1867, p.73). Owen (1878) stated that "the protuberance from the under part of the par-pleurapophysis [tuberculum costolaterale and costal process] of the fifth and sixth cervicals shows the "catapophysis" [carotid process] of Mivart in the seventh; and, each converging towards its fellow, the pair of inferior processes become distinct in the ninth, approximate in the eleventh, and blend into the single median hypapophysis in the twelfth vertebra" (p.88).

In cervicals five to fourteen the transverse processes extend lateral to the articular faces of the prezygapophyses. The lateral end of each transverse process of cervicals six and seven possesses a dorsally projecting tubercle. The dorsal margin of the transverse process is located at a level approximately halfway up the articular face of the prezygapophysis in cervicals eight to ten, and at a level with its ventral margin in cervicals eleven, thirteen and fourteen.

Claessens *et al.* (2015) stated that the placement of the neural arch in the seventh cervical is proportionately slightly more caudal than in preceding vertebrae, the encroachment of the cranial articular face of the centrum onto its dorsal face (that is to say the ventral part of the neural canal), combined with "the orientation of the prezygapophyseal articular facets", appears "to indicate a change in the angle at which the neck was held at rest, marking the start of cervical dorsal flexion leading up to the trunk" (p.53). In cervicals nine to eleven the articular surface of the centrum also curves from the cranial face onto the dorsal surface of the centrum, the associated potential for dorsoflexion marking a "change in orientation of the cervical vertebral column toward the subhorizontal vertebral orientation in the trunk" (Claessens *et al.* 2015, p.54). Claessens *et al.* added that, on examination of the vertebral column of Thirioux's Port Louis skeleton

> Taking the point when there is no longer any overlap between the zygapophyseal facets or, if encountered sooner, the moment when portions of adjacent vertebrae collide at the

---

[72] The figure given by Woodruff (2014, fig.13f) shows the skeleton of the dodo (Owen 1871b, pl.lxiv), but the fifth cervical of *Pezophaps* (cranial aspect; Newton & Newton 1869, pl.xv, fig.14).

[73] In Dromornithidae neural spines are absent in the post-axial vertebrae, but instead there are deep interzygapophysial grooves which probably channelled a continuous interspinous ligamant "functionally similar to the ligamentum nuchae in long-necked mammals" (Murray & Vickers-Rich 2004, p.187).

> maximum range of flexion, it is apparent that the neck of the dodo was likely capable of significant dorsiflexion and ventriflexion (*ibid*., p.81).

This great degree of potential dorsiflexion and ventriflexion is shown in their fig.65. The number of cervical vertebrae has been suggested to be linked primarily to the required degree of flexibility of the neck, rather than its length (Hiraga *et al*. 2014).

Cervical ribs (ossa costalia vera) are developed on the third to eleventh cervicals in *Raphus* (a stubby projection on the twelfth vertebra could be considered a costal process); in *Pezophaps* they are present on the third or fourth to twelfth. In R*aphus* the cervical ribs extend caudally for more than half the length of the centrum in the sixth to tenth cervicals (they extend about halfway in the eleventh). They are longest in the tenth and eleventh cervicals in *Pezophaps*. The articular faces of the prezygapophyses are largest in the tenth to thirteenth vertebrae in both genera; those of the postzygapophyses are largest in the ninth to thirteenth vertebrae. The prezygapophyses of the proximal cervical vertebrae are very oblique and the transverse diameter of their articular faces is at least equal to their longitudinal diameter (Milne-Edwards 1866b). The articular faces of the prezygapophyses of *Pezophaps* are directed slightly more cranially compared with those of *Raphus* and other columbids. The articular faces of the postzygapophyses appear to be more ventrolaterally directed in *Raphus* compared with *Pezophaps*, and are more elongated in proportion to the width in the latter genus. The distinct cristae transverso-obliquae, which provided attachment for the mm. intercristales, can also be seen in the mid cervicals of both *Raphus Pezophaps*. In the fifth to sixth cervicals of *Raphus* they are caudolaterally directed, as they are in the cervicals of *Pezophaps*. However, in the seventh to tenth cervicals their proximal ends are laterally directed in *Raphus*. The neural spines are more developed in the upper cervicals of *Raphus* compared to those of *Pezophaps* (Newton & Newton 1869, pl.xv, figs.6-12). In *Pezophaps* the neural spines gradually decrease in size from the axis to the fifth cervical, where only a pair of tubercles remains; this pair of tubercles persists up to the ninth cervical. The transverse processes are sometimes roughened, presumably for the attachment of mm. intertransversarii. The areae ligamenti elastici of the axis and third cervical are apparently less developed in *Pezophaps* (and *Columba* and *Didunculus*) than in *Raphus*; those of *Caloenas* are more like those of *Raphus* in their development (Claessens *et al*. 2015). In the proximal cervical vertebrae the area ligamenti elastici is not very prominent and is located at the cranial end of a 'V'-shaped ridge (Milne-Edwards 1866b). The lateral surface of the centrum may also show caudoventrally directed crests (crista lateralis arcus of Landolt & Zweers 1985), which may have provided attachment for m. longus colli ventralis or mm. intertansversarii.

Newton & Newton (1869) stated that in the collection of solitaire bones examined by them (containing 161 vertebrae) "there is such a great numerical preponderance of specimens of the eighth, ninth, and tenth cervicals (Plate XV. Figs.24-34) [probably the seventh, eighth and ninth vertebrae], counting backwards, that one is at first led to suppose that *Pezophaps* must have been endowed with more [than nineteen presynsacral vertebrae], till a diligent study of each example compels belief that no other presumption will meet the case equally well, and an explanation of the curious fact that the specimens of each of these three vertebrae are nearly twice as numerous as most of those of the rest must be sought elsewhere" (p.332).

The well-developed muscle and ligaments attachment areas of the occiput and cervical vertebrae in the dodo are in agreement with the long and robust skull in that bird (Claessens *et al*. 2015).

The following description of the free (unfused) vertebrae of the dodo owes much to the descriptions of Claessens *et al*. (2015), as this work describes vertebrae presumed to be from a single individual (Thirioux's Port Louis skeleton; see above); this allows the positional identification of each vertebra to be ascertained. However, it should be noted that the positional identification of isolated vertebrae (that is, not from Thirioux's Port Louis skeleton or the Durban skeleton, which also potentially contains vertebrae from one individual) may be a matter of conjecture.

Atlas

C1 (*Raphus*: Newton & Gadow 1893, pl.xxxvi, figs. 2-4; Claessens *et al*. 2015, fig.18, pls.PL5, D5. *Pezophaps*: Newton & Newton 1869, pl.xv, figs.1-5)

The atlas of *Raphus* is known in UMZC 415.H, UMZC 415.KK, the MNHN and Lausanne collections, the Durban skeleton, Thirioux's and Sauzier's skeletons at Port Louis and MAS 2010 20.064.

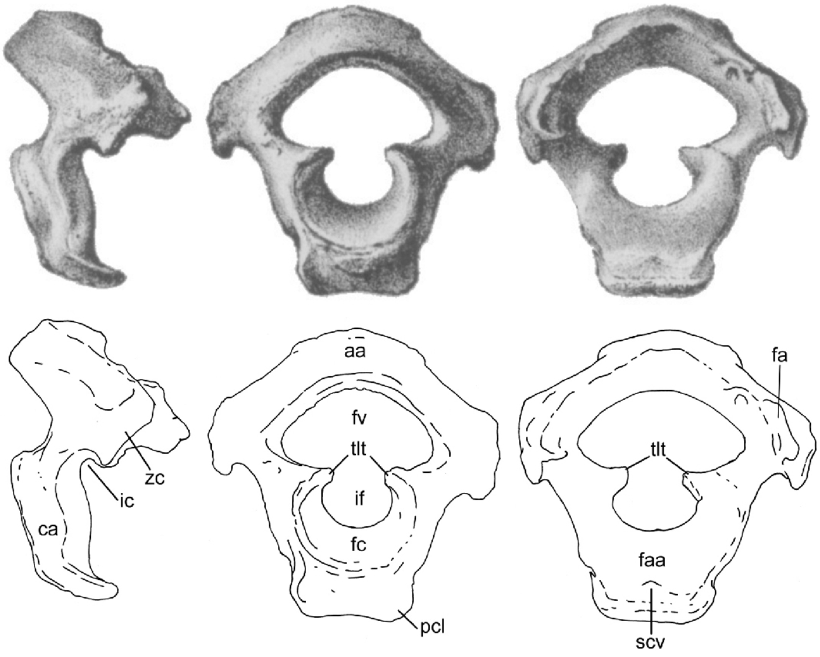

The atlas of *Raphus* in lateral, cranial and caudal views (lithographs: Newton & Gadow 1893, pl.xxxvi, figs. 2-4; "Cambridge Engraving Company").

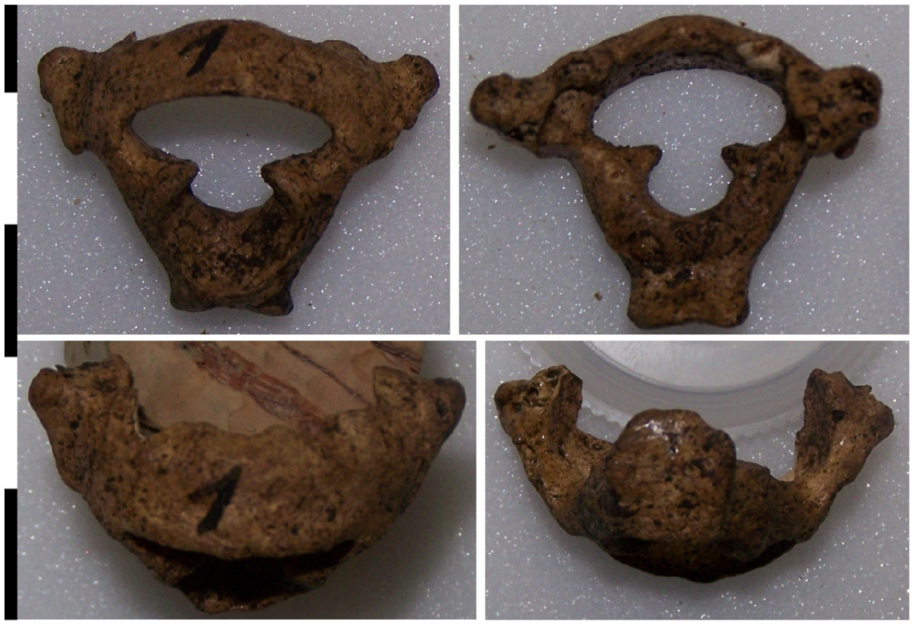

The atlas of *Raphus* in cranial, caudal, dorsal and ventral views (UMZC 415.KK; scale in cm; ○ Jolyon C. Parish, December 2008).

The atlantes of *Raphus* and *Pezophaps* resemble those of other pigeons, being small and ring-like. The atlas is notched, for the reception of the dens (odontoid process) of the axis, by the incisura fossae, which emarginates the dorsal border of the condyloid fossa. The incisura fossae is slightly more than semicircular, with a tuberositas ligamenti transversi forming a medially pointing stubby projection at each dorsal extremity. In both *Raphus* and *Pezophaps* the condyloid fossa is deep. The fossa in *Pezophaps* is more U-shaped compared with that of *Raphus*, and each tuberositas ligamenti transversi is not as pointed as in the former. The neural canal is of rounded semicircular form. Its dorsal margin is formed by the arcus atlantis (neural arch) and ventrally it is open to the incisura fossae. The neural spine is in the form of a very low long ridge on the dorsal surface of the arcus atlantis. The postzygapophyses lie on the caudal aspect of the atlas, at the lateral ends of the arcus atlantis. The postzygapophyses in *Pezophaps* project further backward compared with *Didunculus* and in this character it resembles *Goura* (Newton & Newton 1869).

The ventral part of the atlas is approximately rectangular, with the rounded caudolateral processes projecting slightly from the centrum of the atlas to form the ventral rounded corners. The ventral part of the articular face for the axis has a wide sulcus (sulcus caudoventralis), created by the projection of the caudolateral processes. When articulated with the axis, the ventral part of the atlas projects under the cranioventral part of the latter. The hypapophysis is not developed in the dodo and solitaire (although there is a slight ventral protuberance in some specimens of *Pezophaps* (NHMUK 76.1.28.68) and *Raphus* (the Durban skeleton: Claessens *et al*. 2015, fig.17; MAD specimen: Janoo 1997, pl.17, figs.a-d; MAS 2010 20.064). In a specimen of *Pezophaps*, figured by Newton & Newton (1869, pl.xv, figs.1-5), the atlas is joined to the axis possibly by partial ankylosis (*ibid*.).

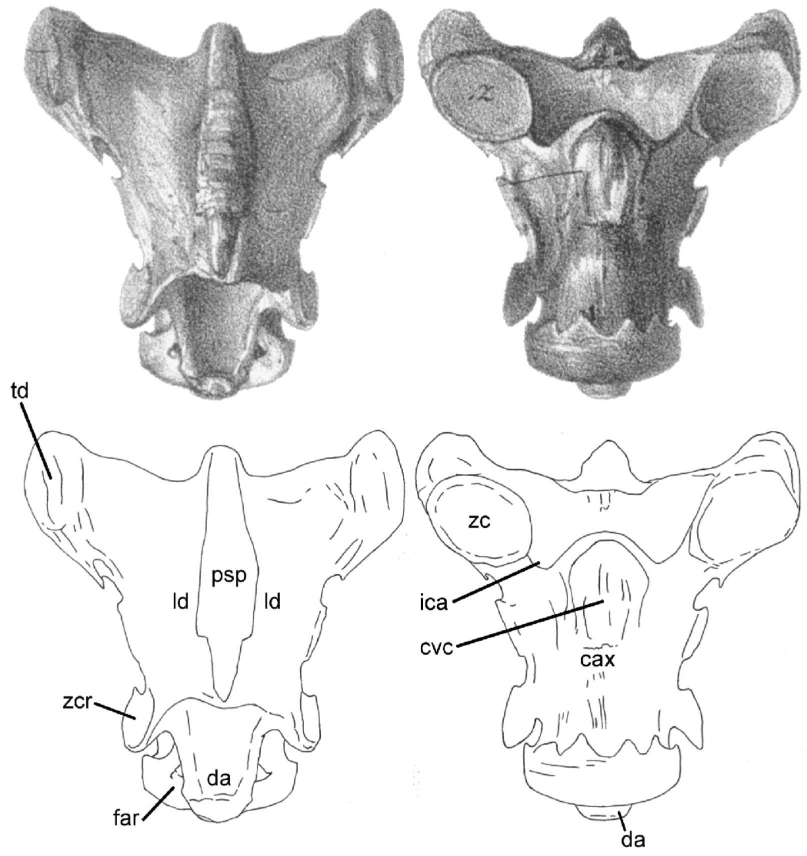

The axis of *Raphus* in dorsal and ventral views (lithographs: Owen 1867, pl.xvii, figs.12, 13; artist: James Erxleben; “From nat on Stone , by J Erxleben” “M & N Hanhart , imp”).

Axis

C2 (*Raphus*: Owen 1867, pl.xvii, figs.12, 13; Claessens *et al*. 2015, fig.18, pls.PL5, D5. *Pezophaps*: Newton & Newton 1869, pl.xv, figs.1-5)

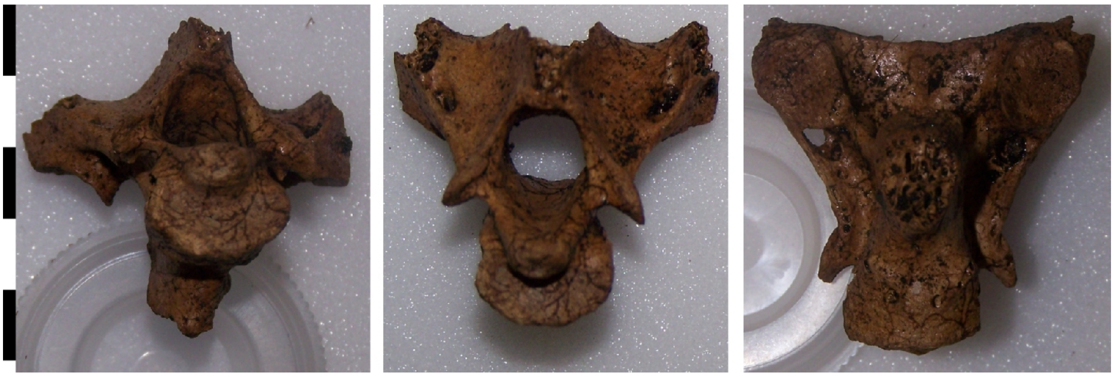

The axis of *Raphus* in approximately cranioventral, craniodorsal and ventral views (UMZC 415.KK; scale in cm; ○ Jolyon C. Parish, December 2008).

The axes of *Raphus* and *Pezophaps* are similar to those of other pigeons, wider caudally, at the postzygapophyses, than cranially. The anterior aspect, dorsally, shows a trident form, with the postzygapophyses forming the lateral points and the neural spine the median one. The rounded apex of the dens displays the fovea ligamenti collateralis atlantoaxialis. The dorsal surface of the dens is continuous with that of the ventral concave surface of the margin of the neural canal. In *Pezophaps* the dens projects much less than it does in *Raphus*, "hardly at all beyond the anterior upper portion" (Newton & Newton 1869, p.333). The neural canal is wider than it is high. Claessens *et al*. (2015) stated that "the angle of its floor above the facies articularis caudalis [is] inclined approximately 25° ventrally in comparison with the dorsal margin of the dens and the more cranial part" (p.51).

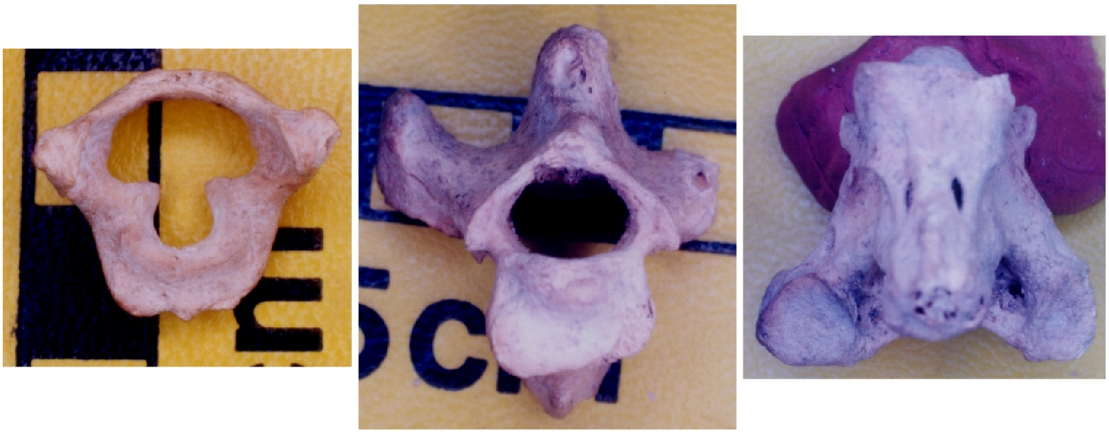

Atlas and axis of *Pezophaps* (NHMUK 76.1.28.68). *Left*: atlas in caudal view, *middle*: axis in cranial view, *right*: axis in ventral view (scales in cm; ○ Jolyon C. Parish).

The prezygapophyses are small and project craniolaterally from the neural arch. The cranial articular face of the centrum faces outward and slightly upward and is of modified oval shape. An interzygapophysial bar (Owen 1878) passes from the caudal part of the prezygapophysis to the cranial base of the postzygapophysis. In both *Raphus* (as in UMZC 415.KK, MGL 20106 and the Durban skeleton; Claessens *et al*. 2015) and *Pezophaps* this defines a foramen (the interzygapophysial foramen of Owen 1878). However, in the axis figured by Owen (1867, pl.xvii, figs.12, 13) the bar is incomplete and the foramen on each side forms an incisure. In *Pezophaps* the bar is present on the right side of the axis figured by Newton & Newton (1869, pl.xv, figs. 4 and 5), but incomplete on the left side. In *Raphus* the transverse foramen is small and directed dorsoventrally (Claessens *et al*. 2015).

The articular surface of the postzygapophysis is approximately three times the size of that of the prezygapophysis and is concave transversely. It faces downward and slightly outward. The anapophysis (tuberculum dorsalis) of the postzygapophysis is a large, approximately oval, tubercle.

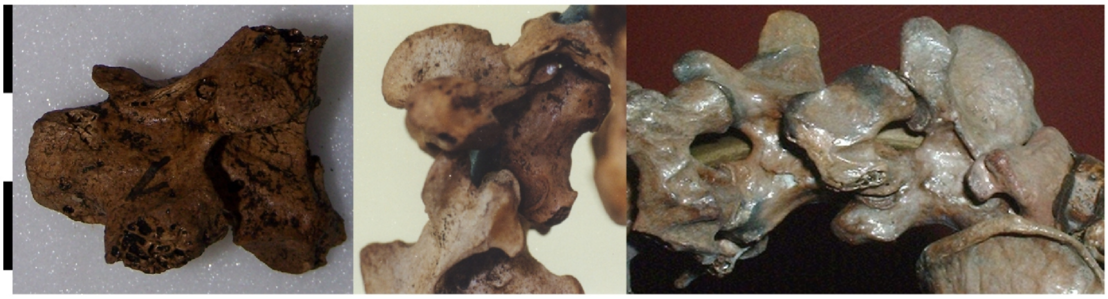

Cervical vertebrae of *Raphus*. *Left*: axis (UMZC 415.KK in approximately ventrolateral view; scale in cm; ○ Jolyon C. Parish), *middle*: atlas, axis and cranial part of C3 in lateral view (Thirioux's Port Louis skeleton; © Jan den Hengst), *right*: axis, C3 and cranial part of C4 in lateral view (NHMUK A.9040; ○ Jolyon C. Parish).

The large neural spine is longitudinally elongate and is longer than it is tall. It has a convex dorsal margin and projects much further caudally in *Pezophaps* than it does in *Raphus*, as do the postzygapophyses. The cranial border of the neural spine is inclined caudodorsally, as is the caudal border, albeit to a lesser extent. Caudally there is a deep area ligamentum elastici at the base of the neural spine. The caudal articular surface of the centrum of the axis is concave vertically and very convex transversely, "being continued upon the sides of the posterior part of the centrum" (Owen 1867, p.56), and is taller than wide. The hypapophysis is thick and prominent. In *Pezophaps* a pair of small longitudinally elongate foramina are present on either side of the midline of the ventral surface of the centrum, approximately halfway between the cranial and caudal margins (NHMUK 76.1.28.68, see also Newton & Newton 1869, pl.xv, fig.5).

Third cervical

C3 (*Raphus*: Owen 1867, pl.xxiii, fig.2?[74] Claessens *et al*. 2015, fig.19, pls.PL6, D6. *Pezophaps*: Newton & Newton 1869, pl.xv, figs.6-8)

The third cervical vertebra is of approximate quadrate shape in dorsal view, with the articular processes forming the four rounded corners. The vertebra is slightly wider caudally, at the postzygapophyses, than it is cranially; the same is true for *Pezophaps*. The cranial articular face of the centrum curves around onto the ventral surface, indicating that the articulation between the axis and the third cervical was capable of significant ventral flexion (Claessens *et al*. 2015).

The caudally-located neural spine is developed, longer than it is tall. Its craniodorsal margin is rounded. The area ligamentum elastici is well-developed at base of the cranial face of the neural spine and forms a deep fossa at the base of the neural spine on the caudal aspect of the vertebra. The large neural spine in *Pezophaps* is wider, but shorter, than that of the axis. The incisura arcus caudalis is deep as in the succeeding vertebrae. The caudal part of the centrum projects more ventrally than the cranial part, as in the axis. In *Raphus* a small triangular cervical rib is present (in Thirioux's Port Louis and the Durban skeletons; see also Newton & Gadow 1893, pl.xxxvi, fig.1), but is not well developed in Owen's figure (1867, pl.xv) or NHMUK A.9040. The figure of the third cervical of *Pezophaps* given by Newton & Newton (1869, pl.xv, figs.6-8) shows a weakly developed cervical rib, but in other specimens (such as NHMUK A.3506) it is more developed, forming a triangular projection, as in *Raphus*. In the dodo an interzygapophysial bar enclosing a foramen (foramen arcocostalis cranialis) is present on each side of the third cervical (seen for example, in a vertebra in the Thirioux Collection and Thirioux's Port Louis skeleton); it is slightly more robust than that of the axis (Claessens *et al*. 2015). Newton & Newton's (1869) figures also show the interzygapophysial bar in *Pezophaps*, which encloses a sub-elliptical foramen on the left side and is notched on the right by an incomplete foramen. The articular surfaces of the postzygapophyses are large and face ventrolaterally. The hypapophysis is large. A pneumatic foramen (or foramina; *ibid*., pl.xv, fig.8) is present on the third cervical of *Pezophaps*, dorsomedially, within the transverse foramen. The third cervical of *Raphus* also possesses pneumatic foramina (pers. obs. UMZC 415.K).

---

[74] Owen (1867, pl.xxiii, fig.2) figured a sagittally sectioned cervical vertebra, which he stated (p.84) was a third cervical (although on page 55 he stated that the third cervical is depicted in figure 3 – this an error, as figure 3 actually shows a thirteenth, or possibly a twelfth, vertebra. This was corrected in handwritten notes added to the copy of Owen & Broderip (1866) in the NHMUK General Library (Owen Coll. 55): on page 24 'third' is underlined and 'penultimate' written beneath it). However, fig.2 of pl.xxiii (Owen 1867) differs from that of the third vertebra depicted by Claessens *et al*. (2015, fig.19).

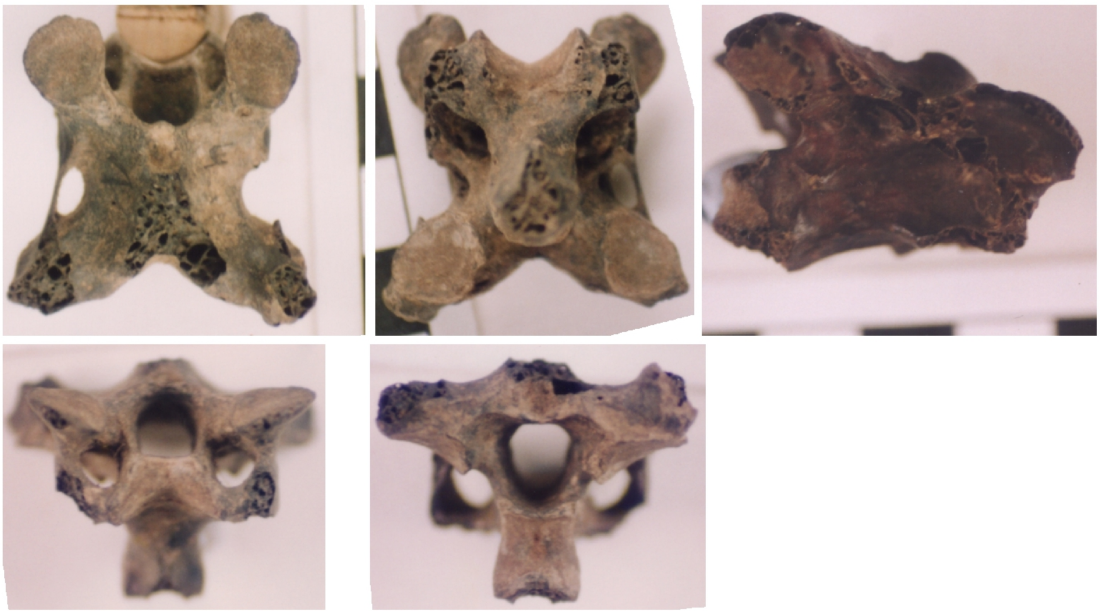

C3 of *Raphus* in dorsal, ventral, lateral, cranial and caudal views (UMZC 415.K specimen; © E. C. Parish).

Fourth cervical

C4 (*Raphus*: Owen 1867, pl.xx, fig.3; Claessens *et al*. 2015, fig.20, pls.PL6, D6. *Pezophaps*: Newton & Newton 1869, pl.xv, figs.9-12)[75]

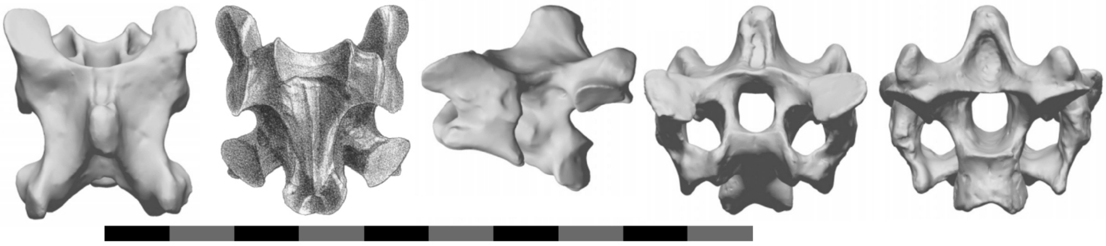

C4 of *Raphus* in dorsal, ventral, lateral, cranial and caudal views (scale in cm; © Aves 3D, except ventral view which is from Owen 1867, pl.xx, fig.3; "From nat on Stone by J Erxleben" "M & N Hanhart , imp").

In both *Raphus* and *Pezophaps* the fourth cervical has a thick, low neural spine, similar in form to that of the third cervical. Overall, the fourth cervical vertebra is similar in form to that of the preceding vertebra but has longer, more caudally projecting, postzygapophyses. The caudal part of the centrum does not project ventrally as does that of the axis or third cervical, and, in addition, there are no foramina enclosed by the interzygapophysial bar as in the preceding vertebra (except on the right side in *Pezophaps* UMZC 415.R). The transverse foramina are also slightly larger than those of the preceding vertebra (Claessens *et al*. 2015).

---

[75] There are two vertebrae in the UMZC 415.K collection joined together by a string and bearing the label "No 4". At least one of these appears to actually be a third cervical (comparing with Claessens *et al*. 2015, figs.19, 20), as, amongst other things, it is wider caudally than cranially, possesses a pair of foramina arcocostales craniales.

The cranial articular face of the centrum curves from the cranial face to the ventral face, although less so than in the third cervical; the fovea cranioventralis is well developed, indicating that the articulation between the third and fourth cervicals was capable of a significant amount of ventral flexion (Claessens *et al*. 2015). The caudal articular face of the centrum is higher than wide (*ibid*.).

The articular faces of the prezygapophyses face craniodorsomedially and are slightly larger than those of the postzygapophyses. The hypapophysis is also not developed, although there is a thin sagittal ridge. The cervical ribs are more developed than in the third cervical. The fourth vertebra is wider cranially than it is caudally. In both *Raphus* and *Pezophaps* the cranial and caudal aspects of the vertebra shows the well developed pit, the area ligamenti elastici, at the base of the neural spine (see Newton & Newton 1869, pl.xv, fig.10). The neural spine appears to be taller and more slender in *Raphus* (Owen 1867, pl.xv) than in *Pezophaps* (Newton & Newton 1869, pl.xv, fig.9) and is directed slightly caudodorsally. The postzygapophysis bears an anapophysis (tuberculum caudale of Claessens *et al*. 2015).

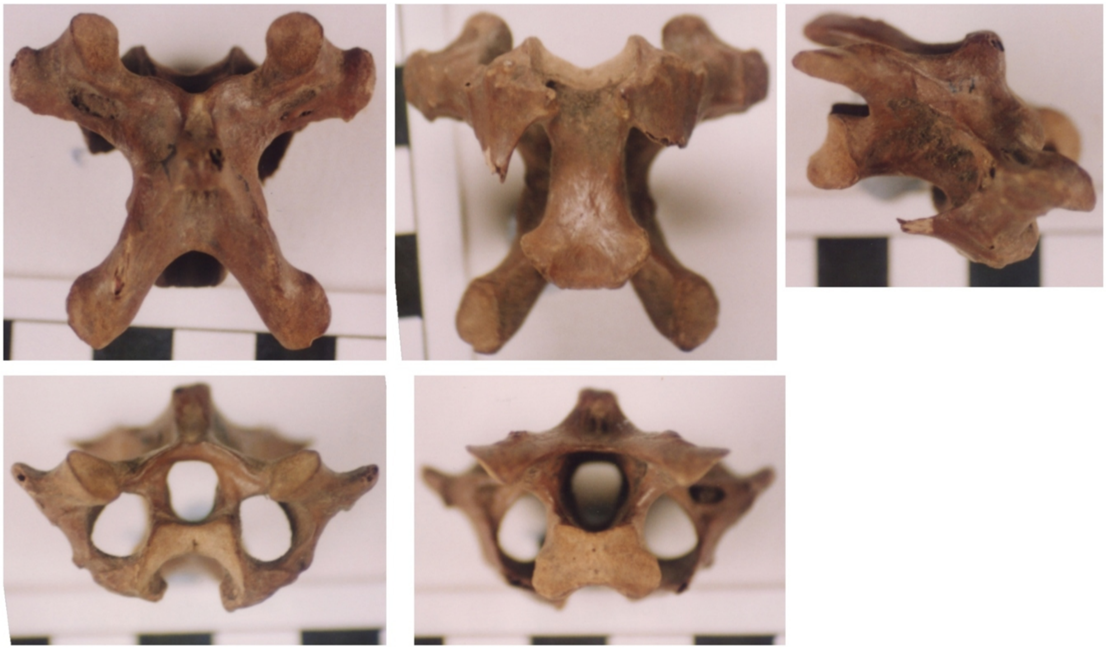

C5 of *Raphus* in dorsal, ventral, lateral, cranial and caudal views (UMZC 415.K specimen; © E. C. Parish).

Fifth cervical
C5 (*Raphus*: Owen 1867, pl.xx, fig.2; Claessens *et al*. 2015, fig.21, pls.PL7, D7. *Pezophaps*: Newton & Newton 1869, pl.xv, figs.13-16; Woodruff 2014, fig.13f)

The cranial articular face of the centrum curves from the cranial onto the ventral surface. The transverse foramina are slightly larger than in the preceding vertebrae (Claessens *et al*. 2015). The articular surfaces of the prezygapophyses face craniodorsomedially. The transverse processes project laterally to these, as in succeeding vertebrae, but not as in cervicals three or four.

In *Raphus* the neural spine of the fifth cervical is tall and proportionately shorter craniocaudally than in the preceding vertebra. In *Pezophaps* the neural spine consists of a pair of longitudinal ridges at the centre of the dorsal surface of the vertebra and is less developed than in the preceding vertebrae. In *Raphus* the caudal area ligamentum elastici is much deeper than the cranial one; in *Pezophaps* they are both deep. The cervical ribs are well developed. The carotid processes are developed, forming the lateral borders to the carotid sulcus. The caudal articular face of the centrum is wider than high (Claessens *et al*. 2015).

The articular surfaces of the postzygapophyses are elongate craniocaudally. The postzygapophyses themselves are long, and extend proportionately further caudally than those of the preceding vertebra. On the dorsal surface of each postzygapophysis is an elongate crista transverso-obliqua. In other respects the fifth vertebra is quite similar to the fourth. In dorsal and ventral views the vertebra appears cruciform, with the transverse processes forming the cranial arms and the postzygapophyses forming the caudal arms. The vertebra is wider than it is high. The caudoventral border of the centrum is convex transversely. The ventral surface of the bone is concave transversely.

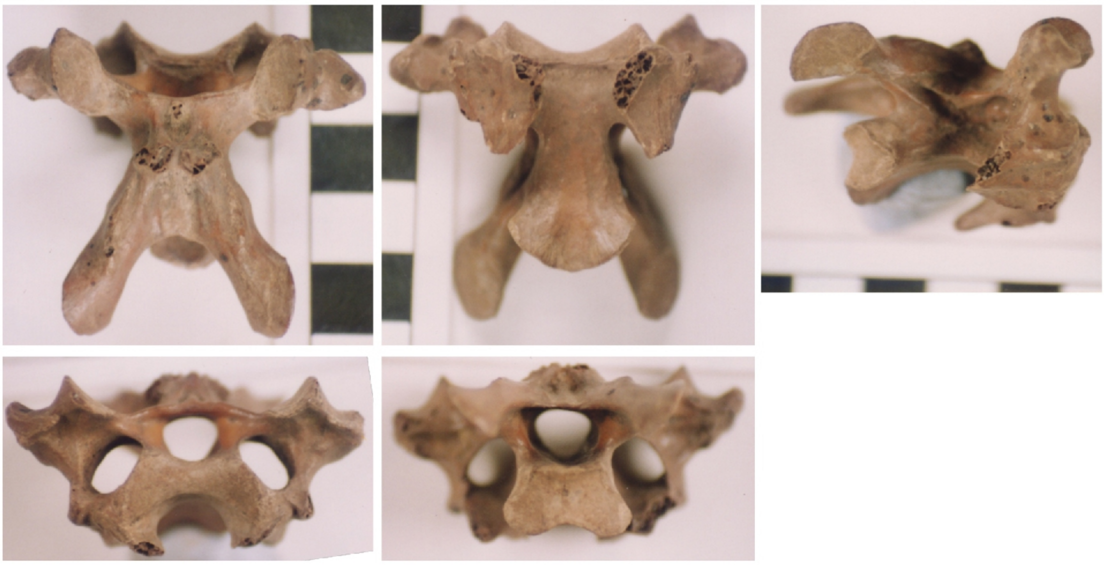

C6 of *Raphus* in dorsal, ventral, lateral, cranial and caudal views (UMZC 415.K specimen; © E. C. Parish).

Sixth cervical

C6 (*Raphus*: Claessens *et al*. 2015, fig.22, pls.PL7, D7. *Pezophaps*: Newton & Newton 1869, pl.xv, figs.17-20)

The centrum of the sixth cervical is longer than each of those of cervicals three to five. The costal process is long – extending for a length greater than half that of the centrum, in contrast to the condition in the preceding vertebrae where the process is less than half the centrum length (Claessens *et al*. 2015). The transverse foramen is of similar diameter to that of cervical five (*ibid*.). There is a shallow fovea cranioventralis on the ventral surface of the centrum (*ibid*.). The carotid processes are proportionately longer than in the fifth cervical. The narrow transverse processes extend lateral to the articular faces of the prezygapophyses. Each has a deep sulcus on its dorsal face, bordered laterally by craniocaudally-elongate ridge. In *Raphus* the neural spine of the sixth cervical is much smaller than that of the fifth. In *Pezophaps* the neural spine of the sixth cervical is also more reduced than it is in the fifth, forming two small tubercles on a pair of longitudinal ridges.

The sixth cervical is similar to the preceding one, but the vertebra is narrower behind the transverse processes. The caudoventral margin of the articular face of the centrum is transversely convex in *Raphus*. In *Raphus* the prezygapophyses have a more rounded dorsal margin, when seen in lateral view, than those of *Pezophaps*. The carotid processes are well developed, and in anterior view the carotid sulcus has a slightly greater than semicircular outline. Claessens *et al*. (2015) stated that compared with *Raphus*, the prezygapophyses in *Pezophaps* are "directed further laterally and [are] laterally more expanded, less pointed" and that "the sulcus on the processus transversus [is] deeper" (p.53). The postzygapophyses are also slightly proportionately more elongate in *Pezophaps*.

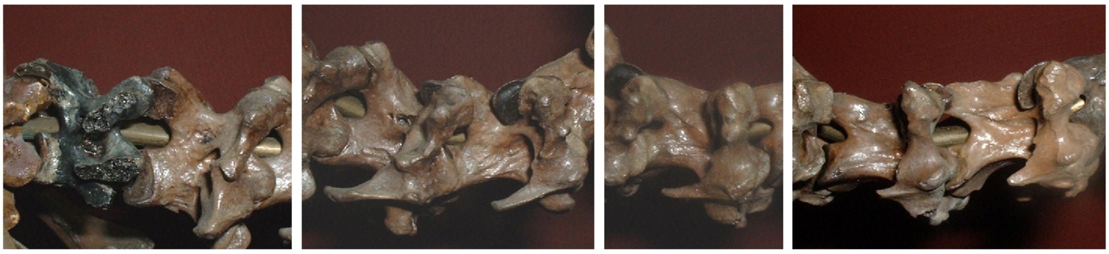

Cervical vertebrae of *Raphus* (NHMUK A.9040) in lateral view. *Right to left*: C6 and C7, C8, C9 and C10, C11 and C12 (○ Jolyon C. Parish).

Seventh cervical

C7 (*Raphus*: Grihault 2005, p.83 (cf. C7?); Janoo 2005, figs.2d, g (cf. C7?); Claessens et al. 2015, fig.23, pls.PL8, D8. *Pezophaps*: Newton & Newton 1869, pl.xv, figs.21-23, and 24-26?[76])

The seventh vertebra is similar to the sixth in form. The seventh cervical vertebra is dorsoventrally compressed, being wider than it is high. The narrow transverse processes extend lateral to the articular faces of the prezygapophyses. The cranial margin of the neural arch is located relatively further caudally than in preceding vertebrae (Claessens *et al*. 2015). The cranial articular face of the centrum is slightly taller than that of the sixth and the fovea cranioventralis curves from the cranial face onto the ventral face. The postzygapophyses project caudally, further than the caudal margin of the centrum. Their articular surfaces face ventrolaterally.

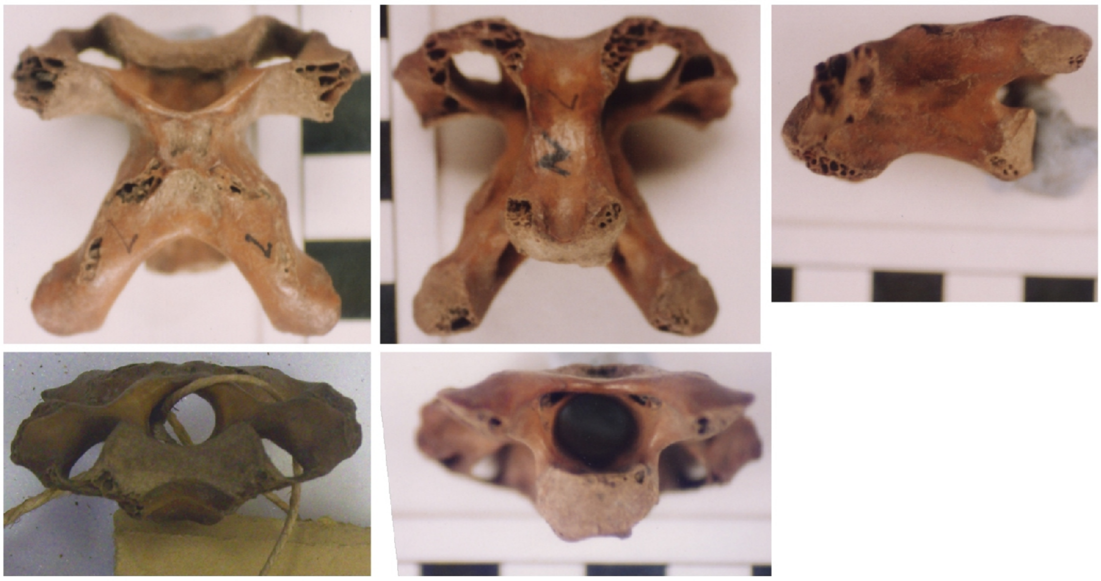

C7 of *Raphus* in dorsal, ventral, lateral, cranial and caudal views (UMZC 415.K specimen; © E. C. Parish, except cranial view which is ○ Jolyon C. Parish). Note: although this is labelled as C7, the form of the caudal articular face of the centrum and the articular faces of postzygapophyses resemble those of C6 of the Durban skeleton (Claessens *et al*. 2015, fig.22) more than those of C7 of the same skeleton (*ibid*., fig.23).

In *Pezophaps* the neural spine is reduced to a pair of very small tubercles. Compared with the preceding vertebra, the neural spine is of a similar size, although the postzygapophyses are shorter, in other respects it is very similar. The carotid processes are well developed. The postzygapophyses appear to be slightly more laterally directed in *Raphus* compared with *Pezophaps* (comparing a UMZC 415.K specimen with Newton & Newton 1869, pl.xv, figs.22-23).

---

[76] Newton & Newton (1869) figure nineteen vertebrae between the skull and the pelvis, which is one too many for *Pezophaps*. Therefore, one of the figured vertebrae is supernumerary to the series. It appears that there may be two seventh cervical vertebrae figured (figs.21-26), although this is not certain.

Eighth cervical

C8 (*Raphus*: Owen 1867, pl.xx, fig.1; Claessens *et al*. 2015, fig.24, pls.PL8, D8. *Pezophaps*: Newton & Newton 1869, pl.xv, figs.27-30?)

The eighth cervical is more robust than the preceding one. The articular faces of the prezygapophyses are larger than in the seventh cervical (Claessens *et al*. 2015) and face more dorsally than those of the sixth and seventh cervicals. The ansa costotransversarium is robust and the dorsal margin of the transverse process is located at a level approximately halfway up the articular face of the prezygapophysis and thus situated more ventrally than in the seventh cervical (Claessens *et al*. 2015). The transverse foramina are of similar size to those of the preceding cervicals. The cranial margin of the neural arch is located relatively further caudally than in the seventh cervical (Claessens *et al*. 2015). The articular surface of the centrum curves from the cranial face slightly onto the dorsal surface of the centrum.

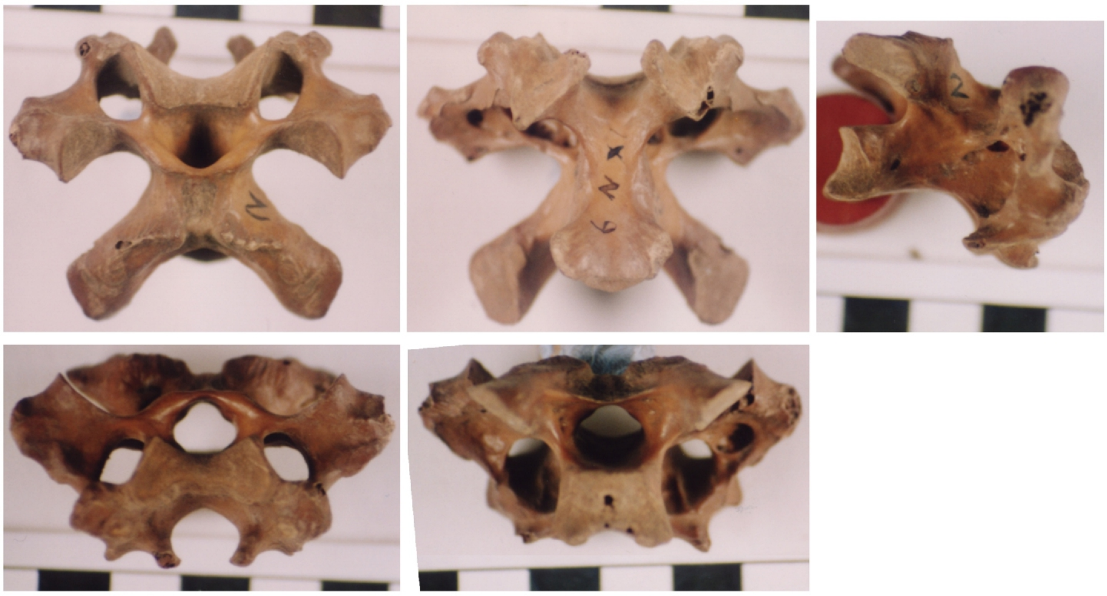

C8 of *Raphus* in dorsal, ventral, lateral, cranial and caudal views (UMZC 415.K specimen; © E. C. Parish).

The neural spine is absent. Instead, in Thirioux's Port Louis skeleton, there is a low sagittal ridge bordered by a bilateral pair of fossae; lateral to these, on each side, is a low ridge (Claessens *et al*. 2015). The cristae transverso-obliquae are developed and the postzygapophyses are dorsally enlarged. The caudal articular face of the centrum is more square than in preceding vertebrae, although it is still wider than tall.

The middle cervical vertebra of *Raphus* figured by Owen (1867, pl.xx, fig.1), in dorsal view, may be an eighth vertebra. It shows well-developed carotid processes (labelled as '*p*', "plates of the parapophysis"), and the carotid sulcus nears enclosure, with only its ventral part open.

The eighth cervical is proportionately shorter and higher in *Raphus* than in *Pezophaps*. The postzygapophyses seem to be slightly more caudolaterally directed in *Raphus* than in *Pezophaps*, with the lateral concavity of the centrum being narrower. In the former genus the cranial margins of the articular surfaces of the postzygapophyses are in line with the cranial margin of the incisura arcus caudalis, whereas in the latter genus they are more cranially placed (see Newton & Newton 1869, pl.xv, fig.27).

Ninth cervical

C9 (*Raphus*: Milne-Edwards 1866b, pl.14, fig.4-4c; Claessens *et al*. 2015, fig.25, pls.PL9, D9. *Pezophaps*: Newton & Newton 1869, pl.xv, figs.31-34)

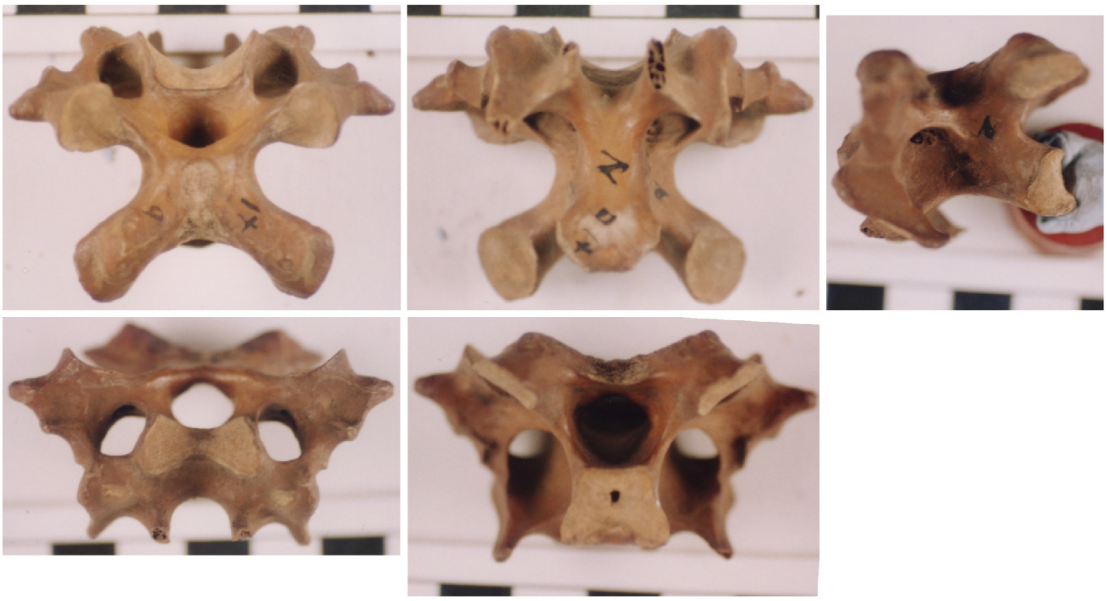

C9 of *Raphus* in dorsal, ventral, lateral, cranial and caudal views (UMZC 415.K specimen; © E. C. Parish).

The ninth cervical is more robust than the preceding one. The dorsal margin of the transverse process is at a level approximately halfway up the articular face of the prezygapophysis.[77] The ansae transversaria are robust and the transverse foramina are slightly larger than in the preceding cervicals (Claessens *et al*. 2015). The cranial articular surface of the centrum is narrow medially and expanded laterally; it curves onto the dorsal surface, indicating a potential for significant dorsoflexion (*ibid*.). A neural spine is not present, or at least is very reduced. The cervical ribs of the ninth vertebra in *Raphus* are long and pointed, extending caudally for more than half the length of the centrum. The cranial border of the neural arch is slightly caudal to the cranial articular face of the centrum (*ibid*.). The carotid processes are long and curved ventromedially; in most specimens the carotid sulcus is not completely closed over, however in Thirioux's Port Louis skeleton it is closed ventrally by a thin lamina (*ibid*.).[78] In both *Raphus* and *Pezophaps* the cristae transverso-obliquae are developed into low rounded tubercles. The postzygapophyses are proportionately shorter than in the preceding vertebra and the articular faces of the postzygapophyses are subcircular. The caudal articular face of the centrum is even more square-shaped than that of cervical eight.

The vertebra of *Raphus* figured by Milne-Edwards (1866b, pl.14, fig.4, 4a-c) appears to be a ninth cervical (or perhaps an eighth cervical).

The figure of Newton & Newton (1869, pl.xv, fig.31, and NHMUK A.3505) of the ninth cervical of *Pezophaps* shows a well-developed tuberculum ansae, for the attachment of mm. intertransversarii.

Tenth cervical

C10 (*Raphus*: Claessens *et al*. 2015, fig.26, pl.PL9. *Pezophaps*: Newton & Newton 1869, pl.xv, figs.35-37)

In Thirioux's Port Louis skeleton the cervical ribs of the tenth cervical are longer than those of the ninth (Claessens *et al*. 2015). The ansa costotransversarium is robust. The cranial border of the neural arch is slightly caudal to the cranial articular face of the centrum (*ibid*.). The cervical ribs are long and slightly pointed. The ventromedially-curving carotid processes are well developed. There is no neural spine. The cristae transverso-obliquae are developed. The caudal articular face of the centrum is slightly taller than wide. The articular faces of the postzygapophyses are subcircular.

---

[77] Claessens *et al*. (2015) described the "dorsal tubercles of the prezygapophyses". However, there are no such features listed by Baumel & Witmer (1993), or other literature consulted, and it is here assumed that it is the dorsal tubercles of the transverse processes which are being referred to. This is confirmed by the mention of the same feature later being described as the "dorsolateral tubercle of the processus transversus" (p.55).

[78] Verheyen (1957) noted that in the ninth cervical of *Treron* the carotid processes can meet and partially cover the carotid sulcus.

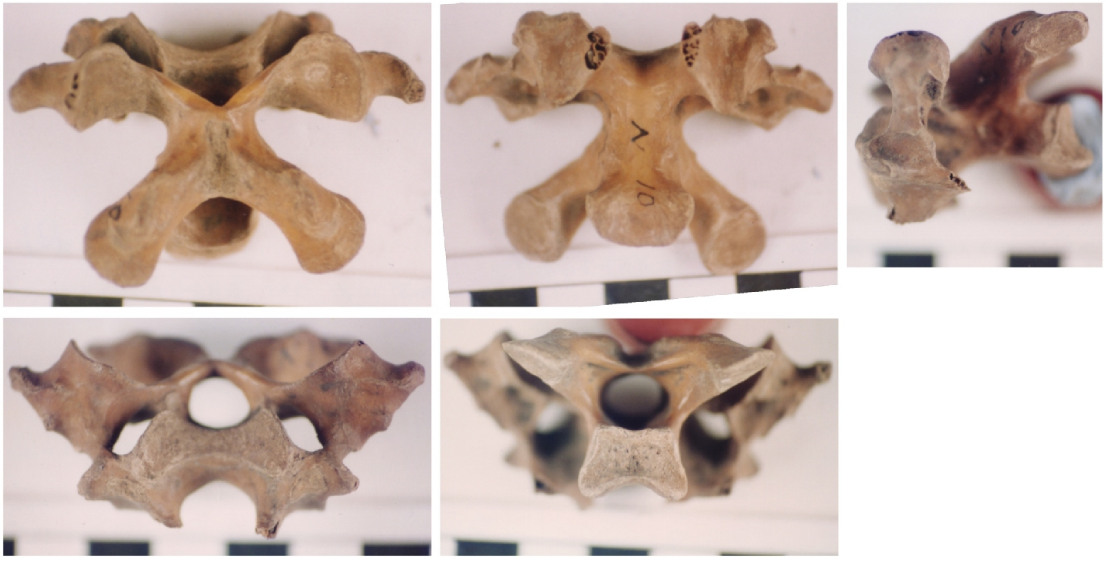

C10 of *Raphus* in dorsal, ventral, lateral, cranial and caudal views (UMZC 415.K specimen; © E. C. Parish).

The tenth cervical of *Pezophaps* resembles that of *Raphus*, although the prezygapophyses appear to be more pointed forwards in lateral view. In *Pezophaps* the length from the cranial extremity of the prezygapophyses to the caudal extremity of the postzygapophyses is greater than the width between the lateral margins of the prezygapophyses; in *Raphus* the opposite appears to be the case. The tenth vertebra of *Pezophaps*, when seen in dorsal view, is 'X' shaped, with all the limbs (formed by the zygapophyses) of approximately equal length; in *Raphus* the prezygapophyses are more laterally directed.

Eleventh cervical

C11 (*Raphus*: Owen 1867, pl.xvii, figs.10, 11 (cf. C11); Janoo 2005, fig.2k (cf. C11); Claessens *et al*. 2015, fig.27, pls.PL10, D10. *Pezophaps*: Newton & Newton 1869, pl.xv, figs.38-41)

The eleventh cervical is distinctive in form, being robust (proportionately shorter than cervicals nine or ten), with the prezygapophyses and anapophyses being almost at the same height, and with a well developed costal process (unlike the twelfth cervical). The ansa costotransversarium is more robust than in preceding cervicals (Claessens *et al*. 2015). The robust blunt cervical ribs extend caudally to approximately halfway along the centrum. The cranial articular surface of the centrum is concave transversely, convex vertically, and wider than it is high. Claessens *et al*. (2015) stated that the "tubercles of the processus transversus" are located at approximately the level of the ventral margin of the articular faces of the prezygapophyses. The transverse foramina are larger than in preceding cervicals (*ibid*.) and are elliptic, with the long axis directed dorsomedially. The cranial margin of the neural arch is located caudal to the cranial articular face of the centrum. The fovea cranioventralis is distinguishable; it is located cranial to the carotid processes (*ibid*.) and indicates a capability for ventroflexion between cervicals ten and eleven. A pair of separate carotid processes is present (although see below); they are straight, project ventrally and are closer together than in preceding vertebrae (*ibid*.). The neural spine is absent. The cristae transverso-obliquae form tubercles and the articular faces of the postzygapophyses are subcircular. The caudal articular face of the centrum is subquadrate, being either square or slightly wider than tall.

A specimen in the UMZC 415.K collection is similar in general morphology, in the narrowness of the ansae costotransversarium and in the subquadrate form of the caudal articular face of the centrum, to the eleventh cervical as figured by Claessens *et al*. (2015, fig.27). However, it possesses a median laterally compressed hypapophysis instead of a pair of carotid processes.

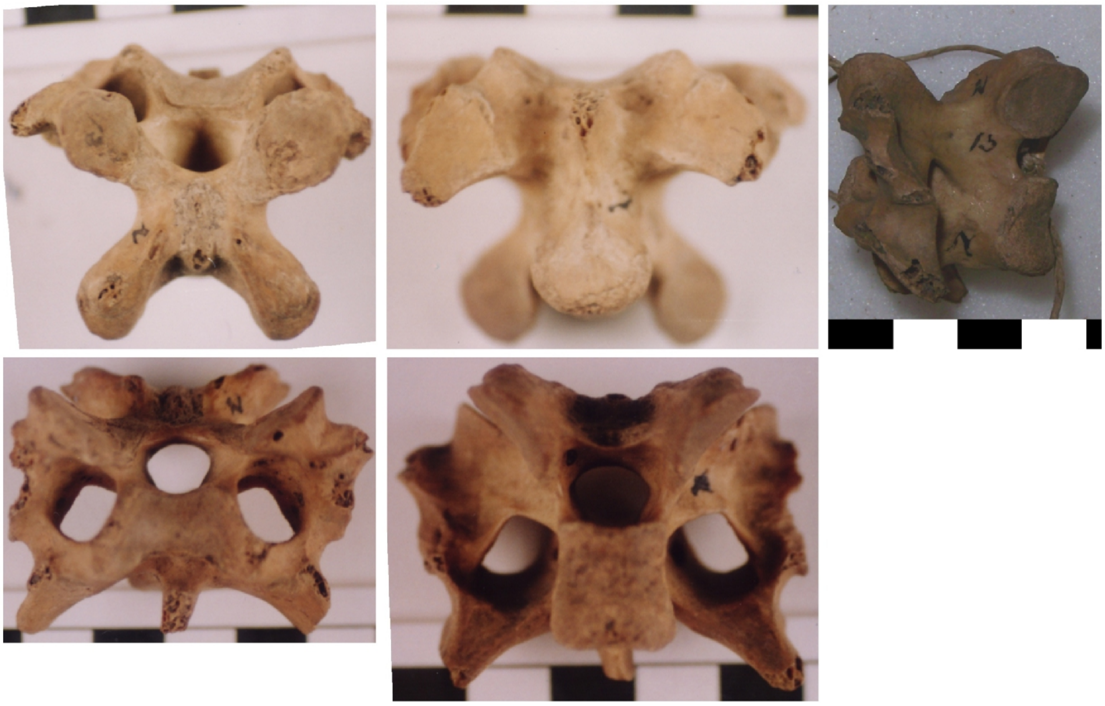

C11 of *Raphus* in dorsal, ventral, lateral, cranial and caudal views (UMZC 415.K specimen; © E. C. Parish, except lateral view which is ○ Jolyon C. Parish).

In *Pezophaps* the eleventh cervical vertebra possesses a pair of carotid processes. These are well developed, with expanded, rounded, slightly roughened extremities and are close together, closer than in the preceding cervical vertebrae. They are inclined caudomedially, with their caudal extremities merging with a pair of ridges which meet in a median longitudinal low ridge. The caudal part of this ridge may form a small cranially directed spur in some specimens (NHMUK A.3505; Newton & Newton 1869, pl.xv, fig.38). The eleventh cervical is the most proximal in the series to show the carotid sulcus bordered by the pair of carotid processes, as the twelfth cervical shows a single median hypapophysis. The prezygapophyses face dorsomedially and slightly cranially. The cervical ribs are long and thick and caudoventrally directed, with blunt, obtuse extremities. The articular surfaces of the postzygapophyses face ventrolaterally. The anapophysis forms a rounded tubercle.

Comparing the eleventh cervical of *Raphus* with that of *Pezophaps*, the vertebra is proportionately shorter in the former. In addition, the eleventh cervical of *Raphus* is wider than it is high; in *Pezophaps* the opposite is the case.

Twelfth cervical

C12 (*Raphus*: Owen 1867, pl.xvii, figs.8, 9 (cf. C12); Chowdhury 2003, fig.VII/27 (cf. C12); Janoo 2005, fig.2a (cf. C12 or C13?); Tschopp *et al*. 2013, fig.10; Claessens *et al*. 2015, fig.28, pls.PL10, D10. *Pezophaps*: Newton & Newton 1869, pl.xv, figs.42-44; Newton & Clark 1879, pl.xliv, figs.5, 6)

The twelfth vertebra of *Raphus* is wider than it is either long or high. The transverse foramina are large. The ansae costotransversaria are thicker than in the eleventh vertebra, especially ventrally. The costal processes are absent, or at least very reduced. The "tubercles of the processus transversus" are located at approximately a level below halfway up the articular faces of the prezygapophyses (Claessens *et al*. 2015). The articular surfaces of the prezygapophyses face dorsally and slightly medially and cranially; those of the postzygapophyses face ventrolaterally. The cranial border of the neural canal is caudal to the cranial articular face of the centrum. The latter is wider than it is tall and has a straight horizontal dorsal margin and a concave ventral one. It curves onto the dorsal face of the centrum, "but not significantly" (Claessens *et al*. 2015, p.60). A fovea cranioventralis is distinguishable, located "immediately caudal" to the cranial articular face and cranial to the hypapophysis (*ibid*.). The ventral margin of the neural canal is more concave than the dorsal one. The neural spine is absent. The large hypapophysis is laterally compressed and is directed cranioventrally. The dorsal margins of the postzygapophyses are more dorsally placed than those of the prezygapophyses. The cristae transverso-obliquae are developed and the articular faces of the postzygapophyses are subcircular. The caudal articular face of the centrum is more oblong than that of the eleventh vertebra, and its ventral width is greater than either its dorsal one or its height.

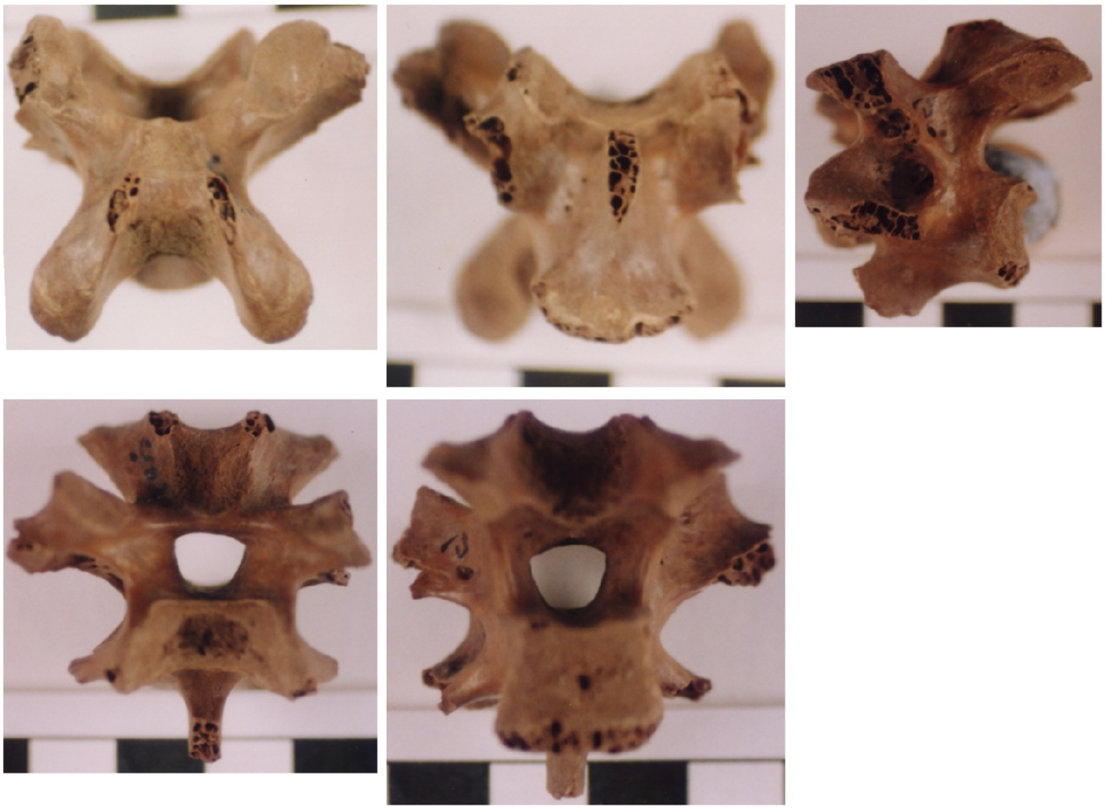

C12 of *Raphus* in dorsal, ventral, lateral, cranial and caudal views (UMZC 415.K specimen; © E. C. Parish). Note: this could be could be C12 or C13, the vertebra being too damaged to allow definitive determination).

A vertebra figured by Owen (1867, pl.xvii, figs.8, 9) might be the twelfth cervical (his "penultimate cervical vertebra" – there are twelve cervicals illustrated in his pl.xv). A hypapophysis is present, which is similar in form to that of the twelfth cervical, as figured by Claessens *et al*. (2015, fig.28) and form of the the neural spine resembles that in Claessens *et al*.'s figure. However, the form of the costal process is quite like that of the eleventh (Claessens *et al*. 2015, fig.27), as is the form of the ansa transversaium and the caudal articular face of the centrum. The middle of the dorsal surface of the neural arch shows an "elliptical, rough, ligamentous surface, which slightly rising in the middle is the sole indication of a neural spine" (Owen 1867, p.55).

The twelfth cervical of *Pezophaps* is similar to that of *Raphus*. It has a very large hypapophysis. The prezygapophyses appear to be longer than in *Raphus* (Newton & Newton 1869, pl.xv, fig.42). The cervical ribs are much reduced and stubby. The anapophyses are also pronounced. The transverse processes are wide and robust (Newton & Clark 1879). Newton & Clark (1879) stated that the "neural processes have not united into a spine, but are present as two thin plates of bone, including a canal" (p.440). As in *Raphus* the twelfth vertebra of *Pezophaps* is wider than it is either long or tall.

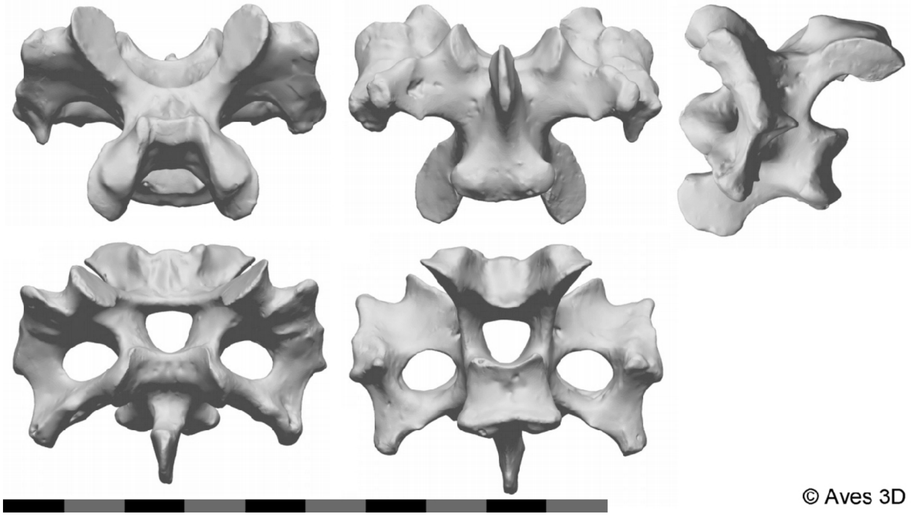

C12 of *Raphus* in dorsal, ventral, lateral, cranial and caudal views (scale in cm; © Aves 3D).

Thirteenth cervical

C13 (*Raphus*: Owen 1867, pl.xxiii, fig.3;[79] Claessens *et al*. 2015, fig.29, pls.PL11, D11. *Pezophaps*: Newton & Newton 1869, pl.xv, figs.45-47; Newton & Clark 1879, pl.xliv, figs.3, 4)

The thirteenth cervical is very similar in form to the twelfth. The ansae costotransversaria are robust, especially ventrally. The costal processes are absent. The transverse processes are located at approximately the level of the ventral margins of the articular faces of the prezygapophyses (Claessens *et al*. 2015). The hypapophysis is developed. The cranial border of the neural arch is located caudal to the cranial articular face of the centrum; the latter does not encroach onto the dorsal surface of the centrum. The fovea cranioventralis is shallow. The neural spine is absent. The articular faces of the postzygapophyses are subcircular. As in the preceding vertebra, the dorsal margins of the postzygapophyses are more dorsally placed than those of the prezygapophyses. The anapophyses are developed. The caudal articular face of the centrum is subsquare, slightly wider than tall.

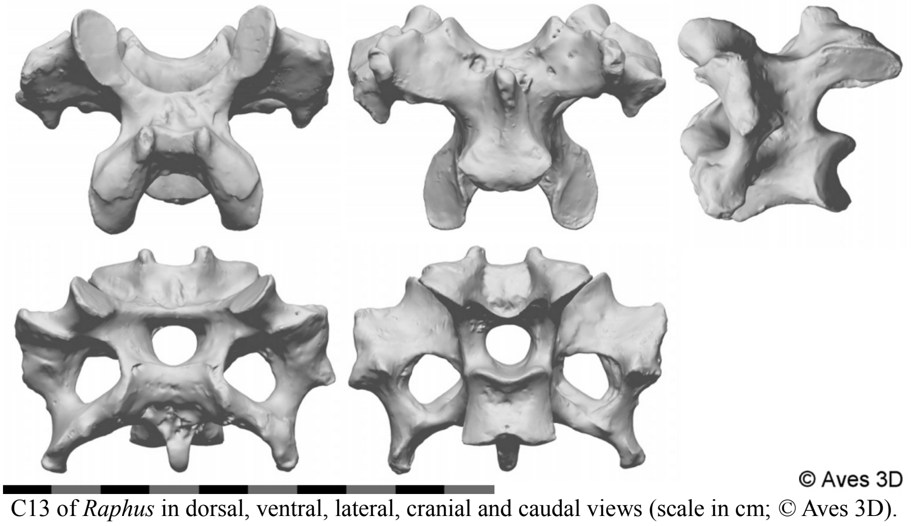

C13 of *Raphus* in dorsal, ventral, lateral, cranial and caudal views (scale in cm; © Aves 3D).

Comparing the vertebral columns of *Raphus* (Thirioux's Port Louis skeleton) and *Pezophaps* (*e.g.*, NHMUK A.3505, A.3506) it would appear that the former has an extra cervical vertebra (giving it fourteen cervicals instead of thirteen found in *Pezophaps*) – this extra vertebra would appear to be the twelfth or thirteenth of the series.

---

[79] This figure appears to depict a sagittally sectioned thirteenth, or possibly twelfth, vertebra (Owen's "lower cervical vertebra") (compare with Claessens *et al*. 2015, figs.28, 29)

The thirteenth cervical of *Pezophaps* resembles the twelfth of *Raphus* and also possesses complete transverse foramina. In NHMUK A.3506 (both sides) and UMZC 415.S, there is a small subtriangular free rib on the thirteenth cervical, whereas that figured by Newton & Newton (1869, pl.xv, fig.45) has complete transverse foramina. Newton & Clark (1879) stated that "in some specimens of this vertebra in the [present] collection [of ten male and twelve female specimens] the canal for the vertebral artery [= transverse foramen] is developed, but in only one instance on both sides" (p.440). The neural spine is similar to that of the first dorsal (the fourteenth vertebra in *Pezophaps*), but is not so developed. It presents dorsally a cranially directed hook (present in both male and female specimens), which may be quite long (as in NHMUK A.3505). The walls of the neural canal are inclined inwards and the dorsal surface arches downwards medially, making its outline sub-cordate. The articular surfaces of the prezygapophyses are elliptical and almost flat; they face dorsomedially and slightly cranially. Those of the postzygapophyses are slightly concave and face ventrolaterally. The hypapophysis is similar to that of the first thoracic vertebra, but is smaller. There are pneumatic apertures on the lateral surface of the thirteenth vertebra between the pre- and postzygapophyses (NHMUK A.3505, A.3506; Newton & Clark 1879, pl.xliv, fig.3).

Fourteenth vertebra

(*Raphus*: Owen 1867, pl.xvii, figs.6, 7; Claessens *et al*. 2015, fig.30, pls.PL11, D11. *Pezophaps*: Newton & Newton 1869, pl.xv, figs.48-50)

The fourteenth of the series is a cervical in *Raphus* and a cervicodorsal in *Pezophaps*.

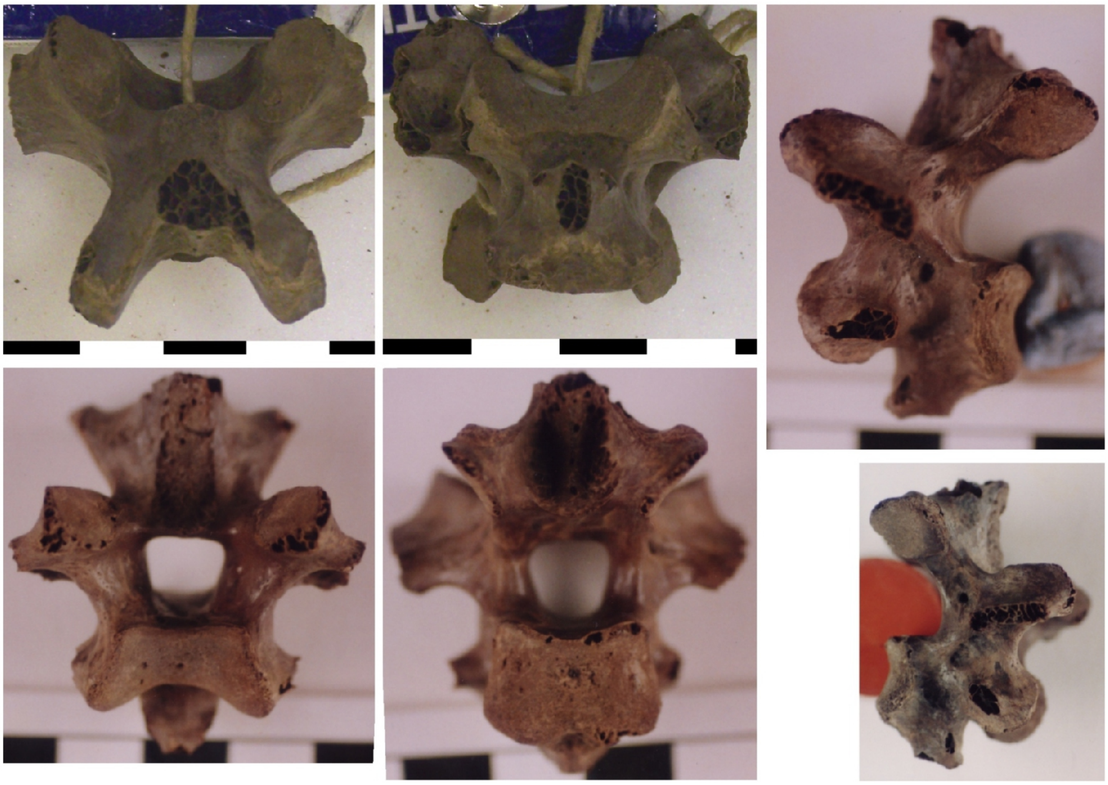

C14 of *Raphus* in dorsal, ventral, lateral, cranial and caudal views (UMZC 415.K specimen; © E. C. Parish, except dorsal and ventral views which are ○ Jolyon C. Parish).

The cranial border of the neural arch is located slightly caudal to the cranial articular face of the centrum and its caudal border projects caudal to the caudal articular face of the centrum (Claessens *et al*. 2015). The neural canal is enlarged cranially and caudally, and is more circular in outline than in the succeeding vertebrae. The neural spine is tall, broad and vertical. The dorsal extremity of this process is slightly pointed, rough and expanded (Owen 1867, pl.xvii, figs. 6, 7). In the Durban skeleton of *Raphus* its dorsal extremity shows a slight, rounded, cranially-directed hook and in Thirioux's Port Louis skeleton and UMZC 415.H the dorsal extremity of the neural spine projects slightly forwards. The cranial margin of the neural spine is longer than the caudal one, which curves to meet the cristae transverso-obliquae or anapophyses. The neural spine shows vertically oblong surfaces cranially and caudally for ligamentous attachment. The transverse processes and robust ansae costotransversaria project lateral to the articular faces of the prezygapophyses (*ibid.*). The tuberculae ansae are developed. The fovea cranioventralis is shallow. The cranial articular surface is approximately twice as wide as tall (*ibid.*). The hypapophysis is ventrally directed, with a slightly expanded and rounded extremity; it is not nearly as large as that of the thirteenth vertebra. The base of the hypapophysis is broad and occupies the middle third of the ventral surface of the centrum; it also presents a pair of laterally directed tubercles at it cranial base (UMZC 415.K; Owen 1867 pl.xvii, fig.7). Claessens *et al*. (2015) stated that the articular faces of the postzygapophyses are directed ventrolaterally[80] "at an angle that is greater than 45° with the horizontal, and are inclined more obliquely than the [articular faces of the postzygapophyses] of the preceding vertebrae, possibly indicating a greater degree of mobility in the sagittal plane" (p.60). Owen (1867) stated that the cranial and caudal articular surfaces of the centrum "indicate freedom and extent of flexure" (p.54). The fourteenth cervical vertebra is much taller and wider than it is long.

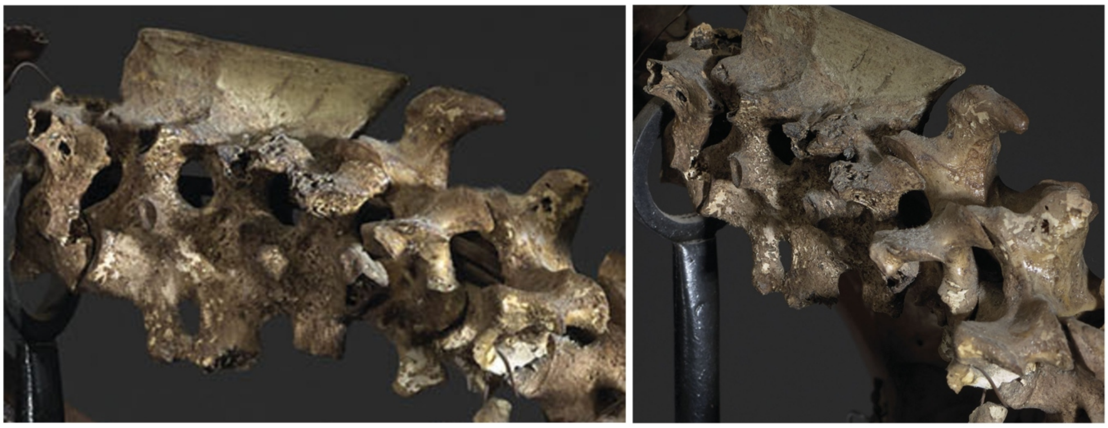

Vertebrae of *Raphus*: 14th and 15th, notarium and 19th (Paul Carié's dodo skeleton (Christie's London, Sale 17492, lot 155; © Christie's 2019).

Owen (1867) referred to the fourteenth vertebra (as shown in his pl.xvii, figs.6, 7) as an "anterior dorsal vertebra" and stated that a pair of free ribs was attached to the vertebra,[81] "indicating the present to be the first of the dorsal series" (p.55). However, the transverse foramina are complete and therefore the fourteenth vertebra is a cervical and not a dorsal, with no free ribs present.

The fourteenth vertebra of *Pezophaps* shows a well-developed neural spine, similar to that of the fifteenth vertebra of *Raphus*, but with a much longer horizontal hook (in both males and females), which is as long as the vertical part of the process. However, the neural spine is not as tall as those of the notarium. In lateral view the vertebra shows three distinct forward pointing projections, that of the centrum, prezygapophysis and hook of the neural spine. The hypapophysis is large and blunt. The transverse processes are well developed, similar to those of the preceding vertebrae. The costal facets are not as well pronounced as in the notarium. The articular surfaces of the prezygapophyses face dorsomedially and slightly cranially; those of the postzygapophyses face ventrolaterally. The incisurae cranialis lamina dorsalis is well developed. The fourteenth vertebra is both taller and wider than it is long.

---

[80] Claessens *et al*. (2015) describe them as facing ventromedially, which does not make sense.

[81] The added outline of the proximal end of an articulating rib ('*pl*') can be seen in pl.xvii, fig.7.

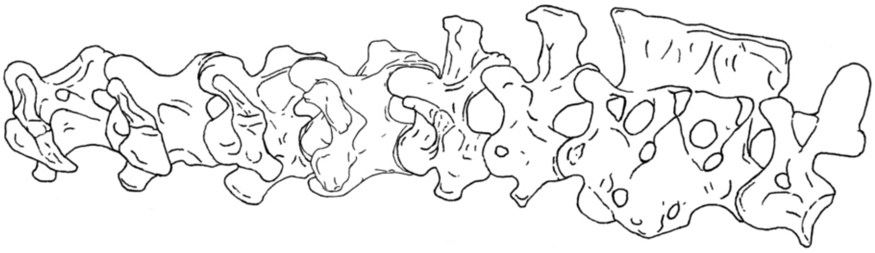

10th to 19th vertebrae of *Raphus* (○ Jolyon C. Parish, 2020).

Cervicodorsal and Thoracic Vertebrae

(*Raphus*: Janoo 2005, fig.2l (centrum))

Raphus has one cervicodorsal (fifteenth of the series) and four thoracic vertebrae. In *Pezophaps* there are two cervicodorsal vertebrae (fourteenth and fifteenth of the series) and three thoracic vertebrae. In *Raphus* the hypapophysis is longest in the seventeenth and smallest in the nineteenth vertebra and *Pezophaps* it is longest in the sixteenth and smallest in the eighteenth vertebra.

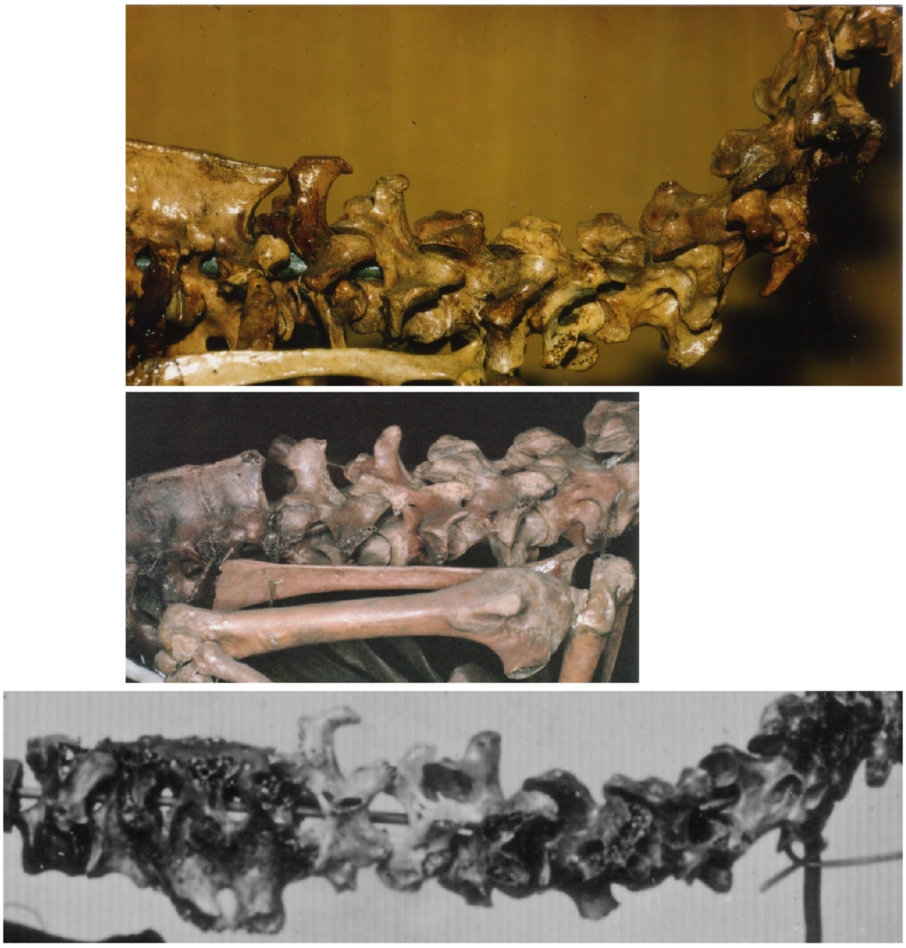

Vertebrae of *Raphus*, lateral view. *Top*: Durban dodo skeleton (© Jan den Hengst), *middle*: UMZC 415.H (○ Jolyon C. Parish, December 2008), *bottom*: a skeleton in Thirioux's collection (photograph (19A) accompanying a letter from E. Thirioux to Alfred Newton, dated 26th December 1901, reversed; © UMZC).

Fifteenth vertebra

(*Raphus*: Claessens *et al*. 2015, fig.31, pls.PL12, D12)

The fifteenth of the series is a cervicodorsal for *Raphus*. The fifteenth vertebra of the series in *Pezophaps* is the first of the notarium (see below).

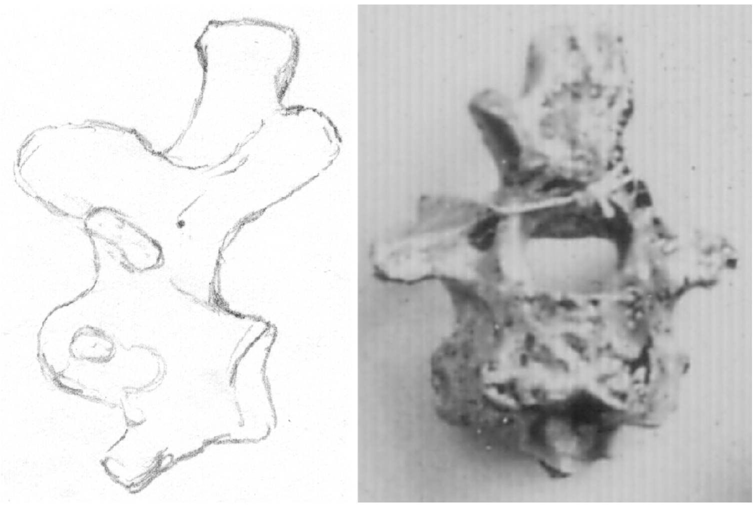

15th vertebra of *Raphus* in lateral and cranial views (lateral: sketch of UMZC 415.H specimen, ○ Jolyon C. Parish; cranial: photograph (14A) accompanying a letter from E. Thirioux to Alfred Newton, dated 14th May 1900, © UMZC).

This vertebra can be seen in *Raphus* in the following skeletons: the Durban, the UMZC (415.H), the two at Port Louis (Thirioux's and Sauzier's), Thirioux's 1902 (see Transcriptions: Thirioux-Newton Correspondence), the MNHN, Paul Carié's, and the Summers Place Auctions, as well as in the Kanaka dodo specimen,[82] and in Newton & Gadow's figure of Sauzier's skeleton (1893, pl.xxxvi, fig.1). The fifteenth vertebra is much taller than it is long, but of near-equal width and height. The fifteenth vertebra is similar to the preceding fourteenth vertebra, but has a taller neural spine with a more pronounced hook. The dorsal extremity of the neural spine is roughened and slightly expanded. The articular faces of the prezygapophyses face craniodorsomedially. The transverse processes are thick and bear the costal articular facets on their ventrolateral faces. The eminentia costolateralis is located on the lateral face of the centrum. The articular faces of the centrum are subsquare. The cranioventrally directed hypapophysis is subrectangular. The articular faces of the postzygapophyses are "relatively round" (Claessens *et al*. 2015, p.61).

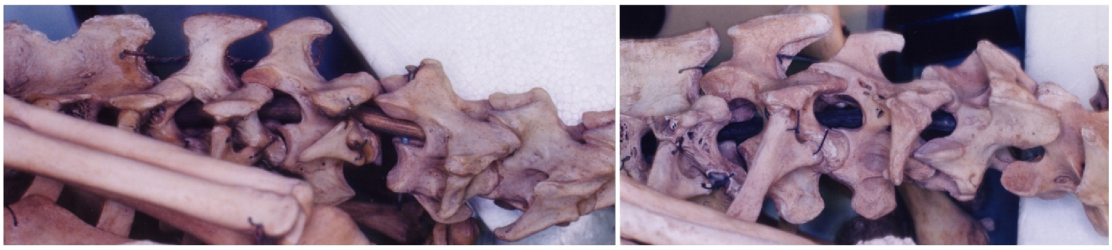

Vertebrae of *Pezophaps*, lateral view. *Left*: NHMUK A.3506 (female), *right*: NHMUK A.3505 (male) (○ Jolyon C. Parish).

Notarium

(Os dorsale) 16th, 17th, 18th (*Raphus*: Owen 1867, pl.xvi, fig.1, pl.xvii, figs.1-5. Claessens *et al*. 2015, fig.32, pls.PL12, D12). 15th, 16th, 17th (*Pezophaps*: Newton & Newton 1869, pl.xv, figs.51-55)

The notarium consists of three ankylosed vertebrae in *Raphus* (the sixteenth, seventeenth and eighteenth) and *Pezophaps* (the fifteenth, sixteenth and seventeenth), fused by their articular faces and neural spines. In *Raphus* the notarial vertebrae are thoracic vertebrae, that is they articulate with ribs whose sternal parts articulate with the sternum. In *Raphus* the cranial articular surface of the centrum is

---

[82] Cf. fifteenth vertebra (pers. obs. from photograph).

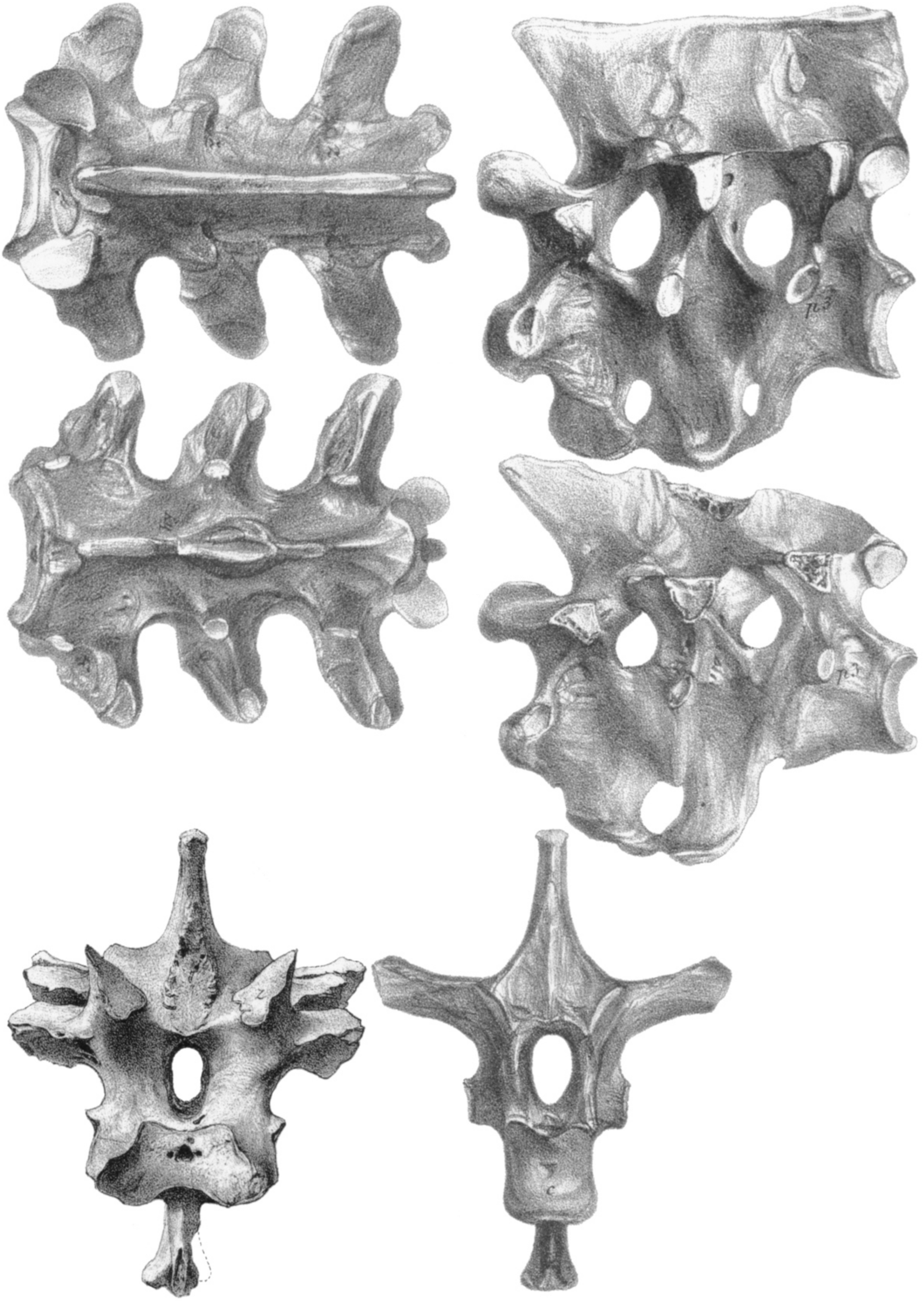

Notarium of *Raphus*, dorsal, lateral, ventral, lateral, cranial and caudal views (Owen 1867, pl.xvi, fig.1; pl.xvii, figs.1-5. Artists: pl.xvi: Edward William Robinson, “E W Robinson del” “W West imp”; pl.xvii: James Erxleben. “From nat on Stone, by J Erxleben” “M & N Hanhart , imp”).

concave transversely in the medial three-fifths and convex transversely in the lateral two-fifths; it is slightly convex vertically (Owen 1867). The articular face is wider ventrally than dorsally and wider than it is tall. The medial portions of its dorsal and ventral borders are concave. The caudal articular surface of the centrum is sub-quadrate, and slightly taller than it is wide. Transversely it is convex and vertically concave. Its dorsal border is concave medially, below the neural canal. The centra of the three notarial vertebrae are wedge-shaped, compressed, and slightly expanded at their ankylosed extremities.

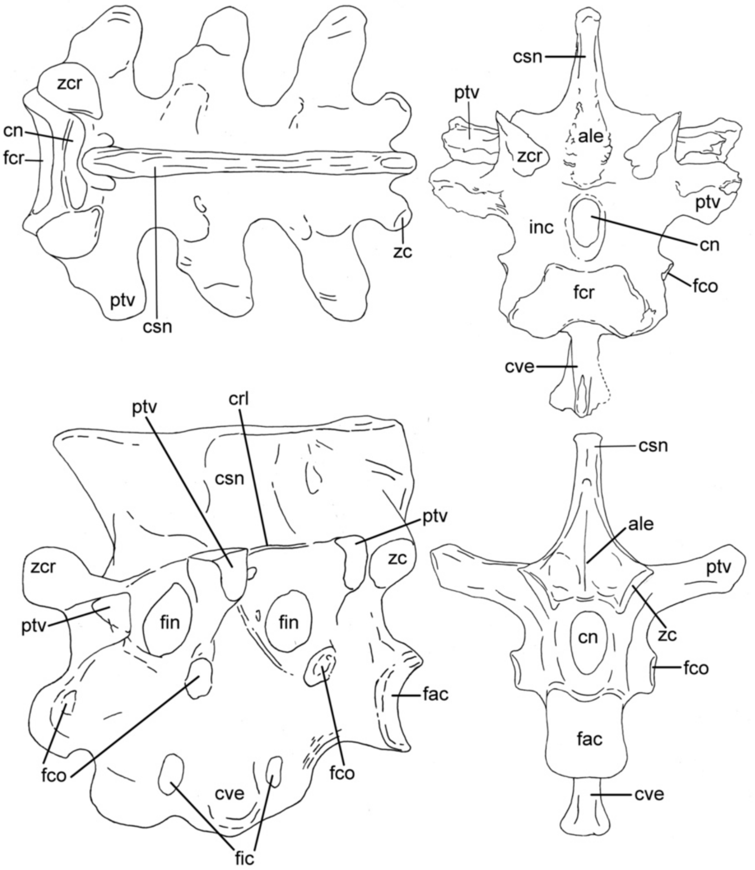

Notarium of *Raphus* (traced from Owen 1867, pl.xvi, fig.1; pl.xvii, figs.1, 2, 4).

The hypapophysis is sub-quadrate in the sixteenth and seventeenth vertebrae; that of the eighteenth is smaller and restricted to the cranial part of the ventral surface of the vertebra. The hypapophyses of the sixteenth and seventeenth vertebrae, and usually the eighteenth, are fused ventrally to form the ventral crest of the notarium (MAD 633; Owen 1867, pl.xvii, fig.1). In so doing they enclose elliptical foramina (foramina intercristata) between them. In some specimens (MAD 6397; Owen 1867, pl.xvii, fig.5) the hypapophysis of the eighteenth vertebra forms only a small forward pointing sharp projection, which is not fused to the preceding hypapophysis.[83] The hypapophysis of the seventeenth vertebra is the longest of the three. Of thirteen notaria examined, nine possessed one foramen (*i.e.*, the hypapophyses of the sixteenth and seventeenth vertebrae were joined) and four had two foramina (the hypapophyses of the sixteenth, seventeenth and eighteenth vertebrae were joined).

The articular surfaces of the prezygapophyses face dorsomedially and slightly cranially; they are oval and flat. Those of the postzygapophyses face ventrolaterally and are oval and very slightly concave. The transverse processes are well developed and long, projecting laterally and slightly caudally. Those of the eighteenth are the longest. Their costal facets are subtriangular and almost flat; they face laterally and ventrally. The costal facets of the costolateral tubercles (eminentiae costolateralia) are elliptical and positioned towards the front of each vertebra. The long axis of the costal articular surface is directed from above obliquely cranioventrally (Owen 1867). The cranial opening of the neural (or notarial) canal is elliptical. There is a slight projection medially on the lateral walls of the canal, above the lower third of the canal. The caudal opening of the canal has an ovoid outline, the narrower end pointing downwards. The two intervertebral foramina are completely surrounded by bone. They are large and elliptical, the cranial one being the larger. They are larger in some specimens than in others (Owen 1867; even though in two specimens (pl.xvii, figs.1, 5) examined by Owen the length of the notarium was the same). The neural spines are ankylosed together completely and are tall and well-formed. Together, they form the spinous (dorsal) crest of the notarium. The cranial margin of the neural spine of the sixteenth vertebra projects forwards, whilst the caudal face of that of the eighteenth is more or less in line with the caudal articular face of the centrum. A pronounced roughened area can be seen at the base of the neural spine of the sixteenth vertebra, the area ligamenti elastici. Some small pneumatic foramina are present at the base of the transverse processes (*ibid*., figs.1, 5). The junctions between the notarial vertebrae are apparent in one notarium of *Raphus* figured by Owen (*ibid*., pl. xvii, fig.2). There are small foramina behind the caudal margins of the postzygapophyses of the sixteenth and seventeenth vertebrae which lead to canals that link with the larger notarial (neural) canal (Owen 1867). In *Pezophaps* foramina are present dorsally, located between the neural spines and the zygapophyses (NHMUK A.3505, A.3506; Newton & Newton 1869, pl.xv, fig.54).

---

[83] Claessens *et al*. (2015) stated that the hypapophysis of the eighteenth vertebra in the Durban skeleton "is very small and restricted to the cranioventral margin of the [centrum]" (p.61).

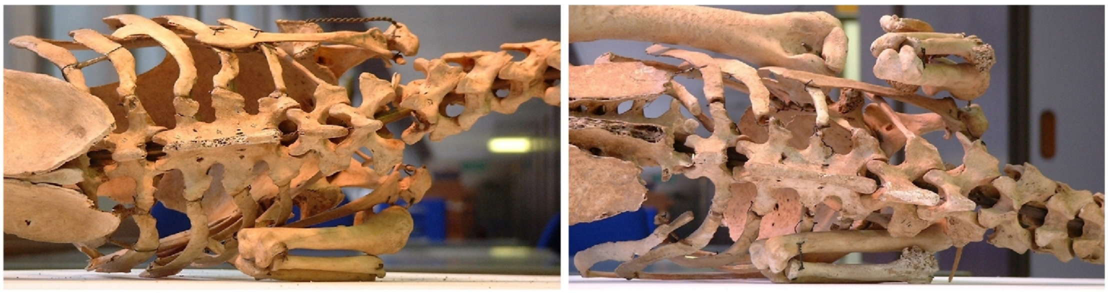

Vertebrae of *Pezophaps*, dorsal view. *Left*: NHMUK A.3506 (female), *right*: NHMUK A.3505 (male) (○ Jolyon C. Parish).

The notarium of *Pezophaps* is very similar to that of *Raphus*, although the articular surfaces and especially the lateral extent of the cranial part of the centrum are proportionately larger in the latter (Newton & Newton 1869). Some specimens of the notarium of male *Pezophaps* are much larger than those of *Raphus*, the ratio of lengths being 10:9 (*ibid*.). Even in the larger specimens the hypapophyses of the fifteenth and sixteenth vertebrae do not join as they do in the dodo. The hypapophysis of the seventeenth vertebra appears to be absent (pers. obs.). The hypapophysis of the sixteenth vertebra is the longest (in both dorsoventral and craniocaudal directions) of the whole vertebral series (pers. obs.; Owen 1878). The cranial projection of the dorsal part of the neural spine of the fifteenth vertebra is hook-shaped, resembling that of the fourteenth, but not quite so well developed, with the dorsal extremity of the neural spine forming a slightly projecting ridge. In some specimens it has a pointed extremity, as in *Raphus* (for example UMZC 415.S; RCSHM/Aves 707; Newton & Newton 1869, pl.xv, figs.51-55), in others it is truncated (UMZC 415.R, NHMUK A.3505). The intervertebral foramina are more round or transversely elliptical compared with those of *Raphus*. The costal facets of the costolateral tubercles can be seen in dorsal view, between the transverse processes; this is not the case in the dodo. The foramina behind the caudal margins of the postzygapophyses of the fifteenth and sixteenth vertebrae appear to be present (see Newton & Newton 1869, pl.xv, fig.54). The cranial and caudal margins of the transverse processes sometimes show irregularities (NHMUK A.3506; Newton & Newton 1869, *ibid*.), which may represent ossified or partly ossified ligaments or tendons. The notarium of *Pezophaps* also shows several pneumatic foramina at the bases of the transverse processes and caudal to the costal foveae (UMZC 635; Newton & Newton 1869, pl.xvi, fig.60).

From the evidence of a damaged notarium (Newton & Newton 1869, pl.xvi, fig.60), it is apparent that the seventeenth vertebra is similar in form to the succeeding free thoracic vertebra (the eighteenth vertebra). UMZC 415.S shows a small foramen between the neural spines of the sixteenth and seventeenth vertebrae and evidence of a suture between the fifteenth and sixteenth vertebrae. Further examples of divisions between the notarial vertebrae are discussed under the section on juveniles (below).

Ultimate presynsacral vertebra

(prepelvic or intermediate vertebra; vertebra thoracica prosynsacralis of Livezey & Zusi 2006) 19th (*Raphus*: Newton & Gadow 1893, pl.xxxvii, fig.2a-c. Claessens *et al.* 2015, fig.13, pls.PL13, D13). 18th (*Pezophaps*: Newton & Newton 1869, pl.xv, figs.56-59; Newton & Clark 1879, pl.xliv, figs.1, 2; Lüttschwager 1961, fig.18)

The last presynsacral vertebra (the nineteenth of the series in *Raphus*) articulates with the notarium cranially and with the synsacrum caudally and is therefore sometimes referred to as the intermediate vertebra. Few specimens of the nineteenth vertebra of *Raphus* are known: those of the Durban and Thirioux's Port Louis skeletons are more complete than that of UMZC 415.H, those of the Thirioux Collection, or that figured by Newton & Gadow (1893, pl.xxxvii, fig.2), and have neural spines and transverse processes present (Chubb 1919a; pers. obs.). Paul Carié's skeleton also has an ultimate presynsacral vertebra and the MNHN skeleton also has a nineteenth vertebra, albeit with an imperfect neural spine. The cranial and caudal articular faces of the centrum are sub-quadrate, with the dorsal border being concave below the vertebral foramen. The caudal articular face has a more rounded outline than the cranial one.

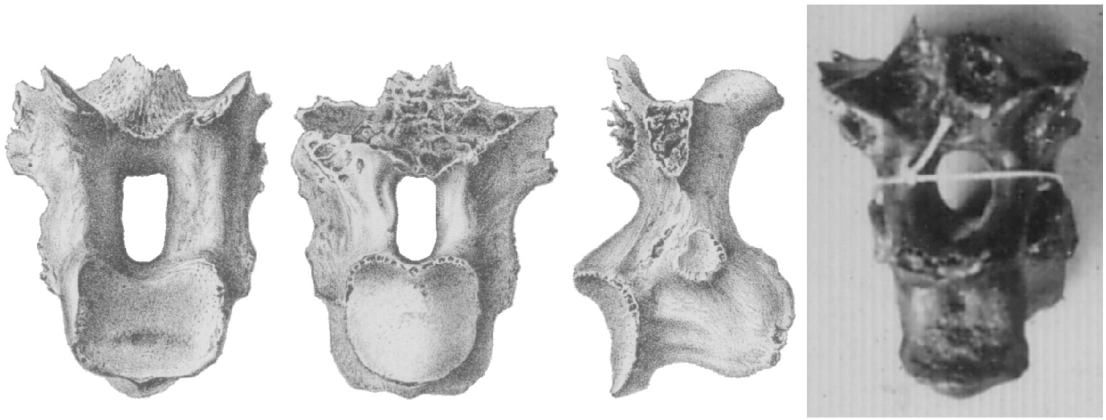

19th vertebra of *Raphus* in cranial, caudal, lateral and caudal views (left three images from Newton & Gadow 1893, pl.xxxvii, fig.2a-c; right image from a photograph (14A) accompanying a letter from E. Thirioux to Alfred Newton, dated 14th May 1900, © UMZC).

The hypapophysis is reduced to a longitudinal ridge. The costal foveae of the costolateral processes are well developed and are located at the base of the neural arch. The neural canal is vertically ellipsoid and slightly rectangular.[84] The neural spine is tall, similar to those of the notarium, and laterally compressed (Thirioux's Port Louis skeleton); in the Durban skeleton its dorsal end is slightly expanded craniocaudally (Claessens *et al.* 2015). In caudal view the last presynsacral shows a pair of slight projections medially on the lateral walls of the neural canal, about halfway up. The articular surfaces of the prezygapophyses face dorsomedially. The transverse processes are well developed.

---

[84] There may be some variation in the form of the neural canal: Thirioux, in a letter to Alfred Newton dated 14th May 1900, stated that one of his specimens of the last presynsacral vertebra ("la 18em vert ou prepelvienne"; now lost) had a round outline to the neural canal, whereas another, as well as that figured by Newton & Gadow (1893, pl.xxxvii, fig.2), had an elongated elliptical one. Furthermore, the length of the nineteenth vertebra in Thirioux's Port Louis skeleton is less than half (10mm) that of the Durban skeleton (21mm), although both have similar widths (50mm and 57mm respectively; Claessens *et al.* 2015, table 5).

In *Pezophaps* the hypapophysis of the last presynsacral vertebra (the eighteenth of the series) is also reduced to a low ridge. The centrum is similar to that of the seventeenth vertebra. The cranial articular surface of the centrum has a semi-circular ventral border, whilst that of the caudal articular surface is more quadrate. Martin (1904) noted that "Remarkably the heart-form of this surface in *Pezophaps* is similar to the form of the cross section of the preceding vertebra" (p.222). Compared with that of *Raphus*, the centrum of the eighteenth vertebra of *Pezophaps* has a more vertically rectangular caudal articular surface. As in *Raphus* the neural canal is vertically ellipsoid, with a slight contraction medially, but it is more circular in outline than that of *Raphus*. The prezygapophyses of the last presynsacral vertebra are more strongly turned inwards in *Pezophaps* than in any other pigeon, including *Raphus* (Martin 1904). The neural spine is slightly longer dorsally than near its base, and is as tall as those of the preceding vertebrae. Its dorsal extremity shows a slight projecting ridge, as in the notarium, and is slightly expanded laterally. The costal facets of the costolateral processes are of sub-reniform shape. The articular surfaces of the postzygapophyses are relatively small and oval, and concave.

It is noteworthy that few specimens of the last presynsacral vertebra are known. The only specimens mentioned in the literature for *Raphus* are in the Durban skeleton and that figured by Newton & Gadow (1893).[85] For *Pezophaps* there were only nine specimens (all damaged) in the collection examined by Newton & Newton (1869), and eleven male and ten female specimens in the collection examined by Newton & Clark (1879). The reason for this bias is not known.

Ribs

The costae incompletae (costae cervicodorsales) articulate with the cervicodorsal vertebrae and the costae completae verae and costae completae spuriae articulate with the thoracic vertebrae.

The allocation and arrangement of ribs in *Raphus* used herein is that of Thirioux's Port Louis skeleton and the Durban skeleton, as these are based on presumed associated material (*i.e.*, from single individuals). In *Raphus* there are one cervicodorsal rib (costa incompleta or costa cervicodorsalis), four true ribs (costae completae verae) and one rib with vertebral and sternal elements in which the latter articulates with the sternal rib cranial to it (costa completa spuria) (Baumel & Witmer 1993).[86]

Pezophaps has six to seven pairs of ribs.[87] The arrangement of ribs in both *Raphus* and *Pezophaps* is given below:

Vertebra	13	14	15	16	17	18	19	20	21	
Raphus			R	RSU	RSU	RSU	RSU	RS*		Thirioux's Port Louis skeleton (Claessens *et al.* 2015)
			R	RSU	RSU	RSU	RSU	RS*	R[88]	Durban skeleton (Claessens *et al.* 2015)
		R	RU	RSU	RSU	RSU	RSU	RS*		Parish (2013, fig.6.1)
Pezophaps		R	RU	RSU	RSU	RS	RS			NHMUK A.3505
	R	R	RSU	RSU	RSU	RSU	R			NHMUK A.3506
		RU	RU	RSU	RSU	RSU	RSU	R		Newton & Gadow (1893, table p.298) ♂
		R	RU	RSU	RSU	RSU	RSU	R		Newton & Gadow (1893, table p.298) ♀

---

[85] Newton & Gadow (1893) stated: "Only one single specimen of this 18th vertebra was found amongst the hundreds of other vertebræ of the Dodo which have passed through our hands. This specimen is unique" (p.302).

[86] According to Verheyen (1957, table pp.21-23), pigeons with thirteen cervical vertebrae have three true ribs, whereas those with twelve cervicals (generally) have four.

[87] Owen (1879) stated, incorrectly, that both *Raphus* and *Pezophaps* have eight pairs of dorsal ribs.

[88] Chubb (1919a) mentions a rib on the right side of the twenty-first vertebra (second synsacral; his twentieth vertebra) and rib facets on the left side. However, this rib is not present in the skeleton today (Claessens *et al.* 2015).

Table summarizing the variation in arrangements of ribs in *Raphus* and *Pezophaps*. Thirioux's Port Louis skeleton (and probably also the Durban skeleton), NHMUK A.3505 and A.3506 were assembled from associated material. Abbreviations: R = vertebral rib only (costa incompleta); RS = vertebral and sternal rib (costa completa vera); RS* = vertebral and sternal rib, the latter not attaching to the sternum but instead to the sternal rib cranial to it (costa completa spuria); U = vertebral rib with an uncinate process. Newton & Gadow's (1893) data for *Pezophaps* was presumably based on UMZC 415.R (♂) and 415.S (♀). Note: the notarium comprises vertebrae 16-18 in *Raphus* and 15-17 in *Pezophaps*; the first two synsacral vertebrae are 20-21 in *Raphus* and 19-20 in *Pezophaps*.

The first (incomplete or cervicodorsal) rib articulates with the fifteenth vertebra in *Raphus* and thirteenth or fourteenth in *Pezophaps*. Sometimes a seventh rib may be present on the twenty-first vertebra (as in the Durban skeleton and a pelvis in the Durban collection), with both vertebral and sternal parts, the latter joining the preceding sternal rib instead of the sternum. Not all individuals possessed the seventh pair of ribs, as the costal facets for their articulation are absent from the twenty-first vertebra in most specimens. Newton & Gadow (1893) stated that the rib of the fourteenth vertebra in male *Pezophaps* has an uncinate process; however, some specimens at least do not (NHMUK A.3505, for example).

The Durban skeleton of *Raphus* has a short rib on the fifteenth vertebra, sternal ribs on the sixteenth to nineteenth vertebrae, an almost sternal rib on the twentieth and a rib on the twenty-first. The rib on the twenty-first is only present on the right-hand side, although the costal facet is seen on the left-hand side (Chubb 1919a). A pelvis in the Durban collection also bears rib facets on the twenty-first vertebra (*ibid.*), and Chubb noted that "in this respect, the Dodo agrees still more closely with *Pezophaps*" (*ibid.*, p.98). However, a rib on the second syndacral vertebra is not a common feature of *Pezophaps*.[89] Owen (1867) stated that the ribs of *Raphus* are broad in proportion to their length, as in pigeons, but are relatively longer in proportion to the dorsal region, "encompassing a more capacious thoracic-abdominal cavity" (p.73).

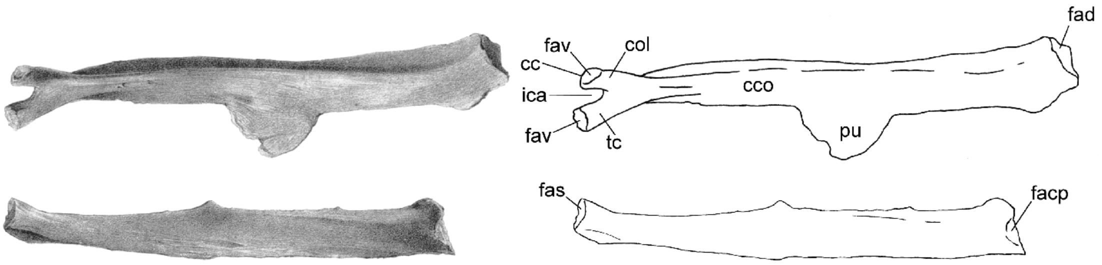

Ribs of *Raphus*. *Top*: vertebral rib, medial view, *bottom*: sternal rib, lateral view (lithographs: Owen 1867, pl.xvi, figs.7b, 3a; artist: Edward William Robinson; "E W Robinson del" "W West imp").

Vertebral Ribs

(*Raphus*: Owen 1867, pl.xv, pl.xvi, figs.2 (in part),[90] 5-11; Claessens *et al.* 2015, figs.16-29, pls.PL16-21, D16-2. *Pezophaps*: Newton & Newton 1869, pl.xvi, figs.62-64; Newton & Clark 1879, pl.xlv, figs.2-6; Ottow 1950, pl.vi, fig.17)

The vertebral ribs are robust, and those of the sixteenth to nineteenth vertebrae possess uncinate processes in *Raphus* (Thirioux's Port Louis skeleton, the Durban skeleton). In *Pezophaps* apparently those of the fifteenth to nineteenth bear uncinate processes (see table above). The uncinate processes in both taxa show variation in size and form, with variation seemingly even occurring between left and right sides (as in Thirioux's Port Louis skeleton; Claessens *et al.* 2015, pls.PL17-PL20): some are flange-shaped whereas others are hook-shaped. The incisure between the head of the rib and the

---

[89] A rib on the twentieth vertebra is seen in UMZC 415.R and is mentioned by Newton & Gadow (1893, table on p.298; male and female skeletons).

[90] It should be noted that one of the vertebral ribs figured by Owen (1867, pl.xvi, fig. 2) is a composite figure. It shows the proximal part of a vertebral rib, but the distal two-thirds actually depicts a pubis (Owen 1871b; although Owen (1867, p.56) stated that this rib was 'entire'); fig.9a likewise depicts a pubis (*ibid.*).

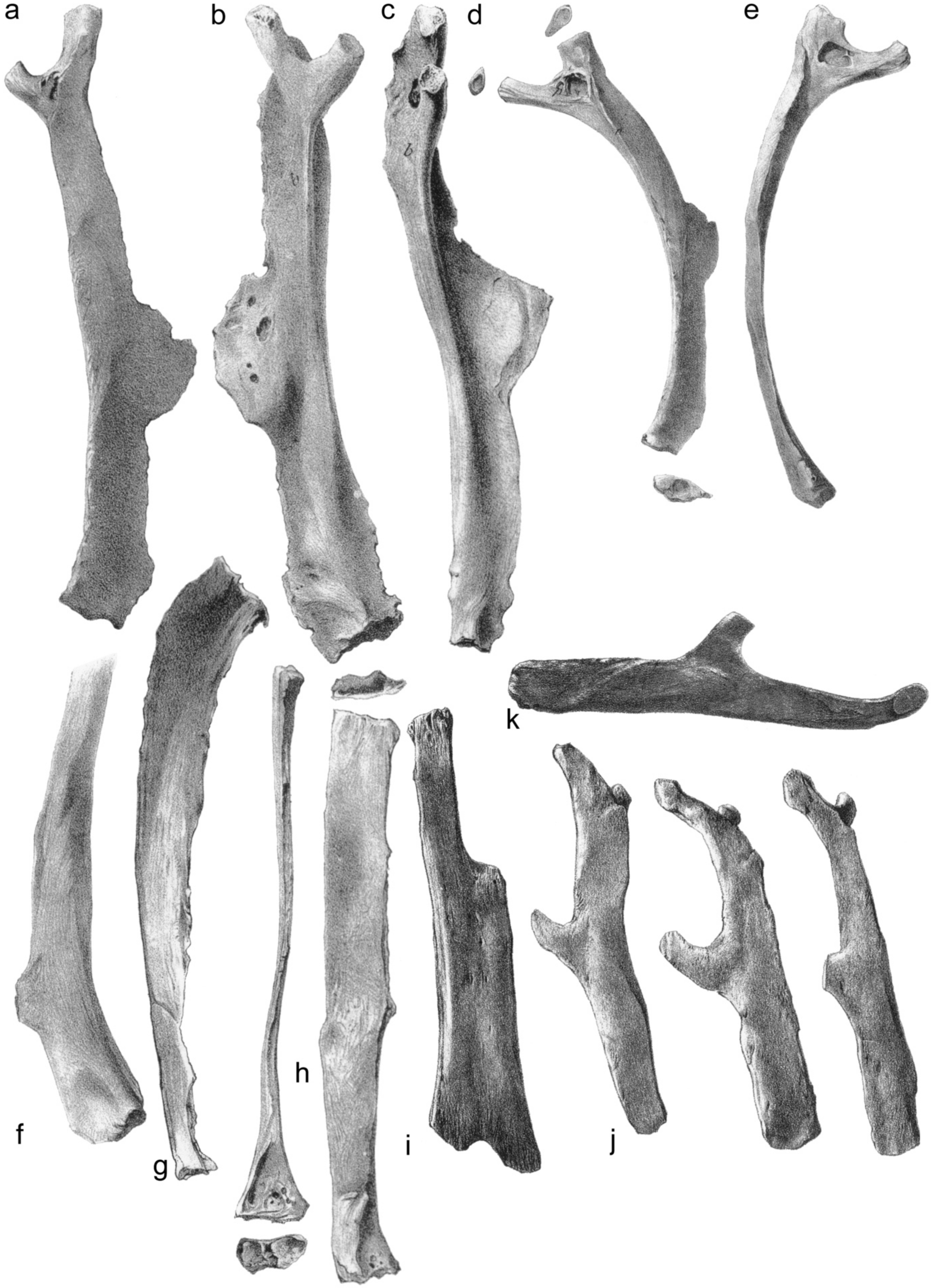

Ribs of *Raphus*: a and d: vertebral rib, lateral and cranial views (Owen 1867, pl.xvi, figs.7, 7a); b and c: vertebral rib, medial and oblique views (Owen 1867, pl.xvi, figs.5, 6); e: vertebral rib, cranial view (Owen 1867, pl.xvi, fig.8); f: distal end of a vertebral rib (Owen 1867, pl.xvi, fig.11); g: sternal rib (Owen 1867, pl.xvi, fig.12); h: sternal rib, cranial, distal, proximal and medial views (Owen 1867, pl.xvi, fig.3d, c, b, e). Ribs of *Pezophaps*: i: sixth and seventh sternal ribs fused together (Newton & Clark 1879, pl.xlv, fig.1); j: fifth, fourth and third vertebral ribs, right side (female; Newton & Clark 1879, pl.xlv, figs.2-4); k: vertebral rib, right side (male; Newton & Newton 1869, pl.xvi, fig.63; artist: George Henry Ford; “G. H. Ford ad nat. lith.” “W. West imp.”). Artists: Owen (1867): Edward William Robinson; “E W Robinson del” “W West imp”; Newton & Clark (1879): “R. Mintern del.” “Mintern Bro^{s}. lith.”

tubercle is wide. In *Raphus* all the ribs have a pneumatic foramen at the cranial face of the proximal extremity of the rib, between the head and the tubercle. Owen (1867, pl.xvi, fig.7) figured a typical vertebral rib: the neck of the rib is lateromedially compressed; its caudal margin is thin, whereas its cranial one is thickened by a "buttress-like ridge" (Owen 1867, p.56) on the medial surface. This ridge passes from the tuberculum down the rib to near its distal end. The medial face of the rib shows a broad depression caudal to the buttress. The caudal edge bears an uncinate process. The distal end is thickened and the facet for articulation with the sternal rib is ellipsoid and rough.

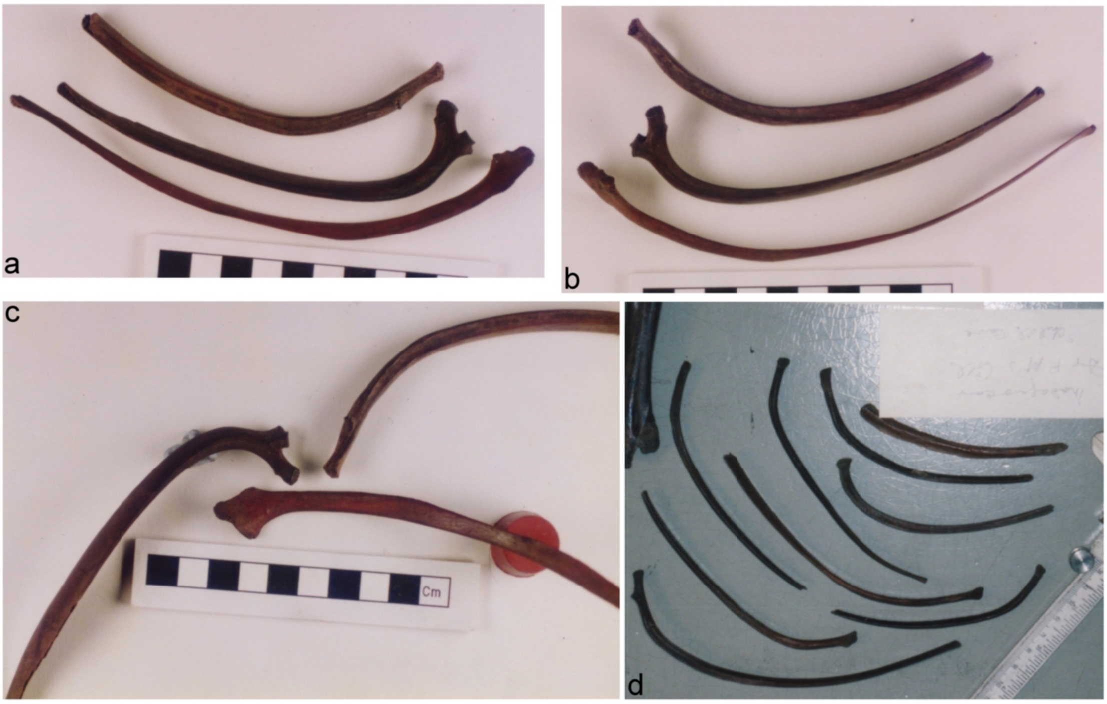

Ribs of *Raphus*. a-c: two vertebral and one sternal (caudalmost sternal) (UMZC 415.K specimens; © E. C. Parish), d: NHMUK specimens (tarsometatarsus at top-left corner; ○ Jolyon C. Parish).

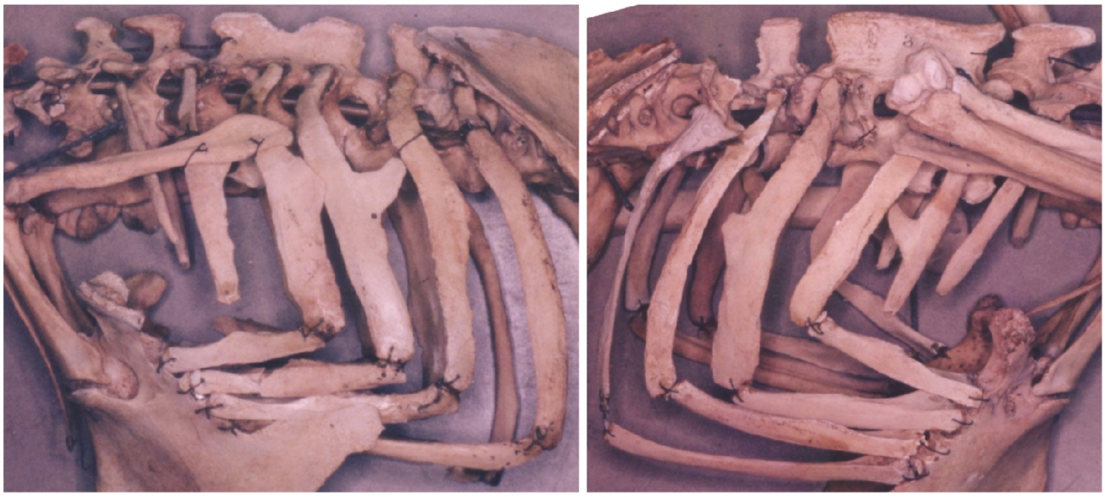

Ribs of *Pezophaps*. *Left*: NHMUK A.3506 (female), left side; *right*: NHMUK A.3505 (male), right side (○ Jolyon C. Parish).

The vertebral rib (the sixth rib in *Raphus*) articulating with the first synsacral vertebra is long. Owen's (1867) deduction that it belongs to the first synsacral vertebra resulted from its length and partial division of the tubercle, and also in the fact that the rib "instead of preserving the regular outward curve of the antecedent one, is more suddenly bent after it emerges beyond the ilium; the lamelliform part thence continued is straighter, and, moreover, shows upon its outer surface a flattened facet, indicative of pressure or friction by the movements to and fro of the thigh over a rib in such a position. Beyond this surface the rib curves in a way not shown in the other specimens" (*ibid*., p.57). Thirioux, in a letter to Alfred Newton (13th November 1901), also mentioned that he had a pelvic rib in his collection. The facet for the sternal rib is almost flat. The rib has neither uncinate process nor any evidence for the former presence of a ligament for the attachment of an uncinate process.

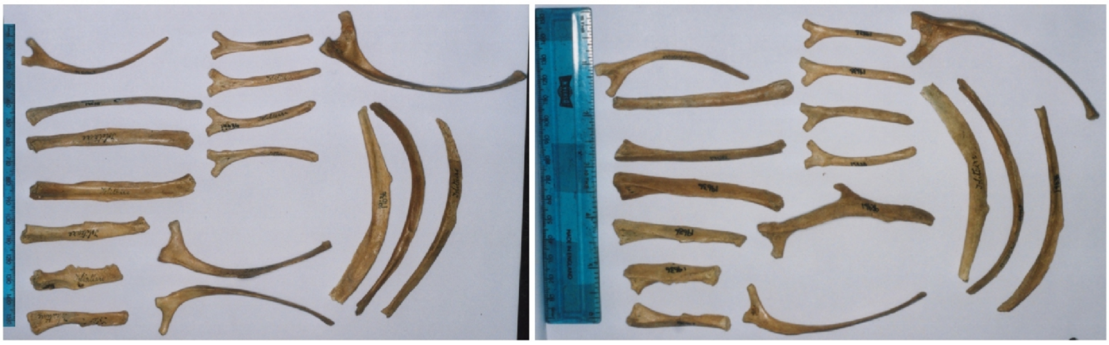

Vertebral and sternal ribs of *Pezophaps* (OUMNH 19636; ○ Jolyon C. Parish, January 2001).

Newton & Newton (1869) stated that the vertebral ribs of *Pezophaps* apparently have proportionately thicker heads and tubercles than those of *Raphus*, especially in specimens from males, many of which are as robust as those of the latter taxon. The pneumatic foramen of the proximal end of the rib is usually present but not always (*ibid*.). The curvature of the ribs is similar to that in *Raphus*, indicating a similar body shape in the two genera. The uncinate processes of *Pezophaps* are generally more slender and hook-shaped than in *Raphus*, with the extremities pointing dorsally in the more developed specimens. Many of the posterior ribs examined by Newton & Newton (1869) showed pressure or friction marks on their outer surfaces, due to movements of the thigh, as sometimes occurs in *Raphus* (see above). As in *Raphus* the second synsacral vertebra sometimes has a rib (Newton & Clark 1879), in, for example, in UMZC 415.R (*ibid*.). The rib of the second synsacral vertebra (Newton & Newton 1869, pl.xvi, fig.64) "appears to have been sometimes coalescent at its sternal extremity with the sternal rib of the preceding" (*ibid*., p.334). This was probably not always the case as a specimen from the opposite side, "most likely from a younger bird" shows (*ibid*., p.334; pl.xvi, fig.61). Caldwell (1875), who found a complete skeleton of a female solitaire in a cavern on Rodrigues, mentioned that in that specimen there were seven vertebral ribs only, with "no trace of the articulation of the eighth dorsal [vertebral] rib [...] though in another specimen there is about ¾ of an inch [19mm] of this rib existing on each side" (p.645).

Sternal Ribs

(*Raphus*: Owen 1867, pl.xv, pl.xvi, figs.3, 12; Claessens *et al*. 2015, figs.16C, D, 37, pls.PL22-26, D22-26. *Pezophaps*: Newton & Newton 1869, pl.xvi, fig.61; Newton & Clark 1879, pl.xlv, figs.7-9; Ottow 1950, pl.vi, fig.17)

Raphus has four to five, and *Pezophaps* four, pairs of sternal ribs which articulate with the costal articular processes of the sternum. In *Raphus* the sternal rib of the twentieth vertebra articulates with that cranial to it, instead of with the sternum (Thirioux's Port Louis skeleton, the Durban skeleton; Claessens *et al*. 2015). An example of this rib may also be present in the UMZC 415.K collection.

In *Raphus* the sternal ribs may be curved or nearly straight. The shortest sternal rib is the most cranial and the longest the most caudal. The articular facet for the vertebral rib is ellipsoid; the sternal end of the rib is expanded. The two convex articular facets for the sternum meet "nearly or quite [...] at an open angle" (Owen 1867, p.57). Owen (1867) mentioned a sternal rib approximately 150mm (6 inches) long – this was probably the fifth sternal rib, which either articulated with the sternum or with the preceding sternal rib.

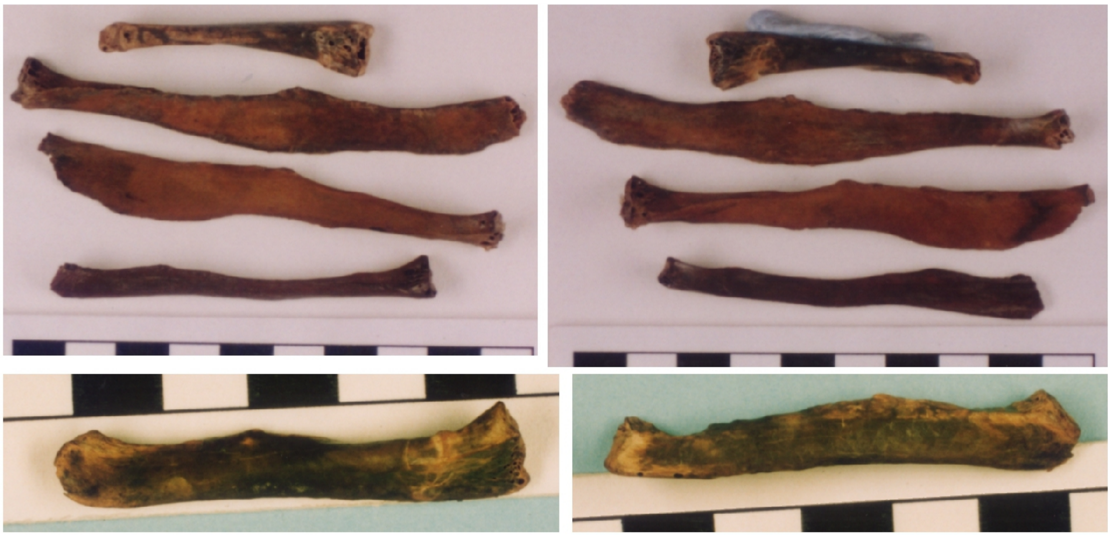

Sternal ribs of *Raphus* (UMZC 415.K specimens; © E. C. Parish).

In *Pezophaps* the sternal rib belonging to the twentieth vertebra, when present, was connected to the preceding sternal rib by a ligament (Newton & Clark 1879): "only three or four examples of these ribs, attached in this manner to each other, have been found, even in the combined collections, and then only on one side or the other. The figure, figure 1 of plate xlv, from a specimen in the British Museum, represents the structure in a very old individual, where the two sternal ribs have become anchylosed" (Newton & Clark 1879, p.440). Figures 7 and 8 of plate xlv of Newton & Clark's (1879) paper represent the first and second ribs on the left side, and figure 9 depicts the third rib on the right side. The sternal ribs of *Pezophaps* are slightly expanded near their middle. The shape of the sternal ribs varies between individuals of *Pezophaps*: in NHMUK A.3506 the first sternal rib shows a rounded triangular projection on its anterior margin at the midlength of the bone; this is much less developed in NHMUK A.3505, which resembles the state seen in *Raphus*.

Synsacrum

(*Raphus*: Claessens *et al*. 2015, fig.34, pls.PL14, D14. *Pezophaps*: Ottow 1950, pl.1, figs.3, 4. See section on pelvis for additional figures)

The synsacrum consists of fused thoracic, lumbar, sacral and caudal vertebrae, and joins with the ilia laterally. Thoracic vertebrae (vertebrae thoracicae; sectio I) are those which possess transverse and costal processes, whereas lumbar vertebrae (vertebrae lumbares; sectio II) lack costal processes. Thoracic and lumbar vertebrae are attached to the preacetabular ilium. Sacral vertebrae (vertebrae sacrales; sectio III) are those with costal processes that extend caudolaterally towards the medial part of the acetabulum. Caudal vertebrae (vertebrae caudales stabiles; sectio IV) also lack costal processes.

The synsacrum is widest near its middle part, decreasing in breadth cranially and caudally. It also decreases in height progressing caudally. Commonly, the synsacrum is composed of seventeen fused vertebrae in *Raphus*[91] and eighteen in *Pezophaps*[92] (see table below). In both *Raphus* (for example, UMZC 415.K) and *Pezophaps* (for example, NHMUK A.1437) there are pneumatic foramina present between the transverse processes on the lateral face of the synsacrum. The fused neural spines of the synsacral vertebrae form the spinous (dorsal) crest of the synsacrum. In *Raphus* the dorsal margin of the ilia meet and fuse together above it; in *Pezophaps* the ilia meet but do not fuse and are separated by a gap, through which the spinous crest can be seen in dorsal view, cranially, and sometimes caudally (as in NHMUK A.3506). Milne-Edwards (1866b) noted that the dorsally extended synsacral crest was a feature found in terrestrial birds.

---

[91] Martin (1904) gave seventeen as the number of synsacral vertebrae in *Raphus*. This number was arrived at by counting the intervertebral foramina, although he states that there may have been individual variation and that sometimes only sixteen vertebrae may be present (see table below).

[92] Martin (1904), Verheyen (1957) and Livezey (1993) stated that *Pezophaps* possessed seventeen synsacral vertebrae, whereas Newton & Newton (1869) and Newton & Clark (1879) gave it eighteen synsacrals. Both totals have been confirmed by personal examination of specimens. Owen (1878) gave the number of synsacrals in *Pezophaps* as sixteen.

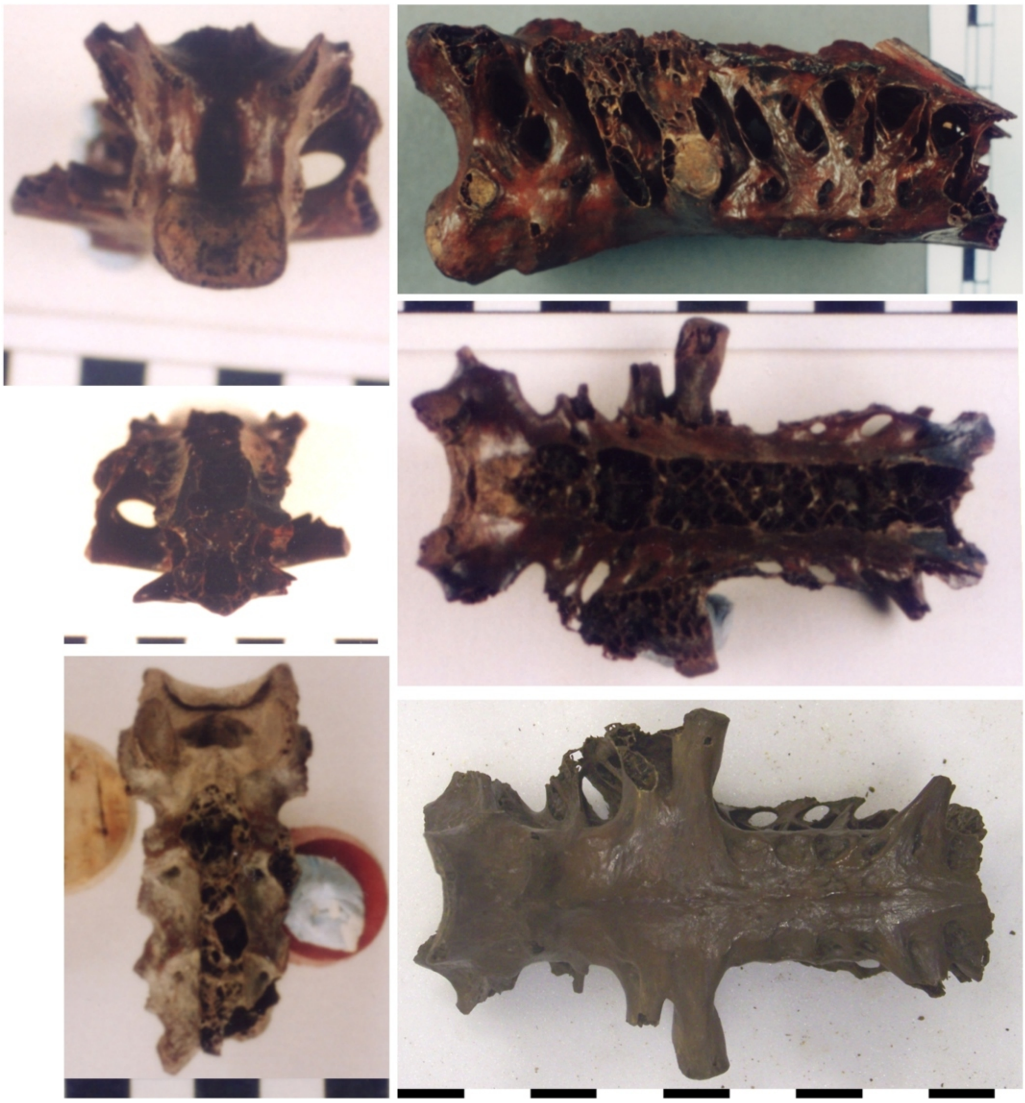

Synsacra of *Raphus* (lacking the caudal ends): cranial, lateral, caudal, dorsal, dorsal and ventral views (UMZC 415.K specimens; scales in cm; © E. C. Parish, except ventral view which is ○ Jolyon C. Parish, December 2008).

Raphus shows strongly developed costal processes on the first and fourth synsacrals, with weaker ones on the second and third synsacrals (Owen 1867, pl.xix, fig.1; UMZC specimens). One exception to this is the pelvis figured by Milne-Edwards (1866b, pl.13, fig.1a), which shows strong costal processes on the first and third synsacrals and a weaker one on the fourth. In *Pezophaps* there are strongly developed costal processes on the first, fourth and fifth synsacrals and weaker ones on the second and third (Newton & Newton 1869, pl.xvii, fig.66; Newton & Clark 1879, pl.xlvi, fig.1). Exceptions to this include NHMUK A.1437 (76.1.28.22), which has reduced costal processes on the fifth synsacral, NHMUK A.3505, in which the first five synsacrals have strongly developed costal processes, and a specimen examined by Newton & Newton (1869) with very thickened costal processes on the fourth synsacral.

The ventral crest of the synsacrum is present as a median narrow longitudinal ridge, most pronounced at its cranial end. In the specimen of the pelvis figured by Owen (1867, pl.xix, fig.1) it is continuous and sharp from the first to the seventh synsacral, and interrupted and not so well pronounced in the succeeding vertebrae; in other specimens (for example UMZC 415.K; Milne-Edwards 1866b, pl.13, fig.1a[93]) it is more or less continuous to the distal end of the synsacrum. That of *Pezophaps* is interrupted and continues to the to fifteenth or sixteenth synsacrals. It is most defined on the first, second, and fourth to eighth synsacrals (NHMUK A.3505, NHMUK A.3506; Newton & Newton 1869, pl.xvii, fig.66; Newton & Clark 1879, pl.xlvi, fig.1). In lateral view the synsacrum of *Pezophaps* (Newton & Clark 1879, *ibid.*) appears to have a more irregular ventral surface of the cranial vertebrae, with transverse rounded ridges marking the boundaries between vertebrae, compared with *Raphus*. The figure of Newton & Newton (1869, pl.xvii, fig.70) shows sharp transverse ridges on the synsacrum of *Pezophaps*, marking the boundaries of the cranial synsacrals, which are cranioventrally directed. *Raphus* (Owen 1867; Milne-Edwards 1866b, pl.14, fig.1; UMZC 415.K) shows a ridge marking the caudal margin of the first synsacral vertebra, which has a short steep cranial face and a long sloping caudal face. The synsacrum of *Raphus* otherwise presents little evidence of transverse ridges demarcating the vertebrae.

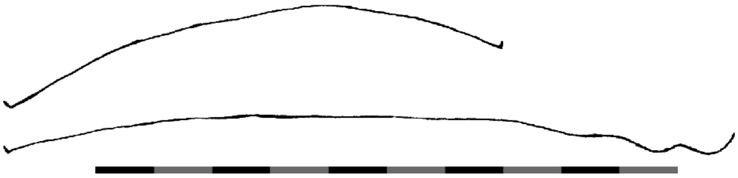

Ventral margins of two synsacra of *Raphus* showing differences in curvature (traced from UMZC 415.K specimens; scale in cm; ○ Jolyon C. Parish).

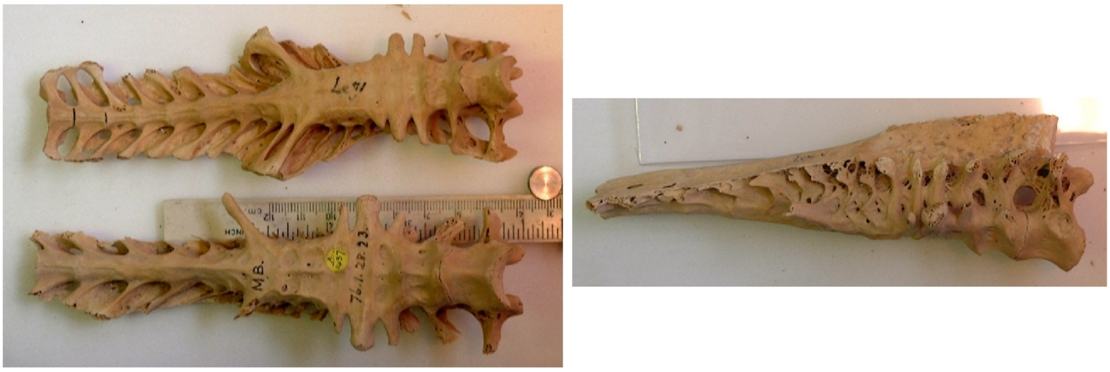

Synsacra of *Pezophaps* in ventral (*left*) and lateral (*right*) views (NHMUK A.1437; ○ Jolyon C. Parish).

The longitudinal curvature of the synsacrum varies: amongst the UMZC specimens (UMZC 415.K) one synsacrum is very slightly concave longitudinally (and has fourteen synsacrals), whereas another is more concave longitudinally.

The proportions of the synsacrum were given by Martin (1904): breadth to length approximately 0.34 for *Raphus* and approximately 0.29 for *Pezophaps*. The table below shows the division of the synsacrum into the types of vertebrae.

	Thoracic	Thoracico-lumbar[94]	Lumbar	Sacral	Caudal	Total
Raphus	1 (2[a])	3 (2)	3-4	1-2	5-9	14-18
	4					

---

[93] Although this specimen is incomplete caudally.

[94] Thoracico-lumbar vertebrae are those with transverse and costal processes but not possessing an articulating free rib.

Pezophaps	1 (2[b])	4 (3)	2-3[d]	1-3[c]	8-9	17-18
	5					

a As in the Durban skeleton and a pelvis in the Durban collections.
b As in UMZC 415.R; Newton & Gadow (1893, table on p.298).
c NHMUK A.1437 (76.1.28.22) has two sacral ribs on the left and one on the right.
d two (n = 1) or three (n = 2).

The following table further enumerates the variation in the numbers of vertebrae comprising the synsacrum in *Raphus*:

	thoracic	lumbar		sacral		caudal				total			
	4	3	4	1	2	5	7	8	9	14	16	17	18
n	27	5	22	15	11	1	6	10	1	1	3	11	2

n = number of specimens exhibiting that number

The first vertebra of the synsacrum (first pelvic, “erste präsacrale Wirbel” of Martin 1904) of *Raphus* resembles that of the preceding free thoracic vertebra (nineteenth). The articular face of the centrum is wider than it is tall, and is transversely concave. The cranially-curving cranial face of the neural spine is roughened by a surface which would have provided ligamentous attachment. The neural spine terminates dorsally in line with the dorsal margins of the cranial part of the ilia, which meet its dorsal extremity laterally. The neural spines of the synsacrum are fused together, their boundaries not being visible in adult specimens, the result being a smooth obtuse longitudinal ridge. The transverse processes are robust and well developed, part of their dorsal surfaces coalescing with the ventral surface of the ilia. Ventrolaterally, at the extremity of each transverse process, is the facet for an articulating rib. The pair of costal foveae are subcircular. The cranial opening of the neural canal is vertically ellipsoid in the majority of specimens (as in a UMZC 415.K synsacrum for example), but is subcircular in some specimens (for example, one examined by Owen 1867; Milne-Edwards 1866b, pl.14, fig.1a; Janoo 1997, pl.24, fig.c). There is a transverse ridge corresponding to the caudal margin of the vertebra. The bilateral depressions cranial to this ridge provided attachment for the caudalmost part of the “subvertebral muscle (longus colli?)” (Owen 1867, p.58).

The second synsacral vertebra (twenty-first in *Raphus*) has both transverse processes and costal processes whose extremities coalesce with the ilia. The costal process is straight and slightly expanded at its base and lateral end. Some specimens show costal foveae for the articulation of a pair of free ribs instead of fused costal processes (for example the Durban skeleton, on both sides, and on both sides of a pelvis in the Durban collections; Chubb 1919a, Claessens *et al.* 2015).[95] However, the vast majority (including Thirioux’s Port Louis skeleton) lack costal foveae on the second synsacral.

The third and fourth synsacral vertebrae (twenty-second and twenty-third in *Raphus*) show robust transverse processes and well-developed straight costal processes, which are thicker and more robust than those of the preceding vertebra. Those of the third synsacral vertebra are directed slightly cranially. Those of the fourth vertebra are thicker. The costal processes of the fourth (UMZC 415.K pelvis; Owen 1867, pl.xix, fig.1), and occasionally the third, synsacrals (UMZC 415.K pelvis; Milne-Edwards 1866b, pl.13, fig.1a, left side) are sometimes not completely fused with the ilia, so that the junctions are visible. The transverse and costal processes of the fourth vertebra form the cranial border of the pars ischiadica of the renal fossa.

The synsacral vertebrae caudal to the thoracic synsacrals decrease in width. The fifth, sixth and seventh synsacral vertebrae (lumbar synsacrals) show no development of costal processes. The transverse processes are thin and long, and slightly caudally and dorsally directed; they also fuse with the ilia. Ventral to, and between, the transverse processes are the pairs of small foramina for the spinal nerves.

Ottow (1950) stated that there is only one sacral vertebra in *Pezophaps*, the second having been converted to a caudal vertebra. However, this feature is subject to variation (see table above). The eighth synsacral vertebra (first sacral vertebra; twenty-seventh of the series) of *Raphus* presents a pair of long costal processes (as seen in the Durban skeleton; Claessens *et al*. 2015),[96] at the widest part of the synsacrum.[97] These costal processes are longer and thinner than those of the fourth synsacral vertebra, and are caudolaterally directed. The lateral extremity of each costal process is expanded and fuses with a prominence on the ventral surface of the ilium which is opposite the caudal part of the acetabulum. In the specimen figured by Milne-Edwards (1866b, pl.13, fig.1a) there appears to be a costal process, as those described above, on the seventh synsacral vertebra, but only on the right side; the eighth has a pair as normal. Occasionally the ninth synsacral possesses costal processes (Martin 1904); this condition is seen in Thirioux's Port Louis skeleton and YPM 2064, where both the eight and ninth synsacrals possess costal processes.[98] The ninth to sixteenth synsacral vertebrae (twenty-eighth to thirty-fifth of the series in *Raphus*) possess only transverse processes (no costal processes being present), which fuse with the ilia laterally. These processes are long and thin, although not as long as those of the eighth synsacral vertebra, and are directed caudolaterally. In the spaces between the transverse processes are sub-elliptical depressions (Owen 1867, pl.xix, fig.1), near the medial ends of which are the elliptical to subcircular foramina intertransversaria, which perforate the synsacrum. These foramina are also visible, to varying degrees, along most of the synsacrum, occurring between the transverse processes. The foramina intertransversaria progressively decrease in number with age in large pigeons, such as *Goura* (Verheyen 1957) and appear to be larger and more numerous in *Raphus* than in *Pezophaps*. The caudal synsacral vertebrae possess no costal processes and are joined to the ilia by their caudolateraly directed transverse processes only. The fused centra of the caudal synsacrals (the ninth to sixteenth synsacrals) are around half the width of those of the preceding vertebrae. Although their width remains roughly constant the centra show a reduction in height, progressing caudally. The caudal articular surface of the centrum of the last, or sixteenth, synsacral vertebra (vertebra synsacri ultima) is transversely oval. The synsacral neural canal of the distal caudals is very small. Thirioux noted[99] that he possessed a synsacrum that did not show any evidence for the attachment of free caudal vertebrae (see Transcriptions: Thirioux-Newton Correspondence).

---

[95] Claessens *et al.* (2015, p.61) mentioned a “fused vertebral rib” on the second synsacral of the Durban skeleton, although from examination of the illustrations the rib does not appear to have been fused to the synsacrum.

In *Pezophaps* the spinous crest of the synsacrum meets the ilia cranially, caudal to this it subsides and then rises slightly and forms a slightly curved ridge, which declines to the caudal extremity of the synsacrum. The crest is more distinct in *Pezophaps* than in *Raphus* (Claessens *et al*. 2015). The cranial articular surface of the centrum of the first synsacral vertebra of *Pezophaps* resembles that of *Raphus*, although it is taller than it is wide, whereas that of the latter is wider than it is tall. The costal facet of the costolateral tubercle, on each side, is placed more cranial than in *Raphus*. The cranial opening for the neural canal is vertically ellipsoid, but sometimes shows a constriction halfway up (Newton & Newton 1869; cf. that of the presynsacral vertebra). The articular surfaces of the prezygapophyses are smaller and directed more cranially and are less vertical than in *Raphus*; the postzygapophyses are also more slender than in the dodo (*ibid*.). The cranial surface of the neural spine is curved and presents a roughened surface for ligament attachment. The first synsacral vertebra is proportionately more elongated in *Pezophaps* compared with that of *Raphus*. In one specimen studied by Newton & Newton (*ibid*.), the costal processes were very thickened, curving ventrolaterally to coalesce with the ventral surfaces of the ilia. This also appears to occur in the second synsacral vertebra figured by Newton & Clark (1879, pl.xlvi, fig.1), in which the costal process on the right side curves caudoventrolaterally, its extremity reaching the ventral margin of the ilium, with which it fuses. The second synsacral vertebra of *Pezophaps* sometimes possesses articular facets for a pair of short free ribs, in both male and female specimens (UMZC 415.R; Newton & Gadow 1893, table on p.298). The second to fourth synsacral vertebrae show much individual variation, as mentioned above; in one specimen studied by Newton &

---

[96] Janoo (1997) stated that it is the seventh synsacral in *Raphus* (fig.11a), and the eighth in *Pezophaps* (fig.11b), which possess costal processes.

[97] The synsacral canal is enlarged where it contains the intumescentia lumbosacralis, forming the bulla intumescentia lumbosacralis (Livezey & Zusi 2006).

[98] As many birds possess two sacral vertebrae, and as Owen's figure (1867, pl.xix, fig.1; Owen & Broderip 1866, pl.vii) depicts only one, Gegenbaur (1871) speculated as to whether either the cranialmost postsacral (postacetabular) vertebra or the caudalmost presacral (preacetabular) vertebra were in fact a 'retrogressed' ('rückgebildeten') second sacral (acetabular) vertebra, but concluded that it was not possible to determine this.

[99] Letter to Alfred Newton (12), 29th November 1900. This specimen is depicted in a photograph (13A) accompanying a letter dated 31st January 1901.

Newton (1869; that mentioned above, with the abnormal costal processes of the first synsacral), the third and fourth synsacrals possessed thickened costal processes. In another specimen examined by them the transverse process of the right side of the fifth synsacral was thickened "so as to present the appearance of a thickened pleurapophysis [= costal process], while on the left it is of the ordinary character" (*ibid*., p.335). The intervertebral foramen is larger in *Pezophaps* than in *Raphus* (Claessens *et al*. 2015).

The costal processes of the fourth and fifth synsacrals do not fuse completely with the ilia, so that the junction between them is visible. The ninth synsacral[100] shows well developed costal processes, at the widest part of the synsacrum. They are caudolaterally directed and expanded towards their lateral ends, their extremities fusing with the ilia directly dorsal to the acetabulum (unlike the case in *Raphus*, where they join the ilia caudodorsal to the acetabulum).

The transverse processes of the caudal synsacrals are stouter and less lamelliform than those of *Raphus*. The sub-elliptical depressions between the transverse processes are shorter than those of *Raphus* due to "the more convex form of the posterior portion of the pelvis" (Newton & Newton 1869, p.336). The fused caudal vertebrae are proportionately wider than those of the dodo, the proportional widening becoming more apparent towards the caudal extremity of the synsacrum (*ibid*.). The last six fused caudals are of the same width, as in *Raphus*, and the first three of these are separated from the ilium on each side by a depression on the dorsal surface in older individuals, and "by a slight interval in younger ones" (Newton & Clark 1879, p.442). The last three synsacral caudals are not attached laterally to the ilia, whereas in *Raphus* they are fused to the ilia on each side. The caudal extremity of the spinous crest of the synsacrum shows a small lozenge-shaped partly articular and partly syndesmotic surface, which joins the cranialmost free caudal vertebra. The centrum of the last synsacral vertebra projects caudally (pers. obs., Newton & Newton 1869). The first free caudal vertebra may become fused to the synsacrum at the ends of the transverse processes and centrum (as seen in NHMUK A.3506), thus increasing the total number of synsacral vertebrae from eighteen to nineteen.

Caudal Vertebrae

(*Raphus*: Chubb 1919a, fig.1.[101] Claessens *et al*. 2015, figs. 16E & F, 35, pls.PL15, D15. *Pezophaps*: Newton & Clark 1879, pl.xlvi, figs.1, 2; Owen 1879, pl.iv, figs.1, 2)

There are six free caudal vertebrae present in *Raphus*. The free caudal vertebrae and pygostyle are known for *Raphus* in the Durban (Chubb 1919a; Claessens *et al*. 2015), the two Port Louis (Claessens *et al*. 2015) and possibly also the Stuttgart skeleton (no. 11910; Stresemann 1958).[102] The skeleton in the UMZC collections (UMZC 415.H) preserves three free caudals and there are also five free caudals in the UMZC 415.KK collection.

The transverse processes of the free caudal vertebrae are well developed and are directed caudolaterally to differing degrees; they are longest in the sixth free caudal (Claessens *et al*. 2015). The neural spines are also developed and are longest on the first three free caudals (Claessens *et al*. 2015). The cranialmost free caudal vertebra[103] of Thirioux's Port Louis skeleton possesses a pneumatic recess on the lateral surface of the centrum. The tail of the Stuttgart skeleton shows well-developed haemal processes on the fifth and sixth free caudals, as in other large birds (Baumel & Witmer 1993) and the first and second free caudals show short caudal zygapophyses.

---

[100] The seventh, eighth or ninth, "most generally in the eighth", according to Newton & Newton (1869, p.335).

[101] The caudal vertebrae and pygostyle the skeleton figured by Owen (1867, pl.xv, fig.1) are guesswork and not based on actual specimens.

[102] The Stuttgart skeleton has six free caudal vertebrae plus a pygostyle. However, they look somewhat different from those of other specimens, especially in the development of the zygapophyses and haemal processes (these latter not seen in any other specimens). The free caudal vertebrae and pygostyle of the Stuttgart skeleton have evidently been painted (presumably to match the pelvis), but whether they are original, casts, or even belong to *Raphus* is unknown. According to Lambrecht (1933; pers. comm. from Fritz Berckhemer to Kalman Lambrecht), the skeleton has only the top of the cranium, the ribs, and the toes restored.

[103] Vertebra caudalis postsynsacralis of Livezey & Zusi (2006).

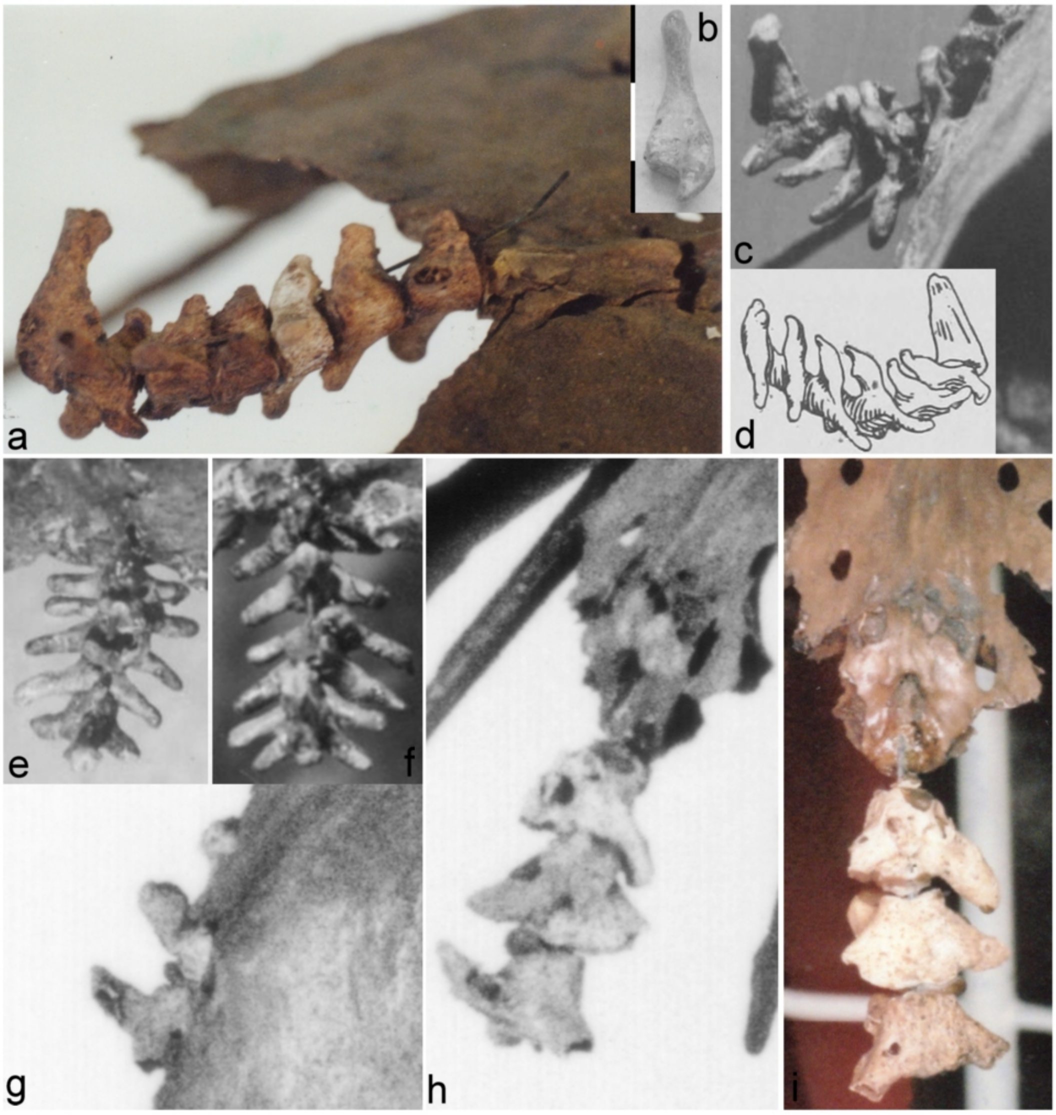

Caudal vertebrae and pygostyle of *Raphus*. a: Thirioux's Port Louis skeleton, lateral view (© Jan den Hengst), b: a pygostyle from Thirioux's collection, lateral view (photograph (13A) accompanying a letter from E. Thirioux to Alfred Newton, dated 31st January 1901, © UMZC), c: Durban skeleton, lateral view (© Durban Natural Science Museum), d: Durban skeleton, lateral view (Chubb 1919a, fig.1), e and f: Durban skeleton, dorsal views (© Durban Natural Science Museum), g and h: UMZC 415.H, lateral views (© UMZC), i: UMZC 415.H, ventral view (with distal synsacrum in dorsal view; ○ Jolyon C. Parish, December 2008).

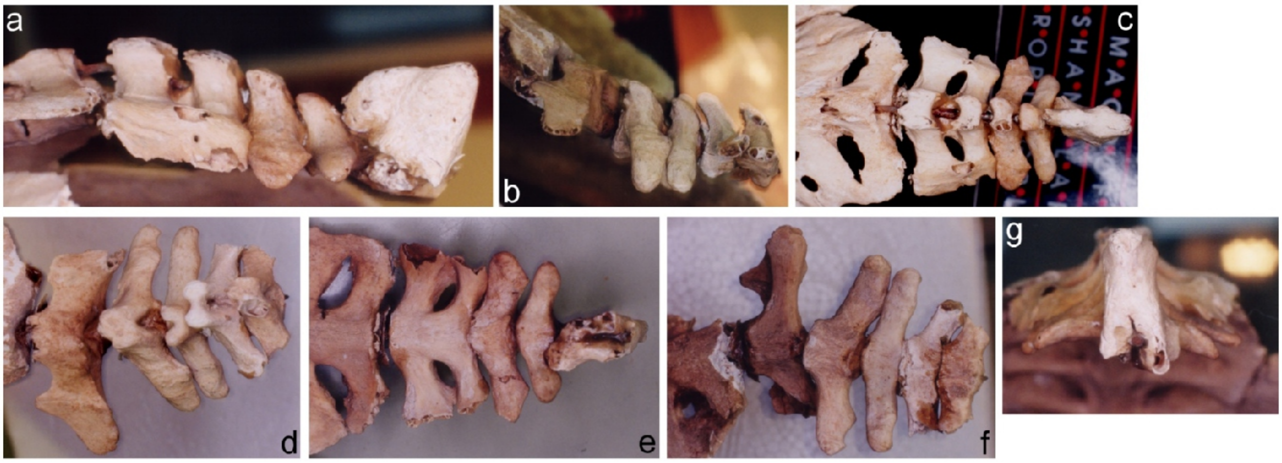

Caudal vertebrae and pygostyle of *Pezophaps*. a and b: lateral views (NHMUK A.3506, A.3505 respectively), c and d: dorsal views (NHMUK A.3506, A.3505 respectively), e and f: ventral views (NHMUK A.3506, A.3505 respectively), g: caudal view (NHMUK A.3506) (○ Jolyon C. Parish).

The pygostyle[104] of *Raphus* is more slender and has a more pointed dorsal end compared with other pigeons, including *Pezophaps*, although there is variation in its form. Claessens *et al*. (2015) described the pygostyle in *Raphus* as "flattened proximally but rounded towards the distal end, with a broad basis pygostyli" (p.61). The pygostyle lamina (lamina pygostyli) has been lost, or at least much reduced, in both *Raphus* and *Pezophaps*, and in the latter the pygostyle has been reduced to a stub of bone. The pygostyle of the Stuttgart skeleton has a small foramen on the lateral surface, dorsal to the articulatory face and another caudal to it. A possible pygostyle was present in the Thirioux Collection, described as "Os inconnu". Thirioux noted that the bone had evidence of an articular surface ("traces d'insertion") at the base.[105]

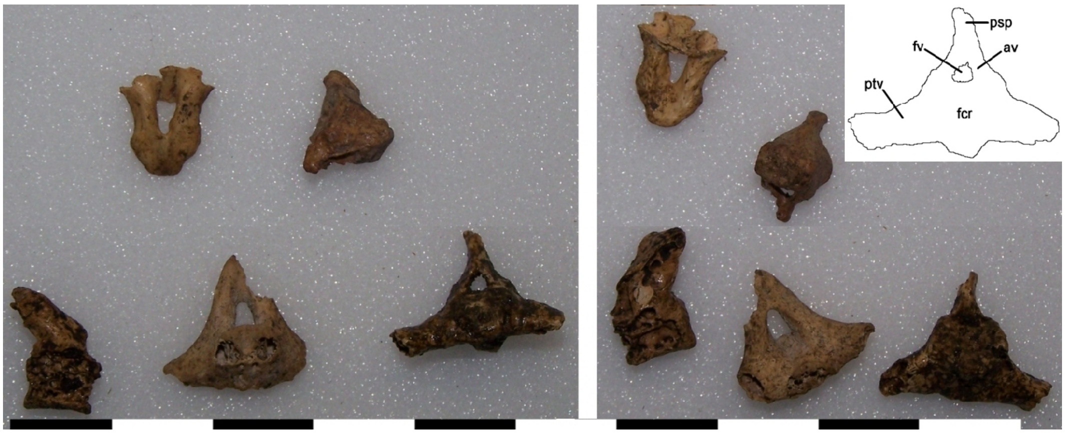

Caudal vertebrae of *Raphus* (UMZC 415.KK specimens; scale in cm; ○ Jolyon C. Parish, December 2008).

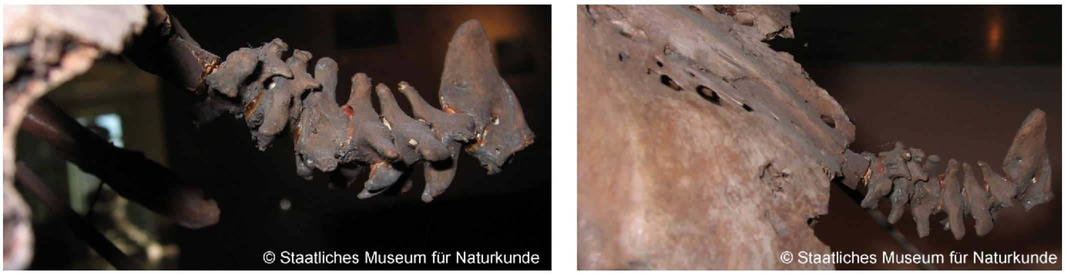
© Staatliches Museum für Naturkunde
© Staatliches Museum für Naturkunde

Caudal vertebrae of the Stuttgart skeleton of *Raphus* (11910), lateral views (© Staatliches Museum für Naturkunde, Stuttgart).

Pezophaps has five (NHMUK A.3505, NHMUK A.3506) or six (RCSHM/Aves 706) free caudals. The neural spines of the caudal vertebrae are weakly developed, similar to that of the last caudal vertebra of the synsacrum. The pygostyle is taller caudally than cranially (caudal height slightly greater than cranial height: Newton & Clark 1879, pl.xlvi, fig.2; caudal height around five-thirds that of the cranial: NHMUK A.3506), and laterally compressed (Newton & Clark 1879, pl.xlvi, fig.2).[106] The length of the pygostyle is almost the same as its height. A slight process projects cranially from its ventral surface under the centrum of the preceding vertebra. Ventrally the pygostyle of NHMUK A.3506 shows a median longitudinal fovea or sulcus, which was presumably vascular (see Livezey & Zusi 2006: 1025). Looking at the figures in Claessens *et al*. (2015, pls.PL15, D15), it appears that *Raphus* may be variable in this character. In *Pezophaps* the transverse processes of the free caudal vertebrae are well developed and are directed laterally and slightly caudally. In NHMUK A.3506 the proximal free caudal is fused to the last caudal of the synsacrum by the extremities of its transverse processes, centrum and partly by its neural spine. The next two free caudals are also fused together at the ends of their transverse processes and centra; the final two caudals are separate. There is no sign of any hypapophyses in the caudals of *Pezophaps*. In Newton & Clark's figure (1879, pl.xlvi, fig.1) the second and third free caudal vertebrae also show fusion at the ends of their transverse processes.

---

[104] Coccyx (Owen 1878).

[105] Letter from Thirioux to Alfred Newton (13A) dated 31st January 1901: "Os inconnu (il porte des traces d'insertion dans l'angle du bas et parait avoir appartenu à ces oiseau".

[106] Slater ("Abstract from H. H. Slater's Report, on Rodriguez-Collection", Royal Society Transit of Venus Expeditions. Correspondence and papers relating to distribution of collections and preparation of reports 1875-1876, DF 202/9, NHMUK General Library) mentioned that he only found a single pygostyle during his searches.

Pelvis (Os coxae)

(*Raphus*: Owen 1867, pl.xv,[107] pl.xvi, figs.2 (in part), 9a, pl.xix, figs.1, 2;[108] Milne-Edwards 1866b, pl.13, figs.1, 1a, pl.14, fig.1, 1a; Newton & Gadow 1893, pl.xxxv, figs.1a, 1b; Martin 1904, fig. S[4]; Rijsdijk *et al*. 2009, fig.3g; Meijer *et al*. 2012, fig.5a; Claessens & Hume 2015, fig.7; Claessens *et al*. 2015, figs.4, 53, 54, pls.PL14, D14; Brown 2020, fig.3. *Pezophaps*: Newton & Newton 1869, pl.xvi, fig.65, pl.xvii, figs.66-69, pl.xviii, fig.70 (same specimen as figs.66-69); Newton & Clark 1879, pl.xlv, fig.13, pl.xlvi, fig.1, pl.xlvii, figs.1, 2; Martin 1904, fig.T[4]; Ottow 1950, pl.ii, figs.5,6)

Complete, or near-complete, pelves are known in the two Port Louis skeletons and the Durban skeleton. The pelvis of *Raphus* is broad and fairly flat in its caudal part.[109] In *Raphus* the preacetabular part of the pelvis is slightly shorter than the postacetabular part (Claessens *et al*. 2015). Martin (1904) gave the ratio of the maximum width of the dorsal surface of the pelvis to the length of the synsacrum for *Raphus* and *Pezophaps* as 0.81 and 0.71 respectively.

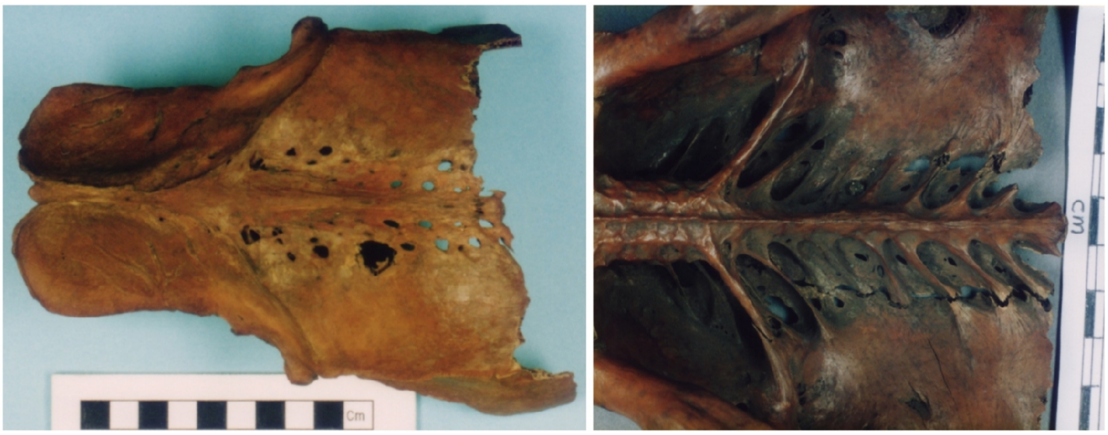

Pelvis of *Raphus* in dorsal and ventral views (UMZC 415.K specimens; © E. C. Parish).

The cranial part of the ilium of *Raphus* is narrow and concave. Its cranial border is slightly thickened and convex cranially, and extends cranially beyond the fused neural spines of the synsacral vertebrae. The rounded angular cranial margin provided attachment for m. sartorius and m. iliotrochantericus. The ilia meet medially above the second and third synsacral vertebrae and fuse with these (pers. obs.; Owen 1867). The pronounced dorsomedial edges of the preacetabular ilia (the dorsal iliac crests) join to from the median dorsal crest (carina iliacae dorsales: Livezey & Zusi 2006). Progressing caudally they diverge, forming the ridge dividing the cranial from the caudal part of the ilium on each side. Where the ilia meet the spinous crest of the synsacrum[110] the roof of the iliosynsacral canals are formed. These canals, on each side of the synsacral spinous crest, widen and open cranially between the transverse

---

[107] The cranial and acetabular parts of the pelvis figured by Owen (1867, pl.xv) are accurately depicted. The caudal end, however, is not, as this part was unknown at the time of drawing due to the imperfection of specimens to hand.

[108] It should be noted that the vertebral rib figured by Owen (1867) in plate xvi, figures 2 is a composite figure. The distal two-thirds of the figure actually shows a pubis. Figure 9a likewise depicts a pubis (Owen 1871b).

[109] This feature is apparent in many contemporary illustrations of the dodo, such as Van-der-Venne (1626), Savery-BM and the sketches of the *Gelderland* artists (1601) (see Parish 2013)..

[110] Crista spinosa synsacri. The crête iliosynsacrale of Janoo (1997).

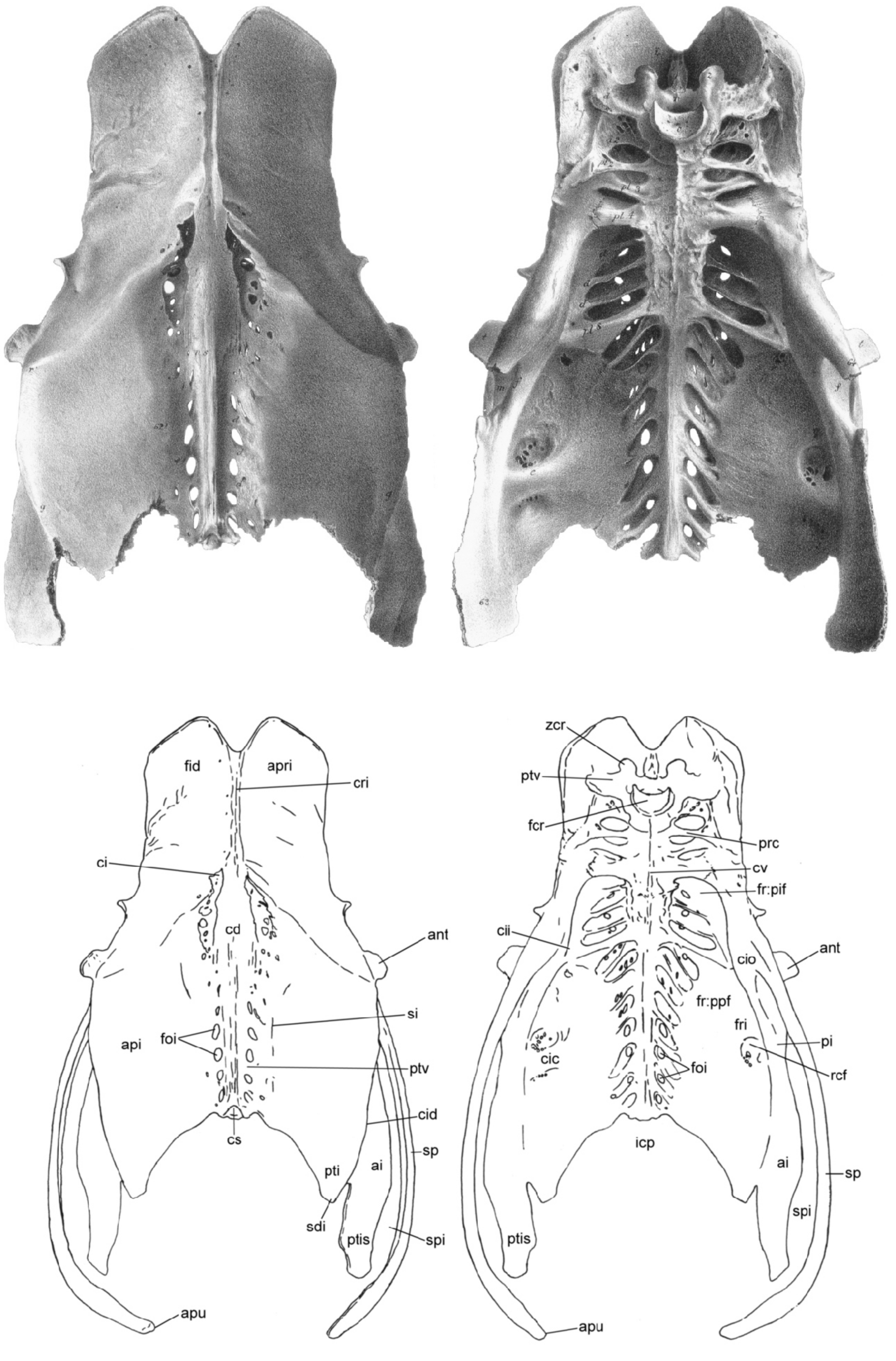

Pelvis of *Raphus* in dorsal and ventral views (lithograph: Owen 1867, pl.xix, figs.1, 2; “J Smit lith” “M & N Hanhart , imp”).

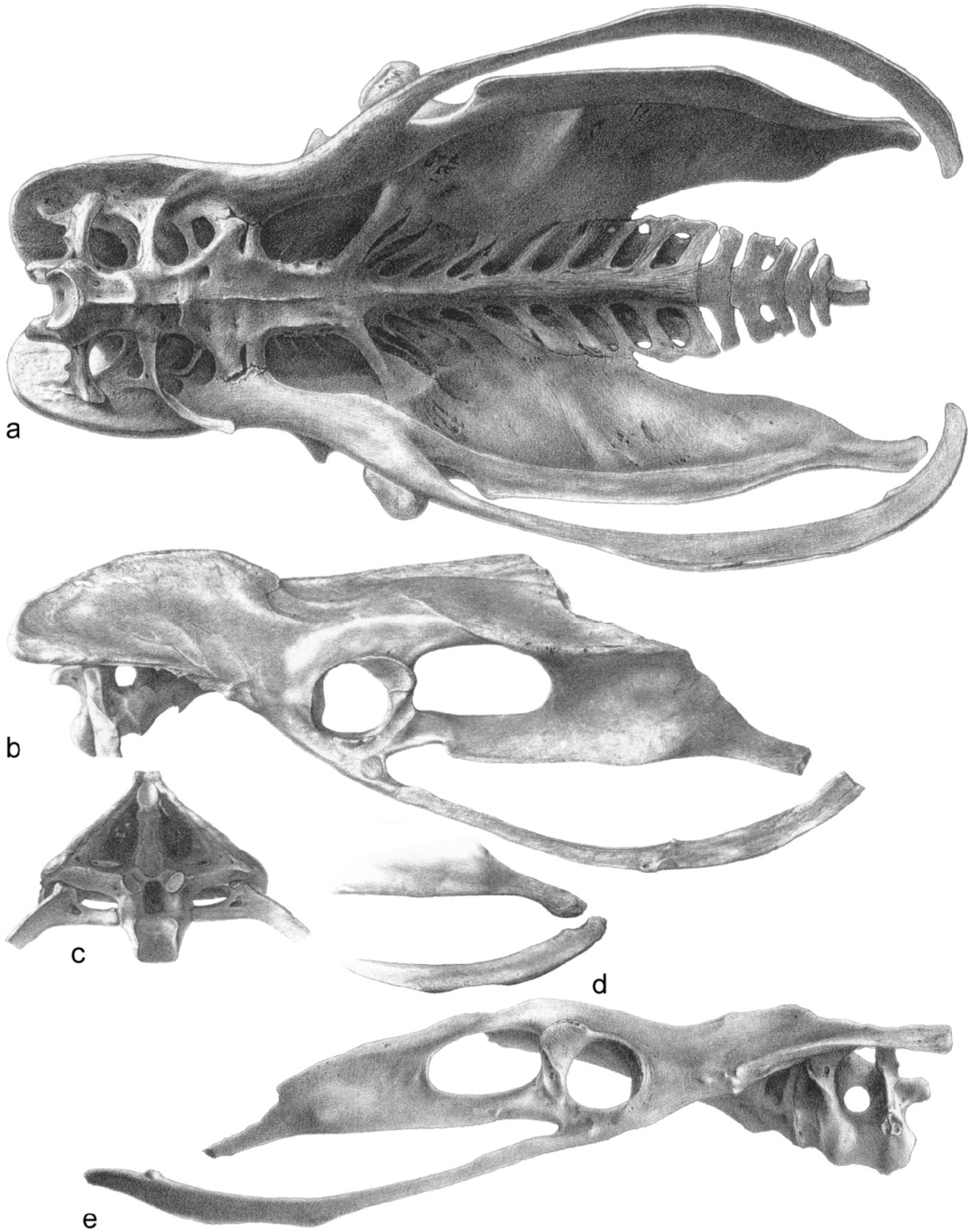

Pelvis of *Pezophaps*. a: ventral view, male (Newton & Clark 1879, pl.xlvi, fig.1), b: lateral view, female (Newton & Newton 1869, pl.xviii, fig.70), c: cranial view, female (Newton & Newton 1869, pl.xvii, fig.67), d: caudal ends of ischium and pubis in lateral view (Newton & Clark 1879, pl.xlv, fig.13), e: lateral view (Newton & Clark 1879, pl.xlvii, fig.1). Newton & Newton (1869): artist: George Henry Ford; “G. H. Ford ad nat. lith.” “W. West imp.” Newton & Clark (1879): “R. Mintern del.” “Mintern Bro^{s}. lith.”

processes and neural spine of the first synsacral vertebra and, dorsolaterally, the ilia. They transmitted the epaxial muscles in life. Caudally they open into depressions either side of the spinous crest of the synsacrum (UMZC 415.K; Owen 1867, pl.xix, fig.2). Sometimes they may be closed completely caudally (UMZC 415.K; Milne-Edwards 1866b, pl.13, fig.1). Of 27 pelves examined, seventeen had iliosynsacral canals that were closed caudally, two had canals closed only on the right side and eight had canals that were open caudally.

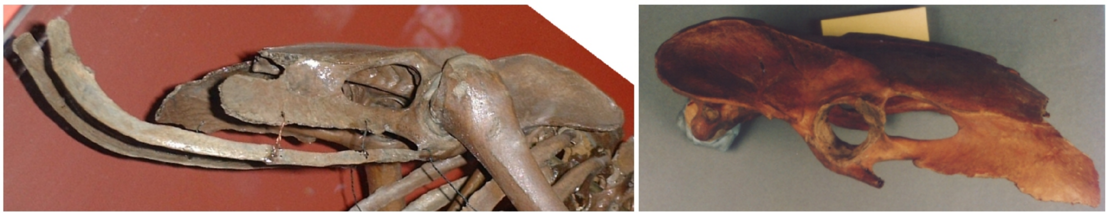

Pelvis of *Raphus* in lateral views. *Left*: NHMUK A.9040 (○ Jolyon C. Parish), *right*: UMZC 415.K specimen (© E. C. Parish).

The concave surface of the cranial part of the ilia may show dendritic impressions of vascular channels. Progressing towards the acetabulum the ilia thicken. The caudal part of the ilium is wider than the cranial part, and is slightly convex. The crista dorsolateralis ilii,[111] separating the caudal part of the ilium from the cranial part, runs from where the ilia diverge from the medial line towards the acetabulum, turning more caudally nearer this area; in some specimens it has a more angular bend as it progresses to the acetabulum (Owen 1867). On each side this ridge continues above the acetabulum, passing dorsal to the ilioischiadic foramen to the terminal process of the ilium. M. iliofibularis, m. iliofemoralis, m. iliotibialis and m. semitendinosus were attached to the crista dorsolateralis ilii in life. The dorsal iliac crest is well defined and prominent. The ilia converge caudally, as the synsacrum becomes narrower, to the fifteenth sacral vertebra; they then diverge slightly at the sixteenth synsacral (Owen 1867). The medial borders of the caudal part of the ilia coalesce with the transverse processes of the synsacral caudal vertebrae.[112] The ventral surface of the caudal part of the ilium presents a buttress, the crista caudalis fossae renalis, which has its lateral extremity behind the ilioischiadic foramen. The iliac recess cranial to the crista caudalis fossae renalis presents several pneumatic foramina; a few pneumatic foramina are also found in the depression caudal to the crista. There are also pneumatic foramina behind the iliac fusion with the costal processes of the sacral synsacral vertebra (Owen 1867). These groups of pneumatic foramina are also found in *Pezophaps*. The dorsal surface of the ilium, corresponding to the iliac recess ventrally, is slightly raised (UMZC 415.K).

The circular acetabulum is closer to the cranial than to the caudal extremity of the pelvis. The cranial border of the acetabulum is well developed and its dorsal margin is sharp. The medial face of the acetabular region has a rounded subtriangular pneumatic fossa, just cranial to the acetabulum. There is also a pneumatic fossa caudal to upper part of acetabulum. The face dorsal to the acetabulum (portion sus-cotyloïdienne of Milne-Edwards 1866b) is almost vertical. The antitrochanter has an approximately oval surface and is composed of the ilium cranially and the ischium caudally; it is directed obliquely cranioventrally. The antitrochanter angle (Hertel & Campbell Jr 2007) is low. Pneumatic foramina are found behind the antitrochanter (Owen 1867). A pneumatic fossa may sometimes be present on the dorsal surface of the pelvis, just medial to the acetabulum; in some specimens only foramina are present (UMZC 415.K). In some specimens of *Raphus* (*e.g.*, UMZC 415.K specimens) round fenestrae paired with medial intertransverse foramina of the synsacrum are present on the medial margin of the dorsal face of the postacetabular ilium (see Livezey & Zusi 2006: 1851). These are also apparent in *Pezophaps*.

---

[111] Janoo (1997, fig.10) referred to the the caudal portion of crista iliaca dorsalis as crête intermédiaire.

[112] Milne-Edwards (1866b, p.365) stated that the "anterior iliac fossae [fosses iliaques antérieures]" are bounded caudally by the transverse processes of the caudalmost thoracico-lumbar synsacral vertebrae, and that these latter "constitute the upper portion of the anterior pelvic strait [détroit pelvien antérieur]" (p.366).

The ischium is long and its lateral surface caudal to the ilioischiadic foramen is slightly concave vertically. In both *Raphus* and *Pezophaps* the ischium is proportionately longer than in other columbids. The caudal expansion of the ischium would have provided a large area of attachment for m. ischiofemoralis. The ilioischiadic foramen is longitudinally sub-oval in outline, being wider cranially than caudally. The ischium ventral to the foramen is trihedral in transverse section, concave laterally and convex medially. Ventral to the foramen the ischium shows a projection, the obturator process, forming the dorsal part of the caudal boundary of the open ischiopubic fenestra. This projection is variably developed: it usually has a well-defined cranial margin (as in Milne-Edwards 1866b, pl.14, fig.1; Durban skeleton; Thirioux's Port Louis skeleton). However, the process is not developed in Newton & Gadow's figure (1893, pl.xxxvii, fig.1b) and is slightly developed both cranially and caudally in Owen's figure (1867, pl.xv). The ischiopubic fenestra is longitudinally sub-oval and is open caudally. The foramen obturatum merges with the spatium ischiopubica. The ventral surface of the ischium shows a low obtuse longitudinal ridge running from the acetabulum to the pelvic cavity, becoming thinner as it does (Owen 1867).

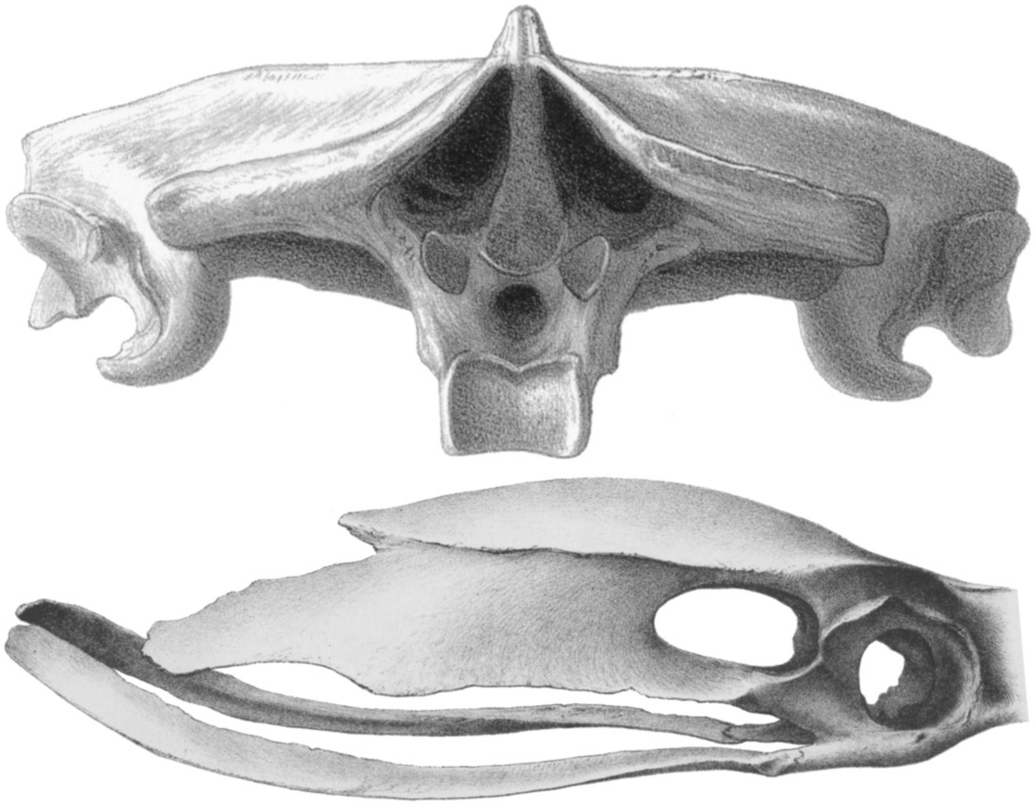

Pelvis of *Raphus*. *Top*: cranial view (Milne-Edwards 1866b, pl.14, fig.1a; "Louveau del et lith." "Imp. Becquet à Paris"), *bottom*: caudal part of pelvis in lateral view (Newton & Gadow 1893, pl.xxxv, fig.1b).

The renal fossa is divided into two parts: cranially the pars ischiadica (fosses rénales antérieures of Milne-Edwards 1866b), and caudally the pars pudenda (fosses rénales postérieures of Milne-Edwards 1866b). The pars ischiadica lies, on each side, lateral to the lumbar synsacral vertebrae. It is deep and divided by the transverse processes of these vertebrae. The pars pudenda is wide and shallow. The crista iliaca intermedia, with which the costal process of the sacral vertebra articulate, is developed and laminar in *Raphus* and *Pezophaps*. In a specimen in the UMZC 415.K collection the junction between the crest and the costal process is visible on each side of the pelvis. The preacetabular tubercle (apophyse iliopectiné of Milne Edwards 1866b; pectineal process) is absent in both *Raphus* and *Pezophaps*, as it is in other columbids.[113]

---

[113] *Contra* Lüttschwager (1959b), who stated that the pectineal process is present in *Raphus* and *Pezophaps*, although only slightly developed.

The pubis is long, and the scapus is not fused to the ischium. Cranially, its ventral surface is smooth and convex. Internally it has a pneumatic structure (Owen 1867). In dorsal aspect of the pelvis the pubes of *Raphus* and *Pezophaps* curve lateral to the ischium before curving medially at their caudal ends; in other columbids the pubis lies ventral, or just ventrolateral, to the ischium. The distal extremities of the pubes are closer together than are those of the ischia.

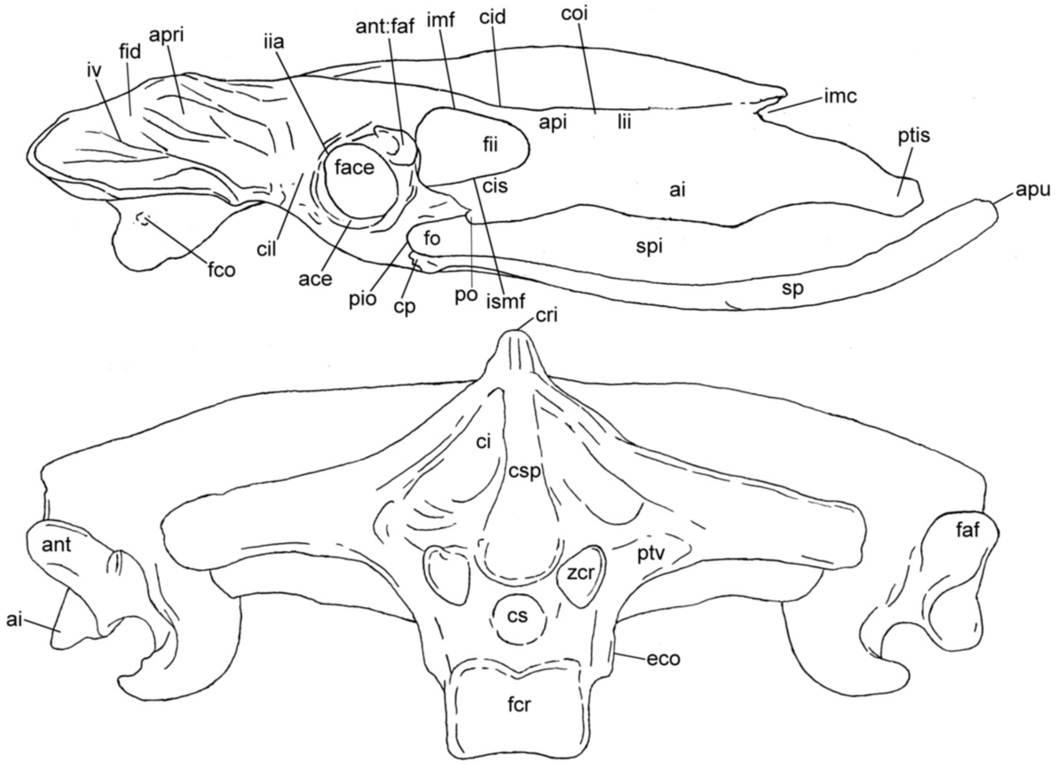

Pelvis of *Raphus*. *Top*: lateral view, *bottom*: cranial view (traced from Milne-Edwards 1866b, pl.14, fig.1a).

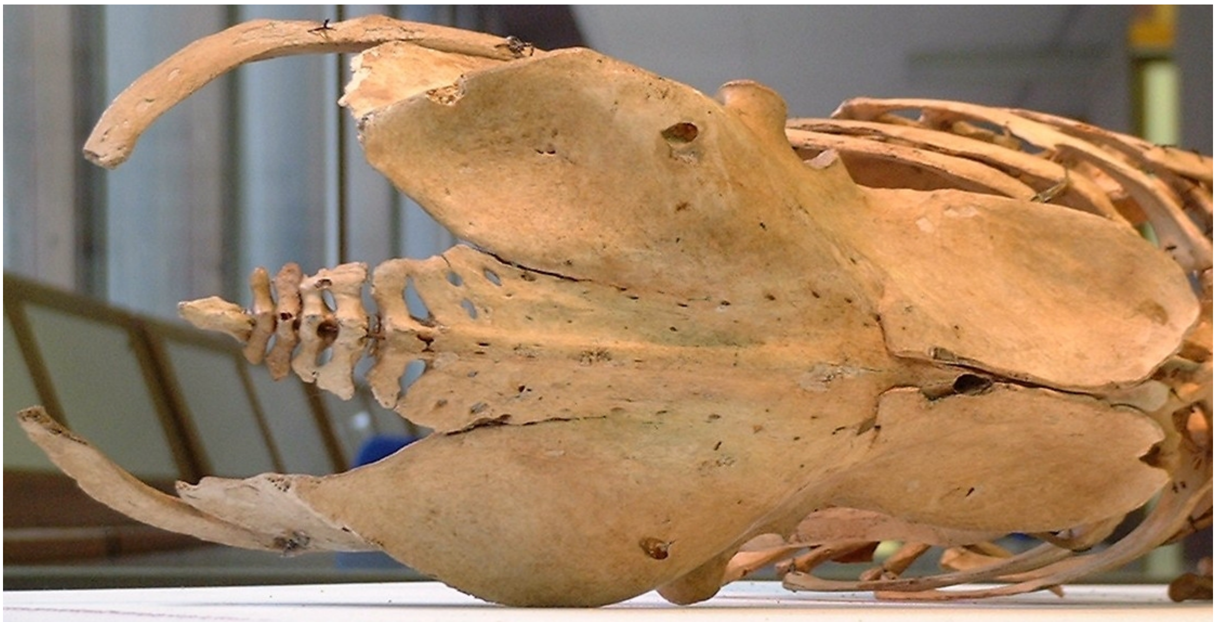

Pelvis of *Pezophaps* in dorsal view (NHMUK A.3506; ○ Jolyon C. Parish).

The ilia of *Pezophaps* are proportionately narrower than those of *Raphus*, especially in the postacetabular region. The crista dorsolateralis ilii is not developed as it is in the latter genus. The preacetabular ala of the ilium is less concave and is narrower than in *Raphus*, and the postacetabular ala is more convex and also narrower. The cranial margin of the ilium is convex and thick; the most convex part is nearer the ventral margin than is the case in *Raphus* (Newton & Newton 1869). The crista iliaca dorsalis is less developed than that of the dodo. The dorsal margins of the preacetabular alae meet in the midline behind the neural spine of the first synsacral vertebra. Their ventromedial edges are joined for a length until, passing caudally, almost above the pars ischiadica of the renal fossa, they diverge and turn downwards. In some specimens studied by Newton & Newton (*ibid.*) they then turned abruptly forwards, before turning backwards, progressing towards the part dorsal to the acetabulum and disappearing after a short length. The openings of the iliosynsacral canals are much smaller than those in *Raphus* and are usually circular in outline (*ibid.*). Newton & Newton (1869, p.336) noted that "the trochanterian surface is narrower, more prominent, and directed more forward" in *Pezophaps* compared to *Raphus*. The sulcus antitrochantericus is proportionately deeper than in *Raphus* (Claessens *et al.* 2015). Dorsal to the antitrochanter, on each side, lateral to where the synsacrum is widest, the ilium rises and curves convexly without producing a ridge. In one specimen examined (NHMUK A.3506) there are a pair of pneumatic foramina (foramen pneumatique dorsale of Janoo 1997, fig.10) on the dorsal surface of the postacetabular ilium, just caudomedial to the antitrochanters. The ilia slope downward, passing caudally to around the region of the fourteenth synsacral vertebra, becoming much closer medially, but not as much as in *Raphus* (*ibid.*); caudal to this they diverge again. The medial surface of the ilium is also thickened caudal to the ilioischiadic foramen, but less than in *Raphus*. Martin (1904) remarked that the acetabular region is broadened and more prominent than in other pigeons.

The ischium of *Pezophaps* resembles that of *Raphus* to a large extent, although the body of the ischium (corpus ischii) is less concave than in *Raphus* (Claessens *et al*. 2015). It is concave cranially and then becomes convex from around a measure of the length of the ilioischiadic foramen from its caudal border. The obturator process is variably developed, as in *Raphus*; it is commonly developed cranially (as in Newton & Newton 1869, pl.xviii, fig.70; NHMUK A.3506), but is only very weakly developed in Newton & Clark's figure (1879, pl.xlvii, fig.1). A shallow depression just cranial to the cranial margin of the obturator foramen in *Pezophaps* (seen in Newton & Newton 1869, pl.xviii, fig.70) may have provided attachment for m. obturator externus. The terminal process of the ischium is long, narrow, and concave; "its lower margin sloping downward and outward, as if to pass and avoid the pubic style [scapus pubis], which is here directed upward and inward in a different plane" (Newton & Newton 1869, p.336). The end of the terminal process of the ischium in a specimen studied by Newton & Clark (1879, pl.xlvi, fig.1) turned medially and slightly upwards as it approached the pubis, "making a hook-like process" (Newton & Clark 1879, p.442). The ilioischiadic foramen is proportionately longer than in *Raphus*, but of a similar shape.

There are pneumatic foramina on the medial surface above the acetabulum. The cranial margin of the ischiopubic fenestra lies ventral to the acetabulum in *Pezophaps*, whereas in *Raphus* it lies caudal to it (pers. obs.; Newton & Newton 1869). The pubis diverges ventrolaterally from the ischium, and curves by differing amounts in different specimens, making the width of the ischiopubic fenestra variable: it is wide in some specimens (Lüttschwager 1960, fig.16 (Zoologisches Museum, Kiel skeleton: A 3166); Newton & Newton 1869, pl.xviii, fig.70), and narrower in others (Newton & Clark 1879, pl.xlvii, fig.1), where it resembles the condition seen in *Raphus*. Cranially it is trihedral in transverse section and also shows a sharp ridge on its dorsolateral margin, which disappears as it progresses caudally (Newton & Newton 1869). The pubis widens as it progresses caudally and the dorsal margin becomes thickened (Newton & Newton 1869). Caudal to the synsacrum, the pubis curves dorsally and the dorsal edge turns slightly medially, and the "bevel turning to the inner side disappears" (*ibid*., p.336). The caudal extremities of the ischium and pubis of UMZC 415.R (Newton & Clark 1879, pl.xlvi, fig.1), that of a very large male, show articular surfaces, suggesting that the ischium and pubis may have met. Likewise, Owen (1878) stated that in one male skeleton there was a rough tuberosity on the dorsal part of the pubis which formed a syndesmosis with the ischium.[114] Comparison of the complete extremities of these bones in a male (Newton & Clark 1879, pl.xlv, fig.13) and a female (*ibid.*, pl.xlvii, fig.1) specimen examined by Newton & Clark (1879) shows there is variation present. In another specimen (*ibid.*, pl.xlvi, fig.1) studied by the above authors the pubis bends medially, caudal to the terminal process of the ischium; the distal apex of the pubis is blunt, terminating slightly medial to the end of the ischium. In the male *Pezophaps* skeleton RCSHM/Aves 706 the distal end of the pubis curves gently ventrally.

Sternum

(*Raphus*: Owen 1867, pl.xv; pl.xvi, fig.4; pl.xviii, figs.1-3; pl.xxiii, fig.4; Milne-Edwards 1866b, pl.14, fig.2; pl.15, figs.1-1b; Hume & Steel 2013, fig.5C; Claessens *et al.* 2015, figs.38, 39, pls.PL27, D27. *Pezophaps*: Strickland & Melville 1848, pl.xiii, figs.5, 6; Newton & Newton 1869, pl.xviii, figs.71-74; Newton & Clark 1879, pl.xlviii, figs.1, 2, pl.xlix, figs.1, 2; Meijer *et al.* 2012, fig.4a; Hume & Steel 2013, fig.5D)

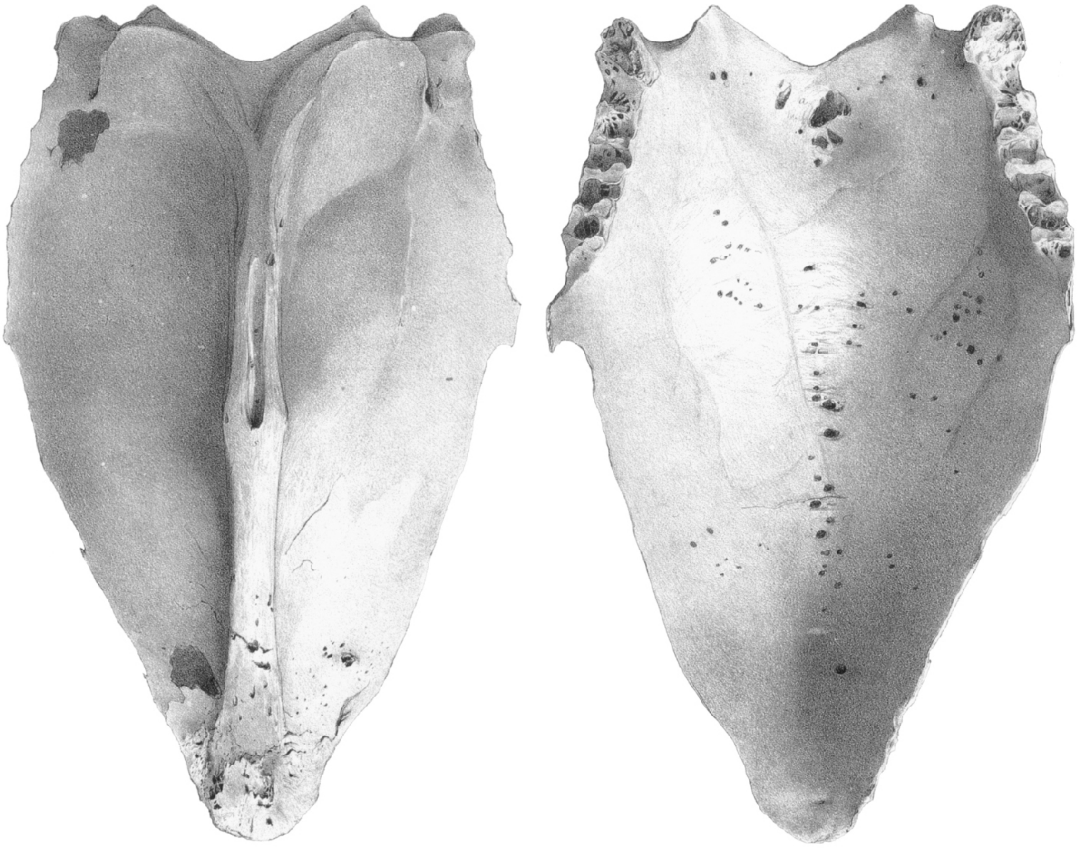

Sternum of *Raphus*, ventral and dorsal views (Owen 1867, pl.xviii, figs.1, 2; artist: Edward William Robinson; "E W Robinson del" "W West imp").

The sternum of *Raphus* is bowl-like, and proportionately much smaller than that of extant pigeons. It is approximately the same length as the synsacrum (Claessens *et al.* 2015). Fürbringer (1888) stated that the sterna of *Raphus* and *Pezophaps* corresponded in length to 4.7 dorsal vertebral lengths. According to Owen (1867), the sternum is "expanded and excavated for the support of the larger gizzard with its heavier grindstones" (p.75). The rostrum of the sternum is absent, as is the case in *Pezophaps*.[115] The sternal carina is proportionately much reduced in both *Raphus* an *Pezophaps* compared with volant columbids. Claessens *et al.* (2015) stated that "the depth to length ratio of the sternum is only about a quarter of the depth to length ratio of volant columbids" such as *Caloenas*, *Columba*, *Didunculus* and *Goura* (p.64). The apex of the carina is not well developed as in volant columbids, and therefore the cranial margin of the sternum forms an obtuse angle with its base in *Raphus* and *Pezophaps*, as opposed to an acute one in pigeons capable of flight. However, the apex is somewhat more developed in *Pezophaps* than in *Raphus*, leading Claessens *et al.* (2014) to speculate that the latter displayed less intraspecific antagonistic behaviour than the former, which used its wings in combats. The spatium intercoracoidale forms a sulcus (intercoracoidal sulcus; échancrure intercoracoïdienne of Milne-Edwards 1866b) on the cranial aspect of the sternum that is well developed due to the coracoidal sulci being widely spaced.[116] It is deeper medially than laterally and of subtriangular form.

---

[114] There may have been a synchondrosis between the distal ischium and pubis (Livezey & Zusi 2006: 1952), but data is limited.

[115] Gervais (1867-1869) erroneously stated that the spina externa ("apophyse épisternale") was present in *Pezophaps*.

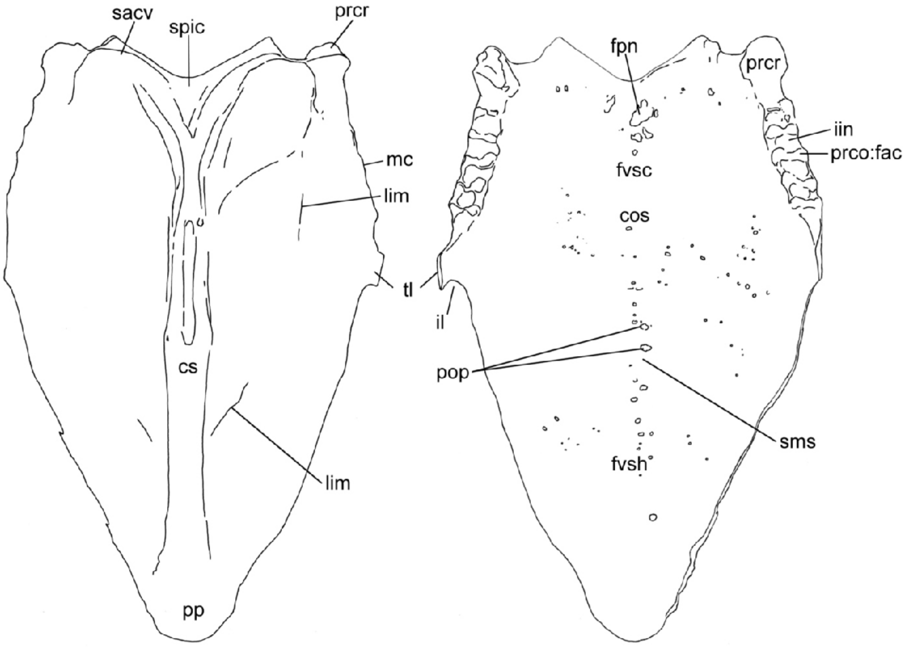

Sternum of *Raphus* (traced from Owen 1867, pl.xviii, figs.1, 2).

The carina is low and thick. On each side the pila carinae progresses from the ventromedial end of the coracoidal sulcus, and forms the lateral boundary of the intercoracoidal sulcus, below which the two parts join to form the single median carina. The carina has a maximum depth around the middle of the sternum (at approximately 60% of its length: Claessens *et al.* 2015) and gradually decreases in height as it passes caudally, disappearing just cranial to the caudal margin of the sternum. Owen's figures (1867, pl.xviii, fig.1; pl.xvi, fig.4) show a longitudinal median depression in the carina, approximately a quarter of the length of the sternum. The caudal end of the depression lies near the middle of the carinal length, which is slightly widened. Milne-Edwards' figure (1866b, pl.15, fig.1) only shows a slight groove in this position, as do several other specimens (for example a sternum in the UMZC 415.K collection); it appears to be present in the Durban skeleton (Claessens *et al.* 2015, fig.40B). In GUEMG: A1767 the median depression forms a distinct elongate pneumatic sulcus. This depression, or part of it, may have provided attachment for the sternoclavicular ligament. Towards the caudal part of the sternum the carina widens and flattens out. In lateral view the lower border of the carina, which is flat, forms an approximate regular curve, the carinal apex not being well developed. The dorsal base of the carina broadens and merges into the rest of the sternum.

---

[116] Claessens *et al.* (2015) referred to this as the sulcus carinae and stated that the carinal sulcus is absent in *Pezophaps*. Livezey & Zusi (2006: 1207) termed the ridges bordering this sulcus bilateral cristae carinae and noted that the crista lateralis carinae "[e]vidently serves as one of several ancorae for membrana sternocoracoclavicularis" (p.193).

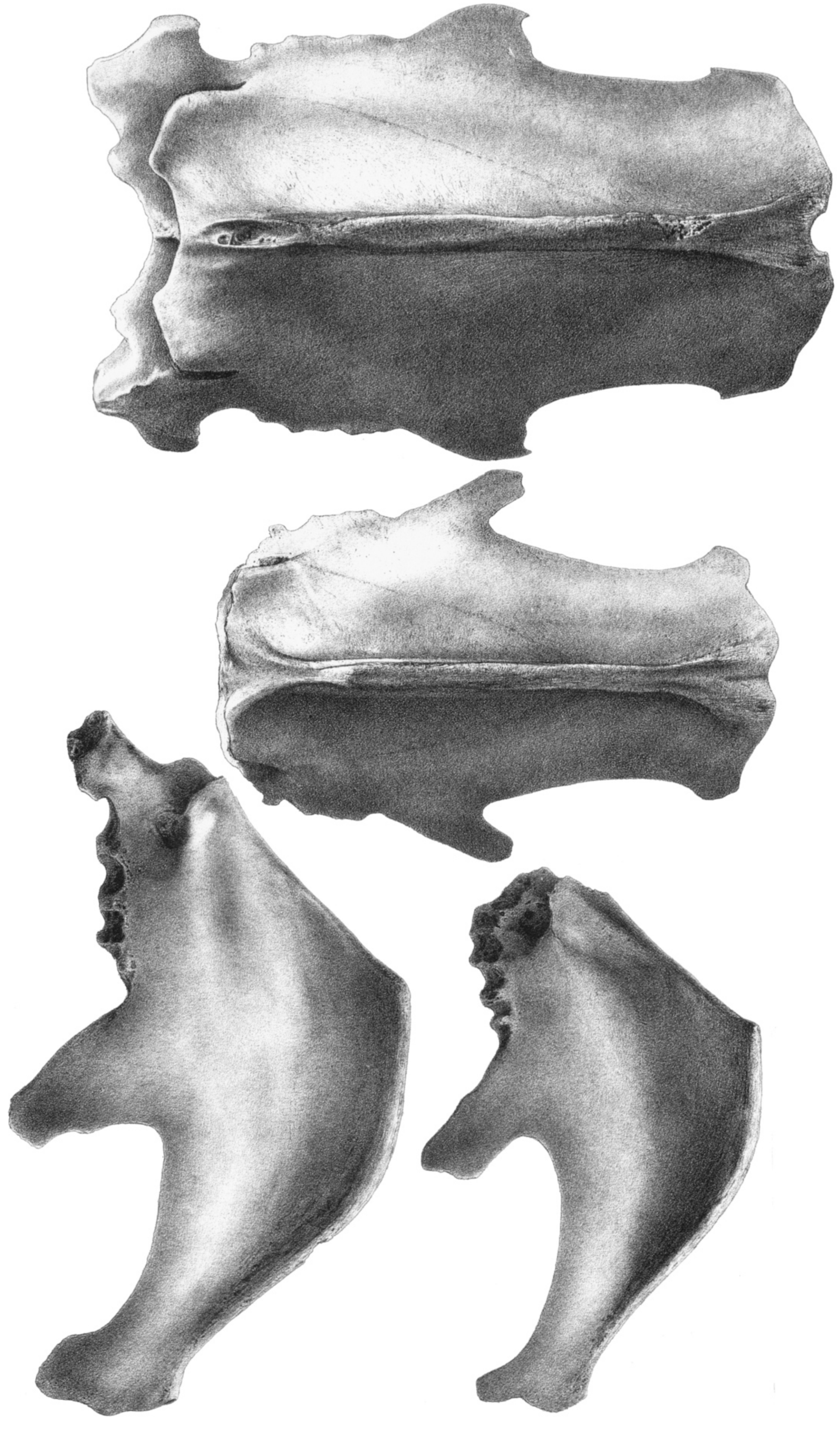

Sternum of *Pezophaps* in lateral and ventral views, male (larger) and female (smaller) (Newton & Clark 1879, pls.xlviii, xlix; “R. Mintern del.” “Mintern Bro^{s}. lith.”)

The coracoidal sulci are proportionately small. The ventral border (labrum ventralis) of each sulcus is ridge-like and convex; it passes into the craniodorsal part of the carina. The dorsal border (labrum dorsale) is deeper and forms a prominence between the craniolateral process and the midline of the sternum. Dorsal to the dorsolateral end of each of the ventral margins of the coracoidal sulci is a depression containing pneumatic foramina. The robust craniolateral processes project dorsally and slightly craniolaterally, broadening from the costal margin. Each bears a distinct oval pit (Claessens *et al*. 2015). The caudal face of each craniolateral process is concave, the concavity continuing to the first costal process; the medial face is convex and smooth. As with other parts of the sternum, the craniolateral processes are reduced compared with those of *Caloenas*, *Didunculus* and *Goura* (*ibid*.). The weak sternocoracoidal impression is situated on the ventral surface of the craniolateral process and provided origin for m. sternocoracoideus, which inserted on the coracoid.[117]

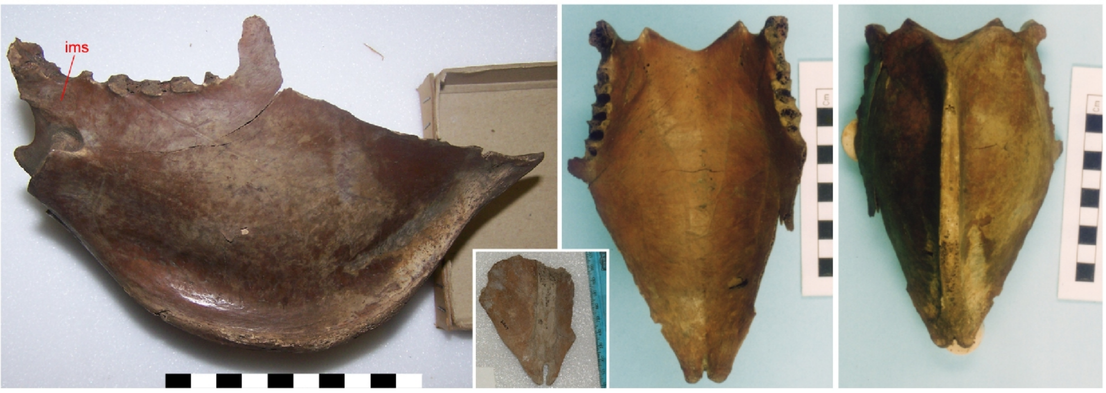

Sternum of *Raphus* (UMZC 415.K specimen, lateral, dorsal and ventral views; YPM 2064 (inset), ventral view. Scales in cm (○ Jolyon C. Parish, except dorsal and ventral views of UMZC 415.K which are © E. C. Parish).

In Thirioux's Port Louis skeleton and the Durban skeleton the costal margin, caudal to the craniolateral process on each side, presents four costal processes (articular ridges of Owen 1878) (Claessens *et al*. 2015). These are bilobed, having a lateral and a median part. However, in *Raphus* the number costal processes is variable: Owen (1867, pl.xviii, fig.2) described a specimen with five costal processes on each side, the cranial one being simple (unilobed) whilst the caudal four are bilobed. Milne-Edwards' figure (1866b, pl.15, fig.1a) shows a specimen with five bilobed facets on the left side and four bilobed and one single one on the right. Newton & Newton (1869) stated that in one specimen of *Raphus* there were five costal facets on the left side and four on the right,[118] and that in another specimen all five facets were bilobed on the left and only the cranialmost on the right side was simple in form. The intercostal spaces (incisurae intercostales) are fairly deep and present several pneumatic foramina (Owen 1867, Claessens *et al*. 2015).

The lateral trabecula projects dorsally and slightly laterally, caudal to the costal border. It is lamelliform and its dorsal end is expanded, with a backward pointed process (as seen in a specimen in Thirioux's collection[119]). The lateral trabecula defines the cranial margin of the lateral incisure.[120] The margin of the sternum caudal to the lateral trabecula (the 'xiphosternum' of Fürbringer 1888 and Martin 1904)[121] is thin and is not notched or fenestrated.[122] The caudal end of the sternum is rounded and flattened into a well-developed planum postcarinale. In some specimens (UMZC 415.K, YPM 2064) the caudal margin is bilobed, each lobe formed from the caudal end of each half of the sternum with a notch between them (the “meso-xiphoid (primordial) notch” of Parker 1868, p.186),[123] whereas in others it is not bilobed (Owen 1867, pl.xviii, figs. 1, 2). On the convex lateral surface of the sternum is the longitudinal intermuscular line (which separated the attachment of m. supracoracoideus dorsally from m. pectoralis ventrally), which runs from the lateral end of the coracoidal sulcus caudomedially to near the caudal third of the carina.[124]

---

[117] Fürbringer (1888, p.114) stated that the length of the lateral margin of the 'precostal' portion ("praecostalen Abschnittes") of the sternum compared to that of the lateral margin of the whole 'costosternum' was 2/5 in *Raphus*.

[118] This would appear to be a specimen in the UMZC 415.K collection (pers. obs.).

[119] Photograph (9A) accompanying a letter to Alfred Newton, 5th September 1900.

[120] Fürbringer (1888) referred to the lateral incisurae, between the lateral processes and the caudal end of the sternum, as "Incisura [inc], Incisura lateralis resp. I. intermedia) (Xiphosternum biincisum s. bifurcum)" (p.119).

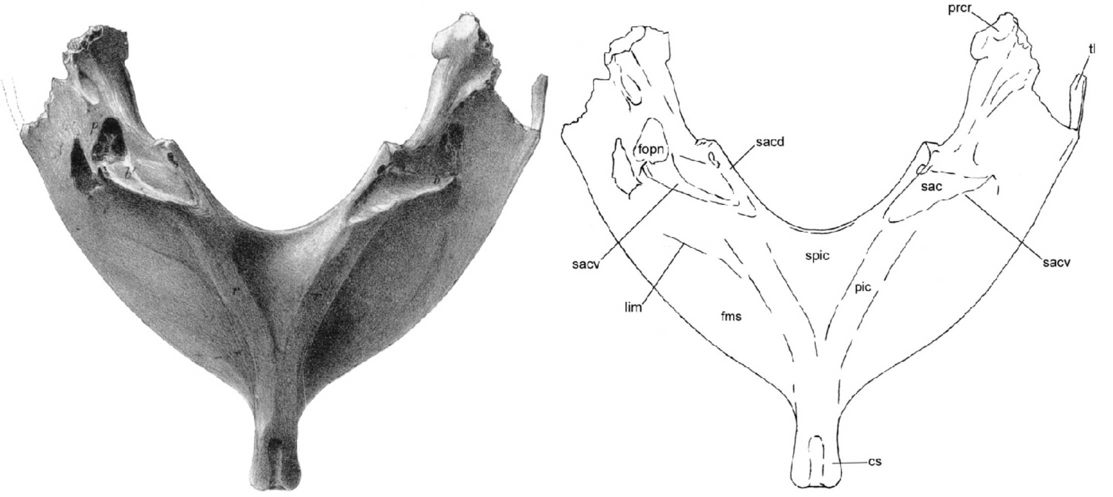

Sternum of *Raphus* (lithograph: Owen 1867, pl.xvi, fig.4; artist: Edward William Robinson; “E W Robinson del” “W West imp”).

The concave dorsal, or visceral, surface presents several pneumatic foramina, with larger ones at the cranial end and smaller ones in approximately the middle third of the sternum (Owen 1867, pl.xvii, fig.2). The majority of these foramina lie in the midline. The size, number, and distribution of the foramina vary between individuals: Owen’s figure (1867, pl.xviii, fig.2) shows large median cranially placed pneumatic foramina and smaller ones caudal to these, whereas a sternum in the UMZC 415.K collection shows very few pneumatic foramina. The large pneumatic foramina at the cranial part of the sternum are obliterated in some specimens of *Raphus* (see Milne-Edwards 1866b, pl.15, fig.1a). The intermediate trabecula and medial fenestra are absent, as they are in *Pezophaps*. Janoo (1997) recognized a small cranial depression, pars cardiaca, on the visceral surface and noted the lack of a median sulcus (as also in *Pezophaps*). He added that towards the caudal part of the sternum the parasagittal impression of two mesenteric vessels (“vaisseaux mésentériques”) were visible.

In transverse section it can be seen that the sternum is very pneumatized. It increases in thickness behind the costal border from the sharp lateral margins to the midline. It is proportionately thicker than in volant pigeons. Above the base of the carina the bone shows a “fine pneumocancellous texture” (Owen 1867, p.62; see *ibid*., pl.xxiii, fig.4).

Newton & Newton (1869) commented that the “very near affinity of *Pezophaps* to *Didus* is nowhere better shown than on comparison of the sterna of the two forms; and it is self evident on the most

---

[121] Parker (1868, p.186) mentioned the “common ‘meso-intermediate xiphoids’” of the sternum. See Appendix 1 for further details.

[122] Fürbringer (1888) stated that there is a tendency in flightless birds to “fill in” the sternal incisures and to create a solid ‘xiphosternum’, citing *Raphus*, *Pezophaps*, *Pinguinus impennis* and *Cnemiornis calcitrans* as examples. He added that many flightless and poorly-flying birds have a simpler form to the caudal end of the sternum (his ‘xiphosternum’) compared with their volant relatives and also that larger birds (regardless of whether they are poor fliers or not) often have a simpler ‘xiphosternum’ than their smaller relatives.

[123] Fürbringer (1888), referring to Parker (1868), referred to this notch as “a true Incisura posterior (xiphoidea) mediana” (p.121). He also called this feature the “Incisura xiphoidea mediana” and “Incisura mediana sterni”.

[124] Fürbringer (1888) stated that in Raphini (his ‘Dididae’) the sternal origin of m. sternocoracoideus extended ⅔-¾ of the sternal length.

cursory inspection of them" (p.338). The sternum of *Pezophaps* shows the same helmet-like shape as that of *Raphus*, although it is proportionately narrower at the level of the costal margin than in *Raphus* (Claessens *et al*. 2015). The intercoracoidal sulcus is not as proportionately large as in the latter. The carina shows the median longitudinal depression on the anterior part, as in the dodo, probably for attachment of the sternoclavicular ligament. The carina is deeper in *Pezophaps* that in *Raphus*, indicating that it possessed more developed sternal musculature; this may be related to the use of the wings of the latter in intraspecific combats. As in the dodo the carina widens and flattens out at the caudal end of the sternum. The coracoidal sulci are deeper and wider than in *Raphus* and closer together medially. At the inner extremity of each sulcus in most specimens there is "a deeper depression, almost a little pit [...] in a line and, occasionally, to some degree confluent with it" (Newton & Newton 1869, p.338). In one specimen examined by Newton & Newton (1869), there is another smaller subtriangular shallow depression above the former one. There is a deep depression at the base of the craniolateral process, on each side, cranially. The thick, wide craniolateral processes are slightly expanded dorsally and also concave dorsally, as in *Raphus*, but with a well-defined ridge crossing the concavity (Melville 1848). The caudal surface, facing the sternal ribs, is sub-concave and trihedral. There are, almost without exception, four costal processes on each side, each bilobed. However, Slater[125] remarked: "Four is the normal number of sternal ribs, as Prof. Newton thought, but one specimen [I found] has four on one side and three only on the other." The costal processes and intercostal spaces are closely spaced, especially the third and fourth (Owen 1878). The thin lateral trabecula is wider at its base than at its extremity and projects dorsally and slightly laterally and caudally. According to Owen (1878), it partly overlaps the caudal two sternal ribs when they are articulated with the sternum, although this is not the case in the present skeletal reconstruction. The lateral trabecula shows individual variation (Newton & Clark 1879). The caudal end of the sternum is slightly expanded laterally, with a pair of broad, blunt laterally projecting processes, the remnants of the intermediate trabecula (the medial fenestrae having become obsolete). There are no caudal fenestrae, but there is sometimes a slight rounded median incisure in the caudal margin (seen in Newton & Clark 1879, pl.xlix, figs.1 and 2). This incisure lies between the two ridges which mark the lateral margins of the caudal end of the carina. The caudal end of the sternum is relatively wider in *Pezophaps* than it is in *Raphus*. The intermuscular lines resemble those of *Raphus*, extending from the coracoidal sulci to the base of the carina. As in *Raphus*, the planum postcarinale is well developed.

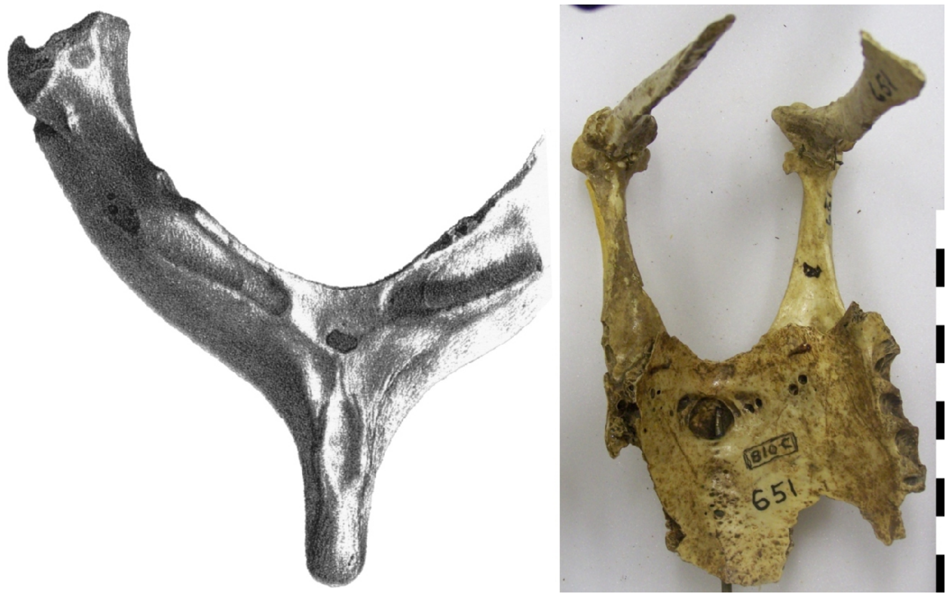

Sternum of *Pezophaps*. *Left*: cranial view, female (Newton & Newton 1869, pl.xviii, fig.71; artist: George Henry Ford; "G. H. Ford ad nat. lith." "W. West imp."), *right*: UMZC 651, approximately dorsal view of cranial portion of sternum, with articulated coracoids and scapulae, scale in cm (○ Jolyon C. Parish).

---

[125] "Abstract from H. H. Slater's Report, on Rodriguez-Collection", Royal Society Transit of Venus Expeditions. Correspondence and papers relating to distribution of collections and preparation of reports 1875-1876, DF 202/9, NHMUK General Library.

The dorsal surface of the sternum is concave and shows pneumatic foramina as in *Raphus*. In *Pezophaps* there is a deep depression at the cranial part of the dorsal surface. In some specimens (including five out of seven specimens (including the large Paris specimen; Strickland & Melville 1848, pl.xiii, figs.5, 6) studied by Newton & Newton 1869) this pit may be so excavated that it pierces the sternum and a foramen is formed (for example in Newton & Newton 1869, pl.xviii, figs.71, 73, 74). This foramen (foramen rostri sterni of Janoo 1997)[126] opens cranially ventromedial to the medial ends of the coracoidal sulci, and lies at the ventral end of the intercoracoidal sulcus, and in one particular specimen studied by the above authors the foramen is very large. It appears to be separate from the pneumatic system of the sternum (Newton & Newton 1869), and does not occur in the dodo, even the largest specimens. The median sternal sulcus (sulcus medianus sterni) is less developed than it is in *Raphus* (Claessens *et al*. 2015).

Scapular Arch

The scapular arch consists of the coracoid, scapula and clavicle. Usually these three bones are separate, as in Thirioux's Port Louis skeleton and the Durban skeleton. However, in *Raphus* the coracoid and scapula may be occasionally fused to form a scapulocoracoid (as in NHMUK A.1351, UMZC 415.H (right), some UMZC 415.K specimens and AMNH 3852). Sometimes the clavicle may also fuse with the scapulocoracoid (as in NHMUK A.1341; UMZC 415.H (left) and Owen 1867, pl.xx, figs.8, 9), or with just the coracoid (as in NHMUK A.1351; Owen 1867, pl.xx, figs. 4, 5).[127] Commonly all three bones are separate and unfused. Of 66 scapular arch elements examined the enumeration was as follows:

scapula n = 40 (24 left, sixteen right)
coracoid n = 9 (six left, three right)
clavicle n = 2
coracoid with fused clavicle n = 0
scapulocoracoid n = 10 (one left, nine right)
scapulocoracoid with fused clavicle n = 5 (three left, two right)

The angle between the coracoid and scapula in *Raphus*, determined by measurement of scapulocoracoids, is obtuse: approximately 100° (AMNH 3852) to 110° (UMZC 415.K specimen). The angle cannot be determined precisely for *Pezophaps*, as no examples of a fused scapula and coracoid are known, but Newton & Newton (1869) stated that "to the best of our judgement, however, it cannot have been much less than it is in *Didus*" (p.341). This obtuse angle is a characteristic of flightlessness, and is found in other flightless birds.

Coracoid

(*Raphus*: Owen 1867, pl.xx, figs. 4, 5,[128] 8-11; Claessens *et al*. 2015, figs.40, 41, pls.PL28, D28. *Pezophaps*: Newton & Newton 1869, pl. xix, figs. 76-83, pl.xx, fig.136; Ottow 1950, pl.ii, figs.7, 8, pl.viii, fig.22; Hume & Steel 2013, figs.7C, D)

The coracoid of *Raphus* is similar to that of other columbids, although it is generally more slender than in volant pigeons and *Pezophaps*. Claessens *et al*. (2015) stated that the minimum transverse width to length ratio of the coracoid of *Raphus* is *c*.0.25.[129] Fürbringer (1888) stated that the coracoid of *Raphus*

---

[126] Janoo (1997) stated that this "deep pneumatic foramen (*foramen rostri sterni*) opens just below the manubrial spine" (p.105). However, the rostrum sterni (manubrium sterni) is absent in both the dodo and the solitaire.

[127] George Clark, the discoverer of many specimens of *Raphus* (see Parish 2013, pp.236-242), remarked "I only found one coracoid with the furcula and scapula (which three bones in the Dodo were anchylosed together) entire, but I met with several to which the latter was attached" (1866, p.143).

[128] Note: Owen (1867, plate xx, fig.5) actually shows the coracoid and clavicle of the right side turned over to show their dorsal aspect, and not, as Owen stated, the left coracoid and clavicle.

[129] It is here presumed that "minimum transverse width" refers to the width of the sternal end. In a specimen listed by Livezey (1993) the ratio is 0.32. In *Pezophaps* the ratio is around 0.37-0.38 (NHMUK A.1373, although other specimens may vary). Claessens *et al*. added that the "relative transverse width of the sternal extremity of the coracoid in *Raphus*, which is around a third of total coracoid length, is approximately equal to those of other volant

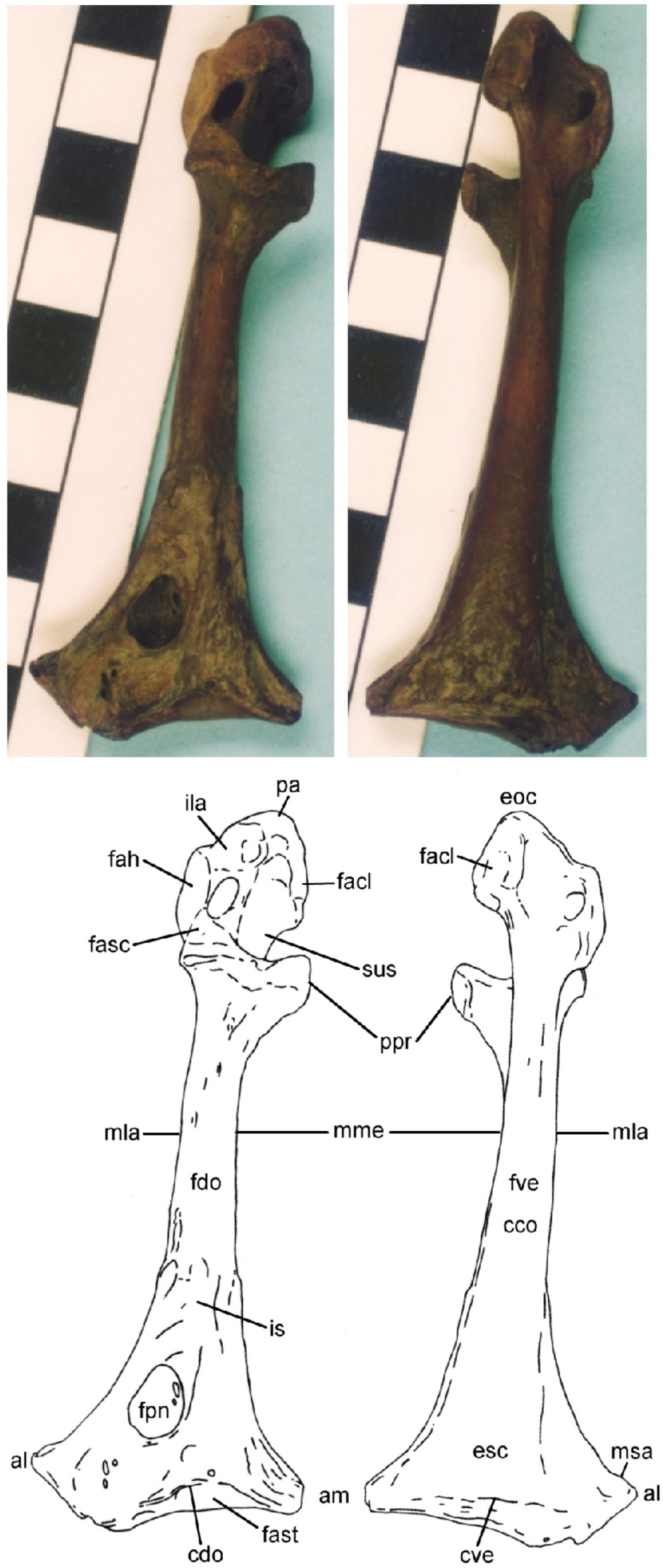

Coracoid of *Raphus* in dorsal and ventral views (UMZC 415.K specimen; photograph: © E. C. Parish)

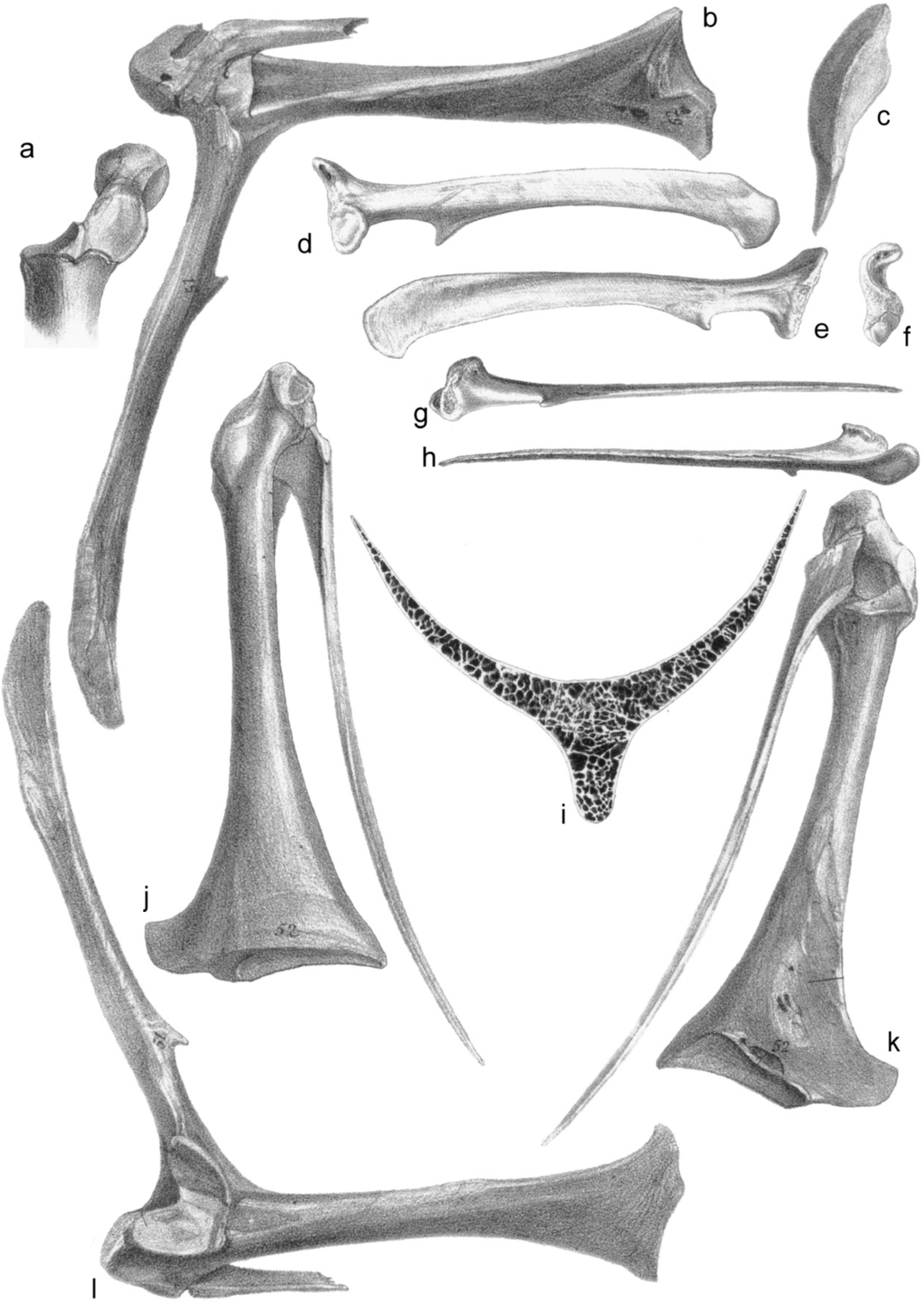

Coracoid, scapula, clavicle and sternum of *Raphus*. a: right coracoid, omal end (Owen 1867, pl.xx, fig.10); b: left scapulocoracoid with proximal end of clavicle fused, medial view (Owen 1867, pl.xx, fig.9); c: right coracoid, sternal view (Owen 1867, pl.xx, fig.11); d-h: left scapula, lateral, medial, proximal, dorsal and ventral views (Milne-Edwards 1866b, pl.17, figs.2-2d); i: sternum, transverse section (Owen 1867, pl.xxiii, fig.4); j and k: right and left coracoids and clavicles, ventral and dorsal views (Owen 1867, pl.xx, figs.4, 5); l: left scapulocoracoid with proximal end of clavicle fused, lateral view (Owen 1867, pl.xx, fig.8). Owen (1867), plate xx: “From nat on Stone by J Erxleben” “M & N Hanhart , imp”; pl.xxiii: “J Smit lith” “M & N Hanhart imp”. Milne-Edwards (1866b): “Louveau del et lith.” “Imp. Becquet à Paris.”

and *Pezophaps* was equivalent in length to 4.0 dorsal vertebrae. The medial angle of the sternal end is well developed: it may be pointed (as in NHMUK A.1351) or truncated (as in OUMNH 19619). The lateral process is also well-developed. When in articulation with the sternum, the lateral process extends laterally to cover cranially the pneumatic foramen lateral to the coracoidal sulcus of the sternum. The lateral process itself varies between individuals, being pointed (as in a UMZC 415.K specimen) to truncated (as in NHMUK A.899). The dorsal edge of the lateral process, extending from its extremity up to about a third of the coracoid's length, is narrow. The medial edge, extending dorsally from the medial angle, is more rounded. Claessens *et al.* (2015) stated that there is "a small ridge [...] situated on the ventral surface [...] where it connects to the sternum" (p.66). The ventral face of the sternal end of the coracoid is convex and smooth. A line, or slight ridge, on the ventral face of the coracoid (seen distinctly in *Pezophaps*, NHMUK 76.1.28.43) may have provided attachment for m. coracobrachialis caudalis. A ridge running along the medioventral border of the coracoid in (as seen in *Raphus* NHMUK A.1351, *Pezophaps* NHMUK A.3505), from near the sternal end towards the scapular articulation, may have provided attachment for the membrana sternocoracoclavicularis. The dorsal surface is flatter, more irregular, and presents small pneumatic foramina, which vary in abundance from several (NHMUK A.1352) to very few (NHMUK A.1351). In the case of a specimen in the UMZC 415.K collection, a large sub-oval pneumatic sulcus is present, situated centrally on the dorsal face. Dorsal to the pneumatic foramina is the shallow impression and roughened surface for m. sternocoracoideus. The shaft of the coracoid has a sub-cylindrical form and is oval in transverse section.

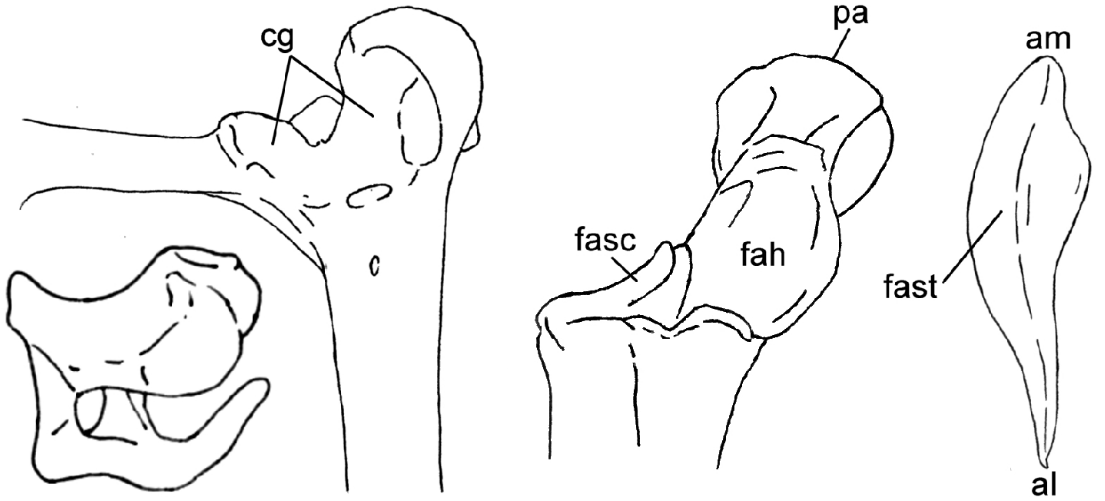

Coracoid and scapula of *Raphus*. *Left to right*: left coracoid, omal view; right scapulocoracoid, lateral view; right coracoid, omal end; right coracoid, sternal view.

The procoracoid process is well developed. Its ventral margin curves downwards into the shaft. It is slightly craniodorsally directed and its apex is either truncated (UMZC 415.K) or pointed (NHMUK A.899). In top (omal) view the compressed plate of the procoracoid process is visible, which is bent slightly ventromedially. In some specimens of the coracoid and scapulocoracoid of *Raphus* the procoracoid process is absent (as in a UMZC 415.K specimen) or very reduced (as in NHMUK A.1352); in Thirioux's Port Louis skeleton and the Durban skeleton it is short. Verheyen (1957) stated that in *Raphus* the acrocoracoid and the procoracoid process are occasionally joined by synostosis and Janoo (1997) recorded that the lig. acrocoraco-claviculare is ossified in some specimens (as in Owen 1867, pl.xx, figs.8, 9). The cotyla for the scapula is concave and oval to subtriangular with the apices of the face rounded off; the upper part of the procoracoid process is roughened for articulation with the scapula also. The articular face for the humerus is large and oval to semicircular. The ligamental attachment impressions of the omal end of the coracoid are much more defined in *Raphus* (as in, for example, a UMZC 415.K specimen) compared with *Pezophaps* (for example, NHMUK A.1373). The

---

columbids" (p.66).

impression for the acrocoracohumeral ligament on the medial part of the ventral face of the omal extremity is large, although less excavated than in *Raphus*. The acrocoracoid process is rounded.

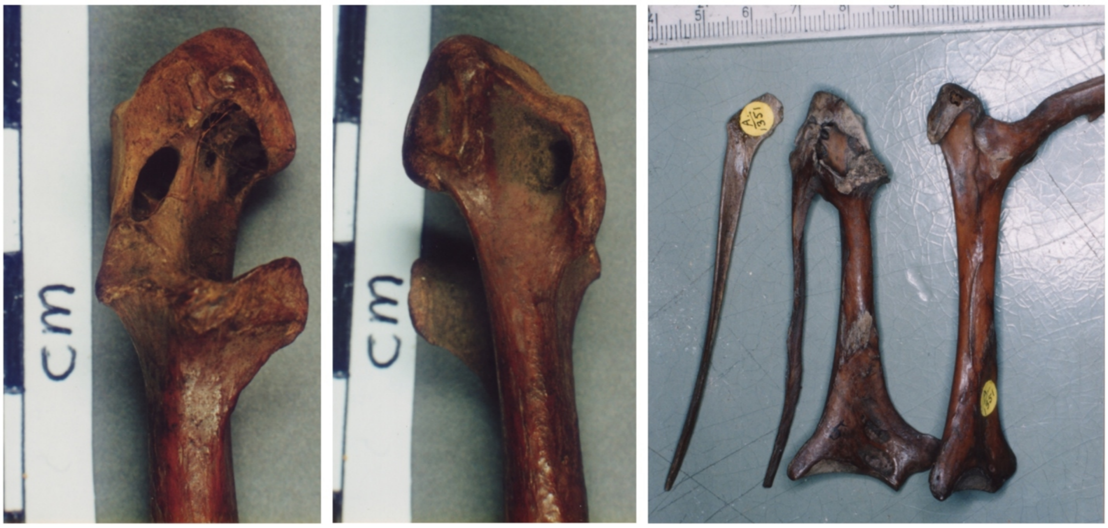

Pectoral girdle elements of *Raphus*. *Left* and *middle*: left coracoid, dorsal and ventral views of omal end (UMZC 415.K specimen; © E. C. Parish), *right*: clavicle, right coracoid with fused clavicle (a scapulocoracoid lacking the scapula; dorsal view) and right scapulocoracoid (NHMUK A.1351; ○ Jolyon C. Parish).

In one specimen of the coracoid in the UMZC 415.K collection there is a pneumatic fossa present dorsal to the scapular cotyla and pneumatic foramina just distal to the acrocoracoid process. These foramina are variably present in *Raphus*. In the same specimen there is also a deep, fairly large, circular hollow on the ventral side, immediately opposite the humeral articular face. Medial to this, a small subcircular to sub-oval impression on the sternal end of the ventral face of the acrocoracoid might represent the attachment of m. bicipitalis. The articular surface for the clavicle is oblong and narrow in outline, and its ventral end is not well developed as it is in volant columbids. It is not hooked as it is in some pigeons (Worthy & Wragg 2008). On the dorsal face, just above the upper apex of the sulcus m. supracoracoidei, is a sub-oval impression, perhaps for a ligament connecting the acrocoracoid and the scapula.

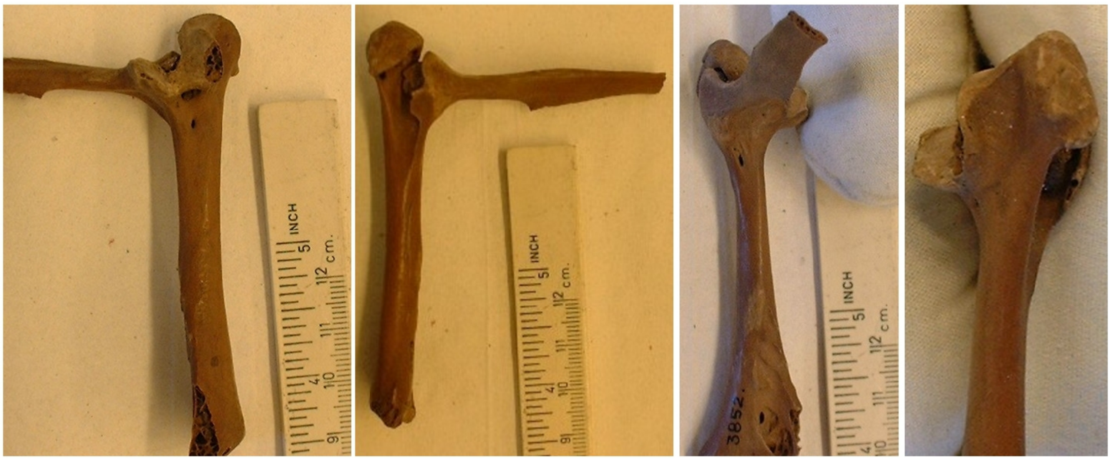

Scapulocoracoids of *Raphus* (AMNH 3852; ○ Jolyon C. Parish).

The coracoid of *Pezophaps* differs slightly in form from that of *Raphus*. It is more robust, thicker and proportionately wider, especially at the sternal and scapular ends, and is also generally smoother. The lateral process of the sternal end is bluntly truncated, and is reduced in *Pezophaps* in comparison with *Raphus* and even more so compared with many volant columbids, due to the reduction of m.

sternocoracoideus ("to few, probably tendinous fibres (roughness on the dorsal surface of the coracoid)": Martin 1904, p.241). The medial process may be bluntly pointed (as in USNM 19450; Newton & Newton 1869, pl.xix, fig.79) or truncated (as in USNM 1871). In some specimens the process is slightly elongated (Newton & Newton 1869, pl.xix, figs.76-79). The sternal articulation is proportionately broader, relative to its length, compared with that of *Raphus* (Janoo 1997). The ventral surface of the sternal end is more convex than in *Raphus*, and the dorsal one less flattened. The dorsal surface usually shows a few small pneumatic foramina in the impressio m. sternocoracoidea (NHMUK A.1373; Newton & Newton 1869, pl.xix, fig.79), which vary in size and number and are sometimes absent altogether (*ibid*.). The ridge and roughened area for the attachment of m. sternocoracoidei are less developed than those of the coracoid of *Raphus*, although the ridge is present in all specimens (*ibid*.). The scapular end (omal extremity) resembles that of the coracoid of *Raphus*, but with a more robust appearance. The articular surface for the scapula is also proportionately larger than in the dodo. In *Pezophaps* the scapular cotyla extends out onto the procoracoid process. According to Newton & Newton (*ibid*.), in most larger (probably male) specimens the cotyla is sub-quadrate, whereas in smaller (probably female) specimens it is triangular.

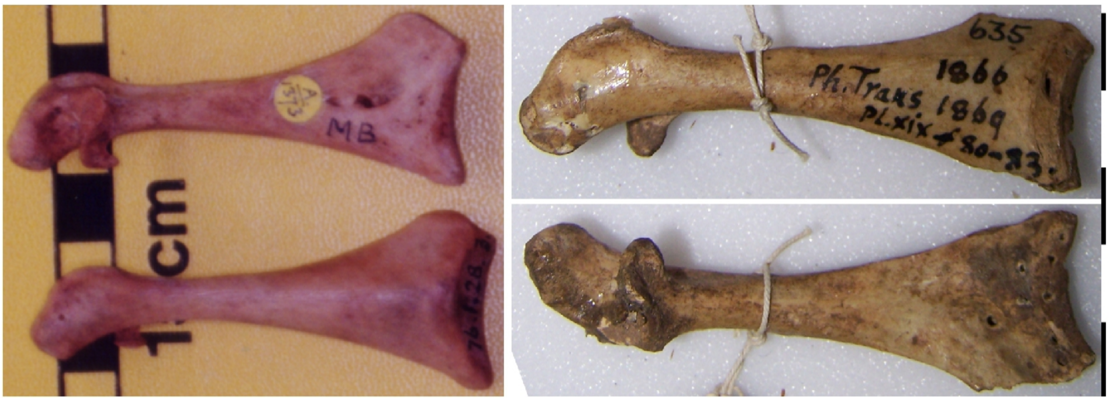

Coracoid of *Pezophaps*. *Left*: left and right sides, ventral and dorsal views (NHMUK A.1373); *right*: left side, dorsal and ventral views (UMZC 635, female). Scales in cm (○ Jolyon C. Parish).

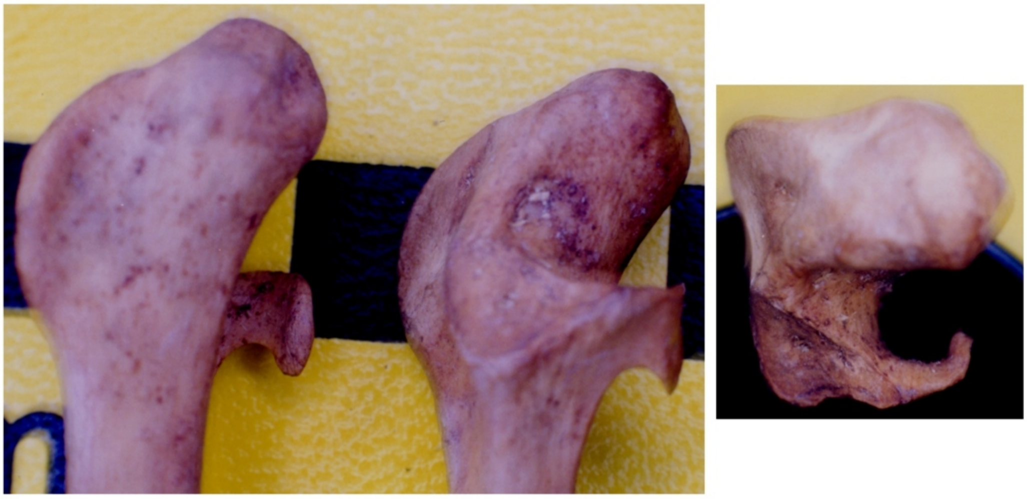

Coracoid of *Pezophaps*. *Left*: right and left sides, omal ends, ventral and dorsal views; *right*: left side, omal view (NHMUK A.1373; ○ Jolyon C. Parish).

The procoracoid process is directed either medially (as in Newton & Newton 1869, pl.xix, fig.83) or medially and slightly upwards (as in *ibid*., fig.79). In some specimens there is a sternally directed flange on its sternal edge (as in USNM 19450, NHMUK A.1373), which curves back into the shaft. The shape of the procoracoid process varies between individuals, being more truncated or rounded in some specimens. In omal view the process curves similar to that in *Raphus* and other pigeons. The sulcus m. supracoracoidei does not appear to be as hollow and as excavated as in *Raphus* and is less pneumatized. As in *Raphus* it is located centrally, rather than medially, on the dorsal face of the coracoid. The articular surface for the humerus is not as well defined as it is in *Raphus*, and is usually semi-lunar in shape and not as smooth; it is directed less ventrally than in the dodo (Claessens *et al.* 2015). This face usually shows two or three depressions due to the presence of pneumatic foramina, which can be seen in some specimens but are obliterated in others (Newton & Newton 1869). The articular face for the clavicle is shorter and wider than it is in *Raphus*. Claessens *et al.* (2015) stated that the acrocoracoid process is more sharply pointed in *Pezophaps* than in the dodo, although the process seems to be variable in form in the latter (pers. obs.). There are no pneumatic foramina under the acrocoracoid process.

No specimens of *Pezophaps* display any fusion of the coracoid with either the scapula or the clavicle, although Newton & Newton (1869) stated that “in many of the larger (male?) ones, there is a considerable bony development on the edges of the articular surfaces, as if resulting from the partial ossification of the integument, which may perhaps be an approximation to that condition of the three bones which seems usually to have existed in *Didus*” (p.341). An example of this is seen in NHMUK 76.1.28.43, which shows bony growths on the scapular cotyla and procoracoid process. Owen (1871b) followed this by noting that “the absence of any example of confluence of scapula and coracoid [in the specimens of *Pezophaps* examined by the brothers Newton] indicates a more habitual and powerful use of the appendage of the arch than was exercised by *Didus*” (p.518).

Scapula

(*Raphus*: Owen 1867, pl.xx, figs. 6-9; Milne-Edwards 1866b, pl.17, figs.2-2d; Meijer *et al.* 2012, fig.4c; Claessens *et al.* 2015, figs.40, 42, pls.PL29, D29. *Pezophaps*: Newton & Newton 1869, pl.xix, figs.84-86, 97-99, pl.xx, figs.132-133)

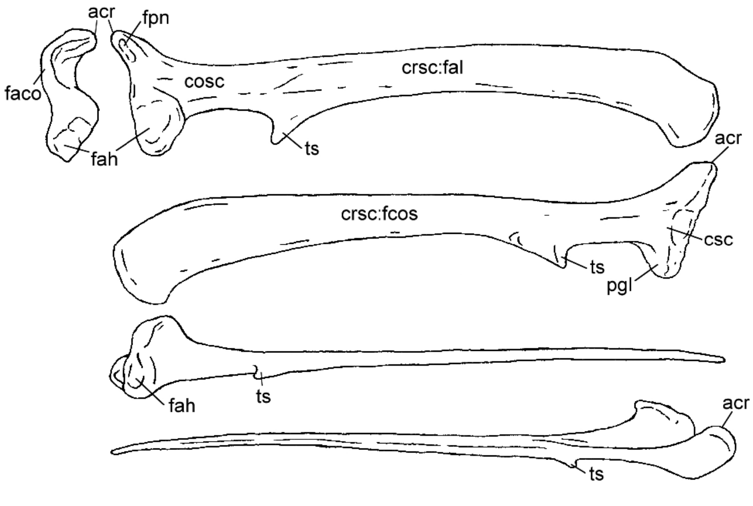

Scapula of *Raphus*: proximal, lateral, medial, ventral and dorsal views (traced from Milne-Edwards 1866b, pl.17, figs.2-2d).

The scapula of *Raphus* is slightly recurved, with a truncated distal end. The body of the scapula is sabre-shaped and the distal end is slightly expanded and decurved. The caudal margin is curved. There is some slight variation between individuals in the shape of the distal end. The lateral face is slightly concave for its caudal two-thirds and shows muscular attachment areas. The medial face is slightly convex and smooth for its caudal two-thirds (Owen 1867). Progressing cranially from the cranial third of the scapula the bone becomes convex, broader and slightly thicker. On the ventral margin there is a small cranioventrally directed process which probably corresponds to the tuberculum m. scapulotricipitis.[130] The form of this tubercle is variable: in some specimens it is pointed (as in

---

[130] Milne-Edwards (1866b) thought that the tubercle provided attachment for the scapulotriceps portion of m. triceps brachi (“la longue portion du triceps brachial”) and suggested that “the corresponding part of the extensor

NHMUK A.436, A.1351; Thirioux's Port Louis skeleton), in others it forms a rounded ridge (NHMUK A.9040; the Durban skeleton).

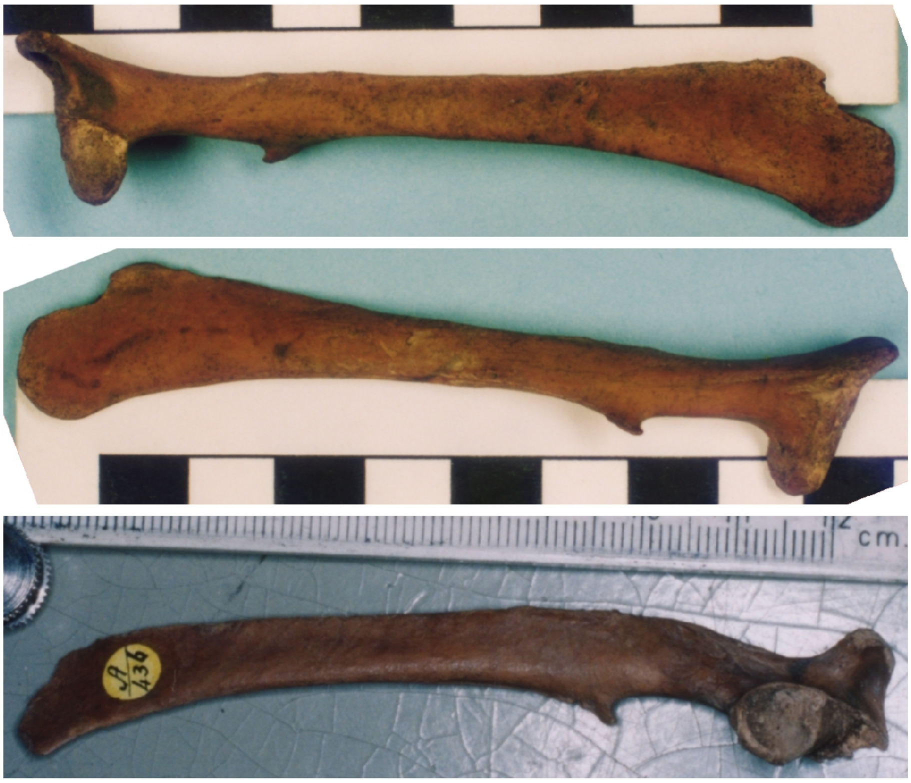

Scapula of *Raphus*. *Top* and *middle*: left side, UMZC 415.K specimen, lateral and medial views (© E. C. Parish); *bottom*: right side (from a scapulocoracoid), NHMUK A.436, lateral view (○ Jolyon C. Parish).

A short, defined ridge running along the dorsal edge of the scapula of *Raphus*, dorsal to the tuberculum scapulae (seen in NHMUK A.436, Thirioux's Port Louis skeleton and the Durban skeleton) may represent the attachment site for m. rhomboideus. The articular surface for the humerus is quite large, almost flat, and subcircular. It faces laterally and slightly dorsally and cranially. The coracoidal articular face is narrower and oblong, and is broad and rough (Milne-Edwards 1866b). The acromion projects cranially and is pointed but with a rounded extremity; it curves towards the coracoid. In the deep depression on the acromion there is a pneumatic foramen (or foramina), which is present in all specimens (pers. obs.; Newton & Newton 1869). In the Durban skeleton the pneumatic foramina are large (Claessens *et al*. 2015, fig.40B).

The scapula of *Pezophaps* differs somewhat from that of *Raphus*, "instead of being sabre-shaped and curved decidedly backward, it is rather straight, or, if anything, inclining generally forward – a character not known by us to exist in any other bird, and only pointing backward and inward at its extremity when it becomes spatulate in form" (Newton & Newton 1869, p.339). The scapula is more robust than that of the latter genus, especially proximally and shows significant individual variation. The muscle attachment areas are not as well marked as in *Raphus*, and so the lateral and medial surface appear similar. The distal part of the lateral surface does not usually show the slight concavity as in *Raphus*, and is convex in many cases. The medial surface is, in almost all specimens, concave, albeit to differing extents (*ibid*.). The tuberculum scapulae is slightly developed (as a low rounded (*ibid*., pl.xix, figs.84-86) or pointed (*ibid*., pl.xix, figs. 132, 133) process) on the ventral margin, marking the end of a ridge, which progresses caudally to form the edge of the distal end. The proximal end of the scapula is proportionately thicker in *Pezophaps* than in *Raphus*, and the articular face for the coracoid is proportionately larger. The humeral articular surface is proportionately smaller, as is the acromion,

---

apparatus of the wing had relatively considerable power" (p.369).

which is less curved and does not possess a pneumatic foramen in the depression on it. The humeral articular surface is also less circular than in *Raphus* (Claessens *et al*. 2015), at least in some specimens.

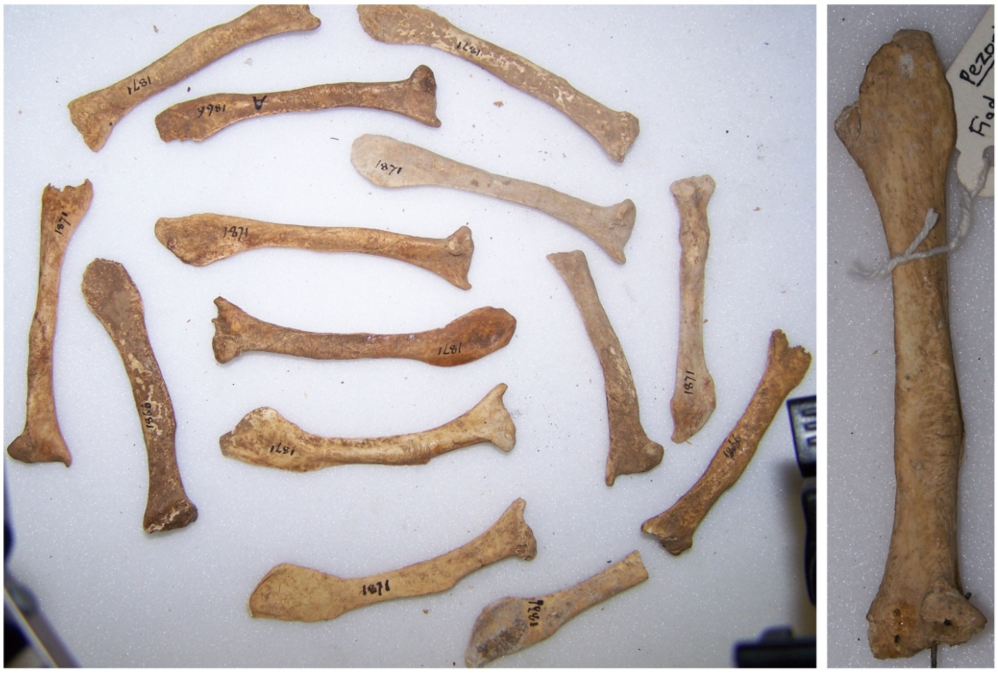

Scapula of *Pezophaps*. *Left*: UMZC specimens, left and right sides, lateral and medial views, *right*: UMZC 634 (male), left side, lateral view. (○ Jolyon C. Parish).

As noted above, the scapula of *Pezophaps* displays variation in the form of the distal end, as evidenced in the collection of scapulae UMZC 653. The distal flanging (expansion) is very developed in some specimens, less so in others. Some specimens have very rounded distal ends, whereas others have more pointed or rounded hooked ends. Slater[131] remarked: "The scapulæ of Pezophaps are extremely curious: their [*sic*] is such an extreme amount of variability in the shape of their free extremities that I do not believe that the two belonging to the same bird were necessarily alike in shape."[132]

Clavicle

(*Raphus*: Owen 1867, pl.xx, figs.4, 5, 8, 9; Newton & Gadow 1893, pl.xxxvi, fig.1; Claessens *et al*. 2015, figs.40, 43, pls.PL27, D27. *Pezophaps*: Newton & Clark 1879, pl.xlvii, fig.3, pl.l. fig.7)

In *Raphus* the clavicles frequently remain as separate slender splints (as in NHMUK A.1351).[133] The Durban and Thirioux's Port Louis skeletons of *Raphus* each possess a complete furcula, with the distal ends of the clavicles joined medially. In Thirioux's Port Louis skeleton the length of the clavicles is slightly greater than that of the coracoids (Claessens *et al*. 2015). In *Pezophaps* the pair of clavicles also often fuse medially, at their distal ends, to form a furcula.

---

[131] "Abstract from H. H. Slater's Report, on Rodriguez-Collection", Royal Society Transit of Venus Expeditions. Correspondence and papers relating to distribution of collections and preparation of reports 1875-1876, DF 202/9, NHMUK General Library.

[132] Claessens *et al*. (2015) stated: "In *Raphus*, the excavation between acromion and facies articularis humeralis is shallower, contains less pneumatic foramina, and the shaft is straighter and lacks a ridge on the dorsal surface distal to proximal end compared with *Pezophaps*. Moreover, in *Raphus*, the shaft is straighter and lacks a ridge on the dorsal surface distal to proximal end" (p.66). However, *Pezophaps* shows variation in the development of the fossa between the acromion and humeral articulation surface (UMZC specimens) and is apneumatic (pers. obs.; Newton & Newton 1869). The straightness of the scapular shaft also varies in *Pezophaps*. As stated above, a ridge on the dorsal surface of the scapula (speculated herein to be for m. rhomboideus) is present in *Raphus*.

[133] Claessens *et al*. (2015) stated that NHMUK A.9040 also has unfused clavicles, although they are not present in the mounted (composite) skeleton. The lack of fusion of clavicles and coracoids, however, is evident from the form of the latter.

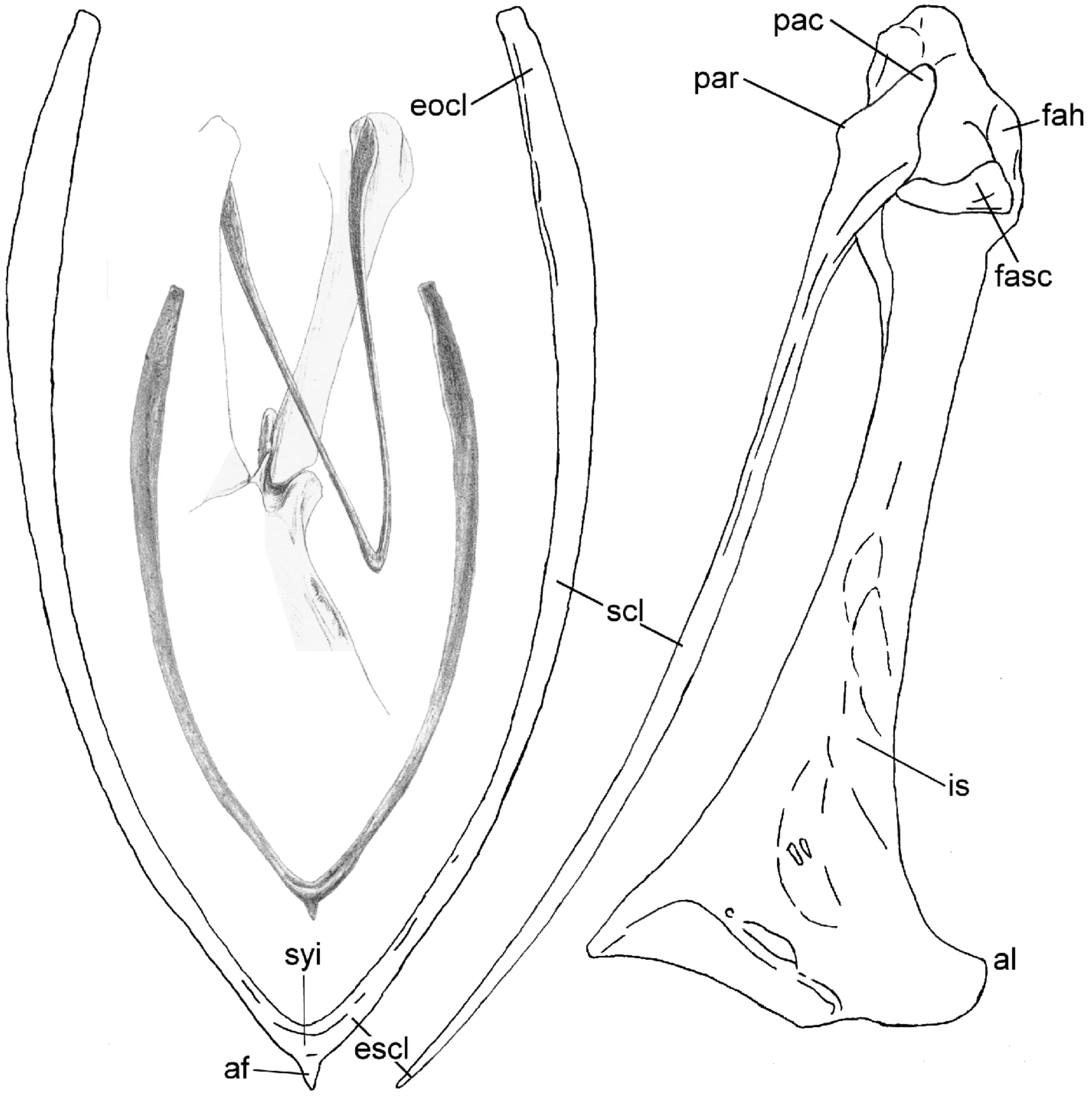

Left: furcula of *Pezophaps* (lithographs: Newton & Clark 1879, pl.l, fig.7; pl.xlvii, fig.3). *Right*: left coracoid with clavicle of *Raphus* (traced from Owen 1867, pl.xx, fig.5). Newton & Clark (1879): “R. Mintern del.” “Mintern Bro^{s}. lith.”

The proximal, or scapular (omal), end of the clavicle of *Raphus* is slightly expanded craniocaudally and flattened, with a blunt recurved extremity, the acrocoracoid process, which articulates with the coracoid. The acromial process is rounded. The clavicle is slightly curved and its distal end is pointed. In some specimens it is fused with the coracoid (as in NHMUK A.1351), and, as in one specimen examined by Owen (1867, pl.xx, figs.8, 9), it is fused with the coracoid and with the acromion of the scapula via synostosis (*ibid*.). The distal end of the furcula, when present, is rounded off; “this may, however, be a case of individual variation, considering that in the male specimen of the Cambridge *Pezophaps* there is likewise no apophysis [hypocleideum], while there is one, although small, in the female specimen. Hence, Professor Owen’s restored drawing of this part in the British Museum specimen of *Didus* cannot be pronounced to be incorrect” (Newton & Gadow 1893, p.296).

The clavicles in *Raphus*, when unfused, meet at an acute angle distally, as can be seen in Owen's figure (1867, pl.xx, figs. 4, 5). When present the furcula is U-shaped, with the apex rounded. In those specimens where the furcula is formed there is no hypocleideum.[134] Fürbringer (1888) stated that in *Raphus* the clavicle is removed from the carina sterni (his crista sterni) around 1.25 dorsal vertebral lengths. The furcula of *Pezophaps* (as seen in NHMUK A.3505, NHMUK A.3506; RCSHM/Aves 706, 707) resembles that of most volant columbids, but differs in not being quite as U-shaped, although it is more so than in *Raphus*. The hypocleideum varies in its development between individuals. It can be seen in Newton & Clark's figure (1879, pl.l, fig.7), as a small pointed process, but is absent in another specimens (NHMUK A.1467; *ibid*., pl.xlvii, fig.3). In some specimens of *Pezophaps* the clavicles are separate (for example, NHMUK A.1467, NHMUK 76.1.28.59); these are similar in form to those of *Raphus*.[135]

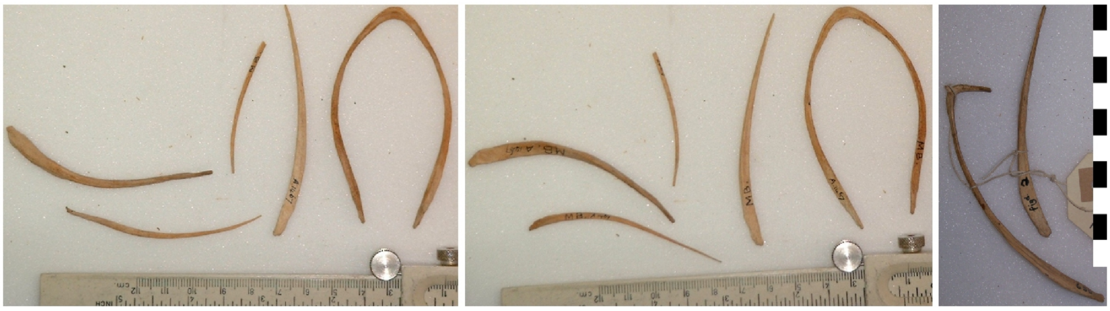

Clavicle and furcula of *Pezophaps*. *Left* and *middle*: NHMUK A.1467, *right*: UMZC 650, broken furcula; scale in cm). (○ Jolyon C. Parish).

Pectoral Limb

(*Pezophaps*: Rand 1954, fig.1I)

The wing is proportionately shorter in *Raphus* than in volant pigeons: the total wing skeleton length is around one-and-two-thirds synsacral length in the former, and over four times synsacral length in *Caloenas* (Claessens *et al*. 2015).

Hume & Steel (2013) stated that the wing (humerus, radius, ulna, carpometacarpus) of *Raphus* was reduced in overall size compared with that of *Pezophaps*, but gave no evidence to support this. This may be true when comparing average males of the two species, but apparently not average females, judging from Livezey's (1993) data.

Based on measurements of Thirioux's dodo skeletons (Port Louis and Durban) given by Claessens *et al*. (2015) the wing element length proportions of humerus : radius : carpometacarpus : phalanges of digit II are: 42%:30%:17%:11% (Port Louis, right side); 41%:30%:16%:12% (Durban, right side).[136] In *Caloenas* the ratios are approximately 30%:32%:21%:17% (USNM 322384). These ratios reflect the progressive proximal to distal shortening of wing elements in the dodo, and in flightless birds in general (Livezey 1992, 1995). The brachial index (humerus length to ulna length) is 1.25-1.26 in

---

[134] However, for those specimens in which a furcula is present (Thirioux's Port Louis skeleton and the Durban skeleton) the ventral ends have been at least partially reconstructed (very reconstructed in the Durban skeleton) (Claessens *et al*. 2015).

[135] Claessens *et al*. (2015) suggsted that "the possibility exists that unfused clavicles may belong to young individuals" (p.67). However, the separate clavicles in both *Raphus* and *Pezophaps* do not show evidence of juvenile bone grain (pers. obs.), and furthermore, unfused clavicles are present in *Otidiphaps nobilis* and *Ducula goliath* (Glenny & Amadon 1955) and clavicles either absent or reduced in Mesitornithidae. Gadow (1893b) stated that in both *Raphus* and *Pezophaps* "the clavicles are reduced to narrow splints, which in *Pezophaps* closely approach, and which in *Didus* even touch, the coracoids" (p.151). However, it is not known what Gadow meant by this.

[136] Livezey (1993) gave the proportions of the pectoral limb bones as: *Raphus*: humerus 44.7%, ulna 36.4%, carpometacarpus 19.0%; *Pezophaps*: humerus 47.1%, ulna 34.0%, carpometacarpus 18.9%. He gave the wing length (humerus, ulna, carpometacarpus) as 227.4mm for *Raphus* and 234.2mm for *Pezophaps* (unweighted mean of sexes) (*ibid*.). However, these were not based on associated specimens.

Raphus (Thirioux's Port Louis skeleton; Claessens *et al.* 2015) and 1.31-1.32 in *Pezophaps* (NHMUK A.3506, A.3505; Claessens *et al.* 2015). These ratios are similar to those of other flightless birds:[137] *Aphanapteryx bonasia* 1.44 (MU 923; Hume 2019) and *Xenicibis xympithecus* 1.40 (Longrich & Olson 2011), and also Anseriformes 1.15±0.15 (Nudds *et al.* 2004). The fact that the ulna is not as reduced as in some other flightless birds supports the idea that the wing was habitually used in both *Raphus* (perhaps for display) and *Pezophaps* (for combat).

According to Armstrong (1953), the dodo, like the solitaire, had thickening of the wing bones; this has not been confirmed by the present author due to lack of data.

Humerus

(*Raphus*: Owen 1867, pl.xx, figs.12-14, pl.xxiii, fig.5; Janoo 2005, fig.2m; Meijer *et al.* 2012, fig.4d; Hume & Steel 2013, fig.7E; Claessens *et al.* 2015, figs.44, 45, pls.PL30, D30; Angst *et al.* 2017, fig.3a; Serrano *et al.* 2020, figs.4, 5, 6B [graphs]. *Pezophaps*: Strickland & Melville 1848, pl.xiv, figs.1-3; Strickland 1853, pl.55, figs.1, 2; A. Newton 1865a, pl.viii, fig.3; Newton & Newton 1869, pl.xix, figs.91, 92; Ottow 1950, pl.iii, fig.9, pl.viii, fig.22; Lüttschwager 1961, fig.20;[138] Hume & Steel 2013, figs.5A, B, 7A, B)

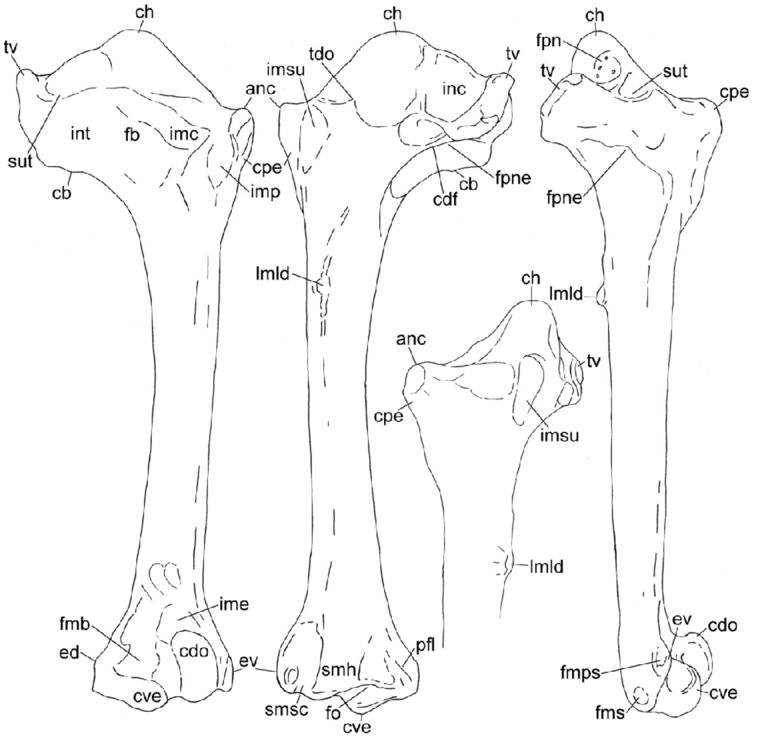

Humerus of *Raphus*, left side; cranial, caudal, dorsal (proximal end) and ventral views (traced from Owen 1867, pl.xx, figs.12-14).

The humerus of *Raphus* is similar to those of volant columbids. However, it is less robust than those of volant columbids (Serrano *et al.* 2020), with a proportionately more elongate shaft. Serrano *et al.* attributed this to "an apparent reversal towards the plesiomorphic condition" due to the release of the functional contraints of flight (p.13). According to Owen (1867), the muscle attachment areas are as developed in *Raphus* as they are in volant pigeons. As in other columbids the proximal end of the humerus projects slightly ventrally. It has an elongate ovoid form, with the larger end toward the dorsal

---

[137] The ratio is 0.88±0.10 for Columbiformes (Nudds *et al.* 2004). It is 0.80-0.81 for *Caloenas*, 0.80-0.84 for *Goura*, and 0.84 for *Didunculus* (Verheyen 1957).

[138] Lüttschwager (1961, fig.20) figured a humerus of a juvenile solitaire ('Jungtier'). However, this specimen does not belong to *Pezophaps*, but instead to a white-tailed tropic bird (*Phaethon lepturus*) (Pieper 1987).

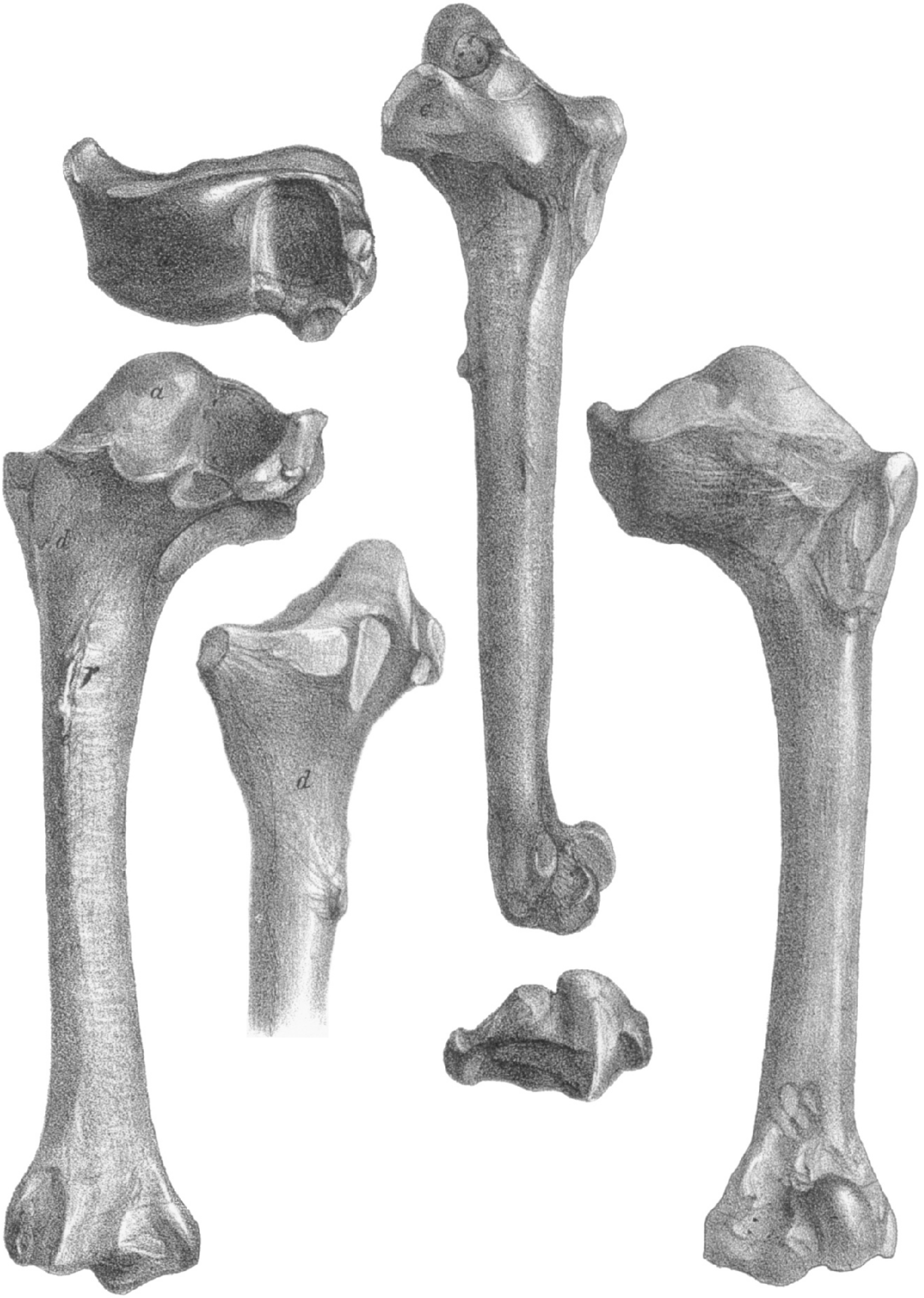

Humerus of *Raphus*, left side; proximal, ventral, caudal, dorsal (proximal end), distal and cranial views (Owen 1867, pl.xx, figs.12-14; artist: James Erxleben; “From nat on Stone by J Erxleben” “M & N Hanhart , imp”).

side, convex caudally, and more flattened cranially. The proximal extremity of the head lies just ventral to the level of the ventral margin of the diaphysis (Claessens *et al*. 2015). The incisura capitis is well developed, rounded and wide, and impresses the ventral margin of the articular surface and the dorsal base of the ventral tubercle. It presents pneumatic foramina proximally and distally (as seen in OUMNH 19619). The dorsal tubercle is small, but distinct, and is slightly proximodistally elongate; it provided attachment for the tendon of m. supracoracoideus. The deltopectoral crest is variably developed, but proportionately shorter than in volant columbids; it is triangular and curved slightly craniodorsally. In some specimens the deltopectoral crest is prominent (as in Owen 1867, pl.xx, figs.12-14; Thirioux's Port Louis skeleton, the Durban skeleton), whereas in others (for example UMZC 415.K) it is only a slight rounded projection. The impressio m. supracoracoidei, on the caudal surface at the base of the deltopectoral crest, is elongate. The ventral tubercle is oblong and its ventral border is convex; it is directed proximally and slightly ventrally. In one specimen (OUMNH 19619; left side), the ventral tubercle projects very prominently proximally, due partly to the recession of the proximal part of the cranial wall of the incisura capitis. Livezey (1993) stated that the proximal end of the humerus, including the bicipital crest and ventral tubercle, is displaced ventrally relative to the axis of the humeral shaft; in this respect *Raphus* differs from *Pezophaps*. The bicipital crest projects caudally. The junction between the bicipital crest and the shaft is curved in some specimens, but more angular in others (OUMNH specimens). The angle between the distal border of the bicipital crest and the long axis of the humerus is smaller in *Raphus* than it is in *Pezophaps* and *Caloenas* (Claessens *et al*. 2015; pers. obs.). The relative distance from the proximal extremity of the humerus to the distal border of the bicipital crest is similar to that of *Pezophaps* and *Goura*, but a little less than in smaller pigeons such as *Caloenas* and *Didunculus* (Claessens *et al*. 2015; pers. obs.). A ridge passes from the bicipital crest distally, ending on the caudal face at a level about a third of the way down the shaft (Claessens *et al*. 2015). There is a shallow impressio coracobrachialis and sulcus ligamentum transversus visible on the cranial face. The sulcus n. coracobrachialis is not present (*ibid*.). The pneumotricipital fossa, which impresses the distal base of the ventral tubercle, is deep and contains a pneumatic foramen or foramina.[139] The fossa varies in depth between individuals. The intumescentia, opposite to this pneumatic fossa, is wide and convex. The shaft of the humerus has a subcircular cross-section, and on its caudal face, at around the proximal third of the bone, it presents the distinct longitudinal ridge of the linea m. latissimi dorsi. The development of the attachment for m. latissimus dorsi suggests that the wing was habitually used, perhaps in display. The distal end of the humerus is similar to those of extant columbids. The dorsal epicondyle is present as a longitudinally elongate tubercle. The dorsal condyle is pronounced, as it is in volant columbids. The ventral condyle is rounded and the ventral epicondyle is broader than its dorsal counterpart. The sub-trapezoidal fossa for the attachment of m. brachialis is shallow, yet large and well defined. In *Raphus* and *Pezophaps* the distance the brachial fossa extends proximally (measured from the distal margin of the humerus) is greater than the distal width of the humerus (a feature also seen in *Natunaornis* and *Goura*). Adjacent (dorsal) to the attachment surface for m. brachialis (and proximoventral to the dorsal condyle), and separated from it by a narrow ridge, is a shallow depression that may have been for the attachment of the ventral head of m. extensor carpi radialis. In *Pezophaps* this impression is not well differentiated from that of m. brachialis. A processus supracondylaris dorsalis is not present in either *Raphus* or *Pezophaps*. A slight subcircular depression on the ventral side of the distal part of the ventral epicondyle probably corresponds to the fossa m. pronator superficialis. The processus flexorius is rounded; it provided attachment for m. flexor carpi ulnaris (Baumel & Witmer 1993). The humerotricipital sulcus is wider than the scapulotricipital sulcus; the latter curves from the caudal face onto the distal face (Claessens *et al*. 2015). Claessens *et al*. (2015) stated that there is a pneumatic foramen proximal to the humerotricipital sulcus.

In longitudinal section the head of the humerus shows "a fine cancellous structure" internally (Owen 1867, p.63). Distal to this, the foramina of the pneumatic fossa open into a large space traversed by a transverse thin osseous bar in Owen's figure (1867, pl.xxiii, fig.5). The internal structure of the deltopectoral crest and other proximal processes of the humerus also shows an arrangement of crossing trabeculae. The inside of the shaft of the humerus comprises a large space, with no trabeculae; the walls of the shaft are thicker than those of the proximal and distal ends of the bone, "but not exceeding that which is characteristic of the long air-bones in birds" (*ibid.*, p.63). The distal end of the humerus also presents a cancellous internal structure.

---

[139] In Thirioux's Port Louis skeleton it contains one large pneumatic foramen (Claessens *et al*. 2015).

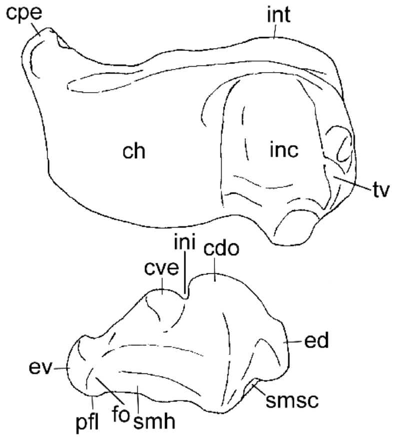

Humerus of *Raphus*, left side; proximal and distal views (traced from Owen 1867, pl.xx, figs.14a, c).

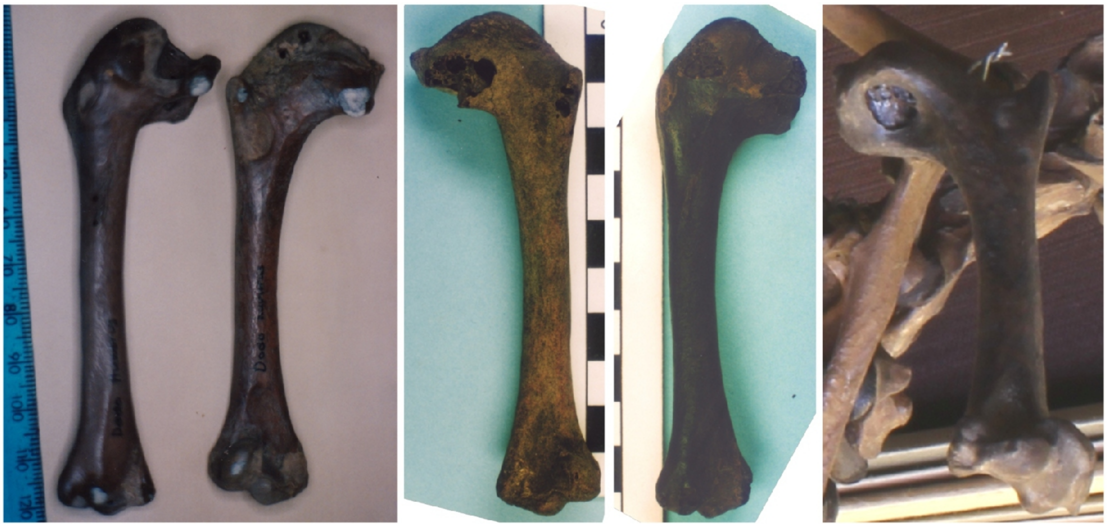

Humerus of *Raphus*. *Left*: left and right sides, caudal and cranial views (OUMNH 19619; ○ Jolyon C. Parish, January 2001); *middle*: two left humeri, cranial and caudal views (UMZC 415.K specimens; © E. C. Parish); *right*: left humerus, oblique distal view (3221, World Museum, Liverpool; © David Gonzalez).

In Thirioux's Port Louis skeleton and the Durban skeleton the right humerus is slightly longer and more robust than the left (Claessens *et al*. 2015).[140] Martin (1904) noted that the angle between the long axis of the dorsal condyle and that of the shaft of the humerus was less in *Raphus* and *Pezophaps* than in volant columbids, and that the distal part of the shaft of the humerus was proportionately broader.

The humerus of *Pezophaps* is similar to that of *Raphus*, although the processes for muscle attachment are less well developed. The proximal end is more rounded and bulbous, and not as proximally projecting as in *Raphus* and other columbids, and "the oval convexity of the articular head [is] absolutely (even in the smallest specimens) more elongated outwardly"(Newton & Newton 1869, p.341). The cranial face of the head is more transversely concave compared with that of *Raphus* (*ibid.*). The rounded deltopectoral crest is only very slightly developed, and the dorsal tubercle is hardly developed at all. The ventral tubercle, also, is not as well developed as in *Raphus*. The incisura capitis is narrower, and presents a pneumatic foramen (as in NHMUK A.1379). The pneumotricipital fossa is much narrower and contains a much larger pneumatic foramen (UMZC 415.R; Newton & Newton 1869). The bicipital crest is less prominent ventrally and its distal border curves gently into the humeral shaft. The impressio coracobrachialis is deeper in *Pezophaps*, particularly distal to the dorsal tubercle (Claessens *et al*. 2015). In some specimens the linea m. latissimi dorsi is faint and not as well formed as in *Raphus*, and is sometimes not present (Newton & Newton 1869; pers. obs.), although in many specimens (*e.g.*, UMZC 635) it is as at least as well developed as that of *Raphus*. The origin for m. brachialis is, as in *Raphus*, less defined than in volant pigeons, although it is deeper than in the dodo. The other muscle attachments of the distal end of the humerus resemble those of *Raphus*. The humeral shaft is slightly wider in transverse diameter than cranio-caudal one (A. Newton 1865a). The humerotricipital and scapulotricipital sulci are relatively shallower than in *Raphus* and the processus flexorius is not as prominent caudally (Claessens *et al*. 2015). Newton & Newton (1869) stated that "the cancellous structure of either end [of the humerus] is perhaps rather less developed in *Pezophaps* [than in *Raphus*]" (p.341). Strickland (1853) described the internal structure of the proximal end of the humerus as "coarsely interlacing cancellous fibres" (p.192).

---

[140] Thirioux's Port Louis skeleton: left 106mm, right 107mm; the Durban skeleton: left 105.5mm, right 106mm (Claessens *et al*. 2015).

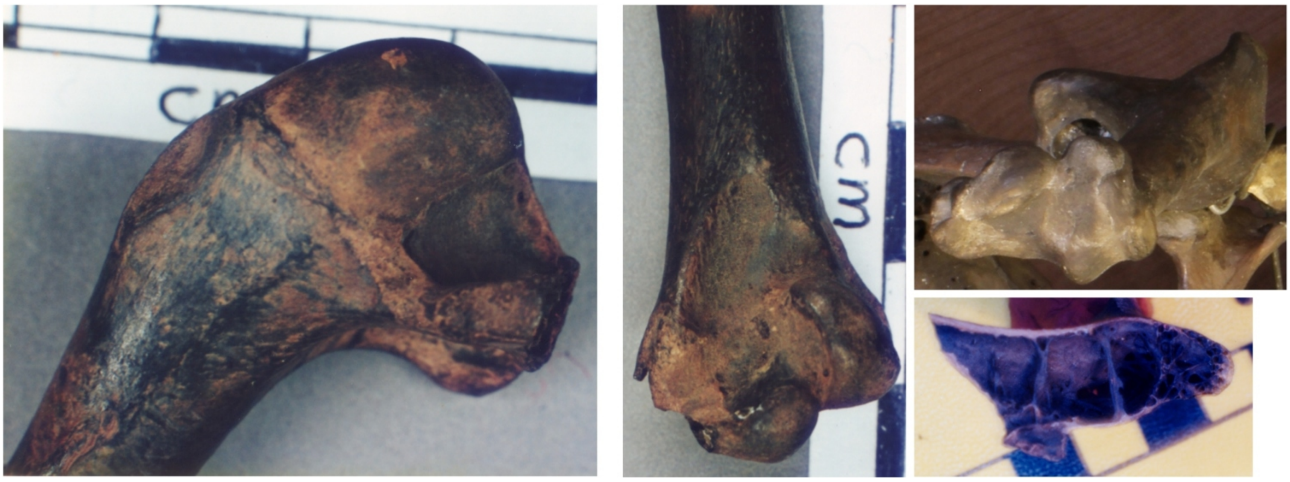

Humerus of *Raphus*. *Left*: left side, caudal view of proximal end; *middle*: left side, cranial view of distal end (both UMZC 415.K specimen; © E. C. Parish); top right: left side, distal view (3221, World Museum, Liverpool; © David Gonzalez); *bottom right*: right side, sagittal section of proximal end (NHMUK A.1338; ○ Jolyon C. Parish).

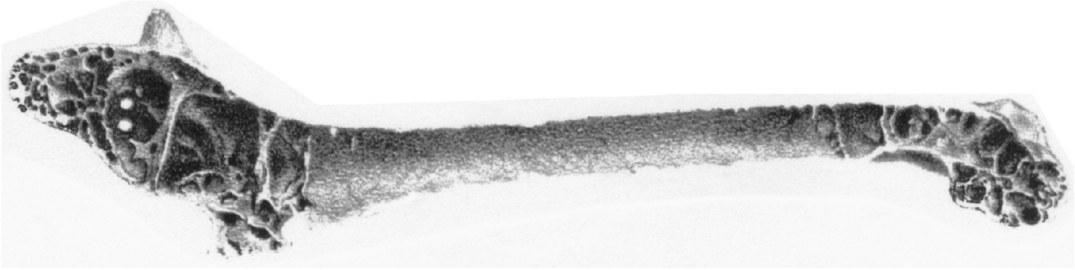

Humerus of *Raphus*, longitudinal section (Owen 1867, pl.xxiii, fig.5; "J Smit lith" "M & N Hanhart imp").

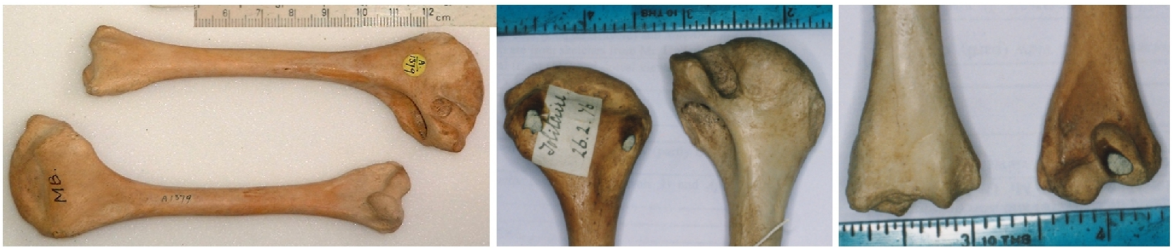

Humerus of *Pezophaps*. *Left* to *right*: left and right sides, caucal and cranial views (NHMUK A.1379); left and right sides, cranial and caudal views of proximal ends (OUMNH 19631); right and left sides, caudal and cranial views of distal ends (OUMNH 19631). (○ Jolyon C. Parish).

Ulna

(*Raphus*: Owen 1867, pl.xx, figs.16, 17; Hume & Steel 2013, fig.5E; Claessens et al. 2015, figs.44, 47, pls.PL32, D32. *Pezophaps*: Newton & Newton 1869, pl.xix, figs.93, 96, pl.xx, figs.134, 135; Lucas 1895, fig.1; Ottow 1950, pl.iii, fig.10, pl.iv, fig.11, pl.viii, fig.21; Ottow 1951, fig.3; Lüttschwager 1961, figs.18, 20; Hume & Steel 2013, figs.5A, B, 7E, F)

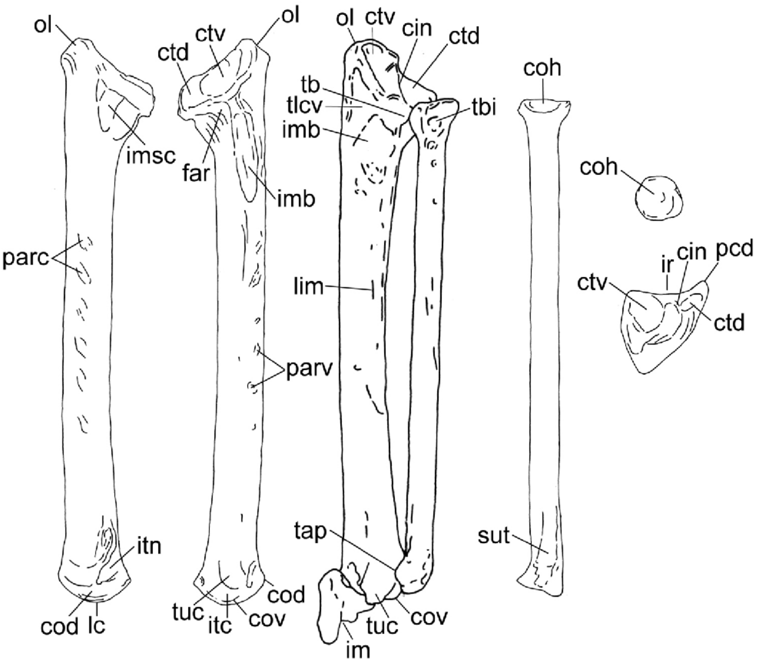

Radius, ulna and ulnare of *Raphus*. Right ulna, dorsal and ventral views; left radius, ulna and ulnare; right radius, dorsal and proximal views; right, proximal view. (Traced from Owen 1867, pl.xx, figs.15, 16, 17; except the articulated radius, ulna and ulnare which are traced from a photograph (10A) sent by E. Thirioux to Alfred Newton, dated 5th October 1900).

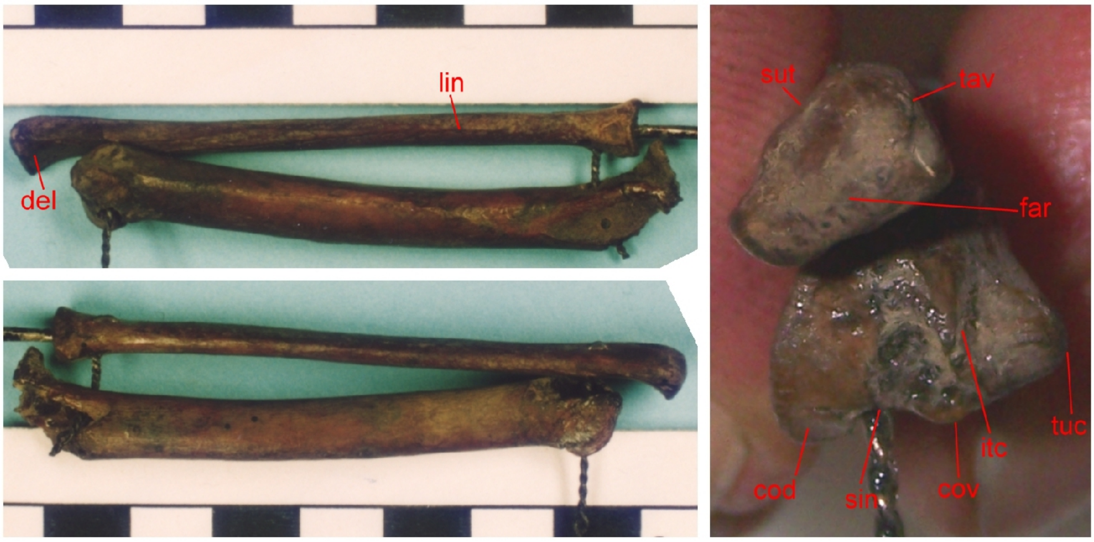

Radius and ulna of *Raphus*, right side (UMZC 415.K specimen; © E. C. Parish).

The apneumatic[141] ulna of *Raphus* is almost straight, whereas those of volant columbids are slightly curved. It is also slightly more robust than in the latter. The degree of curvature varies slightly, being less curved in the ulna described by Owen (1867) than in the ulnae of Thirioux's Port Louis skeleton and the Durban skeleton (Claessens *et al*. 2015). The proximal end of the ulna in Thirioux's Port Louis skeleton and the Durban skeleton is "fairly curved" and the distal portion "somewhat straighter" (*ibid*., p.84). In the dodo the impression for m. brachialis is elliptical and well defined; it resembles that of volant pigeons, extending longitudially from the proximal part of the shaft. Lydekker (1891) stated that the "great development of the ridge forming the outer boundary of the surface for the insertion of the brachialis anticus [= m. brachialis] is remarkable in a bird incapable of flight" (p.130). The margin of the dorsal cotyla shows a prominent dorsal cotylar process, as in extant pigeons; on the dorsal face of the process is the impressio scapulotriceps. The dorsal cotyle is smaller and less deep than the ventral cotyle (*contra* Claessens *et al*. 2015). The ventral margin of the incisura radialis is marked by a ridge (Claessens *et al*. 2015).

---

[141] Although see below.

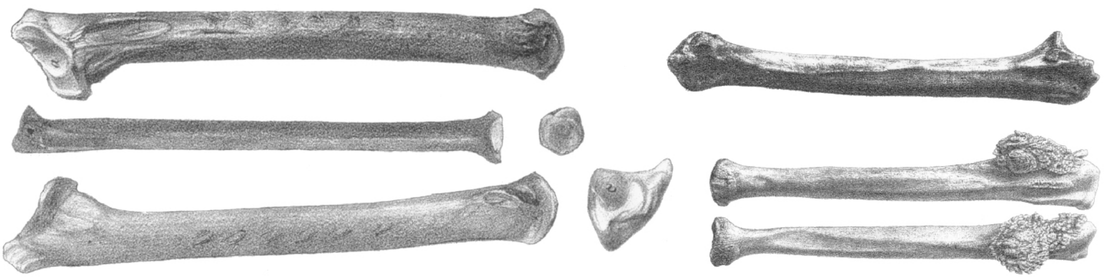

Left: right ulna and radius of *Raphus*, ventral, dorsal and proximal views of ulna, dorsal and proximal views of radius (Owen 1867, pl.xx, figs.15, 16, 17; artist: James Erxleben; "From nat on Stone by J Erxleben" "M & N Hanhart , imp"). *Right*: ulna and radius of *Pezophaps*: right ulna (male), ventral view; right radius (male), dorsal and cranial views (Newton & Newton 1869, pl.xix, fig.96; pl.xx, figs.137, 138; artist: George Henry Ford; "G. H. Ford ad nat. lith." "W. West imp.")

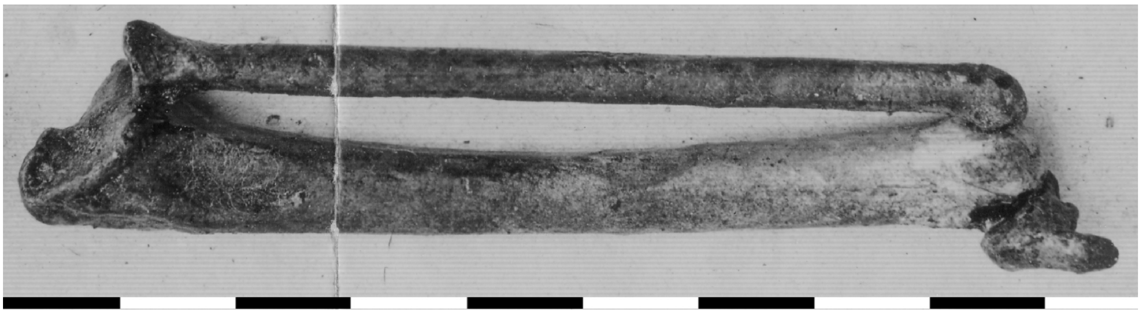

Radius, ulna and ulnare of *Raphus*, left side (from a photograph (10A) sent by E. Thirioux to Alfred Newton, dated 5th October 1900; scale in cm; © UMZC).

The olecranon, for the attachment of m. humerotriceps, forms a short stub. The foramen for the medullary artery is just proximal to the middle of the shaft, and its canal inclines distally (Owen 1867). The caudal remigeal papillae (six? in Owen 1867, pl.xx, figs.16, 17; six in Thiroux's Port Louis skeleton: Claessens *et al*. 2015)[142] for the secondaries, can be seen on the slightly curved caudal face and are more prominent in *Raphus* than in volant columbids (*ibid*.). The ulna illustrated in Owen's work appears to show both caudal and ventral remigeal papillae. In both *Raphus* and *Pezophaps* the ulna is shorter than the humerus; in volant columbids the reverse is the case (pers. obs.; Livezey 1993). In addition, Owen (1867) stated: "the rough depression for the insertion of the chief flexor is less deep and less defined [in *Goura*, compared with *Raphus*]. The plumed winglet of the Dodo would seem, therefore, to have been frequently and more forcibly moved" (p.78).

The depressio radialis is oval and the intercondylar sulcus is well developed. The dorsal and ventral condyles are convex and separated by a shallow sulcus (Claessens *et al*. 2015; pers.obs.). The incisura tendineus is well-marked. The incisura tuberculum carpalis is deep and narrow; according to Claessens *et al*. (2015), it includes small pneumatic foramina in Thirioux's Port Louis specimen. However, Owen

---

[142] There are eight in *Columba palumbus* (pers. obs.).

(1867) stated that the ulna had no pneumatic foramina (although he evidently only examined two specimens) and the ulna is apneumatic and marrow-filled in *Columba* (Müller 1908; pers. obs.).

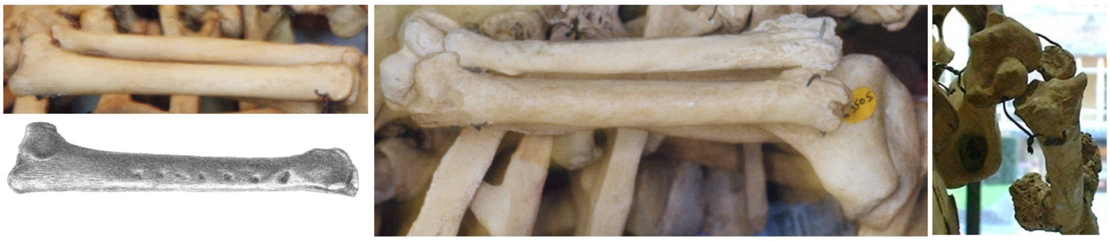

Radius and ulna of *Pezophaps*. *Top left*: right side (female; NHMUK A.3506), *bottom left*: right ulna (female), dorsal view (Newton & Newton 1869, pl.xx, fig.134; artist: George Henry Ford; "G. H. Ford ad nat. lith." "W. West imp."); *middle*: right side (male; NHMUK A.3505); *right*: right side, oblique distal view (UMZC 415.R). (All (except Newton & Newton 1869 image) ○ Jolyon C. Parish).

The ulna of *Pezophaps* is cylindrical, straighter and proportionately thicker than that of *Raphus*. The olecranon is less projecting. The crista intercotylaris is less extensive and directed less dorsally, and the impressio scapulotricipitis is shallower in *Pezophaps* (Claessens *et al*. 2015). The impression for m. brachialis is smaller, less well defined, and located more distally than in the dodo (Newton & Newton 1869). There may be up to ten remigeal papillar impressions in some specimens (*ibid*.), with, also on the caudal surface of the ulna, "three elongated and transversely-directed depressions towards the distal end" (*ibid*., p.342). Cranial to these depressions, Newton & Newton (1869) found, in two or three large specimens, a small bone tuberosity (*ibid*.). The tuberculum carpale is located proportionately further proximally in *Pezophaps* than in *Raphus* (pers. obs.) and the depressio radialis is relatively deeper (Claessens *et al*. 2015).

Radius

(*Raphus*: Owen 1867, pl.xx, fig.15; Meijer *et al*. 2012, fig.4e; Hume & Steel 2013, fig.5E; Claessens *et al*. 2015, figs.44, 46, pls.PL31, D31. *Pezophaps*: Newton & Newton 1869, pl.xix, figs.94,95, pl.xx, figs.137, 138; Lucas 1895, fig.1; Ottow 1950, pl.iv, fig.12, pl.v, fig.13, pl.vii, fig.19; Ottow 1951, fig.2; Lüttschwager 1961, fig.20; Fuller 2002, p.163; Hume & Steel 2013, figs.5A, B, 6B)

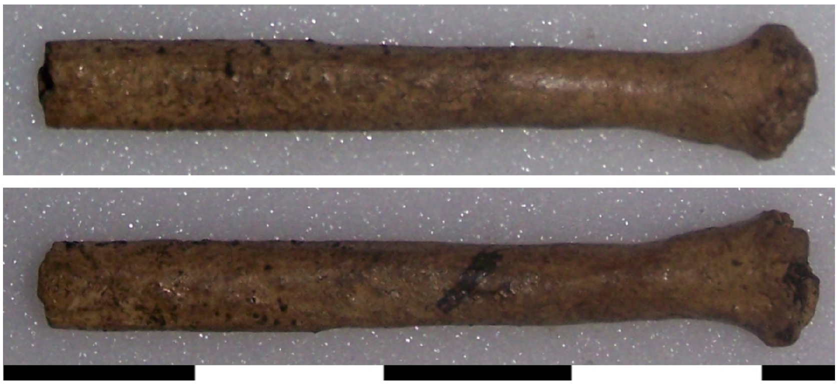

Radius of *Raphus*, distal end of left side, dorsal and ventral views (UMZC 415.KK specimen; ○ Jolyon C. Parish, December 2008).

The radius of *Raphus* is straight and slender and is more robust than those of volant columbids. The proximal (humeral) articular surface is subcircular and fairly concave. The articular face for the ulna is small and flat and located adjacent to the articular face for the humerus, which is bordered by ridges (Claessens *et al*. 2015). At the distal end of the ulnar articular face is the small bicipital tubercle, to which m. biceps brachii was attached in life. Two intermuscular lines run longitudinally on the caudal face of the radius, one of these joins with the tuberculum aponeurosis ventralis. Another intermuscular line passes from the bicipital tubercle to the tendinal sulcus at the distal end. The facies articularis radiocarpalis is bordered by a ridge (Claessens *et al*. 2015). The distal end of the radius is expanded to the same width as the proximal; it is compressed dorsoventrally and curves slightly caudally. The distal end of the radius shows an indistinct crest in *Raphus*, which is more defined in male *Pezophaps* as an exostosis (pers. obs., Verheyen 1957). The tendinal sulcus is wide and shallow. The depressio ligamentosa, for lig.interosseum radioulnare distale, is visible on the ventral side.

In Thirioux’s Port Louis skeleton and the Durban skeleton the right radius is slightly more robust than the left (Claessens *et al*. 2015).

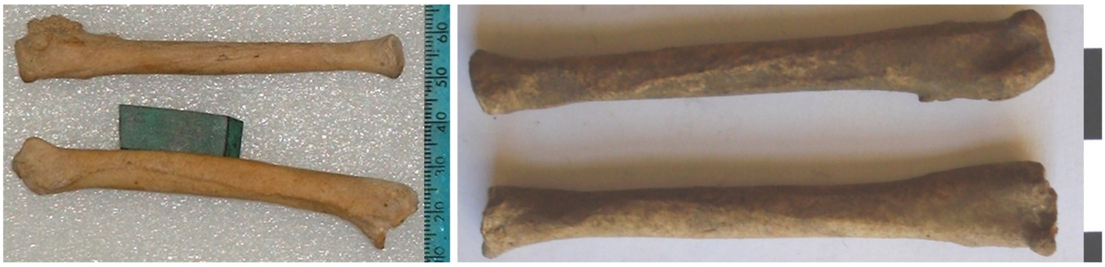

Radius and ulna of *Pezophaps*. *Left*: right radius and left ulna, ventral views (YPM VP.057037; ○ Jolyon C. Parish, May 2001); *right*: two radii (Natural History Museum, Dublin; © David Gonzalez).

The radius of *Pezophaps* is robust, nearly straight and sub-cylindrical. It shows little similarity to that of *Raphus*. The radius of *Pezophaps* is proportionately thicker than in *Raphus*, particularly near the distal end (Newton & Newton 1869). The radius thickens from near the proximal end, and widens laterally towards the distal end, where it is almost twice the width of the middle of the shaft. It has a straight shaft with a round proximal extremity and a larger, wider and flatter distal one. The proximal articular surface is similar to that of *Raphus*, though larger, and the ridges bordering the articular face for the humerus are less developed (Claessens *et al*. 2015). The bicipital tubercle is also less distinct. The intermuscular lines on the caudomedial face are distinct. The distal end shows a marked and relatively deep tendinal sulcus for the extensor tendons of the carpus (see, for example, NHMUK A.3505), indicating that the carpus was habitually moved. In male specimens it is often bordered dorsally by a large exostosis; a smaller exostosis may also occur on the ventral side of the sulcus, opposite the larger one. The tuberculum aponeurosis ventralis is more rounded than in *Raphus*. The facies articularis radiocarpalis is less distinct and less rounded than in *Raphus* and the depressio ligamentosa is shallower (Claessens *et al.* 2015). The female radius is generally much more gracile and thinner than that of the male.

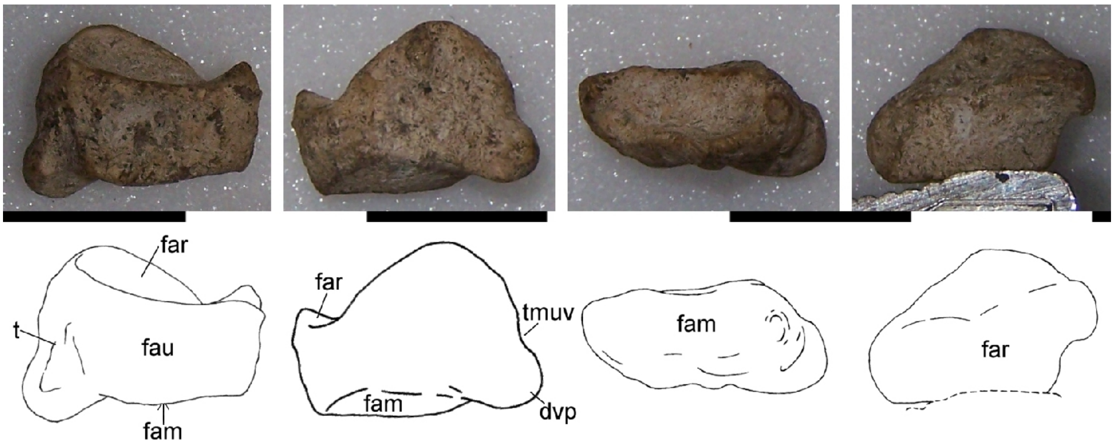

Radiale of *Raphus*, right side (UMZC 415.KK specimen; ○ Jolyon C. Parish, December 2008).

Radiale

(*Raphus*: Claessens & Hume 2015, fig.6A; Claessens *et al*. 2015, figs.48, 50, pls.PL33, D33)

The radiale is only known in *Raphus* in the Durban (both wings: Chubb 1919a; Claessens *et al*. 2015) and Thirioux's Port Louis skeletons (both wings), in the UMZC 415.KK collection (right radiale) and also apparently in the MNHN skeleton (left wing). The articular face for the radius is slightly concave, as is that for the carpometacarpus.

A possible radiale is known for *Pezophaps* in the UMZC 653 collection.[143]

Ulnare
(*Raphus*: Claessens *et al*. 2015, figs.44A-B, 48, 49, pl.PL33. *Pezophaps*: Hume & Steel 2013, fig.5A)

The ulnare of both *Raphus* and *Pezophaps* is similar to those of extant columbids. In *Raphus* the ulnare is known only from Thirioux's Port Louis skeleton (left and right sides), Paul Carié's skeleton (right side only) and Thirioux's collection.[144] The dorsal ramus is larger than the ventral one and the the articular surface for the ulna is slightly concave (Claessens *et al*. 2015). The ulnare is known in *Pezophaps* in NHMUK A.3505 and A.3506 and in the UMZC 653 collection. The dorsal ramus is proportionately longer, compared to the ventral ramus, in *Pezophaps* than in *Raphus*. In NHMUK A.3505 the ulnare bears some exostotic growth.

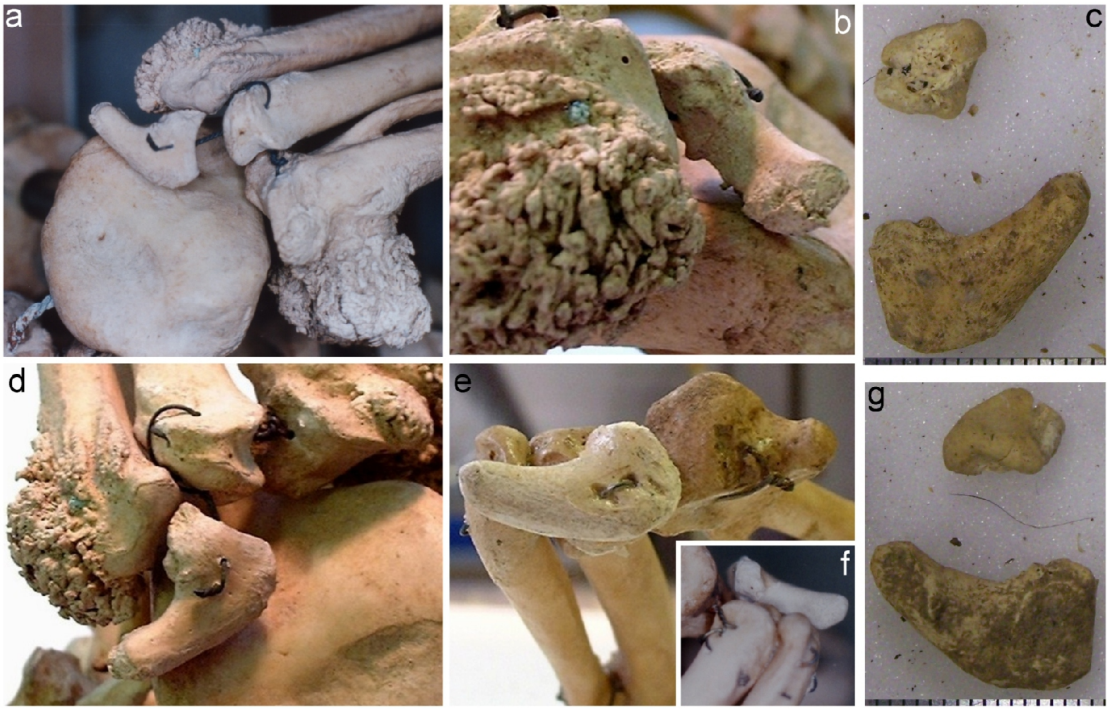

Carpal bones of *Pezophaps*. a, b and d: left wing of NHMUK A.3505 (male), showing ulnare; c and g: ulnare and possible radiale (UMZC specimens); e and f: left wing of NHMUK A.3505 (female), showing ulnare. ○ Jolyon C. Parish.

---

[143] Slater ("Abstract from H. H. Slater's Report, on Rodriguez-Collection", Royal Society Transit of Venus Expeditions. Correspondence and papers relating to distribution of collections and preparation of reports 1875-1876, DF 202/9, NHMUK General Library), however, stated that he did not find a single radiale ('radial') during his searches.

[144] Thirioux mentioned that he possessed "le 2 os de posterieure du metacarpien" (the 2 bones of the posterior of the carpometacarpus): presumably the radiale and ulnare (see Transcriptions: Thirioux-Newton Correspondence, letter 17, dated 13th November 1901). He also sent Alfred Newton a photograph of an ulnare in his collection (letter 10A, dated 5th October 1900). The carpal bones, carpometacarpus and alar phalanges of *Raphus* figured by Owen (1867, pl.xv, fig.1) are interpolations, as they were unknown at the time.

Carpometacarpus

(*Raphus*: Newton & Gadow 1893, pl.xxxvi, fig.5; Meijer *et al*. 2012, fig.4f; Hume & Steel 2013, fig.5E; Claessens *et al*. 2015, figs.44A-D, 48, 51, pls. PL34, D34. *Pezophaps*: Newton & Newton 1869, pl.xix, figs.87-90, pl.xx, fig.131, pl.xxii, fig.148; Lucas 1895, fig.1; Abel 1935 figs.474, 475; Ottow 1950, pl.v, figs.14, 15, pl.vi, fig.16, pl.vii, fig.20; Ottow 1951, fig.1; Lüttschwager 1961, fig.19; Hume & Steel 2013, figs.3, 4, 5A, B, 6A)

Carpometacarpi are known for *Raphus* in UMZC 415.H, UMZC 415.KK, the NHMUK collection (Hume & Steel 2013), the Musée d'Elbeuf collection (18.0.67), the MNHN and Durban skeletons, Thirioux's and Sauzier's skeletons at Port Louis, Paul Carié's skeleton, the Summers Place Auctions skeleton, MCZ 340825, MCZ 341170, CM Av6279, MAS 2005-10, MAS AG 62, and in Thirioux's collection.[145]

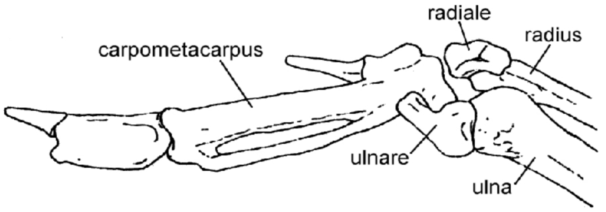

Carpus of *Raphus* (traced from a photograph of Thirioux's Port Louis skeleton; right side, reversed).

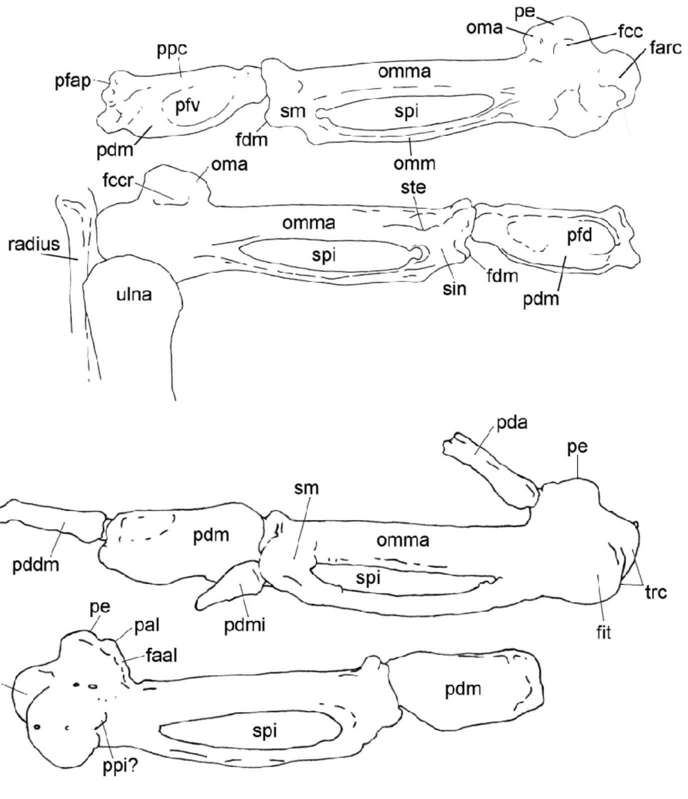

Carpus of *Raphus*. *Top*: ventral and dorsal views (traced from Newton & Gadow 1893, pl.xxxvi, fig.5); *bottom*: right and left carpi, ventral views (traced from a photograph (10A) sent by E. Thirioux to Alfred Newton, dated 5th October 1900).

---

[145] See Thirioux-Newton Correspondence, photographs (10A, 13A) accompanying letters dated 5th October 1900 and 31st January 1901.

The carpometacarpus of *Raphus* is similar to those of extant columbids. The extensor process is block-like and simple and the alular process is indistinct. The intermetacarpal space is proportionately shorter than in volant columbids, and in one specimen (Newton & Gadow 1893, pl.xxxvi, fig.5) its distal margin shows a circular notch in *Raphus*. In addition, the distal metacarpal synostosis is proportionately longer than in volant pigeons. The pisiform process is variably present in *Raphus*: it is present, albeit small, in Thiroux's Port Louis skeleton and the Durban skeleton (Claessens *et al.* 2015), but absent in the UMZC 415.KK carpometacarpus and evidently in a specimen in Thirioux's collection.[146]

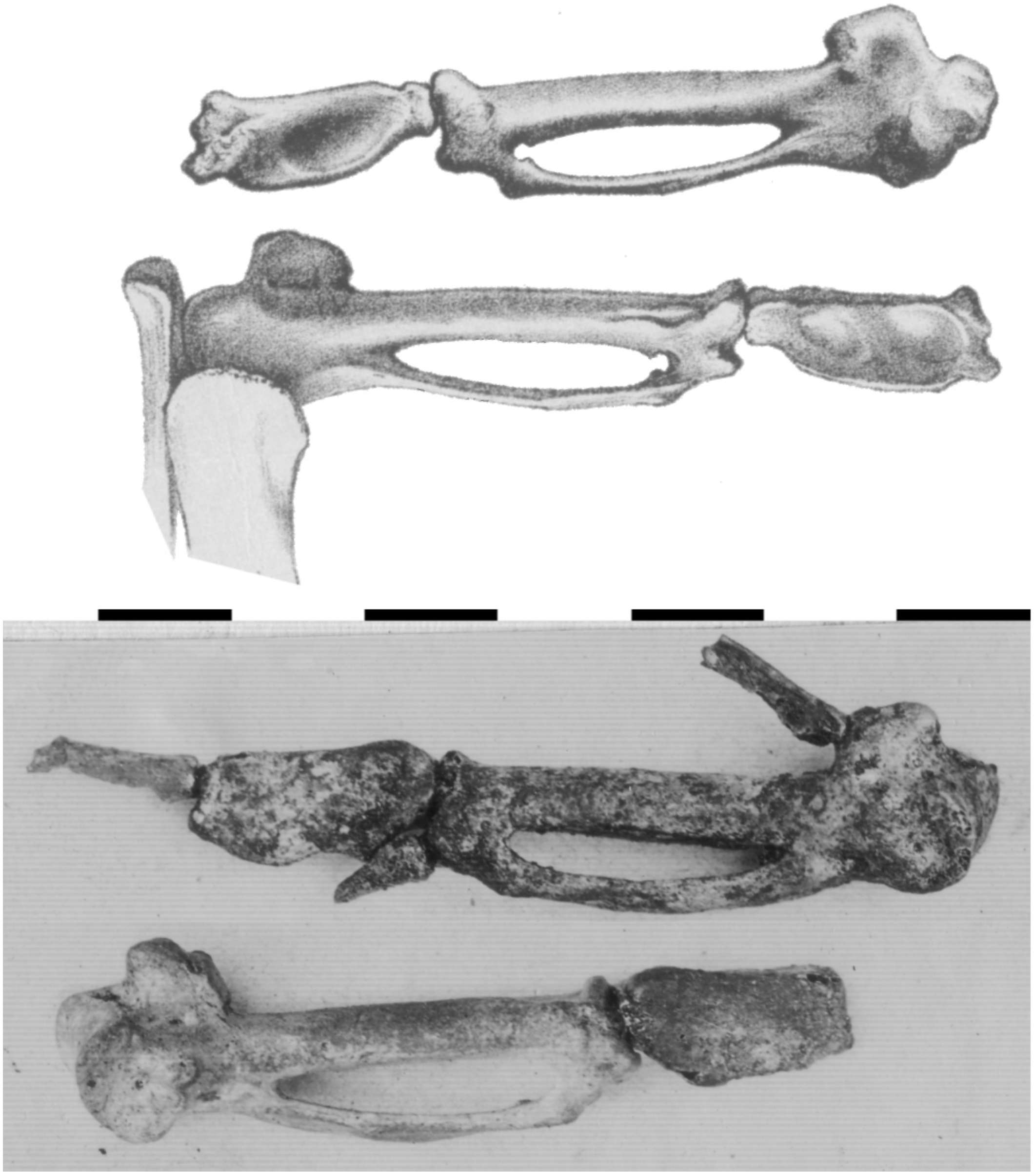

Carpus of *Raphus*. *Top*: ventral and dorsal views (Newton & Gadow 1893, pl.xxxvi, fig.5); *bottom*: right and left carpi, ventral views (from a photograph (10A) sent by E. Thirioux to Alfred Newton, dated 5th October 1900; © UMZC). Scale in cm.

The minor metacarpal (os metacarpale minus) of *Raphus* is also proportionately more slender than in *Pezophaps*; it is craniocaudally compressed. The major (os metacarpalia majus) and minor metacarpals are comparatively long, slender and cylindrical compared with those of *Pezophaps*. The major metacarpal extends further distally than the minor in *Raphus*; in some specimens of *Pezophaps* the minor metacarpal extends slightly further distally. In both taxa the distal end of the minor metacarpal joins with that of the major metacarpal on the ventral side of the caudal face of the latter, as in other columbids. Verheyen (1957) stated that there was some degree of exostotic development in the region of the base of the first metacarpal in *Raphus*, similar to, but far less developed, than that of *Pezophaps*;[147] this has not been confirmed. The sulcus interosseus is deep and (in Thirioux's Port Louis skeleton) its border is marked by small ridges on its cranial side (on the major metacarpal) (Claessens *et al*. 2015). The supratrochlear fossa is shallow. The sulcus tendineus is bordered by a ridge (Claessens *et al*. 2015; see Newton & Gadow 1893 pl.xxxvi, fig.5).

---

[146] See Thirioux-Newton Correspondence, photographs (10A, 13A) accompanying letters dated 5th October 1900 and 31st January 1901 (right carpometacarpus).

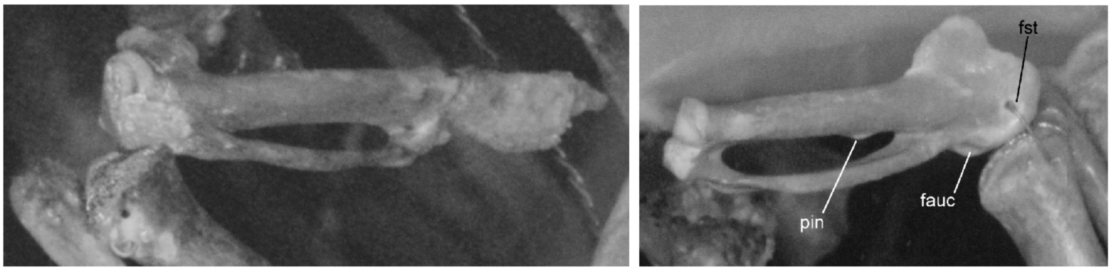

Carpometacarpus of *Raphus*, right and left sides (UMZC 415.H; ○ Jolyon C. Parish, December 2008).

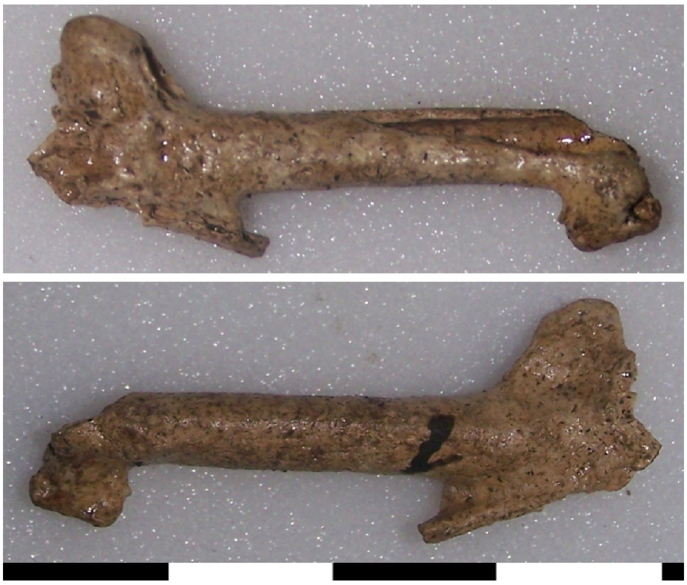

Carpometacarpus of *Raphus*, left side, ventral and dorsal views (UMZC 415.KK specimen; ○ Jolyon C. Parish, December 2008).

Apart from the bone deformities, the carpometacarpus of *Pezophaps*, especially that of the female, shows close resemblance to those of extant columbids. The female carpometacarpus is smaller and more gracile than that of the male. The carpometacarpus of *Pezophaps* has been well documented in the literature, mainly due to the presence of exostoses developed on the extensor process,[148] which provide an example of where the description of François Leguat (1708) has been proved correct (see Parish 2013). Owen (1878) stated that "if a single specimen of a metacarpal bone [= carpometacarpus] of some unknown animal [...] had previously come into the hands of a palæontologist, he would have concluded the bony tumour to have been of morbid nature and origin, and set it down as an exceptional pathological phenomenon. Any other opinion (above all, one holding such tumour to be a constant structure, functional in the healthy individual, and of moment in guiding to a knowledge of the species or sex) would have hazarded the estimate of such palæontologist's standing in his science" (p.93). Although it occurs frequently in *Pezophaps*, the carpal knob, or exostosis, of the carpometacarpus is indeed a pathological phenomenon (and is further discussed in the section on pathologies, below). The large exostosis of the carpometacarpus was considered, by Owen (1878) and others, to be used in fighting between male *Pezophaps*, as Leguat's description mentions. All complete specimens of the male carpometacarpus of *Pezophaps* examined by Newton & Newton (1869) showed, on the cranial (radial) side, a "more or less spherical bony knob or callus-like mass developed immediately beyond the proximal end and the pollex [= phalanx digiti alulae], which last would appear to be thrust away by it to some extent" (*ibid*., p.342). These exostoses display much individual variation, both in morphology, and to a lesser extent, in size. In all specimens studied by Newton & Newton (*ibid*.) the exostosis was more or less pedunculate. In some specimens the exostosis projects downward rather than laterally (*ibid*.). In large male specimens the exostosis is up to around half the length of the carpometacarpus, and its transverse width is not much less (*ibid*.). The carpometacarpus is pneumatic and light, the largest specimen examined by the above authors "weighing, the [carpal] knob and all, just about quarter of an ounce [= 7g]; but the knob, which has been broken off from another specimen, weighs as much as the remainder" (*ibid*., p.342). They also stated that the exostosis was probably covered by a cartilaginous, or horny, integument in life, which may have extended to those of the ulna and radius. The exostoses have a tuberous, porous surface like that of diseased bone and the carpal knob itself may have one, two, or, less commonly, three lobes (Hume & Steel 2013). The surface texture of the carpal knobs of females and smaller males is smoother than that of the males and the knobs are unlobed (*ibid*.).

---

[147] "The fused carpometacarpus shows at the base of the first metacarpal a very projecting exostosis in the males of *Pezophaps solitaria* [...] It is also observed, but with a degree of much less development, in *Raphus*, *Goura*, *Gallicolumba* and *Caloenas* where it answers a callosity of the skin" (p.18).

[148] Such a callosity on the extensor process is also seen in *Natunaornis* (Worthy 2001) and *Goura* (*ibid*.; pers. obs.), although developed to a much lesser extent than seen in male *Pezophaps*.

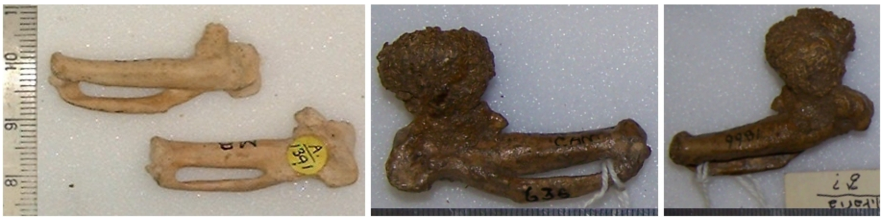

Carpometacarpus of *Pezophaps*. *Left*: left and right sides (female), dorsal and ventral views (NHMUK A.1391); *middle* and *right*: left side (male), ventral and dorsal views (UMZC 636). Scales in cm and mm. ○ Jolyon C. Parish.

All of the carpometacarpi (28 male and seven female) studied by Ottow (1950) showed more-or-less developed exostoses. These were almost always found on the extensor process, and were usually large and extensive; they displayed a very distinct rugose pitted surface. The largest exostosis studied by Ottow measured approximately 29 x 23mm wide and 24mm high, whereas the largest measured by Hume & Steel (2013) was 32.9mm in diameter, although its peduncle was only 14mm wide. There were also other types of bone alteration, and more diffused exostotic growths were also found at the distal end of the carpometacarpus, as well as on the shafts of the metacarpals. Parts of the carpometacarpus were also thickened and swollen. The inner structure of the mass was observed in some specimens where the exostoses had been broken off, showing the core of spongy and compact bone, the area where it had been broken off showed only a small internal space (marrow cavity) (*ibid*., pl.v, fig.14). Hume & Steel (2013) examined 24 male and female carpometacarpi, which were enumerated as follows:

♂ with carpal knob = six
♂ without carpal knob = seven
♀ with carpal knob = four
♀ with carpal knob = seven.

The difference in length between the male carpometacarpi with a carpal knob and those without was statistically significant. However, that of the female carpometacarpi was not.[149]

---

[149] Total length of ♂ carpometacarpi with (48.2 ± 1.45mm, n=6) and without (42.7 ± 1.88mm, n=7) a carpal exostosis. Total length of ♀ carpometacarpi with (39.0 ± 1.18mm, n=4) and without (38.3 ± 1.11mm, n=7) a carpal exostosis (mean ± standard deviation; Hume & Steel 2013).

Female carpometacarpi also show exostoses, usually on the extensor process, although they are generally proportionately smaller than those of the male. In general, the bone irregularities of the female are less developed than those of the male. The exostoses of the female carpometacarpi measured by Ottow (1950) were 10 x 9 x 9mm or smaller. One of the female carpometacarpi he studied was almost normal, with only a small exostosis on the middle of the cranial part of the major metacarpal (*ibid*., pl.vi, fig.16a; NHMUK A.1441). In some female specimens there were also low swellings, which Ottow considered to be dysplastic (*ibid*., fig.16a,c). In radiographic analysis (*ibid*., pl.vii, fig.20, four male carpometacarpi) the more-or-less dense bone structure and the endostal and periostal development of the exostoses could be seen.

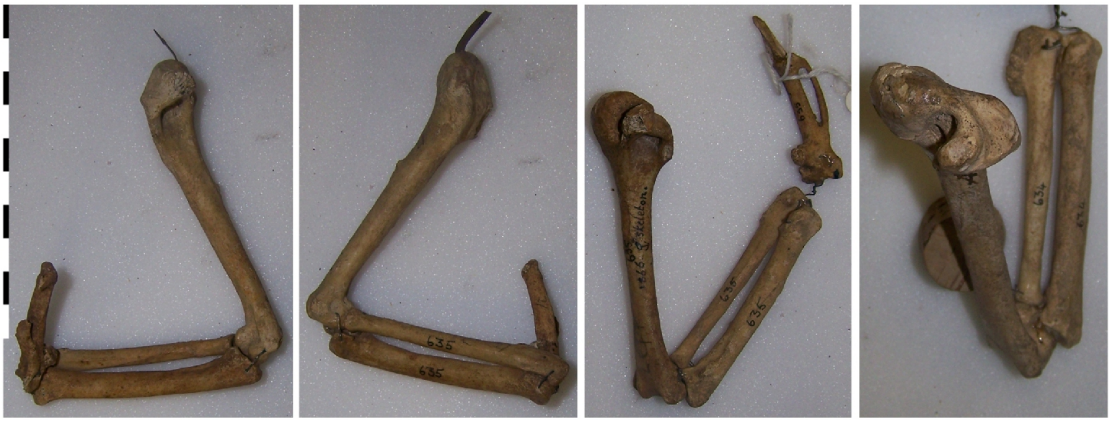

Wing of *Pezophaps*. *Left*: right side, ventral and dorsal views; *right*: left side. (UMZC 635; female; scale in cm (for all images); ○ Jolyon C. Parish, December 2008). Note the projection on the caudal face of the right humerus shaft.

The carpometacarpal and radial exostoses are composed of "highly cancellous woven bone, containing numerous osteocyte lacunae" and resembling a fracture callus (Hume & Steel 2013, p.5). The microscopic structure of an exostosis was described by Joseph Gedge.[150]

> On removing a portion of the exterior (after reducing it to a sufficient tenuity) it presented under a low power the cancellous appearance of moderately old callus. On examining it with high power the [osteocyte: Hume & Steel 2013] lacunæ were for the most part irregular in form; some round with jagged edges, others irregularly stellate, connected together by processes from the lacunæ without the intervention of true canaliculi. A few normal lacunæ and a few vascular canals existed; but there was no lamination. The osseous matter was arranged so as to give an unusually fibrillated aspect to the bone. Irregularity in the form of the lacunæ may not unfrequently be observed in the exterior portion of osseous outgrowths (*e.g.* spavin), when the structure of the interior in no way departs from the ordinary characters of normal bone. It is, however, a character which belongs only to bone which has passed through the stage of rudimental fibrous tissue, and which has not been taken up and laid down again. This growth I consider to be of a nature that might have been produced by irritation of the periosteum, and its formation would appear to have been physiologically analogous to the commonest form of callus (*ibid*., p.343).

Abel's (1935) suggestion that the carpometacarpi of male and female nestlings could have possessed exostoses seems indeterminable. Determining which gender the bones of nestlings belong to is near impossible, and as far as the present author is aware, no carpometacarpi of juvenile *Pezophaps* have ever been found.

---

[150] Joseph Gedge (d. 1870). Admitted to Gonville and Caius College, Cambridge, 1869.

Hume & Steel (2013) remarked: “No growth marks are visible, which indicates that growth did not pause or follow any kind of cycle, but was continuous. We cannot determine how rapidly it grew, but highly cancellous and disorganized tissue typically forms when bone growth is rapid” (p.5).

The pisiform process is either absent in *Pezophaps* (as evidenced by UMZC 635, NHMUK PVA9046), or is at least very reduced (NHMUK PVA9045; Hume & Steel 2013, fig.4D). The major and minor metacarpals are, compared with those of *Raphus*, shorter and flatter, with a rectangular cross-section. The extensor process shows a slight hollow on its dorsal surface. Livezey (1993) stated that the distal end of the carpometacarpus is deflected cranially relative to the long axes of the metacarpals (also a derived character), whereas this is not the case in *Raphus*. However, this character would appear not to apply to all specimens of *Pezophaps* (pers. obs.). The intermetacarpal space is similar to those of volant pigeons, and is widest in the middle of its length or nearer the distal end. The intermetacarpal process is either vestigial or, more commonly, absent in *Pezophaps* (as in Ottow 1950, pl.v, fig.14b). The supratrochlear fossa is more distinct and relatively deeper – at least in some specimens (*e.g.*, UMZC 635), the sulcus interosseus relatively deeper and the sulcus tendineus is less distinct in *Pezophaps* compared with *Raphus*.

Alar phalanges

(*Raphus*: Newton & Gadow 1893, pl.xxxvi, fig.5; Claessens & Hume 2015, fig.6B; Claessens *et al*. 2015, fig.44, pls.PL35, D35.[151] *Pezophaps*: Hume & Steel 2013, fig.5A)[152]

A complete carpus of *Raphus* (carpometacarpus and alar phalanges), in addition to a carpometacarpus and first phalanx of the second digit, is recorded from the Thirioux collection.[153] The alular phalanx is known in Thirioux’s Port Louis skeleton.[154] The first phalanx of the second digit is known in the MNHN, Durban (left and right sides) and Thirioux’s Port Louis (left and right sides) skeletons and in Sauzier’s skeleton (Newon & Gadow, pl.xxxvi, fig.5), and the second phalanx of the second digit is known in Thirioux’s Port Louis (right side) and the Durban skeletons. The phalanx of the third digit is known in the Durban skeleton (only on the right side: Chubb 1919a; Claessens *et al*. 2015) and in the UMZC 415.KK collection. In addition, UMZC 415.H possesses the right alar phalanges 1 and 2 of digit II (right side) and the MNHN skeleton possesses alar phalanges 1 of digit II and an alar phalanx 2 of digit II (left side).

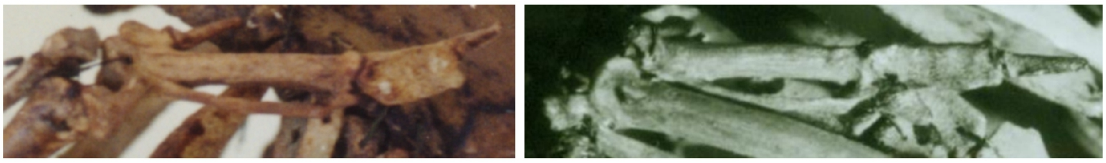

Carpus of *Raphus*. *Left*: Thirioux’s Port Louis skeleton, right side (© Jan den Hengst); *right*: Durban skeleton, right side (2366; © Durban Natural Science Museum).

In males at least, the development of the carpometacarpal exostosis indicates that the alular phalanx was absent in *Pezophaps*. The first phalanx of the second digit of *Raphus* exhibits variation, even in the limited number of specimens known, especially in the development of the distal process. This bone is also known in *Pezophaps* (NHMUK A.1452, A.3506). These specimens resemble those of *Raphus*, although are more robust. Hitherto, this bone has been regarded as being unknown in *Pezophaps*

---

[151] As with the carpometacarpus, the alar phalanges illustrated in Owen’s monograph (1867, pl.xv) are guesswork as these elements were unknown at the time.

[152] The alar phalanges of the male skeleton of *Pezophaps* figured by Owen (1878, pl.vii, fig.1) are apparently extrapolations, as they are not present in the original specimen (NHMUK A.3505; pers. obs.).

[153] See Thirioux-Newton Correspondence, photographs (10A, 13A) accompanying letters dated 5th October 1900 and 31st January 1901 (right carpus).

[154] An alular phalanx was listed by Chubb (1919a) – this does not appear to still be present (pers. obs.), although the phalanges of the second digit, not listed by Chubb (1919a), are. Moreover, an alular phalanx does not appear to be present in the photographs of the Durban skeleton given in Chubb’s articles (1919a, b).

(Ottow 1950), although Slater (1879, p.295) mentioned that "the first phalange of wing" had been found with other solitaire bones in a cave on 6th November 1874. The second (terminal) phalanx of digit II is pointed distally. In *Pezophaps* it is known in a female specimen (UMZC 635).[155]

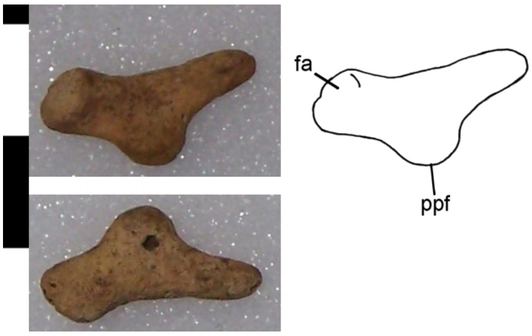

The phalanx of the third digit of *Raphus* (UMZC 415.KK specimen; scale in 5mm units; ○ Jolyon C. Parish, December 2008).

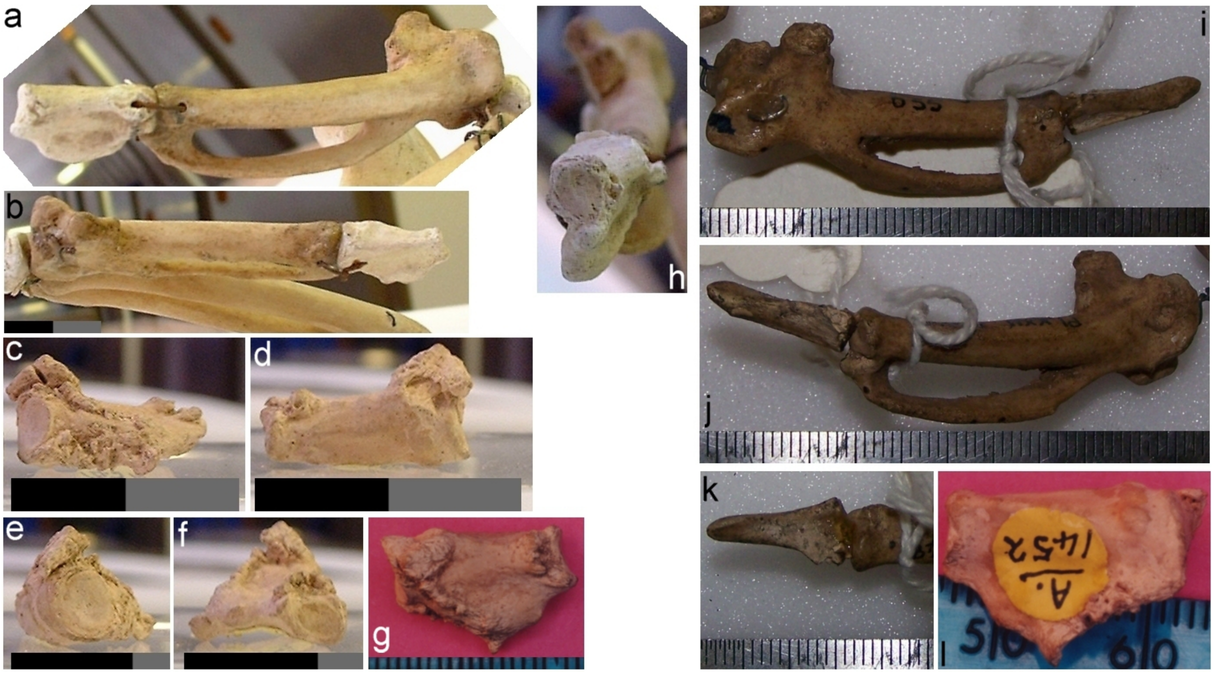

Alar phalanges of *Pezophaps*. a, b and h: left side (NHMUK A.3506; female); c-g and l: phalanx 1 of digit II (NHMUK A.1452); i-k: left carpometacarpus with phalanx 2 of digit II (UMZC 635). Scale bars in cm and mm. ○ Jolyon C. Parish.

A probable phalanx digiti minoris is found in the UMZC 415.KK collection. It has a facet at one end. It differs from the phalanx digiti minoris of the Durban skeleton and from the same element in a photograph of the manus in the Thirioux-Newton Correspondence (accompanying a letter of 31st January 1901). However, it resembles the same element in volant pigeons such as *Goura* (pers. obs.).

Livezey (1993) estimated the proportions of the two phalanges of the major digit as 7.7% and 4.2% of wing length (humerus + ulna + carpometacarpus + alar phalanges), based on data from volant columbids. Using measurements of Thirioux's Port Louis skeleton (Claessens *et al.* 2015) gives 6.8% and 4.2% for the respective length proportions of phalanges 2 and 3 of digit II.

---

[155] The phalanx is glued to the distal end of the left carpometacarpus in this specimen. As the first phalanx of digit II is known elsewhere (see above) and possesses an articular fact at the distal end, it is assumed that this is an incorrect placement.

Pelvic Limb

The pelvic limb of *Raphus* and *Pezophaps* was adapted for terrestrial locomotion. Compared with other columbiforms (particularly *Goura*) the pelvic limb in the dodo and solitaire shows only a slight increase towards graviportality (Livezey 1993). Compared with volant columbids,[156] *Raphus* has disproportionately short tarsometatarsi and *Pezophaps* has disproportionately short pedal phalanges. Claessens *et al*. (2015) found that the hindlimb bones of the dodo are slightly more robust than those of volant columbids, with the mid-shaft width being around 10-15% greater. However, the hindlimb bones of *Raphus* are not particularly peramorphic (Claessens *et al*. 2015, *contra* Livezey 1993)[157] and neither *Raphus* nor *Pezophaps* show a reduction in the proportionate length and corresponding increase in robustness of the femur, as seen in more graviportal birds (*e.g.*, *Aepyornis*).

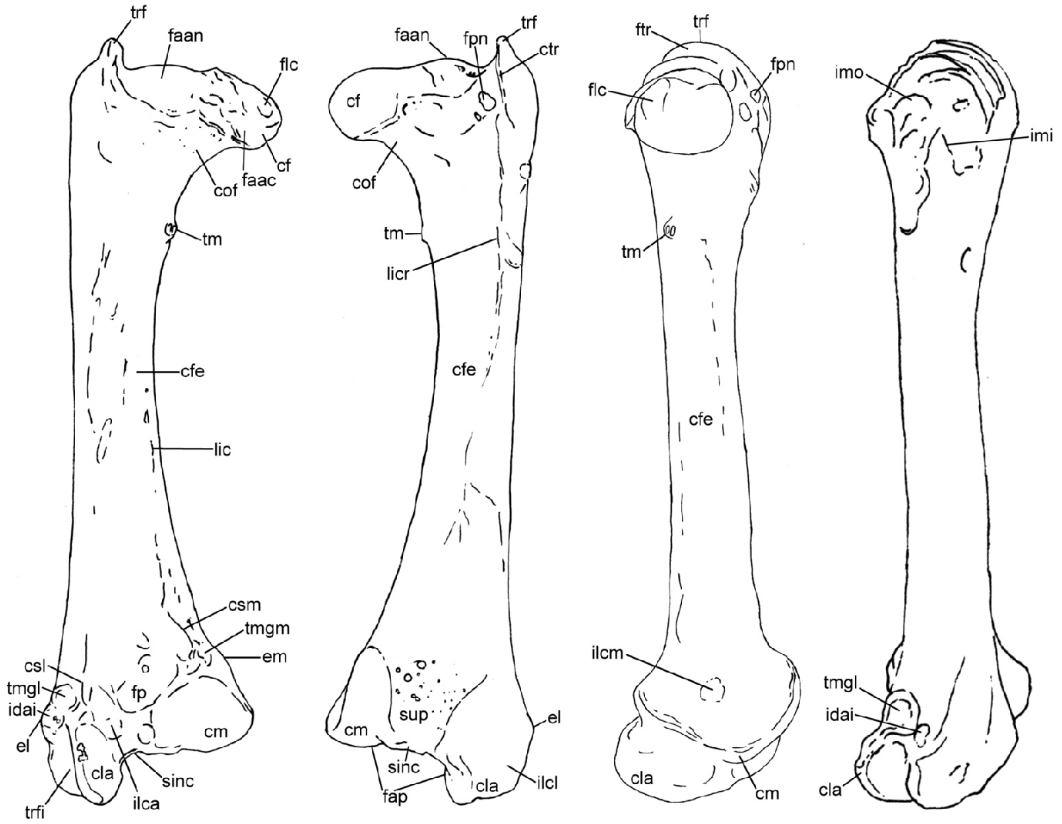

Femur of *Raphus*, left side, caudal, cranial and medial views; right side, lateral view (traced from Owen 1867, pl.xxi, figs.1-3; Milne-Edwards 1866b, pl.16, fig.2b).

In Thirioux's Port Louis skeleton the ratio of femur : tibiotarsus : tarsometatarsus is 30.8%-31.1% : 44.0%-44.2% : 24.8%-24.9% (data from Claessens *et al*. 2015). For *Pezophaps* the ratio is 28.8 : 43.1 : 28.1 (NHMUK A.3506) to 29.1 : 42.4 : 28.5 (NHMUK A.2505; data from Claessens *et al*. 2015). *Raphus*, with its proportionately short tarsometatarsi, resembles *Caloenas* (29.5 : 44.7 : 25.8) in its ratio, whereas *Pezophaps*, with relatively longer tarsometatarsi, resembles *Goura*.[158]

---

[156] Livezey (1993) used *Columba livia*, *Didunculus strigirostris*, *Geopelia cuneata* and *Goura cristata* for metric comparison.

[157] According to Livezey (1993), the relative shaft widths (mean ± standard deviation) of the hindlimb bones are significantly larger in *Raphus* (tibiotarsus 7.2 ± 0.2, tarsometatarsus 11.5 ± 0.5) and *Pezophaps* (tibiotarsus 6.9 ± 0.3, tarsometatarsus 8.6 ± 0.4) than in volant columbids.

[158] Fürbringer (1888) gave the following ratio (femur : tibiotarsus : tarsometatarsus) for *Raphus*: 30 : 45 : 25 (noting a similarity to that of *Apteryx* 30-33 : 45-48 : 20-24). Kitchener (1993) gave the pelvic limb bone proportions for *Raphus* as: femur 30.8%, tibiotarsus 43.7%, tarsometatarsus 25.5% (measured from fig.4). Livezey (1993) gave the proportionate lengths of the hindlimb as: *Raphus*: femur 26.7%, tibiotarsus 36.2%, tarsometatarsus

The ratio of tarsometatarsus to tibiotarsus is 0.56 in *Raphus* (Thirioux's Port Louis skeleton) and 0.65-0.67 in *Pezophaps* (data from Claessens *et al*. 2015). For comparison, it is around 0.56-0.61 in *Natunaornis* (data from Worthy 2001), 0.58 in *Caloenas* (data from Claessens *et al*. 2015), 0.69-0.71 in *Goura*, 0.63 in *Didunculus* and 0.64 in *Otidiphaps* (data from Meyer 1879-1888).

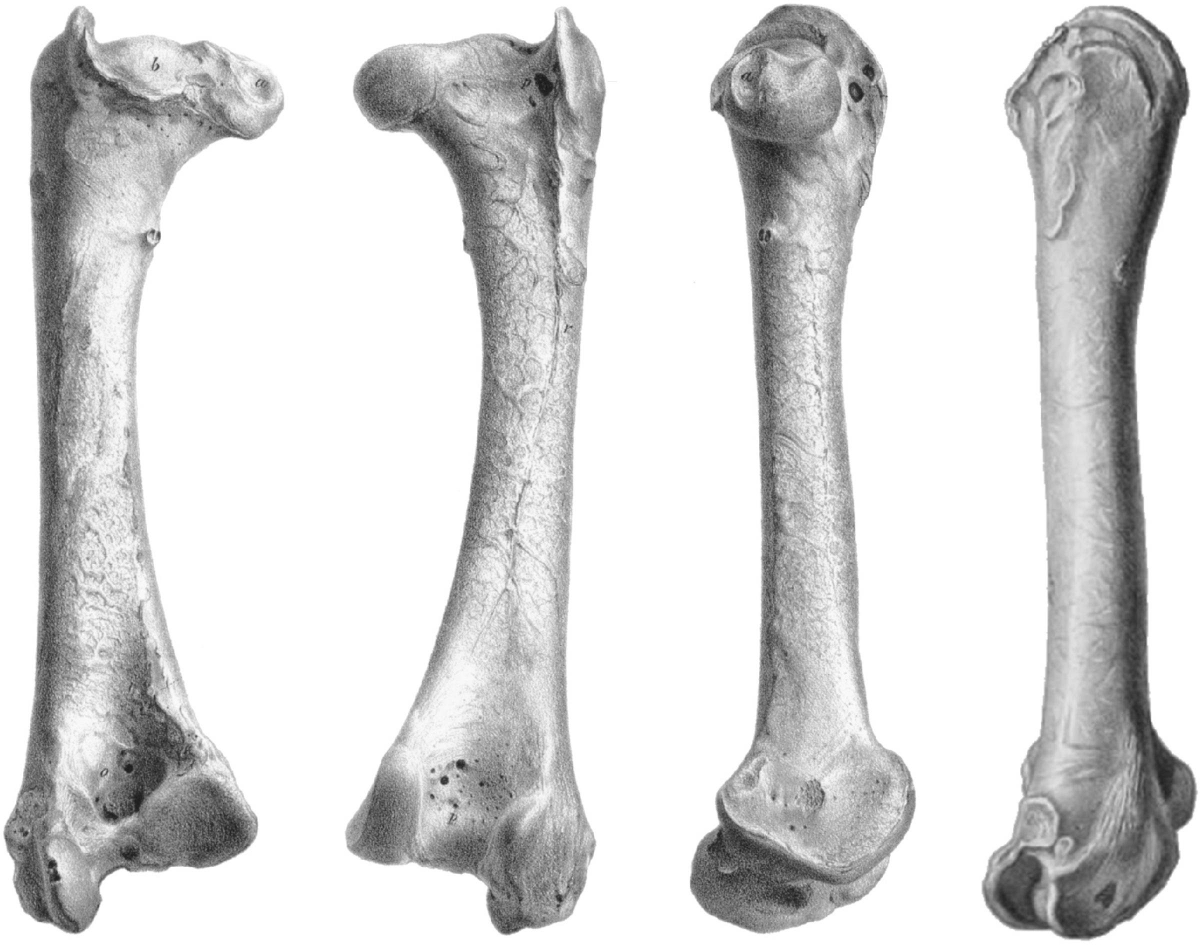

Femur of *Raphus*, left side, caudal, cranial and medial views (Owen 1867, pl.xxi, figs.1-3: "J Smit lith" "M & N Hanhart ,imp"); right side, lateral view (Milne-Edwards 1866b, pl.16, fig.2b: "Louveau del et lith." "Imp. Becquet à Paris.")

The angles between the hindlimb elements formed when the dodo was in "easy standing position" were apparently similar to those of living columbids (Claessens *et al*. 2015). In their digitally repositioned 3D scan of Thirioux's Port Louis skeleton the angles (relative to the horizontal ground surface) given by Claessens *et al*. were: femur 20°, tibiotarsus 60°, tarsometatarsus 75°. Thus, the femur does not appear to have been habitually held in a more vertical position compared with volant columbids (*contra* Kitchener 1993a, b).

Femur

(*Raphus*: Owen 1867, pl.xxi, figs.1-5, pl.xxiii, figs.6, 7; Milne-Edwards, pl.16, fig.2; Lüttschwager 1961, fig.17; Janoo 2005, fig.2b; Rijsdijk *et al*. 2009, fig.3g; Meijer *et al*. 2012, figs.5b, 6;

22.4%, digit III 14.9%; *Pezophaps*: femur 24.8%, tibiotarsus 37.0%, tarsometatarsus 25.0%, digit III 13.2%. He added that *Raphus* shows a relatively long femur, a normally proportioned tibiotarsus (similar in proportion to that of medium-sized terrestrial pigeons, such as *Didunculus*), a short tarsometatarsus, and a long digit III. *Pezophaps* has a normally proportioned femur, relatively long tibiotarsus (similar in proportion to that of *Goura*), long tarsometatarsus, and short digit III.

Rijsdijk *et al.* 2015, fig.7B; Claessens *et al.* 2015, figs.55, 56, pls.PL36, D36; Van Heteren *et al.* 2017, fig.1. *Pezophaps*: Strickland & Melville 1848, pl.xiv, figs.4-10, A. Newton 1865a, pl.viii, fig.1; Strickland 1853, pl.55, fig.3; Lüttschwager 1961, fig.17; Ziswiler 1996, p.68; Fuller 2002, p.123; Kallio 2005, p.27)

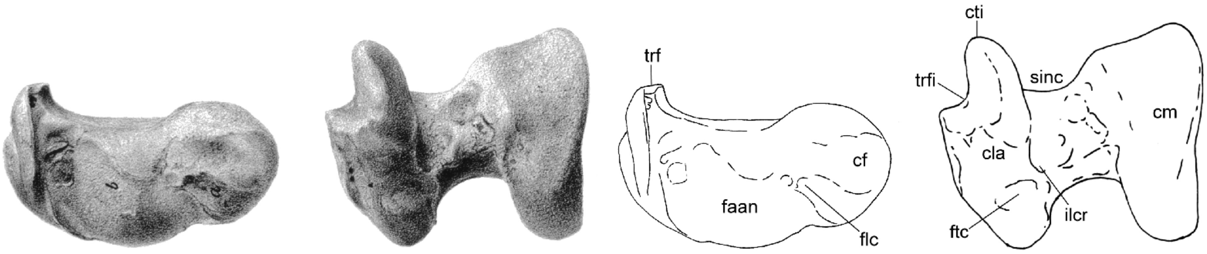

Femur of *Raphus*, left side, proximal and distal views (lithographs: Owen 1867, pl.xxi, figs.4, 5: “J Smit lith” “M & N Hanhart ,imp”).

The femur of *Raphus* is robust, yet not as stout as in graviportal species such as *Aepyornis*. On the medial face of the femoral trochanter, in a line laterally with the head of the femur, there is invariably at least one small, or occasionally one large, pneumatic foramen. These foramina are usually located within a shallow fossa, the fossa trochanteris. Pneumatic foramina may also be present on the medial face of the proximal end of the trochanter. The head of the femur is rounded and presents, dorsocaudomedially, the well-defined fovea lig. capitis, for the attachment of lig. capitis. The antitrochanterian articular face is large and convex dorsally; it is well-defined, especially caudally, where its ventral margin is marked by a low ridge. Martin (1904) stated that on the caudal face the articular surface extends distally for half to two-thirds of the collum in *Raphus* and *Pezophaps*, and is most extensive in the latter, where it corresponds to the position of the antitrochanter. The femoral trochanter rises dorsally, its dorsal extremity is rounded off. Its caudal face is convex and merges with that of the shaft; the cranial face shows the longitudinal trochanteric crest, extending proximodistally from its dorsal extremity; this ridge subsides as it passes distally and eventually becomes the linea intermuscularis cranialis. This well-defined intermuscular line curves gently medially. On the caudal face of the proximal part of the femur, at the base of the femoral trochanter, are the linear obturator impressions. In the specimen figured by Owen (1867, pl.xxi, figs.1-5) there is a small subcircular tubercle (developed in some specimens as a ridge), the “small trochanter” (trochanter minor of Owen 1867), on the medial face of the femur, within its proximal third. This trochanter, perhaps for the attachment of m. iliofemoralis internus, is variably developed and is not present in all specimens (for example it is absent in AMNH 3852 and UMZC 415.K specimens). In the specimen figured by Owen (*op. cit.*) the face of the tubercle is directed caudomedially. In this specimen there is a very small medullary foramen in the middle of the femur, on the caudal face. On the medial side of the caudal face is the longitudinal linea intermuscularis caudalis, well defined in the distal half of the femur. The popliteal fossa is relatively deep, and is elongated parallel to the transverse axis of the distal extremity of the femur; it presents a few small pneumatic foramina. It is separated from the lateral condyle by a subtriangular rough flat surface, on the distal part of which is probably the subcircular impressio ligamenti cruciati caudalis.[159] The lateral condyle itself is rounded and elongate; the medial one is less elongate and is larger. Dorsal to the lateral condyle is the well defined, rough and slightly elevated tuberculum m. gastrocnemialis lateralis. Just distal to, and touching the tuberculum m. gastrocnemialis lateralis is the impressio distalis ansae m. iliofibularis.[160]

---

[159] Identification of the attachments of the cruciate ligaments was made with reference to Cracraft (1971) and Baumel & Witmer (1993) with comparative material comprising femora of *Columba palumbus* (author’s collection).

[160] Claessens *et al.* (2015) stated that “linea intermuscularis caudalis is distinct and connects with an extensive, deeply excavated impressio ansae m. iliofibularis”(p.74). However, the caudal impressio ansae m. iliofibularis is not particularly deep, although it is distinct, and does not appear to connect with the linea intermuscularis caudalis (pers. obs.).

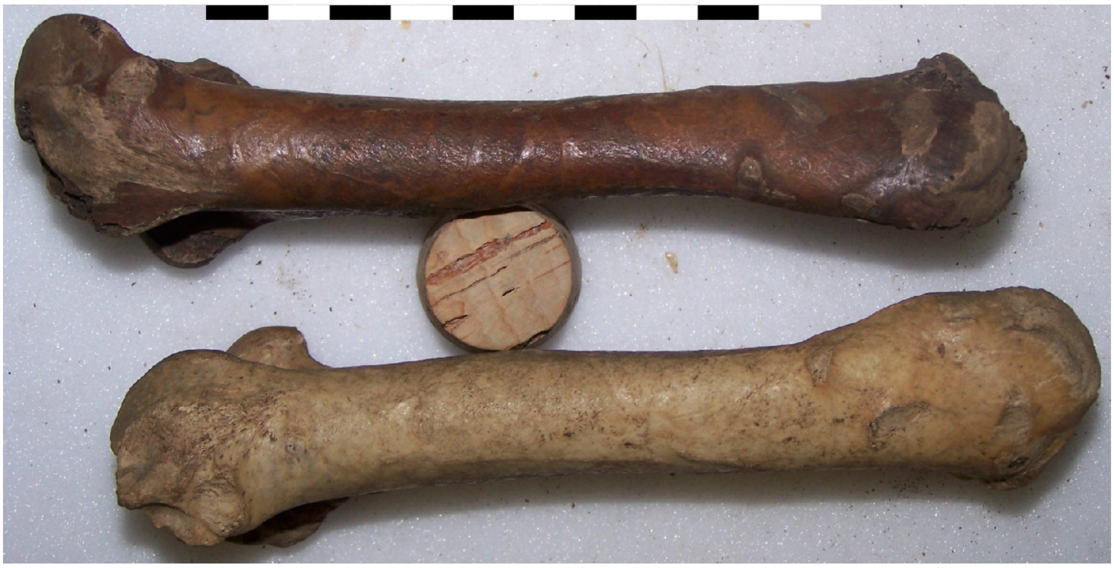

Femur of *Raphus*, right (upside-down) and left sides, lateral views (UMZC 415.K specimens; scale in cm; ○ Jolyon C. Parish).

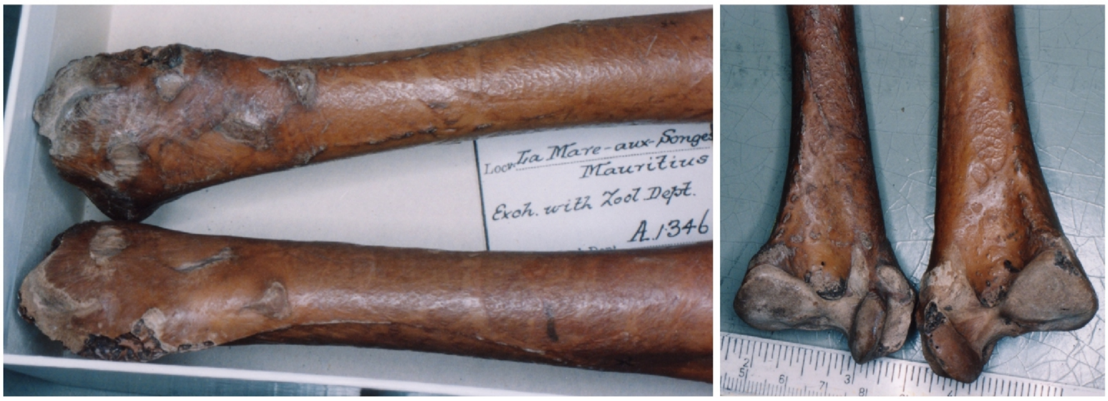

Femur of *Raphus*. *Left*: right and left (upside-down), lateral views of proximal ends; right: right and left, caudal views of distal ends. (NHMUK A.1346; scale in inches and cm; ○ Jolyon C. Parish).

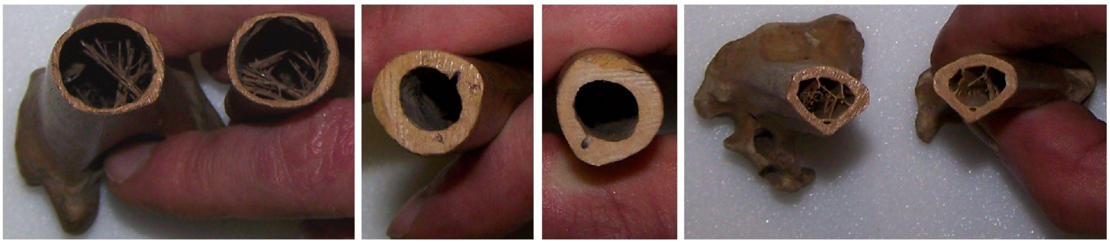

Femur (left side), tibiotarsus (left side) and tarsometatarsus (right side), transversely sectioned (by Andrew Kitchener, 1990) (UMZC 415.K specimens; ○ Jolyon C. Parish, December 2008).

Dorsal to the medial condyle is the rough surface of the tuberculum m. gastrocnemialis medialis. Running proximally from the tuberculum m. gastrocnemialis medialis is the fairly rounded medial supracondylar crest. On the lateral face of the distal end of the femur is the shallow depression of the impressio ligamenti collateralis lateralis; on the medial face of the distal end is the corresponding impressio ligamenti collateralis medialis. The intercondylar sulcus is deep and wide. At the lateral part of the cranial end of the intercondylar sulcus, and just caudal to the patellar sulcus, is a deep circular depression, the impressio ligament cruciati cranialis. The patellar sulcus itself is deep and relatively wide, proportionately more so than in volant columbids; its medial border (formed by the medial condyle) is less rounded than its lateral one. Within the sulcus are a number of pneumatic foramina, varying in size. A slight impression (see Owen 1867, pl.xxi, fig.1) on the proximomedial side of the patellar sulcus may be the impressio proximalis ansae m. iliofibularis. On the distal surface of the lateral condyle is the deep depression of the fovea tendinis m. tibialis cranialis, located almost at the same level distally as the fovea tendineus m. tibialis cranialis (Claessens *et al*. 2015). The tibiofibular crest is long and well developed, and the lateral epicondyle is ridge-like and reaches proportionately further distally than in volant columbids (Claessens *et al*. 2015). The fibular trochlea is rounded and well developed. The fibular angle (Hertel & Campbell Jr 2007) is 35° in *Raphus* and 36° in *Pezophaps*. The femur differs from that of extant columbids, which show a slight caudomedial curvature of the distal part. In *Raphus* and *Pezophaps* this has been almost completely lost (Martin 1904),[161] which Martin attributed possibly to a return to a raising up of the hind extremity.[162] The lateral condyle extends further distally than the medial one, making the transverse axis of the distal end of the femur oblique to the sagittal axis. This angle is more pronounced than in volant columbids. This may be related to the larger size of the dodo and its relatively wider torso, with the femur being held more craniolaterally (*i.e.*, with greater abduction of the distal end); a larger lateral condyle is also seen in some ratites (Claessens *et al*. 2015).

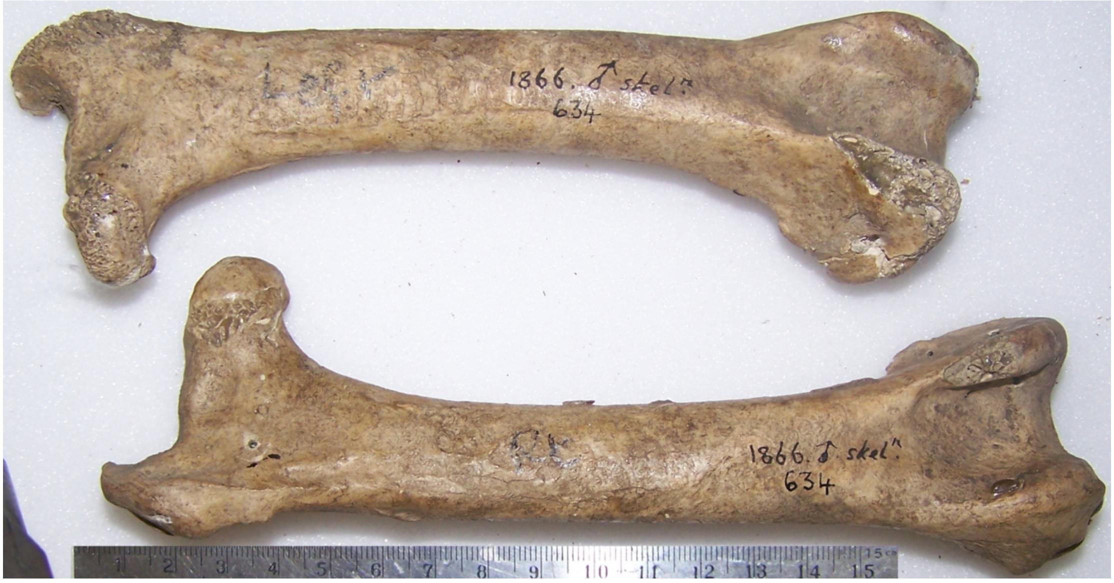

Femur of *Pezophaps*, left and right sides, cranial views (UMZC 634; male; scale in cm; ○ Jolyon C. Parish, December 2008).

The internal structure of the femur (Owen 1867, pl.xxiii, figs.6, 7) shows a pneumatic cancellous structure at the extremities. The wall of the bone is thin and compact on the upper part and sides of the head, neck and femoral trochanter and thickens “at the under part of the neck and lower and back part of the trochanter” (*ibid*., p.65). The walls of the shaft are thickened and the internal structure of the majority of the shaft consists of a few thin struts traversing the internal cavity. At the ends of the shaft the cancellous structure is limited to the outer part of the cavity (*ibid*.). The femoral shaft walls are thinner than would be expected, giving the femur a low cantilever strength (Kitchener 1993a, b; see Parish 2013, pp.297-298). However, the medial wall is somewhat thicker than the lateral, cranial and caudal walls.

Farke & Alicea (2009) CT-scanned a femur of *Raphus* and one of *Pezophaps* and calculated the following:

---

[161] Claessens *et al*. (2015) noted that the femur of *Raphus* “has a dorsoventral curvature on the distal half of the shaft” (p.73). However, the descriptors dorsal and ventral are not usually applied to the femur and it is not clear what they were referring to.

[162] “Der Verlust der Krümmung ist vielleicht auf ein Aufrichten der Extremität zurückzuführen” (p.318).

	TA	CA	PCA	$I_{\max}$	$I_{\min}$	$I_{\max}/I_{\min}$	P	Mass	FL
Raphus	246.6	103.8	42.1	3739.2	2683.2	1.39	59	10.83	137
Pezophaps	239.8	142.3	59.3	4808.1	3017.4	1.59	59	10.79	156

TA = total cross-sectional area (mm^2); CA = cortical area (mm^2); PCA = percent cortical area; $I_{\max}$ = maximum second moment of area (mm^4); $I_{\min}$ = minimum second moment of area (mm^4); P = perimeter (mm); m = mass (kg), estimated from femoral circumference using Anderson *et al*. (1985); FL = femoral length (mm). Data for *Raphus* taken from YPM 2064, that for *Pezophaps* from YPM 1154.

As can be seen above, the cortical area is slightly greater in *Pezophaps* than in *Raphus*. The $I_{\max}/I_{\min}$ value for the flightless birds (palaeognaths plus the dodo and solitaire), excluding *Struthio camelus* (value 2.16), was 1.34, with the value for the solitaire (1.593) being somewhat above average. Farke & Alicea concluded "that cross-sectional properties should be used with caution in determining the posture and behaviors of extinct animals, and only in conjunction with other morphological information" (p.1406).

The femoral splay angle (Hertel & Campbell Jr 2007) is around 13° in *Raphus* (measured from Cleassens *et al*.'s (2015) digitally repositioned Thirioux's Port Louis skeleton).

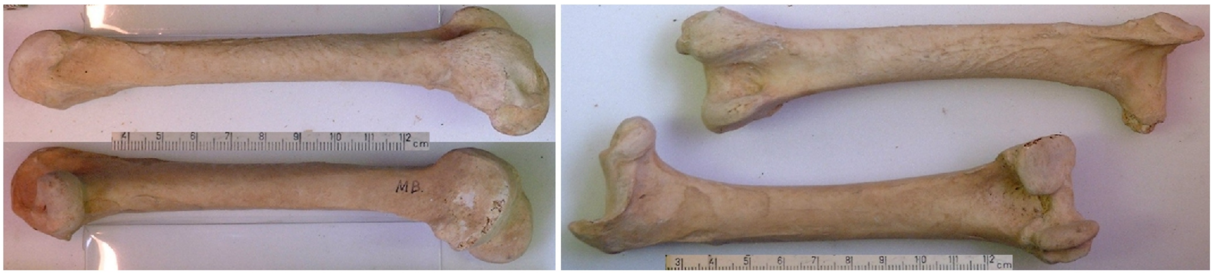

Femur of *Pezophaps*, right and left sides, lateral, medial, cranial and caudal views (NHMUK specimens; ○ Jolyon C. Parish, December 2008).

The femur of *Pezophaps* is very similar to those of volant columbids (Melville 1848). It differs from that of *Raphus* in being less robust and of a more constant thickness and not decreasing as much towards the middle or proximal third (Newton & Newton 1869). The muscle attachment areas are also more developed in *Pezophaps* than in *Raphus*. The facies articularis acetabularis is flatter than in *Raphus*. The fovea ligamenti capitis is relatively larger in *Pezophaps* than in *Raphus* (Claessens *et al*. 2015). The femoral trochanter ascends higher above the neck of the femur in the former and its lateral face, as seen in cranial/caudal view, has a distinct angle (the lateral face is more rounded in *Raphus*). There is no pneumatic foramen on the craniomedial part of the base of the trochanter as there is in the dodo; in this respect *Pezophaps* resembles the majority of columbids. However, in several specimens examined by Newton & Newton (1869) there was a fairly large (probably) pneumatic foramen on the caudal face of the neck of the femur, ventral to the ridge defining the lower part of the articular face for the antitrochanter. This foramen is not present in all specimens of *Pezophaps* (for example in NHMUK A.1392 it is absent), nor in *Raphus*, but there may be several smaller foramina of variable position in this area in some specimens of the latter (*ibid*.; Owen 1867, pl.xxi, fig.3). The impressions iliotrochantericae are less distinct than in *Raphus*. The shaft of the femur shows a less concave medial border in *Pezophaps*, compared with *Raphus*. The linea intermuscularis caudalis is more raised and prominent than in the dodo. The popliteal fossa is relatively shallower than in *Raphus*, but larger (Claessens *et al*. 2015). Newton & Newton (1869) stated that the popliteal fossa "generally presents at least one large, and often two or three smaller pneumatic orifices" (p.344). However, often only a few very small pneumatic foramina are present (as in NHMUK A.1392, OUMNH 19626). The patellar sulcus is relatively deeper than that of *Raphus* and either shows a few minute pneumatic foramina (A. Newton 1865a, pl.viii, fig.1) or none. The transverse section of the femur at mid-shaft is subcircular, being only slightly craniocaudally compressed, the ratio of transverse diameter to cranio-caudal diameter being 0.75-0.8 (data from Strickland 1853; A. Newton 1865a). The walls of the shaft of the femur are thick: according to Strickland (1853), the thickness of the shaft wall is 1¼ lines (2.65mm).

Internally, the femur exhibits the cancellous structure extending "into the medullary cavity for a short distance at each end, and chiefly along the inner wall inferiorly; and the medullary cavity is lined by a thin osseous lamina, with a few and minute perforations" (Melville 1848, p.117).

A fragment of a distal male right femur (NHMUK A.1358; Strickland 1853, pl.55, fig.3) shows a rugged surface, and Strickland thought this bone might be from a very old individual. Another femur (NHMUK A.1359) also shows a rugose bone surface and was likewise supposed by Strickland to be from an aged individual (*ibid.*). However, this rugosity may be due to taphonomic processes (pers. obs.).

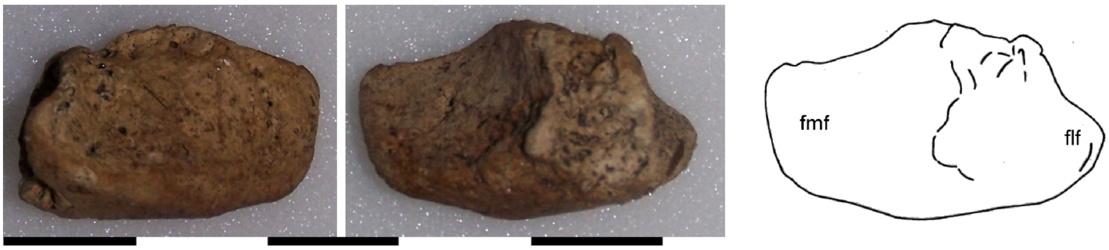

Patella of *Raphus*, right side (UMZC 415.KK specimen; ○ Jolyon C. Parish, December 2008).

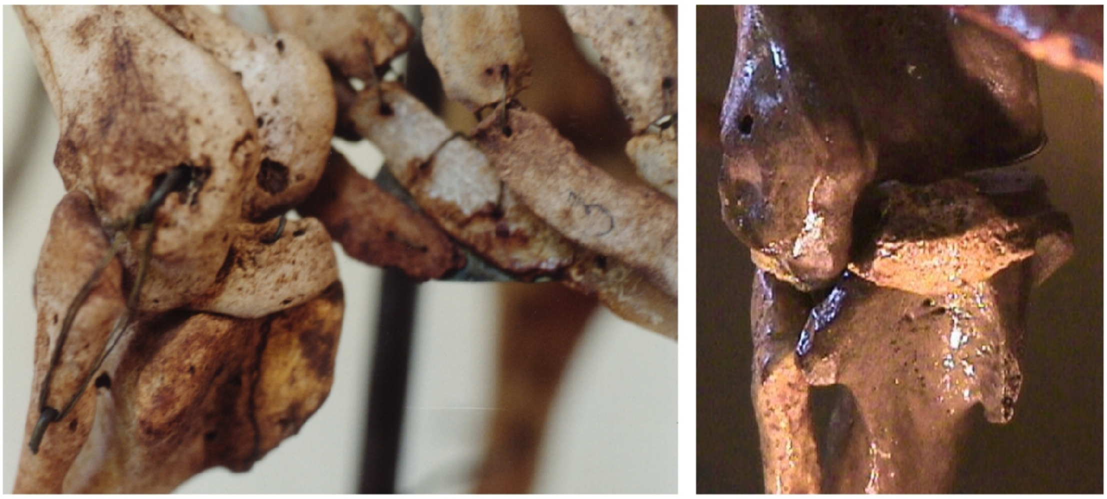

Patella of *Raphus*. *Left*: Thirioux's Port Louis skeleton, right side (© Jan den Hengst); *right*: Durban skeleton, right side (2366; © David Allan, Durban Natural Science Museum).

Patella

(*Raphus*: Claessens & Hume 2015, fig.6C; Claessens *et al*. 2015, figs.55, 57, pls.PL37, D37)

The patella (the sesamoid bone of the tendon of mm. femorotibiales and m. iliotibialis) is known for *Raphus* in the Durban (Chubb 1919a) and Thirioux's Port Louis skeletons (both sides in each skeleton) and from the UMZC 415.KK collection (right side). Thirioux mentioned two or three pairs in his collection.[163] The patella is has a concave cranial surface. The bone is deeper medially than laterally. The ventral surface of the medial side forms a wide concavity, the medial articular face. The lateral articular face of the ventral surface is likewise concave and in between these concavities is a somewhat rugose prominence. The medial border of the lateral articular face is "more upright" than the lateral border of the medial articular face (Claessens *et al*. 2015, p.74), the latter facing more ventromedially. Claessens *et al*. (2015) noted that "[t]here is no prominent impression for the m. ambiens" (p.74). M. ambiens is absent in *Goura*, but present in *Caloenas* and *Didunculus* (Beddard 1898). The dorsal and distal surfaces are smooth with some pitting. Several specimens of patellae are known for *Pezophaps* (NHMUK A.1442, A.3505, A.3506; RCSHM/Aves 706 (right), 707 (left and right)) and the element is similar to that of *Raphus*. Patellae are also present in volant columbids, including *Goura*, *Chalcophaps*, *Ducula*, *Ectopistes*, *Ocyphaps*, *Phaps*, *Scardafella*, *Starnoenas* and *Treron* (Verheyen 1957, Shufeldt 1901; pers. obs.).

---

[163] Letters from Thirioux to Alfred Newton, dated 25th May 1901 (Letter 15): "Aussi plusieurs rotules de Dronte, elles sont un plus fortes et diff. que chez le Solitaire [Also several patellae of the Dodo, they are a stronger and different than in theSolitaire]" and 13th November 1901 (Letter 17): "2 ou 3 paires rotules (supposé du Dronte) [2 or 3 pairs of patellae (assumed to be from Dodo)]".

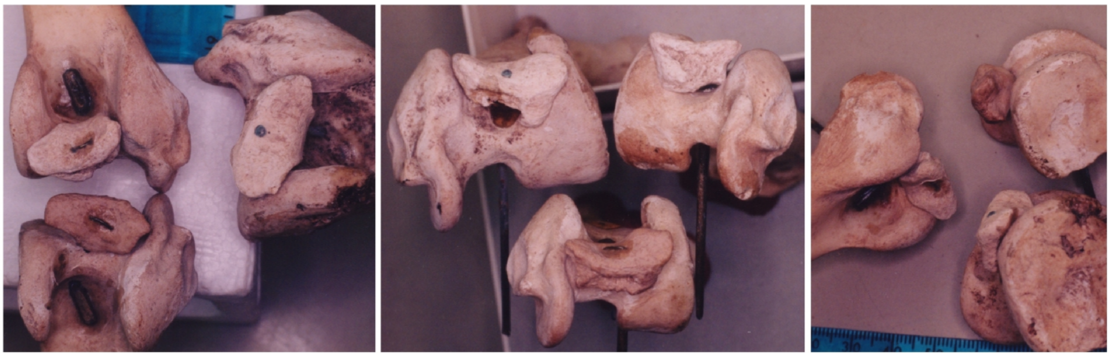

Patella of *Pezophaps*, left and right sides (NHMUK A.3505 (male), A.3506 (female)) (○ Jolyon C. Parish).

Tibiotarsus

(*Raphus*: Owen 1867, pl.xxii, figs.1-5, pl.xxiii, figs.8, 9; Milne-Edwards 1866b, pl.17, fig.1; Lucas 1895, pl.ci, fig.2; Janoo 2005, figs.2c, f; Rijsdijk *et al*. 2009, fig.3g; Meijer *et al*. 2012, fig.5c; Rijsdijk *et al*. 2015, figs.7A, E; Claessens *et al*. 2015, figs.2, 55, 58, pls.PL38, D38. *Pezophaps*: Strickland & Melville 1848, pl.xv, fig.1; Strickland 1853, pl.55, fig.4; Newton & Newton 1869, pl.xx, figs.100, 102; Lucas 1895, pl.ci, fig.1; Ziswiler 1996, p.68; Fuller 2002, p.123; Kallio 2005, p.27)

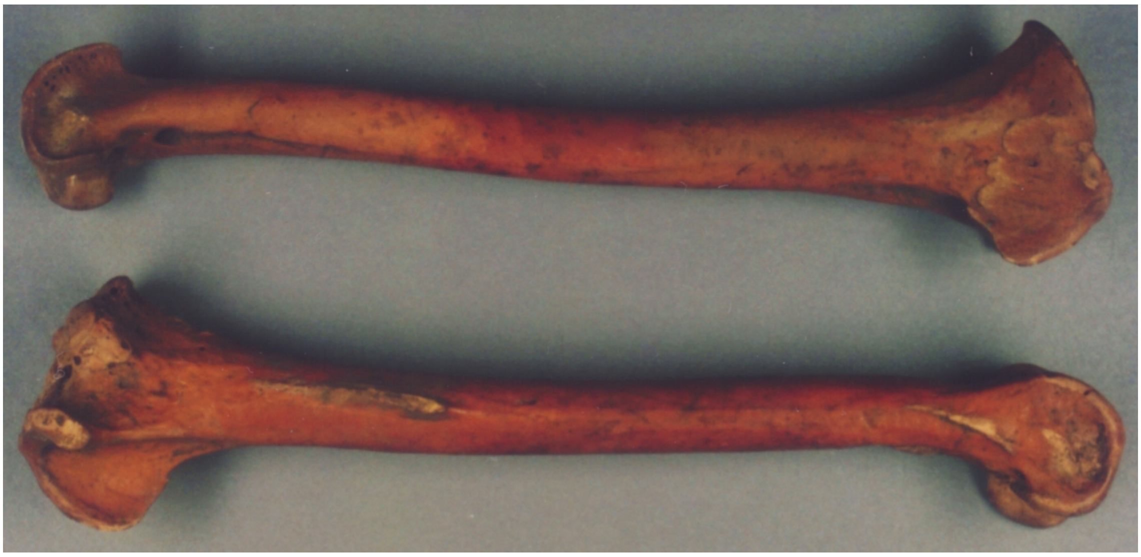

Tibiotarsus of *Raphus*, left side, medial and lateral views (UMZC 415.K specimens; © E. C. Parish).

The cranial cnemial crest of the tibiotarsus of *Raphus* is subtriangular, its base being longest and its apex rounded; it curves slightly laterally. Its proximal margin is expanded and thickened and its craniodistal one is thinner. The medial surface of this crest, the gastrocnemial face, shows an irregular line or ridge for the attachment of m. gastrocnemius medialis. A ridge runs distally from the distal end of the cranial cnemial crest to the tuberositas proximalis retinaculi mm. extensorum, its distal end forms part of the medial border of the sulcus extensorius. The cranial cnemial crest is offset laterally from the medial margin of the medial articular face in both *Raphus* and *Pezophaps*. The lateral cnemial crest is thicker and shorter than the cranial one, its apex is rough. Between the cnemial crests is the intercnemial sulcus, which provided attachment for m. extensor digitorum longus (Baumel & Witmer

1993). It has a small pneumatic foramen and is relatively shallower than in volant columbids such as *Caloenas*, *Didunculus* and *Goura* (Claessens *et al*. 2015). The patellar crest, for the attachment of lig. patellae, is obtuse and well defined, especially caudally. It rises rises to a rounded angle at its junction with the cranial cnemial crest, just above the articular surfaces of the proximal end of the tibiotarsus. Between the lateral cnemial crest and the lateral articular surface is the shallow incisura tibialis, for the caput femorale of m. tibialis cranialis (Baumel & Witmer 1993). Pneumatic foramina may be present in the fossae retrocristales, on the proximal face of the tibiotarsus. On the caudal face of the proximal end of the tibiotarsus is the fairly well defined flexorial fossa, which provided origin for m. flexor digitorum longus (*ibid.*), it is subtriangular, pointing distally, and contains pneumatic foramina.

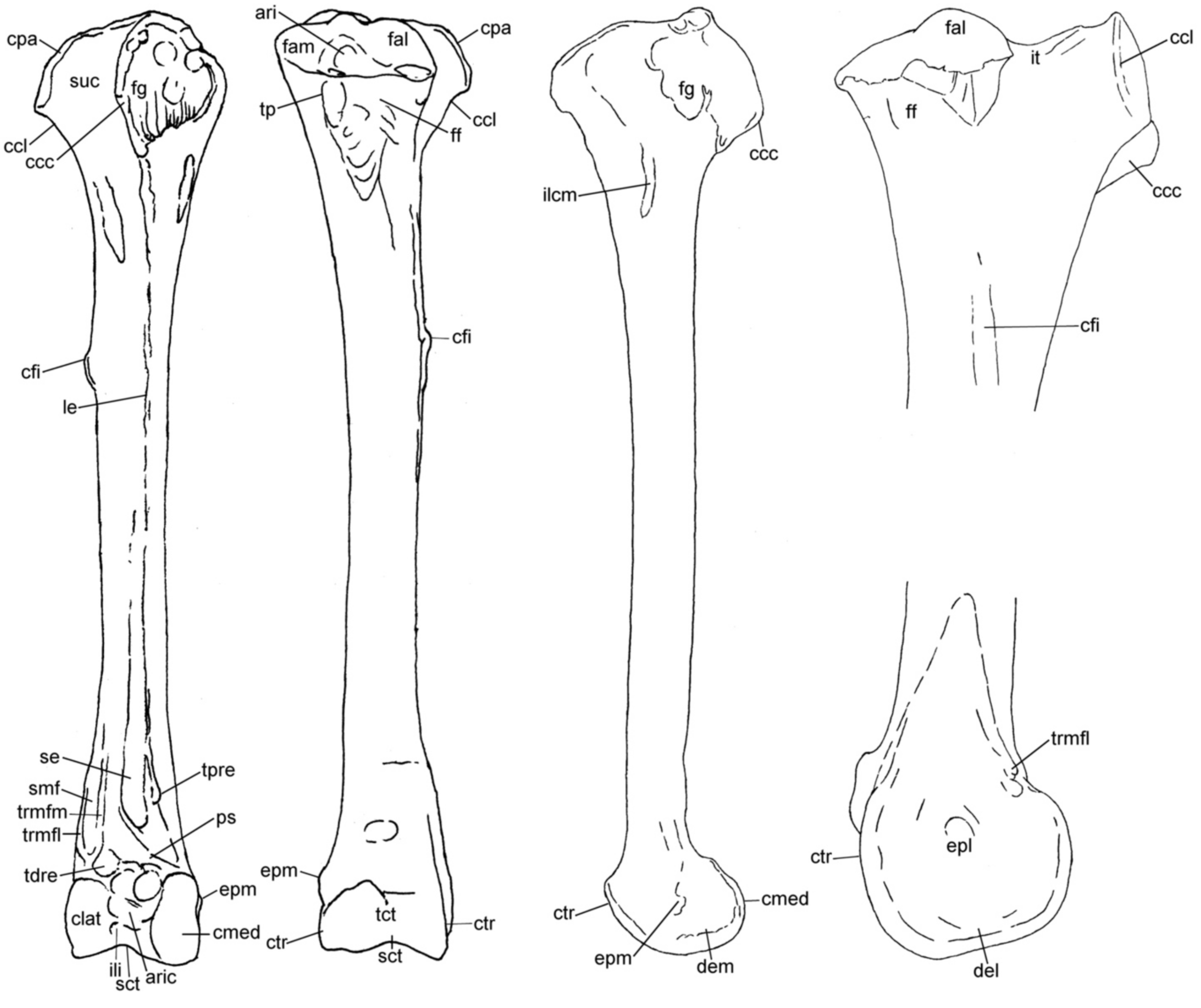

Tibiotarsus of *Raphus*, cranial and caudal views (right side); medial view (left side); lateral view of proximal and distal ends (right side). (Traced from Milne-Edwards 1866b, pl.17, figs.1, 1a; Owen 1867, pl.xxii, fig.2; photograph of a UMZC 415.K specimen; Milne-Edwards 1866b, pl.17, fig.1c).

The fibular crest is longitudinal and prominent; it is better defined distally than proximally and is inclined slightly obliquely, so that its distal end is slightly more cranial than its proximal one (pers. obs.; Owen 1867). It lies along the proximal third of the tibiotarsal shaft. Continuing distally from the fibular crest is the linea m. fibularis, which runs longitudinally to near the distal end of the tibiotarsus. The impressio ligamenti collateralis medialis comprises a short longitudinal ridge at the proximal part of the medial surface of the shaft. Some tibiotarsi exhibit minute longitudinal striations on the shaft (for example, some UMZC 415.K specimens). The extensor sulcus is developed distally, becoming less distinct proximally. It is bridged near its distal end by the supratendineal bridge. The sulcus curves slightly medially. The end of the sulcus distal to the supratendineal bridge consists of a subcircular

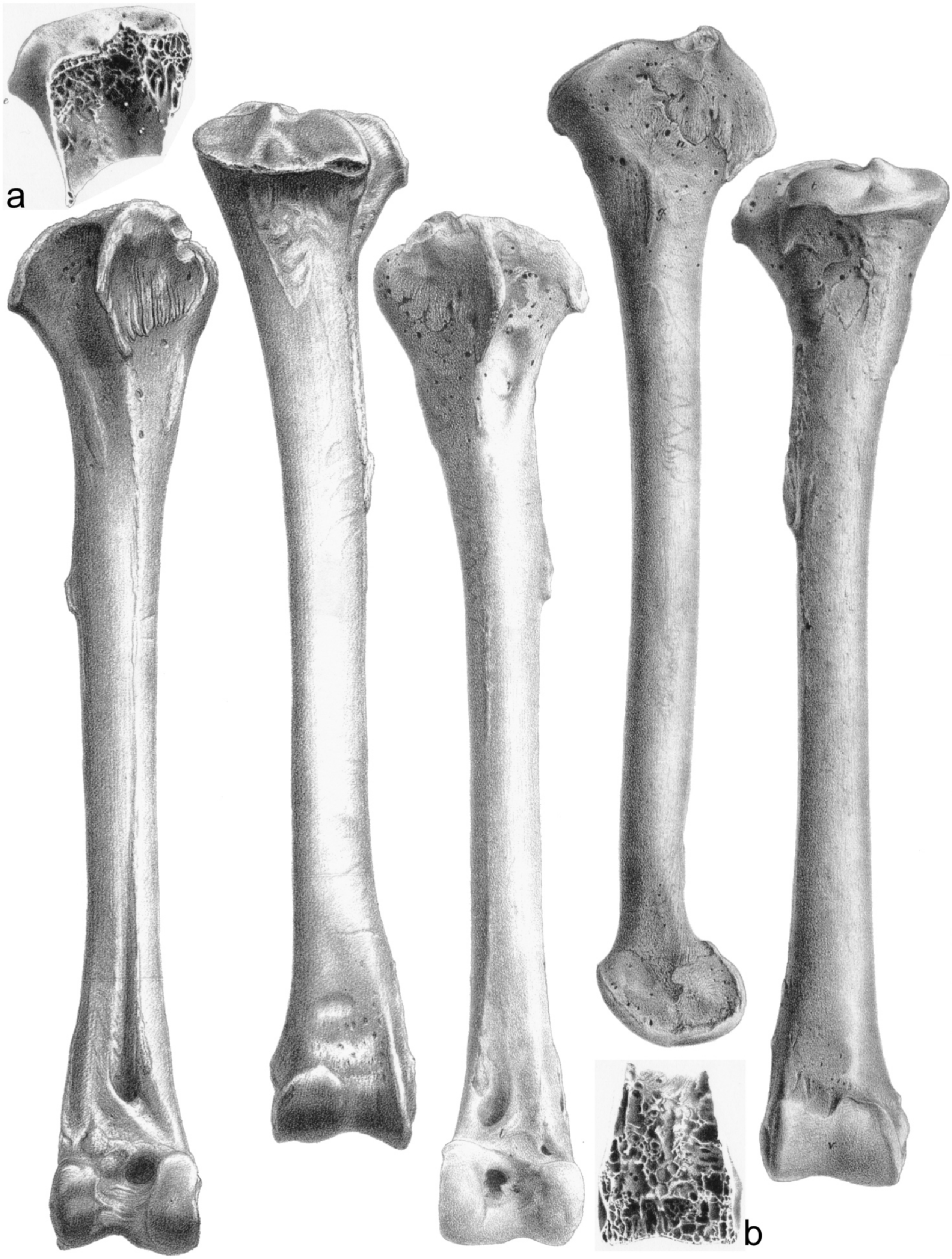

Tibiotarsus of *Raphus*: cranial and caudal views (right side; Milne-Edwards 1866b, pl.17, figs.1, 1a; “Louveau del et lith.” “Imp. Becquet à Paris”); cranial, medial and caudal views (left side; Owen 1867, pl.xxii, figs.1-3; “J Smit lith” “M & N Hanhart imp”). a and b: longitudinally sectioned tibiotarsus, proximal (not to scale) and distal ends (Owen 1867, pl.xxiii, figs.8, 9; “J Smit lith” “M & N Hanhart imp”).

opening, which lies just lateral to the proximal part of the medial condyle. On the lateral side of the cranial face of the distal end of the tibiotarsus is the shallow longitudinal groove, the sulcus m. fibularis, which ends distally just lateral to the supratendineal bridge. In some specimens at least, it has a pneumatic foramen (Claessens *et al*. 2015). The medial condyle of the tibiotarsus projects more cranially than the lateral one. The condyles project only slightly caudally beyond the caudal face of the distal end of the tibiotarsus. In some specimens (for example Owen 1867, pl.xxii, figs.1-5; UMZC 415.K; AMNH 3852; Thirioux's Port Louis skeleton) there is a small foramen proximal to the lateral condyle and lateral to the supratendineal bridge, this is absent in other specimens (such as Milne-Edwards 1866b, pl.17, fig.1; UMZC 415.K). A single minute foramen (or occasionally two, one proximal to the other) is sometimes present medial to the lateral condyle, on the cranial face of the distal tibiotarsus (as in a UMZC 415.K specimen). The lateral epicondyle is not well developed. The tuberositas proximalis retinaculi mm. extensorum comprises a distinct longitudinal wide ridge. In *Raphus* and *Pezophaps* it is located distally, the distance from its distal extremity being less than one-and-a-third times the distal width of the tibiotarsus. The tuberositas distalis retinaculi mm. extensorum comprises a wide tuberosity. According to Worthy (2001), there is variation in the orientation of the flat surface lateral to the tuberositas distalis retinaculi mm. extensorum: in CM Av6280 (a larger specimen, length 129.3mm) it faces craniolaterally, whereas in CM Av8228 (a smaller specimen) it faces mainly cranially. The tuberositates retinaculi m. fibularis are ridge-like. In both taxa the tuberculum lateralis retinaculum m. fibularis is aligned craniocaudally. A tuberculum medialis retinaculum m. fibularis appears to be present in both *Raphus* and *Pezophaps*. The width of the distal end of the tibiotarsus is slightly greater cranially than caudally. The depth of the medial condyle is greater than the caudal width of the distal end of the tibiotarsus in both taxa. The tibiotarsus itself is very slightly curved in both *Raphus* and *Pezophaps*, as in other columbids. Lüttschwager (1959b), in contrast, stated that the tibiotarsi of these taxa were straight[164]

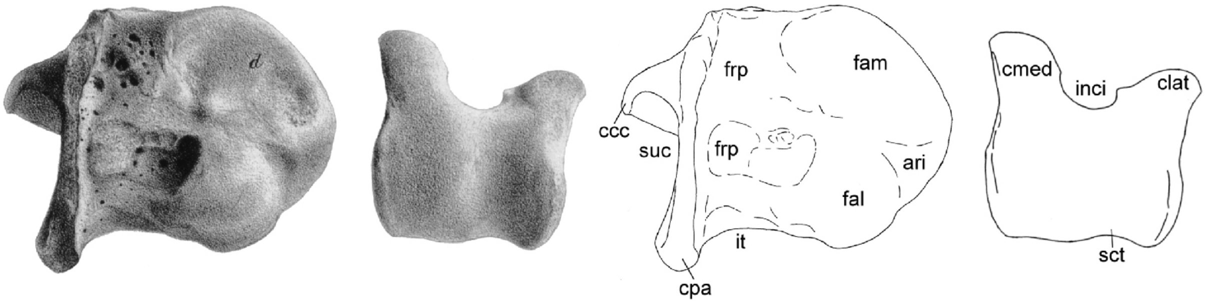

Tibiotarsus of *Raphus*: proximal and distal views (left side) (lithographs: Owen 1867, pl.xxii, figs.4, 5; "J Smit lith" "M & N Hanhart imp").

The internal structure of the tibiotarsus of *Raphus* shows cancellous composition at the proximal and distal ends ("limited to an extent of about half an inch [= 12.7mm] from the proximal articular surfaces [...] and to about an inch and a half [38.1mm] from the distal end of the line": Owen 1867, p.65). The inside of the shaft shows a large space, the walls of the shaft are thick and compact. The thickness of the wall at the proximal third is half a line [1.1mm], "gradually increasing to about a line [= 2.1mm] at the lower fourth, until the cancellous structure is reestablished" (*ibid*.). A transverse plate at the distal end of the inside of the tibiotarsus represents the boundary of the epiphysis of the tibia (*ibid*.). In transverse section the shaft is almost circular, with the medial wall being thickest and the caudal wall thinnest.

The cranial cnemial crest is as well developed in *Pezophaps* as it is in *Raphus* and in several specimens it is thicker than in that genus, although it varies between individuals, as it does in the dodo (Newton &

---

[164] Describing the tibiotarsus of *Raphus* and other columbids, Milne-Edwards (1866b) remarked that the "the internal part of the patellar gutter is strongly reinflated and ascends much [la partie interne de la gouttière rotulienne est fortement renflée et remonte beaucoup]" (p.376). However, there is no "patellar gutter" of the tibiotarsus and it is here assumed that this is an error for another feature. In describing the tibiotarsus of birds of prey he stated: "Behind, the patellar gutter is broad and is regularly widened [En arrière, la gouttière rotulienne est large et régulièrement évasée]" (*ibid*.).

Newton 1869). The junction of the cranial cnemial crest and the patellar crest projects more proximally in *Pezophaps*, at least in some specimens (*e.g.*, NHMUK A.1398). The lateral cnemial crest is very thick at its proximal edge. In *Pezophaps* it is almost directly laterally directed and forms a deep furrow with the fibula (Martin 1904). The flexorial fossa is relatively deeper in *Pezophaps* than in *Raphus* (Claessens *et al*. 2015). The longitudinal slight ridge defining the medial boundary of the sulcus m. fibularis is better defined than it is in the dodo. The tuberositas distalis retinaculi mm.extensorum, lying dorsal to the lateral condyle, is well defined, more so than in *Raphus*. The linea extensoria is also more developed in *Pezophaps* than in *Raphus* (Martin 1904). The foramen proximal to the lateral condyle is either absent or very small in *Pezophaps*. The distal opening of the sulcus extensorius is proportionately larger in *Pezophaps* than in *Raphus*, although the sulcus itself appears to be relatively shallower. The distal condyles are slightly proportionately smaller in *Pezophaps* than in the dodo. The width of the distal end of the tibiotarsus is greater cranially than caudally. The thickness of the shaft wall of a male *Pezophaps* tibiotarsus is about 2mm (Melville 1848).

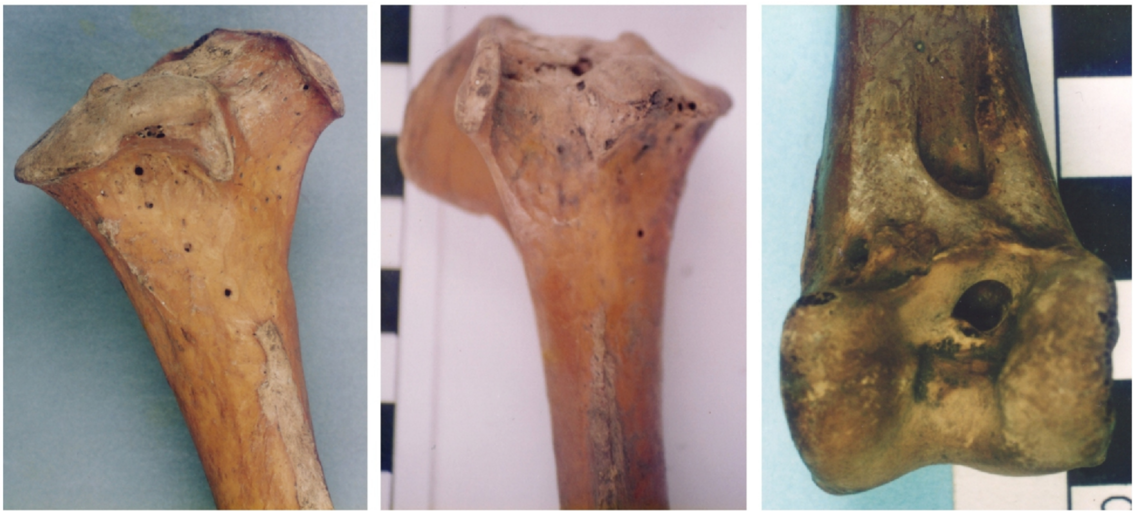

Tibiotarsus of *Raphus*. *Left*: right side, lateral view of proximal end; *middle*: left side, lateral view of proximal end; *right*: right side, cranial view of distal end (UMZC 415.K specimens; scale in cm; © E. C. Parish).

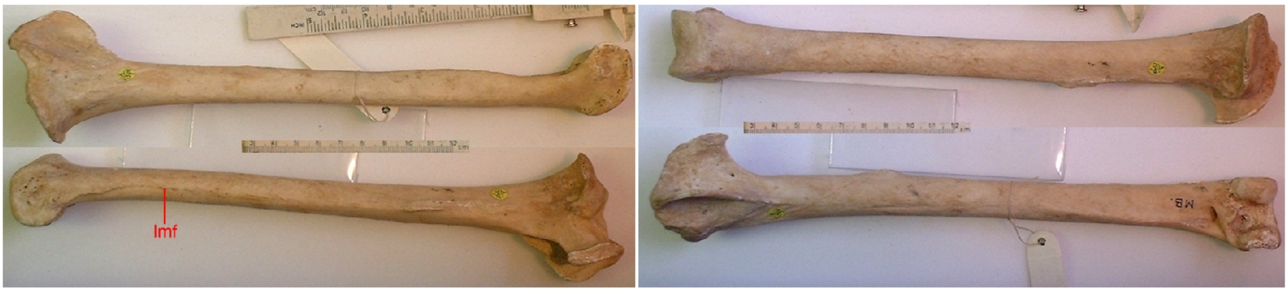

Tibiotarsus of *Raphus*. *Left*: left and right sides, medial and lateral views; *right*: right and left sides, caudal and cranial views (NHMUK A.1398 (male); scale in cm; ○ Jolyon C. Parish).

Fibula

(*Raphus*: Owen 1867, pl.xxii, figs.6-8; Milne-Edwards 1866b, pl.14, fig.3; Rijsdijk *et al*. 2009, fig.3g; Meijer *et al*. 2012, fig.5c; Claessens *et al*. 2015, figs.55, 59, pls.PL39, D39. *Pezophaps* Newton & Newton 1869, pl.xx, figs.100-103; Ottow 1950, pl.vi, fig.17)

The head of the fibula is lateromedially flattened. The articular face for the femur articulated with the femoral trochlearis fibularis in life. The articular face for the tibiotarsus is long. The fovea m. poplitei is shallow. On the caudal part of the lateral surface of the head of the fibula is a depression, which Lambrecht (1933) labelled as the “fossa lig. art. ext.” (fig.21), which may have been for the attachment of lig. collaterale laterale. The fibular spine is around two-thirds of the length of the tibiotarsus (a complete fibula is preserved in Thirioux's Port Louis skeleton: Claessens *et al*. 2015). In cranial/caudal aspect the fibula is kinked slightly near its midlength. On the caudal part of the shaft of the fibula of *Raphus* is the tubercle for the insertion of m. iliofibularis. The crista articularis tibialis is longitudinally elongate.

The fibula of *Pezophaps* is more robust than that of *Raphus*. In proximal view the head of the fibula of *Pezophaps* is more triangular (*contra* Claessens *et al*. 2015) and less craniocaudally flattened. Newton & Newton (1869) stated that the fibula of *Pezophaps* may have a smoother surface than that of *Raphus*, but "two or three of the examples [of the collection of 59] have their ridges and depressions as strongly marked as any of those of *Didus* which we have seen" (p.344).

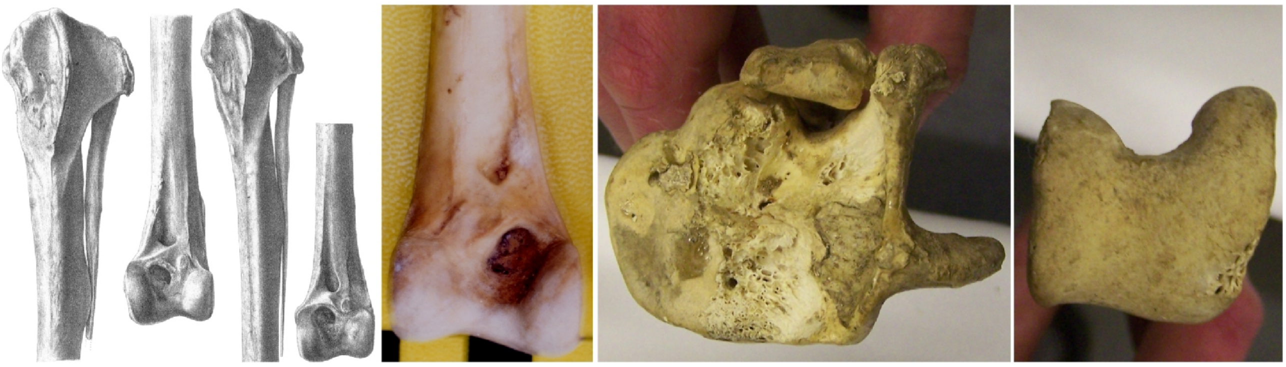

Tibiotarsus of *Pezophaps*. *Left* to *right*: right (male) and left (female) sides (Newton & Newton 1869, pl.xx, figs.100, 102; artist: George Henry Ford; "G. H. Ford ad nat. lith." "W. West imp."); right side, distal end, cranial view (NHMUK A.1375; female; scale in cm); left side, proximal view (with fibula attached; UMZC 634; male); left side, distal view (UMZC 634; male). ○ Jolyon C. Parish (except Newton & Newton 1869 image).

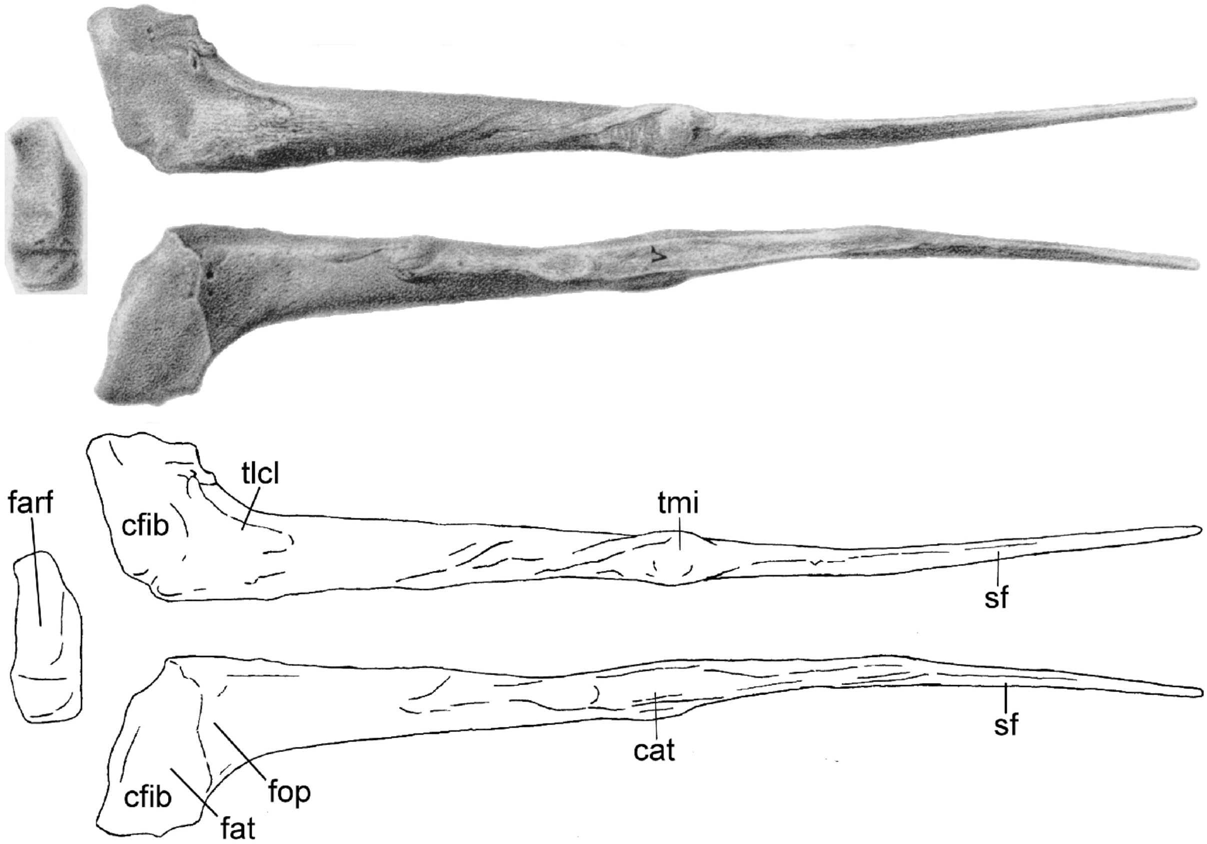

Fibula of *Raphus*, left side, proximal, lateral and medial views (lithographs: Owen 1867, pl.xxii, figs.6-8; "J Smit lith" "M & N Hanhart imp").

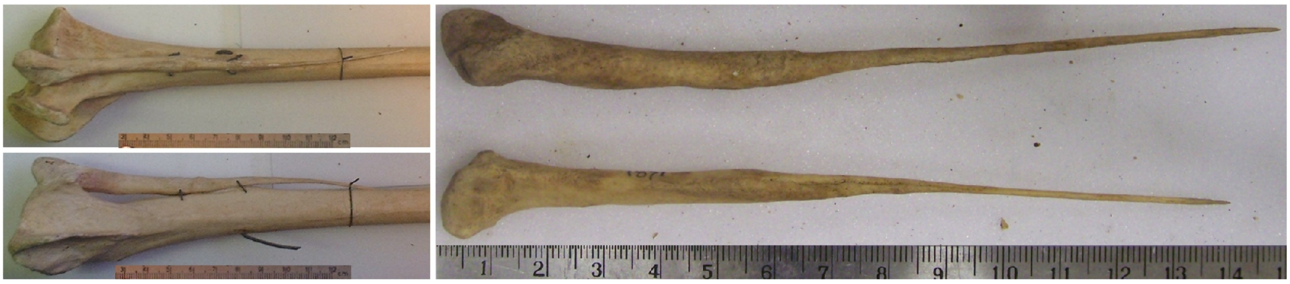

Fibula of *Pezophaps*. *Left*: left side, lateral and cranial views (NHMUK A.3505; male); *right*: left side, lateral and medial views (UMZC specimen). (○ Jolyon C. Parish).

Intertarsal sesamoid
(*Raphus*: Claessens & Hume 2015, fig.6D; Claessens *et al*. 2015, figs.60A, 61, pls. PL37, D37)

Intertarsal sesamoid bones are known in Thirioux's Port Louis and the Durban skeletons (left and right sides for both skeletons) and also from the UMZC 415.KK collection (right side).[165] In addition, D'Emmerez de Charmoy, in a letter to Alfred Newton dated 30th January 1906 (Letter 26), mentioned that he had many sesamoid bones of the dodo ("os Sesamoïdes du Dodo, j'en possède beaucoup ils sont situés à la partie postérieure de l'articulation tarso tibiale"). The sesamoid is longer proximodistally than lateromedially and its surface is rough and pitted. A sesamoid bone is known for the ankle region of *Pezophaps* (NHMUK A.3506;[166] UMZC 653; RCSHM/Aves 706, both left side).[167] It is sub-oval in caudal view and craniocaudally compressed; it is curved to adapt to the trochlea cartilaginis tibialis of the distal end of the tibiotarsus. In life, lig. metatarso-sesamoideum connected the intertarsal sesamoid bone with the tarsometatarsus. Intertarsal sesamoids are also found in other columbids (Claessens *et al*. 2015) and members of the Pteroclidae (Mourer-Chauviré 1993).

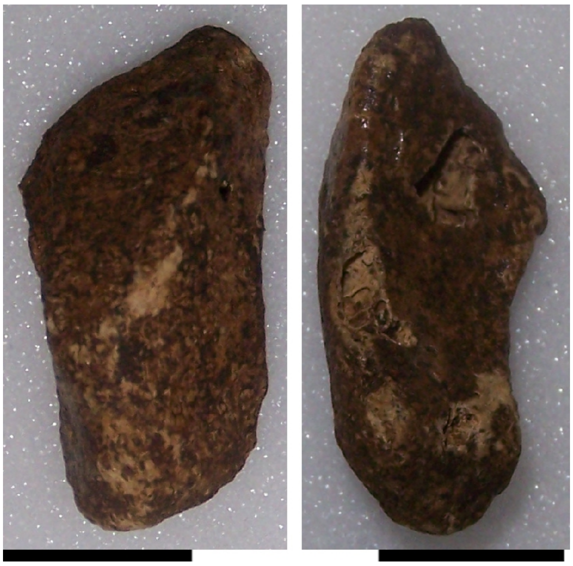

Intertarsal sesamoid of *Raphus*, right side (UMZC 415.KK specimen; scale in cm; ○ Jolyon C. Parish, December 2008).

---

[165] Side determined from comparison with Claessens *et al*. (2015, pls.PL37S, D37M).

[166] Claessens *et al*. (2015) also list NHMUK A.3505, although this has not been confirmed by the present author.

[167] An intertarsal sesamoid bones was also mentioned in a list of previously unknown bones given in a MS. by Slater and a sketch of one was given (Abstract from H. H. Slater's Reports on Rodriguez – Collection. 9pp. In: Royal Society Transit of Venus Expeditions Correspondence and papers relating to distribution of collections and preparation of reports 1875-1876, NHMUK Archives, DF 202/9).

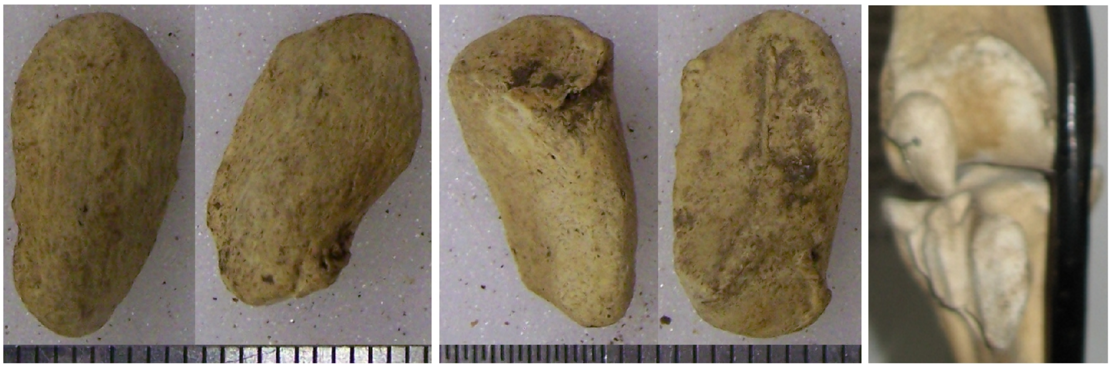

Intertarsal sesamoid of *Pezophaps*. *Left four images*: UMZC specimens; scale in mm; ○ Jolyon C. Parish, December 2008); *right*: left side, in articulation with the tibiotarsus and tarsometatarsus (RCSHM/Aves 706; Simon Chaplin, pers. comm., 20th March 2008; © The Hunterian Museum at the Royal College of Surgeons).

Tarsometatarsus

(*Raphus*: Strickland & Melville 1848, pl.xi, figs.1-6, pl.xii, fig.1, 1b; Owen 1846, pl.xlix, fig.1, pl.l, fig.1; Owen 1867, pl.xxiii, fig.10; Milne-Edwards 1866b, pl.16, fig.1; Owen 1871b, pl.lxvi, figs.8-11, 14-17; Lydekker 1891, fig.31; Lüttschwager 1961, fig.21; Janoo 2005, figs.2e, h; Hume 2006, fig.21; Middleton 2008, photo 15; Rijsdijk *et al.* 2009, figs.2b, 3g; Meijer *et al.* 2012, figs.2, 5d; Hume 2013, fig.5b; Claessens & Hume 2015, fig.6E; Claessens *et al.* 2015, figs.55, 60, 62, pls.PL40, D40. *Pezophaps*: Strickland & Melville 1848, pl.xv, figs.2-4; Strickland 1853, pl.55, figs.5-7; A. Newton 1865a, pl.viii, fig.2; Newton & Clark 1879, pl.xliv, fig.7; Lüttschwager 1961, fig.21; Ziswiler 1996, p.68; Fuller 2002, p.123; Kallio 2005, p.27)

The proximal end of the tarsometatarsus of *Raphus*, as seen end-on, shows the articular surfaces for the tibiotarsal condyles. The medial cotyla is larger and deeper than the lateral one. The medial margin of the medial cotyla is more rounded than the lateral margin of the lateral cotyla. The intercotylar area is depressed behind the articular surfaces and has a semicircular cranial border. The intercotylar eminence is approximately hemispherical and prominent. The cranial margin of the lateral cotyla slopes downwards and shows, cranially at the base of the intercotylar eminence, a depression for the "external semilunar cartilage" (Melville 1848; = meniscus lateralis?). On its caudodorsal[168] surface, the caudolateral extremity of the margin of the lateral cotyla provided attachment for m. fibularis brevis. Cranial to the attachment of m. fibularis brevis is a wide shallow indent, which in life was covered by a synovial membrane (Melville 1848). Slightly distal to this notch is the oval slightly raised impression for the lig. collaterale laterale. Just below the cranial margin of the lateral cotyla is a small transversely elongate tubercle.

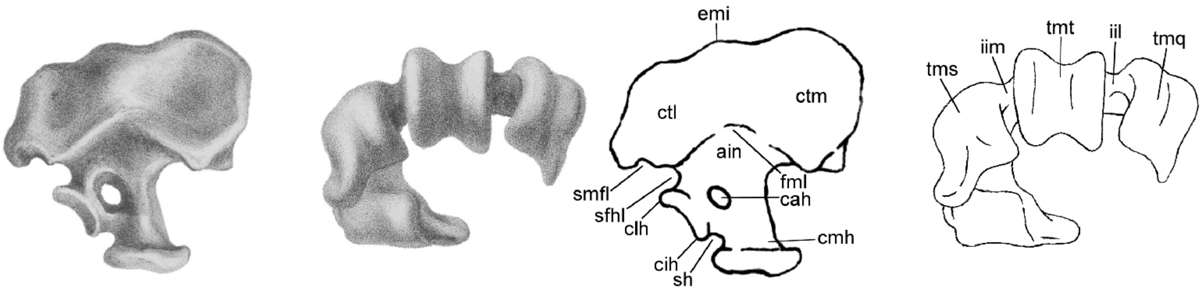

Tarsometatarsus of *Raphus*, left side, proximal and distal views (the latter showing articulated first metatarsal. Lithographs: Strickland & Melville 1848, pl.xi, figs.5, 6; artist: Joseph Dinkel; "Dinkel, del. et lith." "Reeve, Benham & Reeve lith.")

---

[168] The term 'caudal' is used here instead of 'plantar' (as used by Baumel & Witmer 1993) so as to conform with the terminology of the other hindlimb elements.

The hypotarsus is monocanaliculate. The medial crest of the hypotarsus[169] is well developed with an expanded 'foot'; it projects caudally from the middle of the caudal part of the tarsometatarsus. Its dorsal surface is smooth and rounded and shows a slight convexity in the middle (Melville 1848). The 'foot' of the crest (calcaneal tuberosity of Melville 1848) is rough and of rounded subtriangular form when viewed in caudal aspect. It overhangs the peduncle of the crest all the way around and provided attachment for the tendon of m. gastrocnemius. On the medial face of the medial crest of the hypotarsus, under its dorsal margin, is "a curved oblong concavity," which may have contained a haversian gland in life (*ibid*., p.105); between it and the medial parahypotarsal fossa is a sharp ridge. The lateral crest of the hypotarsus is shorter than the medial one and is caudolaterally directed. Its caudolateral end is expanded, overhanging the peduncle craniolaterally and distally. Between the lateral and intermedial hypotarsal crests is a sulcus, facing caudolaterally. Between the intermedial and medial hypotarsal crest is a bridge closing off the hypotarsal canal. The canal is slightly narrowed distally and leading from its distal opening is a short triangular groove on the medioplantar crest. The hypotarsal canal conducted the tendon of m. flexor digitorum longus. Caudal to the hypotarsal canal is the longitudinal groove, the sulcus hypotarsi, which carried the tendon of m. flexor perforatus digiti II cranially, and that of m. flexor perforans et perforatus digiti II caudally; in life this groove would have been closed over by a fibro-cartilaginous bridge. Lateral to the hypotarsal canal is the longitudinal groove for the tendon of m. flexor hallucis longus.[170] This groove was also covered over in life by a fibro-cartilaginous bridge, extending from the lateral lip of the groove to a slight short ridge on the "external and outer angle of the proximal extremity" (Melville 1848, p.105). Lateral and cranial to this groove is another short and shallow one, covered with synovial cartilage in life, over which the tendon of m. fibularis longus moved. These grooves become shorter cranially to caudally. In life there was a wide shallow groove extending from the lateral margin of the 'foot' of the medial crest of the hypotarsus to the lateral margin of the groove for the tendon of m. flexor hallucis longus. The lateral wall of the groove was formed by the fibro-cartilaginous bridge covering over the groove for m. flexor hallucis longus, the caudolateral part was formed by that covering the groove for m. flexor perforatus digiti II and m. flexor perforans et perforatus digiti II. Between these the wall was formed by the shallow groove between the lateral and intermedial crests of the hypotarsus. A fascia was attached to the margins of the wide groove to form a canal, which carried cranially the tendon of m. flexor perforatus digiti III and caudally that of m. flexor perforans et perforatus digiti III and m. flexor perforatus digiti IV. Lateral to the lateral hypotarsal crest is the shallow depression of the lateral parahypotarsal fossa; m. abductor digiti IV was attached to it. Laterally it is bounded by the ridge on the lateral margin of the shaft.

The caudomedial face of the margin of the medial cotyla is sub-vertical and oblong. Its distomedial part is directed slightly proximally and provided attachment for the "ligament of the great tibio-metatarsal sesamoid fibro-cartilage [= cartilago tibialis]" (Melville 1848, p.105; probably lig. metatarso-sesamoideum). A sharp ridge runs from it to the lateral surface of the medial parahypotarsal fossa. Cranial to this, and forming the craniomedial face of the proximal end of the tarsometatarsus, is a subtriangular area. The distally directed apex of this area is rough and served as attachment for lig. collaterale mediale; it passes distally into the sharp medial ridge running to the facet for the first metatarsal. Just distal to the cranial border of the medial cotyla is the distinct oval tubercle of the impressio retinaculus extensorius. There is also a longitudinal rough ridge ("entocondylar tuberosity" of Owen 1871b) marking the medial boundary of the dorsal infracotylar fossa. Between the tubercle and the ridge is a shallow groove directed proximolaterally, ending just under the rim of the medial part of the medial cotyla.

---

[169] Newton & Newton (1869) stated that the medial hypotarsal criest is "regarded as the head of the third (anchylosed) metatarsal", and referred to Gegenbaur (1863, 1864) as the source. Owen (1871b), however, disageed: "the process, as its name implies, is only a part of the head of the third or mid metatarsal" (p.524).

[170] The canal for the tendon of the flexor hallucis longus is open in *Caloenas* (pers. obs.; Martin 1904, fig.U^{4}a) and *Goura* (pers. obs.; Strickland & Melville 1848, pl.xi, fig.14; Milne-Edwards 1869-1871, pl.137, fig.4) but closed over in *Didunculus* (Strickland & Melville 1848, pl.x, fig.9d; Martin 1904, fig.U^{4}b) and some individuals of *Goura* (Claessens *et al*. 2015).

The proximal third of the cranial surface shows the medial elongated sub-oval depression of the dorsal infracotylar fossa, the floor of which is composed mainly of the third metatarsal. This depression is deepest proximally, below the intercotylar eminence. The proximal vascular foramina open into the depression – these are a pair of longitudinally oval apertures which open caudally on the caudal surface. The medial one is around double the size of the lateral one. Slightly distal to the medial foramen is the longitudinally sub-oval rough tubercle for the attachment of m. tibialis cranialis. This prominent tubercle lies on the medial margin of the fossa and shows a deep groove on its proximal end. Proximomedial to the medial proximal vascular foramen, and on the medial border of the dorsal infracotylar fossa, is a rough area: the impressiones retinaculi extensori. Distal to the dorsal infracotylar fossa the cranial surface of the fourth metatarsal is inclined slightly caudally towards the broad lateral margin. The cranial surface of the second and third metatarsals, distal to the fossa, "is more rapidly rounded off centrally towards the inner [= medial] edge" (Melville 1848, p.103). Dividing the lateral third of the cranial surface, "which twists on itself above, where it forms the outer [= lateral] wall of the concavity [the dorsal infracotylar fossa]", from the medial two-thirds is an intermuscular line. This slight ridge extends from the medial edge of the distal part of the lateral proximal vascular foramen to the medial edge of the distal vascular foramen.

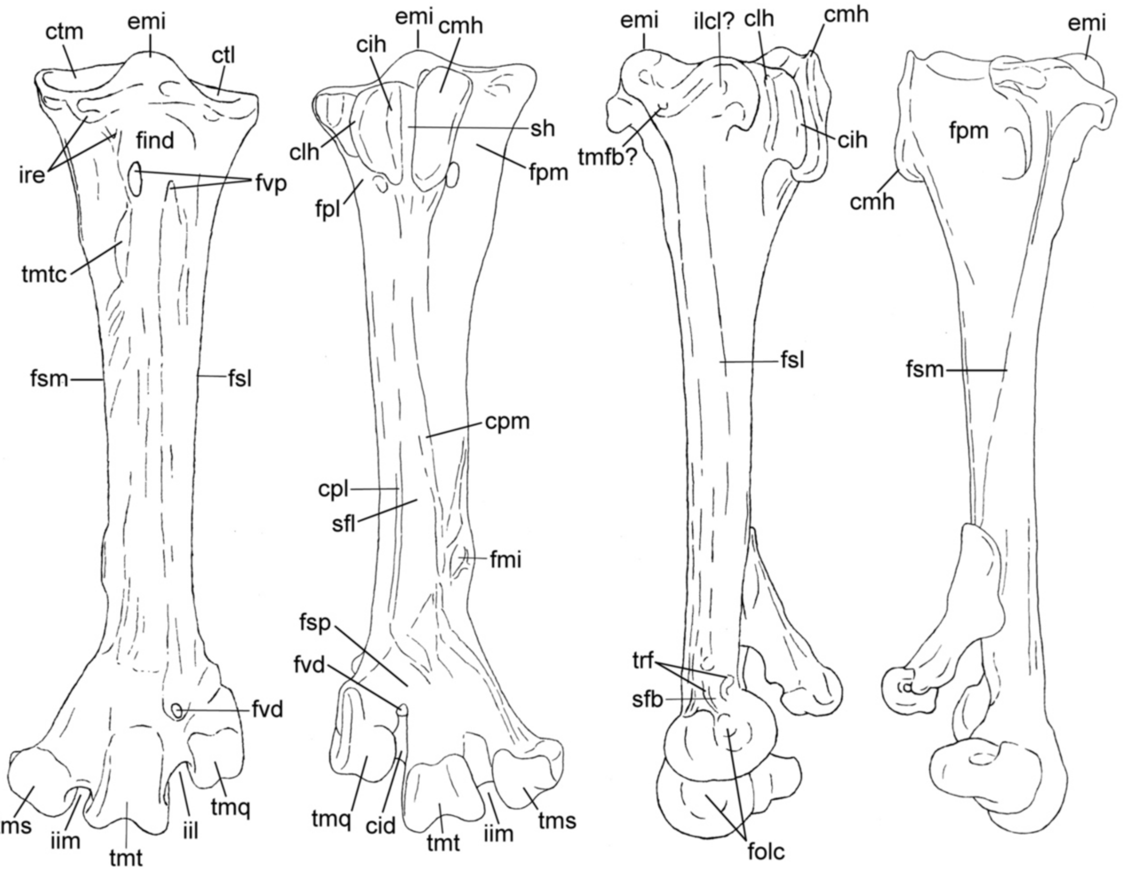

Tarsometatarsus of *Raphus*, left side, cranial, caudal, lateral and medial views (traced from Strickland & Melville 1848, pl.xi, figs.1-4).

The shaft of the tarsometatarsus is of approximately the same width along most of its length, expanding at its proximal and distal ends. Its medial border is slightly more concave than its lateral one. The shaft is triangularly pyramidal in its proximal two-thirds and craniocaudally compressed in its distal third. In OUMNH 11605, slightly lateral to the intermuscular line extending from the lateral proximal vascular foramen, and around halfway down the shaft on the cranial surface, is a small medullary foramen, which is directed distally. Another intermuscular line ("outer interosseal ridge" of Owen 1871b) extends from between the proximal vascular foramina towards the medial trochlea (trochlea metatarsi tertii), increasing slightly in width distal to the middle of the shaft. It terminates proximal to the medial trochlea, and provided attachment for m. extensor brevis digiti III and/or m. extensor proprius digiti III (George & Berger 1966; see section on musculature). The intermuscular line[171] for the attachment of m. abductor digiti II progresses distally from the m. tibialis cranialis tubercle. The proximomedial boundary of the impression for m. abductor digiti II is marked by a ridge, which passes distomedially from the m. tibialis cranialis tubercle to the medial margin, near the midlength of the tarsometatarsus. Dorsal to this narrow ridge is the surface for the attachment of m. extensor hallucis longus, on the cranial surface of the second metatarsal. In OUMNH 11605 this surface is "deeply pitted on either side of a raised subcentral line, and below exhibits two or three faint grooves parallel to its lower boundary" (Melville 1848, p.103). The attachment surfaces for m. extensor brevis digiti III and/or m. extensor proprius digiti III and m. abductor digiti II are very pitted in this specimen, especially distally (Melville 1848). The subcutaneal lateral surface of the tarsometatarsus, that which was not covered by muscle, increases in width passing proximally from just above the trochlea of metatarsal II. Progressing proximally this surface turns to face more cranially. Its cranial border is not well defined, but its caudal one is more distinct and defines the lateral boundary of the attachment surface of m. abductor digiti IV. Distally the caudal border becomes less well defined and converges towards the cranial one. The medial surface presents a sharp well-defined ridge running caudodistally, from the proximomedial corner of the tarsometatarsus to the lateral margin of the fossa for the first metatarsal. In its proximal third the ridge is directed laterally and distal to this it faces more caudally, so that the craniolateral face of the tarsometatarsus in this area is rounded. The proximal part of the medial surface of the bone shows a large but shallow subtriangular depression – the medial parahypotarsal fossa – the apex of which points distally. This depression provided attachment for m. flexor hallucis brevis. Opening into the cranial part of the depression is the caudal opening of the medial proximal vascular foramen.

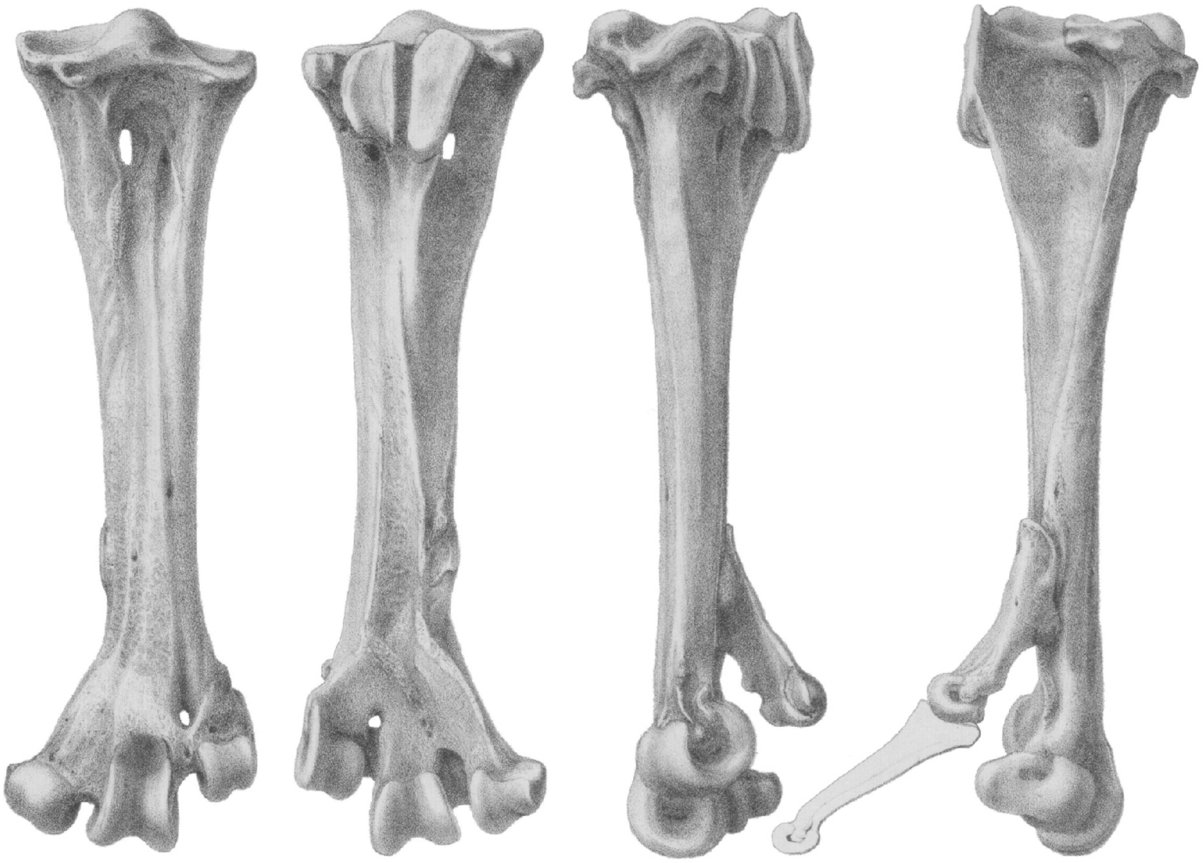

Tarsometatarsus of *Raphus*, left side, proximal and distal views (lithographs: Strickland & Melville 1848, pl.xi, figs.1-4; artist: Joseph Dinkel; "Dinkel, del. et lith." "Reeve, Benham & Reeve lith.")

---

[171] This may correspond to the "entometatarsal ridge" of Owen (1871b). Owen (*ibid.*) stated that this ridge is not present in *Raphus*, but it apparently is in OUMNH 11605 (pers. obs.).

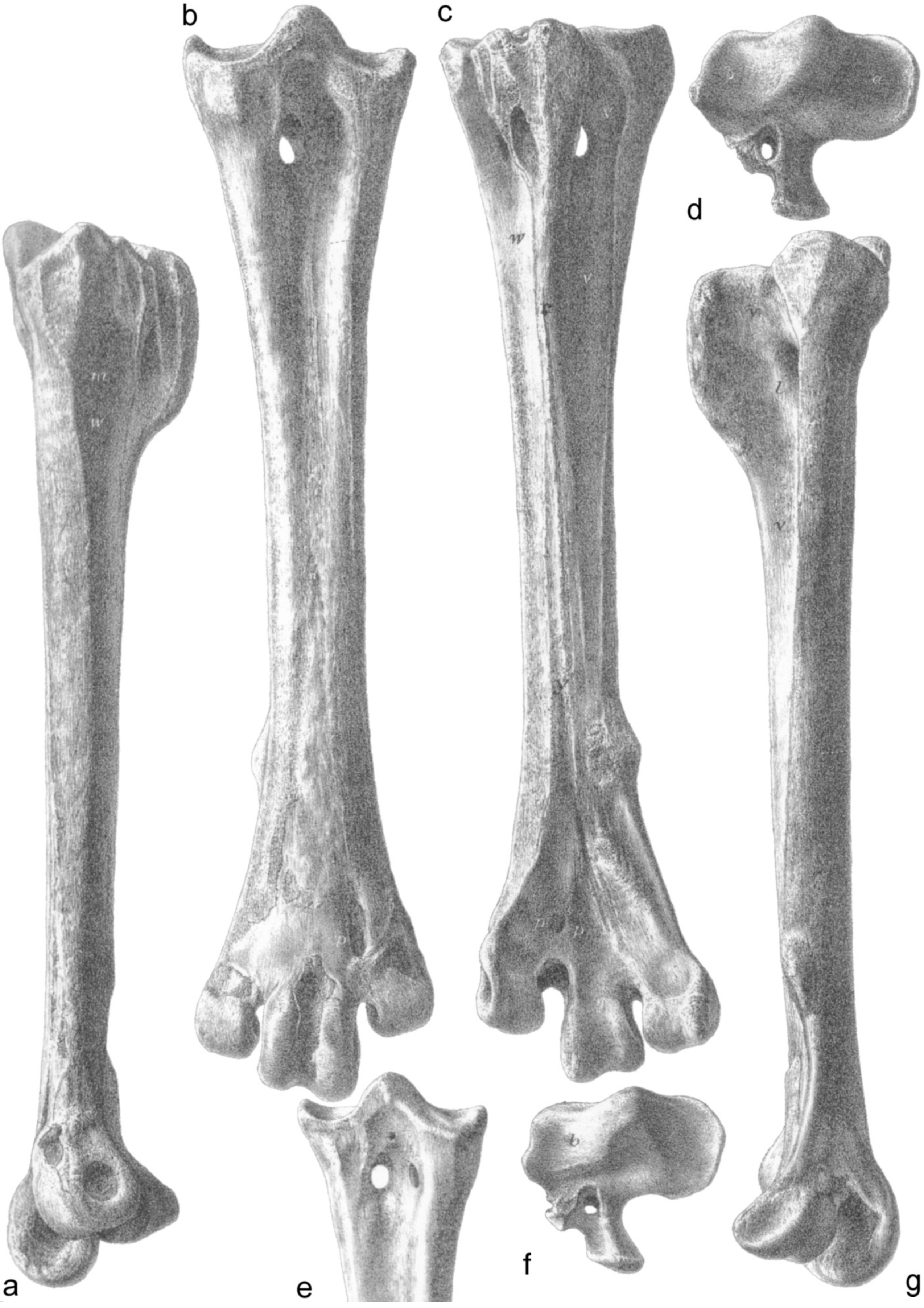

Tarsometatarsus of *Pezophaps*, left sides. a: lateral view (male); b: cranial view (male); c: caudal view (male); d: proximal view (male); e: cranial view (female); f: proximal view (female); g: medial view (male). (Owen 1871b, pl.lxvi, figs.1, 3, 2, 13, 7, 12 and 4 respectively; artist: George Henry Ford; "G. H. Ford" "Mintern Bro.s imp".)

As with the case in other columbids the fossa for the first metatarsal is large and excavated, it projects beyond the medial edge of the tarsometatarsal shaft (Worthy 2001). The fossa is positioned comparatively higher in *Raphus* than in *Pezophaps* and other raphines, the ratio of the distance from the distal end of the tarsometatarsus to the proximal end of the fossa to the total length of the tarsometatarsus being around 0.39-0.40 in *Raphus* and around 0.28 in *Pezophaps*.

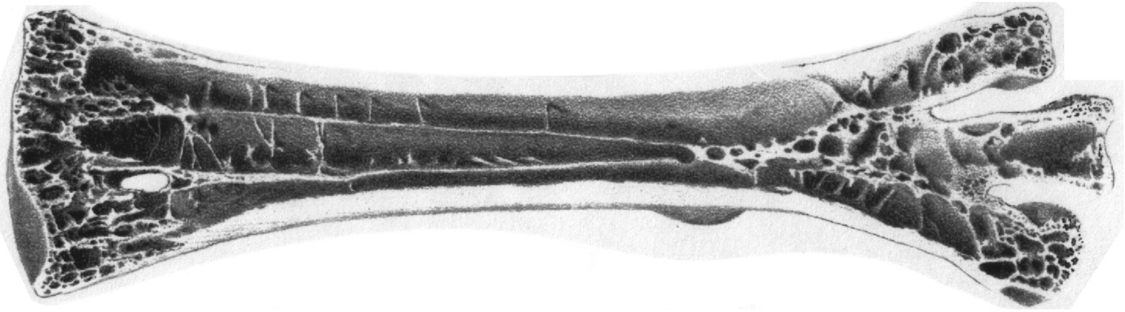

Tarsometatarsus of *Raphus*, left side, section (Owen 1867, pl.xxiii, fig.10; "J Smit lith" "M & N Hanhart imp").

Caudally the shaft presents the medioplantar crest, a longitudinal rounded ridge towards which the medial and lateral surfaces incline. This crest decreases in height from the medial hypotarsal crest, with which it blends, towards the fossa for the first metatarsal. The fossa projects slightly from the medial edge of the tarsometatarsus, and was covered by a "transverse crescentic tract of synovial cartilage" in life (Melville 1848, p.104). The lateral part of the caudal surface of the tarsometatarsus is flat. An intermuscular line (crista plantaris lateralis) passes distally from the lateral proximal vascular foramen, becoming more distinct as it progresses towards the trochlea of metatarsal IV. The origin-attachment for m. abductor digiti IV lies between this intermuscular line and the caudolateral edge of the tarsometatarsus, in a longitudinal area of approximately constant width. An intermuscular line (crista plantaris medialis), medial to the above-described one, descends from the distal part of the medioplantar crest. It runs obliquely to the medial side of the fossa for the first metatarsal. This line becomes faint near the distal part of the medial border of the facet and then becomes more defined as a slightly sigmoidal ridge running to just proximal to the trochlea of the second metatarsal. This ridge provided attachment for "the strong ligament connecting the metatarsi" (Melville 1848, p.104). The area between this intermuscular line and that mentioned above provided attachment for m. adductor digiti II. This area increases in width progressing distally; its proximal end meets the hypotarsus and faces caudolaterally. Distally the area (the tendinal, or intertrochlear, groove of Owen 1871b) is concave and faces caudally. There is an oblique depression between the ridge and the fossa for the first metatarsal, which accommodates the distal part of the articular surface of the proximal end of the first metatarsal. The tendon of m. adductor digiti II passed down a shallow groove between the ridge of the caudomedial margin of the distal part of the second metatarsal and, laterally, a rough elongated impression parallel to it. On the cranial surface of the tarsometarsus is a well-defined groove (canalis m. adductor digiti externus of Lambrecht 1933) leading into the distal vascular foramen. A small foramen or minute foramina or a shallow depression are occasionally present between metatarsals II and III, on the cranial face in the region level with the foramen vasculare distale (as seen in a UMZC 415.K specimen). Depressiones supracondylares trochleares are present at the distal ends of metatarsals III and IV in both *Raphus* and *Pezophaps* (Livezey & Zusi 2006; pers. obs.).

The foramen vasculare distale transmitted the tendon of m. extensor brevis digiti IV in life. The canal for the tendon of m. extensor brevis digiti IV, which runs into incisure between the peduncles of the trochleae of metatarsals II and IV, may be roofed over plantarly (caudally) (as in AMNH 3852; UMZC 415.K; Owen 1871b, pl.lxvi, fig.11) or open, so as to form a sulcus (as in OUMNH 11605)[172]. When roofed over, a there is a foramen created plantarly at its proximal end; this is the caudal ostium of the foramen vasculare distale. Of 114 tarsometatarsi examined, 64 (27 left, 37 right) had the canal roofed over and 50 (25 left, 25 right) had an open sulcus.[173] However, further investigation is needed to ascertain whether there is any correlation between tarsometatarsal size and the morphology of this feature.

---

[172] Worthy (2003) refers to the foramen vasculare distale either having "a single anterior opening leading to a single plantarly-distally aligned groove" or "separate distal and plantar openings" (pp.768, 771). This is incorrect, as only the plantar opening is vascular; the distal opening is for the tendon of m. extensor brevis digiti IV. Janoo (2005) also stated that the "foramen vasculare distale opens both on the plantar surface and in between the trochleae in the incisura intertrochlearis lateralis" (p.172).

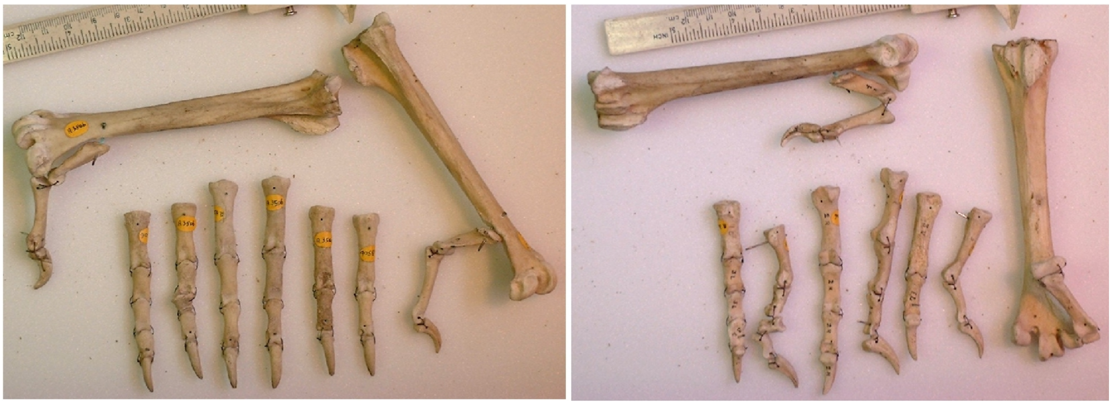

Tarsometatarsus, first metatarsal and pedal phalanges of *Pezophaps*, right and left sides (NHMUK A.3506; female; ○ Jolyon C. Parish).

In transverse section the shaft of the tarsometatarsus is triangular proximally, the apex directed caudally, and transversely oblong or sub-oval distally. The proximomedial part of the cranial surface of the shaft is concave vertically; the rest of the cranial surface is straight longitudinally and convex transversely. The second metatarsal is the most convex of the three fused metatarsals and is slightly cranial to the fourth, which is of greater transverse extent.

In distal end-on view the trochleae are arranged in a slightly convex line. In cranial view the trochleae of metatarsals II and III extend to the same level distally, whereas that of metatarsal IV is shorter and does not extend as far; its distal extremity is around the level of the medial intertrochlear incisure. The trochlea of metatarsal II is slightly medially directed, and that of metatarsal IV slightly laterally directed. Melville (1848) stated that "the elevation of the outer trochlea [that of metatarsal IV], and the abbreviation of the corresponding toe, renders the foot more adapted for progression" (p.105). The oblique peduncle of trochlea of metatarsal II has a right-angled triangular cross-section (*ibid.*). It is transversely convex dorsally and very concave caudally and its caudomedial projection is well developed. The trochlea of metatarsal III shows a well-developed median groove; the medial side of the trochlea is projects further cranially than the lateral, and the lateral side is most developed caudally and distally. The cranial and proximal end of the groove passes into a subcircular depression. As in other columbids the width of the trochlea of metatarsal III width is greater than its craniocaudal depth (Worthy 2001). The trochlea of metatarsal IV shows a slight median groove. The caudal and lateral projection is elongate. Each side of the trochleae shows a depression, the fovea ligamentorum collateralium.

On the lateral surface of the base of the trochlea of metatarsal IV is a groove, the cranial margin of which is marked by a small oval tubercle passing distally into a ridge; the caudal margin is marked by a rough ridge, positioned slightly distal to the tubercle. This groove conducted m. abductor digiti IV and was covered by a fibrous ligament in life (Melville 1848).

---

[173] The open condition is found in the majority of pigeons, as well as in Podargidae, Cuculidae, Trogonidae, Aegothelidae, Coraciidae and Psittaciformes (Livezey & Zusi 2006: 2325; Mayr & Clark 2003; pers. obs.), although in the Cuculidae the tendon for m. extensor brevis digiti IV does not pass through the foramen vasculare distale and in the Aegothelidae, Trogonidae and Psittaciformes the muscle is absent (Steinbacher 1935; Livezey & Zusi 2006: 2701). The plesiomorphic condition for Neornithes (and that found in the majority of bird species) is having the canal roofed over plantarly (Mayr & Clark 2003). Within Columbidae the canal is roofed over plantarly in *Caloenas* (variable), *Didunculus*, *Lopholaimus*, *Nesoenas*, *Ocyphaps*, *Otidiphaps*, and *Trugon* (variable) (pers. obs.).

In longitudinal cross-section (Owen 1867, p.xxiii, fig.10), the tarsometatarsus of the dodo shows the hollow cavities of the metatarsals, with a few transverse struts in the shaft of that bone. The internal boundaries of the metatarsals are reduced to thin walls. The third metatarsal pinches out at around two-thirds of the way down the bone, before expanding again. This is due to the fact that its proximal end is more caudal than its distal end. The lateral wall of the tarsometatarsus is around half the thickness of the medial one (*ibid.*).

The tarsometatarsus of *Pezophaps* is more elongate than that of *Raphus*. The medial cotyla of the proximal end of the tarsometatarsus is deeper and wider craniocaudally than the lateral one, although it is of the same lateral width. It is deeper than that of *Raphus*, with more defined borders. The caudal margin of the medial cotyla extends further in *Pezophaps* compared with *Raphus*, before passing into the medial face of the medial crest of the hypotarsus (Owen 1871b). The intercotylar eminence is well developed, with a rounded apex. Its base covers just over half of the craniocaudal width of the articular surface. The intercotylar eminence is higher and more pointed than that of *Raphus*. Caudal to the intercotylar eminence is the flat subtriangular area of the intercotylar area. Owen (1871b) stated that this was not covered by articular cartilage, as judged by comparing the colour and texture to surfaces which were. Merging with the intercotylar area is the sulcus ligamentosus. The entometatarsal ridge of Owen (1871b, pl.lxvi, fig.4, *e*) may correspond to the ridge demarcating the lateral border of the origin of m. extensor hallucis longus (thus dividing m. extensor hallucis longus from m. abductor digiti II). It passes from the tubercle of the impressio retinaculus extensorius, just distal to the cranial border of the medial cotyla, to about a third of the way down the shaft, although it is not well defined. The ridge forming the medial border of the origin of m. extensor proprius digiti III converges with the lateral one at a level with the lower end of the concavity of the medial margin of the proximal part of the tarsometatarsus (Melville 1848). The entogastrocnemial ridge of Owen (1871b) corresponds to the ridge defining the craniomedial border of the origin of m. flexor hallucis brevis. This ridge is more pronounced and is situated further internally in *Raphus* (*ibid.*). The entocondylar ridge of Owen (*ibid.*) passes from the highest point of the medial border of the medial cotyla distally for a short distance before disappearing or, in some specimens Owen studied, joining, the “entogastrocnemial ridge”. Owen (*ibid.*, p.520) stated that the just below cranial part of the medial cotyla are “two or three oblong tuberosities, in the same transverse line, the outermost of which [...] extends down as a short ridge” and forms part of the medial margin of the dorsal infracotylar fossa. These are the impressiones retinaculi extensorii. The ectometatarsal ridge of Owen (*ibid.*; Crista ectometatarsalis of Martin 1904) probably corresponds to the ridge defining the cranial margin of the origin of m. abductor digiti IV. Owen stated that the medial parahypotarsal fossa is narrower in *Pezophaps* and in female specimens deeper “than in *Didus*, owing to the more posterior position, in *Pezophaps*, of the entogastrocnemial ridge [...] defining that depression internally” (*ibid.*, p.522).

As in *Raphus*, the medial proximal vascular foramen is larger than the lateral one. The medial one is longitudinally elliptical in outline; the lateral one is more vertically slit-like. The elongate rough surface for the insertion of m. tibialis cranialis is not protuberant as it is in *Raphus*. It extends proximally to the medial proximal vascular foramen. Melville (1848) stated that it “extends on both walls of the concavity [the dorsal infracotylar fossa], a deep groove bisecting it; the outer segment is slightly raised, the inner impressed” (p.118). The divisions between the metatarsals are marked by long narrow ridges (*ibid.*). These diverge as they progress distally.

The dorsal infracotylar fossa is deeper in *Pezophaps* than in *Raphus*, with a more “angular floor” (Melville 1848, p.118). It exhibits individual variation, as observed by Strickland (1853), the fossa being shallower and more expanded in a specimen from the former Zoological Society of London collection (NHMUK A.1360) than in a specimen in his collection (UMZC 414.N; *ibid.*, pl.55, figs.5-7), especially distal to the medial proximal vascular foramen, near the insertion of m. tibialis cranialis. The lateral margin of the fossa is only slightly concave. The proximal part of the second metatarsal, medial to the dorsal infracotylar fossa is more transversely convex in *Pezophaps* compared with *Raphus*. The cranial opening of the distal vascular foramen is vertically oblong in outline and is relatively smaller than that of the dodo (Claessens *et al.* 2015); the caudal opening is smaller than the cranial opening and is circular (see below).

The hypotarsus is similar to that of the dodo. It is "developed from the back part of the head of the mesometatarsal [III] and the part of the epiphysis confluent therewith" (Owen 1871b, p.521). The caudal surface of the 'foot' of the medial crest of the hypotarsus is rough, flattened, longitudinally elongate, and wider proximally than distally, as in *Raphus*. The medial crest of the hypotarsus is proportionately slightly smaller than it is in *Raphus* and does not project quite as far caudally. The caudolateral face of the 'foot' of the lateral crest of the hypotarsus is also flattened and rough. The lateral crest is smaller and narrower in *Pezophaps* than it is in *Raphus*; the groove on its lateral face is narrower and defined by a ridge not present in the tarsometatarsus of the latter (*ibid.*). The proximal margin of the medial crest of the hypotarsus is thinner in *Pezophaps* compared with *Raphus* and the hypotarsal canal is smaller, "apparently arising from the greater thickening in the former of the "calcaneal processes [= crests of the hypotarsus]" (Newton & Newton 1869, p.345). Strickland (1853) thought that the medial crest of the hypotarsus was much less developed in *Pezophaps* than in the dodo, however, as Newton & Newton (*op. cit.*) pointed out, this is not the case: "this fact appears to us to be in consequence of the heads of the second and fourth (anchylosed) metatarsals being expanded laterally rather than antero-posteriorly" (*ibid.*, p.345). The hypotarsal sulcus is less deep in the former genus, compared with the latter. In *Pezophaps* the crista medianoplantaris reaches further distally than in *Raphus*. The medial parahypotarsal fossa is similar to that in the dodo. The depression for m. flexor hallucis brevis is narrower and more elongate in *Pezophaps* than in *Raphus*, stretching almost to the fossa for the first metatarsal in the former (Melville 1848). The caudal orifice of the lateral proximal vascular foramen opens into the lateral parahypotarsal fossa. The short longitudinal ridge or process just distal to the medial border of the medial cotyla is less developed in *Pezophaps* than in *Raphus* (Owen 1871b, pl.lxvi, fig.10, *j*); it passes into the ridge of the medial face of the shaft (the "entogastrocnemial ridge") in the former.

Owen's (1871b) "ectometatarsal ridge" (probably corresponding to the ridge marking the cranial margin of the origin of m. abductor digiti IV) is more distinct in *Pezophaps* than in *Raphus*. The ridge marking the lateral margin of the shaft of the tarsometatarsus (Owen's "ectogastrocnemial ridge"[174]) is slightly curved, convex backward, as it progresses distally. Melville (1848) stated that in *Pezophaps* the lateral face of the tarsometatarsus is flatter and wider than that in *Raphus*, and that the lateral margin of the proximal part is vertically concave, whereas in *Raphus* it is slightly convex. The cranial and caudal margins of the lateral face are more angular in *Pezophaps* than in *Raphus*. The ridge forming the ventrolateral edge of the lateral metatarsal, just above the trochlea, is Owen's (1871b) "ectotrochlear ridge"; it marks part of the medial boundary of the attachment of m. abductor digiti IV. The ridge forming the medial boundary of the shaft of the tarsometatarsus (the "entogastrocnemial ridge") progresses distally and ends at the proximal margin of the fossa for the first metatarsal. The medial margin of the proximal third of the shaft is flat with a distinct caudal edge, whereas in *Raphus* it is thinner and more ridge-like. The flat surface in *Pezophaps* faces very slightly outwards (Melville 1848); it ends distally at a medial rough projection. This projection is present in the specimen figured by Melville (*ibid.*, pl.xv, fig.2; Hunterian Museum, Glasgow), but is less developed in many other specimens, as in *Raphus*. Distal to this the medial margin of the tarsometatarsus is convex. The area for the origin of m. adductor digiti II is narrower than in *Raphus*. It curves into the groove running across the supratrochlear fossa, whereas in *Raphus* the junction between the two is angular. Distally the subtriangular crista plantaris, decreasing in height, passes along the lateral side of the fossa for the first metatarsal. This fossa is proportionately approximately the same distance from the distal end of the tarsometatarsus in both *Pezophaps* and *Raphus*, and it is the elongation of the shaft between the fossa and the proximal end of the tarsometatarsus which makes the tarsometatarsus of the former much longer. The medial margin of the shaft distal to the fossa for the first metatarsal is thinner and less concave in *Pezophaps* than in *Raphus*. At the distal end of the tarsometatarsus it is continued by a prominent ridge, which runs obliquely to the medial edge of the medial metatarsal, just above the trochlea. This ridge is Owen's (1871b) "entotrochlear ridge". The tendinal groove mentioned by Owen

---

[174] Owen (1871b) stated that the "ectogastrocnemial ridge" (pl.lxvi, figs.1, 2, *x*; Crista ectogastrocnemialis of Martin 1904), which he mentioned as being external to the postexternal depression (*ibid.*, *w*), terminates on the "ectotrochlear ridge" (pl. lxvi, fig.2, *z*). Judging from his description and figures it does not. Also in figure 8 he labels the "entogastrocnemial ridge" (*g*); this cannot be correct as the figure depicts the lateral face of the tarsometatarsus. The label, *g*, apparently shows his "ectogastrocnemial ridge".

(*ibid*., pl.lxvi, fig.2, B) extending “from the upper and outer part of the oblique [entotrochlear] ridge to or near to the interspace between the ento- [= second] and meso- [= third] trochleae” is that which conducts the tendon of m. adductor digiti II. It is deeper than in *Raphus* (Melville 1848). The groove for m. extensor brevis digiti IV, on the cranial surface of the shaft of the tarsometatarsus, is less developed and shorter in *Pezophaps* compared with *Raphus*, and “indicates a more powerful “adductor muscle”” in the latter (*ibid*., p.522). The medullary foramina are proportionately in approximately the same place on the shaft in *Pezophaps* as they are in the dodo.

The caudal (plantar) supratrochlear fossa is bounded laterally by the “ectotrochlear ridge” and medially by the “entotrochlear ridge” of Owen (1871b). It is shallow and well defined. The trochlea of metatarsal II is convex cranially, and caudally presents a shallow groove. Its caudomedial angle is projecting. The trochlea of metatarsal IV is less concave caudally than the trochlea of metatarsal II and is nearly flat transversely. Its caudolateral angle is less projecting and more rounded than the caudomedial angle of the latter trochlea. The median groove of the trochlea of metatarsal III is deepest cranially. The lateral fovea ligamentorum collateralium is deeper and better defined than the medial one. The trochlea of metatarsal III is larger, proportionately, than those of metatarsals II and IV in *Pezophaps* than in *Raphus*. The lateral fovea ligamentorum (“ectotrochlear depression” of Owen 1871b) of the trochlea of metatarsal IV is distinctly developed. The caudal groove between the peduncles of the trochleae of metatarsals III and IV is invariably bridged over (by the adductor bridge of Owen 1871b), creating a foramen (the caudal ostium of the foramen vasculare distale). Unlike the case in *Raphus*, this bridge is invariably present (pers. obs.).

The articular face for the hallux is located proportionately further distally in *Pezophaps* than in *Raphus* and is relatively smaller.

Strickland (1853) stated that the trochleae are “placed more nearly in the same vertical plane in *Didus* than they are in *Pezophaps*, in which latter bird the two lateral trochleae are placed more obliquely and more posteriorly in reference to the middle one than they are in *Didus*” (p.196). From this he inferred that in *Pezophaps* the lateral toes were more divergent than in *Raphus* and thus the former was able to run faster. Newton & Newton (1869) disagreed, stating that “the large series of examples [of the tarsometatarsus of *Pezophaps*] shows that the angle formed by joining the centres of the three trochleae (of course the only mode of accurately testing the observation) is much more obtuse in the smaller (female?) specimens than in the larger (male?). In this case, if any stress be laid on Strickland’s inference [...] it would follow that the larger (male?) examples of *Pezophaps* did not run so quickly as ordinary examples of *Didus*, while the smaller (female?) attained a greater speed” (p.345).

The tarsometatarsus of *Pezophaps* is absolutely longer than that of *Raphus*, but it is narrower at both ends, making it more gracile. Overall, the tarsometatarsus of the solitaire is very similar to that of the dodo, and Strickland remarked: “the elaborate description given by Dr. Melville of the tarso-metatarsus of the Dodo [...] would apply almost word for word to the bone before us [of *Pezophaps*], and afford the most convincing proof of their close affinity” (1859, p.195). Melville (1848) noted that in “those points in which the [tarso]metatarsus of the Solitaire differs from that in the Dodo [greater elongation, craniocaudal expansion of the central part of the shaft, breadth of the lateral and medial borders], are, in some measure, repeated in *Phaps*, which has nearly the same relation to *Geophaps* that the Solitaire has to the Dodo, in the proportionate lengths of the metatarsi” (p.118). Regarding the functional morphology of the tarsometatarsus in the dodo and solitaire, Owen stated that “the shorter and stronger metatarsus of *Didus* indicates more powerful actions of the foot, in reference to the greater weight of the body to support- perhaps, also, to more habitual and powerful applications in scratching up the soil. The longer and more slender [tarso]metatarsus of *Pezophaps* relates, as Strickland justly observes, to the lighter weight and more active movements of that bird” (*ibid*., p.523).

In transverse section the internal construction of an Andersonian Museum specimen examined by Melville (Strickland & Melville 1848, pl.xv, fig.4) shows the cancellous structure extending “farther towards the middle of the shaft, in the narrow lateral [medial and lateral], than in the wide central division” (*ibid*., p.119). He stated that the wall of the shaft in this specimen is nearly 2mm thick.

First metatarsal

(*Raphus*: Strickland & Melville 1848, pl.xi, figs.7-10; Middleton 2008, photo 14; Claessens *et al*. 2015, fig.63, pls.PL40, D40. *Pezophaps*: Newton & Newton 1869, pl.xx, figs.104, 105; Newton & Clark 1879, pl.xliv, fig.7)

The first metatarsal is “a thick oblong plate, twisted on itself from behind forwards, and from within outwards; the line of flexure corresponding to its diagonal. The channel [canalis flexorius plantaris] thus formed [...] lodges the *flexor* tendons of the hind toe” (Melville 1848, p.109). The canal is wider distally than proximally. The trochlea for the proximal phalanx of digit I is well developed; it is longer than wide and subcylindrical. It is very slightly concave cranially and grooved caudally for the tendon of m. flexor hallucis longus. It is wider medially than laterally, and projects more caudally from the caudal surface of the curved shaft of the bone medially than laterally. The lateral margin of the caudal part of the curved shaft is thin and concave; distolaterally it joins the lateral tubercle, projecting lateral to the trochlea. This process is sub-quadrate and provided attachment for lig. transversum metatarsale. The cranial surface was covered by a thin layer of synovial cartilage in life and a tendon, probably that of m. flexor perforatus digiti II, passed over it. It is more robust in *Raphus* than in volant columbids (Claessens *et al*. 2015).

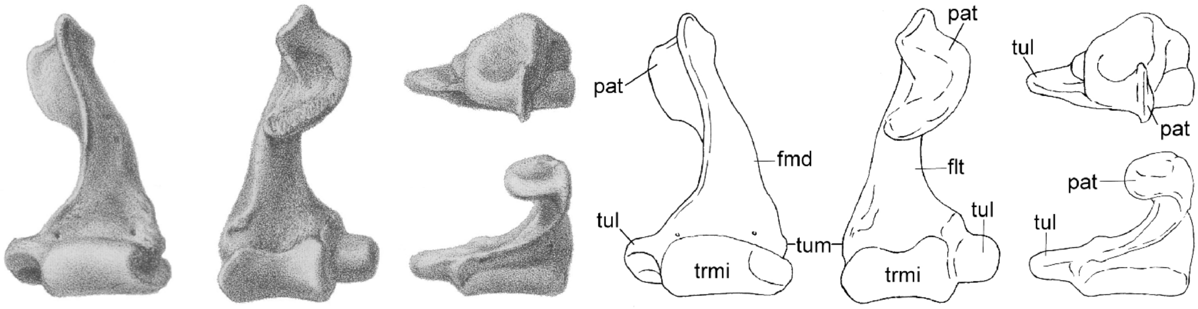

First metatarsal of *Raphus*, left side, caudal, cranial, oblique and distal views (lithographs: Strickland & Melville 1848, pl.xi, figs.7-10; artist: Joseph Dinkel; “Dinkel, del. et lith.” “Reeve, Benham & Reeve lith.”)

The tarsometatarsal articular face of the first metatarsal is relatively flat, and curved, like a boomerang, pointing laterally. Its proximal sub-concave part was covered by articular cartilage in life and “the concavity probably gave origin to some fibres of the *M. adductor indicis* [= m. abductor digiti II]” (Melville 1848, p.109). The articular surface lies on a semicircular lamina, which forms the cranial part of the channel which contained the flexor tendons of digit I. The lateral border is convex, thick and roughened cranially for the attachment of the “strong inter-osseous ligament” of Melville (1848). Melville (*ibid*.) also stated that “the tendon of *M. extensor pollicis* [= m. extensor hallucis longus] passed along the posterior surface [of the first metatarsal], and is bound down immediately above the trochlea by an annular ligament, attached externally by a roughened portion of the outer edge, and internally to a narrow pit close to the inner border”(p.109).

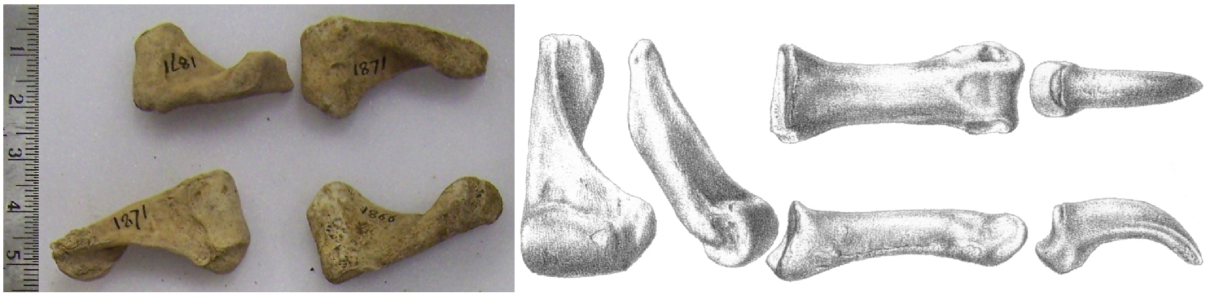

First metatarsal and hallux of *Pezophaps*. *Left*: first metatarsals, left and right sides, cranial and caudal views (UMZC specimens; ○ Jolyon C. Parish); *right*: First metatarsal and hallux, right side, caudal, lateral and dorsal views (Newton & Newton 1869, pl.xx, figs.104-109; artist: George Henry Ford; “G. H. Ford ad nat. lith.” “W. West imp.”)

Comparing specimens of the first metatarsal of *Pezophaps* with figures and a cast of OUMNH 11605, Newton & Newton (1869) concluded that in the former it was larger absolutely, with a smoother surface. They also considered that the canal through which the flexor tendons of the hallux passed was not as deep in *Pezophaps* as in *Raphus*, and that overall the first metatarsal was less twisted in the former. The tarsometatarsal articular face of the first metatarsal is more convex in the middle in *Pezophaps* than in the dodo. Newton & Newton (*ibid.*) stated that "generally this bone in *Pezophaps* would seem to be longer [than that of *Raphus*], which is of course in proportion to the increased length of the lower extremities" (p.345).

As in *Raphus*, the lower part of the articular face is roughened. The lateral tubercle is less pronounced in *Pezophaps* compared with *Raphus*. On the cranial surface of the first metatarsal the lateral tubercle merges with the trochlea so that its margins are poorly defined. "The pit on the inner extremity of the trochlea is to all appearance as deep as in *Didus*" (Newton & Newton 1869, p.345). The medial tubercle is much smaller than the lateral one.

Pedal Phalanges[175]

(*Raphus*: Blainville 1835, pl.iii, figs.vi, vii; Strickland & Melville 1848, pl.xii, figs.1-5;[176] Grihault 2005, p.83; Middleton 2008, photo 14; Meijer *et al*. 2012, fig.5e; Claessens *et al*. 2015, figs.3, 55, 60, 64, pls.PL41-46, D41-46. *Pezophaps*: Newton & Newton 1869, pl.xx, figs.108, 109, 115;[177] Newton & Clark 1879, pl.xliv, fig.7; Ottow 1950, pl.vi, fig.17; Lüttschwager 1961, fig.18)

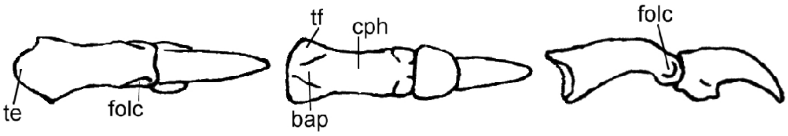

Pedal phalanges of *Raphus*, dorsal, ventral and lateral views (traced from Strickland & Melville 1848, pl.xii, fig.1).

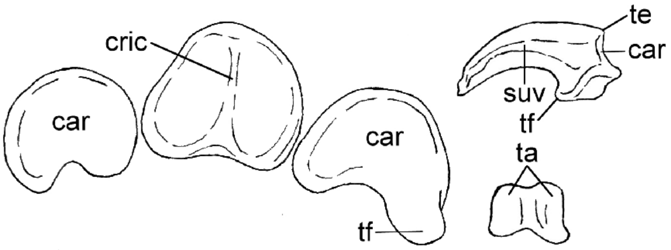

Pedal phalanges of *Raphus*. *Left*: proximal views of proximal phalanges of digits II, III and IV; *top right*: ungual of digit IV, lateral view; *bottom right*: distal view of phalanx 2 of digit IV (traced from Strickland & Melville 1848, pl.xii, figs.2, 4a, 5).

The pedal phalanges of *Raphus* are known from OUMNH 11605, UMZC 415.H, NHMUK A.1352, GLAHM Z1688, the MNHN collection (including a mounted skeleton), Elbeuf (15.0.67, 16.0.67, 17.067, 19.0.67, 20.0.67), the Durban skeleton, Thirioux's and Sauzier's skeletons at Port Louis, Paul Carié's skeleton, the Summers Place Auctions skeleton, the Treize Cantons material (Site 24), the Kanaka cave specimen, the Western Australian Museum skeleton, MAS 2006-61-6, MAS AG 39-40,[178] and a specimen found at a marsh at Flacq (doubtful: Newton 1890; Parish 2013). Both *Raphus* and *Pezophaps* have an anisodactyl foot and the phalangeal formula is 2:3:4:5, as in other pigeons.

---

[175] Note: lateral and medial here refer to the position with respect to the axis of the body, not that of the foot.

[176] In OUMNH 11605 the only ungual phalanx present is that of digit IV, the others have been illustrated by guesswork in the figure given in Strickland & Melville (1848, pl.xii, fig.1) "as to the length from the foot covered with integuments, in the British Museum" (*ibid*., p.110).

[177] Newton & Clark (1879) stated that some of the ungual phalanges figured by Newton & Newton (1869, pl.xx, figs.113-115, 125-127) do not actually belong to *Pezophaps* but to a species of chelonian (only figures 108, 109 and 115 depict those belonging to *Pezophaps*).

[178] According to the Naturalis blog (2007), pedal phalanges were relatively common at Mare aux Songes. Naturalis: Dodo Expeditie Weblogs 2006-2009: www.dodo-expeditie.nl

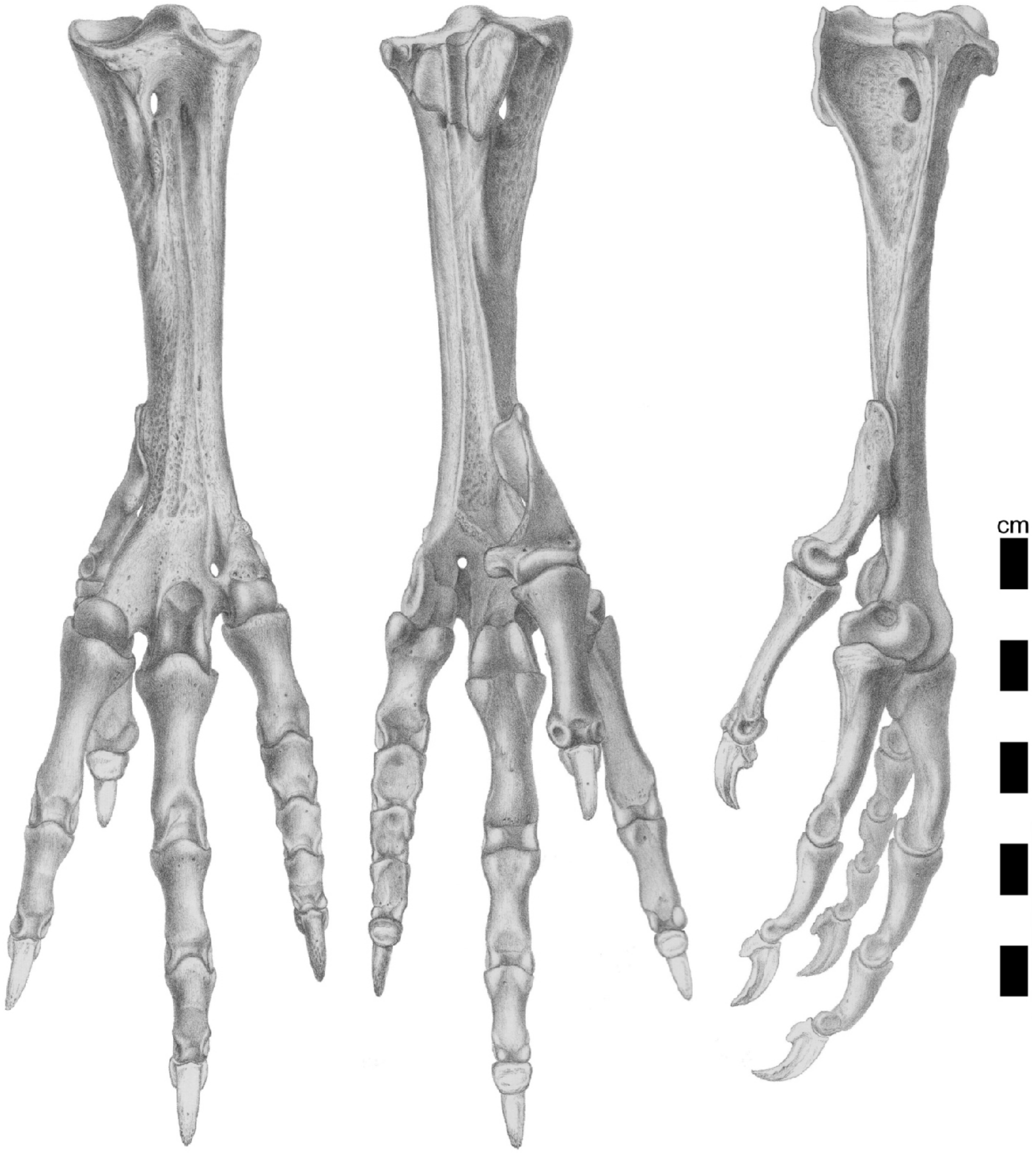

Pes of *Raphus*, left side, cranial, caudal and medial views (Strickland & Melville 1848, pl.xii, fig.1; "Tuffen West, lith." "Reeve, Benham & Reeve, imp.")

The first phalanx of the hallux is at least double the length of the ungual (Melville 1848; pers. obs.). It is longer than that of digit IV, but shorter and flatter than those of digits II and III. The proximal phalanx of the hallux differs from the phalanges of the other digits in the following ways: it shows a projection on the lateral side of the proximal end, a shallow concave proximal articular face, an expansion of the plantar surface of the distal end, the deep foveae ligamentorum collateralia are directed more dorsolaterally and dorsomedially directed than in the phalanges of the other digits, and the intercondyloid ridge is also less developed (*ibid.*). The proximal phalanx of the hallux is more robust in *Pezophaps* than in *Raphus* and the ungual of the hallux is proportionately longer in the former compared with the latter.

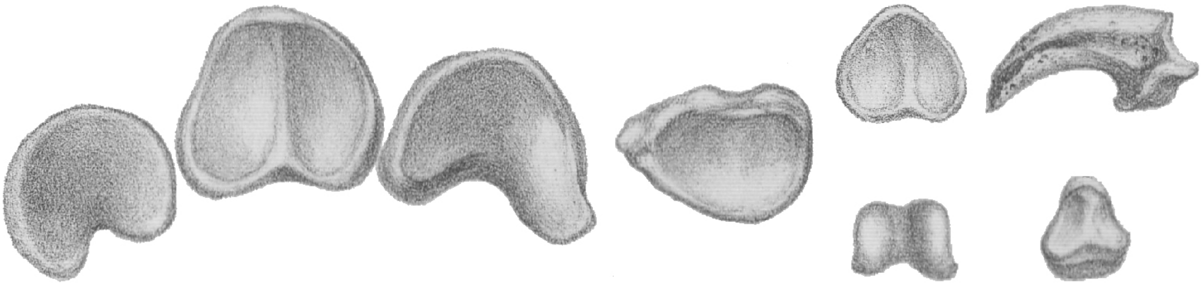

Pedal phalanges of *Raphus*, left side. *Left*: proximal views of proximal phalanges of digits II, III, IV and I; *middle*: proximal and distal views of phalanx 2 of digit IV; *right*: ungual of digit IV, lateral and proximal views (Strickland & Melville 1848, pl.xii, figs.2, 4, 5; "Tuffen West, lith." "Reeve, Benham & Reeve, imp.")

The distal end of the proximal phalanx of digit II is rotated slightly laterally. The lateral margin is more concave than the medial. The articular cotyla is concave and reniform, with the "inner angle being most elongated" (Melville 1848, p.110), and with no intercondyloid ridge. These characters differentiate it from the proximal phalanx of digit III. Its plantar margin is concave for the reception of the flexor tendon. The fovea articularis collateralis is deep and the trochlea articularis has a deep groove (Claessens *et al*. 2015). The axis of phalanx 2 of digit II is rotated slightly laterally. Its proximal end is concave plantarly for reception of the flexor tendon and its distal end is directed slightly medially. Its lateral margin is more concave than its medial one. In lateral view it is more curved than the preceding phalanx. The proximal phalanx of digit II of is approximately the same length as that of digit III, whereas that of *Pezophaps* is the longest in the whole foot (Newton & Newton 1869).

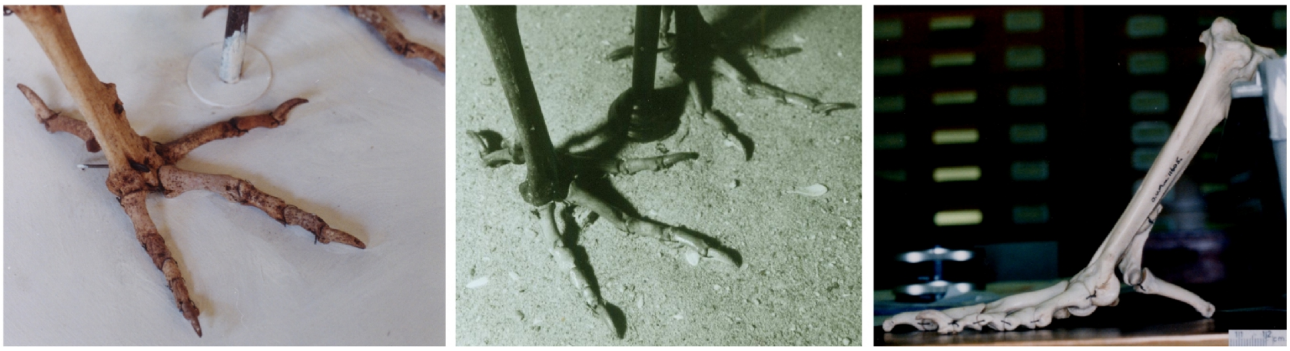

Pes of *Raphus*. *Left*: Thirioux's Port Louis skeleton, right side (© Jan den Hengst); *middle*: Durban skeleton (2366; © Durban Natural Science Museum); *right*: left side, lateral view (OUMNH 11605; ○ Jolyon C. Parish, January 2001).

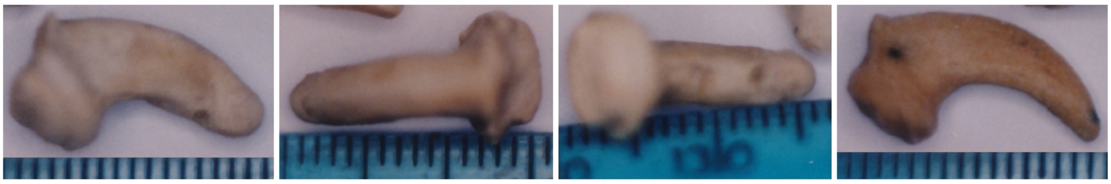

Cast of pedal unguals of *Raphus* (OUMNH 11605). *Left three images*: digit unknown, side, dorsal and ventral views; *right*: digit IV? side view (scale in mm; ○ Jolyon C. Parish, January 2001).

The articular cotyla shows a median intercondylar ridge. This ridge articulates with a groove on the trochlea of metatarsal II of the tarsometatarsus. Claessens *et al*. (2015) noted that "the trochlea metatarsi III–cotyla articularis III-1 joint was more hinge-like and had fewer degrees of freedom than the tarsometatarsal-phalangeal joint of digits I and II, but was also likely able to withstand greater loads" (p.78). The distal end of the proximal phalanx of digit III is rotated slightly laterally. The extensor tubercle is prominent. The articular trochlea of phalanx 1 bears a vertical groove which accommodates the median ridge of the articular cotyla of phalanx 2 (*ibid*.). The trochlea of phalanx 2 bears a groove which is most developed on its plantar face (*ibid*.). The distal ends of phalanges 2 and 3 of digit III are rotated slightly medially. In lateral view phalanx 2 is curved and phalanx 3 moreso. The proximal phalanx of digit III in *Pezophaps* is proportionately longer and thicker than that of *Raphus* and in specimens from males it is absolutely longer. This is the same case with the second and third phalanges of digit III.

The distal end of the proximal phalanx of digit IV is rotated slightly medially. Its articular cotyla bears a vertical ridge. The extensor tubercle is prominent. The medial margin of the phalanx is more concave than the lateral one. Phalanges 2, 3 and 4 of digit IV also have vertical ridges on their articular cotyles. The proximal phalanx of digit IV is the shortest of all the proximal phalanges of the whole foot in *Pezophaps* (Newton & Newton 1869).

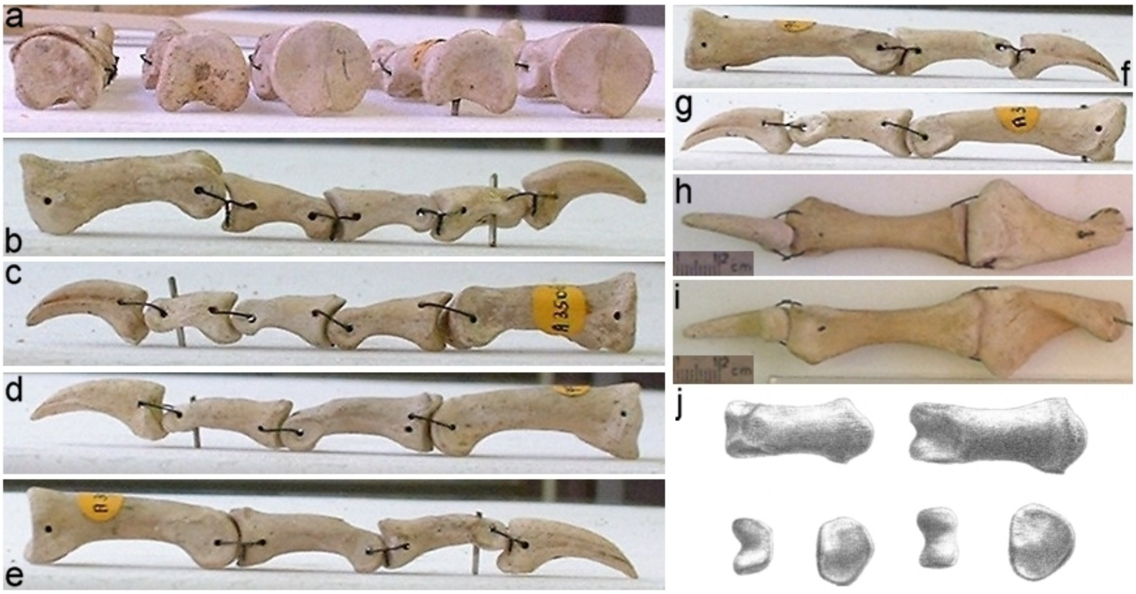

Pedal phalanges of *Pezophaps* (a-i: NHMUK A.3506). a: proximal view; b and c: digit IV; d and e: digit III; f and g: digit II; h and i: first metatarsal with hallux (right side); j: *left*: phalanx 3 of digit III, dorsal, distal and proximal views, *right*: phalanx 2 of digit III, dorsal, distal and proximal views (both right side, male; Newton & Newton 1869, pl.xx, figs.119-124; artist: George Henry Ford; "G. H. Ford ad nat. lith." "W. West imp.") All ○ Jolyon C. Parish, except Newton & Newton (1869) image.

The ungual of digit IV is slightly longer than the preceding phalanx of that digit. It is the smallest of all the ungual phalanges (Claessens *et al*. 2015); its distal extremity is is blunt and slightly laterally compressed. The sulcus vasculorum on the lateral surface is present as a well-developed groove, which almost becomes a canal distally; this groove is well-developed on the unguals of all pedal digits. The tuberculum flexorium (for the insertion of the tendon of m. flexor digitorum longus) is present, but not well developed. The articular cotyla has the form of a rounded equilateral triangle, and is slightly vertically concave (Melville 1848).

The pedal phalanges of *Pezophaps* are known from a number of skeletons (NHMUK A.3505, A.3506; UMZC 415.R, 415.S; RCSHM/Aves 706, 707, for example). Newton & Clark (1879) examined 28 ungual phalanges, stating that it is "almost if not quite impossible to determine their exact position on the foot" (p.444). One pedal phalanx in the UMZC 653 collection has well-developed lateral and medial longitudinal ridges on the ventral face.

Variation

Both *Raphus* and *Pezophaps* show much individual skeletal variation. In his letters to Alfred Newton, Etienne Thirioux suggested that there were two forms of dodo present. In the first form the beak was narrower at its base and in the second it was broader but was of the same length and shape. However, he concluded that attributing the variation to two species was excessive (see Transcriptions: Thirioux-Newton Correspondence). Thirioux also stated that there was variation (sexual or individual) in the cervical vertebrae and remarked that there were two forms of the pterygoid, two forms of notarium (Owen 1867, pl.xvii, figs.1-5) and two forms of the nineteenth (his eighteenth or prepelvic) vertebra, although these bones were damaged. However, without sufficient associated skeletal material it is not possible to ascertain whether there were two forms of dodo or whether these differences were randomly distributed within the population. Both *Raphus* and *Pezophaps* show significant intraspecific size variation (further information is to be found in Appendix 2). Heterochrony is also an important factor in the development of *Raphus* and especially *Pezophaps*, with males being peramorphic with respect to females: presumed males being larger than presumed females in both taxa, and, in the case of *Pezophaps*, showing greater development of exostoses.

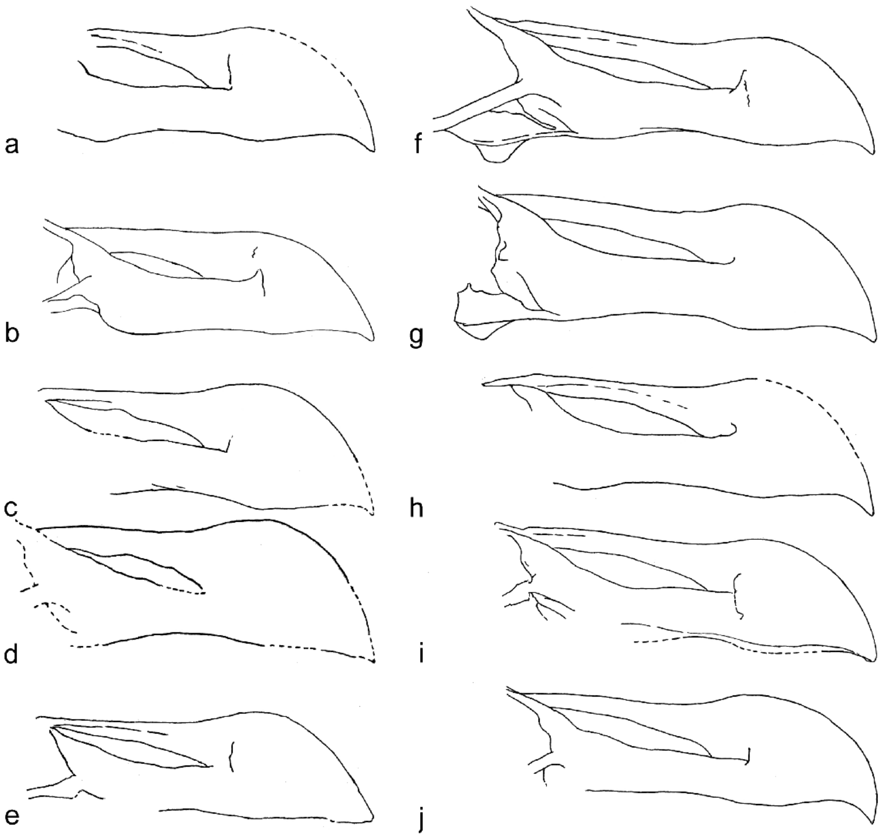

Variation in the shape of *Raphus* beaks: a) Thirioux-Newton Correspondence 10th October 1899 (Letter 2), b) Copenhagen skull (drawn from a cast), c) Thirioux-Newton Correspondence 5th September 1900 (Letter 9B), d) MNHN MAD 6530 (Janoo 1996, fig.2), e) Durban skeleton, f) OUMNH 11605 (Strickland & Melville 1848, pl.viii), g) NMP P6V-004389 (from a photograph by Jiří Moravec), h) Thirioux-Newton Correspondence 5th September 1900 (Letter 9B), i) Thirioux's Port Louis skeleton (from a photograph by Jan den Hengst), j) Owen (1867, pl.xv, fig.1, pl.xxiii, fig.1).

The large variation in size and morphology seen in *Raphus* might be due to intraspecific variation, sexual dimorphism, or perhaps even morphological radiation. Livezey (1992) noted that most skeletal dimensions are more variable (within sexes) in the flightless kakapo (*Strigops habroptilus*) than in its volant relative, the kea (*Nestor notabilis*), adding that "[h]igh mensural variability in the pectoral skeleton of *S. habroptilus* presumably reflects relaxation of stabilizing selection associated with lessened functional importance" (pp.129-130). Absence of predators and of the constraints related to flight probably contributed to decreased selection pressure (at least in these areas), allowing greater variation.

Variable characters in *Raphus* include:

- Variation in beak shape
- Pterygoid with and without peduncle of the pterygobasipterygoid articulation

- Closure, or not, of the carotid sulcus by a ventral lamina in the ninth cervical vertebra
- Variation in development of the hypapophyses and number of foramina of the notarium
- Morphology of the nineteenth (presynsacral) vertebra
- Presence or absence of a rib on the twenty-first (second synsacral) vertebra
- Number and allocation of the synsacral vertebrae
- Degree of ventral curvature of the synsacrum
- Morphology of the caudal vertebrae and pygostyle
- Variability in the fusion of the scapula, coracoid and clavicle
- Fusion, or not, of the clavicles to form a furcula
- Number of ribs attaching to the sternum
- Morphology of the costal facets of the sternum, being bilobed or unilobed
- Development of the deltopectoral process of the humerus
- Degree of curvature of the ulna
- Closure of the ilioneural canals of the pelvis
- Bridging over of the caudally of the channel between the peduncles of the trochleae for digits III and IV of the tarsometatarsus (canal for the tendon of m. extensor brevis digiti IV), or not

These are discussed in the main text.

Variation in bill shape appears to be reflected in the historical depictions of the dodo, with some individuals having a more gracile beak (exemplified by OUMNH 11605) and others a more robust beak (exemplified by MAD 6530) (ratio of distance from mid-eye to distal margin of beak : maximum height of maxillary rhamphotheca (excluding hook) <0.30 vs. ≥0.38; see Parish & Cheke 2018). The bill described by Janoo (1996; MNHN MAD 6530) is more robust than that of OUMNH 11605, has a proportionately wider fissura interpalatina and is proportionately wider at the craniofacial hinge.

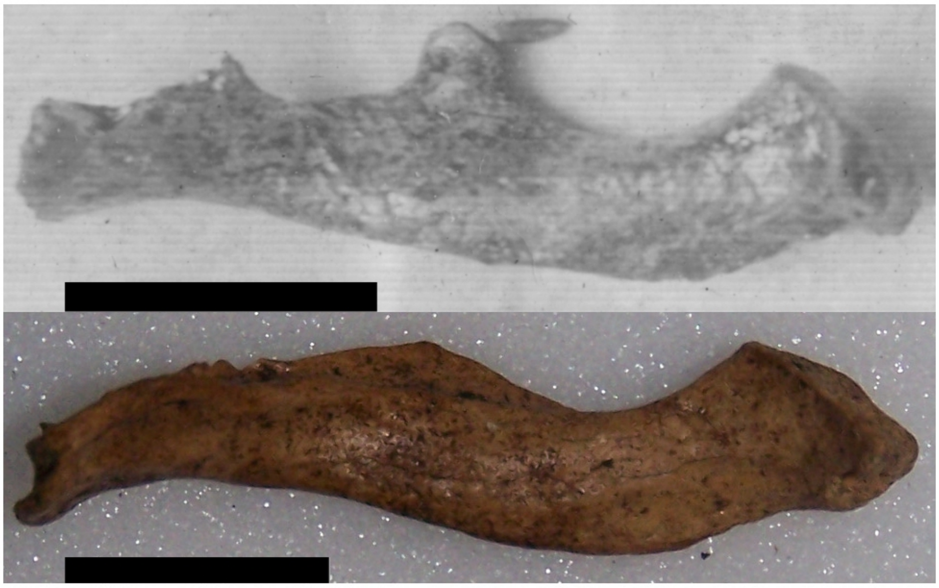

Variation in pterygoid form in *Raphus*. *Top*: a specimen showing a large peduncle of the pterygobasipterygoid articulation (photograph (13A) accompanying a letter from E. Thirioux to Alfred Newton, dated 31st January 1901; © UMZC; image reversed); *bottom*: a specimen without such a developed feature (UMZC 415.KK specimen; ○ Jolyon C. Parish, December 2008). Scale = 1cm.

Etienne Thirioux recognized two forms of pterygoid in *Raphus*, which which he illustrated in photographs sent to Alfred Newton.[179] One of his specimens shows a well-developed peduncle of the pterygobasipterygoid articulation, more prominent than in many other columbids. This specimen is of approximately adult size (determined from the annotation on the photograph: "Os du Dronte. Grandeur ⅔") and the development of the process suggests that it may have contacted the basipterygoid process of the basicranium in life. In another of Thirioux's specimens (UMZC 415.KK) there is only a slight ventromedial projection approximately midway along the pterygoid, a little nearer the quadrate end, which probably represents a remnant of the peduncle of the pterygobasipterygoid articulation.

---

[179] UMZC Thirioux-Newton Correspondence. Photograph accompanying a letter to Alfred Newton, dated 5th October 1900: “Os du Dronte. Grandeur ⅔. [...] 1 pterygoide (nouvelle forme?). [1 pterygoid (new form?)]”

Functional basipterygoid articulations are present in the majority of columbids; however, they are absent in *Ectopistes*, *Patagioenas araucana*, *P. cayennensis*, *P. flavirostris*, *P. picazuro* and *P. subvinacea* (Verheyen 1957).[180] Verheyen also reported that the basipterygoid articulation was frequently lacking in *Goura cristata*: of four specimens examined one had a functional articulation, one lacked an articulation and two had a functional articulation on one side only. He also noted that a similar situation occurred in *Patagioenas maculosa*. Zusi (1993) stated that "[t]he basipterygoid process of ratites, tinamous, and various neognathous birds develops early as a cartilaginous projection of the basisphenoid, enclosed later by the parasphenoid; it articulates with the posterior portion of the pterygoid" (p.402).[181] Zusi added that, in many taxa, the basipterygoid process of the basisphenoid is present in the embryo, but later disappears. Bock (1964) remarked: "The only functions suggested for this structure are ones limiting the amount of movement of the pterygoid and hence the degree of kinetic movement. Almost certainly, the basipterygoid process in birds has lost its functional importance for kinesis and has either acquired other functions in which case it was retained, or has degenerated to a vestigial structure or has been completely lost. However, so little is known about the function of the basipterygoid process that any statements about its evolution would be highly speculative" (pp.6-7). The reduction and disappearance of this basisphenoid-pterygoid articulation allows an increase in the range of movements of the pterygoid (Simonetta 1960). This may facilitate the manipulation and ingestion of large food objects, as was probably the case in *Raphus* and *Pezophaps*.

In addition to that seen in *Raphus* and *Pezophaps*, variation in vertebral number and type is present in other birds (Hiraga *et al.* 2014; Berger 1952, 1956), including columbids (pers. obs.). Berger (1952) stated that in Cuculidae: "[t]here appears to be no significant correlation between the number of fused vertebrae in the synsacrum and the number of free caudal vertebrae" (p.519). Verheyen (1957) recorded variation in the number of cervical, thoracic, notarial, synsacral and caudal vertebrae in a range of pigeon species. He also provided osteometric data, showing variation in bone measurements amongst columbids. Variation in vertebral number and type in birds may be unrelated to genetic diversity in a population (Hiraga *et al.* 2014). Extant pigeons, and other birds, also show variation in the number and form of ribs (pers. obs.).

A notarium in the collections of the Musée d'Elbeuf-sur-Seine described by Buffetaut (2016) shows incomplete fusion of the centra of the cranial two notarial vertebrae (see section on juveniles). Buffetaut ascribed the difference to individual variation. Buffetaut (2016) remarked "[i]t is likely that the notarium of *Raphus cucullatus* is simply a legacy of flying ancestors. The observed variability, which means that in some individuals the fusion of the vertebrae was incomplete (and therefore the rigidity of the notarium less) may have been favoured by less selection pressure on this structure in a non-flying bird" (p.23).

Likewise, in describing *Pezophaps*, Newton & Newton (1869) remarked:

> It is not a very difficult task to describe in great detail a single skeleton, but it is not easy to draw up a description which, while being minute and diagnostic, shall yet fit some

---

(explanation on the reverse with translation by Newton). Photograph accompanying a letter to Alfred Newton, dated 31st January 1901: "[numbers] 2 et 3. Ptérygoïdes 2 var: Dronte". Thirioux also restated his view of two forms of pterygoid in letters to Newton dated 22nd November 1900 ("Vous avez pa voir qu'il y a 2 formes du pterygoïd") and 13th November 1901 ("1 paire Pterigoïdes 2 formes differente").

[180] *Ectopistes* and *Patagioenas* are sister-taxa (Bruxaux 2018).

[181] For a discussion of the development of the basipterygoid process in birds see Zaher & Abu-Taira (2016).

> fifty or more examples. There does not seem to be a single bone in the skeleton of *Pezophaps solitaria* which is not liable to greater or less individual variation of some kind or other [...] the individual variation is not at all confined to absolute size; it extends to the relative proportion of divers parts of the bone, to processes or depressions upon them such as are commonly held to be specifically characteristic, so that it is often utterly impossible to predicate any definite limits of individual modification (p.330).
>
> We have certainly never made a close study of such an extensive series of the bones of any one other species as we have done of the Solitaire, and therefore we are perhaps not in a position to form a true comparison; but it does seem to us that the amount of individual variation both here and in the Dodo is extraordinarily great (p.331).

Newton & Clark (1879) considered “some portion of the wonderful variability observable in the remains of *Pezophaps solitaria*” to be due to specimens being from different time periods, considering some perhaps to be the remains of individuals which “lived at a very remote as well as at a very recent period” (p.451). However, this is unproven, and, moreover, the dodo – of which specimens are known from a single locality (Mare aux Songes) and from a narrow time period (Rijsdijk *et al*. 2009) – also shows morphological variability.

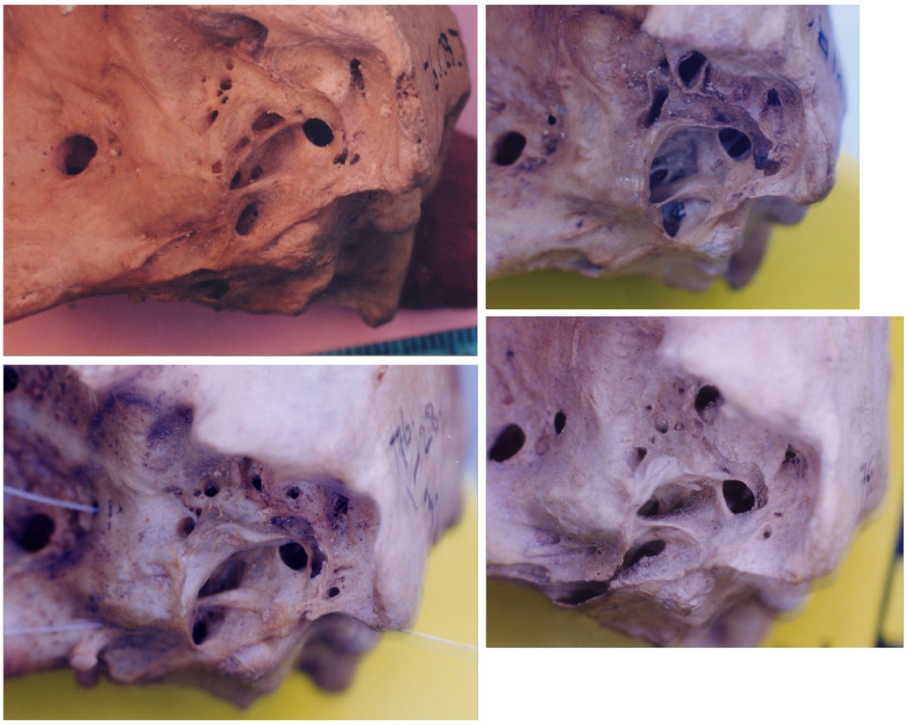

Variation in the auditory region of *Pezophaps*. *Top left*: NHMUK A.1441; *top right*: NHMUK A.1375 (reversed); *bottom left*: NHMUK A.1373; *bottom right*: NHMUK 76.1.28.9. All ○ Jolyon C. Parish.

However, *Pezophaps* appears to have been more conservative in its morphology than *Raphus*. Nevertheless, as stated above, there is still individual variation to be seen. Variable characters in *Pezophaps* include:

- Variation in the morphology of the auditory region of the cranium, including in the number and form of foramina
- Variable development of the basipterygoid processes of the cranium
- Variable fusion of lacrimals to the rest of the cranium
- Presence or absence of a free rib on the thirteenth vertebra
- Number and arrangement of the synsacral vertebrae

- Variability in the form of the distal end of the scapula and shape of the tuberculum scapulae
- Variability in coracoid morphology, particularly in the form of the procoracoid process

Given that the invasion of skeletal elements by the pneumatic system generally occurs relatively late in ontogenetic development, when the individual is almost fully grown (Britt 1997), the paucity of pneumatic foramina in *Pezophaps* in comparison with *Raphus* (and indeed other raphines) is interesting. All juvenile birds have solid, non-pneumatic, bones (Headley 1895), although in some cases pneumatic fossae may be present in juveniles, but disappear in adults (Worthy *et al*. 2016).

Raphus, and to a lesser extant *Pezophaps*, shows variable fusion of skeletal elements. For example, the lacrimal, the frontal processes of the premaxillae, the vertebrae forming the synsacrum, the hypapophyses of the notarium, vertebral ribs, and the elements of the pectoral girdle (scapula, clavicle and coracoid). There is also variable closure of apertures (as in the ilioneural canals) or bridging of tendinal canals (as in the canal for the tendon of m. extensor brevis digiti IV on the distal tarsometatarsus). Such variation may be due to variable timing in the cessation of ontogenetic osteological development (what might be termed late-stage variable ossification), diminished selection pressures due to lack of predators, or factors related to island living (geographical limitations) or the gene pool. A delay in the termination of osteological development may have been responsible for the fusion of the pectoral girdle elements – an early termination might have led to certain elements remaining unfused (lacrimals, for example). However, little is known regarding the ontogeny of the dodo and solitaire.

Berger (1956) stated that “[v]ariation is found in all species of birds; it should be expected” (p.437). Further work needs to be done to assess the amount of osteological variation in columbids, and in birds in general.

Sexual Dimorphism

(see Parish 2013, p.284)

George Clark (1866) thought that the bones from Mare aux Songes could be divided into two distinct groups: “By far the greatest portion of these bones might be divided into two dimensions perceptibly differing, though not very unequal in size, leading to the belief that the diversity in their respective sizes arose from the difference of sex” (p.144). In a letter to Alfred Newton, Thirioux stated that he had found two individuals, without doubt a male and a female (see Transcriptions: Thirioux-Newton Correspondence), suggesting that the two differed in some way, such as size. This is corroborated by the variation in size in the bones examined in the present work (see Appendix 2) and previous works (*e.g.*, Livezey 1993, Van Heteren *et al*. 2014, Angst *et al*. 2017), although more data and more complete statistical analyses are required to ascertain the extent of this variation and whether there are two distinct size groupings.

Livezey (1993) used a K-means statistical method to identify two size groupings in the measurements of dodo bones, which he attributed to males (larger size) and females (smaller size). However, Angst *et al*. (2017) noted that he did not confirm the validity of the clusters and as such his results are not valid.

Van Heteren *et al*. (2014) examined over 750 bones, comprising femora, tibiotarsi and tarsometatarsi obtained from the Dodo Research Project (DRP) excavations and from historical material.[182] Two distinct size groupings were found, one on average 5% larger than the other, which were interpreted as male and female (the male specimens being the larger). However, Angst *et al*. (2017) found that the femoral and tibiotarsal shaft circumferences of the two female specimens (identified by the presence of medullary bone) they examined were "similar to other adult bones in the sample" (p.5).

---

[182] “Kolmogorov-Smirnov Z-tests and Wald-Wolfowitz runs tests were used to examine potential differences between historically collected remains and bones collected by the DRP. Bones from the recent DRP excavations were statistically indistinguishable from the historically collected bones, enabling us to combine these data in further analyses. We performed two-step cluster analyses to search for naturally occurring size fractions in the data, using a log-likelihood distance measure and Schwarz’s Bayesian information criterion. Mann-Whitney-Wilcoxon tests were performed to determine the significance of the obtained fractions” (Van Heteren *et al.* 2014, p.245).

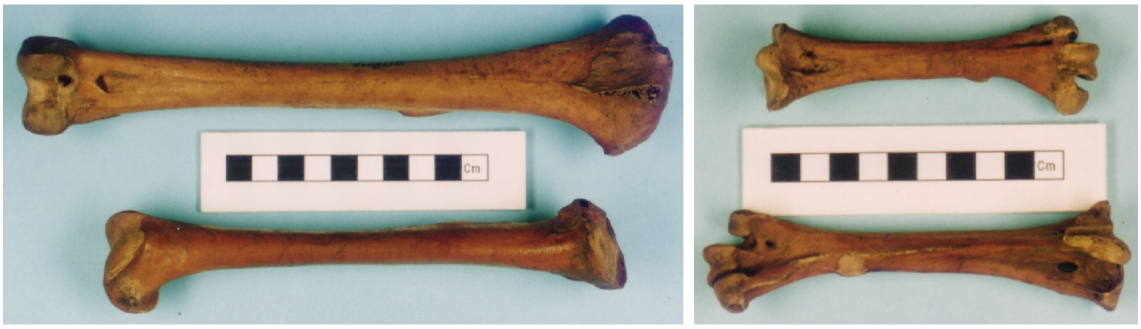

Sexual dimorphism in *Raphus*: longest and shortest bones selected by Andrew Kitchener, 1990, from UMZC 415.K specimens. *Left*: tibiotarsi, *right*: tarsometatarsi. © E. C. Parish.

In some birds the caudal opening of the pelvis is proportionately wider in females than in males. To examine this for the solitaire, Ottow (1952) used the ratio between the following dimensions: length (the distance from the craniodorsal margin of the first synsacral vertebra to the ventral angle between the fused synsacral centra and the costal process of the first sacral synsacral vertebra) to width (the distance from the midline perpendicularly to a point 2.5cm caudal to the cranial margin of the foramen ilioischiadicum along the lateral margin of the ischium).[183] This yielded the following results: one ♂: 9.0cm / 6.1cm and four ♀: 7.0cm / 5.2cm, 7.1cm / 5.3cm, 7.5cm / 5.7cm and 7.3cm / 5.5cm, giving the ratios ♂ 1.48 and ♀ 1.34, 1.33, 1.32 and 1.33. This provided further circumstantial evidence that the smaller series of pelves are female.

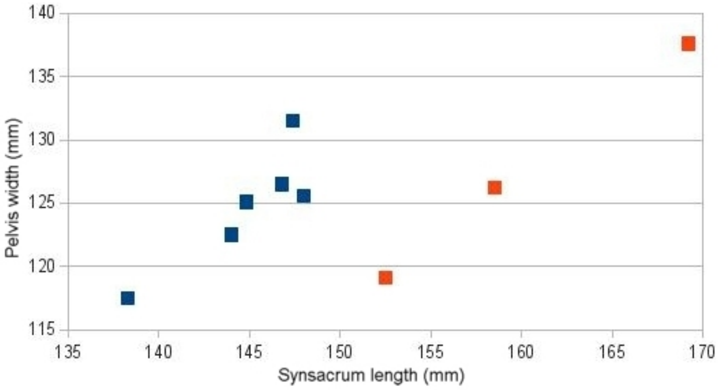

Sexual dimorphism in *Raphus*: plot of pelvis width against synsacrum length. Blue: presumed females, red: presumed males (data from UMZC 415.K specimens).

In *Raphus* a similar dimorphism in pelvic shape can be seen. The ratio of pelvis width to synsacrum length[184] is 0.85-0.89 in presumed females and 0.78-0.81 in presumed males (n = 9; UMZC 415.K specimens; see Appendix 2 for data). The presumed female pelves are also smaller (synsacrum length less than 152.5mm). However, more data is needed to test the validity of these groupings.

Using the above, the Durban skeleton would appear to be from a male (pelvic ratio, tarsometatarsus length), whereas Thirioux's Port Louis skeleton might be from a female (tarsometatarsus length and possibly synsacrum length and pelvic ratio).[185] However, more data is needed to ascertain whether there is meaningful signal as regards sexual dimorphism in bone dimensions, and if so in which elements.

---

[183] "die Entfernung vom oberen Rande des ersten synsakro-thorakalen Wirbels bis zum unteren Winkel zwischen der Beckenwirbelsäule und der hier einzigen synsakro-sakralen Wirbelparapophyse"; "die Entfernung von der Mediane der synsakralen Wirbelsäule zu einem Punkt der 2,5 cm kaudalwärts von dem kranialen Ende des Foramen ovale am lateralen Rande des Ischium" (pp.195-196).

[184] Pelvis width: measured between the lateral margins of the antitrochanters; synsacrum length: measured along the midline.

Size-related sexual dimorphism is greater in *Pezophaps* than in *Raphus*, and in the former it is amongst the greatest in any known neognath. Livezey (1993) found that the mean intersexual differences for twelve main dimensions of limbs and associated girdles for *Raphus* was around 9mm, whereas that for *Pezophaps* was around 22mm. The large degree of sexual dimorphism in *Pezophaps* was observed by Newton & Newton (1869), although some authors (Strickland 1853, Owen 1871b) considered the difference in size to be too great to be sexual, and placed the two size groups into two separate species. *Pezophaps solitaria* was retained for the larger specimens and *P. minor* was erected for the smaller ones. However, only one species is recognized today (*P. solitaria*), with the size differences being due to sexual dimorphism.

Size variation for both *Raphus* and *Pezophaps* is illustrated in Appendix 2, which gives data for the known largest and smallest bone elements.

Specimens of Juveniles

(*Raphus*: Hume 2006, fig.21)

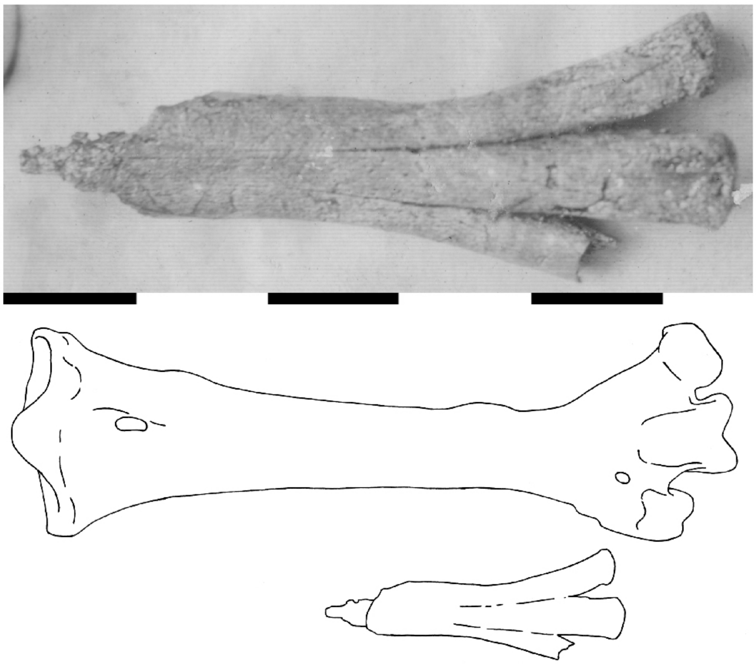

Tarsomentarsus of a juvenile *Raphus* (photograph (13A) accompanying a letter from E. Thirioux to Alfred Newton, dated 31st January 1901; scale in cm (Thirioux stated that the images were very close to natural size); © UMZC). The outline images illustrate difference in size between the juvenile and an adult (adult tarsometarsus traced from Strickland & Melville 1848, pl.xi, fig.1).

Juvenile remains for *Raphus* are very rare. In the Thirioux collection there was a fragmentary tarsometatarsus showing the boundaries between the metatarsals. Gadow remarked that the age of the bird was "not embryonic. Several months old would do very well." Hume (2013) reported a fragment from a juvenile from a cave at La Prairie. The unfused lacrimals present in Thirioux's Port Louis skeleton might be from an immature bird, or they might represent individual variation (cf. unfused lacrimals in *Pezophaps*). Two juvenile 'tarsi' were mentioned by George Clark – these were "unmistakeable, and their bulk was less than one-fourth of that of the adult" (Clark 1866, p.144).

---

[185] Livezey's (1993) data: tarsometatarsus lengths: 'males' 131.6 ± 2.6 (n=72), 'females' 125.1 ± 2.2 (n=65). Durban skeleton tarsometatarsi 133-134mm; Thirioux's Port Louis skeleton tarsometatarsi 123mm (Claessens *et al.* 2015). However, see comment by Angst *et al.* (2017), noted above.

However, these might have been from another pigeon species, given their small size (*mihi*; Anthony Cheke, pers. comm., 10th December 2009).

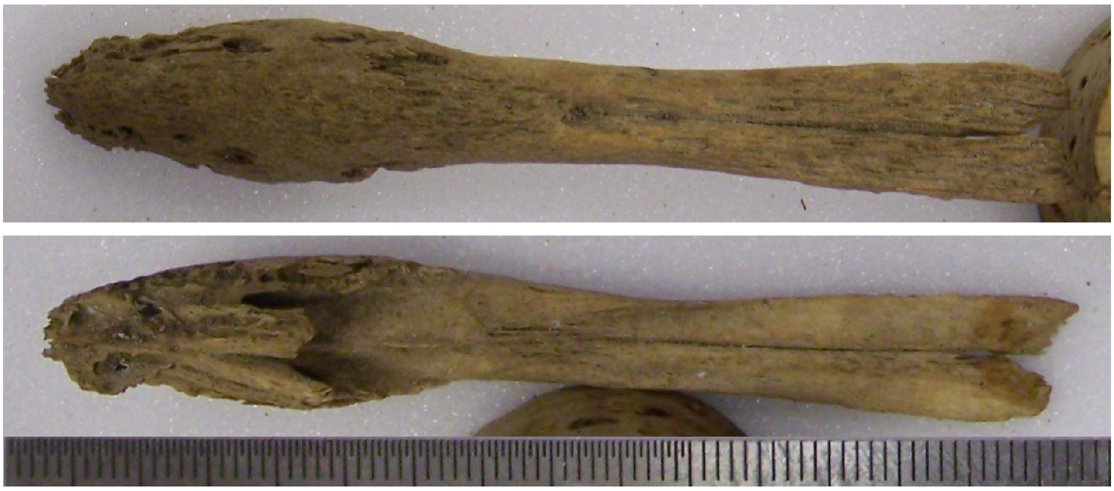

Beak of *Pezophaps*, presumed to be from a juvenile, dorsal and ventral views (UMZC specimen; scale in mm; ○ Jolyon C. Parish, December 2008).

Buffetaut (2016) mentioned a notarium in the collections of the Musée d'Elbeuf-sur-Seine which shows incomplete fusion of the centra between the sixteenth (first notarial) and seventeenth (second notarial) vertebrae. In contrast, the zygapophyses and neural spines are completely fused. However, Buffetaut considered the differences between this specimen and others (such as those figured by Owen 1867) to be due to individual variation (as opposed to being from a juvenile or sub-adult), since it is of near identical size to those described by Owen.

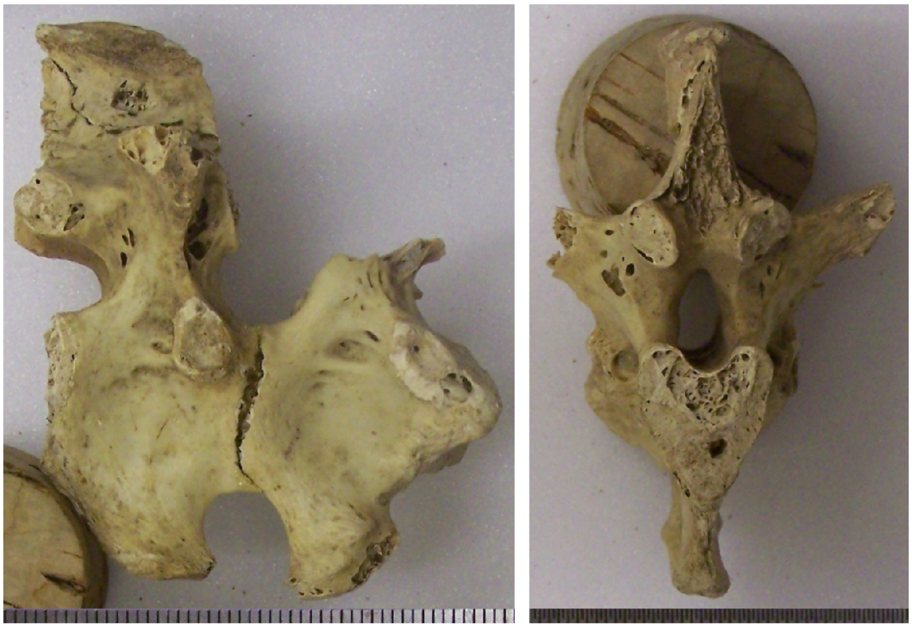

Notarium of *Pezophaps* showing suture between the fifteenth and sixteenth vertebrae (UMZC specimen; scale in mm; ○ Jolyon C. Parish, December 2008). *Left*: lateral view, *right*: caudal view, showing articular faces of sixteenth vertebra.

Angst *et al*. (2017) identified a tibiotarsus (MAS2 - P14965) as coming from a juvenile.[186] This specimen was described as having "a cortex largely comprising of fibrolamellar bone tissue consisting of woven bone with many primary osteons, which suggests a rapid rate of bone deposition. Remnants of the periosteum along the outer surface are preserved and an inner circumferential layer (ICL), without resorption traces, is well developed" (pp.1-2). These features indicate that the individual had undergone a period of rapid growth (rapid deposition of bone during early ontogeny being typical of living birds), but had not reached 'adulthood' and was thus at a late juvenile stage (*ibid*.). However, the well-developed ICL suggested to Angst *et al*. that medullary expansion was complete in this individual.

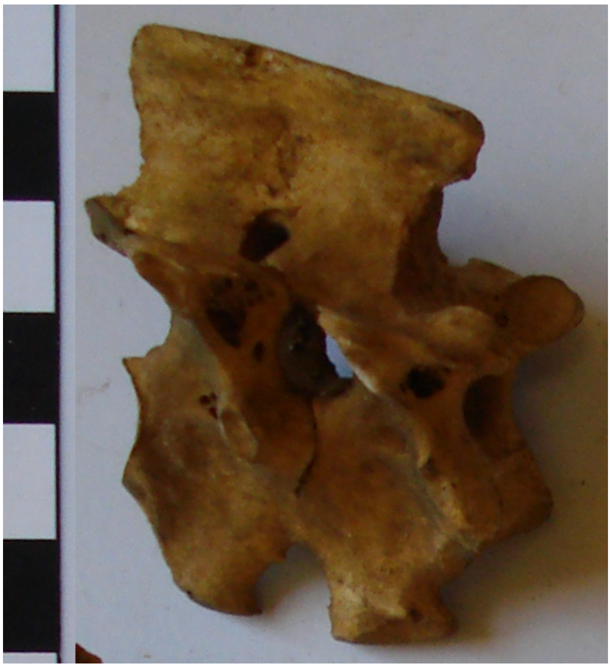

Notarium of *Pezophaps* showing suture between the fifteenth and sixteenth vertebrae (Natural History Museum, Dublin, specimen; scale in cm; © David Gonzalez).

Claessens *et al*. (2015) remarked that there was a possibility that unfused clavicles in *Raphus* and *Pezophaps* may have belonged to young individuals, although these elements do not show evidence of juvenile bone grain (pers. obs.).[187]

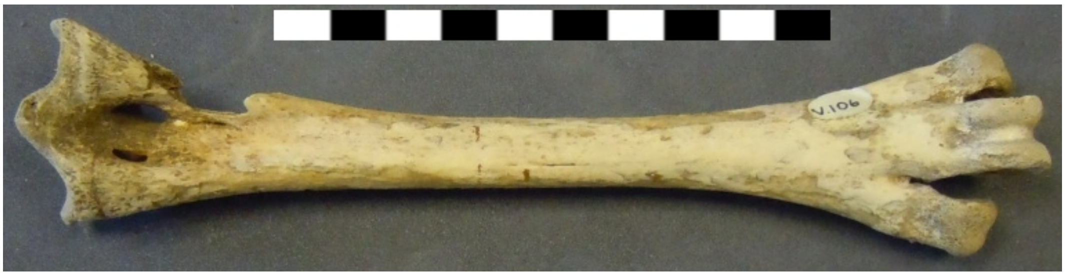

Tarsometatarsus of *Pezophaps* (right side), possibly from a juvenile or subadult (GLAHM V106; scale in cm; © The Hunterian, University of Glasgow).

Juvenile material for *Pezophaps* is likewise rare. Hume (2013) stated that there were no remains of juveniles found. However, there is a premaxilla belonging to a possible subadult bird in the UMZC collections (UMZC 653), which appears to exhibit juvenile bone grain. A notarium also in the UMZC collection (UMZC 652) shows possible evidence of sutures between the vertebrae. This specimen consists of a partial notarium (the fifteenth and sixteenth vertebrae), in which the sutures have partly fused, but fracture has occurred at this weakness and the seventeenth vertebra is broken off completely and is missing. Another notarium of *Pezophaps*, NHMUK A.1435, also shows divisions between the vertebrae. Similarly, a synsacrum belonging to *Pezophaps*, NHMUK A.1437 (76.1.28.22), shows sutures between the sixteenth and seventeenth and seventeenth and eighteenth synsacral vertebrae. In another notarium (Newton & Newton 1869, pl.xvi, fig.60), the junctions between the vertebrae can be seen, as the centra of the notarial vertebrae are not fully fused together. The ankylosis appears to have started at the zygapophyses and neural spine "chiefly between the first and second vertebrae [of the notarium, *i.e.*, the fifteenth and sixteenth], and co-ossification of the centrums is more advanced than between the first and second than between the second and third of these vertebrae" (Owen 1871b, p.514). These instances of incomplete fusion may represent juvenile or subadult individuals (histological evidence is needed to shed further light on this), or they may be examples of individual variation (see above).

---

[186] Angst *et al*. (2017, fig.1a,b). This bone falls within the size range (shaft circumference, largest diameter, smallest diameter, cortex thickness) of the other tibiotarsi studied by Angst *et al*.

[187] See Tumarkin-Deratzian *et al*. (2006) and Watanabe & Matsuoka (2013) for examples of juvenile bone grain.

Melville (1848) described the proximal end of a right *Pezophaps* tarsometatarsus in the Andersonian Museum collections (*ibid*., pl.xv, fig.4) as juvenile. However, this is probably from an adult female. As noted by Pieper (1987), the supposed juvenile humerus figured by Lüttschwager (1961, fig.20) is not from *Pezophaps* but from *Phaethon lepturus*.

Cantilever strengths of hindlimb bones

See Parish (2013, pp.297-298).

Pathologies

See the main text (above) for additional discussion of the exostoses of the carpometacarpus and skull.

Osteopathologies are known for both the solitaire and the dodo.[188] However, it should be noted that there is a potential for bias in the prevalence of specimens of *Raphus* and *Pezophaps* bearing pathologies: individuals whose health had been impaired by injury or disease would have been more likely to become mired in a swamp (such as Mare aux Songes) or fall into a cave and thus be preserved.

History of Research

Newton & Newton (1869) and Newton & Clark (1879) considered the bone abnormalities of *Pezophaps* to be due to healed fractures. However, at the time there was little knowledge of pathological bone disorders and as such the bone abnormalities were considered to be the result of healed mechanical injuries. Slater (1881) thought that solitaires, "fighting with the wings, used by the force of their blows to raise a little callus or knob of diseased bone which in time became hereditary and increased to the size you see. The females had on their wings a small knob also, but it never presented the spongy, diseased appearance you see here, from which it is probable that Leguat was not quite correct in describing the females as fighting among themselves" (p.26). The palaeobiologist Othenio Abel (1912, 1935) examined *Pezophaps* material at Cambridge (UMZC) in February 1911, under the guidance of Hans Gadow, and also regarded the pathologies to be the result of mechanical-traumatic injuries from intraspecific combats (Handlirsch & Pietschmann 1912). He found "numerous severe but rehealed fractures" on the exostotic wing bones of the males, as well as on the hindlimb bones (Abel 1912, p.91). He thought that: "Exostoses are probably in most cases due to traumatic inflammations of the bone-skin [*Knochenhaut*; probably the periosteum]" (*ibid.*) and attributed the healed breaks to the use of the wings as boxing weapons and injuries sustained from conspecifics by kicking with the feet during combats during the breeding season.[189] Abel noted that of the specimens the UMZC collections, the wing bones of the males displayed exostoses and the leg bones showed severe but subsequently healed breaks. In this collection he found many bones with what he regarded as healed break injuries: two coracoids, one humerus, four radii, thirteen ulnae, one fibula and two tarsometatarsi. These breaks, he remarked, were very severe and showed, in for example the humerus, “characteristic features of a fracture scar” (*ibid*., pp.587-588). As the manus and lower arm bones of what he regarded as juvenile males (which would not have been old enough to engage in combats for females) displayed exostoses, he also considered the pathologies to be hereditary, and thus the result of the transmission of acquired characteristics[190] – a hypothesis now known to be incorrect, although some epigenetic effects might have occurred. Abel concluded that the presence of pathologies in alleged juvenile bones was an “unresolved problem”. In contrast, Hume & Steel (2013; see below) stated that the carpal knob developed after skeletal maturity was attained.

---

[188] Ottow (1952) had previously speculated as to whether the dodo, in addition to the solitaire, might also show osteopathologies, but could find no evidence in the specimens available to him (the Kiel material and Stockholm skeleton).

[189] "These injuries are undoubtedly due to mating battles [*Paarungskämpfe*], and they must have been caused by boxing with the wings and kicking with the feet" (Abel 1912, p.588). Lambrecht (1915-1916) added that such could also be observed in *Calidris pugnax* (*Pavoncella pugnax*).

Lambrecht (1933) stated that “exostoses were acquired during mating fights and from severe injuries of the males fighting for the female” (p.602). Benno Richard Ottow (1950) questioned how pathologies could occur through physical-traumatic means (exogenous effects) in bones shielded by others and those covered by thick muscle, and in deep areas, such as the synsacrum. He added that the pathologies also occurred in females as well as males. He responded: “The fact, however, that the large, ponderous and flightless giant pigeons should have ‘fought’ with each other in the mating time by striking with the rudimentary wings and stepping and trampling with the legs so that the extremity bones thereby broke is more than improbable, it is impossible” (1950, p.19); “Todays comparative bone pathology, as well as biological considerations, suggest the aetiological-traumatic interpretation of the exostoses in the skeleton of Pezophaps is more than improbable, indeed it seems impossible” (1952, p.194). Ottow (1952) also noted that similar genetic disorders occur in humans.

From both macroscopical and radiological study Ottow (1950) concluded that *Pezophaps* displayed a genetic disease of the mesenchyme tissues, resulting in exostoses and osteodysplasias[191] (disruption to bone formation), the latter on occasion leading to bone fractures. He (1950, 1951, 1952) termed this genetic condition “osteogenesis dysplastico-exostotica”. He considered that these genetic disorders could have been dispersed throughout the population by geographical isolation, inbreeding and lack of selection. Furthermore, he stated that combats would not produce exostoses. Amadon (1951, p.417) added that the confirmation of the idea that “a harmful genetical condition has become widely established in a small population through random gene fluctuations of the type postulated by the ‘Sewall Wright effect’” could not be definitively determined, and that the specimens sent to Ottow had been specially selected (see Catalogue of Specimens). However, he postulated that the population of *Pezophaps* appeared to be small enough “for deleterious genes to have become established during the tens or hundreds of thousands of years” needed for the evolution of the genus (*ibid*.).[192] Osteopathologies of *Pezophaps* are not present in all individuals, despite the apparent inbreeding and geographical isolation, suggesting to Ottow (1952) that the “gene or chromosome mutation presumably had only a recessive value” (p.199). Ottow (1950) remarked: “the causative gene mutation must have occurred in Pezophaps only after the geological time period in which the fragmentation of a hypothetical closed land territory, to which the Mascarenes may have once belonged, resulted in single island remnants" (p.200) – the idea that the Mascarenes were formerly part of one landmass is now know to be incorrect, although the islands were larger during the last glacial period.

---

[190] “The circumstance is particularly remarkable, that exostoses appear in all the male wing bones in the carpal region [*Handwurzelregion*] and predominantly on the proximal end of the second metatarsal [*sic*] and already in quite young animals. The position, form, and size of these exostoses vary very considerably, but it is clear that these peculiar bone changes are not caused by injuries, but occur on the uninjured bone” (Abel 1912, p.588).

“There are few instances which equally clearly show the direct reaction of the organism to stimuli, and the heredity of acquired traits. Because the development of the exostoses on the bones of the digits and the bones of the forearm is to be seen as a consequence of the boxing bouts of the males; and these exostoses appear again in the male nestlings, which are not yet fighting. Pezophaps solitarius was extinct before the position, form, and size of these exostoses were hereditarily fixed; Choneziphius planirostris [a fossil whale] of the Upper Miocene and Lower Pliocene of Europe and North America, on the other hand, shows us that the pachyostotic and exostotic formation of the snout bone has already occurred as an inherited trait” (*ibid*.).

[191] Herein ‘dysplasie’ is translated as ‘dysplasia’ and ‘dysplasien’ as ‘dysplasias’.

[192] See Parish (2013, p.299) for a discussion of population. Amadon (1951, p.417) stated that it is “hardly likely that the total population of this goose-sized, terrestrial bird exceeded 500 or 1000 pairs and it may have been much less”.

Ottow stated that most of the pathological anomalies seen in *Pezophaps* were due to dysplastic and exostotic alterations of the bone (he did, however, find one specimen of the coracoid which apparently displayed a healed fracture – see below). He also discarded rickets (rachitis, osteomalacia) as the cause of pathologies in *Pezophaps*. However, Hume & Steel (2013), returning to the ideas of Abel and others, suggested an origin for the exostoses in the effects of impacts in combats. Likewise, they considered Ottow's dysplasias to be healed fractures, as opposed to a genetic disorder, and even stated that the numerous specimens exhibiting "healed fractures are testament to the potency of [the carpal] weapon" (p.11). They remarked: "Ottow [1950, 1951, 1952] was incorrect in his interpretation of the carpal knob and other exostoses as a manifestation of a genetic mutation, because such diseases typically do not produce lesions in such a specific region of the skeleton, but cause them to appear in any actively growing bony tissue" (p.9). This will be further discussed below. According to Ottow (1950, 1951), males display more pronounced exostoses on the carpometacarpi and radii and less presumed dysplastic changes, and the females display smaller carpometacarpal exostoses but a greater development of presumed dysplasias of the ulna. This led Ottow to speculate that not only were the pathologies hereditary, but they were also sex-linked to some degree. He also noted that exostoses and presumed dysplasias can occur on the same bone. The former can spread over large areas of small elements (such as the carpometacarpus), whereas the latter are located more in the diaphyseal regions (Ottow 1950).

Lüttschwager (1961) thought that as the wings of *Pezophaps* were not used for flight they would have been less nourished and therefore weaker and more easily damaged in fights. However, further study needs to be undertaken in order to more accurately assess the relative strengths of pectoral elements. Lüttschwager also thought it probable that even juvenile birds fought each other, "play fighting" before their bones had fully strengthened and thus causing broken bones. However, there is little evidence for the presence of juvenile solitaire bones in museum collections, let alone ones with healed breaks.

Hume & Steel (2013) considered the extensor process to possess metaplastic osseous tissue from whence a spur or exostosis has the potential to develop. They posited two mechanisms for the growth of carpal exostoses: in the first, the carpal knob developed due to the effects of combats, to protect the carpus. This would have produced a structure which was more effective in combats and thus was selected for by natural selection. In the second, the carpal knob developed "under the influence of hormones or other signals, when the individual pairs up with a mate and acquires a territory" (p.10). They added that: "A mature male that had successfully held a territory for many years would exhibit pronounced development of a carpal knob and callus growth on the radius and phalanges [...] A female paired with one of these males might also exhibit development of a carpal knob" (p.10). However, Hume & Steel (2013) did not compare the exostoses of *Pezophaps* with neoplastic disorders in order to rule these out as an origin and did not elaborate on the proposed development of exostoses under hormonal (or other) influences.

Discussion

The exostoses of the wing of *Pezophaps* are so common that they were classed as a generic character by Newton & Newton (1869). Exostoses[193] are primarily found on the carpometacarpus and distal radius in male *Pezophaps*. Not all male solitaire carpometacarpi have an exostosis (or exostotic growth), but the greater majority do. As Ottow (1950) pointed out, the exostoses of the carpometacarpi and radii of the males occur symmetrically and are similar in size and form between left and right sides. Some female *Pezophaps* carpometacarpi may also show an exostosis, but these are rarer and are significantly smaller than those of the male, which, in the larger specimens, can have a height approximately equalling half the length of the carpometacarpus. The exostoses of the females (*e.g.*, UMZC 635) generally resemble those of *Goura* (see below), although some specimens (*e.g.*, NHMUK PVA9045) have a morphology similar to those of the males, although smaller. Other bones, such as the ulna, coracoid and leg bones may also present exostoses and what Ottow considered to be dysplastic bone changes. Some bones show healed fractures, or at least structures that resemble such (see, for example, Wood 1941).[194] Bones of *Raphus* have been found that show also healed fractures (Parker 2007).

---

[193] An exostosis is an "abnormal surface projection from bone. Varieties include ossification of muscle attachments, chondromas, osteochondromas, and osteomas" (Sawyer & Erickson 1998, p.33).

That pathologies are found in places such as the synsacrum indicates that they cannot all be purely the result of mechanical-traumatic injuries. Some of the exostoses are formed from the cortical bone[195] and can be compact and without a recognizable medullary cavity (Ottow 1950). The surface texture ranges from relatively smooth to very rugose, the latter possibly indicating a cartilaginous covering in life, at least as regards the carpometacarpal exostoses. In the region of Ottow's presumed dysplasias the cortical bone is irregular, and is thinned or thickened and the os spongiosum (cancellous or trabecular bone) is also affected.

Many bones of *Pezophaps* apparently show evidence of having been broken and healed during life. According to Armstrong (1953), these breaks were undoubtedly due to intraspecific combats. Similar healed fractures of wing bones are also known for the flightless ibis *Xenicibis*, which also possessed modified carpometacarpi likely used in intraspecific combat (Longrich & Olson 2011), and for steamer-ducks (*Tachyeres* spp.; Livezey & Humphrey 1985).[196] However, it is also possible that bones weakened by genetic or nutritional factors might be easily broken under other circumstances. Ottow (1950) noted that dysplastic bones can break and subsequently heal, forming a callus scar, but added that distinguishing a healed break from a strong osteodysplasia can be difficult, even with radiological imaging. The bones most commonly exhibiting healed fractures are the coracoid, radius and ulna (Newton & Newton 1869).[197]

Natural selection can become altered due to the absence of predators, and limitations in population size and habitat area can lead to inbreeding. As a result, genetic diseases can become prevalent in the population. Due to the absence of predators, animals exhibiting genetic diseases may be less frequently removed from the breeding population and can potentially pass on their genes. An absence of predators can also mean that injured individuals are more likely to survive. Ottow (1952) noted that in order for a pathology to become established in a population and not be removed by natural selection special circumstances are required: it must be hereditary, not incapacitating, extensive and there must be "inbreeding-related geographic isolation of the species or populations, that promotes an accumulaton of the pathological mutant genome [*pathologisch mutierten Erbguts*]", and there must be a lack of predators (p.195). He added that under these environmental conditions the preconditions for the preservation and propagation of such a hereditary disease in *Pezophaps* in the wild could take place; this mutation of the genotype caused no further life-threatening disease and resulted in the expression of a genotypical disease of the skeletal system – a "rare event of no small comparative pathological and gentotypical importance" (*ibid*.).

Some pathologies may have even been beneficial to a certain extent, as the wing exostoses would have been advantageous in intraspecific combat, although, as Ottow (1950) stated, the carpometacarpal exostoses did not have any connection with the wing spurs seen in some species of birds. As such certain pathological characters may even have been selected for, although this selection may have also allowed potential pathologies in other parts of the skeleton to develop. Ottow (1950, 1951) noted that in *Pezophaps* there was, perhaps, the first evidence of a genetic disease becoming an almost universal character within a species, a derived vertebrate one at that.

---

[194] Stable, properly aligned fractures heal rapidly in birds, although it has been suggested that pneumatic bones heal slower than medullary bones (Ritchie *et al.* 1994). In cases where a radius or ulna is broken, the adjacent bone of the pair may act as a splint, allowing proper alignment of the broken bone (Wood 1941).

[195] Substantia corticalis.

[196] Livezey & Humphrey (1985) found healed fractures in 13% of the skeletons of *Tachyeres* they examined, and of the 25 'naturally' broken bones 21 were wing and pectoral elements. The carpal knobs of older birds become enlarged, covered by conspicuous bare, and frequently thick and cornified, skin (Livezey & Humphrey 1992). These carpal knobs are used in combat (Nuechterlein & Storer 1985).

[197] An unpublished MS. draft of Newton & Newton (1869) (MSS. ROY Manuscript, General Library, NHM) includes mention of examples of healed fractures that were not discussed in the published version.

Male and female *Pezophaps* display the pathologies differently, suggesting a sex-linkage. Ottow (1950) remarked that carpometacarpal and radial exostoses in the male solitaire may even be invariably present. However, there are some specimens of male carpometacarpus that lack exostoses (for example NHMUK A.3507). Exostoses in other skeletal elements are much less common. The greater development of exostoses in the male solitaire compared with the female may be due to males being more combative, and perhaps also due to peramorphism, with males perhaps having an extended or more rapid growth period.

Pathological fractures may in part be the result of calcium deficiency (hypocalcemia; De Matos 2008), perhaps related to seasonally reduced food resources. Bones already weakened by calcium deficiency would have had greater susceptibility to fracture during intraspecific combat. The elements that most frequently show healed fractures are those that are likely to have been injured in such combats (wing bones, ribs, coracoid, scapula). Hypercalcinosis can lead to calcification of soft tissues although it is not known whether this condition contributed to the pathological ossifications (deposits of excess bone tissue) seen in *Pezophaps*.

Exostoses, similar to those of *Pezophaps*, are known in the extinct caniform carnivorans *Hesperocyon*, *Daphoenus* and *Cynodictis* (Wang & Rothschild 1992). In these taxa an exostosis occurs on the distal end of the radius: in *Hesperocyon* 61% of radii examined by Wang & Rothschild bore exostoses, which were “bilaterally symmetrical in all individuals in which both radii were preserved” (p.387). These exostoses have an uneven surface and are mushroom-shaped, being connected to the body of the bone via a smooth neck or peduncle. Wang & Robinson concluded that the pathologies were the result of multiple hereditary osteochondroma. In humans this condition is such that functional impairment is rare and Wang & Robinson concluded that those extinct canids affected were likewise probably not impaired. In addition, one specimen of *Hesperocyon* the shaft of the radius is also swollen, in another the humerus is pathologically affected and in another a vertebra bears an exostosis (Wang & Robinson 1992; cf. an exostosis seen on the synsacrum of *Pezophaps* – see below). One difference between the case in *Hesperocyon* and *Pezophaps* is that the condition does not appear to be sex-linked in the former. However, the greater development of wing exostoses in males of the latter may be linked to heterochrony, with males being peramorphic with respect to females. Males might have attained osteological maturity later than females (or alternatively, have grown more rapidly), leading to increased size and larger and more developed exostoses.

The carpal exostoses of *Pezophaps* would appear to be hereditary osteochondromas (cartilage-capped osseous growths).[198] Whether these are the same as those seen in humans or other vertebrates, and caused by the same genetic mutations, is uncertain. In humans the presence of multiple osteochondromas “seems to be higher in males (male-to-female ratio 1.5:1)” (Bovée 2008; cf. Wuyts *et al*. 2020). In *Pezophaps* although the exostoses are predominantly found in the wrist region, they are also found elsewhere in the skeleton, as is the case with multiple osteochondromas in other vertebrates. Osteochondromas may be pedunculated or sessile (Taminiau *et al*. 2014). They “grow in size and gradually ossify during skeletal development and stop growing with skeletal maturity, after which no new osteochondromas develop” (Wuyts *et al*. 2020) and “are most frequent around the knee, wrist, hip, shoulder for the long bones and pelvis, scapula and ribs for the flat bones” (Taminiau *et al*. 2014, p.23). They are also usually symmetric (Wuyts *et al*. 2020).

In mammals osteochondromas are commonly associated with long bones, are generally asymptomatic and do not display a tendency for metastasis. However, they can lead to bone fractures, bone deformities and neurological compromise, resulting from, for example, compression of nerves (Laeta

---

[198] “Osteochondroma (osteocartilaginous exostosis) is a cartilage capped bony projection arising on the external surface of bone containing a marrow cavity that is continuous with that of the underlying bone” (Bovée 2008).

et al. 2019). Osteochondromas have been linked to mutations in EXT1 or EXT2 genes[199] in mammals (Kierdorf *et al*. 2017); these genes are also present in birds.[200]

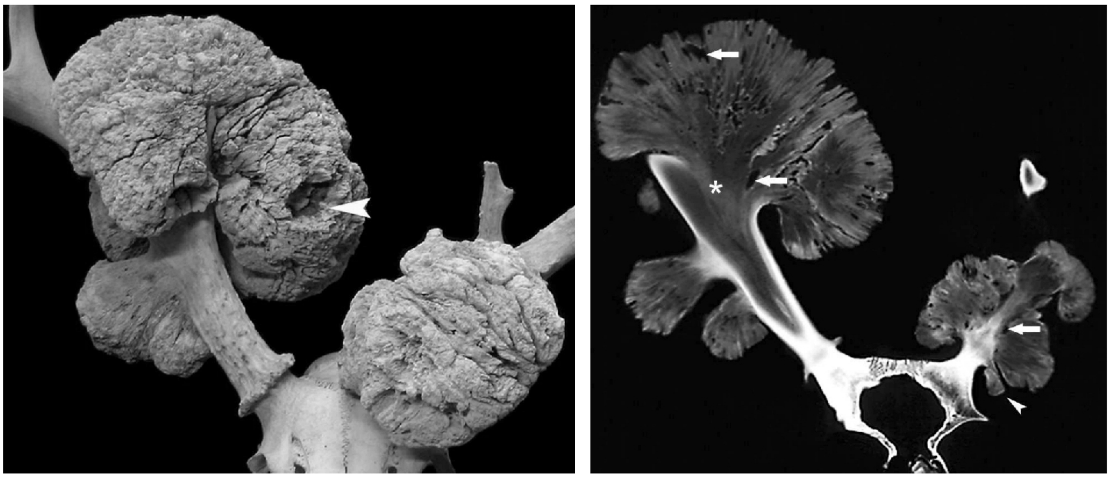

Osteochondromas in a specimen of the deer *Odocoileus virginianus* (Kierdorf *et al*. 2017, figs.1, 4; arrows in original figures; © 2017 Kierdorf *et al*. Creative Commons).

The carpal exostoses resemble the osteochondromas seen in a specimen of the deer *Odocoileus virginianus* (Kierdorf *et al*. 2017), with the surfaces being "rugose and nodular with numerous crevices" (*ibid*., p.5) and the exostoses being lobed. The exostoses of the radii, in contrast, show little or no radiating structure and are much more dense (Ottow 1950, pl.vii, fig.19; Hume & Steel 2013, fig.6B). The carpal exostoses do not resemble ossified haematomas, which have a relatively smooth surface texture and in which, in long-standing lesions, there is bone remodelling and the spaces between the radiating trabeculae are infilled, although their presence can still be distinguished (Mere *et al*. 2010).

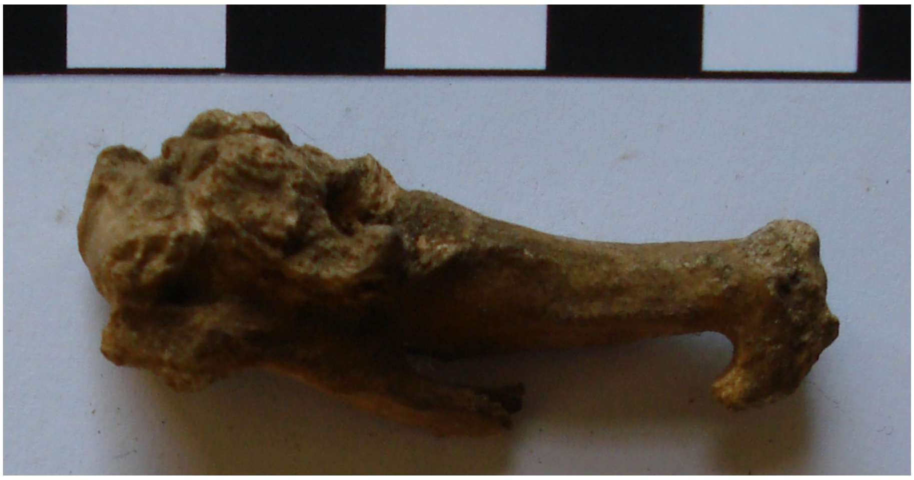

Carpometacarpus of *Pezophaps* in which the carpal knob is broken off and missing (Natural History Museum, Dublin; © David Gonzalez).

However, there are arguments against the homology of the suspected hereditary osteochondromas in *Pezophaps* and those in humans. The exostoses are predominantly site-specific in *Pezophaps*, occuring in the carpal region, with those occuring elsewhere generally either being absent or small. In contrast, in humans, although they may be solitary they are not restricted to one location, and furthermore osteochondromas in humans are often linked to short stature (whereas the exostosis-bearing males of *Pezophaps* are larger than the females). However, this does not appear to be the case for the caniform *Hesperocyon*, in which the osteochondromas do appear to be predominantly site-specific and not linked to smaller body size (Wang & Rothschild 1992).

---

[199] EXT1: exostosin glycosyltransferase 1, EXT2: exostosin glycosyltransferase 2.

[200] https://www.ncbi.nlm.nih.gov/gene/2131/ortholog/
https://www.ncbi.nlm.nih.gov/gene/2132/ortholog/

The radiating trabeculae seen in a section of the carpal exostosis (Hume & Steel 2013, fig.6A) are indicative of rapid growth (Kierdorf *et al.* 2017). Whilst cancellous bone appears to be continuous between the exostosis and the underlying bone (alular metacarpal) in the carpometacarpus (see Ottow 1950, pl.vii, fig.20; cf. Hume & Steel 2013, fig.6A)[201] this does not appear to be the case with the radius (Ottow 1950, pl.vii, fig.19; cf. Hume & Steel 2013, fig.6B). The large lacunae seen in the bone section (Hume & Steel 2013, fig.6A) could "represent areas formerly occupied by unmineralized cartilage that was lost during decomposition" (Kierdorf *et al.* 2017, p.10) as seen in the specimen of *Odocoileus virginianus* described by Kierdorf *et al.* (2017). The radial exostoses resemble parosteal osteochondromas,[202] in which the bone cortex remains intact. As regards the carpometacarpus, the apparent continuity between the cancellous bone of the host and that of the exostosis might argue against the exostoses primarily being a reactionary effect of periosteal trauma. In addition, the exostosis of the distal radius does not appear to disrupt the tendinal sulcus for the extensor tendons of the carpus and, in some specimens at least, exostotic bone is present on both sides of the sulcus. If the exostosis was due to trauma then one might expect the tendinal sulcus to be affected as well as the surrounding bone.

The carpal exostoses, at least, of male *Pezophaps* may well have had a genetic aetiology. Such exostoses might subsequently have been further developed as a reaction to the mechanical damage caused by intraspecific combats (the differing surface textures of the carpal exostoses might possibly reflect varying amounts of modification by trauma-induced reaction). Males, being peramorphic with respect to females, and perhaps defending territory more vigorously than females, would have developed larger exostoses. Further evidence for many of the pathologies being due to combats is that many of the affected elements are forelimb bones (humerus, radius, ulna, carpometacarpus) or ribs – bones one would be expect to have a greater likelihood of being fractured during wing-buffeting combats. However, that bones might have been weakened (and thus be more susceptible to fracture) by other factors (such as hypocalcemia or genetic bone disease) cannot be ruled out.

Arguments against a fracture callus aetiology for the carpal and radial exostoses include surface texture (which is very rugose in at least some specimens, *e.g.*, NHMUK A.3505), lack of incorporated fractured cortical bone or evidence of breakage, and general uniformity of size and morphology (both between left and right sides of the body and between individuals). However, at least some pathologies found elsewhere than the carpometacarpus and distal radius, and showing smooth-surfaced affected areas, do indeed appear to be due to healed breaks (Ottow 1950; pers. obs.).

Competition in periods when resources were scarce may have led to increased territoriality and intraspecific combats, with the development of hereditary exostoses aiding agonistic behaviour. Such competition may have also been a factor in the (presumed) display behaviour of *Raphus*.

Natunaornis also possesses carpal exostoses (Worthy 2001), as does *Tachyeres brachypterus* and some individuals of *Goura* (Hume & Steel 2013; although not all individuals of *Goura*: pers. obs.). However, it is not known whether these have the same aetiology as those of male *Pezophaps*: whether they are hereditary, whether they are solely the result of a response to mechanical damage (due to intraspecific combat), or whether they represent a combination of these factors. Similar exostoses are also found on the extensor processes of some individuals of *Haematopus ostralegus*, *Alectoris rufa*, *Tadorna tadorna*,

---

[201] Ottow (1950): "In some metacarpals where the exostoses have broken off, it can be seen that their interior consists of a spongy, compact bone structure and that there is hardly any marrow canal in the area of the break-off" (p.15).

[202] Parosteal osteoma is a "[r]adiodense, elongated, and lobulated surface bone mass" which is attached to the cortical bone surface with a wide base, although the cortex is not involved in the osteoma. In long bones of humans it occurs more frequently in males. There is also often a dense periosteal reaction in the margins of the osteoma and occasionally cancellous bone may be present (Olvi *et al.* 2015a, p.120).

Anserinae, *Chionis alba* and *Crax fasciolata*.[203] These exostoses are generally relatively small, with a relatively smooth surface (pers. obs.) and may represent ossified haematomas. A skeleton of *Haliaetus albicilla* seen on display (November 2002) at The Paleontological Museum of the Paleontological Institute, Moscow, has a large exostosis on each extensor process of the carpometacarpus. The surface of the exostoses is rough; their aetiology is unknown.

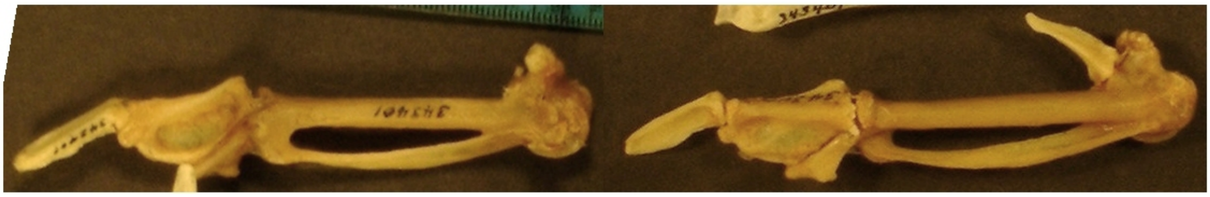

Exostoses on the carpometacarpi of *Goura scheepmakeri* (USNM 343401; ○ Jolyon C. Parish, May 2001).

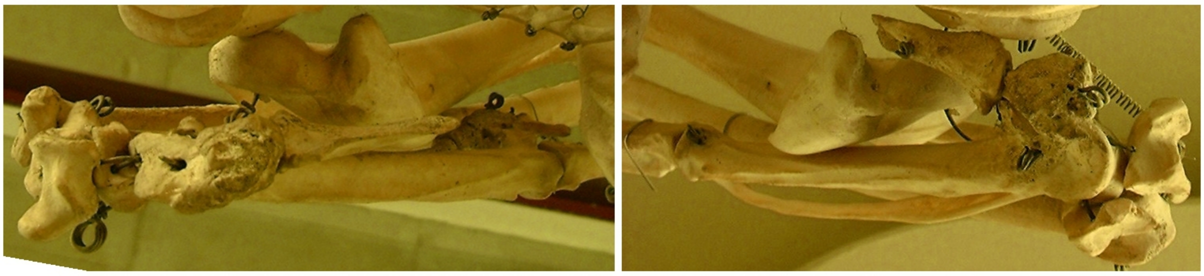

Exososes on the carpometacarpi of a skeleton of *Haliaetus albicilla* seen on display at The Paleontological Museum of the Paleontological Institute, Moscow (○ Jolyon C. Parish, November 2002).

Arguments against a solely trauma-induced origin, and in favour of a neoplastic origin (such as osteochondroma), for the carpal exostoses of male *Pezophaps*, include: surface texture and lobed morphology (especially in specimens such as NHMUK A.3505), large size, and possible continuity between the cancellous bone of the metacarpal and that of the exostosis. It is also of note that although some birds (including *Tachyeres*) exhibiting carpal knobs have wing elements of similar size to, or larger than, those of *Pezophaps*, and with well-developed musculature, none exhibit carpal exostoses anywhere near as large as in the males of the latter. However, at least some of the smaller carpal exostoses of female *Pezophaps* may have formed predominantly as a reaction to trauma, as these resemble the carpal exostoses of other birds (see above). Whether the carpal exostoses of *Pezophaps* are homologous with the calcar alae seen in some other birds is unknown, although their morphology suggests that they are not. Assuming the formation of carpal exostoses of male *Pezophaps* post-sexual maturity (*i.e.*, as a response to the trauma inflicted during combats), if such large exostoses were solely trauma-induced then one *might* expect to see evidence of layering in the internal structure, as a result of sequential breeding seasons, which does not (from the limited data available) appear to be the case.

It is difficult to ascertain whether a pathology is the result of a dysplasia or neoplasm, or is due to physical trauma. Internal examination by means such as radiography and CT scanning is necessary to obtain a diagnosis with any certainty. In conclusion, the osteopathologies of *Pezophaps* are probably due to a combination of factors, including a genetic predisposition to form exostoses on the carpometacarpus and adjacent bones (in males), possible dietary-related calcium deficiency leading to more-easily fractured bones, intraspecific combats causing growth of exostotic bone tissue and fracturing of bones, and infections potentially leading to deposition of bone in other parts of the skeleton. The exostosis of the carpometacarpus resembles hereditary osteochondroma and may have been sexually-selected, or selected for by other means. Further research, for example using radiography and CT scanning, osteometric comparisons (to ascertain whether any laterality was present – if primarily due to mechanical-trauma might exostoses show greater development on one side due to favouring of one limb over another in combat? Is there a correlation between body size and size of the carpal exostosis? Is there a correlation between size and surface texture in carpal exostoses?) and increased sample size, could shed more light on the origin and formation of these pathologies.

---

[203] Author's collection: *H. ostralegus* a.33, *A.rufa* a.38 (exostosis present only on the left carpometacarpus), *T. tadorna* a.52, Anserinae a.83; USNM collection: *C. alba* USNM 488317, *C. fasciolata* USNM 429347. Waterfowl often have a rugose carpal knob covering the extensor process of the carpometacarpus, which is presumed to be used in combat. Genera which almost always possess such a knob include *Alopochen*, *Chloephaga* and *Neochen*, and individuals of *Anser*, *Branta*, *Cygnus*, *Chenopis*, *Hymenolaimus*, *Merganetta*, *Sarkidiornis* and *Tachyeres* are also known to have this feature (Woolfenden 1960).

Instances of skeletal pathologies in the dodo and solitaire are given below.

Skull

The caudal end of the right ramus of a mandible of *Raphus* in the NHMUK collection (A.729) bears a pathology along the ventral part of crest M3 of Van Gennip (1986), perhaps representing a partial ossification of soft tissue.

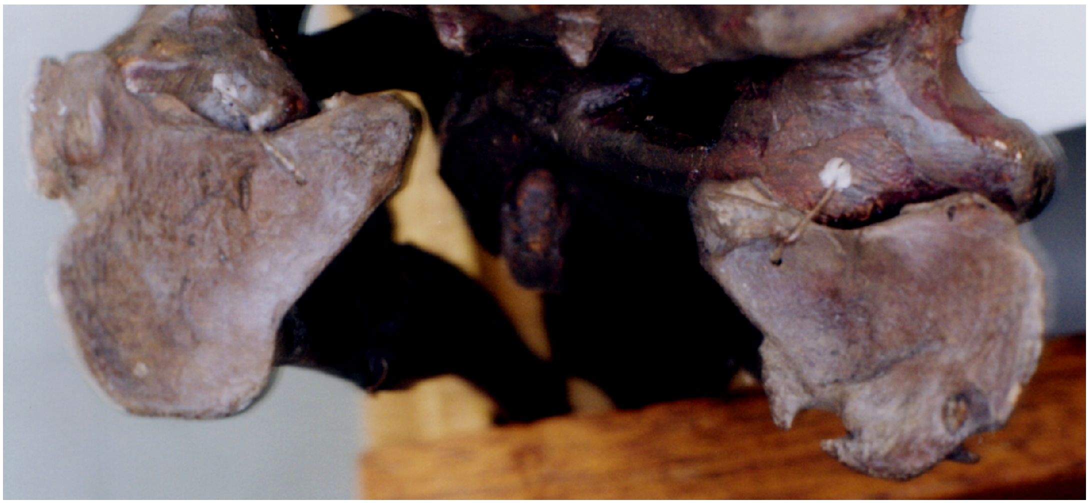

Mandible of NHMUK A.729 in caudal view showing a pathology of the right ramus (○ Jolyon C. Parish, 15th September 1998).

A specimen of a killer whale (*Orcinus orca*), reported by Laeta *et al*. (2019), shows a pair of large bilaterally symmetrical 'cauliflower-like' bony lesions in the occipital region of the skull, which, along with other exostoses on the skull and postcranial skeleton, were interpreted by Laeta *et al*. as osteochondromatosis. Similar exostoses, approximately evenly distributed in the frontal, temporal and nuchal regions of the skull are seen in *Pezophaps*.

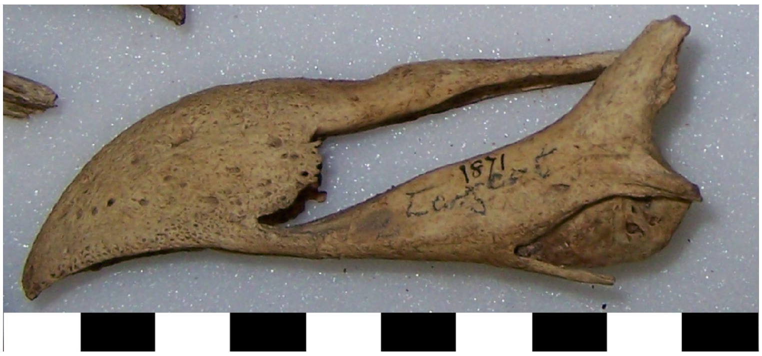

A partial beak (UMZC 653 collection, bearing the pencil annotation 'Largest') with a disrupted nasal bar (scale in cm; ○ Jolyon C. Parish, December 2008).

The lacrimal of the mounted female *Pezophaps* skeleton in the Royal College of Surgeons of England collection (RCSHM/Aves 707) appears to have exostotic irregularities. Nopsca (1923) stated that exostotic bone formation is present in the skull of *Pezophaps*, although Ottow (1950) was unable to confirm this, based on the small sample he studied. Nopcsa was probably referring to the rugosities of the cranio-facial and nuchal regions of the skull.

A partial beak, belonging to a male solitaire, in the UMZC 653 collection has a disrupted nasal bar: the distal portion has been displaced slightly ventrally with respect to the proximal portion.

A mandible of *Pezophaps* in the collections of the NHMUK examined by Ottow (1950, pl.i, figs.1, 2) shows an exostosis on the lateral surface in the marginal area of the dentary, supra-angular and angular. The exostosis is about 30mm in length, 12mm in width and it reaches a height of approximately 10mm. It is very hard and composed of light spongy bone tissue; on the underside shows two small cavities. The surroundings of this exostosis have a disrupted appearance (Ottow 1950). Ottow (1950) considered it to be due osteogenesis dysplastico-exostotica, although its appearance (from Ottow's photographs) also suggests a traumatic origin.

Vertebrae

The two fused pathological vertebrae mentioned and figured in the "Dodo Expeditie Weblog" (20 juni 2006), and stated to belong to the dodo,[204] appear to be cervical vertebrae of *Cylindraspis*, perhaps the seventh and eighth cervicals (see plates in Günther 1877).

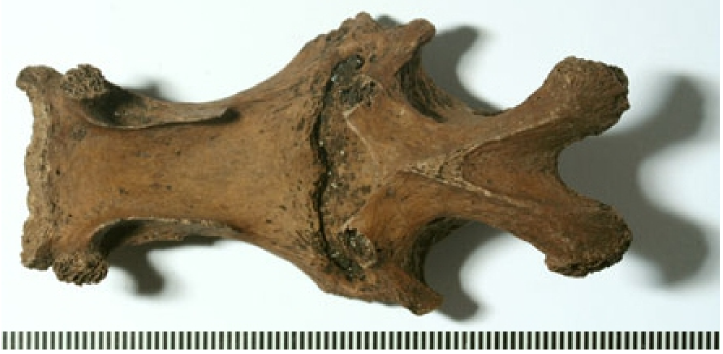

Two fused cervical vertebrae found during the Dodo Research Project excavations and probably belonging to *Cylindraspis* (© Ranjith Jayasena).

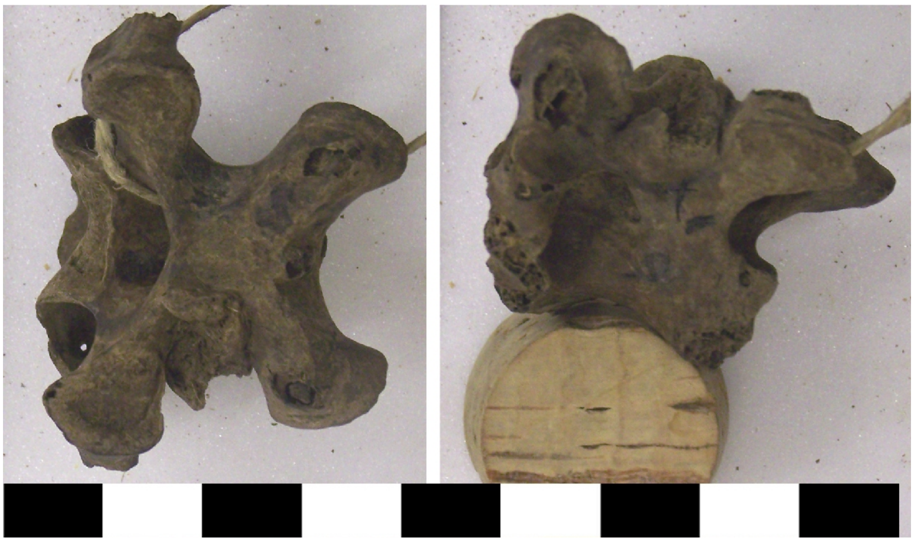

A ninth cervical vertebra of *Raphus* (UMZC 415.K collection) bearing an exostosis (○ Jolyon C. Parish, December 2008).

---

[204] Naturalis. Dodo Expeditie Weblogs 2006-2009: www.dodo-expeditie.nl The find was also mentioned in Parish (2013, pp.260, 261), which used this reference as a source..

A sixth cervical vertebra of *Raphus* in the UMZC 415K collection bears an exostosis on its left lateral face. A seventh and a ninth cervical in the same collection also have pathologies. The eighth cervical of the Durban skeleton shows pathological alteration of the right postzygapophysis with additional bone growth and ventral displacement of the articular face (Claessens *et al*. 2015).

The neural spines of the fourth and fifth cervicals of the Uppsala skeleton of *Pezophaps* display slight exostotic alteration, and are enlarged with a surface covering of small tuberosities (Ottow 1950). In addition, the seventh cervical of the same skeleton has enlarged and irregularly formed transverse processes (*ibid*.). Some irregularities of the transverse processes, exostotic in form, on the eighth cervical are figured by Newton & Newton 1869 (pl.xv, figs.27-30) (Ottow 1950).

Ribs

Owen (1867, pl.xvi, fig.10) illustrated a vertebral rib of *Raphus* with pathology on the shaft: “a fracture which has been healed, with some irregular ossific deposit on the inner surface” (p.57).

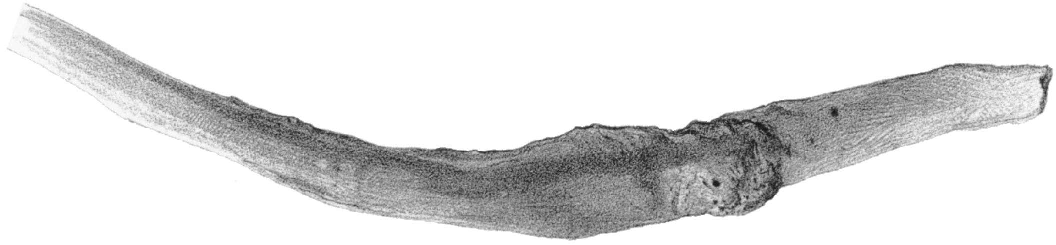

A vertebral rib of *Raphus* with a pathology (Owen 1867, pl.xvi, fig.10; artist: Edward William Robinson; “E W Robinson del” “W West imp”).

The sternal rib of the sixteenth vertebra of Sauzier’s dodo skeleton figured by Newton & Gadow 1893 (pl.xxxvi, fig.1) shows a very expanded posterior border, triangular in shape and overlapping the succeeding sternal rib. The sternal rib itself appears to be bent in around the same region – these characters may have been the result of a healed fracture.

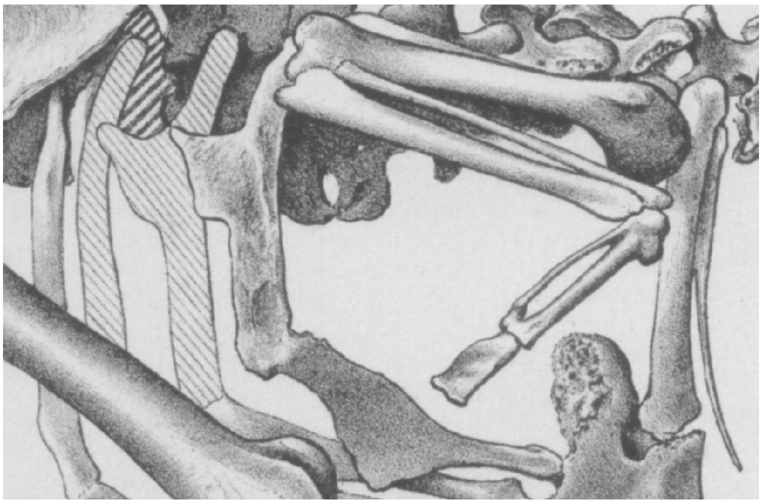

Sauzier’s dodo skeleton at Port Louis, showing a pathological sternal rib (Newton & Gadow 1893, pl.xxxvi, fig.1).

A proximal fragment of a vertebral rib of *Pezophaps* examined by Ottow (1950; NHMUK female[205] specimen) showed a slight bend and a swelling, which Ottow attributed to a dysplasia (*ibid*., pl.vi, fig.17). Four sternal ribs belonging to *Pezophaps* (NHMUK: three male and one ?female), also examined by Ottow (1950), showed pathologic alterations. Two of the male specimens displayed healed fractures, with distinct “dislocatio ad longitudinem”, whereas the other male specimen and the ? female specimen showed only a swelling with slight bending, which again Ottow attributed to a dysplasia (*ibid*., pl.vi, fig.17).

---

[205] Ottow (1950) followed the view of Newton & Newton (1869) that the larger specimens were from males and the smaller ones from females. This is also followed here.

Synsacrum

In a specimen of the synsacrum of *Pezophaps* (NHMUK A.1441) there is a narrow hard tuberous, approximately bean-sized, exostosis on the right side, which extends over the distal lumbar vertebrae and above the costal process of the sacral vertebra. Dorsally it perforates the relatively thin plate of the ilium (perhaps due to pressure-atrophy: Ottow 1950) and projects slightly outwards. The exostosis has a smooth cortical surface and originates on the lateral part of the lumbar vertebrae of the synsacrum. This exostosis must have exerted pressure on the nerve plexus of this region and associated effects must have been observable in the living bird (*ibid*., pl.i, figs.3, 4).

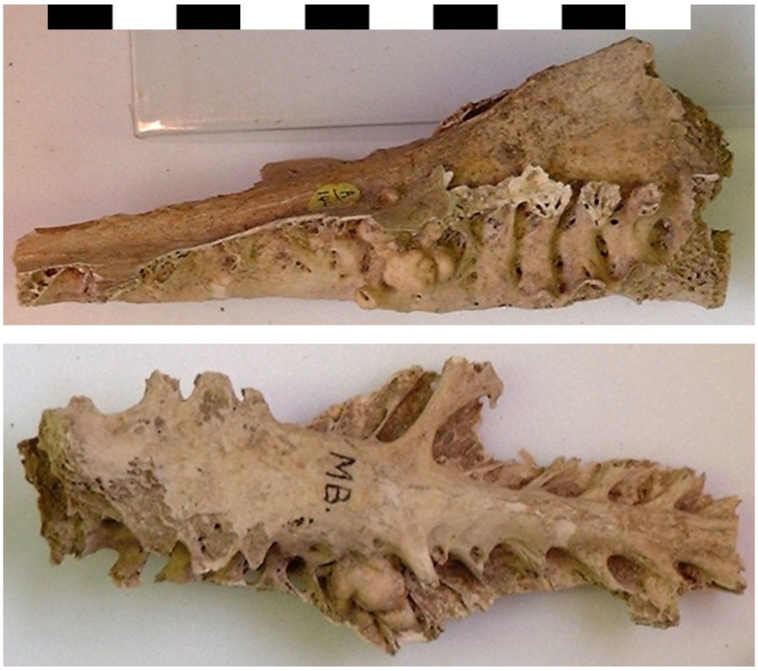

A synsacrum of *Pezophaps* bearing an exostosis on the right side (NHMUK A.1441), lateral and oblique ventral views (scale in cm; ○ Jolyon C. Parish).

Sternum

The Uppsala sternum of *Pezophaps*, examined by Ottow (1950), shows slight deformities at the caudal part, and in the region of the carina. Nopcsa (1923) mentioned that there was an “expansion of the bone rugosity [Ausdehnung der Knochenrauhigkeiten]” of the sternum, as apparent on the cranium (*ibid*.). However, in his paper of 1926 (Nopcsa 1926) Nopcsa referenced Gervais (1867-1869) when mentioning that in some individuals of *Pezophaps* the sternum becomes rugose, suggesting that he mistook the calcareous incrustations on the sternum of the specimen figured by Gervais (MNHN 6400) for bone growths.

Coracoid

The brothers Newton examined a coracoid of *Raphus* which had apparently been broken in life and then healed (Newton & Newton 1869). Hume & Steel (2013) also mentioned a scapulocoracoid with a healed fracture in the AMNH collections (unregistered).

A specimen of the right coracoid of a male *Pezophaps* (UMZC 639), examined by Ottow (1950, pl.ii, fig.7, pl.viii, fig.22), showed a slightly altered shaft, which was, according to him, strongly bent due to a disturbance during its growth. The articular face for the humerus was also roughened. This coracoid was figured by Newton & Newton (1869, pl.xx, fig.136) and they considered it to be the result of a healed fracture. According to Ottow (1950), the continuous cortical bone and the internal bone-structure, seen in the radiograph, confirmed that this was not the case, but that it was “without a doubt just a dysplastic growth disorder” (p.12).

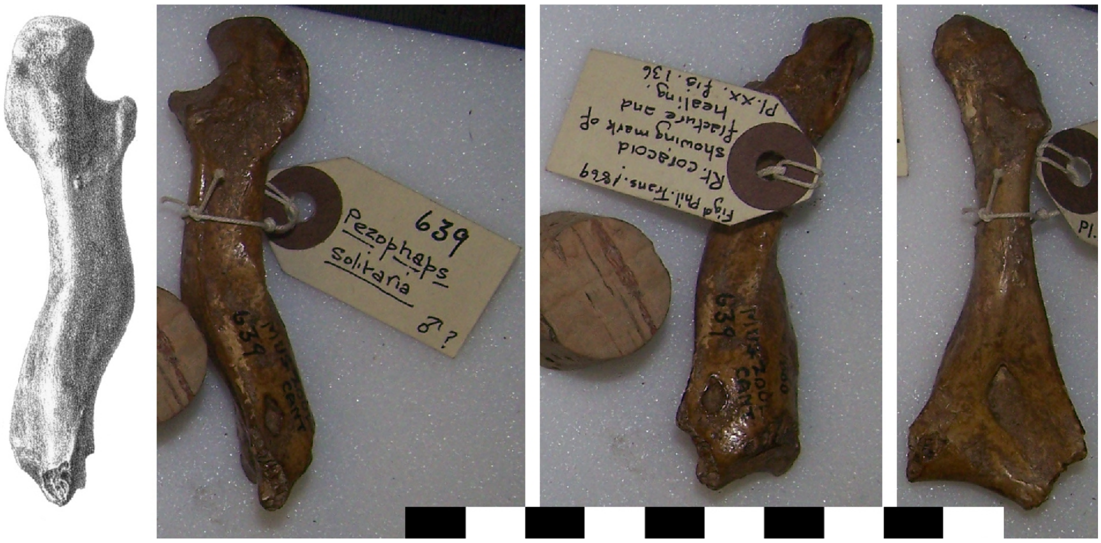

A male right coracoid of *Pezophaps* (UMZC 639) with a bent shaft; scale in cm (*left*: Newton & Newton 1869, pl.xx, fig.136 (artist: George Henry Ford); *middle* and *right*: ○ Jolyon C. Parish, December 2008).

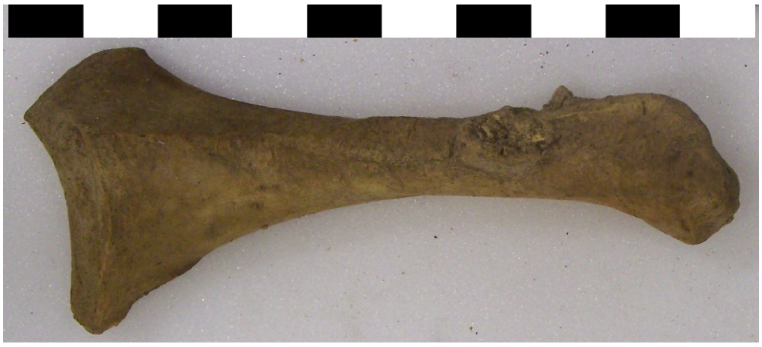

A male right coracoid of *Pezophaps* (UMZC 653 collection) with exostotic development (scale in cm; ○ Jolyon C. Parish, December 2008).

A female *Pezophaps* specimen (NHMUK A.1441.2) studied by Ottow (1950) also showed, according to him, strong dysplastic alteration, with a reduction of the length of the bone to 60mm (as opposed to the normal length of around 70mm). Ottow stated that it displayed dysplastic growth disturbances with exostoses in several places. The walls of the bone were continuous and there was no dislocation (*ibid*., pl.ii, fig.8; Hume & Steel 2013, fig.7C). Running across the bone was a furrow, at the upper and lower ends of which were exostotic growths. Another female specimen (*ibid*., pl.viii, fig.22; UMZC specimen), consisting of only the upper (omal) part,[206] showed, distal to the articular surface, a disruption, although with relatively little callus formation, but with strong *dislocatio ad axin* and *ad peripheriam* fracture (Ottow 1950). There were no dysplastic changes other than the bone scar seen in the radiograph (*ibid*., pl.viii, fig.22). According to Ottow, this specmen showed the only case of a healed fracture in the whole collection he had examined, and he speculated that it might have been caused by the bird being hit by a stick and the fracture subsequently healing. However, intraspecific combat could have also caused such a trauma.

A male right solitaire coracoid in the UMZC 653 collection, shows exostotic development (possible osteochondroma?) on the ventral face, at the level of the scapular articulation. Likewise, a right coracoid of *Pezophaps* (NHMUK 76.1.28.43) displays exostotic development on the ventral part of the procoracoid process and scapular cotyla. A specimen on display in the François Leguat Giant Tortoise and Cave Reserve Museum exhibits what appears to be a healed break.

---

[206] Ottow concluded that the break was *post mortem*, as there was no change in the bone at the break itself.

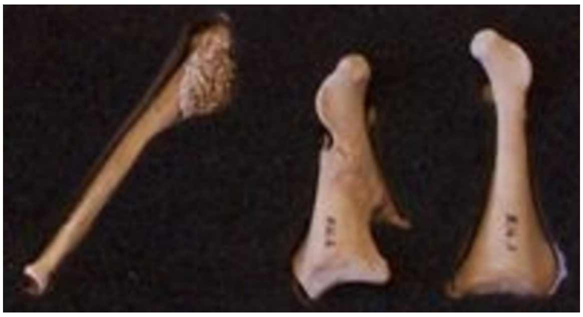

A pathologic right coracoid of *Pezophaps* (*middle*) on display at the François Leguat Giant Tortoise and Cave Reserve Museum. *Left*: a radius with an exostosis, *right*: a normal left coracoid (© Arnaud Meunier, François Leguat Giant Tortoise and Cave Reserve).

Scapula

A specimen of the distal portion of a scapula of *Pezophaps* (♀) examined by Ottow (1950) (NHMUK specimen) was broken in the region of what Ottow considered to be a dysplasia. Another female specimen (UMZC specimen, right side) he thought displayed a distinct dysplastic swelling, and bending along the whole bone below its head. One specimen in the collection UMZC 653 displays displacement of the shaft, whereas others show slight exostotic development around the humeral glenoid.

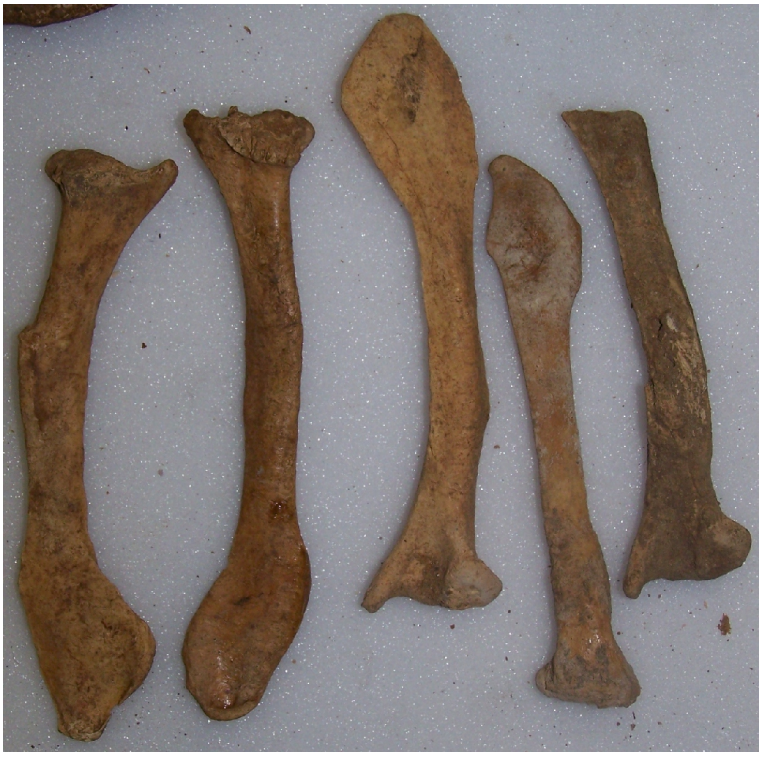

Scapulae of *Pezophaps* (UMZC 653 collection): the left-hand specimen shows a possible healed break and the second from left has exostotic growth around the articular face (○ Jolyon C. Parish, December 2008).

A number of specimens of *Pezophaps* (*e.g.*, OUMNH 19630) bear approximately perpendicular markings on the shaft of the scapula. The origin of these is unknown, although they do show some resemblance to the “ribbed periosteopathy” described by Sawyer & Erickson (1998, fig.8B). Alternatively, they could be of taphonomic or other origin.

A scapula of *Pezophaps* (UMZC 653 collection; scale in cm; ○ Jolyon C. Parish, December 2008).

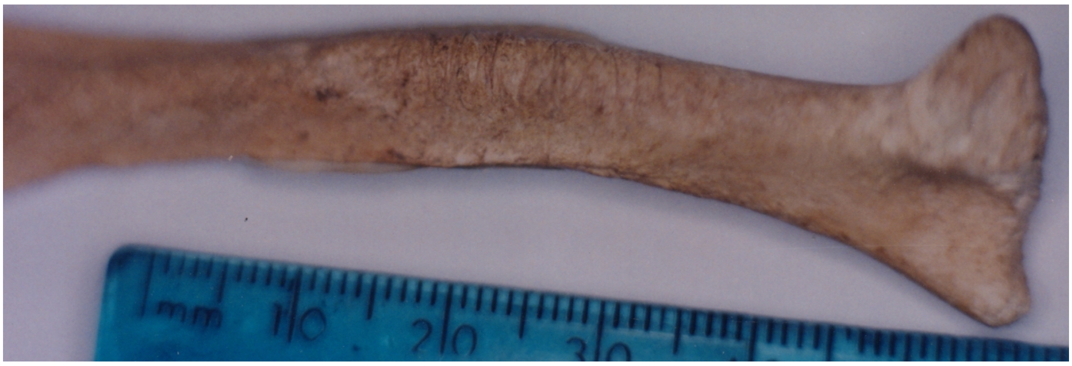

A male left scapula of *Pezophaps* (OUMNH 19630) bearing approximately perpendicular markings on the shaft (○ Jolyon C. Parish, January 2001).

Humerus

Three female *Pezophaps* humeri examined by Ottow (1950) showed what he considered to be dysplastic alterations of the diaphysis. The first female humerus (NHMUK specimen) had what he identified as a dysplastic swelling and a markedly thickened diaphysis (*ibid*., pl.iii, fig.9a). The bone was also shortened, being only 90mm long (as opposed to 95-100mm, *ibid*.). In the area of the presumed dysplasia there were low exostotic irregularities. The second female humerus (NHMUK specimen) had an essentially stronger formed (presumed) dysplastic diaphysial region of around 28mm shaft length, nearer to the ulnar end. The bone structure had been strongly altered, being porous, the cortex appearing as if partially corroded. The bone was broken in the area of the presumed dysplasia *post mortem* (*ibid*., fig.9b). The third female humerus (*ibid*., fig.9c) showed presumed dysplastic features in the middle of its shaft and was fractured in this area during life. The healed fracture was not very serious and had only minor swelling, shortening and bending (“Dislocatio ad longitudinem et latus”). This humerus was figured by Abel (1935, fig.474). The radiograph (Ottow 1950, pl.viii, fig.22) of the third humerus showed compressions of the bone structure in the area of the presumed dysplasias and fracture, in addition to, on one side, a distinct incongruency and shift of the cortical bone, as is common in healed fractures (Ottow 1950). Male humeri with a healed breaks are figured by Lüttschwager (1961, fig.20) and Hume & Steel (2013, fig.7B: NHMUK A.1441.1).

Ulna

Many of the largest (male) specimens of *Pezophaps* show what Newton & Newton (1869) regarded as the results of fracture and healing of the bone. Ottow (1950), however, considered that pathologies of the ulna were genetic. Presumed dysplasias were exhibited by 22 ulnae (three male and nineteen female) examined by Ottow (1950), and of 101 ulnae examined by Hume & Steel (2013), fifteen showed pathologies. Ottow (1950) found no exostoses. However, the distal end of the ulna of NHMUK A.3505 does have some exostotic growth (Hume & Steel 2013). The presumed dysplastic ulnae examined by Ottow showed, around the middle of their shafts and all the way round the bone, a strong swelling of the cortical bone. There was also deformation and bending, and there were alterations of the cortical bone without swellings and disruptions of the structure of the outer bone layer. The bone was shortened, mostly in the shaft. The presumed dysplasia surrounded the shaft like a belt and sometimes occurred nearer the proximal end of the ulna; the distal end, in all 22 specimens, showed no dysplastic alteration. Outside of these main altered areas the bone also showed other alterations, being swollen and bent. One ulna showed evidence of a *post mortem* break in the region of the presumed dysplasia and it could be seen that the internal space was affected in the area of this presumed growth disruption. There was no difference in the form and location of the presumed dysplasias between the sexes, although proportionately more female specimens showed presumed dysplasias than male ones, although this bias could be the result of the limited number of specimens studied.

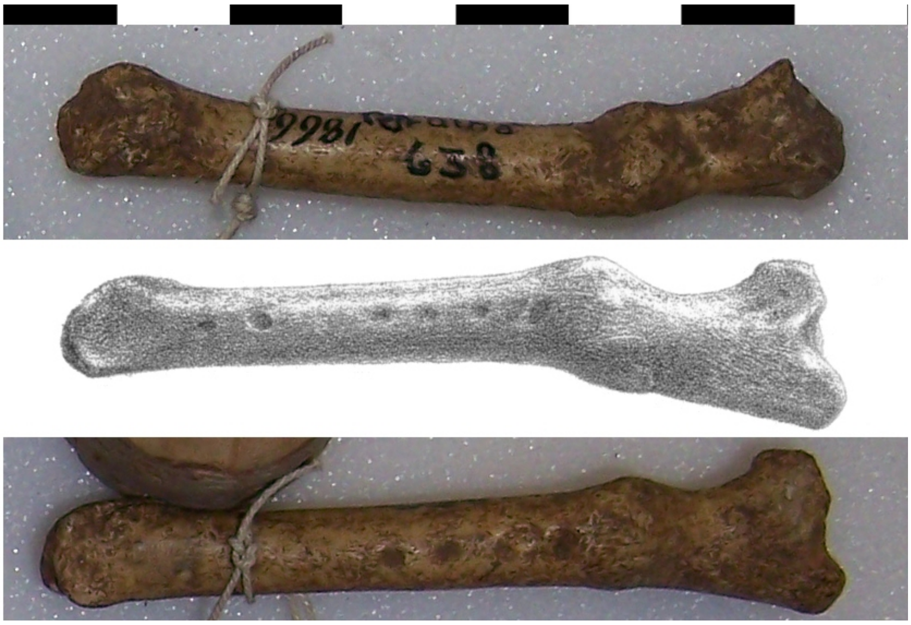

A left ulna of *Pezophaps* (UMZC 638) with swelling and displacement of the shaft; scale in cm (*top* and *bottom*: ○ Jolyon C. Parish, December 2008; *middle*: Newton & Newton 1869, pl.xx, fig.135; artist: George Henry Ford).

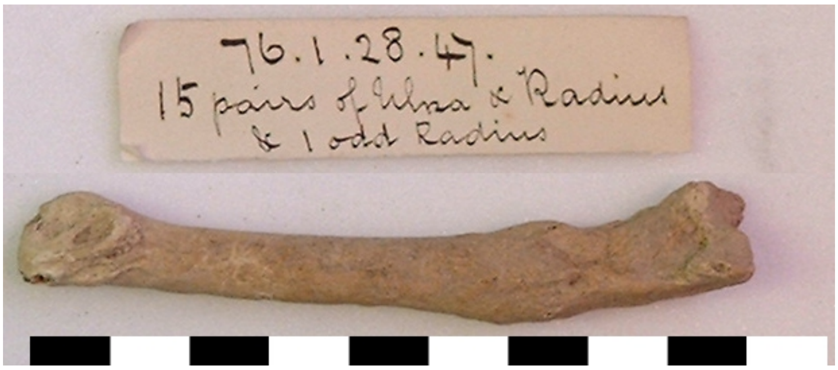

An ulna of a male *Pezophaps* (NHMUK 76.1.28.47) with swelling and bending of the shaft; scale in cm (○ Jolyon C. Parish).

Ottow (1950, pl.iii, fig.10) figured five female ulnae (lengths 66-70mm) with bending of the shaft near to the distal end and what he considered to be strongly formed dysplasias (*ibid.*, pl.iv, fig.11; Ottow 1951, fig.3). Figure 11 of Ottow's work shows six female ulnae with presumed dysplasias and bending more in the middle of the shaft. In some of the specimens figured the impressions for the remigeal papillae can be seen. The radiographs (fig.21) show a complete change in the form of the cortex, including both the periosteal and endosteal bone, in the area of the presumed dysplasias; the male ulnae show presumed dysplasias of the shaft, partly with defective extremities (Ottow 1950). A left specimen (UMZC 638) studied by Newton & Newton (1869, pl.xx, fig.135) shows swelling of shaft near the proximal end and slight displacement. Ulnae with swollen diaphyses were figured by Lüttschwager (1961, figs.18, 20) and Hume & Steel (2013, fig.7F: NHMUK A.9043). Despite Ottow's diagnosis, at least some of the exostoses on the ulnae figured by Ottow (1950, pl.iv, fig.11; pl.viii, fig.21) appear to be ossified haematomas, and in the radiograph images of some specimens a break can be seen in the area of the swelling, suggesting that at least some of the pathologies are indeed healed fractures.

An ulna, belonging to a male solitaire, in the collection NHMUK 76.1.28.47 displays a swelling and slight bending of the proximal diaphysis. A pathological ulna is also present in the collections of the François Leguat Giant Tortoise and Cave Reserve Museum (R272). The collection of the Zoologisches Museum, Kiel, contains three female ulnae (A 4294/143-145), two of which are pathological.

Radius

The distal end of the radius of male *Pezophaps* frequently shows a large exostosis and, along with the carpometacarpi, the radii are the bones that most frequently show pathologies in *Pezophaps*. 37 *Pezophaps* radii were studied by Ottow (1950; 34 male and three female). 32 of the male radii Ottow examined were either exostotic or both exostotic and what he considered to be dysplastic. The three female radii were found to be dysplastic, but not exostotic. In exostotic specimens the distal end of the radius was expanded and showed, on both sides of the bone, distinct small wart- and crest-like structures. The diaphyses of the radii were bent in some specimens and what Ottow considered to be dysostotically thickened. In two male radii there there was very strong presumed dysplastic swelling and changes, of approximately the same kind as in the majority of the female ulnae, in addition to the typical exostoses. Typical exostoses and presumed typical dysplasias of the diaphysis sometimes occurred on the same radius in male specimens. Most of the exostoses were found on the distal end of the radius, usually on the dorsal side. The three female radii showed presumed dysplastic swelling and changes of the shaft. Exostoses may also have occurred in the female radii, as they are present in the carpometacarpi (*ibid*.), but evidence is currently lacking. Ottow's figure (1950, pl.iv, fig.12) shows five male radii (three left and two right) with strongly formed exostoses at their distal ends, but normal shafts (two of these are illustrated in Ottow 1951, fig.2). Another figure (*ibid*., pl.v, fig.13) shows four male and three female radii – the first radius is normal, the second with a slightly roughened exostosis attached, the third and fourth radii with exostoses and also dysplasias of the shaft. The female radii show what Ottow considered to be dysplasias of their diaphyses – the first more at the proximal end, the others in the middle of the shaft. Ottow's figure 19 (pl.vii) shows radiographs of five male radii – one normal and four with large distinct exostoses, with an altered cortex.

Some of the pathologies of the radius illustrated by Ottow (1950, pl.viii, fig.21) could perhaps be ossified haematomas or periosteal pathologies caused by trauma (see Stone 1926). However, the rugose exostosis commonly seen on the distal end of male *Pezophaps* radii may represent a parosteal osteochondroma (see above). Its surface texture, at least in some specimens (*e.g.*, NHMUK A.3505), differs from that of an ossified haematoma (including turret exostosis), that of the latter being more rounded and smoother (see Stone 1926, Rothschild 2010, Cañueto *et al*. 2011).

The collection of the Zoologisches Museum, Kiel, contains two male solitaire radii (A 4294/148-149), one of which is pathological, and also another pathological male radius (A 4294/152). Radii with exostoses were figured by Lucas (1895, fig.1: USNM 18251), Lüttschwager (1961, fig.20) and Hume & Steel (2013, fig.5A). Hume & Steel (2013, fig.6B: FLMR 165.1) figured a thin section of a radius with an exostosis.

Ulnare

The ulnare of NHMUK A.3505 (*Pezophaps*, male) also shows some slight exostotic development.

Carpometacarpus and alar phalanges

The exostosis of the carpometacarpus of *Pezophaps* is noted in the main description, as it is almost invariably present in male specimens. The surface texture of carpal exostosis shows variation in rugosity with some specimens having a less rugose surface than others (see Hume & Steel 2013, fig.3). Newton & Newton (1869) remarked that the appearance of the carpometacarpal rugosity "is so exactly that of diseased bone that one is led to believe that it had its origin in injuries received by the birds in such combats as are mentioned by Leguat, and was aggravated by a continuance of fighting-propensities transmitted from generation to generation" (p.354). Abel (1912) remarked: "the occurrence of exostoses in the carpal region [*Handwurzelregion*] of the extinct solitaire [...] which is also in a completely unmistakable manner a direct consequence of the boxing battles fought by these birds among the males with the carpus [*Handwurzel*] and the forearm" (p.586). Lowther (2002) stated that specimens of *Pezophaps* "show mended fractures in the metacarpus" (p.273).

Ottow (1952) described a male carpometacarpus (Zoologisches Museum, Kiel, specimen) with a mushroom-shaped exostosis on the extensor process 3.5 x 3cm wide and 2cm high. The exostosis consisted of spongy, porous bone (figured: Ottow 1952, fig.1). He also mentioned a female carpometacarpus (also a Kiel specimen) without an exostosis, but with a slightly defective proximal end (figured: Ottow 1952, fig.1).

The fact that the knob was described as "a little round Mass under the Feathers" (Leguat 1708) suggests that it was not covered in keratin (cornified sheath), as is the case with the carpal spurs of Anhimidae. This is further supported by the surface texture of the knob, which is unlike that associated with a keratinous sheath covering (see Hieronymus *et al*. 2009, fig.7). It is probable that the bone of the exostosis was covered by a cartilage cap, which in turn was covered by thick skin, although the latter may have been cornified as a callus formation.

Exostotic *Pezophaps* carpometacarpi (male and female) were illustrated by Newton & Newton (1869, pls.xix, figs.87-90, xx, fig.131), Lucas (1895, fig.1), Ottow (1950, pl.v, figs.14, 15; pl.vi, fig.16; pl.vii, fig.20), Ottow (1951, fig.1), Lüttschwager (1961, fig.19) and Hume & Steel (2013, fig.3a-c [NHMUK A.9047], 3d-f [NHMUK A.3505], 4b [NHMUK A.3505], d [NHMUK A.9045], 5a, b). Hume & Steel (2013, fig.6A: NHMUK A.1387) figured a thin section of a carpometacarpus with carpal knob.

A specimen of the first phalanx of the second digit of *Pezophaps* (NHMUK A.1452) shows some exostotic development and alteration (pers. obs.). A specimen of this phalanx (probably NHMUK A.1452) was figured by Hume & Steel (2013, fig.5A).

Pelvis

A partial male pelvis of *Pezophaps* in the NHMUK collections studied by Ottow (1950) displayed a well-developed bony growth in the region of the left acetabulum (the right side was unaltered), occupying almost its entire circumference. The whole of the antitrochanter also showed exostotic growth similar to that of the cranial periphery of the acetabulum. The structure of the exostosis was very crumbly and spongy and its upper surface showed small lumps. This, to a certain extent, may have been due to its preservation. There was also an exostotic growth on the inside surface of the acetabulum, which was located intraarticularly (*ibid*.). The hip joint was very affected and there must have been severe effects observable in the living bird, with the movement of its hind leg being somewhat hindered. In addition, there were small periosteal disruptions found on the inside of the preacetabular ilium. In some areas the cortical bone of the pelvis was slightly altered (*ibid*., pl.ii, fig.5). Such pathologies might have been due to an infection or osteoarthritis (osteoarthrosis).

In another pelvis (part of the skeleton of *Pezophaps* in Uppsala) the area caudal to the left acetabulum and ventral to the ilioischiadic foramen showed significant thickening and swelling, due to an osteological pathology. This mass was 33mm broad and 20-24mm thick (*ibid*.). Ottow (1950) did not consider the pathology to be a true exostosis, but rather a strong hyperplastic dysplasia.

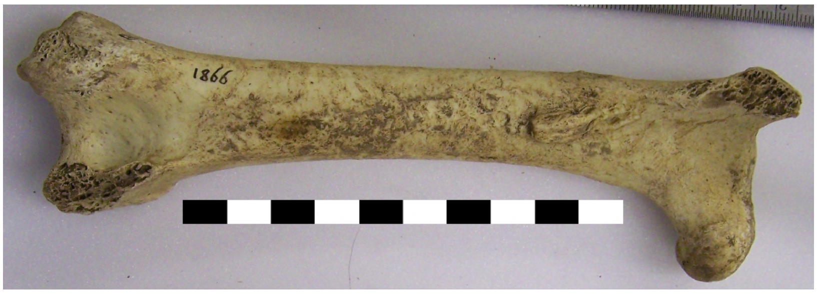

A right male solitaire femur (UMZC 653 collection) with pathology of the shaft; scale in cm (○ Jolyon C. Parish, December 2008).

Femur

Ottow (1952) mentioned a right female *Pezophaps* femur (Zoologisches Museum, Kiel, specimen) with a flat, hard compact exostosis, 9 x 4mm, on the cranial face, just distal to the trochanter (figured: Ottow 1952, fig.3). A right femur of *Pezophaps* in the UMZC 653 collection shows an elongate rugosity on the cranial face of the proximal end of the shaft. A left female femur (also UMZC 653) shows two circular depressions on the cranial face of the distal end of the bone.

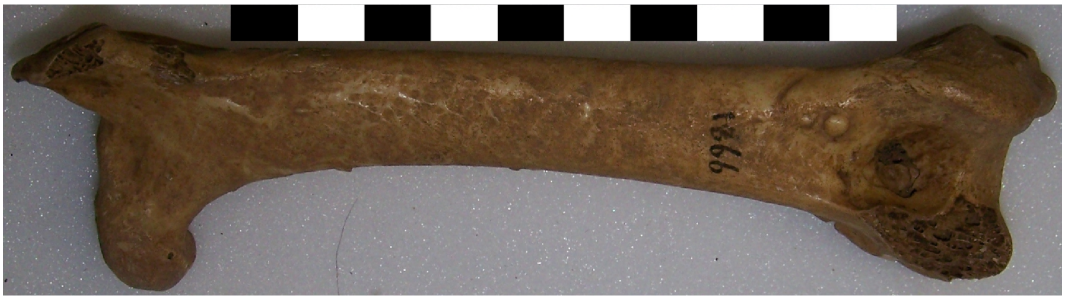

A left female solitaire femur (UMZC 653 collection) with two circular depressions on the distal end of the bone; scale in cm (○ Jolyon C. Parish, December 2008).

Tibiotarsus

A left tibiotarsus of *Raphus* in the YPM collections (YPM 14503) is bowed slightly laterally in the diaphysial region, with the proximal part of the bone bent medially. The shaft also appears to be slightly shortened and the fibular crest enlarged. The bending of the tibiotarsal shaft may be due to a deficiency of calcium, phosphorus or vitamin D3, leading to rachitis (rickets; Ritchie *et al*. 1994), a symptom of which is splaying of the legs (Harcourt-Brown 2002). Such a deficiency might have been caused by poor diet in the young bird (De Matos 2008, Graveland 1996).

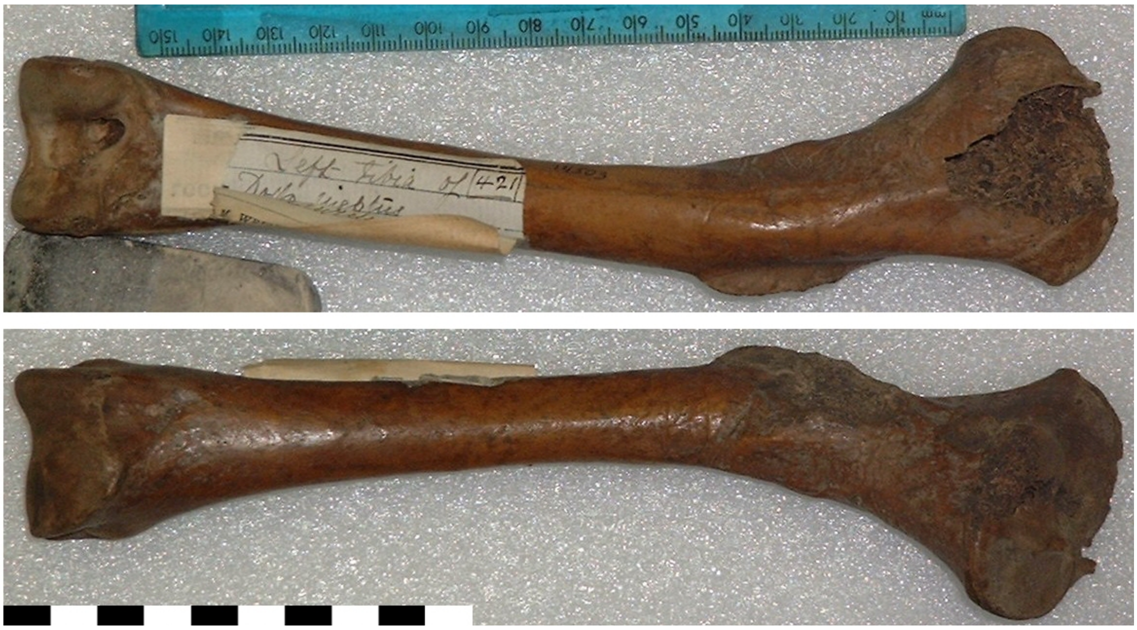

A pathologic left dodo tibiotarsus (YPM 14503; scales in mm and cm; ○ Jolyon C. Parish, May 2001).

The right tibiotarsus of a male skeleton of *Pezophaps* (UMZC 415.R) has what appears to be a slight exostotic growth on the caudomedial edge of the distal end (the medial cristae sulcus), which may represent osteoarthritis (osteoarthrosis).[207] Osteoarthritis is common in birds (both wild and captive), although documented instances are all restricted to the distal tibiotarsus (Rothschild & Panza 2006). Rothschild & Panza (2006) found that it was more common in pigeons than hawks, and more common in arboreal than terrestrial pigeons.

---

[207] "Osteoarthritis was identified on the basis of synovial-lined joint remodeling with spur (osteophyte) formation" (Rothschild & Panza 2006, p.646). UMZC 415.R was on display (behind glass) at the time, and as such was not examined close up.

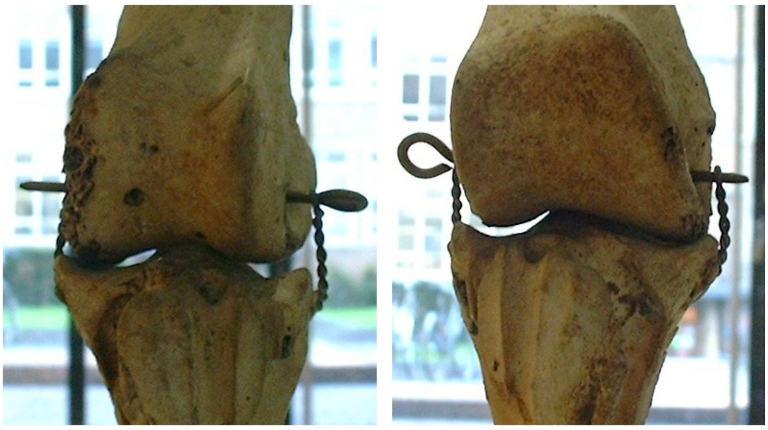

Left: an exostotic growth (likely due to osteoarthritis) on the caudal face of a male right solitaire tibiotarsus, *right*: the left tibiotarsus for comparison (both UMZC 415.R; ○ Jolyon C. Parish).

Fibula

A fibula from a female *Pezophaps* (NHMUK specimen, lacking its distal end) examined by Ottow (1950, pl.vi, fig.17) showed what he considered to be a very strong dysplastic-exostotic alteration of the entire head. In addition, the diaphysis beneath the head of the fibula was slightly bent. Abel (1935, fig.475) figured a fibula which showed what Ottow regarded as a strong dysplastic swelling beneath the head. Ottow (1950) did not study this specimen (from the UMZC collection), although he stated that Abel's assumption that it presented evidence of breaking and healing was incorrect. This specimen may have been one in the UMZC 653 collection – a fibula with swelling of the proximal part of the shaft and displacement.

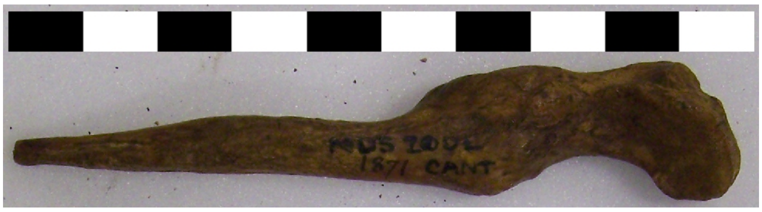

A *Pezophaps* fibula with a swollen and displaced shaft (UMZC 653 collection; scale in cm; ○ Jolyon C. Parish, December 2008).

Tarsometatarsus

According to Melville (1848), the *Pezophaps* tarsometatarsus found in 1786 (MNHN-F MAD6404; see Parish 2013, fig.5.37) shows evidence of "disease similar to those found in the bones of birds dying in menageries" (p.118). The bone structure is opened out along the distal part of the lateral face of the tarsometatarsus and "in a circular space one inch [= 25.4mm] beneath the proximal extremity, so that the bone is more acted upon by atmospheric agencies at thse places; and a small piece of the lower node is removed (Plate XV. Fig.2*a*, 2*b*)" (*ibid*., pp.118-119). The openings of the haversian canals are more apparent than in the normal condition; the bone surface thus has a 'granular' appearance. However, this may be due to weathering of, or damage to, the bone surface (pers. obs.).

Abel (1935) mentioned that there were two *Pezophaps* tarsometatarsi in the UMZC collection showing healed fractures. Unfortunately, Ottow (1950) did not examine these. There are a number of pathological tarsometatarsi in the UMZC 653 collection, including a male right tarsometatarsus with rugosities on the lateral and medial faces of the shaft, a left tarsometatarsus with a distal prolongation of the medial hypotarsal crest into a long slightly exostotic hook (possibly a partial ossification of the tendo m. gastrocnemius), and a right tarsometatarsus with displaced bone or a growth on the medial face of the shaft and extra bone growth on the ventral parts of the hypotarsal crests. A rounded longitudinal bulge on the lateral face of the of the shaft of a right tarsometatarsus in the same collection might represent a periosteopathy,[208] perhaps an osteoid osteoma (*sensu* Olvi *et al.* 2015b),[209] although it is uncertain whether this pathology is due to an injury (such as a fracture or damage to the periosteum; it shows some similarities to an ossified haematoma) or a neoplasm. Information from radiological or CT examination, which could shed light on the origins of these pathologies, is lacking for all these specimens.

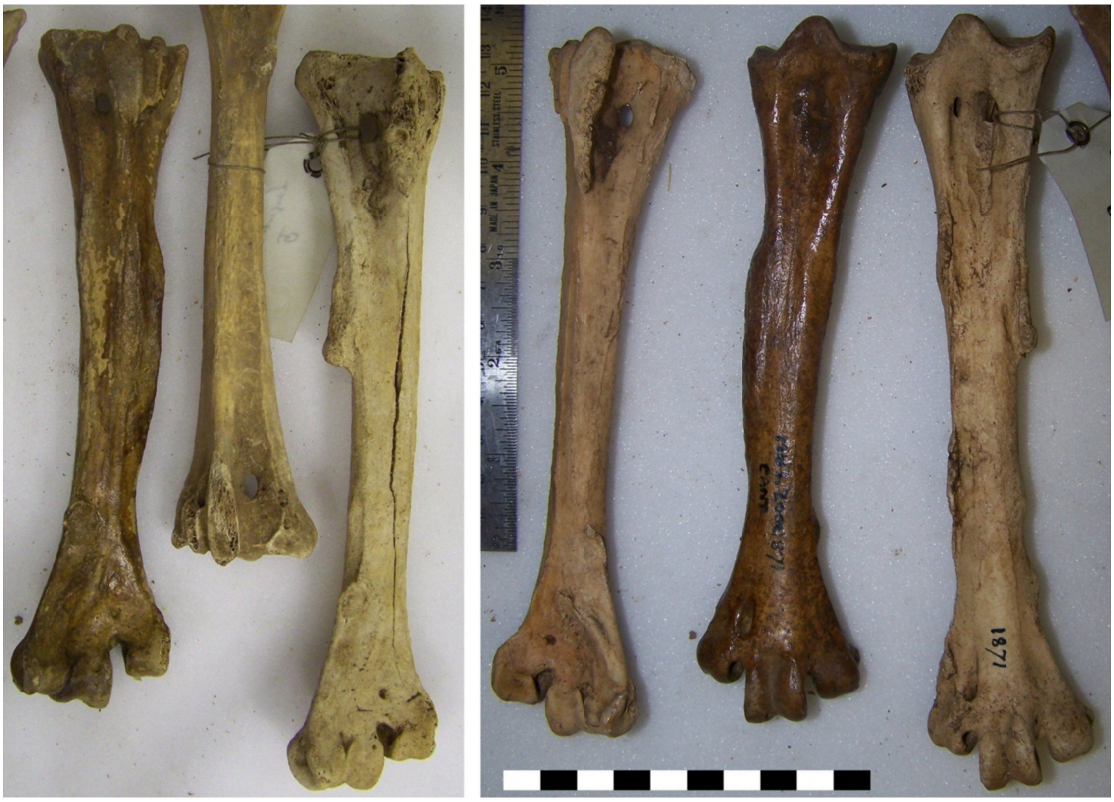

A male right solitaire tarsometatarsus with rugosities on the shaft, a right male tarsometatarsus with a swollen shaft and a left male tarsometatarsus with a distal prolongation of the medial hypotarsal crest (all UMZC 653 collection; scale in cm; ○ Jolyon C. Parish, December 2008).

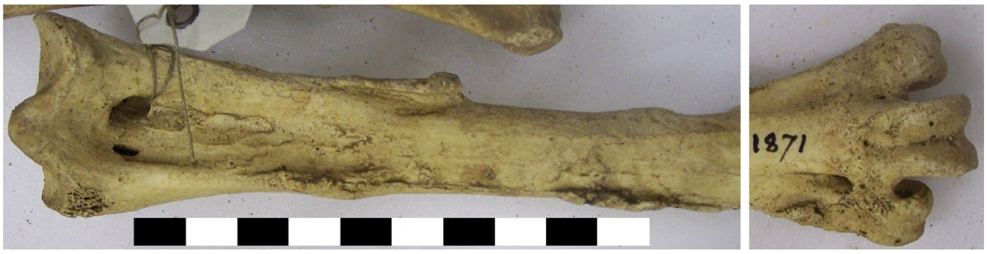

A male right solitaire tarsometatarsus with rugosities on the shaft (see above; UMZC 653 collection; scale im cm; ○ Jolyon C. Parish, December 2008).

---

[208] The swelling on the diaphysis shows some resemblance to avian osteopetrosis, although in that condition the swelling appears more extensive and is caused by a virus (see Holmes 1961, Brothwell 2002), which origin is herein considered unlikely in the case of the solitaire.

[209] An osteoid osteoma is a well-defined osteoma where the nidus is less than 2cm across and is surrounded by sclerosis, which can be quite extensive. In humans it is more common in males than females (2-3:1) and usually occurs in long bones (femur, tibia and humerus, but also in metacarpals, metatarsals and phalanges), usually in the the cortex or subperiosteal region of the metaphysis or diaphysis (Olvi *et al.* 2015b).

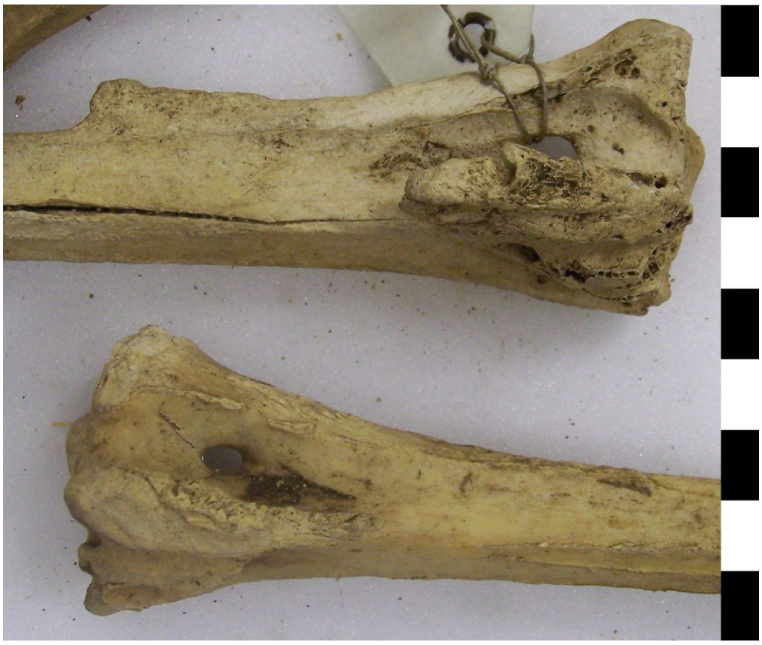

Top: a right solitaire tarsometatarsus with rugosities on the medial crest of the hypotarsus and a growth on the medial face of the shaft, *bottom*: a left solitaire tarsometatarsus with rugosities on and elongation of the medial hypotarsal crest (both UMZC 653 collection; scale in cm; ○ Jolyon C. Parish, December 2008).

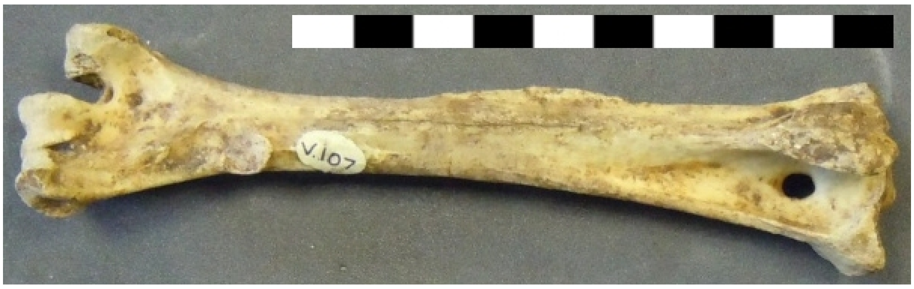

Left female solitaire tarsometatarsus with a pathology on the lateral face of the shaft (GLAHM V107; scale in cm; © The Hunterian, University of Glasgow 2013).

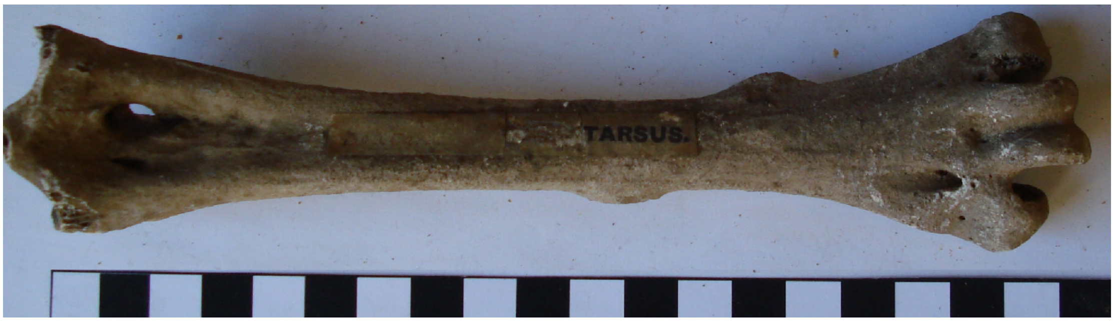

Right male solitaire tarsometatarsus with a pathology on the lateral face of the shaft (Natural History Museum, Dublin; scale in cm; © David Gonzalez).

Pedal phalanges

A hallux (proximal phalanx and ungual) of *Raphus* in the collection of Etienne Thirioux shows a possible pathology, with "some exostoses after injury" according to Hans Gadow (see Transcriptions: Thirioux-Newton Correspondence, 28th February 1901).

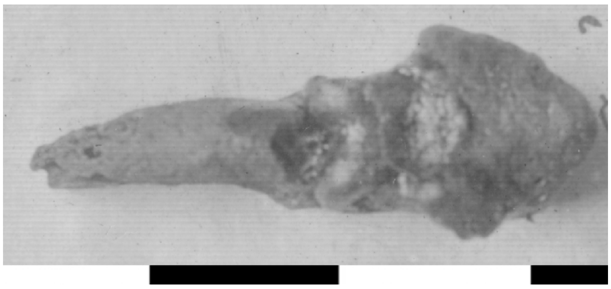

A hallux (proximal phalanx and ungual) of *Raphus* in the Thirioux collection showing a possible pathology (photograph (13A) accompanying a letter from E. Thirioux to Alfred Newton, dated 31st January 1901; scale in cm (Thirioux stated that the images were very close to natural size); © UMZC).

A pedal phalanx of *Pezophaps* from the NHMUK collection examined by Ottow (1950) showed what he considered to be dysplastic-exostotic changes to its distal half (*ibid*., pl.vi, fig.17). An anterior pedal phalanx (Zoologisches Museum, Kiel, specimen, position and sex undetermined), 2.3cm long, was described by Ottow (1952). It had a flat, wart-like exostosis, 1.5 x 1.0cm, on its upper surface and also what he considered to be a slight dysplasia (figured: Ottow 1952, fig.2).

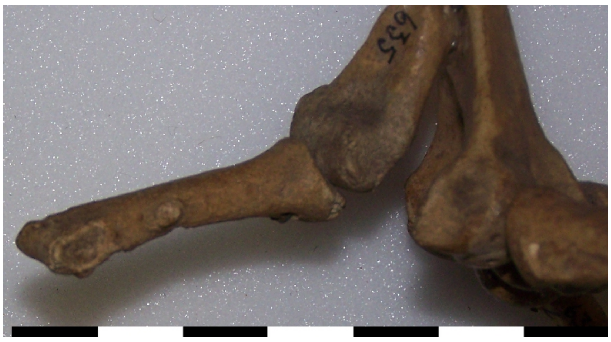

Pes of a female solitaire (UMZC 635) with a small exostosis on the medial face of phalanx 1 of the hallux (scale in cm; ○ Jolyon C. Parish, December 2008).

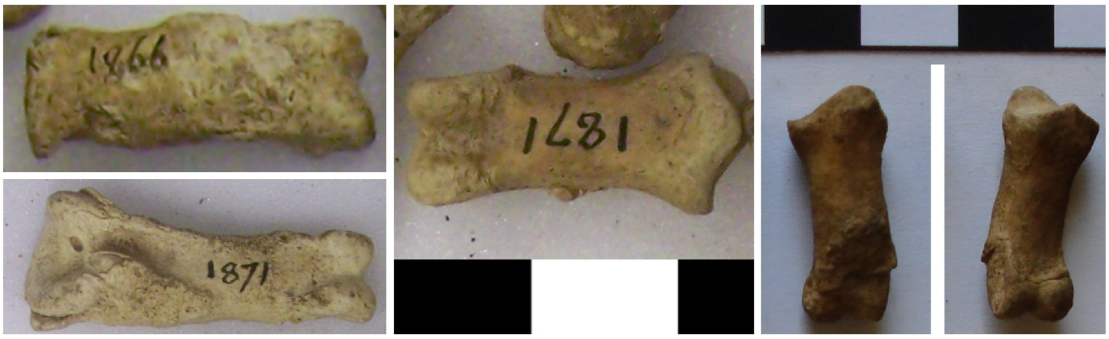

Pathologic solitaire pedal phalanges. *Left* and *middle*: UMZC 653 specimens (*bottom left*: cf. proximal phalanx of left digit II; *middle*: pedal phalanx bearing a small wart-like exostosis) (○ Jolyon C. Parish, December 2008); *right*: solitaire pedal phalanx with a pathology on the dorsal surface, dorsal and ventral views (Natural History Museum, Dublin; © David Gonzalez). Scales in cm.

A pedal phalanx with a large exostosis was also figured by Lüttschwager (1961, fig.18). A number of pedal phalanges in the UMZC 653 collection display exostotic development. Small, round exostoses, such as that seen in UMZC 635 (on the medial face of phalanx 1 of the left hallux), may represent osteoid osteomas ("button osteoma"). Infections, perhaps related to injuries sustained during intraspecific combats or from bones weakened by calcium deficiency, might also be responsible for the some of the pathological deposits of bone around joints seen in some specimens.[210]

---

[210] Deposition of extra bone around joint areas is present in specimens of *Buteo buteo* and *Gallinula chloropus* in the author's collection (a.164 and a.23 respectively). Affected areas include the distal humerus, acetabulum and

Appendix: Osteological material of *Pezophaps* examined by Ottow (1950) (see Catalogue of Specimens for further details):

1) A lower extremity lacking the fibula and toes in the Vertebrate Department of the Swedish Museum of Natural History in Stockholm (derived from UMZC material).
2) Two assembled front extremities lacking phalanges as loans from the UMZC.
3) 71 single exostotic and 'dysplastic' bones of the front extremities, also on loan from Cambridge: one scapula, two coracoids (one ♂, one ♀), one humerus (♂) (although Ottow later (p.12) mentioned two ♂ humeri), fifteen ulnae, thirty radii and 22 carpometacarpi. These specimens included the right wing of UMZC 634.
4) 38 single exostotic and 'dysplastic' bones on loan from the BMNH (now NHMUK): one cranium (76.1.28.11), one mandible, five ribs (one proximal fragment of vertebral rib, four sternal ribs: three ♂, one ?♀), one synsacrum (A.1441), one scapula (♀, distal portion, encrusted), one coracoid (♀), two humeri (both ♀), three radii, eight ulnae, eleven carpometacarpi, two pelves, one fibula (probably ♀) and one pedal phalanx.
5) An almost complete skeleton ("PMU A451") in the Museum of the Palaeontological Institute in Uppsala (Museum of Evolution, Uppsala University).

Some of the bones examined by Ottow still possessed calcareous encrustations from the cave deposits where they were found. He was not able to remove the encrustation from bones on loan and so he preferentially selected bones without encrustation for photographs and radiographs.

Histology

(*Raphus*: Hume 2005, figs.5a, 6a-6b; Steel 2006, fig.3; Rijsdijk *et al*. 2015, fig.7C, D; Angst *et al*. 2017, figs.1-5. *Pezophaps*: Hume 2005, figs.5b, 6c-6d)
See Parish (2013, pp.261, 359, 368-369) for further details.

As in living birds, the cortices of the bone diaphyses of *Raphus* comprise three layers: an outer layer of weakly-vascularized or avascular bone (Outer Circumferential Layer; OCL), a middle layer of fibrolamellar bone, and an inner layer of lamellar bone which was deposited more slowly (Inner Circumferential Layer; ICL) (Angst *et al*. 2017). Both the OCL and ICL contain lamellar bone, which develops more slowly than the tissue of the fibrolamellar bone layer which is deposited rapidly. The former usually develops after the latter, after sexual maturity has been reached (*ibid*.). The histology of *Raphus* differs from that of palaeognaths such as *Casuarius*, *Rhea* and *Struthio* in that the fibrolamellar layer only forms around a third of the cortex, whereas in the former it comprises most of it due to slower growth rates.

Lorna Steel, of the NHMUK, studied the histology of *Raphus* and *Pezophaps* (Steel 2006, 2009). She found that the femur and tibiotarsus of *Raphus* "are composed of rapidly-growing fibrolamellar bone, as is typical of most extant birds [and] do not contain lines of arrested growth, or any growth marks. However, all regions of the cortex are heavily reworked by secondary osteons" (Steel 2009, p.185A). She also found that the hindlimb elements of *Pezophaps* comprise fibrolamellar bone, but display growth marks and lack secondary osteons. Furthermore, she predicted histological differences between the paedomorphic forelimb elements and peramorphic hindlimb elements and possible differences between male and female *Pezophaps*.

Two specimens studied by Angst *et al*. (2017) showed medullary bone: a femur (MAS 39590 CH6-2) and a tibiotarsus (MAS), the medullary bone projecting from the ICL into the medullary cavity – in the former specimen it was approximately 1.5% cortical thickness and sparse, in the latter it was approximately 4.5% cortical thickness. The differences in the amounts of medullary bone between the specimens was suggested by Angst *et al*. to be due to either differences between the bones[211] or due to

---

antitrochanter, and distal tarsometatarsus.

[211] Such differences could include the femur perhaps being more pneumatic than the tibiotarsus, as suggested by the large pneumatic formen on its proximal cranial face and pneumatic foramina elsewhere on the bone (pers. obs.).

the individuals being at different stages in their reproductive cycles: that with less medullary bone being one that had utilized the calcium for making eggshell.

Other specimens examined by Angst *et al.* showed resorption cavities.[212] The resorption cavities were present in the endosteal cortex and occupied 0.01mm^2-0.98mm^2 (0.1-5.9% total bone area). In a number of the larger cavities there was an inner deposit of lamellar bone. The large resorption cavities were suggested to be due to the need for additional calcium, perhaps during periodic moulting. In the specimens with large resorption cavities there are thin lamellar deposits after the last LAG (Line of Arrested Growth) of the OCL which Angst *et al.* considered to be further evidence that moulting began just after the austral summer (see below). In addition there is a significant amount of secondary reconstruction, with numerous secondary osteons. Two tarsometatarsi (Muséum d'Elbeuf collection) displayed significant secondary reconstruction, which had obscured the tripartite layer distinction of the cortex. Angst *et al.* speculated that this could be related to biomechanical adaptations or maybe to the tarsometatarsi being calcium reservoirs.

Specimens[213] from more mature individuals showed a well-developed OCL (7-29% of cortical thickness), and ICR (14-51% cortical thickness) frequently with evidence of endosteal resorption.

Lines of Arrested Growth (LAGs) were also present in some of the specimens examined by Angst *et al.* Specimens[214] attributed to individuals in their first year post sexual maturity showed one LAG and the start of the development of the OCL (comprising 5-20% of cortical thickness). In addition, they showed a well-developed ICL (15-35% of cortical thickness) and evidence of endosteal resorption. Such LAGs may be attributed to reduced food resources during the cyclone season in the summer (November-March) (Angst *et al.* 2017). LAGs have also been reported for moa (Turvey *et al.* 2005).

Angst *et al.* stated: "Assuming that the bone deposition rate is constant between consecutive LAGs, we propose that the thicker the bone deposition between two LAGs, the more time has lapsed since the LAG formed, thereby giving an indication of when the breeding or molting event occurred" (p.7). Examining those specimens with medullary bone, they assumed that as the thickness of bone deposited in the OCL after the last (outermost) LAG was around half that deposited between the previous two LAGs, and as the LAGs are assumed to have formed annually, that the time that had elapsed since the last LAG was six months. Thus, they assumed that the medullary bone (indicative of the breeding season) was deposited six months after the austral summer.

The occurrence of a number of LAGs in the OCL indicate that the dodo had an extended period of growth until reaching skeletal maturity. Protracted growth rates have also been recorded for other insular bird species, such as moa (Turvey *et al.* 2005), aepyornithids and kiwi (Chinsamy *et al.* 2020). Chinsamy *et al.* (2020) noted that in the absence of predators and/or with limitations on food resources, birds can resort to flexible plesiomorphic growth dynamics, with periods of interrupted growth.

Protracted growth might be related to variable fusion of elements in *Raphus*, with elements such as the scapula and coracoid fusing in some individuals but not others. The variation in fusion might suggest that this extended growth period might have had variable termination, with growth terminating earlier in some individuals (lacking fusion of certain elements) than others. This might also be the case in *Pezophaps* (see the section on Juveniles). The lack of secondary osteons noted by Steel (2009) in *Pezophaps* might be linked to the 'juvenile' (*i.e.*, comparatively smooth and unsculptured) appearance of the bones, with little or no secondary reworking of the bone occurring, or could have another explanation.

---

[212] Femur: Omnicane, cave specimen. Tibiotarsi: Muséum d'Elbeuf, MAS.

[213] Femur: Muséum d'Elbeuf. Tibiotarsi: FLMR R2071 (Omnicane), MAS 39589 CH6-1, MAS, Muséum d'Elbeuf (Angst *et al.* 2017).

[214] Humerus: MAS. Femora: MAS1 - P14964, MAS 39590 CH6-2, MAS no number; Muséum d'Elbeuf. Tibiotarsus: MAS (Angst *et al.* 2017).

Musculature and Other Non-osteological Anatomy

The following is a brief description of the muscles of the dodo, with areas of origin and insertion given. The description is mainly limited to muscles where the attachment can be seen on the bone (as an impression, tubercle, *etc*.) and is based on the musculature of other pigeons (data from dissections of *Columba palumbus* and the literature), and it is herein assumed that the dodo had a similar myology.

The skull and foot of *Raphus* (OUMNH 11605) were described in detail by Melville (1848). Melville was writing shortly after the dissection of these elements (see Parish 2013, pp.218, 219) and as such may have had information as to the muscle, ligament and other soft-tissue attachments of the bones. He also softened the tissues of the head of OUMNH 11605 (see Parish 2013, pp.215-216), which might have yielded additional information.

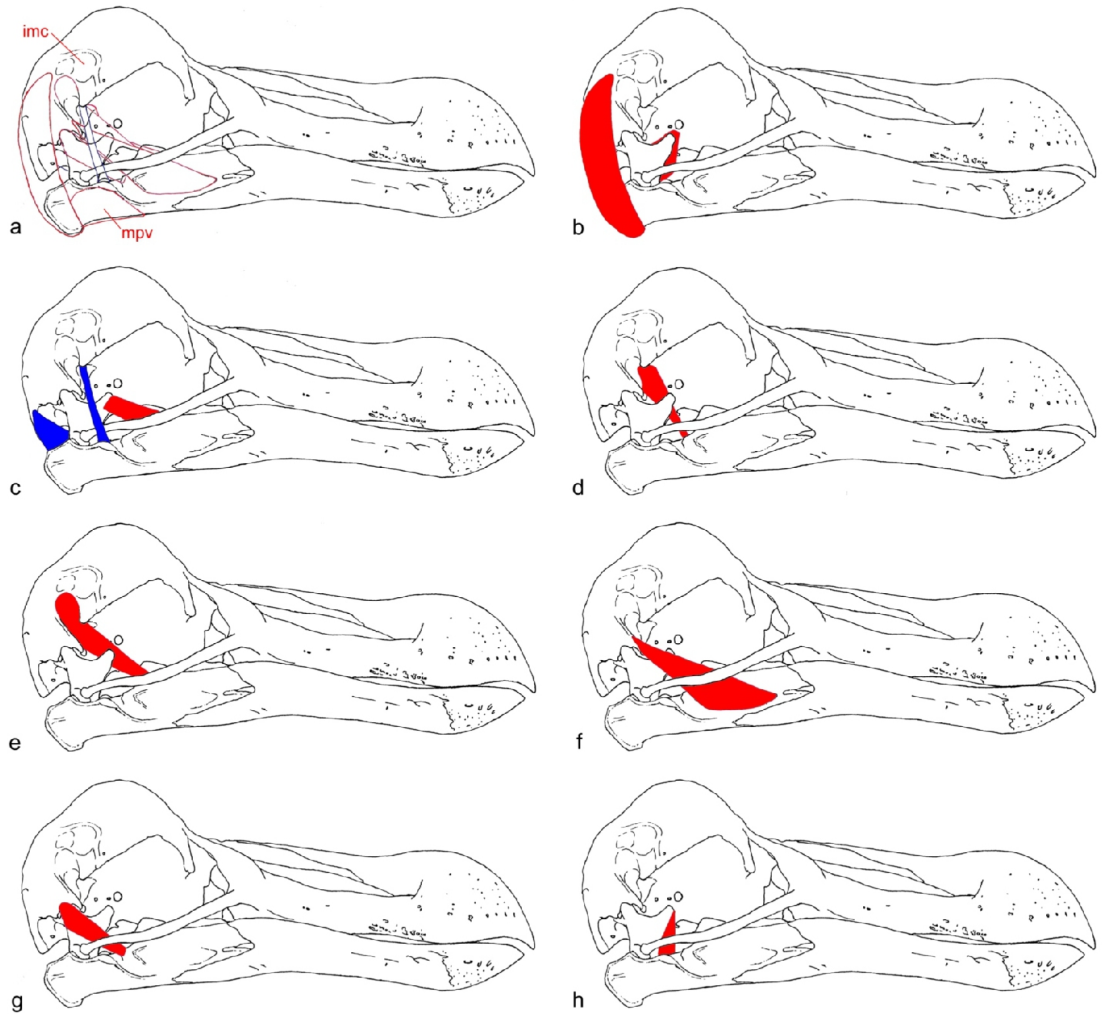

Reconstructed jaw musculature of *Raphus*. a: jaw muscles in outline (see below); b: m. depressor mandibulae and m. protractor pterygoidei et quadrati ; c: m. pseudotemporalis profundus, ligaments (blue): lig. occipitomandibularis and lig. postorbitalis ; d: m. pseudotemporalis superficialis ; e: m. adductor mandibulae externus superficialis ; f: m. adductor mandibulae externus medialis ; g: m. adductor mandibulae externus profundus; h: m. adductor mandibulae posterior (○ Jolyon C. Parish, 2020).

The nomenclature for jaw and lingual musculature primarily follows that of Jones *et al*. (2019) and Bhattacharyya (1989). Reference was also made to Korzun *et al*. (2008), Bhattacharyya (1994), Vanden Berge & Zweers (1993), Van Gennip (1986), Burton (1974), Kuroda (1971), Merz (1963) and Rooth (1953). For biomechanics and cranial kinesis Bock (1960, 1964) and Witmer & Rose (1991) were consulted. Cracraft (1971) provided information on hindlimb musculature and arthrology. An attempt has been made to give the modern synonyms of the muscles and other soft-tissues mentioned by Melville (1848) and others.

The muscle reconstructions figured herein are simplistic due to lack of data (the absence of soft-tissue specimens of *Raphus* and *Pezophaps*, although some soft-tissue does still adhere to the Oxford (OUMNH 11605) and Copenhagen (ZMUK AVES-105485) specimens of the dodo) and the interspecific and intraspecific variation found in Columbidae.

Skull Musculature and Other Soft Tissue

M. depressor mandibulae (m. d. m.). The attachment area of m. d. m. pars superficialis (the digastric muscle of Melville 1848) lies in the caudal part of the parieto-squamosal region (Melville 1848). Its attachment area on the skull is vertically rhomboidal in outline. Its caudal border is separated from the transverse nuchal crest by a narrow area, its rostral border is separated from the temporal notch and the origin of m. a. m. e. superficialis by a narrow area, and its dorsal and rostral extremity touches the caudal margin of the origin of m. cucullaris capitis. Its transverse width is less than a quarter of that of the cranium. Its dorsal and rostral attachments were on crests (C5 and C7 of Van Gennip 1986); these can seen on both the Oxford (OUMNH 11605) and Copenhagen (ZMUK AVES-105485) skulls. In *Pezophaps* the caudodorsal margin of the attachment area is usually marked by a crista (see NHMUK A.1375; Newton & Newton 1869, pl.xxii, fig.149). Pars superficialis inserted on a well-defined crest on the curvature of the caudolateral end of the retroarticular process of the mandible (crest M2 of Van Gennip 1986). This attachment area evidently curved round onto the ventral edge (M4 of Van Gennip 1986) of the caudal end of the mandible, as seen in OUMNH 11605. M. d. m. (the Biventer maxilla muscle of Melville 1848) was also attached to the rough, flattened lateral edge of the paroccipital process, the ala tympanica (Melville 1848). The prominent retroarticular process of the mandible suggests that m. depressor mandibulae was well developed.

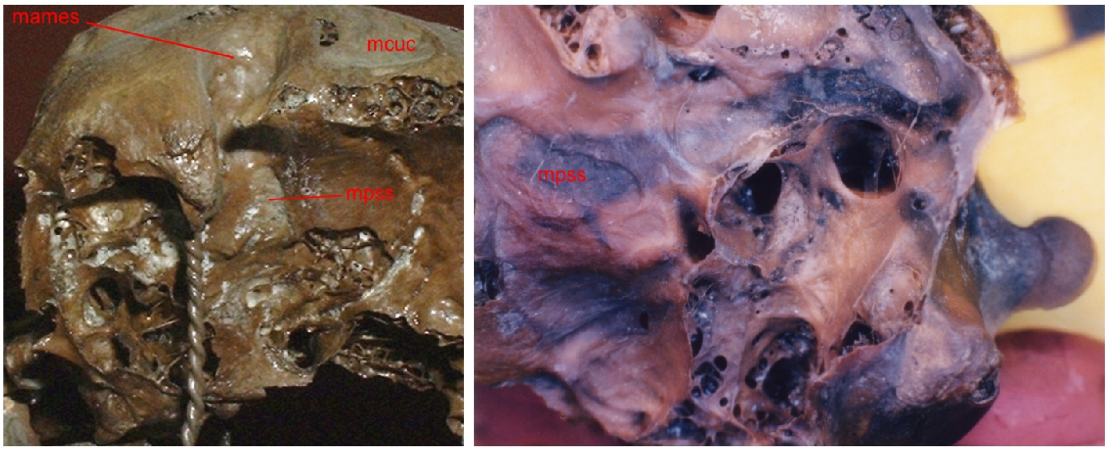

Muscle attachment areas on the cranium of *Raphus*. *Left*: NHMUK A.9040, right side; *right*: NHMUK A.1338, left side (○ Jolyon C. Parish).

M. protractor pterygoidei et quadrati (M. Levator ossi quadrati of Melville 1848). In extant columbids m. protractor pterygoidei originates from the junction of the parasphenoidal rostrum and the interorbital septum, and m.protractor pterygoidei originates from the caudal wall of the orbit medial to the trigeminal nerve foramen and the origin of m. pseudotemporalis superficialis, extending to the rostrovental border of the optic nerve foramen (Merz 1963). In both *Raphus* and *Pezophaps* (NHMUK A.3505, A.3506) there is a distinct depression ventral to the optic foramen (II) and extending caudally to the area ventral to the ophthalmic nerve foramen (V_1), medial to the origin of m. pseudotemporalis superficialis, which was probably for the attachment of m. protractor pterygoidei. In OUMNH 11605 the rostral margin of the triangular attachment area of m. protractor pterygoidei et quadrati lies just caudoventral to the optic foramen, and it extends "over the tympanic convexity, surrounded by a smooth depressed marginal tract of the latter" (Melville 1848, p.83). **Insertion**: in extant columbids m. protractor pterygoidei inserts on the dorsolateral and dorsal surfaces of the caudal half to third of the pterygoid, caudal to the basipterygoid process (Bhattacharyya 1989, Merz 1963, Rooth 1953) and m. protractor quadrati (m. proctaractor quadrati of Janoo 1997) inserts in a depression (depressio protractoris) which deepens into a fossa (fossa basiorbitalis) on the medial face of the quadrate and on a curved crista, running from the otic process to the base of the orbital process, marking its ventral margin. In *Pezophaps* there is a crista on the medial face in this position (NHMUK A.1373; Newton & Newton 1869, pl.xxii, fig.164), which may have provided attachment to m. protractor quadrati. Melville (1848) stated that the insertion of the "M. Levator ossis quadrati" in *Raphus* was located in a "tripartite fossa" on the medial surface of the quadrate, which is "deepest inferiorly, rough throughout; and obliterated towards the extremity of its anterior angle by the expansion of the diploe of the orbital process" (p.95). A deep fossa, the fossa basiorbitalis, is present on the medial face of the quadrate (UMZC 415.KK; Claessens *et al*. 2015, fig.12).

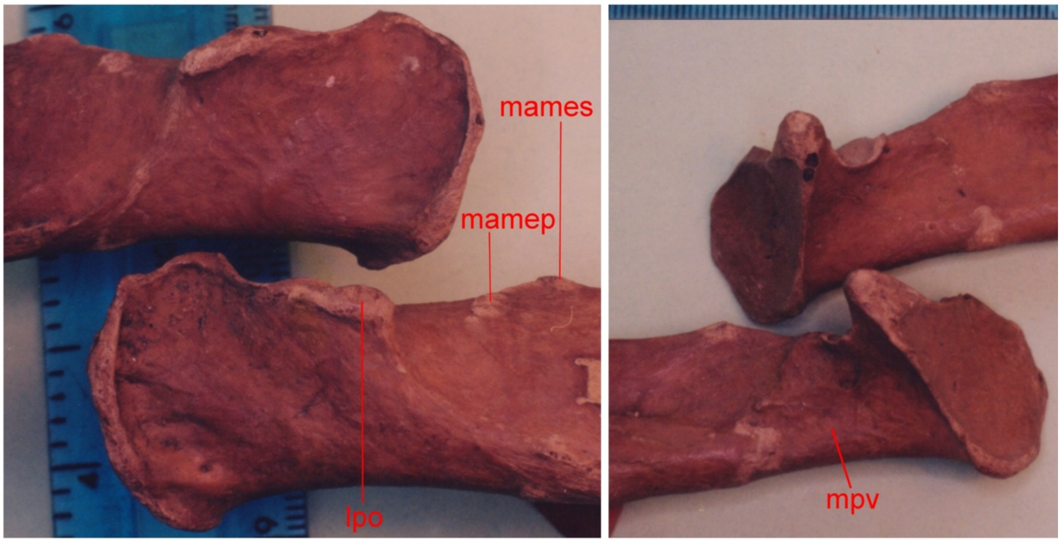

Muscle attachment areas on the proximal end of the mandible of *Raphus*, NHMUK A.1840. *Left*: lateral views; right: medial views (scale in mm). ○ Jolyon C. Parish.

M. pterygoideus. The "internal pterygoid" muscle of Melville (1848) corresponds to the m. pterygoideus (see Merz 1963). Describing OUMNH 11605, Melville (1848) stated that "an oblique line, directed forwards and inwards from the convexity of the crest [crista lateralis] to its inner margin anterior to the subsidence of the palatine process [= crista ventralis], defines the fossa between the crest and the palatine process, which gives attachment to the fleshy fibres of the *internal pterygoid*; the depressed tract on the anterior part of the crest, gives attachment to the tendon of that muscle; its fleshy fibres also arise from the fossa between the nasal process [= crista dorsalis] and crest, which is concave vertically and convex horizontally" (p.94).

Regarding the insertion of the muscle, he noted that the "pitted surface on the inner aspect of the jaw, for the attachment of the *M. pterygoideus internus* is defined anteriorly by an oblique irregular ridge, commencing at the upper edge a little anterior to the [quadrate-mandibular] articular surface, and descending obliquely forwards to a groove, directed obliquely inwards and forwards, across the lower edge of the angular, from the extremity of the dentary to that of the opercular [= splenial]; it extends backwards on the anterior aspect of the inner angle [= medial mandibular process]" (p.96).

M. perygoideus dorsalis anterior. **Origin**: from the dorsolateral surface of the palatine (Jones *et al*. 2019). **Insertion**: via an aponeurosis on the medial surface of the mandible (Van Gennip 1986). A horizontal crista seen in NHMUK A.1840 may mark the site of attachment.

M. perygoideus dorsalis medialis. **Origin**: from the dorsolateral surface of the pterygoid for most of its length (Jones *et al*. 2019, Bhattacharyya 1989). A shallow fossa on the dorsolateral face of the pterygoid in *Raphus* (UMZC 415.KK) and *Pezophaps* (NHMUK A.1454) may have provided attachment for this muscle. **Insertion**: on the medial surface of the mandible, between the insertion areas of m. pseudotemporalis profundus and the quadrate-mandibular articulation (Jones *et al*. 2019).

M. pterygoideus ventralis. **Origin**: from the ventrolateral surface of the palatine (Bhattacharyya 1989). **Insertion:** on the ventral part of the medial face of the caudal portion of the mandible (Van Gennip 1986), continuing along the rostromedial surface to the tip of the medial mandibular process and also extending onto the lateral face of the caudal end of the mandible (Burton 1974, Bhattacharyya 1994, Korzun *et al*. 2008). In NHMUK A.1840 there is a distinct vertical ridge on the ventral part of the medial face of the mandible, caudoventral to the coronoid process. This may have been for the attachment of m. pterygoideus ventralis.

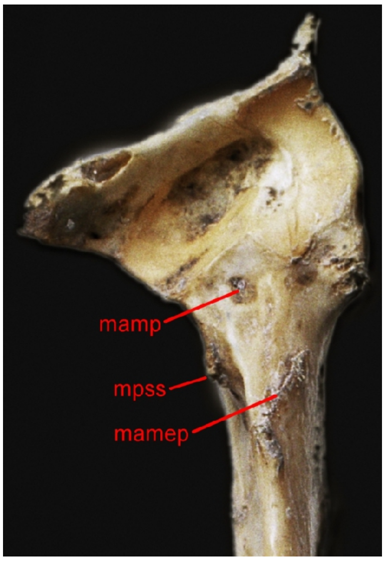

Muscle attachment areas on the proximal end of the mandible of *Raphus*, Copenhagen specimen (ZMUK AVES-105485; © Harri Kallio.

M. pseudotemporalis superficialis. **Origin**: the well-defined attachment area of m. pseudotemporalis superficialis (the internal temporal impression of Melville 1848) lies medial to the origin of m. a. m. e. pars profundus, separated from it by a slight ridge (C13 of Van Gennip 1986). It has the approximate form of a right-angle triangle. The hypotenuse of this triangle, corresponding to the ridge between the origin of m. a. m. e. pars profundus and m. pseudotemporalis superficialis, undulates to the base of the postorbital process. Ventrally it descends towards the maxillomandibular foramen. The attachment site can be seen clearly in both *Raphus* (NHMUK A.1338) and *Pezophaps* (NHMUK A.1375, A.1441). **Insertion**: on the tuberculum pseudotemporale (Baumel & Witmer 1993), located on the medial surface of the rostrodorsal edge of the supra-angular, just caudal to the coronoid process at the base of the medial mandibular process. The mark of the attachment can be seen in the Copenhagen skull.

M. pseudotemporalis profundus (External pterygoid muscle of Melville 1848; muscle ptérygoïdien externe of Janoo 1997). **Origin**: from the ventral and lateral surfaces of the orbital process of the quadrate. The lateral surface of the orbital process of OUMNH 11605 is minutely pitted for m. pseudotemporalis profundus (Melville 1848) except for a narrow area beneath the apex extending caudally along the dorsal margin. The rostrolateral part of the orbital process of the same specimen shows the probable remnants of this attachment. A distinct curved ridge (crista orbitalis) can be seen in Newton & Newton's figure (1869, pl.xxii, fig.163) of the quadrate of *Pezophaps* on the lateral face of the end of the orbital process, extending caudoventrally. **Insertion**: in *Treron* and *Ducula* there are two slips of insertion, an inner and an outer one (Bhattacharyya 1989), whereas in *Otidiphaps* and *Didunculus* there is only an inner one (Burton 1974, Korzun *et al*. 2008). The insertion site of the inner slip of m. pseudotemporalis profundus in OUMNH 11605 is a concave pitted area along the dorsomedial and medial surface of the supra-angular, within the fossa aditus canalis neurovascularis, rostrodorsal to the insertion of m. pterygoideus ventralis lateralis (Melville 1848). The rostral end of the attachment area diminishes to a groove leading to the caudal margin of the mandibular fenestra and the caudal part extends dorsally to the coronoid process (*ibid.*). The outer slip, if present, may have covered the lateral surface of the supra-angular. It appears to have inserted in a slight impression, seen in OUMNH 11605 and also Newton & Newton's figure (1869, pl.xxii, fig.159) of the mandible of *Pezophaps*, extending rostrally to a point just behind the fenestra mandibularis. Caudally the muscle would have overlapped the insertion of m. a. m. e. medialis. If the outer slip of m. pseudotemporalis profundus was not present then m. a. m. e. medialis would have probably occupied the above-mentioned impression.

M. adductor mandibulae externus (M. a. m. e.). M. temporalis of Melville (1848) probably corresponds to part of the m. a. m. e. complex. **Origin:** from the postorbital process and the deep part of the temporal fossa of the braincase. In *Pezophaps* (NHMUK A.3506) a small sub-oval rugosity on the lateral surface of the squamosal, just caudodorsal to the zygomatic process and dorsal to the squamosal head of the quadrate, and also a tubercle on the distal end of the zygomatic process, might have provided attachments for parts of m. a. m. e.

M. a. m. e. superficialis (the crotophyte muscle of Melville 1848). **Origin**: the deep part of the temporal fossa. The rostral margin of the sub-crescentic attachment area lies on the caudal part of the postorbital process. Melville (1848) noted that "the size of the *crotophyte impression* [for m. a. m. e. superficialis], although variable in different species, according to the resistance to be overcome, is very minute when compared with that in the Vulturidae, or even Cathartes; in the Dodo it is exceedingly small, and is not compensated by an increase in the area of the internal temporal surface" (p.74). **Insertion**: the muscle aponeurosis inserted on the coronoid process of the mandible. A distinct rugosity can be seen on the coronoid process of *Raphus* (NHMUK A.1840), which may have provided attachment for m. a. m. e. superficialis.

M. a. m. e. medialis. **Origin**: from the zygomatic process. NHMUK A.1338 (*Raphus*) shows a subtriangular roughened area on the laterodistal part of the zygomatic process, which may have provided attachment for m. a. m. e. medialis. *Pezophaps* does not possess a developed zygomatic process, but there is a tubercle in this region (see also lig. zygomaticomandibulare, below). **Insertion**: on the lateral surface of the mandible, ventral to the coronoid process. OUMNH 11605 shows an angular crista (crista paracoronoidea; Weber & Hesse 1995), with a horizontal dorsal portion and a rostroventrally directed caudal portion, which may have provided an attachment site for this muscle.

M. a. m. e. profundus. **Origin**: from the dorsolateral part of the rostrolateral face of the quadrate (Jones *et al*. 2019). In *Ducula* some muscle fibres also originate from the caudolateral wall of orbital-tympanic part of the cranium, ventral to the zygomatic process (Bhattacharyya 1989). **Insertion**: via an aponeurosis attached to a crista on the rostrodorsal edge of the articular bone of the mandible, rostral to the articular surface for the quadrate. This crista is more distinct in *Raphus* than in *Pezophaps*. The attachment site is visible in the Copenhagen skull.

M. a. m. posterior. **Origin**: in *Ducula* from the rostral, rostrolateral and rostroventral surfaces of the quadrate, extending from the orbital process to the margin of the lateral condyle of the quadrate at its articulation with the mandible (Bhattacharyya 1989). In a specimen of the quadrate of *Pezophaps* (NHMUK A.1373) there is a ridge on the medial face of the orbital process, near to and parallel with its rostroventral border, which may have provided attachment for m. a. m. posterior (alternatively it may have been for m. pseudotemporalis profundus). **Insertion**: within the fossa rostralis articularis of Bhattacharyya (1989) of the rostromedial part of the articular and the caudomedial part of the supra-angular of the caudodorsal end of the mandible.

M. stylohyoideus, m. serpihyoideus. These muscles may correspond to the muscles of the tongue mentioned by Melville (1848, p.96), which were attached to a triangular, concave and deeply pitted surface, bounded rostrally by a rostroventrally directed ridge, separating it from the attachment area of m. a. m. e.[215]

M. genioglossus. **Origin**: from the inner mediodorsal aspect of the mandibular symphysis on either side of the mandibular line. The mandibles of *Raphus* (for example UMZC 415.K) and *Pezophaps* (for example NHMUK 76.1.28.12) show a depression on either side of the midline at the caudal part of the mandibular symphysis which might have provided attachment for m. genioglossus.

M. cucullaris capitis (dermomastoideus muscle of Melville 1848). **Origin**: from the pyriform impression on the dorsolateral surface of the cranium,[216] rostrodorsal to the origin of m. a. m. e. superficialis. This depression is deeper and larger rostrally. Its apex is truncated in line with the caudal margin of the temporal notch (which lies between the postorbital and zygomatic processes). Melville (1848) stated that this sub-pyriform area was probably for the origin of the ‘dermo-mastoideus,’ a cutaneous muscle “inserted into the integument of the posterior surface of the neck” (p.86). Owen (1848a) stated that the temporal fossa extends above the postorbital process (his postfrontal) “and forms there a reniform depression, either for a gland, or what is less likely, for a co-extension of the origin of the temporal muscle” (p.4). Anwar Janoo (pers. comm., 1998) has suggested that this impression is indeed for an extension of the temporal musculature, as it seems too deep and extensive to be for a cutaneous muscle. However, several features suggest that this impression is actually for the attachment of dermal musculature. First, it is in the same location as the origin of m. cucullaris capitis in other columbids[217] and second, its rostroventral margin is separated from the orbital rim by a “narrow scabrous tract” (Melville 1848, p.86), which appears not to have had musculature attached to, or running over, it. Thus, a mandibular muscle originating from this fossa would have to curve around the postorbital process rather than passing over it. In *Pezophaps* the origin of m. a. m. e. is expanded, with its rostral extremity passing dorsal to the postorbital process. The attachment of m. cucullaris capitis appears to form a narrow area rostral and dorsal to the origin of the mandibular musculature. The margins of these attachment areas are marked by a well-defined ridge, the crista temporalis, which shows a varying degree of development (compare Owen 1879, pl.v, fig.1 with NHMUK A.3506), although is generally more prominent than in *Raphus*. **Insertion**: the muscle would have fanned out and inserted on the deep part of the skin of the neck. Its purpose was to raise the feathers of the head and neck, “and push forwards the hood-like cutaneous ridge” (Melville 1848, p.86).

M. rectus capitis ventralis (Recti capiti antici muscles of Melville 1848). **Origin**: from the ventral surface of the atlas and hypopophyses of several succeeding cervical vertebrae (George & Berger 1966). **Insertion**: pars medialis was attached to the rostral part of the basisphenoid plate. Pars lateralis inserted on the lateral surface of the basitemporal plate. Melville (1848, p.79) stated that “the insertion of the fleshy fasciculi of the *Recti capitis antici* muscles” was in a lozenge-shaped concavity on the basisphenoid, deepened caudolaterally adjacent to the rostral surface of the lateral basilar tubercle.

M. rectus capitis dorsalis (M. recti capitis laterales majores of Melville 1848). **Origin:** from the craniolateral surface of the atlas and the costal processes of the transverse processes of C1-C6 (Snively & Russell 2007; Jones *et al.* 2019). **Insertion**: on the basilar tubercles of the basicranium (Baumel & Witmer 1993; Snively & Russell 2007). Melville (1848) stated that “the basilar protuberances [were] for the insertion of the *M. recti capitis laterales*” (p.97). The lateral and medial basilar tubercles provided attachment for lateral and medial parts of the aponeurosis of insertion of m. rectus capitis dorsalis respectively (see Zusi 1962). The attachment of the m. rectus capitis dorsalis muscles on the basilar tubercles can be seen in OUMNH 11605.

---

[215] “An elongated tubercle extends downwards and forwards from the centre of the outer projecting border of the external segment of the articular surface, and its anterior angle is prolonged into a ridge, passing forwards to the extremity of the lower dentary limb. The outer surface of the posterior segment is thus divided diagonally, into two subequal surfaces; the posterior of which is triangular, most concave, and deeply pitted; it gives attachment to the muscles of the tongue, while the anterior furnishes insertion to the *M. temporalis* [= m.a.m.e. externus]” (p.96).

[216] This impression is part of the fossa temporalis of Baumel & Witmer (1993)

[217] See Martin (1904, figs.B-F) for an illustration of the m. temporalis in several columbid species.

Lig. occipitomandibulare. Lig. occipitomandibulare connects the cranium with the dorsal margin of the caudal face of the mandible. On the cranium it attaches to the rostral edge of ala tympanica (Van Gennip 1986). In OUMNH 11605, on the ventral part of the squamosal dorsal to the quadrate, is a slight crista, which was probably either for the attachment of either m. d. m. medialis or lig. occipitomandibulare. Part of the occipitomandibular ligament can still be seen in OUMNH 11605, connecting the ventromedial edge of the paroccipital process with the caudodorsal edge of the medial mandibular process.

Lig. postorbitale. Lig. postorbitale runs from the postorbital process to the dorsolateral side of the lateral process of the mandible; it passes on the lateral side of the jugal arch, to which it also attaches (Van Gennip 1986). Lig. postorbitale was well-developed in *Raphus*. The mandible shows a distinct tubercle for the attachment of the postorbital ligament rostrolateral to the articulatory fossa for the quadrate.

Lig. **zygomaticomandibulare** (external mandibular ligament of Melville 1848?). This ligament extends from the zygomatic process to the coronoid process of the mandible (Baumel & Witmer 1993). Describing OUMNH 11605, Melville (1848) stated that the outer edge of the zygomatic process is rough and provided attachment for the "external mandibular ligament" (p.83), and that the outer edge of the jugal arch rostral to the "the groove for the attachment of the capsular ligament [probably a jugomandibular ligament]" was covered by articular cartilage, over which the "external mandibular ligament" would have moved (p.93). However, in *Raphus* the zygomaticomandibular ligament would presumably have passed on the medial (inner) side of the jugal arch, owing to the lateral curvature of that element. It would have been the postorbital ligament which would have passed on the lateral (external) side of the jugal arch.

Membrana atlantooccipitales (posterior atlanto-occipital ligament of Melville 1848). This membrane was perforated by the v. occipitalis interna (probably the "large branch communicating with the posterior cerebellar sinus" of Melville 1848).

A. carotis cerebralis. *Raphus* and *Pezophaps* likely had carotid arteries with the X-type of intercarotid anastomosis (anastomosis intercarotica), as in many other columbids (Baumel & Gerchman 1968, Gold *et al*. 2016).[218]

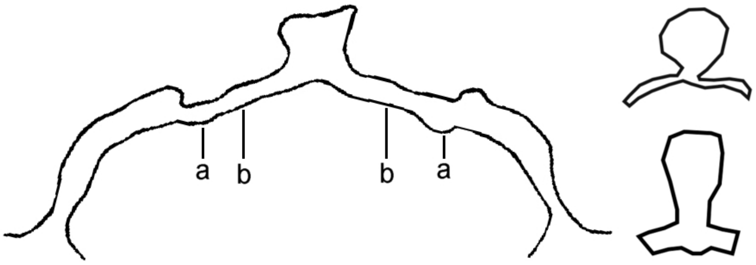

Left: outline of the carotid canals of *Raphus* in rostral/caudal view (combined image traced from CT data of OUMNH 11605; Warnett *et al*. 2020; ○ Jolyon C. Parish). Regions in which the ostia of vascular canals open: a: that of A. sphenopalatinus, b: that of A. sphenomaxillaris. *Right*: line drawings of the pituitary body and cranial carotid arteries of *Raphus* (*top*) and *Pezophaps* (*bottom*) (after Gold *et al*. 2016, fig.8).

V. occipitalis externa (lateral venous sinus of Melville 1848).

V. ophthalmica externa (venous sinus of the Membrana tympani of Melville 1848?).

---

[218] Although all the columbids examined by Gold *et al*. (2016) had the X-type, Baumel & Gerchman (1968) found *Columba livia* to have the I-type (four specimens) or the H-type (one specimen).

A. ophthalmica externa. A. ophthalmica externa was transmitted from the parabasal fossa via the canalis ophthalmicus externus to the orbit. The canalis ophthalmicus externus also carried the external ophthalmic vein (Melville 1848).

Membrana tympani. The membrana tympani was attached laterally to the quadrate, caudally to the paroccipital process, ventrally to the basioccipital plate, and dorsally to the squamosal (Kühne & Lewis 1985). According to Melville (1848), "the paroccipital process presents a shallow groove at its base anteriorly, which widens as it ascends; its floor is cellular above, behind the inferior tympanic facet [= otic articular surface for the quadrate]; below it curves inwards, and passes into a rounded orifice which perforates the outer wall of the canal just mentioned; the groove lodges the sinus of the memrana tympani [= v. ophthalmica externa?], which transmits blood to the internal jugular vein; its outer edge is undefined, the inner sharp and gives attachment to the membrana tympani" (p.83). He added that the outer wall of the fossa parabasilis (containing the foramina of the carotid canal and cranial nerve IX) is perforated "a line [2.1mm] above its margin, by a rounded aperture leading to a broad groove on the base of the paroccipital process anteriorly; it transmits the venous sinus of the membrana tympani [= v. ophthalmica externa] to the internal jugular vein" (p.79).

Brain (Endocasts)

(*Raphus*: Gold *et al*. 2016, figs.2A, 3A, 4A, 5A-B, 7A, 8A. *Pezophaps*: Newton & Clark 1879, pl.l, fig.14; Gold *et al*. 2016, figs.2B, 3B, 4B, 7B, 8B; Walsh & Knoll 2018, fig.5.3, no.48)

According to Owen (1867), in *Raphus* "the division of the cranial cavity appropriate to the cerebrum proper is less in proportion to that for the cerebellum and optic lobes, at least in vertical and longitudinal diameters, than in any other known bird" (p.69).

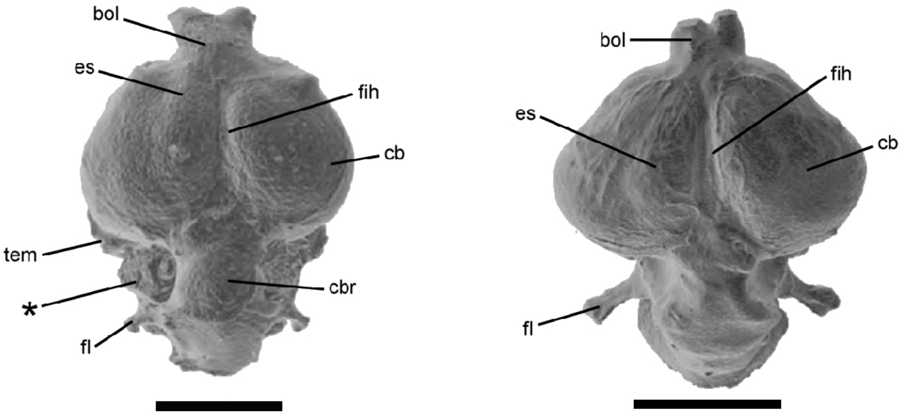

Digital endocasts of *Raphus* (*left*) and *Pezophaps* (*right*) in dorsal view (scale = 15mm; after Gold *et al*. 2016, fig.3).

Edward Newton and John Willis Clark had an endocranial cast of *Pezophaps* made (UMZC 415.Q). They stated that it "seems to have been rather small in proportion to the size of the bird; but comparison with that of a tame Pigeon (*Columba livia* var. *domestica*) shews that it closely resembles it in general shape, and especially in the great breadth of the central lobes" (1879, pp.448-449). Burne (1902) also described an endocranial cast of *Pezophaps* (RCSHM/D 186): "The hemispheres are of moderate size with but slight indications of dorsal longitudinal furrows. They are widely separated mesially, especially in their posterior parts, and extend back over the anterior half of the optic lobes. The latter are well developed and strongly depressed towards the ventral surface. The cerebellum is of some size; its peduncles lie about midway between the anterior and posterior extremities. In front it extends between the hinder ends of the hemispheres. The hypophysis is small and narrow" (p.137).

In both *Raphus* and *Pezophaps* the olfactory bulb is large and wide; rostrally it forms the pair of olfactory lobes from which the olfactory nerves originate. Gold *et al*. (2016) described the dorsal aspect of the brain thus: "At the midpoint of the sagittal eminence, the cerebrum pinches medially to meet the cerebellum. This creates a pyriform-like point on the telencephalon" (p.6). The sagittal eminence[219] is well-developed in both *Raphus* and *Pezophaps*; it lies in "a rostral to rostral-central position" (*ibid*., p.6). In *Raphus* and *Pezophaps* it is expanded more laterally and caudally than in other columbids.[220] The telencephalon of *Raphus* and *Pezophaps* has an approximately hexagonal outline in dorsal view (*ibid*.).

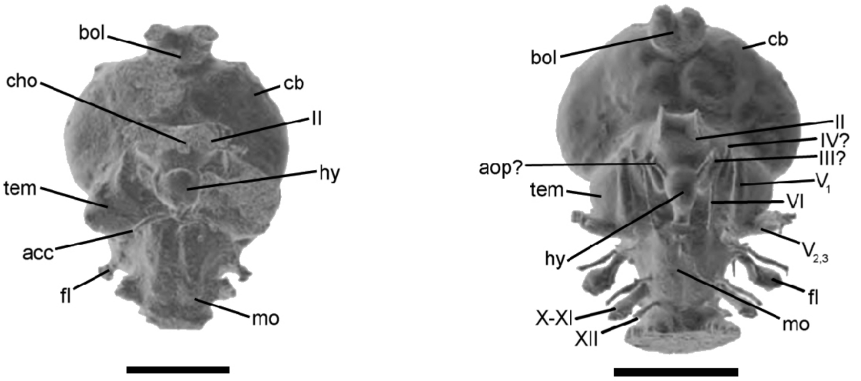

Digital endocasts of *Raphus* (*left*) and *Pezophaps* (*right*) in ventral view (scale = 15mm; after Gold *et al*. 2016, fig.7).

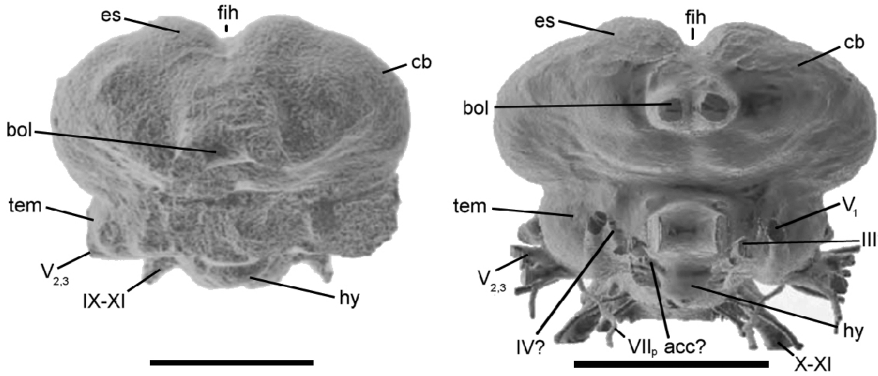

Digital endocasts of *Raphus* (*left*) and *Pezophaps* (*right*) in rostral view (scale = 15mm; after Gold *et al*. 2016, fig.2).

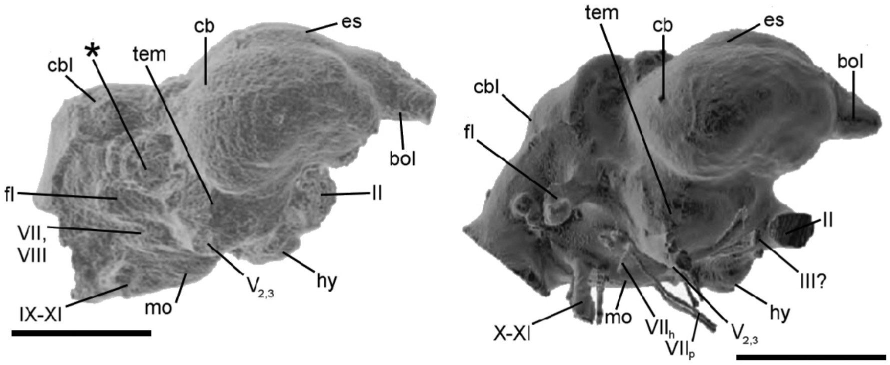

Digital endocasts of *Raphus* (*left*) and *Pezophaps* (*right*) in lateral view (scale = 15mm; after Gold *et al*. 2016, fig.4).

---

[219] The sagittal eminence (Wulst) is involved with visual integration, somatosensation, learning and cognition.

[220] In addition to *Raphus* and *Pezophaps*, the other columbids studied by Gold *et al*. (2016) were: *Caloenas nicobarica*, *Chalcophaps indica*, *Columba livia*, *Didunculus strigirostris*, *Gallicolumba luzonica*, *Goura cristata* and *Phaps chalcoptera*.

Both *Raphus* and *Pezophaps* have Type 1 optic foramina (Hall *et al.* 2009): that is to say, "a discrete optic foramen present in each orbit that probably reflects the size of the optic nerve" (p.1831). Other columbids have either Type 2 ("a single, central optic foramen is present that probably reflects the size of the optic foramen") or Type 3 ("an optic foramen is present that, although discrete, is too large to reflect the optic nerve") foramina (*ibid.*; Gold *et al.* 2016; pers. obs.).

Gold *et al.* (2016) stated that the hypophysis of *Raphus* is proportionately wider than in the other columbids studied and that it protruded from the remainder of the brain to a lesser extent. However, they added that asymmetry in the skull of *Raphus* studied (NHMUK A.9040) "makes it difficult to assess whether this is a result of damage or is an actual characteristic of the skull" (p.6). The hypophysis of *Pezophaps* is approximately the width of the chiasma opticum (*ibid.*). Edinger (1942) noted that the hypophysis is enlarged in giant forms of animals. However, information is limited and the exact relation of hypophysis size to body size as regards gigantism and loss of flight is unknown. Indeed, *Pezophaps* (both males and females) was larger than *Raphus* yet had a proportionately smaller hypophysis (Gold *et al.* 2016).

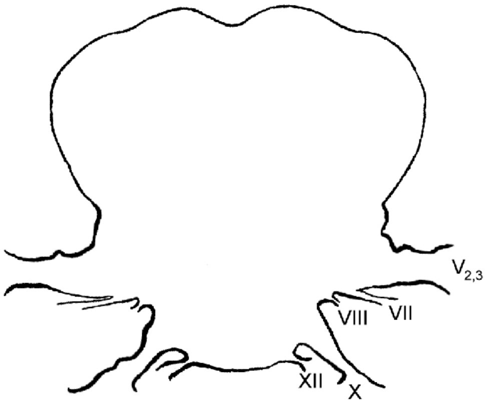

Outline of the endocranial cavity of *Raphus* in rostral/caudal view (combined image traced from CT data of OUMNH 11605; Warnett *et al.* 2020; ○ Jolyon C. Parish).

In *Raphus* and *Pezophaps* the tectum mesencephali is approximately oval in form and "rather small relative to the cerebrum" (Gold *et al.* 2016, p.6). According to Gold *et al.* (2016) the rostral portion of the semicircular vein is visible in the digital endocast of *Pezophaps* they studied; it runs approximately dorsoventrally along the caudal part of the tectum mesencephali.

In dorsal aspect the cerebellum of *Raphus* is longer than wide and narrows slightly rostrally (Gold *et al.* 2016). In dorsal view the cerebellum of *Pezophaps*, and to a lesser extent that of *Raphus*, narrows laterally, "forming an hourglass shape" (*ibid.*, p.7).

The flocculus of *Raphus* and *Pezophaps* is of proportionately similar size to those of *Caloenas nicobarica*, *Chalcophaps indica*, *Columba livia* and *Phaps chalcoptera* (Gold *et al.* 2016). In *Pezophaps*, *Caloenas nicobarica*, *Didunculus strigirostris* and *Goura cristata* it is angled at approximately 45° caudolaterally, whereas in *Raphus* it projects more laterally (*ibid.*).

The trigeminal fossa (fossa ganglii trigemini) does not open into the fossa for the medulla oblongata (fossa medullae oblongatae) (Gold *et al.* 2016). In *Raphus* and *Pezophaps* (as in other columbids) the trigeminal ganglion (ganglion trigeminale) and the base of the trigeminal nerve are contiguous with the tectum mesencephali (*ibid.*).

Tracheal rings

Cartilage 'C'-shaped rings are known for *Pezophaps* (NHMUK A.1453, OUMNH specimens, NMING:F21701/97).

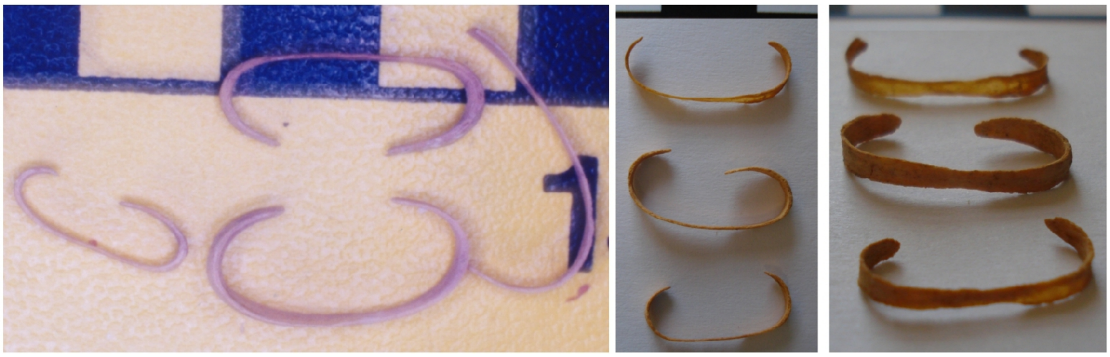

Tracheal rings of *Pezophaps*. *Left*: NHMUK A.1453 (○ Jolyon C. Parish); *right*: NMING:F21701/97 (© David Gonzalez). Scales in cm.

Skin

On the dorsal margin of the soft tissue of the lower jaw of the Tradescant specimen, in the region of the angulus mandibulae, is an area of dense tissue (showing greater X-ray opacity than the surrounding tissue, suggesting calcification; Warnett *et al*. 2020, fig.3). This area is around 3.5mm long and is seen on both sides of the lower jaw, although it is not visible with the naked eye (Warnett *et al*. 2020). A corresponding, but smaller, area is seen in the adjacent part of the soft tissue of the upper jaw.

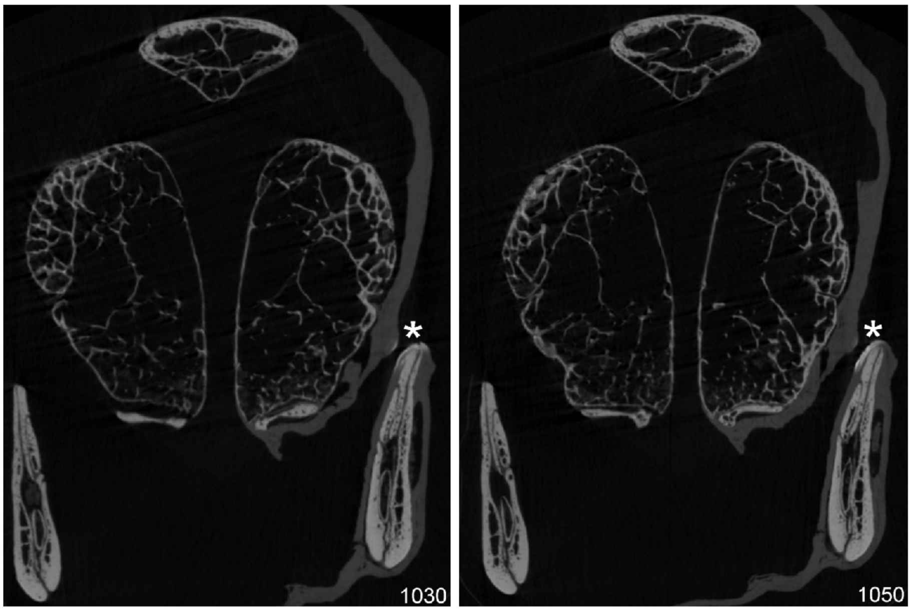

Denser (lighter grey in the above images) areas in the soft tissue of the upper and lower jaws of *Raphus* (OUMNH 11605), indicated by * (CT data relating to Warnett *et al*. 2020; MorphoSource Media: M55320).

Wing Musculature

The lateral process of the coracoid is reduced in *Goura* and this reduction is particularly apparent in *Pezophaps*. According to Martin (1904) this is due to the reduction of m. sternocoracoideus. The sternum of both *Raphus* and *Pezophaps* has a developed carina and large area for the attachment of pectoral musculature. Indeed, early accounts mention that the breast was good to eat (Anon. 1601a; Clusius 1605). The medial intermuscular line of the sternum terminates more cranially in *Raphus* and *Pezophaps* than in volant columbids; in the latter it progresses to the caudal part of the sternum, whereas in the former taxa it ends just caudal to the sternal midlength. The linea (eminentia) m. latissimi dorsi is well developed in *Raphus*, more so than in *Goura* and *Didunculus* (where it is absent). *Raphus* may have used its wings in display in a similar way to *Goura* (see Parish 2013, p.299) and *Pezophaps* is known to have used its wings in intraspecific combat (see Parish 2013, pp.298, 300).

M. supracoracoideus. **Origin**: from the dorsal part of the lateral surface of the sternum. The area of origin is defined ventrally by an intermuscular line. **Insertion**: in *Raphus* the insertion site is marked by a rounded triangular impression (impressio m. supracoracoidei; see Owen 1867, pl.xx, fig.12).

M. pectoralis major. **Origin**: from the carina of the sternum. The dorsal margin of the origin site is marked by the intermuscular line mentioned above. **Insertion**: on the deltopectoral crest (crista deltopectoralis, tuberculum dorsalis) of the humerus. The deltopectoral crest, is variably developed in *Raphus*, and is reduced in *Pezophaps* (see NHMUK A.1375).

M. coracobrachialis cranialis. **Origin**: from the lateral surface of the apex of the coracoid. **Insertion**: the insertion site is marked by an impression on the head of the humerus, just ventral to the deltopectoral crest.

M. scapulotriceps (M. anconaeus scapularis of Fürbringer 1888). **Origin**: in part from the tuberculum m. scapulotricipitis, which is well-developed in *Raphus*. Rolleston (1870) erroneously thought that this tubercle provided attachment for m. serratus superficialis (his "serratus anticus"; p.670). **Insertion**: on the dorsal part of processus cotylaris dorsalis of the ulna.

M. latissimus dorsi. **Origin**: in *Columba livia* this muscle originates from the neural spine of the last cervical (including cervicodorsal vertebrae) and first dorsal vertebra and from the cranial tip of the neural spine of the second dorsal vertebra (George & Berger 1966). This was presumably also the case in *Raphus* and *Pezophaps* **Insertion**: on the linea m. latissimi dorsi of the shaft of the humerus (seen in Owen's figure (1867, pl.xx, fig.12) of the humerus of *Raphus*). In *Raphus* the linea is well-developed, suggesting that the wing was habitually used. In *Pezophaps* the linea is variably developed.

M. brachialis. **Origin**: from the fossa m. brachialis of the distal end of the cranial face of the humerus (seen in Owen's figure (1867, pl.xx, fig.14) of the humerus of *Raphus*). **Insertion**: on the depressio m. brachialis of the ventral face of the proximal ulna. This is seen as a well-defined longitudinally sub-oval impression in *Raphus* (Owen 1867, pl.xx, fig.16*c*).

M. pronator superficialis. **Origin**: from the ventral side of the distal part of the ventral epicondyle of the humerus. In *Raphus* a slight subcircular depression probably corresponds to the attachment site. **Insertion**: on the cranioventral surface of the radius.

M. flexor carpi ulnaris. **Origin**: from the processus flexorius of the humerus. **Insertion**: on the ulnare.

M. extensor carpi radialis. **Origin**: in *Raphus* a shallow depression dorsal to the origin of m. brachialis may represent the origin site for m. extensor carpi radialis. **Insertion**: on the extensor process of the carpometacarpus.

Musculature of the Pelvis and Hindlimb

Milne-Edwards (1866b) remarked: "The upper end [of the tibiotarsus] is relatively larger than that of the majority of the pigeons, and the osseous projections indicate a very great power in the muscles of the thigh and the leg" (p.371). The Garrod formula for the leg muscles of the dodo and solitaire would probably have been ABCDEFGXYV (Am), as in most pigeons. It is not known whether m. ambiens was present or not and it is therefore placed in parentheses (Am).[221]

The large muscles of the hindlimb would have made it powerful. The large iliotibialis lateralis would have provided a strong force for extending the tibiotarsus. The long ischium would have provided a large area for the attachment of m. obturator medialis and m. ischiofemoralis, both of which are femoral retractors. M. iliofibularis, m. iliofemoralis, m. iliotibialis and m. semitendinosus were attached to the crista dorsolateralis ilii in life. M. iliotibialis lateralis would have been very well developed in *Raphus* and *Pezophaps*.

---

[221] M. ambiens is absent in *Goura*, but present in *Caloenas* and *Didunculus*.

Melville (1848) remarked that “the arrangement of the tendons in the foot of the Dodo, is precisely the same as in that of Pigeons &c.; but throws no special light on its affinities” (p.111). Likewise, Zinoviev noted that the development of the pedal muscles is typical for Columbidae. As in other columbids, *Raphus* and *Pezophaps* would have probably possessed a Type I arrangement of deep plantar tendons, where flexor digitorum longus and flexor hallucis longus cross and are joined by a simple viniculum (allowing m. flexor hallucis longus to assist in the flexion of all the digits), the tendon of m. flexor hallucis longus inserting on the hallux and that of m. flexor digitorum longus trifurcating and providing offshoots to digits II, III and IV (Beddard 1898, George & Berger 1966).

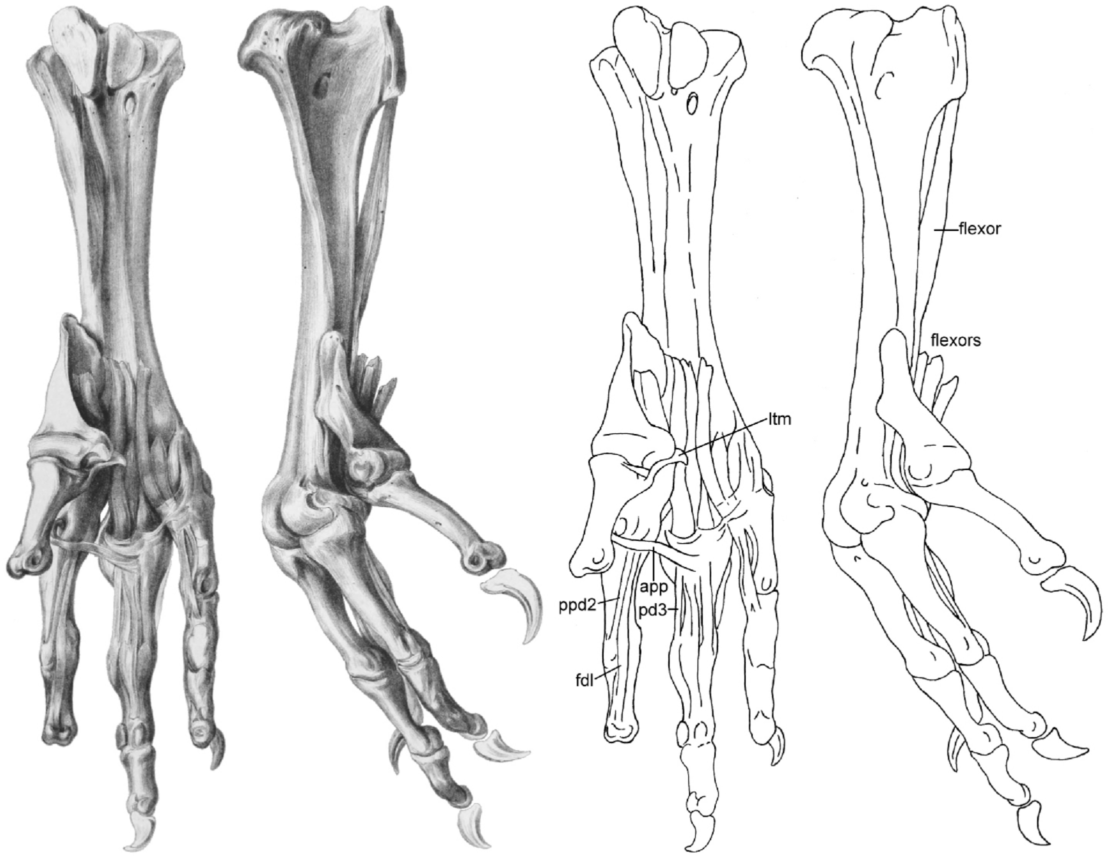

Pes of *Raphus* (OUMNH 11605) showing some soft tissue still remaining (lithographs: Owen 1846, pls.xlix, l; artist: James Erxleben; “J. Erxleben. Zinc.” “Day & Haghe lith^{rs} to the Queen”).

In the UMZC collections there is a wax cast of the Oxford foot (OUMNH 11605) made prior to the complete loss of soft parts (UMZC 415; cf. Owen 1846, pls.xlix, l), which shows some of the muscles and ligaments.

Mm. iliotrochanterici. **Origin**: on the preacetabular ilium. Milne-Edwards (1866b) speculated from examination of the insertion impressions that the elevator muscles of the thigh must have had great power.

M. iliotrochantericus cranialis. **Insertion**: on the craniolateral surface of the femur. Mm. iliotrochanterici were attached to the impressiones iliotrochantericae of the femur (see Owen 1867, pl.xv; Milne-Edwards 1866b, pl.16, fig.2b).

M. iliotrochantericus medius. **Insertion**: on the craniolateral surface of the femur, between those of mm. iliotrochantericus cranialis and caudalis.

M. iliotrochantericus caudalis. **Insertion**: on a ridge on the lateral surface of the femur, distal to the trochanter.

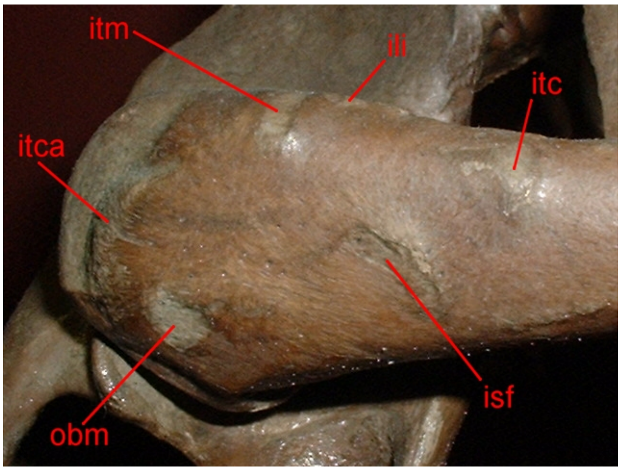

Muscle attachment areas on the proximal end of the femur of *Raphus*, lateral view (NHMUK A.9040; ○ Jolyon C. Parish).

M. ischiofemoralis. **Origin**: on the lateral surface of the ischium. The large area of origin, due to the caudally expanded ischium, would have made m. ischiofemoralis a powerful muscle. **Insertion**: on the lateral surface of the proximal end of the femur. The insertion site is on an impression situated caudal to the distal end of the impressiones iliotrochantericae.

M. femorotibialis externus. **Origin**: from a long area on the lateral and craniolateral surfaces of the femur and from the caudolateral and lateral surfaces, nearer the distal end of the femur.

M. femorotibialis medius. **Origin**: from the cranial intermuscular line of the femur, and from most of the cranial surface of that bone.

M. femorotibialis internus. **Origin**: from the medial surface of the proximal part of the shaft of the femur. **Insertion**: on an impression on the dorsal extremity of the medial face of the tibiotarsus, at the craniomedial corner of the head of the bone.

M. flexor cruris medialis. **Insertion**: probably on a short longitudinal ridge on the medial face of the proximal end of the tibiotarsus (see Owen 1867, pl.xxii, fig.2, *n*).

M. fibularis longus (Peroneus medius of Melville 1848). **Origin**: from an aponeurosis (in *Columba livia*: George & Berger 1966), shared with m. flexor perforans et perforatus digiti III, attached to the crest on the cranial edge of the lateral cnemial crest of the tibiotarsus. **Insertion**: the tendon of m. fibularis longus moved over the synovial cartilage lining the groove on the caudal face of the lateral part of the proximal end of the tarsometatarsus, before fusing with the tendon of m. perforans digiti III, just distal to the lateral crest of the hypotarsus.

M. caudo-ilio-femoralis. **Insertion**: pars iliofemoralis inserted on the caudal surface of the femur, on an impression located about a third of the way down the bone, on the caudolateral side.

M. pubo-ischio-femoralis. **Insertion**: in *Columba livia* pars lateralis (externa) inserts on the caudal face of the femur, just distal to that of m. caudo-ilio-femoralis pars iliofemoralis, medial to that of m. femorotibialis externus, and medial to that of m. flexor cruris lateralis pars accessorius (George & Berger 1966). Pars interna also inserts on the caudal surface of the femur, just medial to the insertion of pars externa. There is an impression on the caudal face of the femur of *Raphus*, about half to two-thirds of the way down the bone, which may have provided insertion for pars medialis (see Milne-Edwards 1866b, pl.16, fig.2a).

Mm. obturator lateralis et medialis. **Insertion**: the tendon of m. obturator medius inserted on the caudal face of the proximal end of the femur. There is a distinct rounded impression just distal to the antitrochanteric articular face which is probably the insertion site of this muscle (see Owen 1867, pl.xxi, fig.3; Milne-Edwards 1866b, pl.16, fig.2a).

M. iliofemoralis internus. **Insertion**: it inserted on the medial face of the proximal shaft of the femur. Some faint impressions on the caudomedial part of the proximal shaft of the femur, seen in Milne-Edwards' figure (1866b, pl.16, fig.2a), may represent part of the insertion site. In some specimens it might have originated from the "small trochanter" ("trochanter minor") of Owen (1867, pp.64, 78; pl.xxi, fig.3, *d*).

M. popliteus. **Origin**: from the caudomedial surface of the head of the fibula. **Insertion**: on an impression on the caudal surface of the proximal end of the tibiotarsus, just distal to the proximal articular surface.

M. tibialis cranialis (M. tibialis anticus of Melville 1848; muscle tibial antérieur of Milne-Edwards 1866b). **Origin**: the superficial or tibial head originated from the cranial edge of the cranial cnemial crest, the patellar crest, and the medial surface of the lateral cnemial crest. The deep or femoral head originated from the fovea tendinis m. tibialis cranialis on the lateral condyle of the femur (seen in Milne-Edwards' figure (1866b, pl.16 fig.2c)). **Insertion**: the tendon of insertion was held in place to the distal end of the tibiotarsus by a transverse ligament (retinaculum extensorium tibiotarsi). The tendon passed over the cranial surface of the ankle joint and inserted on the tuberositas m. tibialis cranialis on the cranial surface of the proximal end of the tarsometatarsus. The tendon of m. tibialis cranialis (or perhaps that of m. extensor digitorum longus) appears to be visible in Shaw & Nodder's (1792-1794) plate depicting the British Museum foot, although it is not evident in later images of the specimen.

M. iliofibularis. **Insertion**: the tendon passed through the ansae m. iliofibularis and inserted on a tubercle (tuberculum m. iliofibularis) on the caudal part of the fibula. Lambrecht (1933) labelled this attachment area as "apophysis m. iliofibularis" (see his fig.21).

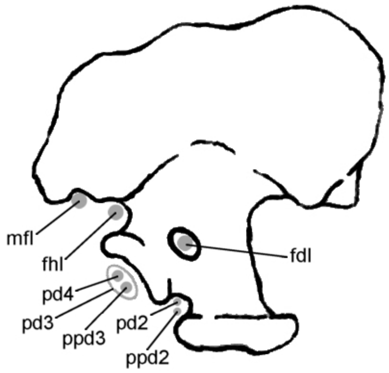

Proximal view of the tarsometatarsus of *Raphus* (left side) showing, in diagrammatic fashion, the positions of the tendons of the pes (partly based on Cracraft 1971, fig.11; ○ Jolyon C. Parish, 2020).

M. gastrocnemius. **Origin**: M. gastrocnemius is divided into three parts – pars lateralis (pars externa; ectogastrocnemius muscle of Owen 1867; gastrocnemius externa of Owen 1871b), pars intermedia (pars media), and pars medialis (pars interna; gastrocnemius internus of Owen 1871b). **Pars lateralis** originated from a subcircular depression on the caudodistal part of the femur, proxial to the lateral condyle and just proximal to the impressio distalis ansae m. iliofibularis (seen in Owen 1867, pl.xxi, fig.3). **Pars intermedia** arose from the intercondylar region of the distal femur and from the caudal surface of the medial condyle. **Pars medialis**, the largest of the three parts, originated from the whole of the medial surface of the cranial cnemial crest of the tibiotarsus (see Owen 1867, pl.xxii, fig.2, *n*) and, in *Columba livia*, originates from the proximal part of the shaft. The origin-impression is well developed, and the origin from the shaft is from a short longitudinal ridge. The tendons of these parts joins to form the tendo achillis. **Insertion**: in *Columba*, the tendo achillis runs over the caudal surface of the cartilago tibialis and inserts on the caudal face of crista medialis hypotarsi. It then continues distally and inserts on the caudolateral ridge of the tarsometatarsus throughout most of its length (George & Berger 1966). A strong aponeurotic sheath ("strong ligamentous aponeurosis" of Owen 1871b, p.521; probably vagina fibrosa flexoria) or fascia joined with the distal part of the tendo achillis to form a fibro-osseous canal for the flexor tendons of the toes. This fascia was attached to the lateral and medial margins of the tarsometatarsus, to the "ectogastrocnemial" and entogastrocnemial" ridges of Owen (1871b).

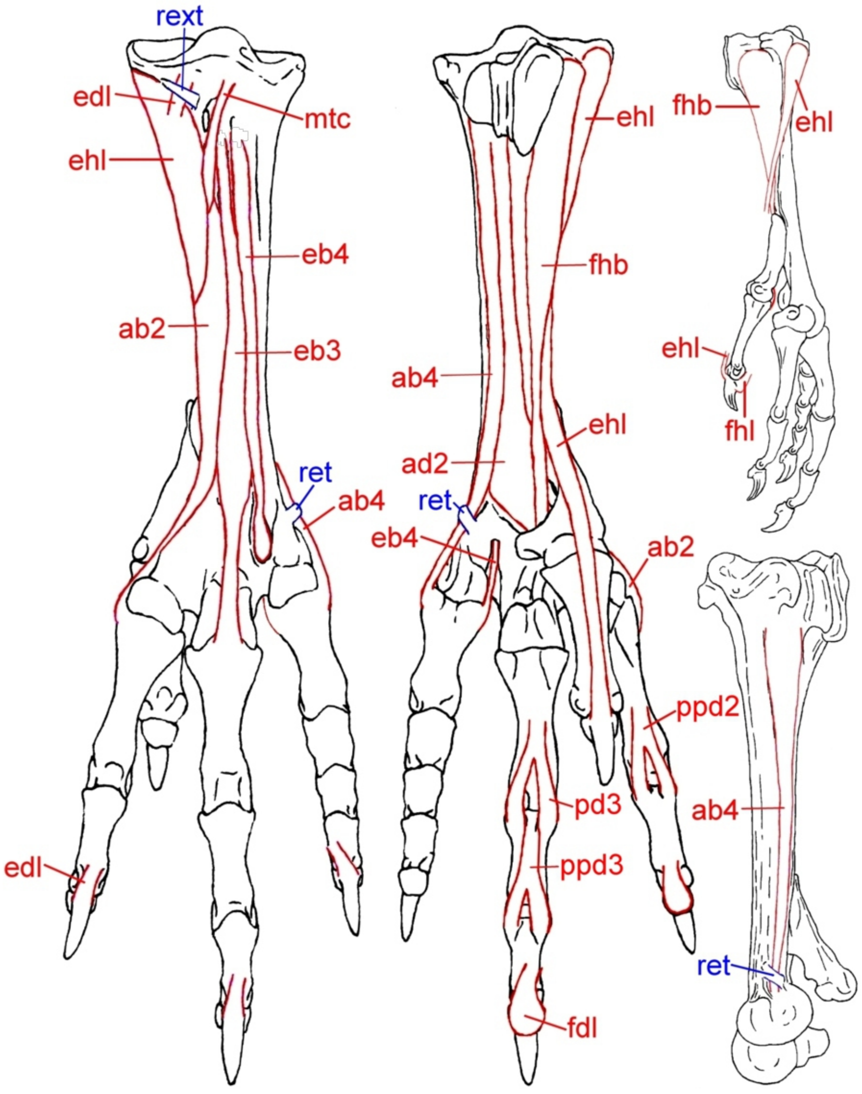

Reconstructed musculature of the foot of *Raphus* (left side), cranial, caudal, medial and lateral views (○ Jolyon C. Parish, 2020).

M. extensor digitorum longus (M. extensor communis digitorum of Melville 1848; tendon du muscle extenseur des doigts of Milne-Edwards 1866b). **Origin**: in *Columba livia* it originates from the patellar crest, medial surfaces of the cranial and lateral cnemial crests, and from a long narrow line on the craniolateral surface of the tibiotarsus. In Milne-Edwards' figure (1866b, pl.17, fig.1) there is a longitudinal slightly raised area which may have provided attachment for m. extensor digitorum longus; in Owen's figure (1867, pl.xxii, fig.1) this area corresponds to a depression. **Insertion**: the tendon passes under the supratendinal bridge of the distal end of the tibiotarsus and then under the retinaculum extensorium tarsometatarsi.[222] In *Columba livia* the tendon splits into four parts – one goes to digit II, one to digit IV, and two to digit III. The tendons of digits II and IV insert on the dorsal surfaces of the bases of the terminal phalanges, with attachments to the proximal ends of intermediate phalanges as well. The tendon of digit III inserts mainly on the terminal phalanx, but also on the intermediate phalanges of digit III (George & Berger 1966).

M. fibularis brevis. **Origin**: from the lateral surface of the tibiotarsus and cranial surface of the fibula. There is a longitudinal slight ridge, continuing from the distal end of the fibula, on the lateral face of the tibiotarsal shaft, which may have provided attachment for m. fibularis brevis. The muscle lay in a shallow longitudinal groove on the lateral side of the cranial face of the distal end of the tibiotarsus – the sulcus m. fibularis – and was restained by the retinaculum m. fibularis. **Insertion**: the tendon inserted on the caudodorsal surface of the caudolateral extremity of the margin of the lateral cotyla of the tarsometatarsus.

M. flexor perforans et perforatus digiti III (M. flexor medii perforans et perforatus of Melville 1848). **Insertion**: the tendon passed through the cartilago tibialis and then through the canal formed by the attachment of a fascia to the caudolateral face of the proximal end of the tarsometatarsus. Within this canal the tendon passed caudal to that of m. flexor perforatus digiti III and medial to that of m. flexor perforatus digiti IV. M. flexor perforans et perforatus digiti III inserted on the medial and lateral corners of the proximal end of the third phalanx of digit III (Melville 1848; George & Berger 1966).

M. flexor perforans et perforatus digiti II (M. flexor indicis perforans et perforatus of Melville 1848). **Origin**: possibly from a small subcircular impression on the lateral surface of the lateral condyle of the femur, distal to that of the ansae m. iliofibularis (see Milne-Edwards 1866b, pl.16, fig.2b). **Insertion**: the tendon of this muscle passed through the cartilago tibialis and then ran through the longitudinal groove caudal to the hypotarsal canal. Within this groove it passed caudal to the tendon of m. flexor perforatus digiti II. M. flexor perforans et perforatus digiti II inserted on the medial corner of the base of the second phalanx of digit II.

M. flexor perforatus digiti II (M. flexor indicis perforatus of Melville 1848; m. flexor perforans digiti II of Claessens *et al*. 2015). **Insertion**: the tendon passed through the cartilago tibialis and then ran through the groove caudal to the hypotarsal canal. Within this groove it ran cranial to the tendon of m. flexor perforans et perforatus digiti II. It inserted on the medial and lateral corners of the base of the proximal phalanx of digit II. The tendon of this muscle probably corresponds to the superficial flexor tendon of the inner toe of Melville (1848), which moved over the synovial cartilage on the cranial surface of tuberositas lateralis of the first metatarsal. Claessens *et al*. (2015, fig.62E) stated that this muscle passed along the sulcus between the lateral and intermedial hypotarsal crests; this would appear to be an error (see entry for m. flexor perforatus digiti III).

M. flexor perforatus digiti III (Flexor medii perforatus of Melville 1848). **Origin**: in *Columba livia* the femoral head arises from the medial part of the intercondyloid region of the distal femur. **Insertion**: the tendon passed through the cartilago tibialis and through the canal mentioned above. Within this canal it passed cranial to the tendon of m. flexor perforatus digiti IV and m. flexor perforans et perforatus digiti III. It inserted on the medial and lateral corners of the base of the second phalanx of digit III (Melville 1848; George & Berger 1966).

M. flexor perforatus digiti IV (Flexor annularis perforatus of Melville 1848). **Origin**: in *Columba livia* the femoral head of this muscle originates from the lateral part of the intercondyloid region of the distal femur, distal to the origin of m. accessorius semitendinosi and lateral to that of m. gastrocnemius pars media. **Insertion**: the tendon passed through the cartilago tibialis and then ran through a canal formed by the attachment of a fascia to the margins of a wide groove on the caudolateral part of the proximal end of the tarsometatarsus. Within this canal it lay lateral to the tendon of m. flexor perforans et perforatus digiti III and superficial to that of m. flexor perforans digiti III. It inserted on the plantar surface of the second phalanx of digit IV and on the medial and lateral surfaces of the bases of the third and fourth phalanges of digit IV (Melville 1848; George & Berger 1966).

---

[222] "Beneath the anterior and internal angle is the oblique oval prominent tubercle, for the insertion of a ligamentous band, binding down the tendon of the *M. extensor communis digitorum*; internally, it is attached to a short rough ridge, along the inner margin of the anterior concavity, separated from the preceding by a groove leading upwards and outwards, and impressing the anterior edge of the internal condyloid fossa, as it rises into the intercondyloid tubercle" (Melville 1848, p.105).

M. flexor hallucis longus (Flexor perforans pollicis, deep flexor of the hind toe of Melville 1848). **Origin**: from the caudal face of the distal end of the femur, perhaps from an area proximomedial to the lateral condyle, at, or bordering, the popliteal fossa. **Insertion**: the tendon passed through the cartilago tibialis and then ran through the longitudinal groove lateral to the hypotarsal canal. It inserted on the plantar surface of the base of the distal phalanx of the hallux. In Columbidae the tendon of m. flexor hallucis longus is joined to that of m. flexor digitorum longus by a viniculum. The groove on the lateral part of the hypotarsus was covered over in life by a fibro-cartilaginous bridge, extending from the lateral lip of the groove to a slight short ridge on the "external and outer angle of the proximal extremity" (Melville 1848, p.105). M. flexor hallucis longus inserted mainly on the plantar surface of the base of the distal phalanx of the hallux. The tendon of this muscle may also correspond to the deep flexor tendon of the hind toe of Melville (1848), which ran through in the groove on the cranial[223] surface of the trochlea of the first metatarsal. The flexor tendons of the hallux passed through the channel formed by the curvature of the first metatarsal.

M. flexor digitorum longus (M. flexor perforans digitorum of Melville 1848; m. flexor digitorum perforans of Lambrecht 1933). **Origin**: the fibular head arose from the caudal part of the head, neck and shaft of the fibula (from the "apophysis m. flexor digitorum perforans" of the fibula of Lambrecht 1933). The tibiotarsal head originated from the caudal surface of the shaft of the tibiotarsus, from the fossa flexoria (and possibly also the "apophysis m. flexor digitorum perforans" of the tibiotarsus of Lambrecht 1933), which is well defined. **Insertion**: in *Columba* the tendon passes through the hypotarsal canal and then trifurcates and gives offshoots to digits II, III and IV, where each attaches to the tuberculum flexorium of its respective ungual phalanx.

M. flexor hallucis brevis (M. flexor brevis pollicis of Melville 1848; fléchisseur propre du pouce of Milne-Edwards 1866b). This muscle was proportionately larger than in other columbids, being more developed in birds with a long hallux (Zinoviev 2014). **Origin**: from the medial parahypotarsal fossa, and from the caudal part of the shaft of the tarsometatarsus extending from the apex of the fossa to the facet for the first metatarsal. Melville (1848) stated that the faint ridge defining the origin for m. adductor digiti II medially provided attachment for the intermuscular ligament from which m. flexor hallucis brevis originated. **Insertion**: a large area of the plantar surface of the base of the proximal phalanx of the hallux.

M. extensor hallucis longus (M. extensor pollicis of Melville 1848). **Insertion**: "the tendon of *M. extensor pollicis* [= m. extensor hallucis longus] passes along the posterior surface [of the first metatarsal], and is bound down immediately above the trochlea by an annular ligament, attached externally by a roughened portion of the outer edge, and internally to a narrow pit close to the inner border"(Melville 1848, p.109).

M. abductor digiti II (M. adductor indicis of Melville 1848). **Origin**: it was attached to an intermuscular line which progresses distally from the m. tibialis cranialis tubercle. **Insertion**: Melville (1848) stated that the concave part of the upper part of the cranial surface of the first metatarsal "probably gave origin to some fibres of the *M. adductor indicis*" (p.109). The tendon passed between the trochleae of digits II and III and inserted on the lateral surface of the base of the proximal phalanx of digit II (George & Berger 1966).

M. adductor digiti II (M. abductor indicis of Melville 1848). **Origin**: from the lateral surface of the base of the hyoptarsus. The fleshy belly lay between two intermuscular lines and extended down to the region of the facet for the first metatarsal. The tendon passed along a shallow groove between the ridge of the caudomedial margin of the distal end of the second metatarsal and a second ridge running parallel to it. The tendon then ran between the trochleae of the second and third metatarsals. **Insertion**: on the lateral surface of the base of the proximal phalanx of digit II.

---

[223] Melville (1848, p.109) stated that the distal end of the first metatarsal: "supports the transversely elongated trochlea, which is very slightly concave in front, but behind, it is grooved for the deep *flexor* tendon". However, the flexor tendon would have passed on the cranial (front) side of the first metatarsal, whereas the extensor tendon would have passed on the caudal (back) side.

M. extensor brevis digiti III (Extensor medii of Melville 1848).[224] **Origin**: from the infracotylar fossa, between the distal ends of the proximal vascular foramina (Melville 1848) to nearly the distal end of the tarsometatarsus. The muscle lay between m. extensor brevis digiti IV and mm. extensor hallucis longus and abductor digiti II. **Insertion**: on almost the whole dorsal surface of the base of the proximal phalanx of digit III (George & Berger 1966).

M. extensor proprius digiti IV. Attachment site identified by Zinoviev (2014).

M. extensor brevis digiti IV (M. adductor annularis of Melville 1848; tendon of the adductor muscle of the fourth toe (IV) of Owen 1850b; adductor digiti externi of Owen 1871b; muscle adducteur annulaire of Janoo 1997). **Origin**: from the dorsal infracotylar fossa. **Insertion**: the tendon passed through the canal of the distal vascular foramen, following the interosseous tendinal canal, and inserted on the medial surface of the base of the proximal phalanx of digit IV. In *Raphus* this canal is roofed over caudally in some specimens (as it is in *Pezophaps*), but not in others (see main text).

M. abductor digiti IV (M. abductor annularis of Melville 1848; abducteur du doigt externe of Milne-Edwards 1866b). **Origin**: from the caudolateral surface of the proximal part of the tarsometatarsus, lateral to the lateral hypotarsal crest. The lateral boundary of the origin attachment area is defined by the sharp caudal border of the proximal part of the lateral surface of the tarsometatarsus. The medial boundary is marked by an intermuscular line passing distally from the lateral proximal vascular foramen, towards the trochlea of digit IV. **Insertion**: on the ventrolateral corner of the base of the proximal phalanx of digit IV. The tendon of the muscle passed through a groove on the lateral surface of the base of the trochlea of the fourth metatarsal. It was retained by a fibrous oblique retinacular ligament attached to a tubercle on the cranial margin of the groove and a rough ridge on the caudal margin (Melville 1848).

Note: Melville (1848) appears to have got the abductor and adductor muscles of digit II the wrong way round. Meville also used terms for the pectoral limb (*pollicis*, *M. digitorum communis*) when referring to the foot (so pollicis = hallucis, M. digitorum communis = m. digitorum longus).

Lig. capitis (“ligamentum teres” of Owen 1867). This ligament was attached to fovea lig. capitis of the femoral head.

Ansae m. iliofibularis. This ligament was attached to the impressio distalis ansae m. iliofibularis, a small subcircular impression immediately distal to that of m. gastrocnemialis lateralis (tuberculum m. gastrocnemialis lateralis). The impressio ansae m. iliofibularis is not well marked in all specimens. The tendon of m. iliofibularis passed through the ansae.

Lig. collaterale laterale. This ligament may correspond to the “lig. art. ext.” of Lambrecht (1933), which was attached to the “fossa lig. art. ext.” on the caudal part of the lateral surface of the head of the fibula.

Retinaculum extensorum tibiotarsi. This retinaculum was attached to the tuberositas proximalis retinaculi mm. extensorum, a longitudinal ridge on the medial border of the extensor sulcus on the cranial face of the tibiotarsus, and to the tuberositas distalis retinaculi mm. extensorium, a rounded tuberosity just proximal to the proximal end of the lateral condyle. The retinaculum was obliquely oriented, and retained the tendon of m. tibialis cranialis and, more deeply, that of m. extensor digitorum longus, in place in the extensor sulcus.

---

[224] See Vanden Berge & Zweers (1993, fig.6.18). The area of origin may also have included that of m. extensor proprius digiti III (see Holmes (1962), who says that “it appears that in most birds one of these two muscles has become reduced and fused with the other or lost completely” (p.488). This would appear to be m. extensor proprius digiti III of Cracraft (1971) and Kuroda (1971).

Retinaculum m. fibularis. This retinaculum was attached to the tuberositates retinaculi m. fibularis, longitudinal ridges on either side of the sulcus m. fibularis on the distal end of the tibiotarsus. The retinaculum retained the tendon of m. fibularis brevis in the sulcus.

Lig. meniscotibiale. This ligament was attached to an impression in the intercondylar incisure of the distal tibiotarsus, cranioproximal to that of lig. intercondylare tibiometatarsale. The ligament bifuracted distally.

Lig. intercondylare tibiometatarsale. This ligament was attached to an impression in the intercondylar incisure of the distal tibiotarsus, caudodistal to that of lig. meniscotibiale. On the tarsometatarsus it was attached to the intercondylar eminence.

Cartilago tibialis ("the great tbio-metatarsal sesamoid fibro-cartilage" of Melville 1848). The mediodistal part is ossified to form the os sesamoideum intertarsale (which is known in both *Raphus* and *Pezophaps*).

Ligg. collaterale laterale et mediale (ligaments latéraux de l'articulation tibio-tarsienne of Milne-Edwards 1866b). These ligamants were attached to the epicondyles of the distal tibiotarsus, which are well developed.

Meniscus lateralis (external semilunar cartilage of Melville 1848?). The meniscus lateralis was attached to the cranial surface of the proximal end of the tarsometatarsus. Melville (1848) mentioned a pit at the lateral part of the base of the intercondylar eminence, on the cranial face of the tarsometatarsus which, he stated, was for the external semilunar cartilage. This appears to correspond to the attachment area for the meniscus lateralis (Baumel *et al.* 1979).

Retinaculum extensorium tarsometatarsi ("ligamentous band, binding down the tendon of the *M. extensor communis digitorum*" of Melville 1848). The retinaculum was a fibrous arch that restrained and acted as a pulley for the tendon of m. extensor digitorum longus. It was attached to a distinct oval tubercle (impressiones retinaculi extensorii), situated just distal to the cranial border of the medial cotyla.

Ligg. collaterale laterale et collaterale mediale (external lateral ligament of Melville 1848). On the tibiotarsus, lig. collaterale laterale was attached to a raised area on the lateral face of the lateral condyle. Its tarsometatarsal attachment was to an oval slightly raised impression on the lateral border of the lateral cotyla. Lig. collaterale mediale was attached to a raised area on the medial face of the medial condyle of the tibiotarsus, and to the cranial part of the medial surface of the proximal end of the tarsometatarsus.

Lig. metatarso-sesamoideum et Lig. collaterale mediale. These may correspond with the "ligament of the great tibio-metatarsal sesamoid fibro-cartilage [= cartilago tibialis]" of Melville (1848), which he stated was attached to the sub-vertical and oblong caudomedial face of the margin of the medial cotyla of the tarsometatarsus. The lig. metatarso-sesamoideum joined the os sesamoideum intertarsale (the ossified mediodistal part of cartilago tibialis) to the tarsometatarsus, just distal to the rim of the medial cotyla, caudal to the attachment of lig. collaterale mediale (Baumel *et al.*1979).

Lig. transversum metatarsale (Annular ligament of Melville 1848). This ligament was attached medially to the tuberositas lateralis of the distal end of the first metatarsal and to the proximal phalanx of digit I, and laterally to the lateral epicondyle of the trochlea of metatarsal IV of the tarsometatarsus. It acted as a retinaculum and restrained the flexor tendons of the digits against the caudal surface of the tarsometatarsus (Baumel *et al.* 1979).

Ligg. plantaria ("sesamoid or glenoid fibro-cartilages on the plantar aspect of the metatarso-phalangeal articulations" of Melville 1848, p.111. Figured: Strickland & Melville (1848, pl.xii, fig.3). The ligg. plantaria of digits II, III and IV of OUMNH 11605 are shown in Strickland & Melville's plate (1848, pl.xii, fig.2 a, b, c). They were attached to the proximal phalanx by a ligament, and, less strongly, to the "peduncle of the trochlea by a reflected synovial memebrane" (Melville 1848, p.111). Cranially they were moulded to the trochlear surface. Their plantar surfaces show sulci for the flexor tendons, which were held in place by fibrous flexor sheaths (vaginae fibrosae) that transformed the grooves into canals (see Cracraft 1971, fig.16). "The internal fibro-cartilage is acted on directly by the attachment of the *perforated flexor* tendon [= tendon of m. flexor perforatus digiti II] of the inner toe to the theca [= vagina fibrosa?], just as the corresponding sesamoid fibro-cartilage at the tibio-metatarsal articulation is moved by the *Plantaris*: in the hind toe, the corresponding glenoid ligament was probably without a definite figure" (*ibid*., p.111). The "grooved surface of the external glenoid ligament [= lig. plantaris] with the portion of the theca [= vagina fibrosa?] still attached to it slit open" is shown in Strickland & Melville (1848), plate xii, figure 3, at the top.

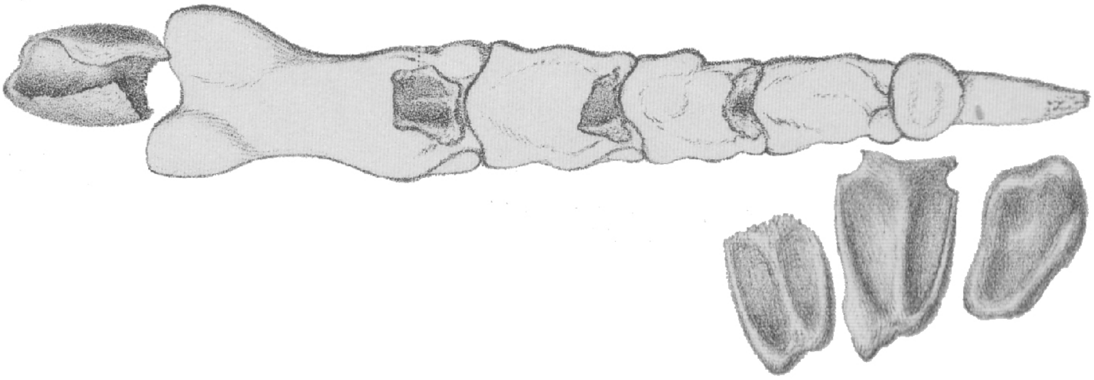

Top: caudal (plantar) view of digit IV (left side) of *Raphus*, showing the ligg. plantaria; *bottom*: ligg. plantaria of digits II, III and IV (left foot) (Strickland & Melville 1848, pl.xii, figs.3 and 2 respectively; "Tuffen West, lith." "Reeve, Benham & Reeve, imp.")

Ligg. plantaria were found at all the interphalangeal joints, except the distalmost ones (joints relating to the ungual phalanges). Each one was joined with the collateral ligaments (lateral ligaments of Melville 1848), strongly attached to the distal phalanx, and moulded to the capitulum of the proximal phalanx of the joint in question. The tendon of m. flexor digitorum longus was attached to each. At the distal phalangeal joint they were not well developed and were almost membranous (Melville 1848). Melville stated that in OUMNH 11605 "these fibro-cartilages [= ligg. plantaria] remain, but are shrunk and indurated, and when covered by varnish [...] they very much resemble irregularly-shaped sesamoid bones" (*ibid*., p.111).

Carus (1845) stated: "I drew the attention of [John] Kidd to a particular form of the ossified [*verknöcherten*] tendons of the flexor-muscles [*Beugemuskeln*]. *) [*) The bony [*knöchernen*] tendons disintegrate [or divide] into several pieces, which are connected by joints [= internodia? of Melville (1848)]. A mechanism, which otherwise on such tendon-bones [*Sehnenknochen*] is not known to me]" (p.375). Melville (1848) added that "the supposed anomaly, however, disappears on moistening the foot, and examining the glenoid ligaments by transmitted light" (p.112). These 'tendon-bones' were probably parts of the ligg. plantaria; Cracraft (1971) noted that "[i]n *Columba* very little ossification takes place and is usually absent" (p.212).

There was also a "fibro-cartilaginous thickening of a crescentic form, with the concavity directed forwards [...] in the dorsal fibrous capsule of the joint connecting the first two phalanges of the middle toe [digit III], the tendon of the *Extensor communis digitorum* [= m. extensor digitorum longus] gliding over it (*ibid*., p.112).

Gastrolith[225]

(*Raphus*: Van Wissen 1995, p.79; Ziswiler 1996, p.70; Staub 1996, pl.4b; Grihault 2005, p.100; Parish 2013, fig.6.12. *Pezophaps*: Newton & Clark 1879, pl.l, figs.4-6; Oliver 1891, frontispiece; Parish 2013, fig.6.13 [casts])

It is interesting to note that only a handful of gastroliths belonging to *Pezophaps* have been found: three by George Jenner's men (Jenner 1871), four by Thomas Morris and William James Caldwell (Caldwell 1875)[226] (see Parish (2013, pp.250-251, 293-294) – these are now lost – and a selection in the François Leguat Giant Tortoise and Cave Reserve Museum (R175, R176, R178). Slater (1879a) reported that he had not found a single gastrolith during his excavations, despite finding representatives of almost every skeletal element. There is only one supposed gastrolith known for *Raphus*, that of Pierre Bourgault du Coudray (see Parish 2013, pp.292-293, fig.6.12). The scarcity of gastroliths may be explained by the fact that when a body decomposes the gastroliths often drop out and become separated from the specimen (Wings 2004).

Gastrolith of *Pezophaps* in three aspects (Newton & Clark 1879, pl.l, figs.4-6; "R. Mintern del." "Mintern Bro^{s}. lith.")

Diamond *et al*. (1999) found that in the frugivorous birds of New Guinea "those practising geophagy tend to be the largest in their order, family or group" (p.186). Ostriches are known to display variation in gastrolith size between individuals, with some birds prefering gravel-sized stones and others cobble-sized stones (Wings 2004). As *Raphus* and *Pezophaps* evidently had only a single gastrolith, this potentially could have been quite large. The average mass of gastroliths in the ostrich is between 1.04% (n = 212) and 1.05% (n = 135) of body-mass (Wings 2004). Using this approximation would give 83.2-84g (8kg body-mass) to 187.2-189g (18kg body-mass) for *Raphus*, which compares to 90g for Pierre Bourgault du Coudray's stone. For *Pezophaps* this would be 156-158g (15kg female body-mass) to 166-168g (16kg female body-mass) and 270-273g (26kg male body-mass) to 291-294g (28kg male body-mass).[227] This compares to 49g for one of Caldwell's stones – a large discrepancy.

Conclusions

The dodo probably fed on large food items such as fruits and seeds. Supporting evidence for this includes reduction or loss of functional basipterygoid processes, allowing greater flexibility of the jaw. Reduced, or a lack of, basipterygoid processes are also seen in other columbids which have a diet which includes large food items – for example, *Ducula* and *Ectopistes* (Bhattacharyya 1994, Gibbs *et al*. 2001). The attachment for m. depressor mandibulae is particularly large in the dodo. This muscle is the main depressor for the mandible and is active during the grasping, stationing and transport phases of feeding, especially when large food items are ingested (Bout & Zeigler 1994). The skull of both the dodo and solitaire was prokinetic and the mandible, at least of the latter, likely had some degree of mid-ramal flexion, allowing the ingestion of large food items. A large gastrolith, present in both birds, would have aided in the breakdown of fruits and seeds. A large posterior, seen in the images of Mansūr and the *Gelderland* (Parish 2013), suggests that a significant amount of hindgut digestion took place in the dodo. Large olfactory bulbs (bulbus olfactorius) and large olfactory chambers (regio olfactoria) indicate that the dodo and solitaire both had a developed sense of smell, which was presumably used in detecting food, such as fallen fruits. The pelvic girdle and limb was well developed in both taxa, allowing efficient cursorial locomotion.

---

[225] 'Geo-gastrolith' (Wings 2007).

[226] One of these is probably that formerly in the UMZC (UMZC 415.P). Casts of this specimen still exist (UMZC 415.T).

[227] *Raphus* body-mass from Van Heteren *et al*. (2017), *Pezophaps* body-mass from Parish (2013).

In the dodo, pars intermedia of the mandible was reinforced by a bony 'brace' formed by the rostral projection of the supra-angular ventral to the mandibular fenestra. Combined with the apparently calcified soft tissue present on the lower and upper jaws this would have allowed the manipulation of large and hard food items and perhaps even the crushing of softer items (although probably not hard items such as tambalacoque seeds) at mid-mandible, closer to the quadrate-mandible hinge than between the distally located rhamphothecae.

The bifurcated neural spines (particularly evident in *Pezophaps*) – providing passage for a strong elastic interspinal ligament – and strong muscle attachment sites on the vertebrae indicate habitual powerful movements of the large head and long neck. The muscle attachment sites of the vertical occiput also indicate the presence of strong neck musculature. *Raphus* (at least in some individuals) has an extra cervical vertebra compared with the majority of other columbids (exceptions being due to individual variation), although the biomechanical effects of this have not been investigated and the modal number of presynsacral vertebrae not known for either *Raphus* or *Pezophaps*. The well-developed pelvic limb in the dodo and solitaire would have enabled effective cursorial movement. An increased postacetabular region of the pelvis, compared with that of volant columbids, would have provided increased muscle attachment area for muscles powering the hindlimb.

The naked face of the dodo, combined with its long beak and large cucullus, may have been used in display. The pneumatization and related inflation skull of the dodo would have increased the facial area. The skull shows that the cucullus muscles were well developed, which agrees with the suggestion of long head feathers in some images of the bird (see Parish 2013). Some contemporary accounts describe the wing feathers as yellow, and some of Roelandt Savery's painting show dark-tipped wing coverts (see Parish 2013), which may have been used in display, perhaps in similar way to that seen in *Goura*. The wing bones, which have developed muscle attachment sites (for example, that of m. latissimus dorsi) and show a proportionately longer ulna than in other flightless species such as *Aphanapteryx* and *Xenicibis*, indicate that they were habitually used: perhaps for display in the dodo and for combat in the solitaire. The bowl-like sternum would have also provided significant muscle attachment area.

Evidence for intraspecific combat in the solitaire is found in the presence of well-developed exostoses on the carpometacarpus and radius. The presence of healed breaks, particularly in the forelimb and pectoral girdle, provide further evidence for combats.

The solitaire is herein postulated to have displayed hereditary osteochondroma, similar to the condition seen in the extinct caniform *Hesperocyon*. Although mainly focussed on the carpal region, the exostoses of *Pezophaps* were also located on the skull and occasionally in other regions, including the vertebrae and pelvis. The effects of this condition (the development of carpal exostoses), which apparently generally did not inhibit the bird, might have been preferentially selected for, thus making it widespread within the population. Characters such as large carpal exostoses would have been an advantage in competition for resources during times of scarcity.

Both the dodo and the solitaire show significant osteological variation, as documented herein. A lack of predators may have allowed the survival of more individuals with pathologies (including healed fractures) and could have led to greater morphological variation in the population as individuals with potentially detrimental characters were not removed. A bowed specimen of dodo tibiotarsus may provide evidence for nutritional deficiency, which may be related to food shortages caused by cyclones or drought (see Angst *et al*. 2017).

Understanding the skeletal morphology of the dodo and solitaire, including adaptations for feeding and locomotion, individual variation, sexual dimorphism, and pathologies, can shed light on the evolution of flightlessness and terrestriality, insular evolution, and the effects of an absence of predators, in birds. It is hoped that this work has provided some small contribution.

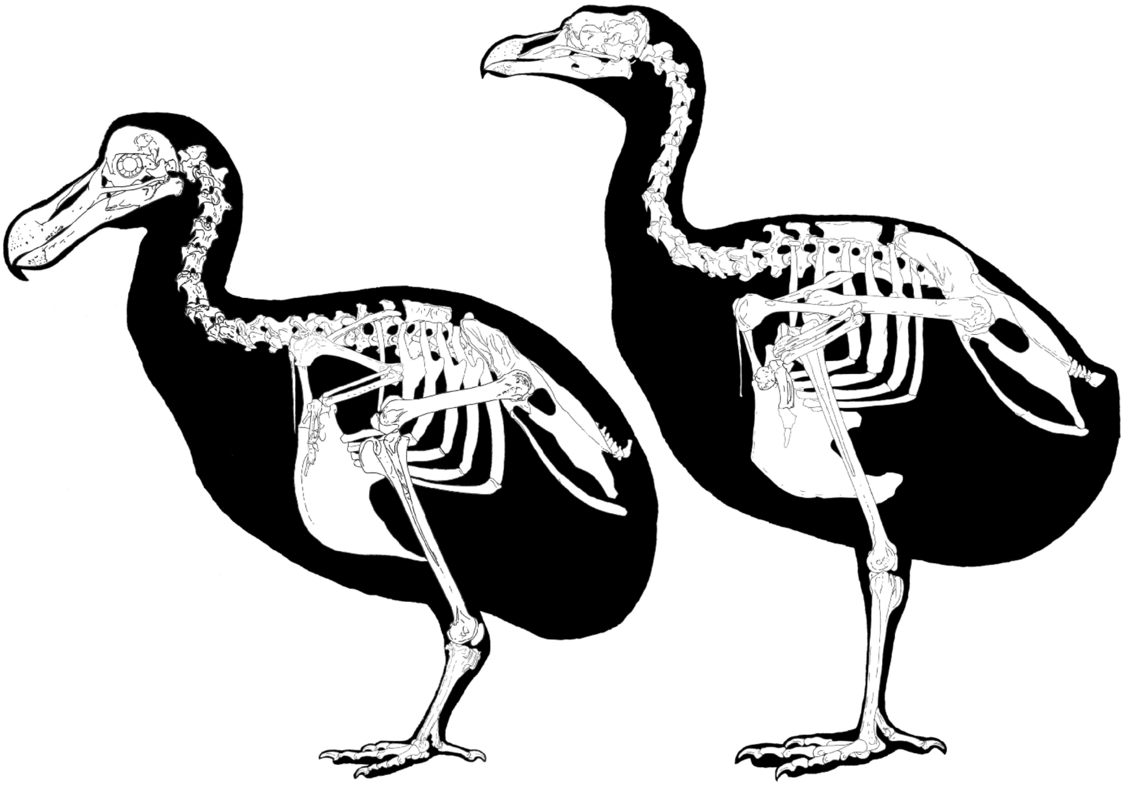

Reconstructed skeletons of the dodo (*Raphus cucullatus*; *left*) and male solitaire (*Pezophaps solitaria*; *right*) with body outlines added. ○ Jolyon C. Parish, 2020.

Ethics

No birds were killed for this study: comparative specimens of birds examined in the author's own collection were from individuals found already dead. However, this may not necessarily be the case for museum specimens. The present author does not condone killing. A number of specimens examined in the present study are from overseas collections and while the study of them was not the primary reason for travel to the museums where they are housed, the use of industrial means of travel (for example, aeroplanes) was involved.

Richard Benno Ottow (1884-1975), who described the pathologies of *Pezophaps*, was a eugenicist and member of the *Erbgesundheitsgericht* of the Third Reich (Hansson *et al*. 2011). It is not known to what degree his beliefs affected his views on the osteological pathologies of the solitaire. The work of Bout & Zeigler (1994), referenced herein, used live pigeons. The present author is opposed to the use of animals in experiments.

There are ethical concerns relating to the sources of the CT data of the Tradescant dodo head (OUMNH 11605) created by the Warwick Manufacturing Group (WMG), as the latter "has long-term relationships with", and has received funding from, arms companies, including BAE Systems, Airbus and Rolls-Royce.[228] Furthermore, the research was funded by the Engineering and Physical Sciences Research Council (EPSRC), an organization well known for its funding of military projects (Hersh

---

[228] https://www.studywarnomore.org.uk/documents/warwick.pdf
https://theboar.org/2011/11/warwick-university-creates-closer-relations-worlds/
https://blog.uiin.org/2018/01/wmg-empowering-smes-cutting-edge-science-capacity-building/

2015).[229] The present author is opposed to the manufacture and trade in arms and military equipment. Similarly, a number of dodo bones are housed at Mon Desert Mon Tresor Sugar Estate (owned by Omnicane). The sugarcane industry causes significant pollution, uses herbicides and pesticides, and requires large amounts of resources and land.[230] This situation is part of a wider occurrence in that many museums, libraries and other institutions have been built upon a foundation created from the proceeds of exploitation; indeed, exploitation is inherent in civilization itself.

Hansson, N., Peters, A. & Tammiksaar, E. 2011 Sterilisierungsoperateur und Forscher: Leben und Karriere Benno Ottows (1884-1975), *Medizinhistorisches Journal*, vol.46, pp.212-237.

Hersh, M. 2015 Ethics, Scientists, Engineers and the Military, *in* Hersh, M. (ed.) Ethical Engineering for International Development and Environmental Sustainability, *London: Springer-Verlag*, pp.325-360.

Acknowledgements

This work would not have been nearly as comprehensive if it were not for the generous assistance provided by curators and others. In particular I would like to thank: Sandra Chapman (NHMUK), Simon Chaplin (RCSHM), Ann Charlton (UMZC), Anthony Cheke, Leon Claessens (University of Maastricht), John A. Cooper (Booth Museum), James Dean (USNM), Belinda Eisenhauer (formerly at the Durban Natural Science Museum Library), Mark S. Florence (USNM), Adrian Friday (UMZC), David Gonzalez, Owen Griffiths (The François Leguat Giant Tortoise and Cave Reserve Museum), Jan den Hengst, Harri Kallio, Lumka Ludwaba (Librarian, Durban Natural Science Museum), Jiří Moravec (Národní Muzeum), Malgosia Nowak-Kemp (OUMNH), Paul Sweet (AMNH), Ray Symonds (UMZC), Ralfe Whistler, Larry Witmer (Ohio University) and Kristof Zyskowski (YPM). Edward Parish took many of the photographs of UMZC specimens used herein.

In addition, the artists of the lithographs illustrating the bones of the dodo and solitaire should be acknowledged:

E. Benham, Lovell Augustus Reeve (1814-1865) and F. Reeve, lithographers (Strickland & Melville 1848)
Day & Haghe [William Day (1797-1845, or his son of the same name born *c*.1824) and Louis Haghe (1806-1885)], lithographers (Owen 1846)
Joseph Dinkel (*c*.1806-1891), artist and lithographer (Strickland & Melville 1848)
James Erxleben (1830-1890), Dutch artist and lithographer (Newton 1865a; Owen 1846, 1867, 1871b, 1879)
George Henry Ford (1809-1876), artist (Newton & Newton 1869;[231] Owen 1871b, 1879)[232]
Louveau, artist and lithographer (Milne-Edwards 1866b)
R. Mintern, artist, one of the Mintern brothers (Newton & Clark 1879)
Edward William Robinson (1835-1877), artist (Owen 1867)
Joseph Smit (1836-1929), lithographer (Owen 1867)

---

[229] See also: Street, T. & Beale, M. 2007 Study War No More. Military involvement in UK universities, *Campaign Against Arms Trade and The Fellowship of Reconciliation*.
https://www.studywarnomore.org.uk/documents/studywarnomore.pdf
Get Your Bombs Off Our Lawn. The Arms Industry and the University of Liverpool (2015)
http://138.253.13.50/media/livacuk/engage/Get,Your,Bombs,Off,Our,Lawn.pdf
Langley, C. & Parkinson, S. 2009 Science and the corporate agenda. The detrimental effects of commercial influence on science and technology, *Folkestone: Scientists for Global Responsibility*.
www.sgr.org.uk/SciencePolicy/SGR_corp_science_full.pdf

[230] See, for example: http://omnicane.com/ir2016/reports/sustainability-report.pdf

[231] Newton & Newton (1869): "figures nearly all of the natural size, and drawn most carefully by the artist, Mr. Ford" (p.331).

[232] Melville (1848) mentioned the "the unrivalled lithographs of the skull of the Dodo (Plates VIII, IX, IX*), from the pencil of my esteemed friend Mr. Ford, (to whom I beg to return my sincere thanks,)" (p.100). However, plates vii-xii were drawn by Joseph Dinkel, and although there is correspondence by George Henry Ford in the UMZC "Dodo Book" Archive, Ford did not contribute any plates to Strickland and Melville's (1848) work (Rookmaker 2010).

Tuffen West (1823-1891), artist and lithographer (Strickland & Melville 1848)

Dedication

In memory of Ray Symonds, collections manager at the UMZC, who died on 13th August 2014.

Additional References

References used in the present work but not found in the *Bibliography of the Didinæ* are listed here:

Anderson, J. F., Hall-Martin, A. & Russell, D. A. 1985 Long bone circumference and weight in mammals, birds and dinosaurs, *Journal of Zoology*, vol.207, pp.53-61.

Barnikol, A. 1953 Studien am Kopf der Opisthocomiformes, Musophagidae, Galli, Columbae und Cuculi, *Zoologisches Jahrbuch. Abteilung für Systematik, Ökologie und Geographie der Tiere*, vol.81, pp.487-526.

Baumel, J. J. 1993 Systema Cardiovasculare, *in* Baumel J. J., King, A. S., Breazile, J. E., Evans, H. E. & Vanden Berge, J. C. (eds) Handbook of Avian Anatomy: Nomina Anatomica Avium, *Publications of the Nuttall Ornithological Club*, 23, pp.407-476.

Baumel, J. J. & Gerchman, L. 1968 The Avian Intercarotid Anastomosis and its Homologue in other Vertebrates, *American Journal of Anatomy*, vol.122, pp.1-18.

Baumel, J. J. & Witmer, L. M. 1993 Osteologia, *in* Baumel J. J., King, A. S., Breazile, J. E., Evans, H. E. & Vanden Berge, J. C. (eds) Handbook of Avian Anatomy: Nomina Anatomica Avium, *Publications of the Nuttall Ornithological Club*, 23, pp.45-132.

Beddard, F. E. 1898 The Structure and Classification of Birds, *London: Longmans, Green, and Co*.

Berge, J. C. vanden & Zweers, G. 1993 Myologia, *in* Baumel, J. J., King, A. S., Lucas, A. M., Breazile, J. M. & Evans, H. E. (eds.) Nomina Anatomica Avium, *London: Academic Press*, pp.189-247.

Berger, A. J. 1952 The Comparative Functional Morphology of the Pelvic Appendage in Three Genera of Cuculidae, *American Midland Naturalist*, vol.47, no.3, pp.513-605.

Berger, A. J. 1956 Anatomical Variation and Avian Anatomy, *The Condor*, vol.58, pp.433-441.

Bhattacharyya, B. N. 1989 Functional morphology of the jaw muscles of two species of Imperial Pigeons, *Ducula aenea nicobarica* and *Ducula badia insignis*, *Morphologisches Jahrbuch*, vol.135, pp.573-618.

Bhattacharyya, B. N. 1990 The functional morphology of the lingual apparatus of two species of Imperial pigeons, *Ducula aenea nicobarica* and *Ducula badia insignis*, *Proceedings of the Zoological Society of Calcutta*, vol.43, pp.65-92.

Bhattacharyya, B. N. 1994 Diversity of feeding adaptations in certain columbid birds: A functional morphological approach, *Journal of Biosciences*, vol.19, no.4, pp.415-427.

Bock, W. J. 1960 Secondary Articulation of the Avian Mandible, *Auk*, vol.77, pp.19-55.

Bock, W. J. 1964 Kinetics of the Avian Skull, *Journal of Morphology*, vol.114, no.1, pp.1-42.

Bout, R. & Zeigler, H. P. 1994 Jaw muscle (EMG) activity and amplitude scaling of jaw movements during eating in pigeon (*Columba livia*), *Journal of Comparative Physiology* A, vol.174, pp.433-442.

Bovée, J. V. M. G. 2008 Multiple osteochondromas, *Orphanet Journal of Rare Diseases*, 2008, 3:3. DOI:10.1186/1750-1172-3-3

Britt, B. B. 1997 Postcranial Pneumaticity, *in* Currie, P. J. & Padian, K. (eds.) Encyclopedia of Dinosaurs, *Academic Press*, pp.590-593.

Brothwell, D. 2002 Ancient avian osteopetrosis: the current state of knowledge, *Acta zoologica cracoviensia*, vol.45 (special issue), pp.315-318.

Burton, P. J. K. 1974 Jaw and tongue features in Psittaciformes and other orders with special reference to the anatomy of the Tooth-billed pigeon (*Didunculus strigirostris*), *Journal of Zoology*, vol.174, pp.255-276.

Butendieck, E. & Wissdorf, H. 1981 Beitrag zur Benennung der Ossa cinguli membri thoracici und der Ossa alae beim Truthuhn (*Meleagris gallopavo*) unter Berücksichtigung der Nomina Anatomica Avium (1979), *Zoologische Jahrbücher Anatomie und Ontogenie der Tiere*, 106, pp.121-143.

Butendieck, E. & Wissdorf, H. 1982 Beitrag zur Benennung der Knochen des Kopfes beim Truthuhn (*Meleagris gallopavo*) unter Berücksichtigung der Nomina Anatomica Avium (1979), *Zoologische Jahrbücher Anatomie und Ontogenie der Tiere*, 107, pp.153-184.

Butendieck, E., Wissdorf, H. & Ballman, P. 1981 Beitrag zur Benennung der Ossa cinguli membri pelvici und der Ossa membri pelvici beim Truthuhn (*Meleagris gallopavo*) unter Berücksichtigung der Nomina Anatomica Avium (1979), *Zoologische Jahrbücher Anatomie und Ontogenie der Tiere*, 106, pp.449-470.

Cañueto, J., Santos-Briz, A., Yuste-Chaves, M., Nieto, G. & Unamuno, P. 2011 Exostosis de Turret: osteocondroma adquirido [Turret Exostosis or Acquired Osteochondroma], *Actas Dermosifiliográficas*, vol.102, pp.474-475.

Chinsamy, A., Angst, D., Canoville, A. & Göhlich, U. B. 2020 Bone histology yields insights into the biology of the extinct elephant birds (Aepyornithidae) from Madagascar, *Biological Journal of the Linnean Society*, vol.130, issue 2, pp.268-295.

Cracraft, J. 1971 The Functional Morphology of the Hind Limb of the Domestic Pigeon, *Columba livia*, *Bulletin of the American Museum of Natural History*, vol.144, article 3.

Curtis, E. L. & Miller, R. C. 1938 The Sclerotic Ring in North American Birds, *The Auk*, vol.55 pp.225-243.

Diamond, J., Bishop, K. D. & Gilardi, J. D. 1999 Geophagy in New Guinea birds, *Ibis*, vol.141, pp.181-193.

Dubbeldam, J. L. 1993 Systema Nervosum Periphericum, *in* Baumel J. J., King, A. S., Breazile, J. E., Evans, H. E. & Vanden Berge, J. C. (eds) Handbook of Avian Anatomy: Nomina Anatomica Avium, *Publications of the Nuttall Ornithological Club*, 23, pp.555-584.

Early, C. M., Iwaniuk, A. N., Ridgely, R. C. & Witmer, L. M. 2020 Endocast structures are reliable proxies for the sizes of corresponding regions of the brain in extant birds, *Journal of Anatomy*. 15pp. DOI: 10.1111/joa.13285

Eyton, T. C. 1867Osteologia Avium; or, A Sketch of the Osteology of Birds, *Published by R. Hobson, Wellington, Salop*.

Eyton, T. C. 1869 Supplement to Osteologia Avium; or, A Sketch of the Osteology of Birds, *Published by R. Hobson, Wellington, Salop*.

Edinger, T. 1942 The Pituitary Body in Giant Animals Fossil and Living: A Survey and a Suggestion, *The Quarterly Review of Biology*, vol.17, issue 1, pp.31-45.

Ewald, J. R. 1892 Physiologische Untersuchungen ueber das Endorgan des Nerves Octavus, *Wiesbaden: Verlag von J. F. Bergmann*.

Fisher, H. I. 1955 Some Aspects of the Kinetics in the Jaws of Birds, *The Wilson Bulletin*, vol.67, no.3, pp.175-188.

Gegenbaur, C. 1863 Vergleichend-anatomische Bemerkungen über das Fussskelet der Vögel, *Archiv für Anatomie, Physiologie und Wissenswchaftliche Medicin*, pp.450-472.

Gennip, E. M. S. J. van 1986 The Osteology, Arthrology and Myology of the Jaw Apparatus of the Pigeon (*Columba livia* L.), *Netherlands Journal of Zoology*, vol.36, no.1, pp.1-46.

George, J. C. & Berger, A. J. 1966 Avian Myology, *New York and London: Academic Press*.

Gibbs, D., Barnes, E. & Cox, J. 2001 Pigeons and Doves. A Guide to the Pigeons and Doves of the World, *Sussex: Pica Press*.

Glenny, F. H. & Amadon, D. 1955 Remarks on the Pigeon, *Otidiphaps nobilis* Gould, *Auk*, vol.72, pp.199-203.

Graveland, J. 1996 Calcium Deficiency in Wild Birds, *The Veterinary Quarterly*, vol.18, supplement 3, pp.S136-S137.

Günther, A. C. L. G. 1877 The Gigantic Land-Tortoises (Living and Extinct) in the Collection of the British Museum, *London: Printed by Order of the Trustees* [of the British Museum].

Hall, M. I., Iwaniuk, A. N. & Gutiérrez-Ibáñez, C. 2009 Optic Foramen Morphology and Activity Pattern in Birds, *The Anatomical Record*, vol.292, pp.1827-1845.

Harcourt-Brown, N. H. 2002 Orthopedic Conditions That Affect the Avian Pelvic Limb, *Veterinary Clinics of North America: Exotic Animal Practice*, vol.5, no.1, pp.49-81.

Haswell, W. A. 1880 Notes on the Anatomy of Birds, *Proceedings of the Linnean Society of New South Wales*, iv, pp.303-310.

Headley, F. W. 1895 The Structure and Life of Birds, *London and New York: Macmillan and Co*.

Hertel, F. & Campbell Jr, K. E. 2007 The Antitrochanter of Birds: Form and Function in Balance, *The*

Auk, vol.124, no.3, pp.789-805.

Hieronymus, T. L., Witmer, L. M., Tanke, D. H. & Currie, P. J. 2009 The Facial Integument of Centrosaurine Ceratopsids: Morphological and Histological Correlates of Novel Skin Structures, *The Anatomical Record*, 292, pp.1370-1396.

Hiraga, T., Sakamoto, H., Nishikawa, S., Muneuchi, I., Ueda, H., Inoue, M., Shimura, R., Uebayashi, A., Yasuda, N., Momose, K., Masatomi, H. & Teraoka, H. 2014 Vertebral Formula in Red-Crowned Crane (*Grus japonensis*) and Hooded Crane (*Grus monacha*), *Journal of Veterinary Medical Science*, vol.76, no.4, pp.503-508.

Holmes, E. B. 1962 The Terminology of the Short Extensor Muscles of the Third Toe in Birds, *The Auk*, vol.79, no.3, pp.485-488.

Holmes, J. R. 1961 Radiological Changes in Avian Osteopetrosis, *British Journal of Radiology*, vol.xxxiv, no.402, pp.368-377.

Hume, J. P. 2019 Systematics, morphology and ecology of rails (Aves: Rallidae) of the Mascarene Islands, with one new species, *Zootaxa*, 4626 (1), pp.1-107.

Jollie, M. T. 1957 The Head Skeleton of the Chicken and Remarks of the Anatomy of This Region in Other Birds, *Journal of Morphology*, vol.100, no.3, pp.389-436.

Jones, M. E. H., Button, D. J., Barrett, P. M. & Porro, L. B. 2019 Digital dissection of the head of the rock dove (*Columba livia*) using contrast-enhanced computed tomography, *Zoological Letters*, 5: 17. DOI: 10.1186/s40851-019-0129-z

Kierdorf, U., Miller, K.V., Flohr, S., Gomez, S. & Kierdorf, H. 2017 Multiple osteochondromas of the antlers and cranium in a free-ranging white-tailed deer (*Odocoileus virginianus*), *PLoS ONE*, 12(3): e0173775. https://doi.org/10.1371/journal.pone.0173775

Korzun, L. P., Erard, C., Gasc, J.-P. & Dzerzhinsky, F. J. 2008 Bill and hyoid apparatus of pigeons (Columbidae) and sandgrouse (Pteroclididae): A common adaptation to vegetarian feeding? *Comptes Rendus Biologies*, vol.331, pp.64-87.

Kühne, R. & Lewis, B. 1985 External and middle ears, *in* King, A. S. & McLelland, J. (eds.) Form and Function in Birds, *New York, London: Academic Press*, vol.3, pp.227-271.

Kuroda, N. 1971 [A myological illustration of *Columba livia* (Appendicular and caudal muscles)], *Journal of the Yamashina Institute for Ornithology*, vol.6, no.4 (no.36), pp.321-355. [in Japanese]

Laeta, M., Kompanje, E. J. O., Watson, A., Souza, S. M. F. M., Dittmar, K., Cuenca, S. C., Hassel, L. B. & Siciliano, S. 2019 Osteochondromatosis (multiple cartilaginous exostoses) in an immature killer whale *Orcinus orca*, *Diseases of Aquatic Organisms*, vol.134, pp.209-213.

Lemmrich, W. 1931 Der Skleralring der Vögel, *Jenaische Zeitschrift für Naturwissenschaften*, vol.65, pp.513-586.

Livezey, B. C. 1992 Morphological Corollaries and Ecological Implications of Flightlessness in the Kakapo (Psittaciformes: *Strigops habroptilus*), *Journal of Morphology*, vol.213, pp.105-145.

Livezey, B. C. & Humphrey, P. S. 1985 Territoriality and Interspecific Aggression in Steamer-ducks, *The Condor*, vol.87, pp.154-157.

Livezey, B. C. & Humphrey, P. S. 1992 Taxonomy and Identification of Steamer-Ducks (Anatidae: Tachyeres), *Lawrence, Kansas: Museum of Natural History, The University of Kansas*, Monograph No.8.

Longrich, N. R. & Olson, S. L. 2011 The bizarre wing of the Jamaican flightless ibis *Xenicibis xympithecus*: a unique vertebrate adaptation, *Proceedings of the Royal Society B*, vol.278, pp.2333-2337.

Lowe, P. R. 1924 On the Anatomy and Systematic Position of the Madagascan Bird Mesites (Mesœnas), with a Preliminary Note on the Osteology of Monias, *Proceedings of the Zoological Society of London*, no.lxxiv, pp.1131-1152.

Matos, R. de 2008 Calcium Metabolism in Birds, *Veterinary Clinics: Exotic Animal Practice*, vol.11, pp.59-82.

Mayr, G. 2020 The otic region of the skull of neognathous birds: on the homology and comparative morphology of some neurovascular and muscular foramina and other external skeletal structures, *Vertebrate Zoology*, vol.70, no.1, pp.69-85.

Mere, A. E. van der, Maat, G. J. R. & Steyn, M. 2010 Ossified haematomas and infectious bone changes on the anterior tibia: histomorphological features as an aid for accurate diagnosis, *International Journal of Osteoarchaeology*, vol.20, no.2, pp.227-239.

Merz, R. L. 1963 Jaw musculature of the mourning and white-winged doves, *University of Kansas Publications. Museum of Natural History*, vol.12, pp.521-551.

Meyer, A. B. 1879-1888 Abbildungen von Vogel-Skeletten, *Dresden*. Band I, II.

Midtgård, U. 1984 The Blood Vascular System in the Head of the Herring Gull (*Larus argentatus*), *Journal of Morphology*, vol.179, pp.135-152.

Milne-Edwards, A. 1869-1871 Recherches Anatomiques et Paléontologiques pour servir a l'histoire des Oiseaux Fossiles de la France, *Paris, Librairie de G. Masson, Place de l'École-de-Médicine*.

Milne-Edwards, A. & Grandidier, A. 1879, 1881 Histoire Physique, Naturelle et Politique de Madagascar, *Paris: L'Imprimerie Nationale*. Volumes XII (Histoire Naturelle des Oiseaux Tome I), XV (Histoire Naturelle des Oiseaux Tome IV. Atlas III).

Mourer-Chauviré, C. 1993 Les gangas (Aves, Columbiformes, Pteroclidae) du Paléogène et du Miocène inférieur de France, *Palaeovertebrata*, 22, pp.73-98.

Müller, B. 1908 The air-sacs of the pigeon, *Smithsonian Miscellaneous Collections*, vol.50, part 3, pp.365-414.

Nudds, R. L., Dyke, G. J. & Rayner, J. M. V. 2004 Forelimb proportions and the evolutionary radiation of Neornithes, *Proceedings of the Royal Society B* (Suppl.), 271, pp.S324-S327.

Nuechterlein, G. L. & Storer, R. W. 1985 Aggressive Behavior and Interspecific Killing by Flying Steamer-Ducks in Argentina, *The Condor*, vol.87, no.1, pp.87-91.

Olvi, L. G., Lembo, G. M. & Santini-Araujo, E. 2015 Parosteal Osteoma, *in* Santini-Araujo, E., Kalil, R., Bertoni, F. & Park, Y. K. (eds.) Tumors and Tumor-Like Lesions of Bone: For Surgical Pathologists, Orthopedic Surgeons and Radiologists, *London: Springer-Verlag*, pp.119-126.

Olvi, L. G., Lembo, G. M. & Santini-Araujo, E. 2015 Osteoid Osteoma, *in* Santini-Araujo, E., Kalil, R., Bertoni, F. & Park, Y. K. (eds.) Tumors and Tumor-Like Lesions of Bone: For Surgical Pathologists, Orthopedic Surgeons and Radiologists, *London: Springer-Verlag*, pp.127-149.

Owen, R. 1866 On the Anatomy of Vertebrates, *London: Longmans, Green and Co*. Vol. II Birds and Mammals.

Porter, W. R. & Witmer, L. M. 2016 Avian Cephalic Vascular Anatomy, Sites of Thermal Exchange, and the Rete Ophthalmicum, *The Anatomical Record*, vol.299, issue 11, pp.1461-1486. https://doi.org/10.1002/ar.23375

Ritchie, B. W., Harrison, G. J. & Harrison, L. R. 1994 Avian Medicine: Principles and Application, *Lake Worth, Florida: Wingers Publishing, Inc*.

Rooth, J. 1953 On the correlation between the jaw muscles and the structure of the skull in *Columba palumbus palumbus* L. II, *Proceedings of the Koninklijke Nederlandse Akademie van Wetenschappen*, C56, pp.251-264.

Rothschild, B. 2010 Macroscopic Recognition of Nontraumatic Osseous Pathology in the Postcranial Skeletons of Crocodilians and Lizards, *Journal of Herpetology*, vol.44, no.1, pp.13-20.

Rothschild, B. M. & Panza, R. 2006 Osteoarthritis is for the birds, *Clinical Rheumatology*, vol.25, pp.645-647.

Rotthowe, K. & Starck, J. M. 1998 Evidence for a phylogenetic position of button quails (Turnicidae: Aves) among the Gruiformes, *Journal of Zoological Systematics and Evolutionary Research*, vol.36, pp.39-51.

Sawyer, G. T. & Erickson, B. R. 1998 Paleopathology of the Paleocene Crocodile *Leidyosuchu*s (= *Borealosuchus*) *formidabilis*, *The Science Museum of Minnesota*, Monograph Volume 4: Paleontology.

Shufeldt, R. W. 1901 On the Osteology of the Pigeons (Columbæ), *Journal of Morphology*, vol.xvii, no.3, pp.487-514.

Smith, N. A. & Clarke, J. A. 2012 Endocranial Anatomy of the Charadriiformes: Sensory System Variation and the Evolution of Wing-Propelled Diving, *PLoS ONE*, 7 (11): e49584. 22pp. DOI: 10.1371/journal.pone.0049584

Snively, E. & Russell, A. P. 2007 Functional morphology of neck musculature in the Tyrannosauridae (Dinosauria, Theropoda) as determined via a hierarchical inferential approach, *Zoological Journal of the Linnean Society*, vol.151, pp.759-808.

Starck, J. M. 1995 Comparative Anatomy of the External and Middle Ear of Palaeognathous Birds, *Berlin; Heidelberg: Springer-Verlag*. (Advances in Anatomy Embryology and Cell Biology Vol.131).

Steinbacher, G. 1935 Funktionell-anatomische Untersuchungen an Vogelfüßen mit Wendezehen und Rückzehen, *Journal für Ornithologie*, 83, Heft 2, pp.214-282.

Stone, C. A. 1926 Ossifying Hematoma, *Journal of the American Medical Association*, vol.87, no.23, pp.1885-1888.

Taminiau, A. H. M., Bovée, J. V. M. G., Van Rijswijk, C. S. P., Gelderblom, H. A. J. & Van de Sande, M. A. J. 2014 Cartilage-Forming Bone Tumours, *in* Bentley, G. (ed.) European Instructional Lectures. European Instructional Lectures, vol.11, pp.23-44. DOI: 10.1007/978-3-642-34746-7_206

Tsuihiji, T. 2004 The Ligament System in the Neck of Rhea americana and its Implications for the Bifurcated Neural Spines of Sauropod Dinosaurs, *Journal of Vertebrate Paleontology*, vol.24, no.1, pp.165-172.

Tumarkin-Deratzian, A. R., Vann, D. R. & Dodson, P. 2006 Bone surface texture as an ontogenetic indicator in long bones of the Canada goose *Branta canadensis* (Anseriformes: Anatidae), *Zoological Journal of the Linnean Society*, vol.148, pp.133-168.

Turvey, S. T., Green, O. R. & Holdaway, R. N. 2005 Cortical growth marks reveal extended juvenile development in New Zealand moa, *Nature*, vol.435, pp.940-943.

Verheyen, R. 1955 Note sur la Variabilité des Caractères Ostéologiques chez la Macreuse Noire, Melanitta nigra (L.), *Institut royal des Sciences naturelles de Belgique Bulletin* [*Koninklijk Belgisch Instituut voor Natuurwetenschappen Mededelingen*], Tome xxxi, n° 21, pp.1-19.

Wang, X. & Rothschild, B. 1992 Multiple Hereditary Osteochondroma in Oligocene *Hesperocyon* (Carnivora: Canidae), *Journal of Vertebrate Paleontology*, vol.12, no.3, pp.387-394.

Watanabe, J. & Matsuoka, H. 2013 Ontogenetic change of morphology and surface texture of long bones in the Gray Heron (*Ardea cinerea*, Ardeidae), *in* Göhlich, U. B. & Kroh, A. (eds.) Paleornithological Research 2013. Proceedings of the 8th International Meeting of the Society of Avian Paleontology and Evolution, *Vienna: Naturhistorisches Museum Wien*, pp.279-306.

Weber, E. & Hesse, A. 1995 The systematic position of *Aptornis*, a flightless bird from New Zealand, *Courier Forschungsinstitut Senckenberg*, 181, pp.293-301

Wings, O. 2004 Identification, Distrubution, and Function of Gastroliths in Dinosaurs and Extant Birds with Emphasis on Ostriches (*Struthio camelus*), Dissertation zur Erlangung des Doktorgrades (Dr. rer. nat.) der Mathematisch-Naturwissenschaftlichen Fakultät der Rheinischen Friedrich-Wilhelms-Universität Bonn.

Wings, O. 2007 A review of gastrolith function with implications for fossil vertebrates and a revised classification, *Acta Palaeontologica Polonica*, vol.52, no.1, pp.1-16.

Wissdorf, H. & Butendieck, E. 1982 Beitrag zur Benennung von Columna vertebralis, Cavitas thoracica, Costae und Sternum beim Truthuhn (*Meleagris gallopavo*) unter Berücksichtigung der Nomina Anatomica Avium (1979), *Zoologische Jahrbücher Anatomie und Ontogenie der Tiere*, 107, pp.1-19.

Witmer, L. M. 1990 The craniofacial air sac system of Mesozoic birds (Aves), *Zoological Journal of the Linnean Society*, vol.100, pp.327-378.

Witmer, L. M. & Rose, K. D. 1991 Biomechanics of the jaw apparatus of the gigantic Eocene bird *Diatryma*: implications for diet and mode of life, *Paleobiology*, vol.17, no.2, pp.95-120.

Witmer, L. M. & Ridgely, R. C. 2008 The Paranasal Air Sinuses of Predatory and Armored Dinosaurs (Archosauria: Theropoda and Ankylosauria) and Their Contribution to Cephalic Structure, *The Anatomical Record*, vol.291, pp.1362-1388.

Wood, H. B. 1941 Fractures among Birds, *Bird-Banding*, vol.12, no.2, pp.68-72.

Woolfenden, G. E. 1960 Osteology of the Waterfowl. A Dissertation Presented to the Graduate Council of the University of Florida in Partial Fulfillment of the Requirements for the Degree of Doctor of Philosophy. University of Florida. August, 1960.

Worthy, T. H., Mitri, M., Handley, W. D., Lee, M. S. Y., Anderson, A. & Sand, C. 2016 Osteology Supports a Stem-Galliform Affinity for the Giant Extinct Flightless Bird *Sylviornis neocaledoniae* (Sylviornithidae, Galloanseres), *PLoS ONE*, 11(3): e0150871. DOI: 10.1371/journal.pone.0150871

Wuyts, W., Schmale, G. A., Chansky, H. A. & Raskind, W. H. 2020 Hereditary Multiple Osteochondromas, *in* Adam, M. P., Ardinger, H. H., Pagon, R. A., *et al*. (eds.) GeneReviews® [Internet]. *Seattle (WA): University of Washington, Seattle*. 1993-2020. https://www.ncbi.nlm.nih.gov/books/NBK1235/pdf/Bookshelf_NBK1235.pdf

Zaher, M. M. & Abu-Taira, A. M. 2016 A review on the avian viscerocranium, *The Journal of Basic & Applied Zoology*, vol.75, pp.46-53.

Zusi, R. L. 1962 Structural Adaptations of the Head and Neck in the Black Skimmer *Rhynchops nigra* Linnaeus, *Cambridge, Massachusetts: Publications of the Nuttall Ornithological Club*, No.3.

Appendix 1: Anatomical Abbreviations and Additional Notes

With synonyms from other works in which dodo and solitaire osteology is discussed.

Skull and Mandible

am	*angulus mandibulae*	mandibular angle
an	*os angulare*	angular bone
ano	*apertura nasalis ossea*	nasal aperture[233]
aps	*ala parasphenoidalis*	
ar	*os articulare*	articular bone
bo	*os basioccipitale*	basioccipital bone[234]
bsp	*os basisphenoidale*	basisphenoid bone[235]
can	*canalis neurovascularis mandibulae*	mandibular canal[236]
cc	*canalis caroticus*	carotid canal
cco	*canaliculus cochleae*	
cfi	*crista frontalis interna*	internal frontal crest[237]
cic	*crista intercotylaris*	
cl	*os quadratum: crista lateralis*	
clq	*os quadratum: condylus lateralis*	lateral condyle of the quadrate[238]
cm	*crista marginalis*	
cme	*os quadratum: crista medialis*	
cmq	*os quadratum: condylus medialis*	medial condyle of the quadrate[239]
cns	*crista nuchalis sagittalis*	sagittal nuchal crest[240]
cnt	*crista nuchalis transversa*	transverse nuchal crest[241]
co	*os quadratum: crista orbitalis*	
coc	*condylus occipitalis*	occipital condyle
coca	*canalis orbitalis caudalis*	
coe	*canalis ophthalmicus externus*	
col	*facies articularis quadratica: cotyla lateralis*	lateral mandibular facet
com	*facies articularis quadratica: cotyla medialis*	medial mandibular facet
copmx	*corpus ossis premaxillare*	body of the premaxilla
coqj	*os quadratum: cotyla quadratojugalis*	quadratojugal facet of the quadrate
corb	*canalis orbitalis*	
coro	*canalis orbitalis rostralis*	
cot	*os quadratum: condylus oticus*	otic condyle of the quadrate[242]
cpc	*cristae paracoronoidea rostralis et caudalis*	(Weber & Hesse 1995)
cptq	*os quadratum: condylus pterygoideus*	pterygoid condyle of the quadrate
cq	*os quadratum: corpus quadrati*	body of the quadrate
cqj	*os quadratojugale: condylus quadraticus*	quadrate condyle of the quadratojugal
cqo	*cotyla quadratica otici*	otic cotyla for the quadrate[243]
cqs	*os squamosum: cotyla quadratica squamosi*	quadrate facet of the squamosal
csq	*os quadratum: condylus squamosus*	squamosal condyle of the quadrate[244]

---

[233] Nasal fissure (Melville 1848); Nasenspalte (Brandt 1848).

[234] Occipital bone (Melville 1848)?

[235] Sphenoid bone [in part] (Melville 1848)?

[236] Dental canal / space (Melville 1848).

[237] Falcial ridge (Owen 1867).

[238] Outer mandibular condyle (Melville 1848).

[239] Inner mandibular condyle (Melville 1848).

[240] Infra-occipital ridge, inferior occipital ridge (Melville 1848); Crista sagittalis (Martin 1904); infraoccipital ridge (Janoo 1996).

[241] Supra-occipital ridge, superior occipital ridge (Melville 1848); Crista lambdoides (Martin 1904); (supra)occipital crest (Janoo 1996); crête supraoccpitale (Janoo 1997).

[242] Posterior superior condyle (Melville 1848); opisthotic head of the quadrate (Lowe 1926); condyle prootique (Janoo 1997).

[243] Posterior tympanic facet, inferior tympanic articular surface (Melville 1848); prootic articular facet (Janoo 1996).

[244] Anterior superior condyle (Melville 1848); temporal condyle (Janoo 1996); “segment articulaire mastoïdien” (Janoo 1997, p.103).

ct	*crista tentorialis*	tentorial crest[245]
cte	*crista temporalis*	temporal crest[246]
ctf	*crista transversa fossae*	
ctpmx	*crista tomialis premaxillare*	tomial crest of the premaxilla
cty	*os quadratum: crista tympanica*	tympanic crest
d	*os dentale*	dentary bone
dp	*os quadratum: depressio protractoris*	
dpc	*os quadratum: depressio precondylaris*	
ds	*dorsum sellae*[247]	
eac	*eminentia arcuata canalis semicircularis rostralis*	
ect	*os ectethmoidale*	ectethmoid bone[248]
eo	*os exoccipitale*	exoccipital bone
f	*os frontale*	frontal bone[249]
fac	*fossa auriculae cerebelli*[250]	
facn	*fossa aditus canalis neurovascularis*	mandibular fossa
fafr	*os lacrimale: facies articularis frontonasalis*	
fai	*fossa acustica interna*	internal acoustic fossa[251]
fan	*fenestra antorbitalis*	antorbital fenestra[252]
fapa	*os palatinum: facies articularis parasphenoidalis*	parasphenoid facet of the palatine
faps	*os pterygoideum: facies articularis parasphenoidalis*	parasphenoid facet of the pterygoid
fapt	*os pterygoideum: facies articularis palatina*	palatine articulation of the pterygoid
faq	*os pterygoideum: facies articularis quadratica*	quadrate facet of the pterygoid
fbo	*fossa bulbi olfactorii*	
fc	*fossa caudalis*	
fcc	*fossa cranii caudalis*[253]	
fce	*fossa cerebelli*[254]	
fco	*fenestra cochleae*[255]	
fcr	*fossa cranii rostralis*[256]	
fen	*foramen endolymphaticum*	endolymphatic foramen
fet	*foramen ethmoidale*	ethmoid foramen
fgv	*fossa ganglii vagoglossopharyngealis*	
fip	*fissura interpalatina*	interpalatine fissure[257]
fmc	*foramen m. columellae*	
fmm	*foramen magnum*	foramen magnum
fmr	*fenestra mandibularis rostralis*	mandibular fenestra[258]
fn	*facies nuchalis*	nuchal face[259]
fna	*foramina n. ampullaris*	[see text for details]
fnv	*foramina neurovascularia*	neurovascular foramina
fob	*fossa basiorbitalis*	basiorbital fossa[260]
foc	*fonticulus occipitalis*	supraoccipital foramen[261]

---

[245] Vertical tentorium (Owen 1867)?; postcerebral division (Owen 1867)?; tentorial ridge (Owen 1870b).

[246] Maseteric ridge (Newton & Clark 1879); crista lateralis (Janoo 1996).

[247] Clinoid plate / process (Melville 1848).

[248] Inferior or inflated ala of the ethmoid (Melville 1848).

[249] Stirnbein (Brandt 1848).

[250] Oblong cerebellar fossa / pit (Owen 1867).

[251] Meatus acusticus internus (Melville 1848); multiperforate internal auditory depression (Owen 1867)?; méat auditif externe (Janoo 1997).

[252] Lachrymal fissure / vacuity (Melville 1848); naso-lachrymal orifice (Owen 1878); Thränenspalte (Reuss 1855).

[253] The "petrosal excavation" of Melville (1848) may correspond to the fossa cranii caudalis, or part of it.

[254] Epencephalic compartment (Owen 1867)?

[255] Foramen rotundum (Melville 1848).

[256] Cerebral fossa, prosencephalic chamber (Owen 1867).

[257] Inferior nasal fissure (Melville 1848); Choanenspalte (Brandt 1848); untere Nasenspalte (Reuss 1855); palato-nasal fissure, naso-palatine aperture (Owen 1867); interpalatine vacuity, maxillo-palatal cleft (Owen 1878).

[258] Ramal vacuity (Melville 1848); foramen mandibulaire (Verheyen 1957); foramen mandibulaire rostral (Janoo 1997).

[259] Plaque nuchale (Janoo 1997).

[260] Recessus medialis (Janoo 1997).

[261] Mesial occipital aperture (Melville 1848); foramen supraoccipitale (Martin 1904).

foi	*foramen ophthalmicum internum*	
fol	*foramen orbitonasale laterale*	lateral orbitonasal foramen[262]
fom	*foramen orbitonasale mediale*	medial orbitonasal foramen[263]
fpb	*fossa parabasalis*	parabasal fossa
fpc	*foramen pneumaticum caudale*	caudal pneumatic foramen
fpl	*os frontale: processus lacrimalis*	lacrimal process of the frontal[264]
fpn	*os nasale: processus frontalis*	frontal process of the nasal[265]
fppmx	*os premaxillare: processus frontalis*	frontal process of the premaxilla[266]
froc	foramen for ramus occipitalis of A. ophthalmica externa?	
ft	*fossa temporalis*[267]	temporal fossa
ftm	*fossa tecti mesencephali*	
fve	*fenestra vestibuli*	vestibular fenestra[268]
fvoe	*foramen venae occipitalis externae*	external occipital vein foramen[269]
idnl	*incisura ductus nasolacrimalis*	lacrimal groove
iiq	*os quadratum: incisura intercondylaris*	intercondylar notch of the quadrate
ios	*septum interorbitale*	interorbital septum[270]
iov		canal for internal ophthalmic vessels
j	*os jugale*	jugal bone[271]
jpmx	*os maxillare: processus jugalis*	jugal process of the maxilla[272]
la	*os laterosphenoidale*	laterosphenoid bone[273]
lac	*os lacrimale*	lacrimal bone[274]
ld	*os mesethmoidale: lamina dorsalis*	
lps	*lamina parasphenoidalis*	parasphenoid plate
me	*os mesethmoidale*	mesethmoid bone[275]
mpp	*os maxillare: processus maxillopalatinus*	maxillopalatine process of the maxilla[276]
mppmx	*os maxillare: processus premaxillaris*	premaxillary process of the maxilla
mpq	*os quadratum: processus mandibularis*	mandibular process of the quadrate[277]
mso	*margo supraorbitalis*	supraporbital margin
npm	*os nasale: processus maxillaris*	maxillary process of nasal[278]
nvc	*foramen n. vestibulocochlearis*	
occ	*ostium canalis carotici* [*ostium canalis caroticus cranialis*]	carotid canal foramen
ocnv	*ostium canalis neurovascularis*	opening of neurovascular canal
ocoe	*ostium canalis ophthalimicus externus*	external ophthalmic canal foramen[279]

---

[262] Prefronto-ethmoidal fissure (Melville 1848); fissure préfronto-ethmoïdale (Janoo 1997).

[263] Ant-orbital foramen (Melville 1848).

[264] Ant-orbital process of the frontal (Melville 1848); prefrontal (Newton & Clark 1879); processus orbitalis of the prefrontal (Livezey 1993).

[265] Frontal plate of the nasal (Melville 1848); processus nasalis frontalis (Janoo 1996).

[266] Nasal process of the premaxillary (Melville 1848, Owen 1867, Newton & Newton 1869; Janoo 2000); premaxillary median / mesial process (Melville 1848); Stirnnasentheil des Zwischenkiefers (Brandt 1848); Nasenfortsatze des Zwischenkieferbeins, Frontalfortsatzes des Zwischenkiefers (Reuss 1855); processus nasal des prémaxillaire (Verheyen 1957).

[267] The fossa temporalis is here restricted to the cranial attachment fossa of the m. a. m. e. (the fossa musculorum temporalium of Livezey & Zusi 2006).

[268] Foramen ovale of the vestibule (Melville 1848).

[269] Lateral occipital foramen (Melville 1848).

[270] Septum interorbital (l'orbitosphenoide) (Verheyen 1957).

[271] Malar bone (Melville 1848, Owen 1867); Jochbein (Brandt 1848).

[272] Malar process / style (Melville 1848).

[273] Orbitosphenoid (Martin 1904): "With the ventral section of its caudal edge it limits the For. opticum resp. lacerum ant. forward, its dorsal section grows together with the Alisphenoid [...] in *Didunculus*, *Didus* and *Pezophaps* it limits the exit of the N. olfactorius downward" (p.195).

[274] Prefrontal (Melville 1848); Thränenbein (Brandt 1848); os lacrymaux (Milne-Edwards 1866b); préfrontal, lacrymal (Janoo 1997). "The bone which has heretofore been denominated the lachrymal in birds, is undoubtedly the homologue of the prefrontal in the cranium of fishes and reptiles" (Melville 1848, p.87).

[275] Pre-sphenoid (Parker 1861).

[276] Siebbeinplatte (Brandt 1848); prevomer (Parker 1866).

[277] Condyle mandibulaire (Janoo 1997).

[278] Ecto-nasal limb (Melville 1848); Oberkieferfortsatz der Nasenbeine (Brandt 1848); äusseren Nasalfortsatz (Reuss 1855); processus latéral du nasal, barre latérale du nasal (Janoo 1997).

op	*os opisthoticum: promontorium tympani*	tympanic promontory of the opisthotic bone
otp	*ostium tympanicum tuba pharyngotympanica*	opening of the auditory tube
par	*os parietale*	parietal bone[280]
pat	*os prearticulare*	prearticular bone[281]
pbpt	*os parasphenoidale: processus basipterygoideus*	basipterygoid process[282]
pc	*processus condylaris*	condylar process
pcd	*os palatinum: crista dorsolateralis*	dorsolateral crest of the palatine
pcl	*os palatinum: crista lateralis*	lateral crest of the palatine
pco	*processus coronoideus*	coronoid process
pcr	*os palatinum: processus rostralis choanalis*	
pcv	*os palatinum: crista ventralis*	ventral crest of the palatine[283]
pfdl	*os palatinum: facies dorsolateralis*	dorsolateral face of the palatine
pfv	*os palatinum: fossa ventralis*	ventral fossa of the palatine
pie	*os exoccipitale: processus internus*	internal exoccipital process[284]
pl	*os quadratum: processus lateralis*	
pml	*processus lateralis mandibulae*	lateral mandibular process
pmm	*processus mandibulae medialis*	medial mandibular process
pmpn	*os nasale: processus premaxillaris*	premaxillary process of the nasal[285]
pmxm	*os premaxillare: processus maxillaris*	maxillary process of the premaxilla[286]
pn	*foramen pneumaticum*	pneumatic foramen
pna	*foramen pneumaticum articulare*	
po	*pila otica*	otic pillar
poq	*os quadratum: processus oticus quadrati*	otic process of the quadrate[287]
porq	*os quadratum: processus orbitalis quadrati*	orbital process of the quadrate[288]
ppe	*processus paroccipitalis*	paroccipital process
ppmp	*os palatinum: processus premaxillaris*	premaxillary process of the palatine
ppo	*processus postorbitalis*	postorbital process[289]
pppmx	*os premaxillare: processus palatinus*	premaxillary process of the palatine[290]
pppt	*os palatinum: processus pterygoideus*	pterygoid process of the palatine[291]
pqu	*os pterygoideum: processus quadraticus*	quadrate process of the pterygoid
pre	*processus retroarticularis*	retroarticular process[292]
pro	*os lacrimale: processus orbitalis*	orbital process of the lacrimal
prs	*os parasphenoidale: rostrum sphenoidale*	parasphenoid rostrum
psl	*os parasphenoidale: processus lateralis*	lateral process of the parasphenoid[293]
psm	*processus suprameaticus*	suprameatic process[294]
psp	*os parasphenoidale*	parasphenoid bone[295]
pt	*os pterygoideum*	pterygoid bone[296]
ptb	peduncle of the pterygobasipterygoid articulation	
ptp	*os pterygoideum: pes pterygoidei*	foot of the pterygoid

---

[279] Foramen du processus métotique (Janoo 1997, fig.8, fp)?

[280] Scheitelbein (Martin 1904).

[281] The prearticular forms the “rostrum of the articular element” of Melville (1848, p.96).

[282] Pterygoid process (Owen 1867); pterapophysis (Owen 1878).

[283] Palatine process (Melville 1848); crista palatina interna (Janoo 1997); internal palatine lamina (Janoo 2000).

[284] Vestibular elevation / prominence (Melville 1848).

[285] Ento-nasal plate (Melville 1848); innere Fortsatz des Nasenbeins; inneren Nasenfortsatz, inneren Nasalfortsatz (Reuss 1855).

[286] Nasal process of the premaxillary (Janoo 1996).

[287] Capitulum (Janoo 1997).

[288] Processus orbitaire (Janoo 1997).

[289] Postfrontal process (Owen 1848a, 1867); processus post-orbitaire (Janoo 1997).

[290] Palatine tuberosity (Melville 1848)?

[291] “Éperon épiptérygoidien ou processus pterygoideus (=processus caudalis)” (Janoo 1997, p.176). However, Verheyen (1957) stated that the epipterygoid spur (éperon épiptérygoïdien) is absent in Columbae, suggesting that this refers to a distinct feature and not the pterygoid process itself.

[292] Posterior angular process of the mandible (Janoo 2000: 40).

[293] Lateral basitemporal process (Bock 1960); processus métotique (Janoo 1997).

[294] Mastoid process (Melville 1848)?; post-tympanic process (Owen 1866b).

[295] Sphenoid [in part] (Melville 1848); presphenoid (Owen 1848a, 1867, 1878); basisphenoid (Owen 1848a); basi-presphenoid, basisphenoid (Owen 1878); basi-sphenoid, sphenoid (Newton & Clark 1879).

[296] Flügelbeine (pl.) (Brandt 1848).

pz	*processus zygomaticus*	zygomatic process[297]
qj	*os quadratojugale*	quadratojugal bone[298]
qu	*os quadratum*	quadrate bone[299]
rc	*recessus columellae*	columellar recess[300]
rm	*ramus mandibulae*	mandibular ramus
ro	*regio olfactoria*	posterior olfactory chamber[301]
rom	*rostrum mandibulae*	mandibular symphysis
rtd	*recessus tympanicus dorsalis*	dorsal tympanic recess[302]
rtr	*recessus tympanicus rostralis*	rostral tympanic recess
sa	*os supra-angulare*	supra-angular bone[303]
siq	*os quadratum: sulcus intercondylaris*	intercondylar sulcus of the quadrate
soc	*os supraoccipitale*	supraoccipital bone[304]
sol	*sulcus n. olfactorii*	olfactory sulcus[305]
spl	*os spleniale*	splenial bone[306]
spnq	*os quadratum: sulcus pneumaticus*	pneumatic sulcus of the quadrate
sq	*os squamosum*	squamosal bone[307]
st	*sella turcica*	
svs	*sulcus v. semicircularis*[308]	
tac	*tuba auditiva* [*pharyngotympanica*] *communis*	common auditory/eustachian tube[309]
tbl	*tuberculum basilare laterale*	lateral basilar tubercle[310]
tbm	*tuberculum basilare mediale*	medial basilar tubercle[311]
tm	*tomium mandibulae*	mandibular tomium
tpt	*tuberculum pseudotemporale*[312]	
vf	venous? foramen (see Mayr 2020)	

Cranial nerves / cranial nerve foramina:

I	*foramen n. olfactorius*	olfactory nerve foramen[313]
II	*foramen n. opticus*	optic nerve foramen
III	*foramen n. oculomotorii*	oculomotor nerve foramen
IV	*foramen n. trochlearis*	trochlear nerve foramen[314]
V_1	*foramen n. ophthalmici*	ophthalmic nerve foramen
$V_{2,3}$	*foramen n. maxillomandibularis*	maxillomandibular nerve foramen[315]
VI	*foramen n.abducentis*	abducens nerve foramen
VII	*foramen n. facialis*	facial nerve foramen
VIII	*foramen n. cochlearis*	auditory nerve foramen
IX	*foramen n. glossopharyngealis*	glossopharyngeal nerve foramen
X	*foramen n. vagi*	vagus nerve foramen[316]

---

[297] Post-temporal process of the mastoid (Melville 1848); zygoma (Beddard 1898); processus temporal (Verheyen 1957); temporal process (Janoo 2000); mastoid process (Owen 1848a).

[298] Squamosal (Newton & Newton 1869).

[299] Tympanic (Melville 1848, Owen 1878); Quadratbein (Brandt 1848).

[300] Vestibule (Melville 1848).

[301] Olfactory fossa (Melville 1848); interior fossae bulbi olfactorii (pl.) (Claessens *et al*. 2015).

[302] Superior tympanic / pneumatic aperture / foramen (Melville 1848); upper tympanic recess (Janoo 1996).

[303] Surangular (Melville 1848).

[304] Occipital bone, supra-occipital plate (Melville 1848).

[305] Groove for nasal vessels (Melville 1848).

[306] Opercular (Melville 1848).

[307] Mastoid bone (Melville 1848).

[308] Groove for the lateral venous sinus (Owen 1867).

[309] Ouverture des tromps d'Eustache (Janoo 1997).

[310] Basilar protuberance (Melville 1848); basioccipital tubercle (Owen 1867); tubercule basispénoïdal, tubercule basilaire (Janoo 1997).

[311] "Scabrous tubercle" (Melville 1848); corps mammilaires basisphénoïdaux, tubercule mammillaire (Janoo 1997).

[312] Tubercule pseudotemporal (proc. pseudotemporalis), processus pseudotemporal (Janoo 1997). Janoo (1997, p.178) mistakenly synonymizes the coronoid process (processus coronoïde) and the tuberculum pseudotemporale.

[313] Rhinencephalic foramen (Janoo 1996).

[314] Foramen for patheticus nerve (Melville 1848).

[315] Foramen ovale, foramen rotundo-ovale, foramen lacerum anterius (Melville 1848).

XI	*n. accessorius*	accessory nerve (exits the endocranial cavity with nerve X)
XII	*canalis n. hypoglossi*	hypoglossal nerve canal[317]

3D CT images

aja	*arcus jugalis*	jugal arch
aop	*ampulla ossea posterior*	
aor	*ampulla ossea rostralis*	
cc	*canalis caroticus*	carotid canal
cco	*canaliculus cochleae*	
cfi	*crista frontalis interna*	
chl	*cochlea*	
coca	*canalis orbitalis caudalis*	
coe	*canalis ophthalmicus externus*	
coro	*canalis orbitalis rostralis*	
cosc	*crus osseum commune*	
csa	*canalis semicircularis anterior*[318]	
csl	*canalis semicircularis lateralis*[319]	
csp	*canalis semicircularis posterior*[320]	
ect	*os ectethmoidale*	ectethmoid
f	*os frontale*	frontal
fac	*fossa auriculae cerebelli*	
fbo	*fossa bulbi olfactorii*	
fcm	*fossa cranii media*	
fcr	*fossa cranii rostralis*	
fen	*foramen endolymphaticum*	endolymphatic foramen
fet	*foramen ethmoidale*	ethmoid foramen
fh	*fossa hypophysialis*	hypophysial fossa
fmd	*fossa medullae oblongatae*	
fom	*foramen orbitonasale mediale*	
fpb	*fossa parabasilis*	parabasal fossa
fpn	*os nasale: processus frontalis*	frontal process of the nasal
fppmx	*os premaxillare: processus frontalis*	frontal process of the premaxilla
fve	*fenestra vestibuli*	
idnl	*incisura ductus nasolacrimalis*	lacrimal groove
imc	*impressio m. cucullaris*	
iov		canal for internal ophthalmic vessels
la	*os laterosphenoidale*	laterosphenoid
lac	*os lacrimale*	lacrimal
los	*labyrinthus osseus*	bony labyrinth
mes	*os mesethmoidale*	mesethmoid
npm	*os nasale: processus maxillaris*	maxillary process of the nasal
pal	*os palatinum*	palatine
par	*os parietale*	parietal
pat	*os prearticulare*	prearticular
pco	*processus coronoideus*	coronoid process
pmpn	*os nasale: processus premaxillaris*	premaxillary process of the nasal
pn	*foramen pneumaticum*	pneumatic foramen
psp	*os parasphenoidale*	parasphenoid
pt	*os pterygoideum*	pterygoid
q	*os quadratum*	quadrate
qj	*os quadratojugale*	quadratojugal
rc	*recessus columellae*	
ro	*regio olfactoria*	posterior olfactory chamber
rtc	*recessus tympanicus caudalis*	caudal tympanic recess
scl	*ossa sclerae*	sclerotic ring

---

[316] Foramen for pneumogastric nerve and spinal accessory nerve (Melville 1848).
[317] Condyloid foramen (Melville 1848); precondyloid foramina (Owen 1867).
[318] Superior semicircular canal (Owen 1867); canal semicirculaire rostral (Janoo 1997).
[319] Canal semicirculaire horizontal (Janoo 1997).
[320] Canal semicirculaire caudal (Janoo 1997).

soc	*os supraoccipitale*	supraoccipital
spl	*os spleniale*	splenial
tac	*tuba auditiva communis*	common auditory/eustachian tube
tav	*tuba auditiva*	auditory tube

Endocasts

acc	*a. carotis cerebralis*	
aop	*a. ophthalmica*	
bol	*bulbus olfactorius*	olfactory bulb
cb	*cerebrum*	
cbl	*cerebellum*	
cho	*chiasma opticum*	
es	*eminentia sagittalis*	sagittal eminence[321]
fih	*fissura interhemispherica*	
fl	*flocculus*	
hy	*hypophysis*	pituitary body
mo	*medulla oblongata*	
tem	*tectum mesencephali*[322]	
VII_{h}	*n. hyomandibularis*	
VII_{p}	*n. palatinus*	

* = “damaged portion of endocranium resulting in outpocket of endocast” (Gold *et al*. 2016, p.5). The damage is in the region of the “tentorial tuberosity” of Owen (1867).

Postcranial Skeleton and Soft Tissue

Atlas

aa	*arcus atlantis*[323]	
ca	*corpus atlantis*	
fa	*facies articularis*	
faa	*facies articularis axis*	
fc	*fossa condyloidea*[324]	
fv	*foramen vertebrale*	neural canal
if	*incisura fossae*	
pcl	*processus caudolateralis*[325]	
scv	*sulcus caudoventralis*	
tlt	*tuberositas ligamenti transversi*	
zc	*zygapophysis caudalis*	postzygapophysis[326]

Axis[327]

cax	*corpus axis*	
cvc	*crista ventralis corporis*[328]	hypapophysis
da	*dens axis*[329]	
far	*facies articularis atlantica*	
ica	*incisura caudalis arcus*[330]	
ld	*lamina dorsalis*	
lla	*lamina lateralis arcus*	
psp	*processus spinosus*	neural spine[331]

---

[321] Wulst.

[322] Optic lobe (Gold *et al*. 2016).

[323] Arcus atlantis dorsalis (Janoo 1997). Janoo (1997) mentioned the pair of lateral anses (*ansa latus* Boas 1929) of the atlas. These probably correspond to the arcus atlantis.

[324] Fovea condylus (Janoo 1997).

[325] Tuberculum ventralis (Janoo 1997, pl.16).

[326] Apophyses articulaires: inférieures (Milne-Edwards 1866b); processus ala caudalis, processus arcualis caudalis (of the atlas) (Janoo 1997).

[327] Epistropheus (Newton & Gadow 1895).

[328] Corps hypocentraux [of the caudal vertebral column] (Verheyen 1957)?

[329] Odontoid process (Owen 1867).

[330] Arcuales recessi (pl.) (Janoo 1997)?

td	*tuberculum dorsale*	anapophysis
zcr	*zygapophysis cranialis*	prezygapophysis[332]

Cervical vertebra

ac	*ansa costotransversaria*[333]	
av	*arcus vertebrae*	neural arch[334]
cl	*concavitas lateralis*	
cto	*crista transverso-obliqua*	
cv	*corpus vertebrae*	centrum
fa	*facies articularis*	articular face
fac	*facies articularis caudalis*	caudal articular face of the centrum
fcr	*facies articularis cranialis*	cranial articular face of the centrum
ft	*foramen transversarium*[335]	transverse foramen
fv	*foramen vertebrale*	neural canal
ica	*incisura caudalis arcus*	
icra	*incisura cranialis arcus*	
lda	*lamina dorsalis arcus*	
li	*lacuna interzygapophysialis*	
lla	*lamina lateralis arcus*	
pc	*processus caroticus*[336]	carotid process
pco	*processus costalis*[337]	
psp	*processus spinosus*	neural spine
ptv	*processus transversus vertebrae*[338]	
pvc	*processus ventralis corporis*	
sc	*sulcus caroticus*[339]	
sl	*sulcus lateralis*	
ta	*tuberculum ansae*	
td	*torus dorsalis*[340]	
zc	*zygapophysis caudalis*	postzygapophysis
zcr	*zygapophysis cranialis*	prezygapophysis

Zygapophyses (apophyses articulaires of Milne-Edwards 1866b).

Notarium[341]

ale	*area ligamenti elastici*[342]	
cn	*canalis notarii*	
crl	*crista lateralis*	
csn	*crista spinosa (dorsalis) notarii*	spinous (dorsal) crest
cve	*crista ventralis notarii*	
fco	*fovea costalis*	
fic	*fenestra intercristalis*	
fin	*foramen intervertebrale*[343]	

Vertebral rib[344]

cc	*capitulum costae*
cco	*corpus costae*

---

[331] Spinous process (Newton & Gadow 1895); neurapophyse (Janoo 1997).

[332] Apophyses articulaires: supérieures (Milne-Edwards 1866b).

[333] Par-pleurapophysis (Owen 1879).

[334] Neurapophysis (Owen 1867).

[335] Passages des artères vertébrales (pl.) (Milne-Edwards 1866b); "arterial canal" (Newton & Clark 1879).

[336] Catapophysis (Owen 1879).

[337] Pleurapophysis (Owen 1867).

[338] Apophyses transverses (pl.) (Milne-Edwards 1866b); diapophysis (Owen 1867).

[339] Carotid / haemal canal (Owen 1867).

[340] Anapophysis, anapophysial tubercle (Owen 1867); hyperapophysis (Owen 1879).

[341] Os dorsale (Verheyen 1957).

[342] Surface d'insertion du ligament cervical (Milne-Edwards 1866b).

[343] Conjugational foramen (Owen 1867).

[344] Pleurapophysis (Owen 1867); dorsal rib (Newton & Newton 1869).

col	*collum costae*[345]
fad	*facies articularis costalis distalis*
fav	*facies articularis vertebralis*
ica	*incisura capitulotubercularis*
pu	*processus uncinatus*[346]
tc	*tuberculum costae*

Sternal rib[347]

facp	*facies articularis costalis proximalis*
fas	*facies articularis sternalis*

Synsacrum

cd	*crista dorsalis*	
cs	*canalis synsacri*[348]	
csp	*crista spinosa synsacri*	spinous (dorsal) crest[349]
cv	*crista ventralis*[350]	
eco	*eminentia costolateralis*	
fco	*fovea costalis*	
fcr	*facies articularis cranialis*	cranial articular face of the centrum
prc	*processus costalis*	costal process
ptv	*processus transversus*	transverse process
zcr	*zygapophysis cranialis*	prezygapophysis

Foramina intervertebralia (for spinal nerves): see notarium.

Caudal vertebra

av	*arcus vertebrae*	neural arch
fcr	*facies articularis cranialis*	cranial articular face of the centrum
fv	*foramen vertebrale*	neural canal
psp	*processus spinosus*	neural spine
ptv	*processus transversus vertebrae*	

Pelvis (Os coxae)[351]

ace	*acetabulum*[352]
ai	*ala ischii*
ant	*antitrochanter*[353]
api	*ala postacetabularis ilii*[354]
apri	*ala preacetabularis ilii*
apu	*apex pubis*
ci	*canalis iliosynsacralis*[355]
cic	*crista caudalis fossae renalis*[356]

---

[345] The neck and head of the cervical rib, fused to the cervical vertebra, correspond to the parapophysis of Owen (1867, pl.xii, figs.7, 9). The term ‘parapophysis’ is used in historical literature to refer to the eminentia costolateralis of cervicodorsal and dorsal vertebrae (see Baumel & Witmer 1993).

[346] Epipleural process (Owen 1867); epipleural appendage (Newton & Newton 1869).

[347] Haemapophysis (Owen 1867); “sternal appendage”, “sterno-costal appendage” (Newton & Clark 1879).

[348] Rückenmarkscanal (Martin 1904).

[349] Crête épineuse du sacrum (Milne-Edwards 1866b); composed of coalesced “sacral spines” (Owen 1867); crête synsacrale (Verheyen 1957); composed of fused “spinae dorsales” (Lüttschwager 1959a); crête sacrée médiane, crête dorsale du synsacrum (Janoo 1997); mid-synsacral crest, crista synsacralis (Janoo 2000).

[350] Crête synsacrale ventrale (Janoo 1997).

[351] Innominate bone.

[352] Cavités cotyloïdes (pl.) (Milne-Edwards 1866b).

[353] Facette sus-cotyloïdienne du bassin (Milne-Edwards 1866b); “Trochanterian surface” (Newton & Newton 1869).

[354] Aile postérieure de l’ischion [*sic*] (Janoo 1997, fig.11).

[355] Gouttières vertébrales (pl.) (Milne-Edwards 1866b); ileoneural [*sic*] canal (Owen 1867); ilioneural canal (Newton & Newton 1869); canaux ilio-lombaires (pl.) (Verheyen 1957); Cavum ilio-lumbale dorsale (Lüttschwager 1959b); cavum iliodorsalis, cavum iliolombaire, cavum iliosynsacralis (Janoo 1997); ilio-lumbar canals (pl.) (Janoo 2000).

cid	*crista dorsolateralis ilii*[357]
cii	*crista iliaca intermedia*
cil	*corpus ilii*
cio	*crista iliaca obliqua*
cis	*corpus ischii*
coi	*concavitas infracristalis*
cp	*corpus pubis*
cri	*crista iliosynsacralis*
face	*foramen acetabuli*
faf	*facies articularis femoralis*[358]
fid	*fossa iliaca dorsalis*[359]
fii	*foramen ilioischiadicum*[360]
fo	*foramen obturatum*[361]
foi	*foramina intertransversaria*[362]
fr	*fossa renalis*[363]
fri	*facies renalis ilii*
icp	*incisura caudalis pelvis*
iia	*os ilium: incisura acetabularis*
imc	*incisura marginalis caudalis*
imf	*os ilium: margo foraminis ilioischiadica*
ismf	*os ischium: margo foraminis ilioischiadica*
iv	*impressiones vascularia*
lii	*lamina infracristalis ilii*
pi	*pila ilioischiadica*
pif	*pars ischiadica fossae*[364]
pio	*os pubis: incisura obturatoria*
po	*processus obturatorius*[365]
ppf	*pars pudenda fossae*[366]
pti	*processus ternimalis ilii*
ptis	*processus terminalis ischii*
rcf	*recessus caudalis fossae*[367]
sdi	*spina dorsolateralis ilii*
si	*sutura iliosynsacralis*
sp	*scapus pubis*[368]
spi	*spatium ischiopubicum*[369]

Pre- and postacetabular regions of the pelvis (régions précotyloïdienne et postcotyloïdienne of Milne-Edwards 1866b).

Sternum[370]

cos	*corpus sterni*	

---

[356] "Transverse buttress" (Owen 1867); Crista ichiosacralis [*sic*] (Gegenbaur 1871); crista iliaca caudalis.

[357] Crête sus-ischiatique (pl.) (Milne-Edwards 1866b); Gluteal ridge (Newton & Newton 1869); crista lateralis, crête dorsolatérale (Janoo 1997).

[358] "Trochanterian surface" (Owen 1867).

[359] Fosses iliaques externes (pl.) (Milne-Edwards 1866b).

[360] Trou sciatique (Milne-Edwards 1866b); ischiadic foramen (Owen 1867); foramen ischiadicum (Owen 1878); foramen ischiatique (Janoo 1997); foramen ovale (Ottow 1952).

[361] Trou obturateur (Milne-Edwards 1866b); "Obturator interspace" (Owen 1878); foramen obturatorium (Martin 1904); pars dissaepta du foramen obturatorium (Verheyen 1957).

[362] Foramina interdiapophysaires (Verheyen 1957); foramen transverse (singular) (Janoo 1997).

[363] Fosses rénales antérieures et postérieures (Milne-Edwards 1866b).

[364] Praerenal fossa (Owen 1867).

[365] Processus inferior ossis ischii (Verheyen 1957); processus inferior ischii (Janoo 1997).

[366] Postrenal fossa (Owen 1867).

[367] Recessus iliacus posterior (Gegenbaur 1871); recessus iliacus.

[368] Post pubis (Janoo 1997).

[369] Trou sus-ischiatique (Milne-Edwards 1866b); "Tendinal interspace" (Owen 1878); foramen oblongum (Lüttschwager 1959b).

[370] Brustbein (Brandt 1848).

cs	*carina sterni*[371]	sternal carina
fac	*facies articularis costalis*	
fms	*facies muscularis sterni*	
fopn	*fossa pneumaticum*	pneumatic fossa
fpn	*foramen pneumaticum*	pneumatic foramen
fvsc	*facies visceralis sterni:*[372] *pars cardiaca*	
fvsh	*facies visceralis sterni: pars hepatica*	
iin	*incisura intercostalis*	
il	*incisura lateralis*[373]	
ims	*impressio m. sternocoracoidei*[374]	sternocoracoidal impression
lim	*linea intermuscularis*[375]	
mc	*margo costalis*[376]	
pic	*pila carinae*	
pop	*pori pneumatici*	
pp	*planum postcarinale*	
prco	*processus costalis*	
prcr	*processus craniolateralis*[377]	craniolateral process
sac	*sulcus articularis coracoideus*[378]	coracoid sulcus
sacd	*sulcus articularis coracoideus: labrum dorsale*[379]	
sacv	*sulcus articularis coracoideus: labrum ventrale*[380]	
sms	*sulcus medianus sterni*	
spic	*spatium intercoracoidale*	
tl	*trabecula lateralis*[381]	lateral trabecula

Coracoid

al	*angulus lateralis*	
am	*angulus medialis*[382]	
cco	*corpus coracoidei*	
cdo	*crista dorsalis*[383]	
cg	*cavitas glenoidalis* [of the scapulocoracoid]	articular face for the humerus
cve	*crista ventralis*	
eoc	*extremitas omalis coracoidei*	
esc	*extremitas sternalis coracoidei*	
facl	*facies articularis clavicularis*	
fah	*facies articularis humeralis*[384]	articular face for the humerus
fasc	*facies articularis scapularis* (*cotyla scapularis*)	

---

[371] Carène médiane, carène sternale (Milne-Edwards 1866b); keel (Owen 1867); Crista sterni (Fürbringer 1888, Lambrecht 1933).

[372] Face supérieure (antéro-viscérale) (Janoo 1997).

[373] Ectolateral notch (Owen 1867).

[374] Impressio sternocoracoidea (Lambrecht 1933).

[375] Ligne intermusculaire (Milne-Edwards 1866b); pectoral ridge (Owen 1867); Linea interpectoralis (Fürbringer 1888, Lambrecht 1933).

[376] Costal border / surface (Owen 1867).

[377] Costal process (Melville 1848); apophyses hyosternales (pl.) (Milne-Edwards 1866b); Processus sterno-coracoideus s. praecostalis (Fürbringer 1888); proc. sternocoracoideus (Lambrecht 1933); processus costal (Verheyen 1957).

[378] Rainures coracoïdiennes (pl.) (Milne-Edwards 1866b); coracoid groove (Owen 1867); fossettes coracoïdiennes (pl.) (Gervais 1867-1869); fossa coracoidea (Behn 1868b); “fosse coracoïdienne” (Janoo 1997).

[379] Labrum internum (Lambrecht 1933).

[380] Crête antérieure des rainures coracoïdiennes (Milne-Edwards 1866b); Labrum externum (Lambrecht 1933).

[381] External lateral process (Melville 1848); ectolateral / lateral process (Owen 1867); lames latérales (Milne-Edwards 1866b); posterior lateral process (Lindsay 1885); processus lateralis posterior (Lüttschwager 1959b); processus ectolatéral (Janoo 1997).

[382] “Inner angle” (Owen 1867).

[383] Crista articularis sternalis (Fürbringer 1888).

[384] Cotyle huméral (Janoo 1997, fig.14: there is no ‘ch’ marked in fig.14 and it is here assumed that the feature labelled ‘fh’ is that referred to), facette articulaire glenoidale (Janoo 1997, fig.14: there is no ‘fag’ marked in fig.14 and it is here assumed that the feature labelled ‘fh’ is that referred to).

fast	*facies articularis sternalis (crista articularis sternalis)*	
fdo	*facies dorsalis*[385]	
fpn	*fossa pneumatica*	
fve	*facies ventralis*[386]	
ila	*impressio ligamenti acrocoracohumeralis*[387]	
is	*impressio sternocoracoidei*	
mla	*margo lateralis*	
mme	*margo medialis*	
msa	*margo supra-angularis*	
pa	*processus acrocoracoideus*[388]	acrocoracoid process
pl	*processus lateralis*[389]	
ppr	*processus procoracoideus*[390]	
sus	*sulcus m. supracoracoidei*	

Lateral margin of the processus lateralis of the coracoid (bord hyosternal of Janoo 1997).

Scapula

acr	*acromion*[391]	acromion
cosc	*collum scapulae*	
crsc	*corpus scapulae*	
csc	*caput scapulae*	
faco	*facies articularis coracoidea*[392]	
fah	*facies articularis humeralis*[393]	
fal	*facies lateralis*	
fcos	*facies costalis*	
fpn	*foramen pneumaticum*	pneumatic foramen
pgl	*processus glenoidalis*	
ts	*tuberculum scapulae*	

Furcula

af	*apophysis furculae*	hypocleideum[394]
eocl	*extremitas omalis claviculae*	
escl	*extremitas sternalis claviculae*	
pac	*processus acromialis*	
par	*processus acrocoracoideus*	
scl	*scapus claviculae*	
syi	*synostosis interclavicularis*	

Humerus

anc	*angulus cristae*	
cb	*crista bicipitalis*	bicipital crest[395]
cdf	*crus dorsalis fossae*	
cdo	*condylus dorsalis*	dorsal condyle[396]
ch	*caput humeri*	head of the humerus
cpe	*crista deltopectoralis*	deltopectoral crest[397]

---

[385] Face interne (Janoo 1997).

[386] Face externe (Janoo 1997).

[387] Impressio ligamentum acrocoracoideum, sulcus du ligament acrocoracoïdien (Janoo 1997).

[388] Acrocoracoid (Fürbringer 1888); acrocoracoïde (Verheyen 1957).

[389] "Outer angle" (Owen 1867).

[390] Processus procoracoideum, procoracoïde (Janoo 1997).

[391] Tubérosité claviculaire (Milne-Edwards 1866b); acromial process (Owen 1867).

[392] Surface articulaire coracoïdienne (Milne-Edwards 1866b); "coracoidal surface" (Owen 1867).

[393] Facette glénoïdale (Milne-Edwards 1866b); "humeral surface" (Owen 1867).

[394] Hypocleidium [*sic*] (Newton & Gadow 1893).

[395] Posterior crest (Strickland 1853).

[396] L'épitrochlée (Gervais 1859)?

[397] Anterior crest (Strcikland 1859); saillie deltoïdienne (Gervais 1859); pectoral process / ridge (Owen 1867); crête latérale de l'humérus (Verheyen 1957); crista lateralis (Lüttschwager 1959b); "crête latérale de l'humérus (crista lateralis humeri)" (Janoo 1997, p.182); crête pectorale (Janoo 1997).

cve	*condylus ventralis*	ventral condyle
ed	*epicondylus dorsalis*	dorsal epicondyle[398]
ev	*epicondylus ventralis*	ventral epicondyle
fb	*facies bicipitalis*	bicipital face
fmb	*fossa m. brachialis*	brachial fossa
fmps	*fossa m. pronator superficialis*	
fms	*fossa muscularis*	
fo	*fossa olecrani*	
fpn	*fossa pneumaticum*	
fpne	*fossa pneumotricipitalis*	pneumatic fossa[399]
imc	*impressio m. coracobrachialis*	
ime	*impressio m. extensor carpi radialis*	
imp	*impressio m. pectoralis*	
imsu	*impressio m. supracoracoidei*	
inc	*incisura capitis*	
ini	*incisura intercondylaris*	intercondylar incisure[400]
int	*intumescentia humeri*[401]	
lmld	*linea m. latissimi dorsi*	
pfl	*processus flexorius*	flexor process
smh	*sulcus m. humerotricipitis*	
smsc	*suclus m. scapulotricipitis*	
sut	*sulcus [ligamentosus] transversus*	
tdo	*tuberculum dorsale*	dorsal tubercle[402]
tv	*tuberculum ventrale*	ventral tubercle[403]

Ulna

cin	*crista intercotylaris*	
cod	*condylus dorsalis*	dorsal condyle
cov	*condylus ventralis*	ventral condyle
ctd	*cotyla dorsalis*	dorsal cotyla
ctv	*cotyla ventralis*	ventral cotyla
far	*facies articularis radialis*	
imb	*impressio m. brachialis*	impression for m. brachialis
imsc	*impressio m. scapulotricipitis*	
ir	*incisura radialis*[404]	
itc	*incisura tuberculi carpalis*	
lc	*labrum condyli dorsalis*	
lim	*linea intermuscularis*	
ol	*olecranon*	
parc	*papillae remigiales caudales*	caudal and ventral remigeal papillae[405]
parv	*papillae remigiales ventrales*	
pcd	*processus cotylaris dorsalis*	
sin	*sulcus intercondylaris*	intercondylar sulcus
tb	*tuberculum bicipitale*	
tlcv	*tuberculum ligamenti collateralis ventralis*	
tuc	*tuberculum carpale*	

---

[398] L'épicondyle (Gervais 1859)? The "ectocondyloid tuberosity" of Owen (1867, p.77), probably correspons to the tuberculum supracondylare dorsale.

[399] "Ouverture aérienne" (Gervais 1859); Fossa pneumo-anconaea (Lüttschwager 1959b).

[400] "La gorge qui sépare les deux poulies inférieures du cubitus" (Gervais 1859).

[401] Intumescentia processus medialis humeri (Verheyen 1957).

[402] Radial tubercle / tuberosity (Owen 1867); tubercule radial (Janoo 1997).

[403] Ulnar tuberosity (Owen 1867); tubérosité ulnaire (Janoo 1997). The "petite tubérosité" of Gervais (1859) may correspond to this feature: "L'humérus fossile présente sous sa petite tubérosité une ouverture aérienne [= fossa pneumotricipitalis]" (p.427).

[404] Depressio radialis (Claessens *et al*. 2015)?

[405] Quill-tubercles (Owen 1867); "série anconale des protubérances ulnaires" (Verheyen 1957, p.18).

Radius

coh	*cotyla humeralis*	articular face for the humerus
del	*depressio ligamentosa*	
far	*facies articularis radiocarpalis*	
lin	*linea intermuscularis*	
sut	*sulcus tendinosus*	tendinal sulcus
tap	*tuberculum aponeurosis ventralis*	
tbi	*tuberculum bicipitale*	bicipital tubercle

Radiale (Os carpi radiale)

dvp		distoventral projection (Mayr 2004)
fam	*facies articularis metacarpalis*	
far	*facies articularis radialis*	
fau	*facies articularis ulnaris*	
t		attachment for tendon?
tmuv		notch for tendon of m. ulnometacarpalis ventralis

Ulnare

im	*incisura metacarpalis*

Carpometacarpus[406]

faal	*facies articularis alularis*	
farc	*facies articularis radiocarpalis*	
fauc	*facies articularis ulnocarpalis*	
fcc	*fovea carpalis caudalis*	
fccr	*fovea carpalis cranialis*	
fdm	*facies articularis digitalis minor*	
fit	*fossa infratrochlearis*	infratrochlear fossa
fst	*fossa supratrochlearis*	supratrochlear fossa
oma	*os metacarpale alulare*	
omm	*os metacarpale minus*	minor metacarpal (III)
omma	*os metacarpale majus*	major metacarpal (II)
pal	*processus alularis*	alular process
pe	*processus extensorius*	extensor process
pin	*processus intermetacarpalis*	
ppi	*processus pisiformis*	pisiform process
sin	*sulcus interosseus*	
sm	*synostosis metacarpalis*	metacarpal synostosis
spi	*spatium intermetacarpale*	intermetacarpal space
ste	*sulcus tendineus*	
trc	*trochlea carpalis*	carpal trochlea

Alar phalanges

fa	*facies articularis*
pda	*phalanx digiti alulae*
pddm	*phalanx distalis digiti majoris*
pdm	*phalanx proximalis digiti majoris*
pdmi	*phalanx digiti minoris*
pfap	*phalanx proximalis digiti majoris: facies articularis phalangealis*
pfd	*phalanx proximalis digiti majoris: fossa dorsalis*
pfv	*phalanx proximalis digiti majoris: fossa ventralis*
ppc	*phalanx proximalis digiti majoris: pila cranialis*
ppf	*phalanx digiti minoris: processus flexorius*

---

[406] Metacarpus (Owen 1871b).

Femur

cf	*caput femoris*	head of the femur
cof	*collum femoris*	neck of the femur[407]
cla	*condylus lateralis*	lateral condyle[408]
cm	*condylus medialis*	medial condyle[409]
cfe	*corpus femoris*	
csl	*crista supracondylaris lateralis*	
csm	*crista supracondylaris medialis*	medial supracondylar crest
cti	*crista tibiofibularis*	tibiofibular crest[410]
ctr	*crista trochanteris*	trochanteric crest[411]
el	*epicondylus lateralis*	lateral epicondyle
em	*epicondylus medialis*	medial epicondyle
faac	*facies articularis acetabularis*	
faan	*facies articularis antitrochanterica*	articular face for the antitrochanter[412]
fap	*facies articularis patellaris*	
flc	*fovea lig. capitis*[413]	
fp	*fossa poplitea*	popliteal fossa[414]
fpn	*foramen pneumaticum*	
ftc	*fovea tendinis m. tibialis cranialis*	
ftr	*fossa trochanteris*	
idai	*impressio distalis ansae m. iliofibularis*	
ilcl	*impressio ligamenti collateralis lateralis*	
ilcm	*impressio ligamenti collateralis medialis*	
ilca	*impressio ligamenti cruciati caudalis*	
ilcr	*impressio ligamenti cruciati cranialis*	
imi	*impressiones iliotrochantericae*	
imo	*impressiones obturatoriae*	obturator impressions
lic	*linea intermuscularis caudalis*	caudal intermuscular line[415]
licr	*linea intermuscularis cranialis*	cranial intermuscular line[416]
sinc	*sulcus intercondylaris*	intercondylar sulcus[417]
sup	*sulcus patellaris*	patellar sulcus[418]
tm	*tuberculum*	small trochanter[419]
tmgl	*tuberculum m. gastrocnemialis lateralis*[420]	
tmgm	*tuberculum m. gastrocnemialis medialis*[421]	
trf	*trochanter femoris*	femoral trochanter[422]
trfi	*trochlea fibularis*	fibular trochlea[423]

Lambrecht (1933, fig.20D) labelled the lateral part of the lateral condyle, that forming the cranial wall of the trochlea fibularis, the Condylus fibularis.

Patella

---

[407] Col fémoral (Milne-Edwards 1866b).

[408] Outer condyle (Owen 1867); condylus externus (Lambrecht 1933).

[409] Condyle interne (Milne-Edwards 1866b); inner condyle (Owen 1867); condylus internus (Lambrecht 1933).

[410] Crête péronéo-tibiale (Mine-Edwards 1866b).

[411] Great trochanterian ridge (Owen 1867).

[412] Articulatio iliacalis (Lambrecht 1933).

[413] Fossa lig. teres (Lambrecht 1933).

[414] Fosse poplitée (Milne-Edwards 1866b); Fovea poplitea (Martin 1904).

[415] Linea aspera (Lambrecht 1933).

[416] Linea anterior (Lambrecht 1933).

[417] Intercondyloid notch (Strickland 1853); sulcus intercondyloideus (Lambrecht 1933).

[418] Gorge rotulienne, gouttière rotulienne (Milne-Edwards 1866b); rotular groove / channel (Owen 1867); fossa patellaris (Lambrecht 1933).

[419] Trochanter minor (Owen 1867).

[420] Apophysis m. gastrocnemialis externus (Lambrect 1933).

[421] Apophysis m. gastrocnemialis internus (Lambrect 1933).

[422] Great trochanter (Owen 1867); trochanter major (Lambrecht 1933).

[423] Fibular depression (Owen 1867); sulcus fibularis (Lambrecht 1933).

flf	*facies articularis condylus lateralis femoralis*
fmf	*facies articularis condylus medialis femoralis*

Tibiotarsus[424]

ari	*area interarticularis*	
aric	*area intercondylaris*[425]	
ccc	*crista cnemialis cranialis*	cranial cnemial crest[426]
ccl	*crista cnemialis lateralis*	lateral cnemial crest[427]
cfi	*crista fibularis*	fibular crest[428]
clat	*condylus lateralis*	lateral condyle[429]
cmed	*condylus medialis*	medial condyle[430]
cpa	*crista patellaris*	patellar crest[431]
crt	*crista trochlearis*	
del	*depressio epicondylus lateralis*	
dem	*depressio epicondylus medialis*	
epl	*epicondylus lateralis*	lateral epicondyle
epm	*epicondylus medialis*	
fal	*facies articularis lateralis*	
fam	*facies articularis medialis*	
ff	*fossa flexoria*	
fg	*facies gastrocnemialis*	
frp	*fossa retropatellaris*	
ilcm	*impressio ligamenti collateralis medialis*	
ili	*impressio ligamenti intercondylaris*	
inci	*incisura intercondylaris*	intercondylar incisure[432]
it	*incisura tibialis*	
le	*linea extensoria*	
lmf	*linea m. fibularis*[433]	
ps	*pons supratendineus*	supratendineal bridge[434]
sct	*sulcus cartilaginis tibialis*	
se	*sulcus extensorius*[435]	
smf	*sulcus m. fibularis*[436]	
suc	*sulcus intercnemialis*	intercnemial sulcus
tct	*trochlea cartilaginis tibialis*[437]	
tdre	*tuberositas distalis retinaculi mm. extensorum*[438]	
tp	*tuberositas poplitea*	
tpre	*tuberositas proximalis retinaculi mm. extensorum*[439]	
trmfl	*tuberositas retinaculum m. fibularis lateralis*[440]	

---

[424] Tibia (Melville 1848).

[425] Gorge intercondylienne antérieure (Milne-Edwards 1866b).

[426] Internal ridge (Strickland 1853)?; procnemial ridge / plate (Owen 1867); crista interna (Martin 1904); crista cnemialis interna (Lambrecht 1933).

[427] Ectocnemial process / plate (Owen 1867); crista externa (Martin 1904); crista cnemialis externa (Lambrecht 1933).

[428] Fibular ridge (Strickland 1853); crête péronière (Milne-Edwards 1866b).

[429] Condylus tibialis externus (Lambrecht 1933); laterale Condylus (Lüttschwager 1959a).

[430] Condyle interne de l'articulation du genou (Milne-Edwards 1866b); Condylus tibialis internus (Lambrecht 1933).

[431] Epicnemial process / ridge (Owen 1867).

[432] Intercondyloid groove (Strickland 1853); gorge intercondylienne antérieure (Milne-Edwards 1866b); incisura intercondyloidea (Lambrecht 1933).

[433] Linea intermuscularis m. extensor digitorum (Lambrecht 1933).

[434] Pont sus-tendineux (Milne-Edwards 1866b); Ligamentum transversum ossificatum (Lambrecht 1933).

[435] Gouttière de l'extenseur des doigts (Milne-Edwards 1866b); Tendinal canal (Owen 1867); canalis m. extensor digitorum (Lambrecht 1933).

[436] Canalis m. peroneus profundus (Lambrecht 1933).

[437] Facies patellaris (Lambrecht 1933).

[438] Tuberositas retinaculum extensoris lateralis extensorium (Claessens *et al*. 2015).

[439] Apophysis lig. obliqui (Lambrecht 1933); tuberositas retinaculum extensoris medialis (Claessens *et al*. 2015).

[440] Apophysis lig. obliqui (Lambrecht (1933).

trmfm	*tuberositas retinaculum m. fibularis medialis*	

Fibula[441]

cat	*crista articularis tibialis*	
cfib	*caput fibulae*	
farf	*facies articularis femoralis*	articular face for the femur
fat	*facies articularis tibialis*	articular face for the tibiotarsus
fop	*fovea m. poplitei*[442]	
sf	*spina fibulae*	fibular spine
tlcl	*tuberositas ligamenti collateralis lateralis*	
tmi	*tuberculum m. iliofibularis*[443]	tubercle for m. iliofibularis

Tarsometatarsus[444]

ain	*area intercotylaris*	intercotylar area[445]
cah	*canalis hypotarsi*	hypotarsal canal[446]
cid	*canalis interosseus distalis*	
cih	*crista intermedialis hypotarsi*	
clh	*crista lateralis hypotarsi*	lateral crest of the hypotarsus[447]
cmh	*crista medialis hypotarsi*	medial crest of the hypotarsus[448]
cpl	*crista plantaris lateralis*[449]	
cpm	*crista plantaris medialis*	
crm	*crista medianoplantaris*[450]	
ctl	*cotyla lateralis*[451]	
ctm	*cotyla medialis*[452]	
emi	*eminentia intercotylaris*[453]	intercotylar eminence
find	*fossa infracotylaris dorsalis*	dorsal intercotylar fossa[454]
fmi	*fossa metatarsi I*[455]	articular face for the hallux
fml	*fovea menisci lateralis*	
folc	*foveae ligamentorum collateralium*	
fpl	*fossa parahypotarsalis lateralis*	lateral parahypotarsal fossa[456]
fpm	*fossa parahypotarsalis medialis*	medial parahypotarsal fossa[457]
fsl	*facies subcutanea lateralis*	
fsm	*facies subcutanea medialis*	
fsp	*fossa supratrochlearis plantaris*	plantar supratrochlear fossa[458]
fvd	*foramen vasculare distale*	distal vascular foramen[459]
fvp	*foramina vascularia proximalia*	medial proximal vascular foramen[460]
		lateral proximal vascular foramen[461]

---

[441] Péroné (Milne-Edwards 1866b).

[442] Fossa poplitea, fovea m. poplitea (Claessens *et al*. 2015).

[443] Apophysis m. ilio-fibularis (Lambrecht 1933).

[444] Metatarsus (Melville 1848).

[445] Intercondylar triangular tract (Owen 1871b).

[446] Calcaneal canal (Melville 1848); tendinal canal (Owen 1871b).

[447] Ectocalcaneal process (Melville 1848).

[448] Calcaneal ridge, ento-calcaneal process (Melville 1848); inner calcaneal process (Strickland 1853).

[449] This may correspond to the "postinterosseal ridge" of Owen (1871b, pl.lxvi, fig.2 *y*) and the Crista postinterossea of Martin (1904).

[450] Calcaneal buttress (Melville 1848).

[451] External condyloid fossa (Strickland 1853); ectocondylar cavity / fossa (Owen 1871b).

[452] Internal condyloid fossa (Strickland 1853); entocondylar cavity (Owen 1871b).

[453] Intercondyloid tubercle (Melville 1848); intercondylar process / tuberosity (Owen 1871b); eminentia intercondylaris (Claessens *et al*. 2015).

[454] Anterior interosseous (antinterosseal) depression (Owen 1871b).

[455] Posterior metatarsal articular facet (Melville 1848); hallucial surface (Owen 1871b).

[456] Postexternal depression (Owen 1871b).

[457] Postinternal depression (Owen 1871b).

[458] Posttrochlear depression (Owen 1871b).

[459] Lower interosseal or "adductor" canal (Owen 1871b).

[460] Internal interosseous foramen (Strickland 1853); entinterosseal canal (Owen 1871b).

iil	*incisura intertrochlearis lateralis*	
iim	*incisura intertrochlearis medialis*	medial intertrochlear notch[462]
ilcl	*impressio ligamenti collateralis lateralis*	
ire	*impressiones retinaculi extensorii*	
sfb	*sulcus m. fibularis*	
sh	*sulcus hypotarsi*	hypotarsal sulcus[463]
sfhl	*sulcus m. flexor hallucis longus*	
sfl	*sulcus flexorius*	
smfl	*sulcus m. fibularis longi*	
tmfb	*tuberositas m. fibularis brevis*	
tmq	*trochlea metatarsi quarti*[464]	
tms	*trochlea metatarsi secundi*[465]	
tmt	*trochlea metatarsi tertii*[466]	
tmtc	*tuberositas m. tibialis cranialis*	
trf	*tuberculi retinaculae m. fibularis*	

Hypotarsus (calcaneal process of Owen 1846, 1871b; processus calcanei of Brandt 1848a [divided into ecto- and entocalcaneal processes])
Metatarsal II[467]
Metatarsal III[468]
Metatarsal IV[469]

Milne-Edwards (1866b) mentioned a “gouttière métatarsienne antérieure” (p.370), which is longer in *Goura* than in *Raphus*, where it is also shallow; it is not certain what this feature corresponds to.

Os metatarsale I (first metatarsal)[470]

flt	*facies lateralis*	
fmd	*facies medialis*	
pat	*processus articularis tarsometatarsalis*	
trmi	*trochlea metatarsi I*	
tul	*tuberculum lateralis*	lateral tubercle[471]
tum	*tuberoculum medialis*	medial tubercle

Pedal phalanges

bap	*basis phalangis*	
car	*cotyla articularis*	articular cotyla
cph	*capitulum phalangis*	
cric	*crista intercotylaris*	
folc	*fovea ligamenti collateralis*	
suv	*sulcus vasculorum*	
ta	*trochlea articularis*	trochlea
te	*tuberculum extensorium*	extensor tubercle
tf	*tuberculum flexorium*	

Os sesamoideum intertarsale	*intertarsal sesamoid*

Musculature

---

[461] Ectinterosseal canal (Owen 1871b).
[462] Internal intertrochlear notch (Strickland 1849).
[463] Calcaneal / tendinal groove (Owen 1871b).
[464] External trochlea (Strickland 1853); ectotrochlea (Owen 1871b).
[465] Internal trochlea (Strickland 1853).
[466] Middle trochlea (Strickland 1853); mesotrochlea (Owen 1871b).
[467] Entometatarsal (Owen 1871b).
[468] Mesometatarsal (Owen 1871b).
[469] Ectometatarsal (Owen 1871b).
[470] Posterior metatarsus (Melville 1848).
[471] Styloid process (Melville 1848).

ab2	*m. abductor digiti II*
ab4	*m. abductor digiti IV*
ad2	*m. adductor digiti II*
eb3	*m. extensor brevis digiti III*
eb4	*m. extensor brevis digiti IV*
edl	*m. extensor digitorum longus*
ehl	*m. extensor hallucis longus*
fdl	*m. flexor digitorum longus*
fhb	*m. flexor hallucis brevis*
fhl	*m. flexor hallucis longus*
mfl	*m. fibularis longus*
mtc	*m. tibialis cranialis*
pd2	*m. flexor perforatus digiti II*
pd3	*m. flexor perforatus digiti III*
pd4	*m. flexor perforatus digiti IV*
ppd2	*m. flexor perforatus et perforans digiti II*
ppd3	*m. flexor perforatus et perforans digiti III*

flexor, flexors = flexor muscle(s) of pedal digit(s)

Aponeurosis and Ligaments

app	*aponeurosis plantaris*
ltm	*ligamentum transversum metatarsale*
ret	*retinaculum*
rext	*retinaculum extensorium tarsometatarsi*

Additional Notes

Additional Anatomical Features of the Skull and Their Synonyms

Interorbital region of the frontals [pars interorbita [*sic*] des frontaux (Janoo 1997)]
Upper beak (rostrum) [oberen Kinnlade (Reuss 1855)]
Dorsal bar of the upper beak [mittleren Kinnladenarme, mittleren Kinnladenäste, mittleren Aste (Reuss 1855)]
Lateral bar of the upper beak [lateral beam / stem (Melville (1848); Seitenäste, seitlichen Aste, seitlichen Kinnladenarme, seitlichen Kinnladenäste (Reuss 1855)]
Hook of the beak (Newton & Gadow (1896) [dertrum (Newton & Newton 1869)]
Jugal arch (arcus jugalis) [Jochbogen (Brandt 1848); arcade jugale (Milne-Edwards 1866b)]
Palatine [Gaumenbeine (Brandt 1848)]
Nasal [Nasenbein (Brandt 1848)]
Palatal fissure [Gaumenspalte (Reuss 1855)]
Palatal vessels [Gaumengefässe (Reuss 1855)]
Premaxilla [Zwischenkiefer (Brandt 1848)]
Dorsal surface of pars symphysialis of the mandible [“surface goniale” (Janoo 1997, p.104)]
Pneumatic canal [Luftcanal (Reuss 1855)]
Vessel canal [Gefässcanal (Reuss 1855)]
Neurovascular canal [Gefässcanal (Reuss 1855)]

Miscellaneous Notes on Nineteenth-Century Terminology and Concepts

A note on “cranial vertebrae”

In the nineteenth century some authors considered the skull to be composed of “cranial vertebrae”, this is to say that the skull bones were essentially vertebrae, with the various elements corresponding different vertebral processes. Melville (1848) recognized in the cranium of OUM 11605 three “cranial vertebrae”, “essentially related to the three higher senses” (p.84). He regarded the interorbital septum as “the compressed body of the third and last [or olfactory], or most anterior of the cranial vertebrae” (p.87) and thought that the optic and auditory capsules were “situated between two adjacent vertebrae” (p.89).

Owen (1878) stated that in order to “view the neurapophyses of the nasal vertebra, the nasals, premaxillary, and coalesced part of the frontals must be removed; and then the homologue of the “os en ceinture” of batrachotomy and of the “æthmoid” of anthropotomy is brought into view, with part of the confluent olfactory capsules” (pp.89-90). He added that in birds “the bird strong processes answering to diapophyses are extended outwards from the neurapophysial or essential parts of the prefrontals; and to these the name “prefrontal” is restricted by some who retain the term “æthmoid” for the plates transmitting the olfactory nerves from the rhinencephalon” (p.90). Owen also stated that in the premaxillary processes of the nasals progressing rostrally to meet ventrally in the midline “we have, in the extreme variation of an extreme segment of the vertebral axis, the hæmal spine closing the tubular series by overlapping the neural spine of its own segment” (p.90).

Likewise, Goodsir (1857) remarked:

> The separation of the optic foramina from the pneumatic expansion of the pre-sphenoidal centrum leads me, in the second place, to observe, that the characteristic separation of these orifices in the extinct forms Dido [*sic*], Dinornis, Palapteryx, did not depend entirely on pneumatic expansion of the pre- sphenoidal centrum, nor on such width of that bone as might be attributed to incomplete mesial fusion of a pair of “pre-frontals,” but on the remarkable prolongation backwards on each of its sides of the neurapophyseal walls of the ethmoidal olfactory chambers.
>
> Professor Owen, in his series of graphic and valuable memoirs on these three extinct forms, and in his memoirs on Apteryx, assuming the pre-frontal doctrine regarding the bone in question, and directing special attention to the more or less complete passage backwards of the nasal chambers to the anterior or inferior wall of the cranial cavity, and to the passage of the olfactory nerves into these by a number of orifices, apparently recognises in Apteryx, for instance (although he does not directly make the statement), a completed Mammalian ethmoid. [...] the embryological considerations from which the formation of neither the Mammalian ethmoidal septum, nor the so-called ethmoid of the Ostrich, Dinornis, Dodo, nor Apteryx, can be conceived as resulting from coalesced pre-frontals (p.156).

Owen (1866b, pp.353-354) countered Melville’s concept of the homologies of the avian skull:

> Dr. Melville contends that “the interorbital septum in Birds is the homologue of the Mammalian presphenoid.”[1] But of this presphenoid in Pigeons he describes the “ossified portions of the ethmoid, or olfactory capsule,” to be processes[2]. Moreover, he admits that the ‘interorbital septum’ appears on the upper surface of the cranium “behind the premaxillary, and between the nasals,” “in the Emu and other Struthionidæ.”[3] It is shown in this exposed position in the Ostrich (art. *Aves*, Cyclop. of Anat. vol. i. p. 274, fig. 127, *l*) as part of the ‘ethmoid’, in the Emu (Zool. Trans. vol. iii. pi. 39. figs. 1 & 2, 14) as ‘prefrontals,’ and in the *Rhea* (Zool. Trans. vol. v. pl. 42) as the ‘middle ethmoid’ or ‘perpendicular ethmoid.’
>
> I have not, however, met with any instance, in any class, in which the ‘anterior sphenoid’ afforded attachment to ‘turbinals’ or ossified parts of the olfactory capsule. Anthropotomists describe and figure the homologue of the ‘presphenoid’ as the “’rostrum’[4] of the sphenoid bone, to which is articulated the vomer and the perpendicular part of the ethmoid.”
>
> The ‘rostral’ form and proportions of the ‘anterior sphenoid’ in *Cetacea* approach nearer to those of the ‘rostrum of the sphenoid’ in Birds and Reptiles than in most other mammals. I am unable, therefore, to accept the special homology of the ‘interorbital septum’ in birds proposed or adopted by Dr. Melville. His views of the “general homology” of the part in question are expressed as follows:– “For reasons which cannot be discussed here, I regard the interorbital septum as the compressed body of the third and last or most anterior of the cranial vertebræ.”[5] But, in this case, we have the body or centrum of a vertebra appearing at the upper surface of a neural arch, and displacing the moieties of a neural spine, projecting, *e.g.*, “between the nasals,” as in the Struthious birds already adduced. And beneath this part so

[1] ”Dodo and its Kindred,” ‘Osteology of the Dodo,’ 4to, 1848, p. 87.

> [2] Ibid.
> [3] Ibid.
> [4] 'Anatomy, Descriptive and Surgical,' by H. Gray, 8vo, p. 33, fig. 30.
> [5] *Op. cit.* p. 87.
>
> exposed the alleged 'vertebral body' gives off a process "arching over the foramen, for the transmission of the olfactory and ophthalmic nerves."[1] But this is, surely, a relation rather of a 'neurapophysis' than of a 'centrum' of a vertebral segment.
>
> Some who appeal to developmental phenomena will reject the "general homology" proposed for the interorbital septum by Dr. Melville, on the ground of the non-extension of the 'chorda dorsalis' so far forward in the cephalic blastema of the embryo. I may presume, however, that the arguments for the insufficiency of this ground of objection given in my 'Archetype of the Vertebrate Skeleton' (8vo, p. 6) are held to be conclusive by the learned Professor in Queen's College, Galway. My objections to his view rest on the more decisive and demonstrative homological bases of 'connexion' and 'relative position.'
>
> [1] "Dodo and its Kindred," &c., 4to, p. 87.

The lacrimal, ectethmoid and mesethmoid

Parker (1866) discussed the antorbital elements of the cranium:

> Looking at the antorbital plate of the *Hemipodius* from behind (Pl. XXXIV. fig. 6), we can see it to be composed of three portions connected by a faint, triradiate suture. The external portion of this relatively large cellular mass of bone is formed by the lachrymal (*l.*), which is like that of the Pigeon, but still more like that of the Dodo. The supero-internal portion is the upper prefrontal (*pr.f.*); the infero-internal is autogenous in its cartilaginous state, as well as in its ossified condition. This is the lower prefrontal, the so-called "antorbital" (*a.o.*) of the bird, and the homologue of the "pars plana," or "lamina papyracea," of the Mammal. This perirhinal element is partly coiled upon itself, in many birds, to form the middle turbinal.
>
> In *Hemipodius* these coalesced structures are the tiny counterparts of what we see in the Dodo's skull (p.179).
>
> Between the forks of the nasal bone the aliethmoid can be freely seen in Pigeons, Sandgrouse, and the *Hemipodii* as a convex cellular plate (Pls. XXXIV. & XXXV. fig. 3); only a small portion can be seen in *Vanellus*, and that thin and fibrous like the rest of that bird's skull. The extreme thickness of the cellular descending process of the nasal in the Dodo hides the view of the aliethmoid in this aspect. This is but an exaggeration of a Pigeon-character in that massive bird (p.180).

The "upper prefrontal" would appear to be the ectethmoid and/or the mesethmoid, the 'antorbital' would be the ectethmoid and the aliethmoid may be the ectethmoid, at least in part.

Palate

Based upon the "Modifications of the Basi-sphenoid in Relation to the Pterygo-palatine Apparatus" ("how the palato-maxillary fittings are attached to the rostrum in different birds"), Parker (1861) divided birds into several groups. He defined "Group 3", which included the dodo, *Goura* and *Didunculus*, amongst others, as follows:

> The great fronto-maxillary [= craniofacial] hinge is here composed of splint-like laminæ of the nasal [= frontal] processes of the pre-maxillaries and nasals, which overlap the sphenoido-frontals [= frontals]; or the lacrymals and sphenoido-frontals are adapted to the contiguous bones of the facial sclerotome by a dentate suture, the margin of the hinge being more or less synovial. The rostrum of the basi-sphenoid [= parasphenoid rostrum] in this group is either patched on each side or completely covered with synovial cartilage

> for a definite extent, on which lubricated space the pterygo-palatals glide. Vomer variable (p.285).

Notes on Terms used to Describe the Sternum
Owen (1867) described the sternum as a "mass of coalesced and expanded hæmal spines" (p.72). Milne-Edwards (1866b) remarked: "If the Dodo were a *Colombide* modified to live only on the ground, we should expect to find in it a sternum conformed like that of the pigeons, except more or less great atrophy of the sternal carina, the narrowness of the posterior portion of the entosternal ['l'entosternal'], or the absence of ossification of part of the lateral blades [= trabeculae laterales]" (p.367). The 'entosternal' is the median portion of the sternum, including the keel (Saint-Hilaire 1833, Parker 1866).

In their description of the sternum of *Pezophaps*, Newton & Clark (1879) remarked: "In the former paper [Newton & Newton (1869)] the anterior portions of the 'pleurosteon' were described and figured, [...] but the posterior portion was broken in all specimens. Immediately behind the articulations for the ribs is a short broad 'metosteon,'" (p.442). The 'pleurosteon' corresponds to part of the anlage corporis sterni, whereas the 'metosteon' corresponds to part of the anlage costo-lateralis sterni (Livezey & Zusi 2006).

According to Newton & Gadow (1896):

> Ossification of the Sternum does not begin till after it has attained its final shape, and proceeds from various centres, which, notwithstanding the elaborate studies of Geoffroy St.-Hilaire, L'Herminier and Parker cannot always be recognized in the different groups of Birds, chiefly owing to the variable situation of these centres – one or another being suppressed and its place taken by the extension of its neighbours. As a rule ossification begins earliest where the greatest strength or resistance is needed. Thus in *Rhea*, *Gallinæ*, *Turnix*, *Lestris* and the *Passeres*, each anterior lateral process [= craniolateral processes] has its *pro-osteon* (Parker), but in many other forms, as *Ardea*, *Rallidæ* and *Ibis*, these processes possess no special centre of ossification, and are converted into bone by the extension of the *pleurostea*, which last occur in the majority of Birds, though absent in *Turnix* and the *Gallinæ*, and lie in the lateral margin of the Sternum, where the ribs are attached: *coracostea* occur sometimes at the anterior end of the Sternum, near the articulation of the Coracoids, and in some Birds *metostea* are the centres whence the posterior lateral processes [= lateral processes] ossify, while the *lophosteon* (Parker), which may be single, multiple or paired, is the centre of ossification for the keel (p.910).

In describing "the Gallinaceous Sternum before the middle of incubation (ninth day)", Parker (1868) stated:

> The costal processes pass into the costal region, with its four condyles for the sternal ribs (c. c.); behind the fourth condyle the large, lateral xiphisternum is seen, which bifurcates into the "external" and the "intermediate xiphoid processes" (e. x. and i. x.); the interspace between these is the "external xiphoid notch." Between the "intermediate xiphoid process" and the main part of the Sternum there is a very long notch, with only a moderate tract intervening between it and the anterior notch; if these clefts were perfect, we should have a large separate "entosternum" (e. s.), with the emarginate rostrum in front, the coracoid grooves antero-laterally, a large keel further backwards, and behind the keel the "middle xiphoid process" (m. x.); this process is double, and its halves are separated by the primordial fissure (p.144).

He added:

> The fewest ossifications appear in the Struthionidæ; these, with the exception of the genus *Rhea*, have but one symmetrical pair; these centres being principally related to the costal margin, may each be called "pleurosteon" [...]; they exist in all the Lacertilia and the Crocodiles. In all other Birds, known to me, there is a large azygous centre, which

> arises in the crest of the Sternum [...]; this may be termed the "lophosteon," it is nearly universal in the Bird-class, but has been observed in no other Vertebrates. Behind each "pleurosteon" there is, in the Gallinaceæ [...] and a few other types, in the Crows [...], for instance, another bony centre, the "metosteon;" it ossifies the outer and intermediate xiphoid bars in the Gallinaceæ; this centre exists in the third degree of frequency (*ibid*.).

Fürbringer (1888) identified a cranial part of the sternum, the 'costosternum' (with which the sternal ribs articulate), and a caudal part, the 'xiphosternum' or 'metasternum'.

Saint-Hilaire, E. G. 1833 Sur des Observations Communiquées a l'Académie des Sciences, au Sujet des Sternums des Oiseaux, en ce qu'elles s'appliquent a la théorie des analogies, *Nouvelles Annales du Muséum d'Histoire Naturelle*, Tome Deuxième, pp.1-22.

Appendix 2: Osteometric Data

(Osteometric data: Melville 1848, pp.102, 110, 113, 115-116 (and in main text); Strickland 1853, pp.190, 192, 193, 194, 195; Reuss 1855, p.76; A. Newton 1865a, p.200; Owen 1867; Owen 1878, p.95 (and in main text); Newton & Clark 1879, pp.443, 444, 446, 447; Mertens 1925, p.202; Lüttschwager 1959b, pp.139, 142; Lüttschwager 1961, p.45; Pieper 1987; Brom & Prins 1988, table i; Kitchener 1993a, fig.4; Livezey 1993, tables iv, v; Janoo 1996, table i; Worthy 2001, tables 1, 2, 4; Janoo 2005; Angst & Buffetaut 2010, tableau 1; Angst *et al.* 2011a, fig.1, supplementary material; Angst *et al.* 2011b; Hume & Steel 2013, tables 3, 4; Claessens *et al.* 2015, tables 2-14, 16-24, A2-A10)

The following are osteometric data for *Raphus* and *Pezophaps*. Measurements of dodo and solitaire bones, taken by the author, can be found here:
https://drive.google.com/file/d/18gPfwK8CP2LpdoQfd0r8GE_82jnx7bY0/view

Note: Where original measurements were given in inches and lines these have been converted to metric and the original data given in parentheses.

Author's data (UMZC specimens) for *Raphus*. Bone lengths in mm; n = number of specimens measured; s.d. = standard deviation:

Element	**n**	**Minimum**	**Maximum**	**Mean (s.d.)**	**Median**
mandible length	2	187.0	200.6	193.8 (6.80)	193.8
synsacrum length	11	138.3	169.2	150.0 (9.10)	147.4
scapula length	3	93.0	98.0	96.0 (2.18)	97.1
coracoid length	3	81.2	86.3	84.2 (2.16)	85.0
sternum length	2	162.9	165.8	164.4 (1.45)	164.4
humerus length	6	96.5	106.8	102.3 (3.34)	102.5
ulna length	2	85.1	86.1	85.6 (0.50)	85.6
pelvis width[472]	14	117.0	137.6	124.6 (5.49)	124.8
femur length	27	138.5	161.3	150.7 (6.12)	150.5
tibiotarsus length	24	191.2	243.0	221.4 (10.50)	221.8
tarsometatarsus length	53	110.8	141.1	127.6 (5.69)	127.5

Longest and shortest bones

Bone lengths in mm. % = smallest / largest x 100.

Raphus	**Longest**	**Shortest**	**%**
facial skeleton (beak)	147.0 (NMP P6V-004389)	*c.*139.7 (ZMUK AVES-105485)[a]	95.0
mandible	200.6 (UMZC 415.K)	182 (Claessens *et al.* 2015)	90.7
synsacrum	169.2 (UMZC 415.K)	138.3 (UMZC 415.K)	81.7
scapula	98.0 (UMZC 415.K)	92 (Claessens *et al.* 2015)	93.9
coracoid	95 (Claessens *et al.* 2015)	76.8 (Claessens *et al.* 2015)	80.8
sternum	177.8 (Owen 1867)	159 (Claessens *et al.* 2015)	89.4
humerus	107.2 (Claessens *et al.* 2015)	91.1 (Claessens *et al.* 2015)	85.0
ulna	87 (Claessens *et al.* 2015)	81.3 (Claessens *et al.* 2015)	93.4
carpometacarpus	47 (Hume & Steel 2013)	41.5 (Hume & Steel 2013)	88.3
pelvis width	137.6 (UMZC 415.K)	117.0 (UMZC 415.K)	85.0
femur	161.3 (UMZC 415.K)[c]	138.5 (UMZC 415.K)[d]	85.9
tibiotarsus	243.0 (UMZC 415.K)	191.2 (UMZC 415.K)	78.7
tarsometatarsus	146 (Booth: No.101775)[b]	110 (Brussels: left tmt)[b]	75.3

a: from a photograph of a cast (USNM 16957). As noted in Parish (2013, p.380n9), the bill length given by Livezey (1993) as *c.*118mm is an error. Longest and shortest femora, tibiotarsi and tarsometatarsi of *Raphus* had previously been selected from the UMZC collection by Andrew Kitchener.[473] b: data from Angst *et al.* (2011a). c: Newman (1866, p.98) stated that in *Raphus* "some femurs are nearly seven inches [177.8mm] long". d: the length of 125mm given by Angst *et al*. (2011a) for a left femur (Lyon QV 12) is a mistake; the measurement should be 155mm (Angst *et al*. 2011b). Booth = Booth Museum of Natural History, Brighton; Brussels = Institut royal des Sciences naturelles de Belgique, Brussels. Note: due to potential differences in the ways measurements were taken by different authors they are not necessarily identical.

---

[472] Distance between lateralmost margins of antitrochanters.

The largest individual of *Raphus* the present author has noted is represented by a tarsometatarsus from the Booth Museum collections (Angst *et al*. 2011a), which has a length of 146mm.

Pezophaps	**Longest**	**Shortest**	**%**
cranium	86.3 (Newton & Clark 1879)	72.8 (Newton & Clark 1879)	84.4
humerus	125.8 (UMZC 415.L)	91.0 (UMZC 635)	72.3
ulna	*c*.92 (Ottow 1950)	*c*.66 (Ottow 1950)	71.7
radius	80.6 (Pieper 1987)[a]	62.0 (Pieper 1987)	76.9
carpometacarpus	49.9 (Hume & Steel 2013)	37 (Hume & Steel 2013)	74.1
femur	187.8 (UMZC 415.L)	141.0 (Newton & Clark 1879)	75.1[474]
tibiotarsus	276.9 (Newton & Clark 1879)	212.1 (Newton & Clark 1879)	76.6
tarsometatarsus	189.2 (Newton & Clark 1879)[c]	137.2 (Newton & Clark 1879)	72.5
Caldwell's solitaire skeletons (height)[b]	male: 83.82cm	female: 69.22cm	82.6

a: specimen was pathological (Pieper 1987). b: data from caption to photograph (Item 28, Indian Ocean MS. volume, Balfour and Newton Libraries, University of Cambridge): male 2 feet 9 inches, female 2 feet 3¼ inches. c: Livezey (1993) gives a mean of 183.0 (n = 5, s.d. = 9.3).

Skull

Raphus

Measurements of OUMNH 11605 (Melville 1848):

Distance between ventral points of paroccipital processes 39.2mm (1 inch 6½ lines)

Distance between lateral surfaces of ventral extremities of lacrimals ('prefrontals') 43.4mm (1 inch 8½ lines)

Ventral extremity of lacrimal ('prefrontal') to postorbital process 40.2mm (1 inch 7 lines)

Foramen opticum: diameter 5.3mm (2½ lines); distance between rostral edge of foramen and that of opposite side 14.1mm (6⅔ lines)

Width of cranium: at supraorbital notches 76.2mm (3 inches); at rostral edge 38.1mm (1 inch 6 lines)

Distance between rostral angle of lacrimal ('prefrontal') and caudal edge of occipital face 80.4mm (3 inches 2 lines)

Posterior olfactory chamber ("olfactory fossa"): depth 29.6mm (1 inch 2 lines); width at rostral orifice 10.6mm (5 lines)

Cranial cavity: length from foramen magnum to olfactory septum 45.5mm (1 inch 9½ lines); width between ophthalmic foramina 25.4mm (1 inch); maximum width of cerebral fossa perhaps 44.5mm (1 inch 9 lines); length of fossa for medulla oblongata 26.1mm (1 inch ⅓ line).

Mandible length 196.9mm (7 inches 9 lines)

Owen (1845, measurements of OUMNH 11605 prior to dissection): distance between temporal fossae 70.0mm (2 inches 9 lines). Interorbital space 76.2mm (3 inches) across. "outer apertures of the ears" just over 25.4mm (1 inch) caudoventral to the eyes. Symphysis of mandible 38.1mm (1½ inches) long.

Reuss (1855):

Measurements of Prague beak (NMP P6V-004389). OUMNH 11605 from Strickland & Melville (1848), Copenhagen head (ZMUK AVES-105485) from cast.[475]

---

[473] Notes accompanying UMZC 415.K state that the longest and shortest femora, tibiotarsi and tarsometatarsi were selected from the collection by Andrew Kitchener in November 1989.

[474] Strickland (1853) stated that the ratio of the lengths of the femora and tarsometatarsi of female to male specimens of *Pezophaps* was 0.77.

[475] Conversions calculated using 1 nineteenth-century Paris foot = 32.48cm, giving 1 Paris inch = 27.07mm.

	Prague	Copenhagen	OUMNH 11605
Beak (rostrum) length (following the dorsal margin)	173.25mm (6.4 Paris inches)	158.36mm (5.85 Paris inches)	157.01mm (5.8 Paris inches)
Length of the dorsal bar	109.63mm (4.05 Paris inches)	100.16mm (3.7 Paris inches)*	101.51mm (3.75 Paris inches)
Maximum width of the beak (rostrum) of the caudal end	48.73mm (1.8 Paris inches)	48.73mm (1.8 Paris inches)	42.77mm (1.58 Paris inches)
Maximum perpendicular height of the beak (rostrum) at the lower angle of the caudal end	48.73mm (1.8 Paris inches)	48.73mm (1.8 Paris inches)	39.25mm (1.45 Paris inches)
Width of the caudal margin of the dorsal bar	27.07mm (1.0 Paris inches)	23.01mm (0.85 Paris inches)	27.07mm (1.0 Paris inches)
Minimum width of the dorsal bar	14.89mm (0.55 Paris inches)	14.62mm (0.54 Paris inches)	12.40mm (0.458 Paris inches)
Length of the premaxillary process of the nasal at the lateral edge of the dorsal bar	50.08mm (1.85 Paris inches)	?	44.94mm (1.66 Paris inches)
Width of the premaxillary process of the nasal at the caudal end	7.44mm (0.275 Paris inches)	?	5.63mm (0.208 Paris inches)
Length of the lateral bar at the ventral edge up to the junction of the palatine	73.09mm (2.7 Paris inches)	62.26mm (2.3 Paris inches)	?
Length of the lateral bar diagonally from the rostral end of the ventral edge up to the caudal end of the maxillary process of the nasal	115.05mm (4.25 Paris inches)	109.63mm (4.05 Paris inches)	?
Length of the dorsal concave edge of the lateral bar	104.22mm (3.85 Paris inches)	97.45mm (3.6 Paris inches)	101.51mm (3.75 Paris inches)
Height of the caudal end of the lateral bar	59.55mm (2.2 Paris inches)	62.26mm (2.3 Paris inches)	60.91mm (2.25 Paris inches)
Thickness of the caudal end of the lateral bar at the junction of the jugal arch	18.95mm (0.7 Paris inches)	?	17.87mm (0.66 Paris inches)
Minimum thickness of the two united lateral bars in ventral aspect	17.60mm (0.65 Paris inches)	21.66mm (0.8 Paris inches)	15.70mm (0.58 Paris inches)
Minimum width of each lateral bar in the same place	8.12mm (0.3 Paris inches)	8.66mm (0.32 Paris inches)	7.50mm (0.277 Paris inches)
Height of the whole beak (rostrum) in this place	40.60mm (1.5 Paris inches)	43.31mm (1.6 Paris inches)	33.84mm (1.25 Paris inches)
Length of the nasal fissure	92.04mm (3.4 Paris inches)	79.86mm (2.95 Paris inches)	?
Maximum height of the nasal fissure	16.24mm (0.6 Paris inches)	13.53mm (0.5 Paris inches)	?
Length of the corpus ossis premaxillare from the caudodorsal edge to the termina distalis	78.50mm (2.9 Paris inches)	73.09mm (2.7 Paris inches)	?
Length the same in a straight line measured on the ventrolateral edge	59.55mm (2.2 Paris inches)	56.85mm (2.1 Paris inches)	54.14mm (2.0 Paris inches)
Thickness the same at its caudal margin in ventral aspect	27.07mm (1.0 Paris inches)	27.07mm (1.0 Paris inches)	?
Thickness the same in the middle of the caudal edge before the entrance into the neurovascular canal	36.54mm (1.35 Paris inches)	33.84mm (1.25 Paris inches)	29.24mm (1.08 Paris inches)
Height of the same at the caudal edge	50.08mm (1.85 Paris inches)	45.34mm (1.675 Paris inches)	38.44mm (1.42 Paris inches)
Maximum width of the palatal surface of the corpus ossis premaxillare	25.72mm (0.95 Paris inches)	20.30mm (0.75 Paris inches)	?
Palatine length	52.79mm (1.95 Paris inches)	50.08mm (1.85 Paris inches)	67.67mm (2.5 Paris inches)
Palatine: maximum height	22.47mm (0.83 Paris inches)	24.36mm (0.9 Paris inches)	?

Maximum width of dorsal bar: Prague (NMP P6V-004389): 28.42mm (1.05 Paris inches)

Newman (1866): the ‘tip’ of one upper mandible of *Raphus* is 50.8mm (2 inches) deep and 25.4mm (1 inch) thick.

Pezophaps
Measurements of crania (in mm) (Newton & Clark 1879):

Presumed adult males

Length	86.36mm (3.40 inches)	86.34mm (3.40 inches)	85.34mm (3.36 inches)	85.09mm (3.35 inches)	84.58mm (3.33 inches)
Height	24.13mm (0.95 inches)	23.37mm (0.92 inches)	23.11mm (0.91 inches)	22.86mm (0.90 inches)	22.86mm (0.90 inches)

Presumed adult females

Length	78.74mm (3.10 inches)	77.98mm (3.07 inches)	77.98mm (3.07 inches)	77.72mm (3.06 inches)	77.47mm (3.05 inches)	77.47mm (3.05 inches)	76.20mm (3.00 inches)	74.93mm (2.95 inches)	73.15mm (2.88 inches)	73.00mm (2.87 inches)
Height	20.07mm (0.79 inches)	20.57mm (0.81 inches)	19.30mm (0.76 inches)	19.81mm (0.78 inches)	20.32mm (0.80 inches)	20.32mm (0.80 inches)	19.05mm (0.75 inches)	17.78mm (0.70 inches)	18.80mm (0.74 inches)	17.78mm (0.70 inches)

Presumed adult males

Length from forehead to base of occiput	85.34mm (3.36 inches)	85.34mm (3.36 inches)	85.34mm (3.36 inches)	85.09mm (3.35 inches)	84.58mm (3.33 inches)	85.58mm (3.33 inches)	83.82mm (3.30 inches)
Maximum breadth of skull	71.12mm (2.80 inches)	69.09mm (2.72 inches)	broken	70.10mm (2.76 inches)	71.12mm (2.80 inches)	68.83mm (2.71 inches)	68.33mm (2.69 inches)

Presumed adult females

Length from forehead to base of occiput	79.50mm (3.13 inches)	78.23mm (3.08 inches)	78.00mm (3.07 inches)	77.47mm (3.05 inches)	77.22mm (3.04 inches)	76.71mm (3.02 inches)	76.20mm (3.00 inches)	76.20mm (3.00 inches)	75.18mm (2.96 inches)	74.93mm (2.95 inches)	74.93mm (2.95 inches)	74.17mm (2.92 inches)
Maximum breadth of skull	broken	60.20mm (2.37 inches)	broken	broken	60.45mm (2.38 inches)	59.69mm (2.35 inches)	60.96mm (2.40 inches)	58.42mm (2.30 inches)	broken	broken	60.45mm (2.38 inches)	60.71mm (2.39 inches)

Measurements of MNHN-F MAD6001 (1786 find), including carbonate encrustation (Melville 1848):
Length from occipital condyle to “inter-olfactory septum” 86.8mm (3 inches 5 lines)
Maximum width rostral to postorbital processes 74.1mm (2 inches 11 lines)
Height in centre 42.3mm (1 inch 8 lines)
Distance from occipital face to craniofacial margin 74.1mm (2 inches 11 lines)
Distance from occipital face to rostral margin of the orbit 65.6mm (2 inches 7 lines)
Distance from occipital condyle to optic foramen 38.1mm (1 inch 6 lines)
Distance from optic foramen to rostral margin of orbit 27.5mm (1 inch 1 line)
Distance from rostral margin of temporal notch to rostral margin of orbit 27.5mm (1 inch 1 line)

Maximum width of cast (UMZC 415.La) of MNHN-F MAD6001 (original specimen includes carbonate encrustation): 75.8mm

Sternum

Raphus

Newman (1866): some specimens over 127mm (5 inches) wide and 177.8mm (7 inches) long, the carina is 6.4mm (¼ inch) wide and attains a maximum depth of about 25.4mm (an inch); the sternum is about 19.1mm (¾ inch) thick, thinning toward the edges.

Owen (1867): length 177.8mm (7 inches) (from the craniolateral process to the caudal margin); maximum width 114.3mm (4½ inches) (between the lateral processes).

Clark (1865): "The keel is a quarter of an inch [25.4mm] thick, and about an inch [25.4mm] deep in the deepest part, which is at the centre; and the sternum is there three quarters of an inch [19.1mm] in thickness".

Pezophaps

Paris sternum MNHN-F MAD6400 (Melville 1848): length of sternum fragment 114.3mm (4½ inches), width 101.6mm (4 inches).

Coracoid

Raphus

Coracoid length (Owen 1867): 91.0mm (3 inches 7 lines).

Scapula

Raphus

Scapula lengths (Owen 1867): 91.0mm (3 inches 7 lines), 93.1mm (3 inches 8 lines).

Humerus

Raphus

Humerus length (Owen 1867): 108.0mm (4 inches 3 lines).

Newman (1866): less than 101.6mm (4 inches) long, shaft about 9.5mm (⅜ inch) in diameter and less than 6.4mm (¼ inch) in thickness.

Clark (1865): "The humerus is less than four inches [101.6mm] in length, and the shaft only about three eigths of an inch [9.5mm] in diameter".

Pezophaps

Shaft of left humerus collected by Edward Newton (A. Newton 1865a, pl.viii, fig.3): transverse diameter of shaft 12.7mm (6 lines), craniocaudal diameter of shaft 9.9mm (4⅔ lines) (A. Newton 1865a).

Paris (MNHN) humerus (Melville 1848): length 118.5mm (4 inches 8 lines).

Length of cast of the Paris humerus (UMZC 415.Lc) 125.8mm

Proximal portion of right humerus (NHMUK A.1357): maximum width from pectoral crest to bicipital crest 37.0mm (1 inch 5½ lines), minimum horizontal diameter of shaft 12.7mm (6 lines), minimum vertical diameter of shaft 11.6mm (5½ lines), horizontal diameter of medullary cavity 8.5mm (4 lines), vertical diameter of medullary cavity 6.4mm (3 lines). Measured by W. K. Parker (A. Newton 1865a).

Ulna

Raphus

Ulna length (Owen 1867): 78.3mm (3 inches 1 line).

Clark (1865): "the ulna, under three inches [76.2mm], and less than a quarter of an inch [6.4mm] in thickness".

Pelvis

Raphus

Pelvis, width 25.4mm (1 inch) caudal to the acetabulum (Owen 1867): 127mm (5 inches).

Femur

Raphus

Femur length (Owen 1867): 158.8mm (6 inches 3 lines), 161.9mm (6 inches 4½ lines).

Newman (1866) stated that in *Raphus* "some femurs are nearly seven inches [177.8mm] long and more than an inch [25.4mm] in diameter" (p.98).

Pezophaps

Maximum length of male femur (Strickland 1853): 182.0mm (7 inches 2 lines).

Length of cast of MNHN-F MAD6421 (UMZC 415.Ld) 187.8mm

Nearly perfect, right femur (female?) (NHMUK A.1359): length from sulcus intercondylaris to proximal extremity of neck 127mm (5 inches), transverse diameter of shaft 16.9mm (8 lines), craniocaudal diameter of shaft 13.2mm (6¼ lines), transverse diameter of proximal extremity 37.0mm (1 inch 5½ lines), transverse diameter of distal extremity 35.5mm (1 inch 4¾ lines), minimum circumference 48.7mm (23 lines) (Strickland 1853).

Distal fragment of a right femur (NHMUK A1358): transverse diameter of shaft 21.2mm (10 lines), craniocaudal diameter of shaft 16.9mm (8 lines), transverse diameter of medullary cavity 15.9mm (7½ lines), craniocaudal diameter of medullary cavity 11.6mm (5½ lines), minumum circumference 63.5mm (30 lines) (Strickland 1853).

Right femur (UMZC 632): length from intercondyloid notch to upper surface of neck 152.4mm (6 inches), length from upper edge of trochanter to lateral condyle 171.5mm (6 inches 9 lines), lateromedial width of shaft 21.2mm (10 lines), craniocaudal diameter of shaft 15.9mm (7½ lines), lateromedial width of proximal end 52.2mm (2 inches ⅔ line), lateromedial width of distal end 46.6mm (1 inch 10 lines). Measured by W. K. Parker (A. Newton 1865a).

	Presumed male	Presumed females	
	Imperfect right femur, Andersonian Museum no.8 of Strickland 1853	Perfect right femur (no.14 of Strickland 1853)	Left femur, damaged at extremities (no.15 of Strickland 1853)
Minimum circumference	61.4mm (29 lines)	49.7mm (23½ lines)	48.7mm (23 lines)

(data from Strickland 1853).

	Andersonian Museum			MNHN
	Right femur	Left femur	Right femur, extremities damaged	Left femur MNHN-F MAD6421
Length from sulcus intercondylaris to proximal surface of neck	132.3mm (5 inches 2½ lines)	–	Length, as damaged: 124.9mm (4 inches 11 lines)	160.9mm (6 inches 4 lines)
Length from lateral condyle to extremity of trochanter femoris	146.1mm (5 inches 9 lines)	–	–	186.3mm (7 inches 4 lines)
Transverse diameter of shaft	16.9mm (8 lines)	16.9mm (8 lines)	20.1mm (9½ lines)	23.3mm (11 lines)
Craniocaudal diameter of shaft	13.8mm (6½ lines)	14.1mm (6⅔ lines)	15.9mm (7½ lines)	19.1mm (9 lines)
Transverse diameter of proximal extremity	38.1mm (1 inch 6 lines)	–	–	55.0mm (2 inches 2 lines)
Transverse diameter of caudal extremity	35.3mm (1 inch 4⅔ lines)	–	–	50.8mm (2 inches)

(data from Melville 1848).

Lengths of *Pezophaps* femora (Newton & Clark 1879). Numbers: presumed males 28 left, 41 right; presumed females 38 left, 31 right:

Pezophaps femora	Largest	Smallest
Presumed males	184.9mm (7.28 inches)	167.6mm (6.60 inches)
Presumed females	154.9mm (6.10 inches)	141.0mm (5.55 inches)

Tibiotarsus

Raphus

Tibiotarsus length (Owen 1867): 220.1mm (8 inches 8 lines), 228.6mm (9 inches).

Newman (1866) stated that some tibiotarsi of *Raphus* were 228.6mm (9 inches) long, with upper condyles 50.8mm (2 inches) in diameter.

Pezophaps

Maximum length of *Pezophaps* male tibiotarsus (Strickland 1853): 256.1mm (10 inches 1 line).

Pezophaps tibiotarsi (male) possibly from same individual:

	Left, lacking proximal end (Melville 1848, pl.xv, fig.1, 1a)	Right (NHMUK A1356)
Total length	–	256.1mm (10 inches 1 line)
Transverse diameter of proximal extremity	–	40.2mm (1 inch 7 lines)
Craniocaudal diameter of proximal extremity	–	44.5mm (1 inch 9 lines)
Length of fibular crest	–	57.2mm (2 inches 3 lines)
Distance from distal extremity of fibular ridge to Incisura intercondylaris	165.1mm (6 inches 6 lines)	157.7mm (6 inches 2½ lines)
Minimum transverse diameter of shaft	16.9mm (8 lines)	16.9mm (8 lines)
Minimum craniocaudal diameter of shaft	14.8mm (7 lines)	13.8mm (6½ lines)
Width of distal extremity	32.8mm (1 inch 3½ lines)	33.9mm (1 inch 4 lines)
Craniocaudal diameter of distal extremity	31.8mm (1 inch 3 lines)	32.8mm (1 inch 3½ lines)

Lengths of *Pezophaps* tibiotarsi (Newton & Clark 1879). Numbers: presumed males 41 left, 42 right; presumed females 42 left, 40 right:

Pezophaps tibiotarsi	Largest	Smallest
Presumed males	276.9mm (10.90 inches)	259.1mm (10.20 inches)
Presumed females	236.2mm (9.30 inches)	212.1mm (8.35 inches)

Fibula

Raphus

Fibula length (Owen 1867): 110.1mm (4 inches 4 lines), 114.3mm (4 inches 6 lines).

Tarsometatarsus

Pezophaps

Lengths of *Pezophaps* tarsometatarsi (Newton & Clark 1875). Numbers: presumed males 34 left, 36 right; presumed females 33 left, 29 right:

Pezophaps femora	Largest	Smallest
Presumed males	189.2mm (7.45 inches)	172.7mm (6.80 inches)
Presumed females	156.0mm (6.14 inches)	137.2mm (5.40 inches)

UMZC 633: length from middle trochlear groove to intercondylar eminence 173.6mm (6 inches 10 lines); length from lateral trochlea to lateral cotyla 160.9mm (6 inches 4 lines); length from medial trochlea to medial cotyla 167.2mm (6 inches 7 lines); lateromedial width of proximal end 38.1mm (1 inch 6 lines); craniocaudal width of proximal end 31.8mm (1 inch 3 lines); width of distal end 40.2mm (1 inch 7 lines); projection of medial crista of hypotarsus 16.9mm (8 lines). Measured by W. K. Parker (A. Newton 1865a).

Left tarsometatarsus in the Andersonian Museum (Melville 1848): probable length from distal end of middle trochlea to proximal end of intercondyloid eminence 184.2mm (7 inches 3 lines); transverse width of shaft 16.2mm (7⅔ lines); craniocaudal width of shaft at proximal margin of fossa metatarsi I 11.6mm (5½ lines); transverse width of distal end 39.2mm (1 inch 6½ lines); length from proximal margin of fossa metatarsi I to medial intertrochlear incisure 43.4mm (1 inch 8½ lines) (Melville 1848). Length 184.2mm (87 lines), least circumference 49.7mm (23½ lines) (Strickland 1853).

Right tarsometatarsus in the Andersonian Museum (Melville 1848): craniocaudal width of proximal articular face (to the hypotarsal canal) 14.8mm (7 lines).

Right tarsometatarsus MNHN-F MAD6404 (Melville 1848): length from middle trochlear groove to intercondyloid eminence 179.9mm (7 inches 1 line); length from trochlea of metatarsal IV to lateral cotyla 167.2mm (6 inches 7 lines); length from trochlea of metatarsal II to medial cotyla 169.3mm (6 inches 8 lines); transverse width of proximal end 38.1mm (1 inch 6 lines); craniocaudal width of proximal end 36.0mm (1 inch 5 lines); transverse width of distal end 44.5mm (1 inch 9 lines); projection of medial hypotarsal crista 14.8mm (7 lines); thickness of carbonate encrustation about 2.1mm (1 line).

Length of cast of MNHN-F MAD6404 (UMZC 415.Le) 186.5mm

Strickland (1853):

	UMZC 415.N	NHMUK A1360
Length from distal border of trochlea of metatarsal III to summit of eminentia intercondylaris	143.9mm (5 inches 8 lines)	146.1mm (5 inches 9 lines)
Least circumference	36.0mm (17 lines)	36.0mm (17 lines)
Transverse diameter of shaft	12.7mm (6 lines)	12.7mm (6 lines)
Cranio-caudal diameter of the shaft at the proximal portion of articular surface for posterior metatarsal	8.5mm (4 lines)	8.5mm (4 lines)
Transverse diameter of distal extremity	32.8mm (1 inch 3½ lines)	33.3mm (1 inch 3¾ lines)
Distance from proximal border of posterior metatarsal articular facet to medial intertrochlear incisure	31.8mm (1 inch 3 lines)	33.3mm (1 inch 3¾ lines)
Length from trochlea of metatarsal IV to lateral cotyla	130.2mm (5 inches 1½ lines)	132.3mm (5 inches 2½ lines)
Length from trochlea metatarsal II to medial cotyla	132.3mm (5 inches 2½ lines)	134.4mm (5 inches 3½ lines)
Width of proximal end	29.6mm (1 inch 2 lines)	30.2mm (1 inch 2¼ lines)
Cranio-caudal diameter of proximal end	27.5mm (1 inch 1 line)	–
Projection of medial hypotarsal crest	11.6mm (5½ lines)	–

Pedal Phalanges

Raphus

Maximum lengths of pedal phalanges from OUMNH 11605 (Melville 1848, p.110):

	Hallux (digit I)	Digit II	Digit III	Digit IV
Phalanx 1 (proximal)	33.9mm (1 inch 4 lines)	39.2mm (1 inch 6½ lines)	38.1mm (1 inch 6 lines)	26.5mm (1 inch ½ line)
Phalanx 2		23.3mm (11 lines)	25.4mm (1 inch)	14.8mm (7 lines)
Phalanx 3			19.1mm (9 lines)	12.7mm (6 lines)
Phalanx 4				12.7mm (6 lines)
Phalanx 5 (ungual)				14.8mm (7 lines)

Length of proximal phalanx plus the ungual phalanx of hallux in the British Museum foot: about 50.8mm (2 inches) (Melville 1848).

Skeleton

Owen (1878):

	Pezophaps		*Raphus*
	Male	Female	
Length of vertebral axis (from tip of beak to end of pygostyle, following the curves)	88.9cm (2 feet 11 inches)	78.7cm (2 feet 7 inches)	96.5mm (3 feet 2 inches)
Height in easy standing position	78.7cm (2 feet 7 inches)	66.0cm (2 feet 2 inches)	61.0cm (2 feet)

Length of leg (from proximal end of tibiotarsus to sole)	41.9cm (1 foot 4 inches 6 lines)	33.0cm (1 foot 1 inch)	35.6cm (1 foot 2 inches)

Osteometrics

	Humerus:ulna	Humerus: metacarpal II*	femur: tibiotarsus	femur: tarsometatarsus	humerus:femur	Locomotory Index
Raphus	1.25-1.26	2.41-2.43	0.70-0.71	1.24-1.25	0.69-0.70	0.48
Caloenas	0.80-0.81	1.41-1.51	0.68-0.70	1.14-1.18	1.16-1.17	1.02-1.04

Raphus (Thirioux’s Port Louis skeleton; measurements from Claessens *et al*. 2015)
Caloenas (n=3, data from Verheyen 1957)
Locomotory Index (“Index de locomotion” of Verheyen 1955) = lengths of humerus + ulna + metacarpal II / lengths of femur + tibiotarsus + tarsometatarsus
* For *Raphus* the length of the carpometacarpus is used.

Appendix 3a: Notes on the Skeletal Reconstructions Presented Herein

3a: Dodo

The present skeletal reconstruction is an updated version of that in Parish (2013, fig.6.1). Elements are shown in lateral view and no correction is made for perspective and bones (*e.g.*, the femur) being at an angle to the sagittal midline. However, this makes only a slight difference (cf. Claessens *et al.* 2015, pl.PL2D).

The scapulocoracoid and limb elements were scaled using length measurements of elements (left side) of Thirioux's Port Louis skeleton from Claessens *et al.* (2015): coracoid 94mm, humerus 106mm, ulna 85mm, radius 76mm, carpometacarpus 44mm, femur 152mm, tibiotarsus 218mm, fibula 141mm, tarsometatarsus 123mm. The skull was scaled using the proportions of OUMNH 11605 (tarsometatarsus length to skull length 133.8 : 208.5, based on Strickland & Melville's (1848) data,[476] including plates viii and ix). The standing height of the dodo (based on the reconstructed body outline) is 62.6cm.

Skull: The skull (including mandible) was traced from Strickland & Melville (1848, pl.viii). The proximal hyoid apparatus is not shown as it is unknown. The sclerotic ring was traced from Strickland & Melville (1848, pl.ix*, fig.5) and placed using Mansūr as a reference, with the ring being placed over the eye.

Vertebrae: The atlas was traced from Newton & Gadow (1893, pl.xxxvii, fig.4). The vertebral series from the axis to the tenth cervical vertebra was traced from Owen (1867, pl.xv). The eleventh and twelfth vertebrae were drawn from UMZC specimens (UMZC 415.K) with reference to Newton & Gadow (1893, pl.xxxvi, fig.1). The thirteenth vertebra was traced from Claessens *et al.* (2015, pl.PLD11C), with reference to pl.PL11C in the same work for the hypapophysis. The fourteenth vertebra was drawn from a UMZC specimen (UMZC 415.K) and also from Owen (1867, pl.xvii, fig.6). The fifteenth vertebra was drawn from the UMZC skeleton (UMZC 415.H) with reference to Newton & Gadow (*op. cit.*). The neural spines of the fourteenth and fifteenth vertebrae were drawn with reference to UMZC 415.H and the Durban skeleton. The notarium was traced from Owen (1867, pl.xvii, fig.1) and the nineteenth vertebra was traced from Newton & Gadow (1893, pl.xxxvi, fig.2) with the neural spine traced from Thirioux's Port Louis skeleton (Claessens *et al.* 2015, fig.33). The pygostyle and caudal vertebrae were traced from a photograph of Thirioux's Port Louis skeleton.

Sternum: The body of the sternum was traced from a photograph of UMZC 415.H. The craniolateral process was drawn with reference to UMZC 415.H and Thirioux's Port Louis skeleton and the lateral process was modified from UMZC 415.H.

Scapula, coracoid and clavicle: The scapulocoracoid was traced from Owen (1867, pl.xx, fig.8), with the angles between the scapula and coracoid being approximately 108°. The proximal end of the clavicle was traced from Owen (1867, pl.xx, fig.8), with the length of the clavicle taken from Thirioux's Port Louis skeleton.

Wing: The humerus was traced from Owen (1867, pl.xx, fig.14). The radius was traced from a specimen in the Thirioux collection (Thirioux-Newton Correspondence, UMZC, letter 10A). The ulna was traced (and reversed) from Owen (1867, pl.xx, fig.17). The ulnare and radiale were traced from a photograph of Thirioux's Port Louis skeleton. The carpometacarpus and alar digit II of phalanx 1 were traced from Newton & Gadow (1893, pl.xxxvi, fig.5). Alar digit I, digit II phalanx 2, and digit III were traced from a specimen in the Thirioux collection (Thirioux-Newton Correspondence, UMZC, letter 10A).

---

[476] Skull length 8 inches 2½ lines (208.5mm).

Ribs: The number and arrangement of the ribs were taken from Thirioux's Port Louis skeleton (Claessens *et al*. 2015; see above). The first vertebral rib (that of the fifteenth vertebra) was drawn with reference to Thirioux's Port Louis skeleton (Claessens *et al*. 2015, fig.36). The uncinate processes of the second, fourth and fifth vertebral ribs were traced from a photograph of Thirioux's Port Louis skeleton. The uncinate process of the third vertebral rib was traced from Thirioux's Port Louis skeleton (Claessens *et al*. 2015, pl.18I). The sixth vertebral rib is based on a specimen in the NHMUK collections, although made slightly shorter. The heads of the vertebral ribs were drawn with reference to a photograph of Thirioux's Port Louis skeleton.[477] Sternal ribs: the first sternal rib is based on a UMZC 415.K specimen; the second and third are from a photograph of Thirioux's Port Louis skeleton; the fourth is from a photograph of Thirioux's Port Louis skeleton (and is similar to one in UMZC 415.H); the fifth is based on a UMZC 415.K specimen and articulates with preceding sternal rib instead of with the sternum. The angle between vertebral and sternal ribs is taken from Newton & Gadow (1893, pl.xxxvi, fig.1), which apparently shows a pathologically fused vertebral and sternal rib.[478] The lengths and angles of the ribs allow for a large posterior, as seen in the Mansūr and *Gelderland* images.

Pelvis: The pelvis was traced from Milne-Edwards (1866, pl.14, fig.1) with the pubis and distal ischium and ilium added from Newton & Gadow (1893, pl.xxxvii, fig.1B). The synsacrum was drawn from a UMZC 415.K specimen.

Femur and patella: The proximal part of the femur was traced from Owen (1867, pl.xv) with detail added from Milne-Edwards (1866, pl.16, fig.2b). The distal end of the femur was traced from Newton & Gadow (1893, pl.xxxxvi, fig.1). The femur was positioned using an overlay of the medial aspect of the femur as a guide, fitting the femoral head in the acetabulum. The patella was drawn from a photograph of Thirioux's Port Louis skeleton.

Tibiotarsus, fibula and tarsal sesamoid: The proximal end of the tibiotarsus was drawn from a UMZC 415.K specimen with reference to Newton & Gadow (1893, pl.xxxvi, fig.1); the distal end was drawn with reference to UMZC 415.K specimens, the Cambridge skeleton (UMZC 415.H) and Owen (1867, pl.xv). The proximal part of the fibula was traced from Owen (1867, pl.xxii, fig.7); the distal part (spina fibulae) was traced from Claessens *et al*. (2015, pl.PL2D). The tarsal sesamoid was traced from Claessens *et al*. (2015, fig.61C).

Tarsometatarsus and pedal phalanges: The tarsometatarsus, first metatarsal and phalanx 1 of digit I were traced from Strickland & Melville (1848, pl.xi, fig.4). The remaining phalanges were drawn from OUMNH 11605. The ungual of digit III is a composite of ungual of digit IV from Strickland & Melville (1848, pl.xii) and the ungual of digit IV of UMZC 415.H. The unguals of pedal digits I, II, III match the shape of those of the British Museum foot (Strickland & Melville 1848, pl.vi).

In the present skeleton the approximate angles of the long axes of the main hindlimb bones, relative to the horizontal, are as follows: femur 10°, tibiotarsus 65.5°, tarsometatarsus 65°. In the digitally-repositioned scan of Thirioux's Port Louis skeleton created by Claessens *et al*. (2015) the angles are: femur: 20°, tibiotarsus: 60°, tarsometatarsus: 75°.

Claessens *et al*. (2015) stated that: "The Mansur painting of a living dodo (e.g., Hume, 2006) could not be used for the reconstruction of hind limb joint angles, because it is painted in a naïve style and not to scale" (p.35). However, the scale argument does not stand as the Mansūr image is a collage (Welch 1996). Moreover, Mansūr's illustration shows a good general fit with a reconstructed skeleton (see Parish 2013, fig.3.3) and is considered herein to be an accurate portrayal of the dodo. Welch (1996) described it thus: "This is one of few pictures believed to have been made from direct observation. In fact, Jahāngīr's picture is considered to be the most exact and trustworthy image [...] it is sensitively, knowingly drawn, and painted with finesse" (p.98).

---

[477] Note: The vertebral ribs of the sixteenth to twentieth vertebrae of Thirioux's Port Louis skeleton are all approximately the same length (86-98mm) and are shorter than some specimens in other collections (*e.g.*, UMZC 415.K, NHMUK). Whether this means that not all of the vertebral ribs in the skeleton belong to the same individual, or whether there was significant intraspecific variation in vertebral rib length, is not known.

[478] This angle is similar to that seen in partly articulated specimens of *Goura* (USNM 489410) and *Caloenas* (USNM 322384).

The body outline was created following a reconstruction of the musculature, with illustrations considered to be drawn from life, such as that of Mansūr, used as reference for soft-parts and overall appearance.

3b: Male Solitaire
The elements of the skeleton are shown in lateral view with no corrections made for perspective. The skeleton was scaled using length measurements of elements of NHMUK A.3505 taken from Claessens *et al.* (2015): coracoid 91.5mm, humerus 123.8mm, ulna 93.6mm, radius 87.9mm, femur 182mm, tibiotarsus 265mm, tarsometatarsus 178mm. The standing height for the male solitaire (based on the reconstructed body outline) is 74.2cm.

Skull: The skull was traced from Owen (1879, pl.v, fig.1). The quadrate in NHMUK A.3505 (seen in Owen 1879, pl.v, fig.1) is positioned with the orbital process rotated medially. As such the quadrate was redrawn in a more lateral view. The orbital process was traced from Owen (1879, pl.v, fig.1) and the remainder of the quadrate was drawn from a photograph of RCSHM/Aves 706 (Simon Chaplin, pers. comm., 20th March 2008), with reference made to specimens in the UMZC 653 collection. The mandible was traced from a photograph of NHMUK A.3505, with reference to a photograph of RCSHM/Aves 706 (Simon Chaplin, pers. comm., 20th March 2008) for obscured portions. The skull was scaled using a scaled photograph of NHMUK A.3505. The epibranchial was drawn from a photograph of NHMUK A.3505. The sclerotic ring and columella are not shown (no specimens of the former are known).

Vertebrae: Cervical vertebrae 1-11 were traced from Newton & Newton (1869, pl.xv) with the ends of some of the cervical ribs restored with reference to photographs of UMZC 415.R and RCSHM/Aves 706. The atlas was articulated with the skull with reference to Owen (1878, pl.vii, fig.2). The twelfth vertebra was traced from Newton & Clark (1879, pl.xliv, fig.5). The thirteenth vertebra was traced from Newton & Newton (1869, pl.xv, fig.45) with the upper part from Newton & Clark (1879, pl.xliv, fig.3). The notarium and fourteenth vertebra were traced from Newton & Newton (1869, pl.xv, figs.48 and 51 respectively). The eighteenth vertebra was traced from Newton & Clark (1879, pl.xliv, fig.1). The caudal vertebrae were traced from a photograph of NHMUK A.3505 with the pygostyle copied from a photograph of NHMUK A.3506. Their scaling is approximate.

Ribs: The heads of the vertebral ribs articulating with the fifteenth to seventeenth vertebrae were traced from Newton & Newton (1869, pl.xv, fig.51). The uncinate process and distal end of the vertebral rib of the fifteenth vertebra were traced from a photograph of UMZC 415.R. The vertebral ribs of the sixteenth and seventeenth vertebrae were copied from a photograph of NHMUK A.3505. The vertebral rib of the eighteenth vertebra was drawn with reference a photograph of NHMUK A.3505. The vertebral rib of the nineteenth vertebra and the sternal ribs of the sixteenth to nineteenth vertebrae were copied from a photograph of NHMUK A.3505. The arrangement of ribs is based on that of NHMUK A.3505.

Pelvis: The pelvis was traced from Newton & Newton (1869, pl.xviii, fig.70) with the caudal part drawn with reference to a photograph UMZC 415.R. The distal ends of the ischium and pubis were copied from Newton & Clark (1879, pl.xlv, fig.13).

Pectoral girdle and sternum: The coracoid and scapula were traced from a photograph of NHMUK A.3505. The scapula-coracoid angle is approximately 90°, based on UMZC 651. Newton & Newton (1869) remarked: "The exact angle formed by the axes of the coracoid and scapula at the point where they meet cannot positively be determined. To the best of our judgment, however, it cannot have been much less than it is in *Didus*" (p.341). The position of the coracoid relative to the sternum is based on UMZC 651. The sternum was traced from Newton & Clark (1879, pl.xlviii, fig.1), rescaled with reference to a photograph of UMZC 415.R. The furcula was drawn with reference to a photograph of UMZC 415.R.

Wing: The humerus was traced from a photograph of NHMUK A.1379 and was positioned with reference to a photograph of NHMUK A.3505. The ulna and radius were traced from Newton & Newton (1869, pl.xix, figs.93 and 94 respectively). The carpometacarpus and ulnare were traced from a photograph of NHMUK A.3505. The ulnare was positioned with reference to a specimen of *Columba palumbus* (author's collection). The radiale is not shown. The proximal phalanx of alar digit II was traced from a photograph of NHMUK A.1452 and the distal phalanx from a photograph of a UMZC 635 specimen. The latter was scaled with reference to carpometacarpus length.

Leg: The femur was traced from a photograph of NHMUK A.3505 and was positioned using an overlay of the medial aspect of the femur as a guide, fitting the femoral head in the acetabulum. The patella was traced from a photograph of NHMUK A.3505. The tibiotarsus was traced from a photograph of NHMUK A.1398. The fibula was traced from a photograph of RCSHM/Aves 706, and the shaft straightened. The articulation of the fibula and tibiotarsus is based on a specimen of *Buteo buteo* (author's collection) in which the distal fibula is fused to the tibiotarsus, thus providing information as to the *in vivo* placement of the fibula. The detail of the proximal fibula was traced from Owen (1878, pl.vii, fig.1). The tarsal sesamoid was traced from a photograph of NHMUK A.3506 and scaled with reference to the distal width of the tibiotarsus. The tarsometatarsus was traced from Owen (1879, pl.iii, fig.1). The first metatarsal and hallux were traced from Newton & Newton (1869, pl.xx, figs.105, 107 and 109). The anterior toes were drawn with reference to photographs of UMZC 415.R and RCSHM/Aves 706. The ungual of digit IV was drawn from a photograph of RCSHM/Aves 706.

3c: Notes on Owen's Skeletal Reconstruction of the Dodo

Owen (1867, pl.xv, fig.1)[479] figured a life-size skeletal reconstruction of the dodo (drawn by James Erxleben), "with an outline of the bird as represented in the oil-painting presented to the British Museum by Edwards [...] of the natural size"[480] (p.82). The scapular arch was depicted rotated forwards in order to show the cranial dorsal vertebrae. As there was insufficient material to make up a complete skeleton at the time of writing, Owen extrapolated the missing parts. The inaccuracies in the drawing are: 1) vertebrae: the thirteenth vertebra shows a free rib. The fourteenth and fifteenth vertebrae are (probably) extrapolations. The atlas and caudal vertebrae (including the pygostyle) were not known at the time and were extrapolated. 2) ribs: the arrangement of the vertebral ribs is likely incorrect (see Thiroux's Port Louis skeleton (Claessens *et al*. 2015) for comparison). 3) pelvis: the caudal part of the pelvis, including the distal pubis were unknown at the time and were extrapolated. 4) wing: alar phalanges unknown at the time and were also interpolated. The carpometacarpus was known at the time, as although George Clark mentions finding a single specimen (Clark 1866), Owen (1867) neither described nor figured it and it was not among those bones sent to the British Museum.

○ Jolyon C. Parish 2020. Apart from images created by others (and indicated as such) this work is neither in the public domain nor not in the public domain. The present author's work is neither under copyright nor under Creative Commons, both of which have a legal system integral to them. You are free to use the author's work, but please give acknowledgement when using material provided herein and please use it only for noncommercial, educational purposes.

If this file, or part(s) thereof, is used then the preferred citation is:
Parish, J. C. 2020 The Anatomy of the Dodo (*Raphus cucullatus*) and the Solitaire (*Pezophaps solitaria*): A Description and Atlas, *in* The Dodologist's Miscellany. Available at: http://sites.google.com/site/dodologistsmiscellany/ [date accessed]
This work is part of a larger corpus. Links to other parts can also found on the same site.

28-December-2020

---

[479] "From nat on Stone by J.Erxleben." "M. & N. Hanhart. imp."

[480] The body outline does not accurately match that of the dodo in the British Museum (now NHMUK) painting, and, moreover, the painting itself is larger than life-size (Parish 2013).

http://sites.google.com/site/dodologistsmiscellany/